2015

Landscape forcing mechanisms on Quaternary timescales: The Tabernas Basin, SE Spain

Geach, Martin Roy

Landscape forcing mechanisms on Quaternary time-scales: the Tabernas Basin, SE Spain

by

Martin Roy Geach

A thesis submitted to the University of Plymouth in partial fulfilment for the degree of

DOCTOR OF PHILOSOPHY

School of Geography, Earth and Environmental Sciences

Faculty of Science and Environment

April 2015

Landscape forcing mechanisms on Quaternary time-scales: the Tabernas Basin, SE Spain

Martin Roy Geach

Quaternary landform features and their associated sedimentary assemblages (river terraces and alluvial fans) often provide important records of long-term landscape evolution. The reconstruction of global terrace sequences has enabled the identification of numerous external and internal forcing mechanisms which operate within the Quaternary landscape system. The relative effects of these forcing mechanisms are highly variable over a range of spatial and temporal scales. In this research, a combined study approach is adopted in order to ascertain the significance of external (e.g. tectonics, climate) and/or internal (e.g. lithological thresholds) forcing mechanisms upon patterns of Quaternary landscape development within the Tabernas Basin, SE Spain.

The results of extensive field investigation have developed a four-tiered landform stratigraphy (i.e. basin wide terrace levels) for the Tabernas Basin. Chronological constraints for the Quaternary stratigraphy were obtained from Optically Stimulated Luminescence dating. Age estimations develop a pattern of climatically driven terrace aggradations during glacial phases throughout the Middle to Late Pleistocene. This pattern fits well with regional models of enhanced terrace formation during glacial phases after the Middle Pleistocene.

The Quaternary stratigraphy of the Tabernas Basin was investigated by methods of geospatial interpolation and numerical modelling. The results of conceptual and quantitative modelling approaches highlight the dominance of non-uniform rates of base-level change driven by variable rates of tectonic uplift throughout the Mid-Late Pleistocene. Enhanced uplift in the west of the basin associates well with regional patterns, with tectonically driven base-level changes focused in the eastern Alpujarran Corridor. Internal landscape thresholds were important in the Holocene development of the Tabernas basin. Increased rates of incision in the final stages of basin development were likely attributed to the effects of lithological controls coupled with anthropogenic activity in the basin catchment.

Contents

Chapter 2 Study Area

Chapter 3 Quaternary Landform Record

Chapter 4 Optically stimulated luminescence dating

Chapter 8 Conclusion

Final Word count = 75680

List of figures

Chapter 1 Introduction

Chapter 2 Study Area

List of tables

List of equations

Acknowledgements

Many aspects of undertaking a PhD are like riding a very long, slightly nauseating roller coaster. There are the endless downs that come with the lonely days at a rain soaked Urra, or the uncontrolled sneeze that disperses all of your sand grains anywhere but on the slide you aimed for in Denmark. However, there are also the ups! This research has experienced many 'ups' related to the people who developed the project through its infancy and were pivotal in its success throughout the later stages. My thanks first to Dr Anne Mather, Dr Martin Stokes and Dr Matt Telfer who have offered their true friendship and invaluable experience in developing myself as a geomorphologist, OSL wizard and human surveying pole! Your knowledge, time and efforts were a real drive throughout those dark days and I wish you all great success in your future research. My thanks also to Lindy Walsh for the provision of lodgings at Urra, and most importantly, a few glasses of G&T accompanied by fine conversation and endless motivation during my stays in Spain.

This research was not funded by an extensive research grant, but it was based on an important scholarship from the School of Geography, Earth and Environmental sciences at Plymouth University. Limited funding formed the research foundation which was supplemented by the kindness and charity of numerous institutions and individuals. My thanks to Prof Andrew Murray, Dr Jan-Pieter Buylaert (still struggle to spell this), Dr Kristina Thomsen and Dr Christine Thiel at Risø in Denmark. The provision of fantastic research facilities coupled with the warmth of everyone at the lab made my stays in Denmark truly special; including the odd Schnapps or two at the Christmas party…Skål! My thanks also to Dr Willem Viveen and colleagues at Wageningen University for all your time and efforts in teaching me the joys of FLUVER2 on rainy days in Cardiff!

Finally, a special thank you to my fiancée Inga and awesome family for your support on those days when my brain stopped working. It has been a long and challenging few years but I loved every day!

Author's Declaration

At no time during the registration for the degree of Doctor of Philosophy has the author been registered for any other university award without prior agreement of the graduate committee.

Work submitted for this research degree at the Plymouth University has not formed part of any other degree either at Plymouth University or any other establishment. This study was financed by an internal studentship from the School of Geography, Earth and Environmental Sciences. Optically Stimulated Dating was conducted at the Nordic Centre for Luminescence Research supported by the Technical University of Denmark (DTU) and Aarhus University. Conference attendance was supported by the British Society for Geomorphology (2013) and the Steve Farrell Memorial Fund from the British Sedimentological Research Group (2014). Relevant scientific seminars and conferences were attended at which work was often presented and external initiations were visited for consultation purposes.

Presentations and conferences attended:

- British Society for Geomorphology Annual Conference, Royal Holloway (June 2013)
- 8th Fluvial Archives Group Biennial Meeting, Spain (Sept, 2014)
- Improving Understanding of Fluvial Landscape Development : exploring synergies between field-based and modelling approaches. Workshop, the Netherlands (Dec,2014)

The following peer-reviewed publications were also produced as part of this research:

- Geach, M.R., Stokes, M., Telfer, M.W., Mather, A.E., Fyfe, R.M., Lewin, S., 2014a. The application of geospatial interpolation methods in the reconstruction of Quaternary landform records. Geomorphology, 216(0), 234-246.

- Geach, M.R., Viveen, W., Mather, A.E. , Telfer, M.W., Fletcher, W.J., Stokes, M. (submitted). An integrated field and numerical modelling study of controls on Late Quaternary fluvial landscape development (Tabernas, SE Spain). Earth Surface Processes and Landforms.
- Geach, M.R., Thomsen, K.J., Buylaert, J-P., Murray, A.S., Mather, A.E., Telfer, M.W., Stokes, M. (submitted). A chronological framework for the Quaternary landform records of the Tabernas Basin, SE Spain. Proceedings of the 14th International Conference on Luminescence and Electron Spin Resonance Dating, Quaternary Geochronology.

Word count of main body of thesis: 75,052

Signed: 

Date: 06 July 2015

Chapter 1

1.1 Introduction

In regions which lie beyond the limits of Quaternary ice sheets, fluvial systems are an intrinsic and significant part of the landscape system (Bridgland and Westaway, 2008; Della Seta et al., 2005; Antón et al., 2012; Viveen et al., 2013a). In the Tabernas Basin, southeast Spain, the preserved Quaternary landscape styles and associated sedimentological deposits (river terraces) present a detailed record of the interplay of fluvial processes over a range of spatial and temporal scales (Harvey et al., 2003; Nash and Smith, 2003; Alexander et al., 2008). The forces which promote change occur either externally to the fluvial system, driven by mechanisms of tectonics, climate and/or sea-level change, or internally as a result of self-regulating shifts in channel style and morphology (Stokes et al., 2012a).

In studies of long-term landscape evolution (10^2 - 10^5 yrs.), extensive focus is placed on understanding how external and internal forcing mechanisms influence fluvial system development through space and time (e.g. Bridgeland and Westaway, 2008; Lewin and Gibbard, 2010; Baartman et al., 2011). In particular, current interest is focused on: (i) the application of new or refined absolute dating methods in order to constrain the temporal aspects of landscape change over Quaternary timescales (Cunha et al.,2008; Viveen et al., 2012), and (ii) the use of numerical modelling packages (e.g. LAPSUS, CAESAR, FLUVER2) in an attempt to support our qualitative understanding of how forcing mechanisms effect fluvial systems over long timescales (Baartman et al., 2012; Coulthard and Van de Wiel, 2013; Viveen et al., 2014). The application of these new and developing methodologies has offered valuable insight into the evolution of Quaternary landscapes (e.g. Macklin and Lewin, 2008; Schoorl et al., 2014). However, the approaches used often offer little appreciation of the limitations of the technique applied, with a tendency to oversimplify the intricacies of the landscape system as evidenced from the field record (*sensu* Coulthard and Van de Wiel, 2013).

In this thesis, emphasis is placed on integrating and refining techniques available in assessing patterns of long-term landscape evolution with reference to the complex Quaternary landform record from the Tabernas Basin, southeast (SE) Spain. Throughout the research, the findings from extensive field investigations are qualitatively compared and contrasted with data from absolute dating techniques (OSL dating) and numerical modelling packages (FLUVER2) in order to evaluate the intricate relationships between landscape processes over Quaternary timescales. However, care is taken to assess the limitations and errors of all methods used, with emphasis on the fundamental requirement for a well refined geological/geomorphological understanding of the study area, as based on extensive field investigations.

The Tabernas Basin is utilised as it offers a complex geomorphic setting where the preserved landform record demonstrates the effects of variable tectonic uplift (Harvey et al., 1999; 2003), regional climates cycles (Harvey et al., 2003; Alexander et al., 2008) and internal processes of landscape stabilisation (Nash and Smith, 2003) throughout the Quaternary (as detailed in Chapter 2). Located far from any major continental ice sheets, the landform record represents a complex picture of Quaternary landscape evolution with little influence from post-depositional reworking or destruction, as commonly evidenced in glaciated regions (*sensu* Bridgland and Westaway, 2008). The Tabernas Basin forms just one of a series of interconnected sedimentary basins in the Almería region (Fig.1.1) where the regional response to Quaternary landscape forcing agents has been highly variable over a range of spatial and temporal scales (Harvey and Wells, 1987; Mather et al., 2002; Maher, 2007; Stokes, 2008). Therefore, this study not only offers valuable insight into the localised basin scale responses to forcing agents, but it also allows for further regional correlations where patterns of Quaternary landscape change can be qualitatively compared and contrasted between sedimentary basins across SE Spain and further Iberian Peninsula.

1.2 Study aim, objectives and philosophical approach

1.2.1 Aim

The principal aim of this study is to ascertain the interplay and dominance of external forces (i.e. tectonic uplift and climate cycles) and/or internal controls (e.g. lithological controls) upon the evolution of the Quaternary fluvial system within the Tabernas Basin. These aspects are then qualitatively compared and contrasted with both (i) the regional records of Quaternary landscape change from other sedimentary basins located in the Betic Cordillera region of SE Spain (e.g. Sorbas and Vera Basins) and (ii) further studies of long-term landscape evolution within the Iberian Peninsula.

1.2.2 Objectives

In order to meet the aim of this study the following objectives are proposed:

- Construct a formal geomorphic basin stratigraphy for the Quaternary landform records across the Tabernas Basin;
- Develop and constrain the timing of Quaternary landscape development of the Tabernas Basin by means of optically stimulated luminescence dating of depositional fluvial landforms. This chronology is to be further compared with other regional chronologies in order to assess the significance of timings of climatically driven aggradation phases within the Tabernas Basin against neighbouring basins in the Betic Cordillera region of SE Spain;
- Develop and apply methods of geospatial interpolation in the reconstruction of Quaternary landform records across the Tabernas Basin. Landform reconstructions are used to identify the temporal and spatial patterns of landscape change across the Tabernas Basin;
- Apply the numerical modelling package FLUVER2 alongside the field based terrace record to resolve the importance of major landscape forces (variable tectonic uplift, climate and internal controls) across the Tabernas Basin throughout the Quaternary;

- Integrate field, dating and modelling approaches to explore how patterns of Quaternary landscape evolution in the Tabernas Basin fit with the regional patterns across SE Spain;
- Assess how the findings from studies of long term arid region landscape evolution conducted in SE Spain compare with further records from across the Iberian Peninsula.

1.2.3 Philosophical approach

The philosophical approach adopted in this research is that of a critical rationalist, where multiple 'statements of the problem' are proposed in the development of a research hypothesis (Haines-Young and Petch, 1986). Hypotheses are researched with rigor in an attempt to prove or disprove their truth as based on deductive reasoning. Deductive reasoning supports the approach of a critical rationalist and involves the collection and interpretation of data in order to develop hypotheses (Trochim, 2006). In this study, deductive reasoning includes the collection of empirical evidence (e.g. field data) and the generation of conceptual data (e.g. model outputs) in order to develop a model for landscape evolution. A scientific methodology is adopted to support this research approach. The scientific methodology allows for the description of natural phenomena in such a way as to promote understanding and provide reasoned explanation. Based on the principals of Graziano & Raulin (1989), accurate scientific predictions and/or interpretations are based upon observational relationships between events within the environment. Where events are not observable in current environment, judgements have been made as based on theories, or formalised concepts from organised observations and inferences (Seale, 1999).

As many of the objectives aim to develop methods in both scientific observation and reconstruction, the construct of this thesis diverts from a classical structure (i.e. introduction, methods, results and discussion). Instead, each chapter presents an individual topic of focus (i.e. an objective) and thereby investigates that topic by means of a scientific methodology. Each chapter evolves in approach, developing preliminary findings with the overall goal of

addressing the primary aim (e.g. application of advanced testing protocols in OSL dating in order to increase dating precision). Although each chapter addresses individual objectives great effort is taken to incorporate key findings in order to formalise a understanding of the aim.

1.2.4 General approach

The general approach adopted in this thesis represents the progression of research throughout the scholarship. Three broad areas of focus form essential links to each other: (1) field investigation; (2) application of OSL dating; and (3) geospatial and numerical modelling. The foundation of the research is based on extensive field investigation with focus on developing a stratigraphy for the landforms of the Tabernas Basin. The Tabernas basin was identified an opportunistic study area where localised elements of the Quaternary landscape have been presented in detail, yet not fully integrated at a basin or regional scale (Chapter 2 for detail). The results from field morphological mapping and sedimentological analysis highlight the connections between localised landscape elements and are essential in developing the Quaternary stratigraphy for the basin (presented in Chapter 3).

The Quaternary stratigraphy of the Tabernas Basin forms the primary basis for the application of OSL dating. The sedimentological knowledge and morphological relationships developed in the field aided in the development of a sampling methodology, giving a geomorphological context for the age estimates (Chapter 4). A combination of field and OSL data forms the fundamental inputs in to the geospatial and numerical modelling aspects. For example, methods of geospatial interpolation are based on the reconstruction of field terrace levels of a known relative age. Palaeolandscape reconstructions enable quantification of degradation rates and present a basic model of landscape evolution (Chapter 5) which is investigated by advanced numerical modelling techniques (Chapter 6). The numerical model outputs are then calibrated against the stratigraphic model in order to test the accuracy of model outcomes, in essence highlighting the circular nature of this study, founded in a comprehensive field investigation.

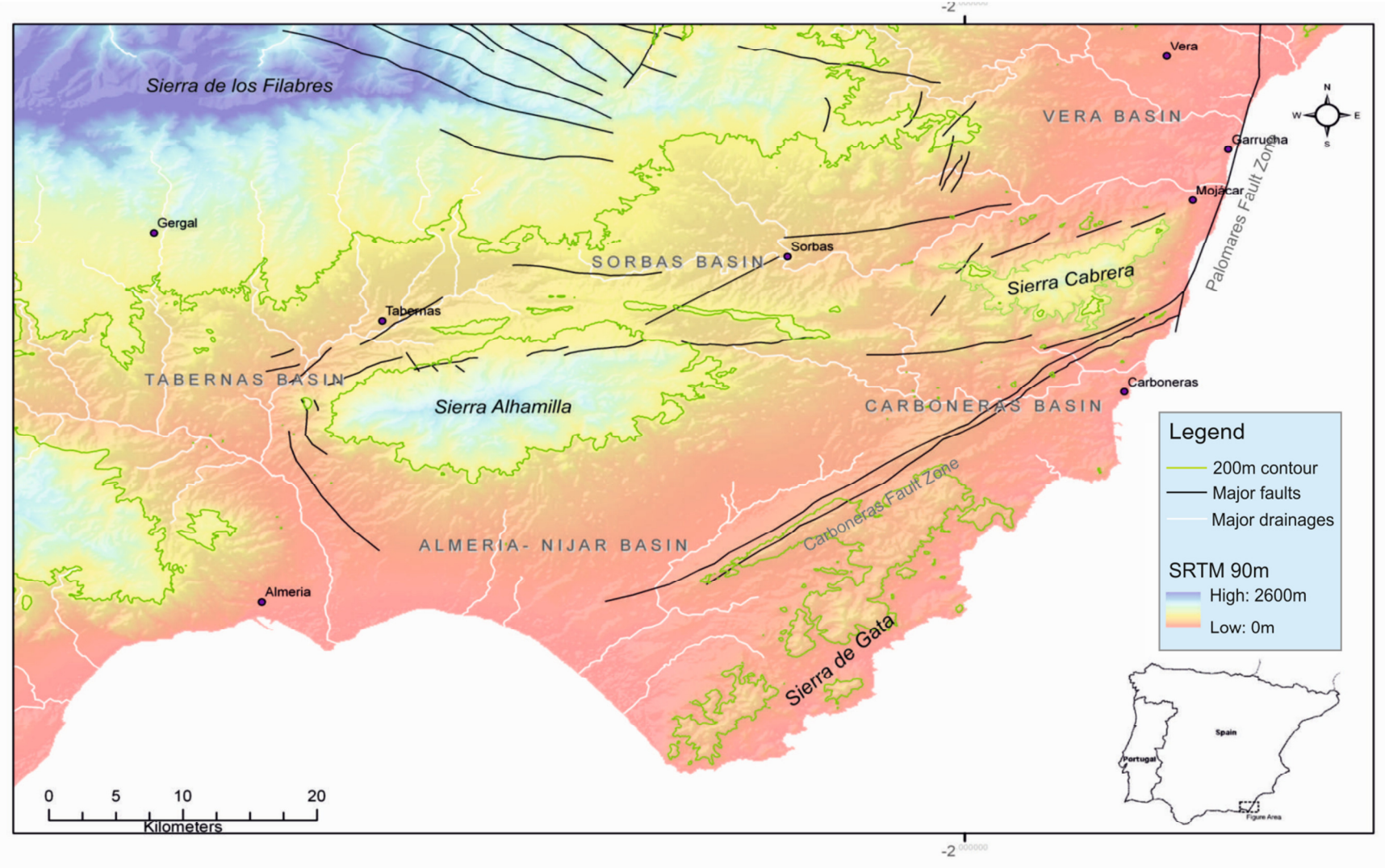

Figure 1.1 Overview map of the Neogene sedimentary basins within southeast Spain. Major fault lines (black lines) and drainages (white lines) are presented over SRTM elevation data (90m resolution).

1.3 The Tabernas Basin

The Tabernas Basin forms one of a series of interconnected Neogene intramontane sedimentary Basins located within the Internal Zone of the Betic Cordillera (Betics) in southeastern Spain (Fig. 1.1). The basin is orientated in an east-west direction, bound to the north by the Sierra de los Filabres and to the south by the Sierra Alhamilla. The current hydrological configuration of the basin was established in the Early Pleistocene-Late Pliocene with the final stages of river capture into the neighbouring Sorbas Basin (discussed in detail in Section 2; Harvey, 1987). The eastern boundary of the basin is relatively indistinct, marked by a small escarpment (<30m) which defines the modern drainage divide with the adjacent Sorbas Basin (Fig. 1.2A). The western margin of the basin is dominated by bedrock foothills of the Sierra de los Filabres, with the current hydrological basin defined by the catchment of the major regional drainage, the Río Andarax (Fig. 1.2A).

The present day basin catchment size is 560 km^2 (~25 km long x 20 km wide), characterised by a thermo-Mediterranean semi-arid climate, with a mean annual temperature of 17.8 ℃ and mean annual precipitation of 218 mm (Lázaro and Rey, 1990). The axial basin drainage, the Rambla Tabernas, drains in an east - west direction, forming a tributary to the larger Río Andarax in the southwest of the basin in the Tabernas-Almería Basin Corridor (Fig. 1.2A). A number of large tributaries such as the Rambla Sierra, Arroyo Verdelecho and Rambla Lanujar drain toward the Rambla Tabernas in the basin centre, adopting a principally north – south drainage direction from the bounding Sierras (Fig. 1.2A). The valley floors of the main tributaries and axial drainage have wide braided channels with a characteristically high transport capacity during flood events (Calvo-Cases et al., 2014). The geomorphology of the basin (as detailed in Chapter 2) records a stark contrast in incisional styles over a small area with 250 m of incision over ~12 km (Fig.1.2B). In the east of the basin, the landscape is dominated by a single depositional surface formed by aggrading alluvial fans that records little incision (<10m; Fig 1.2C). In contrast, the central

and western parts of the basin record substantial amounts of incision (Fig.1.2D), with the formation of a stepped, inset sequence of fluvial terraces, pediment surfaces and badlands which increase in abundance and maturity towards the confluence with the Río Andarax. This variation in geomorphic style across the basin has been attributed to combined interactions of tectonic, climatic and internal controls on base level throughout the Quaternary (Nash and Smith, 1998; Harvey et al., 2003; Nash and Smith, 2003; Harvey, 2007; Alexander et al., 2008; Calvo-Cases et al., 2014). The interactions between these major landscape forces form the basis for this study, with the aim of addressing the significance of each forcing agent upon the landscape system.

1.4 Scientific Context

The following sections introduce the key concepts of long-term landscape evolution with focus on fluvial system development. Firstly, the modes of fluvial terrace formation and the differences in terrace assemblages are presented. The section then develops the principal landscape forces (external and internal) which promote terrace generation and preservation. Patterns of long-term landscape evolution in SE Spain are then presented, demonstrating the significance of process interactions (e.g. a combination of many external and internal forces) upon the Quaternary landscape system. The section aims to develop the context behind this study, highlighting the importance of the Tabernas Basin with regard to: (i) its local position and the understanding of basin scale responses to external and internal driving mechanisms, and (ii) its regional significance when developing patterns of Quaternary landscape change across SE Spain.

1.4.1 Fluvial terraces

Fluvial terraces are common, globally-distributed landforms formed as a result of climatic variations in sediment and water discharge coupled with trends of base-level change acting upon/within the fluvial system through time (Bridgland et al., 2004). The first formative descriptions of terraces were made in the late 19th century, with the description of a series of

flat topped sediment bodies situated at elevations much higher than that of the active channel (Hitchcock, 1824; Lesley, 1878). Moving forward nearly two centuries and river terraces have become of increased academic concern with particular use in studies of reconstructing long-term landscape evolution (e.g. Maddy, 1997; Schumm et al., 2000; Cunha et al., 2008; Westaway et al., 2009; Antón et al., 2012, Viveen et al., 2014).

Individual terrace bodies are generated as a result of switches in periods of aggradation and incision in a fluvially dominated system, such as an active river channel and its floodplain or a hillslope alluvial fan surface (Stokes et al., 2012a). In order to form a terrace body, a primary aggradation stage is required where sediment thicknesses accrue in the river channel, floodplain or fan surface. This aggradation stage is followed by an incisional stage, whereby the ongoing erosion of the river (or multiple rivers) into its bed leads to the isolation of a relic body of sediment above that of the active channel. This relic body of sediment (terrace) provides a geomorphological snap-shot into the fluvial processes that occurred in the reach at the time of deposition (e.g. flow direction, discharge values and channel widths which are commonly calculated from the geomorphic attributes of the terrace, such as terrace sedimentology, tread slope and the vertical and horizontal distances between terrace risers; Miall, 1996).

In order to form a terrace staircase (i.e. an inset series of terraces where multiple stages of aggradation and incision are evidenced) patterns of ongoing base-level lowering must dominate the river system (Stokes et al., 2012a). Base level is defined as the lowermost point within a landscape that a river can erode (Leopold and Bull, 1979). Base-level changes are known to be promoted by external forcing mechanisms such as tectonic uplift, climate variability or relative changes in sea-level driven by either tectonics or climate (Bridgland and Westaway, 2008; Gibbard and Lewin, 2009; Viveen et al., 2014); however, in regions of tectonic quiescence internal processes such as drainage rearrangement and / or major channel avulsions can be of significance (Bishop, 1995; Prince et al., 2011).

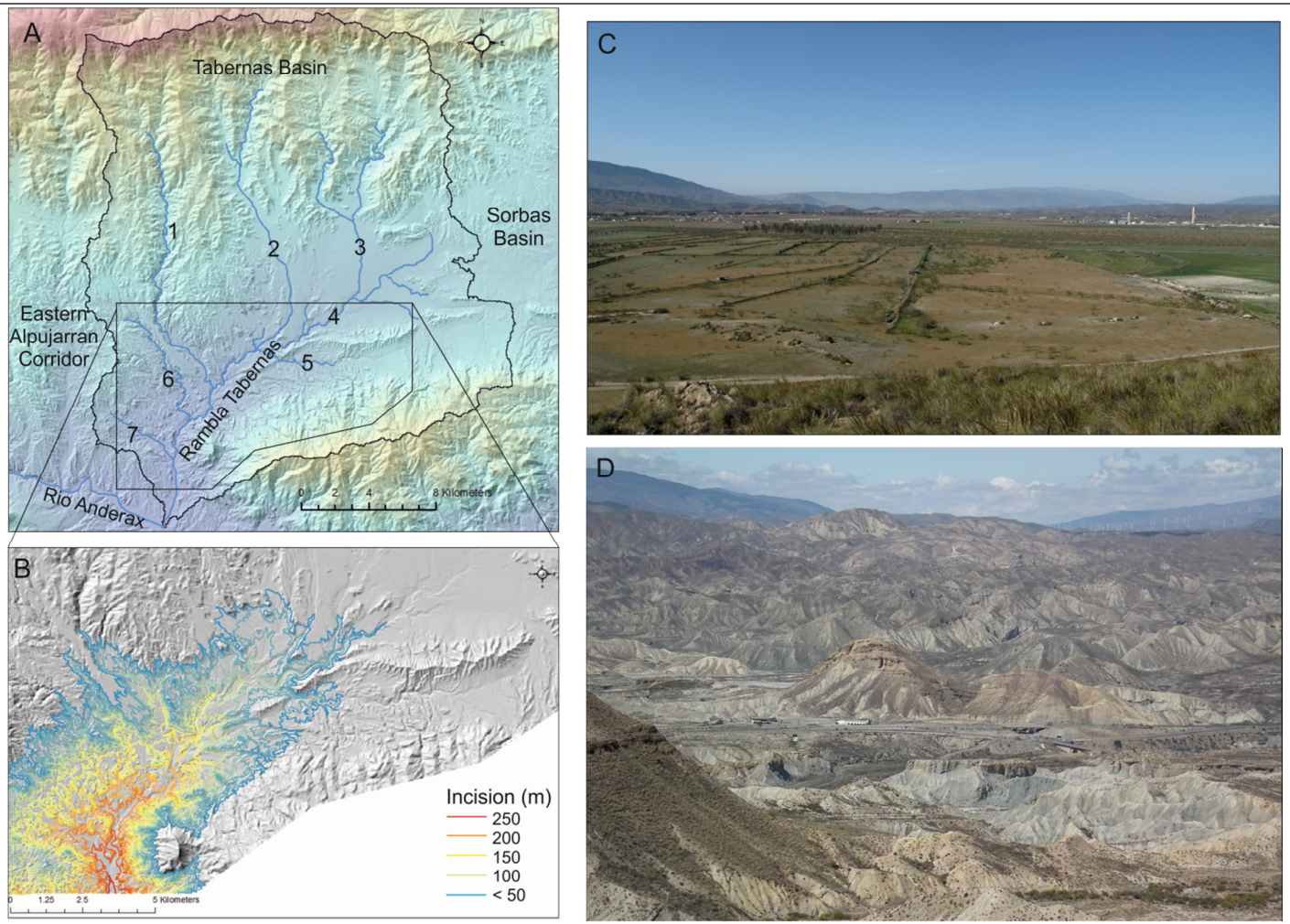

Figure 1.2 (A) Overview map of the Tabernas Basins with major drainages and current catchment defined. Drainage 1 = Arroyo Verdelecho, 2 = Rambla Galera, 3 = Rambla Honda, 4 = Rambla de los Molinos, 5 = Rambla Sierra, 6 = Rambla Lanujar and 7 = Rambla Seca. (B) Patterns of incision across the Tabernas Basin with some 250m of incision over 12km. (C) View from the eastern basin margin over approx. 2 - 3 km of coalescent alluvial fan surfaces with little incision. Photo facing east from UTM 30S 563190/4105784. (D) View point over the El Cautivo badlands in the west of the basin demonstrating the clear incisional landscape style with vertical incision of up to 250m from Pliocene surfaces. Photo facing north from UTM 30S 554964/4096891

In accordance with the variable processes of generation, the morphology of individual terrace bodies and collective terrace staircases can be highly complex and non-uniform. Unfortunately, at present there is not a globally accepted methodology in the description and recording of terrace bodies. However, across Europe consensus appears to conform to the broad grouping of individual terraces based on either an erosional or aggradational method of formation (see Stokes et al., 2012a). Terraces formed under erosional conditions are termed 'strath' terraces (terminology after Leopold et al., 1964), characterised by a distinct sub-horizontal erosional terrace base commonly cut in to underlying bedrock and thin sedimentary thicknesses with respect the river that deposited them (Blum, 1993). In contrast, terraces formed under broadly aggradational conditions are termed 'fill' deposits. A fill terrace is characterised by a thick alluvial deposit which formerly buried the river valley bottom. The base of fill deposits can be sub-horizontal such as in strath terraces; however, it is often common to encounter highly variable basal contacts which commonly overlie units deposited during early stages of terrace formation (Leopold et al., 1964).

The modes of terrace formation within a collective terrace staircase can vary considerably in terms of both spatial and temporal patterns (Lewin and Gibbard, 2010). In the simplest of examples, a river eroding at a constant rate into its bed under conditions of uniform surface uplift will lead to formation of a strath staircase (Fig. 1.3A). However, if rates of tectonic uplift are highly variable or even record subsidence, the terrace staircase record can be highly complex. In such cases terraces can form either; (i) fill - cut sequences (terminology from Lewin and Gibbard, 2010) representing stages of incision into prior fill deposits (Fig. 1.3B), or (ii) cut-fill sequences where fill aggradations occur within formerly incised fill units, in essence recording multiple fill cycles (Fig.1.3C). For both fill sequences, terrace morphology and stratigraphy are often highly variable due to changes in sediment inputs promoted by various feedback mechanisms driven through time (Starkel, 2003; Vandenberghe, 2003).

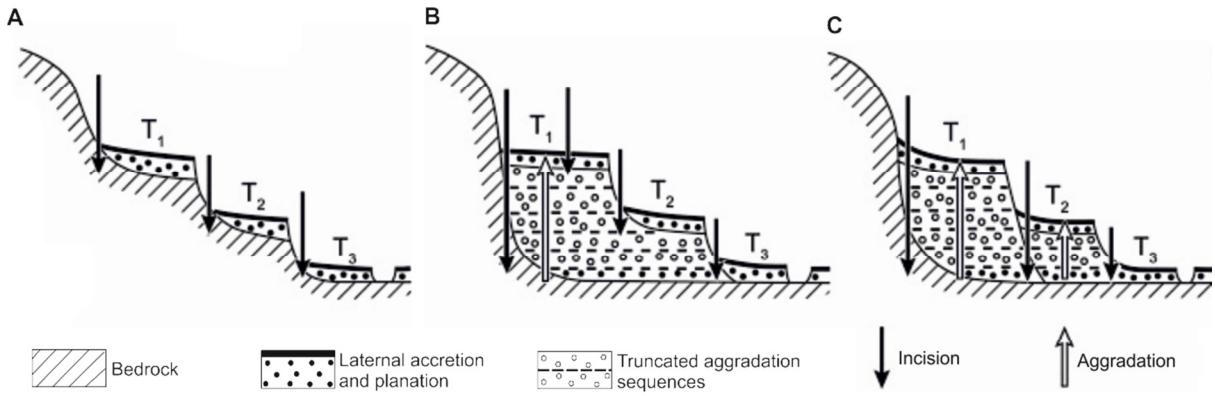

Figure 1.3 Example of terrace staircase formation from Lewin and Gibbard (2010): (A) strath terrace formation under condition of progressive uplift into bedrock, (B) fill-cut formation with a series of incisions prior to valley fills, and (C) cut-fill sequences formed as a result of coupled cut and fill episodes.

1.4.2 External forces: Tectonics

Over long timescales (10^3 to 10^6 yrs^{-1}) the three most important external controls on fluvial system development and resultant river terrace formation are tectonics, climate and sea level change (Veldkamp and Tebbens, 2001). At a primary scale, fluvial systems respond to changes in surface topography and base-level modifications which are driven by active processes of tectonic uplift or subsidence (Westaway, 2006). Active tectonic forcing promotes variations in surface elevation and changes in river gradient, altering the amount of available power within the active system (stream power; Bull, 1991). Although complicated by a multitude of internal feedback mechanisms (e.g. rock strength, fabric and sediment availability), system-wide changes in channel gradient promote either: (i) periods of channel incision under conditions of tectonic uplift or (ii) channel aggradation under conditions of subsidence (Daniels, 2008). This relationship is well evidenced in empirical studies over long timescales (10^3 to 10^5 yrs^{-1}; Schumm, 2000; Bull, 2007) and can be further reproduced in experimental numerical models which demonstrate progressive fluvial network incision under conditions of uniform surface uplift and precipitation (Fig. 1.4).

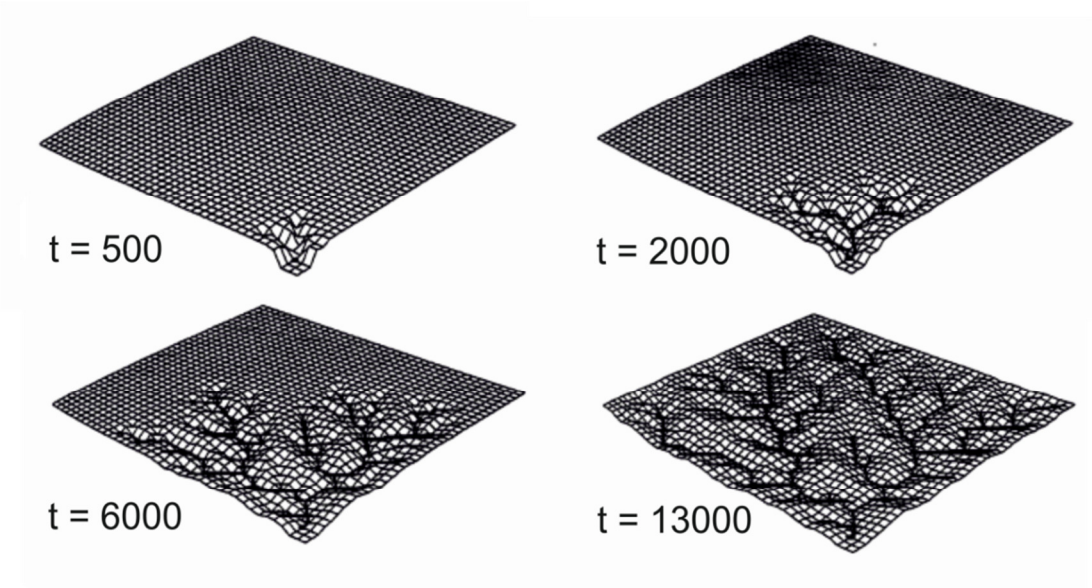

Figure 1.4 Numerical model output demonstrating the development of a fluvial channel network on a planar surface when subjected to uniform rates of tectonic uplift and precipitation with time. Taken from Willgoose et al., (1991). Unit '*t*' is time in years.

The effects of active tectonics in the formation and preservation of river terraces are variable over a range of spatial and temporal scales. On a global scale, terrace formation is most pronounced at or near plate boundaries as associated with large scale base-level changes which occur within zones of orogenic uplift and/or active crustal deformation (Bridgland and Westaway, 2008). At global scales uplift rates are typically non-uniform, such as along the Atlantic margins where uplift is controlled by the variable rates of deformation that occur in accordance with the relative motions of the lithosphere operating over timescales of 1-2 Ma (Cloetingh et al., 1990). On regional or local scales, the effects of active tectonics are often related to individual features such as faults or folds (Trudgill, 2002; Stange et al., 2013). Localised variations in stream gradient occur at or near deformational features which promotes a system-wide response as the active channel attains grade (Twidale, 2004). Fluvial system development often occurs in response to varying mechanisms of active tectonic forcing operating over a range of spatial and temporal scales

(e.g. base-level changes as a result of localised faulting overprinted on to regional patterns of uplift). This often complicates interpretations of landscape evolution and highlights the requirement for a thorough understanding of both the local and regional tectonic setting.

In tectonically quiescent regions, such as areas of low lithospheric mobility, the effects of active tectonics are subdued and resultant river system development is often constrained by the inherited geological structure of the landscape (e.g. structure of stable Archean cratons; Westaway et al., 2009). Passive tectonic controls in the form of fault controlled corridors or faulted basin margins can exhibit an underlying control on drainage pathways and sediment budgets both within and between sedimentary basins (Stokes, 2008). Although rare and occurring at much slower rates than in active tectonic settings, the effects of ongoing incision in passively controlled systems can promote the steady state unloading and eventual reactivation of tectonic features, given a further control on base-level is present (e.g. flexural upwarping of large amplitude fold structures as driven by climatically driven sea-level lowering; Reusser et al., 2004). Even though terrace formation is rare and preservation potential is poor, terrace staircases do form in areas of low tectonic activity. In these locations, terrace records are commonly of complex fill architectures and/or strath forms with little altitudinal spacing (Starkel, 2003), where the effects from active faulting or folding are typically absent or negligible.

As presented in detail in Chapter 2, the effects of both active and passive tectonics have been of upmost importance in the evolution of fluvial system development in the Tabernas Basin. The configuration of the main basin drainage occupies the centre of a broad synclinal feature formed as a result of low amplitude folding across SE Spain during the collision of the African and European plates. Ongoing tectonic uplift and active faulting / folding has further promoted the rearrangement and reactivation of drainage pathways throughout the Quaternary (e.g. Harvey, 2007; Giaconia et al., 2012).

1.4.3 External forces: Climate

Climate has a profound effect upon the geomorphic properties of the landscape system. Climatic cycles promote changes in the weathering and erosional regimes of hillslope systems as a result of variations in vegetation cover and slope stability (i.e. critical power threshold of Bull, 1979 and 1991). Much like tectonics, the effects of climate upon the fluvial system are significant over a range of temporal and spatial scales. For example, instantaneous changes in precipitation rates over localised areas (10^{-1} - 10^{2} m^2), as associated with weather, facilitates a net increase or decrease in fluvial system discharge over experimental to observational timescales (10^{-7} – 10^{-1} yrs; Daniels et al., 2008). At Quaternary timescales, cyclic variations in regional precipitation and air temperature are the primary influence upon fluvial system development as a result of balanced differences in regional sediment and water discharge (Vandenberghe, 2003). During periods of decreased precipitation and temperature (i.e. cold climate cycles) the relative amounts of sediment available to the fluvial system increases as a result of decreases in slope vegetation cover and resultant slope stability (Fig 1.5; Bull, 1991). The balanced increase in sediment discharge (Q_{sed}), compared to relative decreases water discharge (Q_w), leads to the onset of deposition (terrace aggradation) in the channel reach. This process is reversed during periods of increased precipitation and temperature (i.e. warm climate cycles) with relative decreases in sediment availability (Q_{sed}) and relative increases in water discharge which promote incision (terrace abandonment) in the channel reach (Lane, 1955).

Long-term fluctuations in climate are attributed to global cold (glacial) phases and warm (interglacial) cycles established in the Late Cenozoic (~ 2.7 Ma) with the progressive cooling of the globe and the widespread growth of the polar region ice sheets (Bull, 1991; Gibbard and Lewin, 2009). Throughout the early-mid Pleistocene, the dominance of orbital obliquity cycles experienced throughout the late Pliocene (significant at 41 ka), were progressively superseded by the 100 ka rhythm of orbital eccentricity (Fig. 1.6A). The switch to eccentricity cycles was complete by the Middle Pleistocene (~750 ka) with the onset of

cold and warm climate phases of increased intensity and duration when compared with the prevailing Late Cenozoic environmental conditions (Fig. 1.6A; Gibbard and Lewin, 2003; 2009).

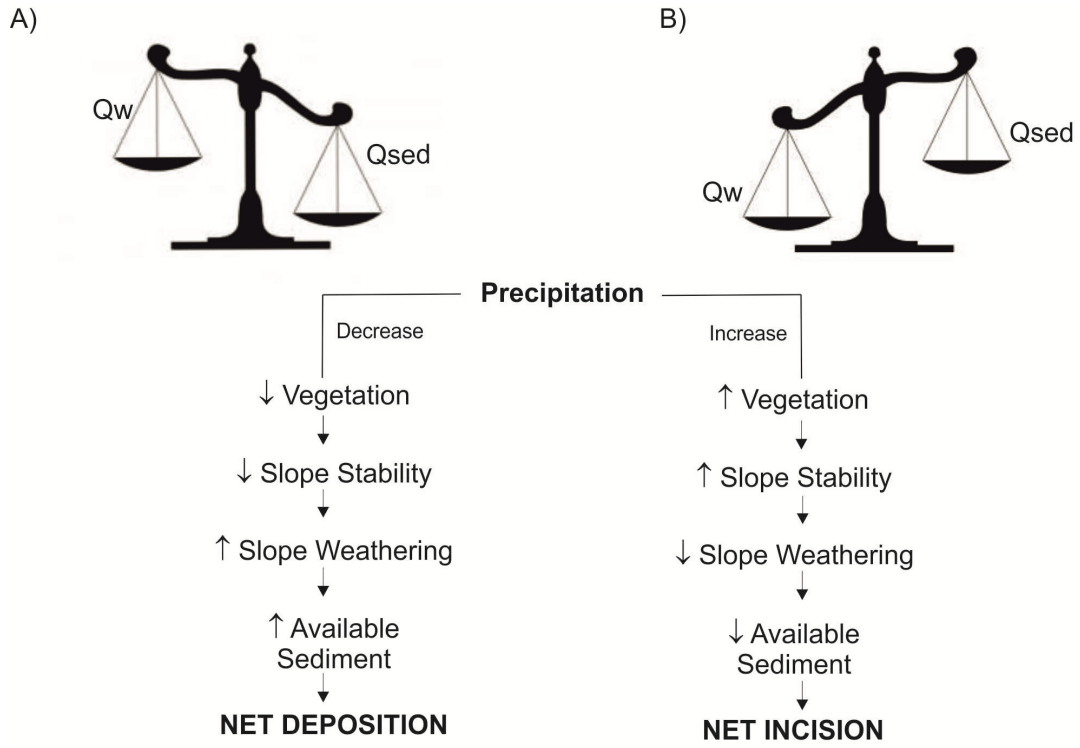

Figure 1.5 Lane's stream power balance models demonstrating the effects of climate, modified from Lane, 1955. (A) During periods of decreased precipitation fluvial systems experience an overall increase in available sediment and net deposition within the system. This process is reversed during periods of increased precipitation (B).

The pronounced severity of cold climate cycles after the Mid Pleistocene, termed the Mid Pleistocene Revolution (MPR), left its mark in the fluvial systems across the globe (Macklin et al., 2002; Vandenberghe, 2003; Bridgland et al., 2004; Bridgland and Westaway, 2008). In northwest Europe, changes in style and number of fluvial terraces evidence the shift to eccentricity driven climate cycles (e.g. the Middle Rhine valley Fig. 1.6B; Frechen et al., 2010). For example during pre-MPR conditions, fluvial terraces were characterised by wide expanses of sediment that record significantly greater valley-floor widths than are seen today, whereas terraces formed under post-MPR conditions record steeper incision and the

narrowing of valleys (Bridgland and Westaway, 2008). In accordance with the increase in absolute chronologies across the region multiple studies established correlations between phases of terrace formation and post MPR climate cycles (e.g. Maddy and Bridgland, 2000; Bridgland et al.,2004). Notably, terrace sedimentation events typically occurred during cold climate (glacial) phases under conditions of sediment excess, and terrace incision during climate transitions under conditions of sediment deficit (Bridgland and Westaway, 2008).

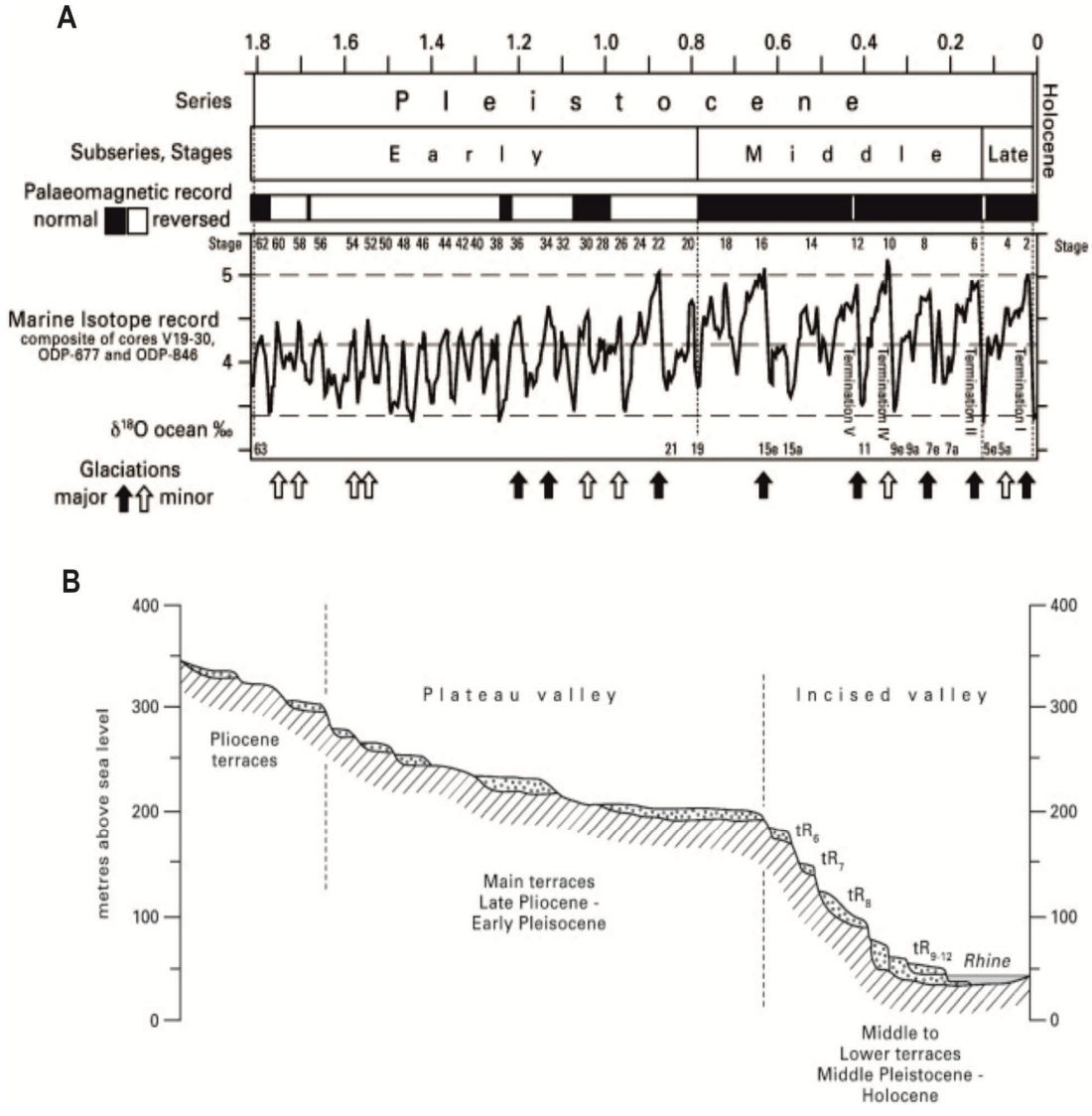

Figure 1.6 (A) Major cold climate events during the Pleistocene evidenced from Marine isotope record with major glacial phases highlighted by arrows. Note the increased intensity of glacial and interglacial phases post MPR at ~ 750 ka. (B) Cross section of the Middle Rhine valley which demonstrates the change in the terrace frequency starting in the mid- Pleistocene, both from Gibbard and Lewin (2009) and references therein.

Assigning river terrace formation to post MPR 100 ka eccentricity cycles correlates well in regional fluvial systems across northwest Europe (e.g. Bridgland, 2000; Maddy and Bridgland, 2000; van den Berg and van Hoof, 2001; Gibbard and Lewin, 2003; Bridgland et al., 2004). However, many disparities occur on both local and regional scales in global fluvial systems which highlight the limitation in assigning terrace formation to climate forcing alone. For example:

1. Local variability occurs in the preservation potential of river deposits based on past and present rates of channel migration which is largely controlled by the internal characteristic of a fluvial landscape (Lewin and Macklin, 2003);
2. In glacial regions, terrace preservation is often poor with many terrace sequences destroyed during subsequent periods of glacial advance such as major glacial stages of MIS 2 and MIS 6 (Lewin and Macklin, 2003; Bridgland and Westaway, 2008);
3. Regional variability in the timing of incisional events within the climate cycle has been noted, with increases in terrace level numbers in systems where incision occurred during both cooling to warming and warming to cooling trends (e.g. River Solent in southern England; Bridgland, 2001);
4. The global significance of climatic setting with relation to changes in processes of terrace formation is also non-uniform. For example, in cooler glaciated regions, patterns of terrace aggradation tend to occur during interglacial-glacial cool to warming and warming to cooling phases in relation changes in temperature and resultant bedload supply. However, in warmer non-glaciated regions terrace aggradations typically occur during major cold stages as a result of changes in precipitation and regional aridity (Bridgland and Westaway, 2008).

Although climatic forcing plays an important role in promoting terrace aggradation and incision cycles, it is common belief that climate alone does not directly facilitate the formation of terrace staircases (Stokes et al., 2012a). This is due to the underlying

requirement for a mechanism of base-level lowering (Fig. 1.7) (Starkel, 2003). Under stable tectonic conditions and assuming no effects from sea-level change, base level is effectively pinned between climatic cycles and resultant terrace staircase formation is limited (Fig 1.7; Starkel, 2003; Bridgland and Westaway, 2008). Recent research has highlighted possible links between the climate system and accelerated tectonic uplift in regions of highly mobile lower crust where increases in climatically driven incision relate to the relative unloading of the Earth's surface (e.g. Westaway, 2006); however, the number of case studies that prove this theory are still limited.

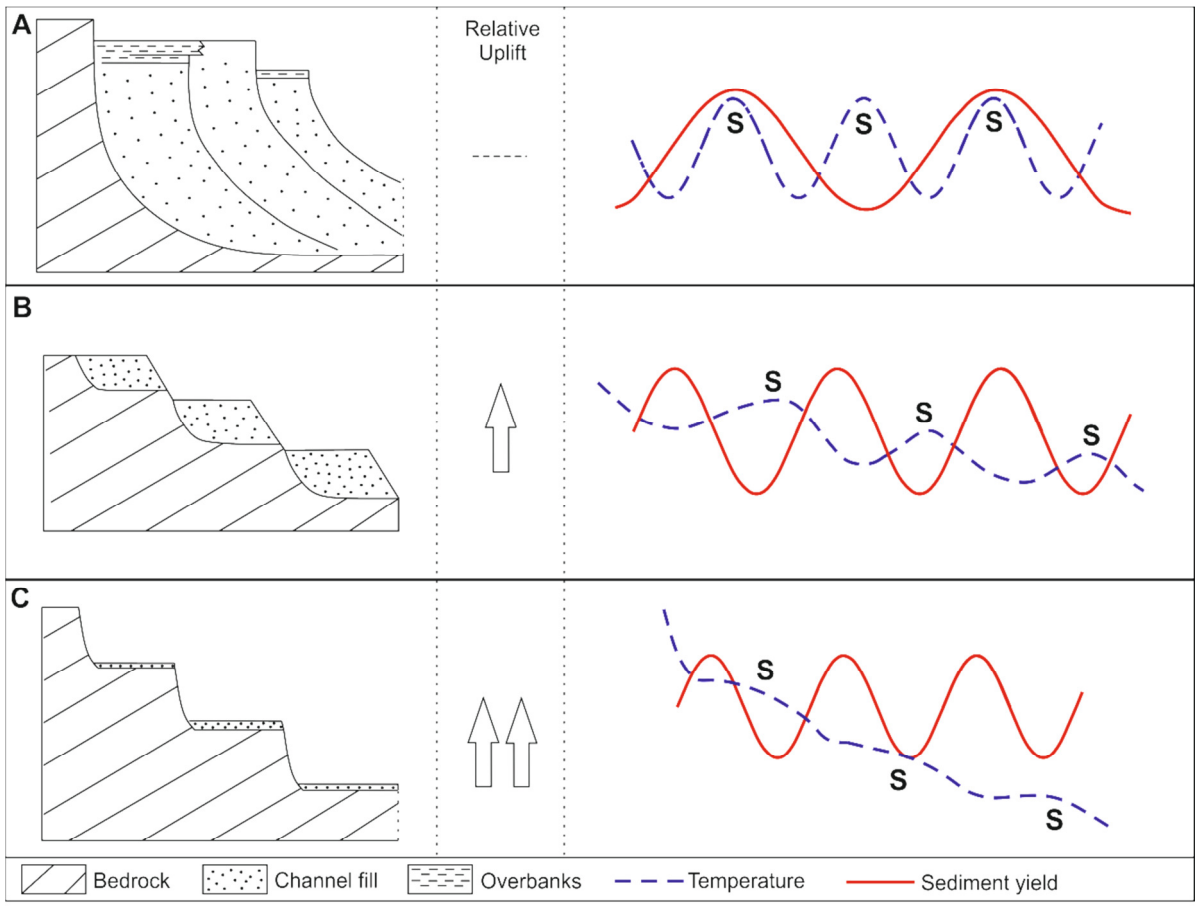

Figure 1.7 Response of fluvial systems to Quaternary climate cycles under varying tectonic regimes, modified from Starkel (2003). (A) Fill sequence formed under conditions of tectonic quiescence, (B) a strath terrace with substantial sediment thicknesses formed as a result of moderate uplift rates, (C) A strath record dominated by thin sedimentary veneers and large degrees of terrace separation formed under intense tectonic uplift. Terrace Sedimentation stages are marked 'S'.

Climatic processes have been highlighted as a major forcing factor in the formation of Quaternary landforms in the Tabernas basin (e.g. Mather and Stokes, 1999; Harvey et al., 2003). The formation of extensive fluvially dominated alluvial fan fronts in the east of the basin occurred as a result of shifts to cold climate conditions when sediment availability from the bounding Sierras would have been high (Harvey et al., 1999; 2003). This pattern of aggradation is further evidenced in the neighbouring Sorbas and Vera Basins (e.g. Miekle, 2008; Schulte et al., 2008). However, in all situations the delivery of sediments to basin is over printed on a trend of variable tectonic uplift and basin wide incision (Harvey et al., 2003; Nash and Smith, 2003; Alexander et al., 2008).

1.4.4 External forces: Sea-level change

Sea level acts as the ultimate base level for all fluvial systems (Leopold and Bull, 1979). Over Quaternary timescales sea level is controlled by climate cycles (~100ka), being low(er) during cold climate periods and high(er) during warm climate periods (Blum and Tornqvist, 2000). Posamentier and Vail, (1988) (refined by Posamentier and Allen,1993) presented a generalised model of fluvial system response to sea-level change where: (i) during early stages of relative sea-level fall, fluvial systems respond by depositing more sediment in their distal channel reaches, which are extended in a seaward direction. (ii) During the later stages of sea-level fall and lowstand, sustained valley incision and sediment bypass occurs, with the overall shift of aggradation centres in an offshore direction on to the marine shelf, and (iii) under conditions of relative sea-level rise, valley wide filling occurs with net aggradation in the coastal reaches of the fluvial system. Blum and Tornqvist (2000) highlight that the impacts of sea-level change upon fluvial system development and resultant terrace formation is principally governed by the proximity of the fluvial system to the coast and the configuration of the offshore shelf, deferring from over simplified models. At some point upstream, fluvial system development occurs completely independent of eccentricity driven cycles of sea-level change (Blum and Tornqvist, 2000). This distance is unique for each river system and is strongly governed by the configuration of the offshore continental

shelf (Blum and Tornqvist, 2000). In situations of a steep and narrow offshore shelf with a sharp shelf break, the upstream effects of base-level changes are relatively limited occurring at scales of less than 10's km (e.g. the Miño system, NW Spain; Viveen et al., 2013a), and in some cases are completely removed from the upstream fluvial system (e.g. the Vera Basin fluvial system; Miekle, 2008). In contrast, for large fluvial systems with broad and expansive shelf margins (e.g. the Mississippi river) the effects of climate related sea-level change can reach some 200 km upstream (Blum and Tornqvist, 2000).

Isostatic changes in surface elevation driven by tectonic uplift or subsidence amplify the effects of eustatic sea-level change upon fluvial system development over a range of spatial and temporal scales (Antoine et al., 2000). At a global scale, changes in Late Pliocene intra-plate stress fields and ocean basin geometry have driven apparent eustatic changes in sea-level which have accelerated fluvial system development within major coastal systems (Cloetingh, 1986; Cloetingh et al., 1990). At regional and local scales, the coupled effects of tectonics and Quaternary eustatic sea-level change have promoted the formation of highly variable terrace records in response to complex interplays of both mechanisms of base-level change (Blum, 1993; Blum and Tornqvist, 2000). For example, under conditions of tectonic uplift and sea-level lowering the degree of base-level change in the upstream fluvial system of the Vera Basin was amplified, with increased landward incision and degradation and reworking of the inland terrace record (Miekle, 2008).

Some major questions still exist about the dominance of sea-level change upon fluvial development at Quaternary timescales. For example, changes in sea-level throughout the Middle - Late Quaternary were driven by climatic cycles (Stokes et al., 2012a). The coupling of sea-level with climate cycles makes it hard to ascertain the true significance of sea-level change alone on processes of terrace formation. In addition, little is known with regard to effects of short duration sea-level changes driven by brief climatic episodes such as Dansgaard – Oeschger events (Blum and Tornqvist, 2000). This is a function of poor

terrace formation, preservation and/or accessibility coupled with the lack of continual high resolution absolute chronologies for coastal terrace sequences (Macklin and Lewin, 2008).

Unlike the dominance of tectonics and climate upon the Quaternary landscape system in the Tabernas Basin, the effects of eustatic sea-level change are non-existent. This is due to: (i) the inland location of the basin, for example in the neighbouring Carboneras Basin the effects of sea-level lowered are only recorded up to 5 km from the current coast line (Maher,2005), (ii) the low gradient of the continental shelf off the Almería coastline, and (iii) the high sediment yield of the major regional drainage (Río Andarax) which limited the transmission of eustatic base-level lowering to immediate coastal areas only (Garcia et al., 2003). However, given that sea level is a dominant control of base-levels in more coastal basins of the Almería region (e.g. Vera and Carboneras Basins) the mechanism is not discredited from discussions as a significant landscape forcing agent.

1.4.5 Internal landscape processes

Internal landscape processes occur as self-organising feedback mechanisms which enhance or reduce fluvial system response to external forcing mechanisms (Schumm and Parker, 1973). The effects of internal feedbacks upon river terrace formation are significant over a range of temporal and spatial scales, however, they are not always directly linear to the response expected from the amount of external forcing applied (e.g. the amplified increases in stream power and resultant river incision which occur as a result of tectonically driven river capture events; Veldkamp and Van Dijke, 2000; Stokes et al., 2002; Bowman et al., 2010; Coulthard and Van de Wiel, 2013).

Instantaneous channel avulsion and river capture events demonstrate how internal self-organisational mechanisms promote variable rates of river activity over Quaternary timescales. Both avulsion and capture events occur when an internal threshold point is crossed in the landscape (Fig. 1.8). In avulsions events, the threshold point is defined by the increase in elevation of the active aggrading channel in relation to its flood plain. In capture events the threshold is related to the breaching of drainage divides between actively incising

fluvial systems. In both instances a resultant change in channel configuration promotes either a period of equilibrium, aggradation, or incision in accordance with local alterations in stream power (Fig. 1.8; Schumm, 1993). If a period of equilibrium or aggradation is achieved net sedimentation will increase the likelihood of terrace formation. However, if a period of incision ensues terrace formation will be limited (Lewin and Macklin, 2003). The extent of terrace aggradation or incision is closely related to the frequency and duration of threshold conditions (Fig.1.8; Bull, 1979).

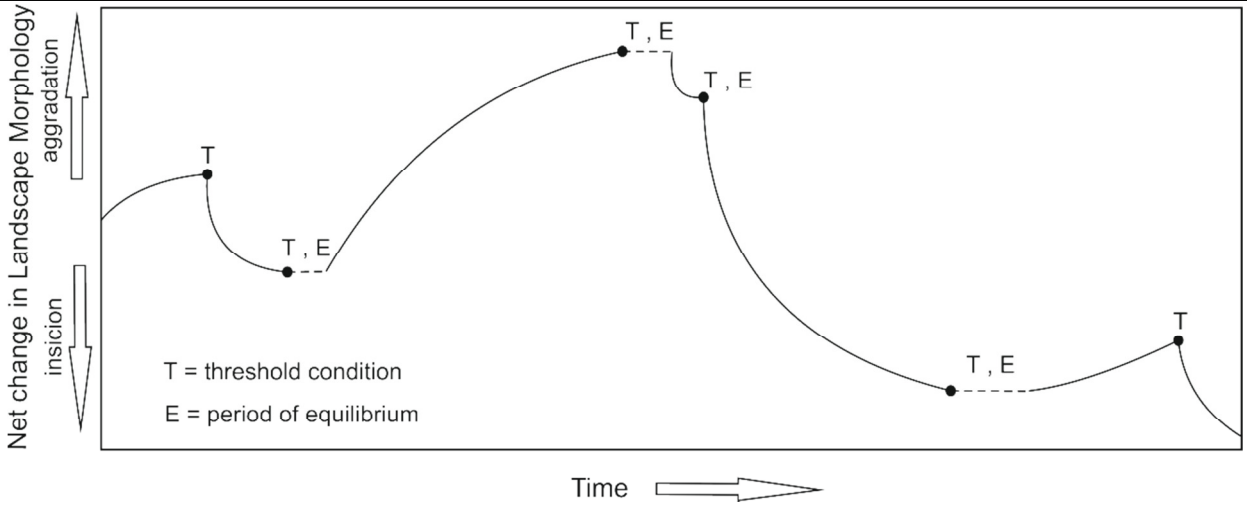

Figure 1.8 Hypothetical model of landscape response for a river system based on the threshold theories of Bull, (1979). Periods of landscape change occur after an internal threshold has been crossed. This can trigger either a period of equilibrium within the channel with no net change in channel elevation (dashed lines) or promote substantial change via increased sedimentation or incision. Terrace formation and preservation is therefore closely associated with the frequency and duration of change promoted once a threshold is crossed.

Further internal controls on fluvial development relate to the ability of a river to store sediment as governed by the amount of accommodation space (Schumm, 1977). As a channel evolves under conditions of tectonic or climatic forcing its discharge grows linearly in accordance with its basin area as it attains grade and a steady-state profile (Hack, 1957). As the channel reaches steady state it begins to widen via processes of lateral channel migration and hence increases the accommodation space. However, the rates of valley incision and widening are fixed by mean discharge, resistance of rock substrate and

sediment flux (Pazzaglia et al., 1998). Rock resistance includes aspects of internal discontinuities, bedding and shear fabrics which occur in the most part as an inherited configuration of the landscape and are of importance in long-term studies. Over long timescales sediment flux is primarily controlled by the self-regulating mechanisms of the system commonly expressed in the channel morphology and type (Coulthard and Van de Wiel, 2013). Sediment and water discharge are the dominant factors controlled by external forcing factors, yet sediment availability is still strongly related to the internal dynamics of the landscape system, especially in the arid region bedrock fluvial systems (Mather, 2009). This demonstrates the complex internal configuration of landscape system whereby numerous feedback mechanisms are of importance in long-term studies of evolution and development.

Internal thresholds conditions and feedbacks have been important in the evolution of the Tabernas basin. In the early stages of development, the piracy of drainages from the neighbouring Sorbas basin led to the formation of the drainage network which exists until this day (Harvey, 1987). Internal controls have also promoted variable rates of basin-wide incision when the axial fluvial system passed through major lithological barriers, such as the crossing of a major sandstone unit in the El Cautivo badlands (Alexander et al., 2008); or the incision through extensive high-strength groundwater calcretes across the basin (Nash and Smith, 1998; 2003).

1.5 Quaternary landscape evolution in the Almería Region, SE Spain

Over Quaternary timescales the effects of tectonics, climate, sea-level change and internal processes have all been of significance upon fluvial system development within the Almería region (Harvey and Wells, 1987; Maher, 2007; Maher and Harvey, 2008, Schulte et al., 2008). At a first order scale, the tectonic evolution of the region is associated with the collision of the African and Iberian plates and the formation of the Betic mountain range (presented in detail in Chapter 2; Larouzière et al., 1988). The characteristic uplifted mountain blocks (Sierra de los Filabres and Sierra Alhamilla) and down-faulted sedimentary

basins of the Inner Betics (e.g. Tabernas, Sorbas and Vera basins; Fig.1.1) formed as a result of regional variations in displacements along major fault lines (Braga et al., 2003; Omodeo Salé et al., 2012) coupled with regional patterns of fold related uplift and subsidence (e.g. Sierras form large low amplitude anticlines and the sedimentary basins form synclines; De Vicente and Vegas, 2009). Ongoing tectonic uplift promoted a spatially variable shift from marine to terrestrial conditions in sedimentary basins throughout the Pliocene (double line of Table 1.1; Mather, 1991; Stokes, 1997). At some point in the Early Pleistocene, basin wide incision initiated in all of the sedimentary basins of the region (see Chapter 2), with the development of extensive Quaternary fluvial systems which record a sustained pattern of variable base-level lowering (dashed line of Table, 1.1; Harvey and Wells, 1987).

Table 1.1 Plio-Pleistocene evolution of the sedimentary Basins of the Almería region, SE Spain, taken from Stokes (1997). The double line depicts the broad boundary between marine and terrestrial conditions; however, it is noted that the transition between units is locally variable within all basins.

<table>
<tr><th>Epoch</th><th>Tabernas-
Almería Basin</th><th>Sorbas Basin</th><th>Vera Basin</th><th>Carboneras- Níjar
Basin</th></tr>
<tr><td rowspan="2">Pleistocene</td><td>Terrace Sequence</td><td rowspan="2">Terrace
Sequence</td><td>Terrace
Sequence</td><td rowspan="2">Terrace Sequence</td></tr>
<tr><td rowspan="2">Gador Formation</td><td rowspan="2">Salmerón
Formation</td></tr>
<tr><td rowspan="3">Pliocene</td><td rowspan="3">Abríoja Formation</td><td rowspan="2">Gochar
Formation</td><td rowspan="2">Polopos Formation</td></tr>
<tr><td>Espiritu Santo
Formation</td></tr>
<tr><td>Cariatiz
Formation</td><td>Cuevas
Formation</td><td>Cuevas Viejas
Formation</td></tr>
</table>

Throughout the Late Pliocene and Quaternary, non-uniform rates of tectonic uplift prompted a highly variable response of fluvial systems across the region (Table, 1.2; Fig. 1.9). Higher rates of uplift in the Sorbas Basin, in comparison to the neighbouring Vera Basin, created steep regional drainage gradients between the basins with the resultant onset of incisional fluvial styles (Fig. 1.9; Harvey, 1987; Mather, 1993; Stokes, 2008). Patterns of aggressive drainage development dominated the region throughout the Quaternary and promoted: (i) multiple drainage rearrangements (e.g. Harvey and Wells, 1987; Fig. 1.9), (ii) increased drainage integrations and (iii) continued network expansion, as evidenced by the Quaternary fluvial terrace records (Harvey and Wells, 1987; Mather et al., 2000; Stokes et al., 2002; Maher, 2007; Ilott, 2013).

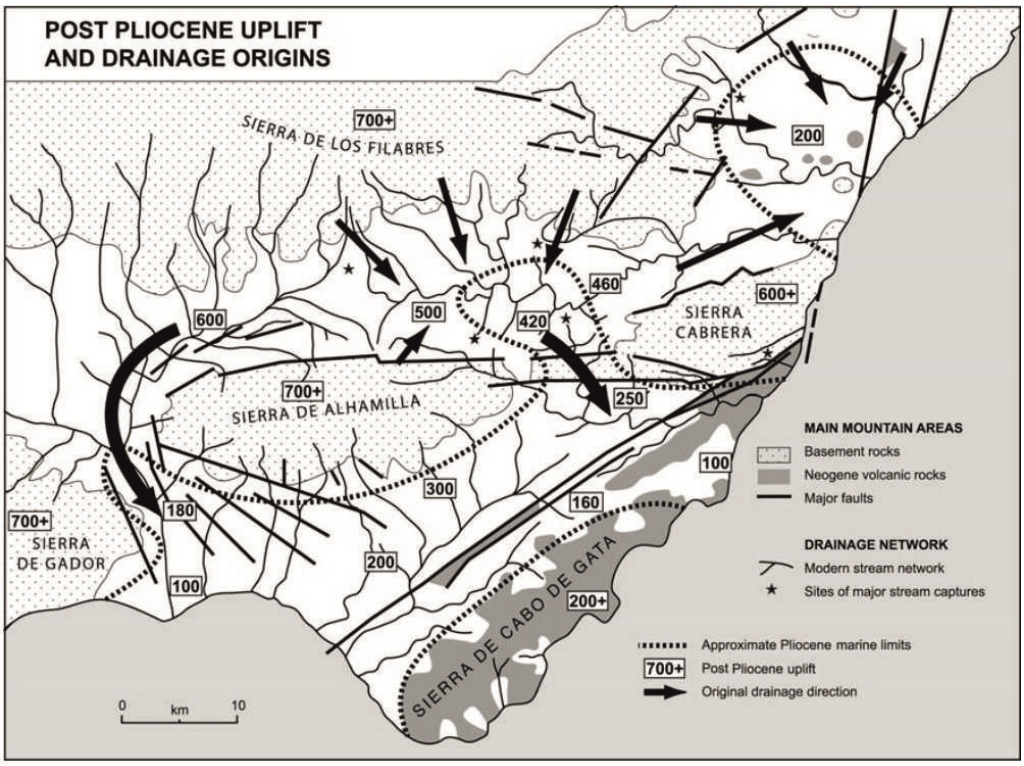

Figure1.9 Uplift patterns since the Late Pliocene for the Almería region from Harvey (2007). High rates of post Pliocene uplift in the Sorbas basin promoted multiple drainage rearrangements as evidenced by original drainage directions (black arrows).

Although tectonic uplift was a dominant control on the Quaternary landscape system, tectonic deformation of landforms (e.g. faults and folds) is sparse across the region. In the

Tabernas Basin, evidence of post depositional deformation is encountered with normal faulting of a fluvial terraces (Nash and Smith, 1998), deformation of terrace sediments in the east of the basin (Harvey et al., 1999) and areas of fault reactivation along the Marchante ridge and northern margins of the Sierra Alhamilla (Giaconia et al., 2012). Across the Sorbas Basin, syndepositional deformation is noted in river terraces along the Marchalico-Inferno lineament of Mather (2000). However, deformation is spatially constrained and temporally restricted to one sub-set of terraces (D2 terraces of Harvey et al., 1995). In the Vera Basin, normal faulting is restricted to the Plio – Pleistocene Salmerón Formation and the oldest Quaternary river terrace deposits (Terrace Level A of Stokes, 1997).

As in the Tabernas Basin, the axial drainages in neighbouring sedimentary basins (e.g. Sorbas and Vera basins) are controlled by passive tectonic features as they follow the strike of low amplitude synclines (Stokes, 2008). In most basins, the drainage networks have exploited the extensive low strength Neogene basin fills which offer few barriers to base-level changes and promote the transmission of waves of incision (e.g. the accelerated headward erosion of the post capture system into weak Neogene Marls in the Sorbas basin; Stokes et al., 2002).

Table 1.2 Pliocene and Quaternary uplift rates for the Neogene sedimentary Basin of SE Spain

Basin	Uplift Rate (m/ka)	Record	Author
Almería Basin	0.04	Quaternary raised beaches	Zazo et al., 2003
Tabernas	0.10 – 0.20	Miocene and Pliocene coastal and marginal marine rocks (e.g. fringe reefs)	Braga et al., 2003
Sorbas	0.07 - 0.10	Miocene and Pliocene coastal and marginal marine rocks (e.g. fringe reefs)	Braga et al., 2003
Sorbas	0.08 - 0.16	Pliocene shorelines/ marine units	Mather, 1991; Mather and Harvey, 1995; Mather et al., 2002
Vera	0.07	Quaternary raised beaches	Miekle, 2008
Vera	0.01 - 0.02	Pliocene shorelines above present	Stokes, 1997; 2008
Eastern Alpujarran Corridor	0.3-0.7	Quaternary (< 500ka) terrace records	García et al., 2003

In addition to tectonic controls, the correlation of dated fluvial sequences from across the Almería region has further demonstrated the effects of orbital forced climate change upon the landscape system (Schulte, 2002; Miekle, 2008; Ilott, 2013). Basin wide aggradation events are typically found to occur during cold / dry climatic periods, significant at 100 ka eccentricity cycles (e.g. last glacial maximum MIS 2 ~ 20ka and MIS 6 at ~ 130 ka). Under cold climate conditions (global glacial stages), relative decreases in Atlantic derived precipitation facilitated the replacement of forest or wooded biomes by steppe vegetation across much of the Iberian Peninsula (Schulte et al., 2008; Fletcher et al., 2008). Decreases in canopy cover increased soil susceptibility and sediment availability under high physical stresses and highly peaked river discharge regimes under cold-climate conditions (Amor and Florschutz, 1964; Macklin et al., 2002; Geach et al., in press.).

Correlations of fluvial archives from across the greater Iberian peninsula with high resolution climate records (e.g. oxygen isotope records) further demonstrate the effects of sub-orbital climatic changes, such as Heinrich events (major periods of ice-sheet rafting) and Dansgaard-Oeschger cycles (a series of abrupt warm periods which following Heinrich events; Maslin et al., 2001) upon terrestrial systems (Macklin and Lewin, 2008). Although limited by the availability of absolute chronologies, the correlation of Iberian fluvial sequences with abrupt climatic events (e.g. H1 at ~ 17 ka and the Younger Dryas ~12ka) suggests that fluvial systems responded to short-term climate change throughout the Late Pleistocene (Macklin and Lewin, 2008). To date, correlations between sub-orbital climate events and fluvial activity across the Almería region are limited. Links have been made with incisional stages during the Younger Dryas (e.g. Schulte et al., 2008). However, these patterns of fluvial system response conflict with regional patterns of terrace formation (i.e. aggradations during cold climate phases) and could evidence the coupled result of climate and sea-level changes upon local fluvial systems, or simply be a facet of limited absolute dates available in the region (Miekle, 2008; Schulte et al., 2008).

The effects of Quaternary sea-level change are limited to the coastal basins and hillslope systems of the region (e.g. Vera Basin, Carboneras Basin and the Cabo de Gata natural park; Fig.1). This is linked to: (i) the relative effects of on-going tectonic uplift in all basins (ii) the distance from the ocean for most inland basins (.e.g. Sorbas and Tabernas Basins) and (iii) the configuration of the offshore shelf around the Almería coastline which is notably narrow when compared with other regions in Iberian Peninsula (e.g. average shelf width of 7km offshore of the Río Almanzora compared with 70km for the Ebro River; Miekle, 2008). Throughout the Quaternary, the morphology of the offshore shelf facilitated the link of the terrestrial fluvial and alluvial systems (e.g. Río Almanzora drainage in the Vera Basin) with the offshore environment during major cold climate lowstands when sea levels could have been some 120m lower then present day (Harvey et al.,1999; Siddall et al., 2003; Miekle, 2008). The effects of sea-level lowering, overprinted on regional trends of tectonic uplift and climatically controlled sediment delivery, triggered accelerated landward incision of the Río Almanzora system in the Vera Basin during the four major cold climate periods of the Middle to Late Pleistocene (MIS 2, 6, 12 and 16). Landward incision was driven by alterations in available stream power which occurred in response to an increase in sediment transportation and system progradation in the seaward direction (Miekle, 2008). The combined effects of tectonics and climatically driven sea-level change also controlled terrace aggradation and incision in the coastal reaches of Río Aguas system, with similar patterns of coastal aggradation during sea-level lowstands (Schulte et al., 2008).

It is clear that the Quaternary evolution of the Almería region has been driven by a complex interplay of active and passive tectonic forces, climate cycles, sea-level change and internal controls / feedbacks over a range of spatial and temporal scales. The evolution of the Tabernas Basin is linked to these complex process-form relationships; however, the local and regional significance of the basin with regard to patterns of Quaternary landscape change are yet to be developed and form the aim of this study.

1.6 Summary

This chapter has introduced the main driving forces which promote fluvial system development over Quaternary timescales. It has shown that global patterns of river terrace aggradation and incision occur as a result of cyclic changes in sediment and water discharge, which are principally controlled by climatic fluctuations in precipitation and temperature throughout the Quaternary (Bridgland and Westaway, 2008). Overprinted on this climatic control is the importance of tectonic forcing in driving base-level changes which promotes terrace staircase formation of either erosional (strath) or depositional (fill) forms (Stokes et al., 2012a). The effects of both climatic and tectonic forcing can be further complicated by sea-level fluctuations which exhibit a dominant control on sediment dynamics in coastal fluvial systems (Blum and Tornqvist, 2000), or by intrinsic controls which control the availability of accommodation space and sediment flux within a system.

The interactions of external and internal controls have been of significance in the evolution of fluvial landscape in SE Spain (Harvey and Wells, 1987; Harvey et al., 1995). The close association between fluvial aggradation stages and cold-climate phases highlights the importance of climate upon terrace formations (Miekle, 2008; Schulte et al., 2008). Variable rates of tectonic uplift have also promoted a highly dramatic incisional landscape style that has in turn driven internal feedbacks such as river capture events (Mather, 2000).

It is likely that the Quaternary landforms of the Tabernas Basin record similar complex responses to external and internal forcing mechanisms throughout the Quaternary. However, in order to assess the importance of such mechanisms it is important to formalise a detailed understanding how the basin evolved to its current day form. The following chapter (Chapter 2) presents a detailed geological and geomorphological background of basin formation, presenting a context for the Quaternary fluvial system which forms the focus of this study.

Chapter 2

2.1 Study Area

This chapter presents a summary of the geological and geomorphological evolution of the Tabernas Basin throughout the Late Cenozoic. Initially, the development of the Almería region is presented with focus on the formation of the Betic mountain range. This regional background is of relevance in understanding the processes behind the formation of the intramontane basins and in developing the inherited form of the regional landscape. The chapter then focuses on the evolution of the Tabernas Basin itself, presenting the local tectonic regime and major bedrock lithologies which have constrained the rates and styles of fluvial system evolution. Finally, the Quaternary geomorphology of the basin is discussed with reference to the significance of variable rates of tectonics, climate and internal forcing mechanisms upon the formation of individual landscape elements across the basin.

2.2 Establishing the Geological Sequence: Regional Setting

2.2.1 Geodynamic evolution of the Betic Cordillera: External and Internal Zones

The Tabernas Basin forms one of a series of interconnected Neogene sedimentary basins located within the Internal Zone of the Betic Cordillera in southeast Spain (Fig. 2.1). The formation, evolution and resultant incision of the basin is closely associated with the geodynamic history of the mountain range (Sanz de Galdeano & Vera, 1992). The Betic Cordillera is a collisional orogenic belt, formed as a result of convergence between the Alborán domain and the south-Iberian and Maghrebian palaeomargins, in the context of N–S to NW–SE Africa–Iberia convergence (Martínez-Martínez and Azañón, 1997). The mountain belt forms over Variscan deformed metasediments and igneous rocks of the Iberian craton (Maldonado et al., 1999). The current topographic configuration is that of a major ENE-WSW trending Alpine thrust and fold belt with westwards vergence (Braga et al., 2003). The broad E-W Alpine trend is common across the Iberian Peninsula and is widely related to the transmission of compressive stresses from collisional centres at the Pyrenean border which

affected the upper crust and the lithosphere, giving rise to higher order folds and regional topographical pattern (De Vincente and Vegas, 2009). However, convergence in the Betics is believed to be further complicated by localised mechanisms of deformation (e.g. westward vergence of the Alborán domain in relation to pure N-S compression; De Vincente and Vegas, 2009).

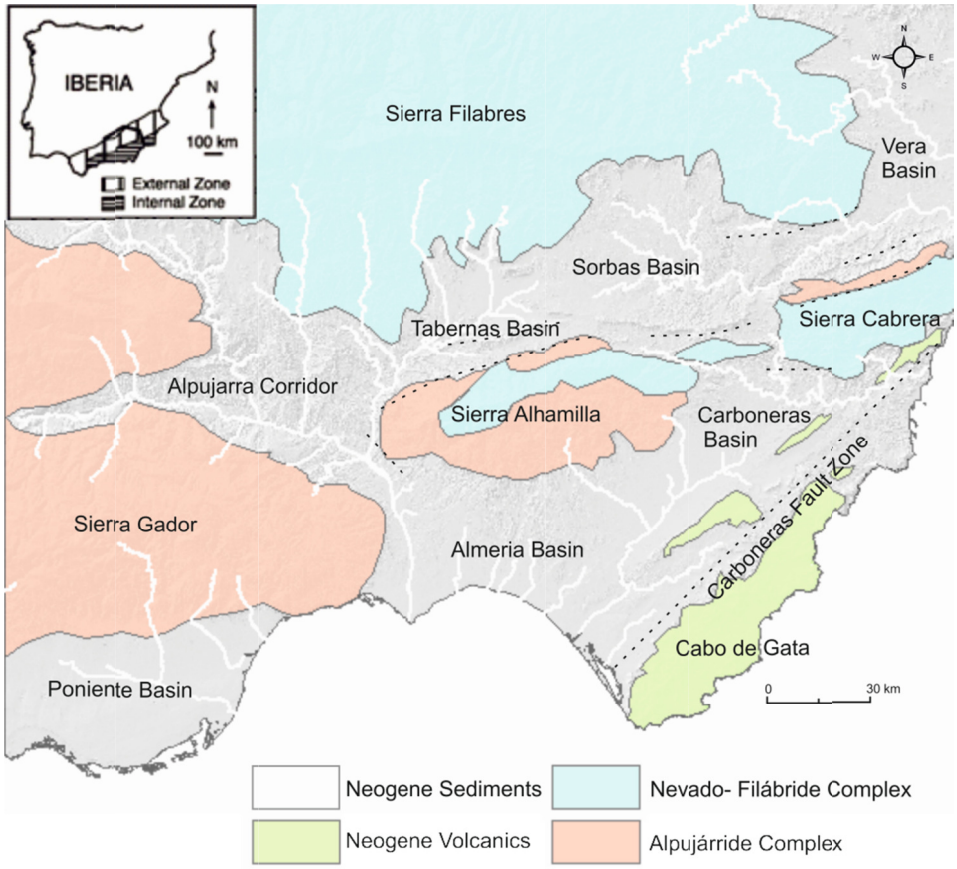

Figure 2.1 Geological map of the Internal and External zones within SE Spain (see inset), with the location of Nappe sequences, Neogene Volcanics and Neogene sedimentary basins (see key for colours), redrawn from Braga *et al., (*2003). Major mountain ranges (Sierras), fault lines (dashed lines), regional drainages (white lines) and sedimentary basins are depicted.

Traditionally, the Betic Cordillera is split into two main domains: the Internal and External Zones based on lithological, tectonic and palaeogeographic criteria (Fig. 2.1 inset) (Braga et al., 2003). The External Zone occurs in the north of the cordillera and is composed of the Sub-Betic and the Pre-Betic Zones, which display Mesozoic and Tertiary sedimentary strata not affected by metamorphism and characterised by thin-skinned tectonics (Sanz de Galdeano & Alfaro, 2004). The Pre-Betic Zone constitutes the external domain where

continental and shallow-marine sedimentation prevailed from the Triassic to the Middle Miocene (Braga et al., 2003).

The Almería region is located within the Internal Zone, commonly termed the 'Betic' Zone, which occurs within the southern part of the cordillera (Fig. 2.1 inset). The Betic Zone is comprised of three main tectonically superimposed thrust sheets or 'Nappe' complexes. From the base upwards these include the Nevado–Filábride, the Alpujárride and the Maláguide complexes (Sanz de Galdeano, 1990). These are differentiated by the extent of deformation as correlated to age of superimposition (Egeler & Simon, 1969). The lower two complexes outcrop in the Tabernas Basin (Nevado- Filábride & Alpujárride) and were subjected to high pressure metamorphism and a succession of ductile and brittle deformational events that have resultantly overprinted previous metamorphic events in the lowermost parts (Gómez-Pugnaire *et al.*, 2012). This suggests that formation of these individual nappe units occurred independently of each other, under differing metamorphic and tectonic conditions (Gómez-Pugnaire *et al.*, 2012). The Maláguide complex does not outcrop in the Tabernas Basin.

2.2.2 Neogene – Quaternary geodynamics: The formation of the Tabernas Basin.

The current geographical representation of the Internal and External Betic Zones is a result of tectonic convergence that has been on-going since the Neogene. During the Early Miocene, the Internal zone possibly situated to the south of present day Sardinia, was thrust westward at the same time as the opening of the Alborán Sea due to the subsidence in the Alborán basin (Weijermars, 1991). The External Zone was deformed by this process, with the Sub-Betic thrusted over the Pre-Betic (Sanz de Galdeano, 1990). After this thrusting stage, and during its westward migration in the Early to Mid-Miocene, the Internal Zone underwent a period of major extension, forming broad anticlinal features (e.g. Sierra de los Filabres) comprising a series of deformed stacked thrust sheets (nappes) (Table, 2.1; Braga et al., 2003). Continued uplift and deformation throughout the Late Miocene (~ 8.5 Ma - 7.2 Ma; Tortonian) was coupled with a regional marine transgression which inundated most of

Betic Cordillera except for areas of elevated topography (e.g. the Sierra Nevada and Sierra de los Filabres; Table 2.1; Sanz de Galdeano & Alfaro, 2004). The transgression resulted in the deposition of substantial marine deposits in regional synclinal features, such as the extensive marine marl and sandstone units in the Tabernas Basin (Weijermars, 1991). Shortly after the onset of the Tortonian transgression, there was a major geodynamic change across the region and the extensional westward shift of the Internal Zone was largely blocked by north-south compressional tectonics focused in the Sierra Nevada (Sanz de Galdeano & Alfaro, 2004).

From the Late Tortonian onwards, the Betics have undergone north-south horizontal compression, oscillating between NNE–SSW and more frequently NNW–SSE, depending on the areas and time (Sanz de Galdeano & Vera, 1992; Montenat & Ott D'Estevou, 1996). Ongoing compression promoted the formation of a series of major strike-slip fault systems, collectively termed the Trans-Alborán Shear Zone, which dominate the Almería region (De Larouzière et al., 1988; Vera, 2001). The shear zone is laterally extensive, running some hundreds of kilometres offshore from Almería to Alicante in a NE-SW orientation and is evidenced by major sinistral strike-slip faults systems, such as the Carboneras (shown on Fig. 2.1) and Palomares fault zones. Variations in displacements along the shear zone from the Late Tortonian / Early Messinian onward coupled with the inherent deformational styles of the region, led to the formation of a series of uplifted mountain blocks (e.g. Sierra de los Filabres, Sierra Alhamilla) and down-faulted sedimentary basins (e.g. Tabernas Basin, Sorbas Basin and Vera Basin) (Table 2.1; Omodeo Salé et al., 2012). Ongoing tectonic uplift of the Betics following nappe emplacement, combined with regional compression throughout the Mid Miocene led to the inversion of many of the Neogene sedimentary basins during the last stages of their evolution (Table 2.1; Mather, 1991; 1993; Stokes, 1997; 2008). Basin inversion was spatially variable facilitating the switch from marine to continental conditions in many of the inland sedimentary basins (e.g. Sorbas and Tabernas Basins) which prevailed throughout much of the Quaternary (e.g. Stokes, 2008).

Table 2.1 Summary of the Miocene evolution of the Almería Region and Betic Cordillera based on work of Braga et al., 2003 and references therein

Epoch/ Stage	Environmental Condition	Geomorphic Activity/Expression	Geological and Stratigraphic Evidence
Late Pliocene	Mainly terrestrial, minor shallow-marine in southern most zones of Almería- Níjar & Poniente basins	• Localised uplift within basins only	• Extensive terrestrial fluviatile deposits across most basins.
Early Pliocene	Terrestrial in north and west with final (3rd) marine transgression and onset of localised marine sedimentation in basins proximal to current Mediterranean sea (Almería-Níjar & Vera basins). Brief sea-level invasion into Sorbas basin followed by regional regression and basins becoming terrestrial from west to east.	• Continued emergence of the eastern portion of the Alpujarran corridor and eastern part of Tabernas Basin concentrated siliclastic sediment from Sierra Nevada/ Sierra de los Filabres chain with formation of delta between Sierra de Gádor and Sierra Alhamilla. • Volcanic relief of the Cabo de Gata completely emergent.	• Marine conglomerates and sandstones, with variable bioclastic and calcarentite content prograding over distal silts and marls recorded marine transgression in Almería-Níjar & Vera basins. • Thin series of laterally persistent brackish-marine marker beds in Sorbas basin- recording brief marine phases.
Mid- Late Messinian	Largely terrestrial with marine regression post early-Messinian transgression and onset of Messinian Salinity Crisis, followed by the re-instatement of marine conditions during late Messinian (2nd transgression)	• N-S highland separated the Tabernas and Sorbas basins. • Sierra Cabrera emerged separating the open-marine Vera basin to the north and the evaporitic Almería-Níjar basin to the south • Erosional down-cutting as sea levels fell	• Deposition of evaporite deposits of irregular thicknesses in areas of first phase sea-level rise (Tabernas, Sorbas) • Marine sedimentation re-instated although much more restricted then previous periods. • Deposition of shallow to deep water successions over lower Messinian reef platforms as sea-level rose.
Early Messinian	Major transgression with localised shallow marine conditions passing to deep- water marine channels in south. A landward shift of coastlines & deep-marine conditions was experienced in southerly basin.	• Landward displacement of shorelines due to global eustatic sea-level rise. • Continued uplift in the Sierra Alhamilla and Sierra de Gádor- radially displacing coastlines from the Sierra axes. • Uplift of Alpujarran corridor and merging of Sierra de la Contraviesa and Sierra de Gádor with Sierra Nevada chain, restricting marine basins to the east. • Re-arrangement of volcanic highs in the Cabo de Gata area.	• Marine deposits restricted to south of the region, occurring in the Tabernas, Sorbas, Vera and Almería- Níjar basins. • Reef units (Bioherms & Fringing reefs) deposited proximal to Sierras passing laterally to marls and turbidite conglomerates and sandstones in south.

Epoch/ Stage	Environmental Condition (cont.)	Geomorphic Activity/Expression (cont.)	Geological and Stratigraphic Evidence (cont.)
Latest Tortonian-early Messinian	Continental in north, shallow marine passing to deep-water marine in south (regression)	• Uplift of northern basins (Granada, Guadix and Almanzora basins) becoming continental. • Uplift of Sierra Alhamilla and Sierra Gádor ranges, restricting marine basins to south of Sierra Nevada/ Sierra de los Filabres chain, and promoting the formation of N-S Andarax Corridor.	• Deposition of fluviatile and lacustrine deposits in Granada and Guadix basins. • Shallow water bioclastic carbonates and local fan-deltas forming proximal to southern margin of Sierra Nevada/ Sierra de los Filabres chain, passing to distal marls and turbidites in far south.
Late Tortonian	As Early Messinian however detailed analysis of coastline positions is not preserved	• Little to no emergence of highlands • Extensive un-roofing and erosion of existing highlands (namely Sierra Nevada). • Main relief associated with Nevada / Sierra de los Filabres chain.	• Narrow fringe of coral reefs and fan deltas rimming Sierra Nevada/ Sierra de los Filabres chain. • Marls deposited on top of continental conglomerates and shallow-marine bioclastics in the laterally connected Tabernas, Sorbas and Vera basins. • Pelagic sedimentation around sierras. • Fan-delta sedimentation around current sierras with formation of coral reefs.
Early Tortonian	Shallow Marine (complicated by disconnected nature of emergent reaches of basin).	• Continued emergence of Sierra Nevada/ Sierra de los Filabres chain. • Subbetic upland areas becoming emergent, forming islands rimmed by shallow water marine platforms.	• Inferred continuous shallow water platforms across much of Internal and External Betic zones. • Carbonate platforms rimming emergent Sierra Nevada/ Sierra de los Filabres chain. • Scattered shallow marine deposits across much of south of region (Tabernas, Sorbas & Vera basins).
Pre-Tortonian / Serravallian	Continental to Shallow Marine in north progressing to coastal shelf/slope in the south (south of current Sierra Alhamilla/ Cabrera).	• Emergence, un-roofing and erosion of Betics. • Presence of a series of islands (Betic islands). • Large emerged upland in Granada basin.	• Upper Langhian coral reefs (south Granada & Vera basins) and coastal conglomeratic facies proximal to emergent Betic islands. • Shallow water carbonates deposited on platform of Iberian Massif changing southwards to slope/basin marls and mass flow deposits. • Terrestrial conglomerates (red) deposited within marine facies across remnant topographic highlands (Sierra de Gádor, Sierra Alhamilla and Cabrera).

In the Tabernas Basin, the dominant N-S / NNW-SSE compressional tectonic regime is evidenced by numerous faults and folds which deform deposits of Late Neogene to Quaternary age (Fig. 2.2) (Sanz de Galdeano *et al.*, 2010). This inherited tectonic form and ongoing tectonic activity is believed to be a primary control upon the Quaternary landscape system, as evidenced by: (i) the variable rates of fluvial incision across the basin (Harvey, 2007); (ii) the passive control of anticlinal features upon drainage pathways; and (iii) the rejuvenation of drainage lines in the south of basin along fault lines in the Northern Alhamilla Fault Zone (NAF) (Fig. 2.2) (Giaconia et al., 2012).

2.3 Geological domains- Tabernas Basin

The strength and structure of the underlying bedrock geology is of primary significance in the evolution of bedrock fluvial systems (e.g. fluvial systems formed in thin or non-existent thicknesses of alluvium; Pazzaglia et al., 1998). Knowledge of the sediment sources (provenance) into and within a basin can offer valuable information with regard to patterns of sediment delivery and flux over long timescales (e.g. Calvache and Viseras, 1997, Stokes et al., 2002). The Quaternary landscape of the Tabernas Basin can be split in to two broad geological domains which encompass both aspects of bedrock geology and sediment sources. These domains comprise: (1) Alpine basement rocks, which form the resistant lithologies of the bounding Sierras (Sierra de los Filabres and Sierra Alhamilla) and are believed to be the major source of sediments to the Tabernas Basin (Harvey, 1987; 1996; 2002); and (2) Neogene basin fills which blanket the basin centres and have been a significant control upon the Quaternary fluvial system (Fig. 2.2); (Harvey et al 2003; Alexander et al., 2008).

The following sections (2.3.1 and 2.3.2) describe the main stratigraphical and lithological relationships between the alpine basement and Neogene basin fill complexes within the Tabernas Basin. Where significant, reference is made to stratigraphic and lithological relationships that extend between sedimentary basins across the Almería region.

This regional geological context is of key importance when developing the intra-basinal relationships across the Almería region throughout the Late Cenozoic.

2.3.1 Alpine basement geology

The Alpine basement geology of the Tabernas Basin is the principal source of hillslope sediment for the Quaternary fluvial system (Harvey, 1987). The bounding mountain ranges (Sierra de los Filabres and Sierra Alhamilla) comprise a series of Mesozoic, Paleozoic and Precambrian metamorphic rocks of the Betic Zone (basement lithologies on Fig. 2.2). As previously presented, the Betic Zone is grouped into a series of characteristic nappe complexes (from oldest to youngest): (1) the Nevado-Filábride complex ; (2) the Alpujárride complex; 3) the Maláguide complex (Gómez-Pugnaire, 2001). In the Tabernas Basin only the Nevado-Filábride complex and the Alpujárride complex are found (Fig. 2.2).

Nevado-Filábride complex

The Nevado-Filábride complex makes up most of the northern boundary of the Tabernas Basin and is characteristic of the Sierra de los Filabres, with minor outcrops in the upper slopes of the Sierra Alhamilla in the south. The complex extends further west to form some of the highest peaks of the Iberian peninsula in the Sierra Nevada (Gómez-Pugnaire, 2001). Classically, the Nevado-Filábride complex is separated into two distinct unconformable lithological units: 'Basement' and 'Cover' (terminology from Egeler et al., 1969). The Basement is simple in stratigraphic form and is made up of extensive thicknesses (>4000 m) of Precambrian / Paleozoic graphite-bearing mica schists (often chlorite and garnet rich) with alternating quartzite beds (Fig. 2.3A - group 5) (Gómez-Pugnaire, 2001; Azañón *et al.*, 2005; Gómez-Pugnaire et al., 2012). In comparison, the Cover consists of four formations which are highly variable in thickness and lithology (numbers correlate to units numbers in Fig. 2.3A):

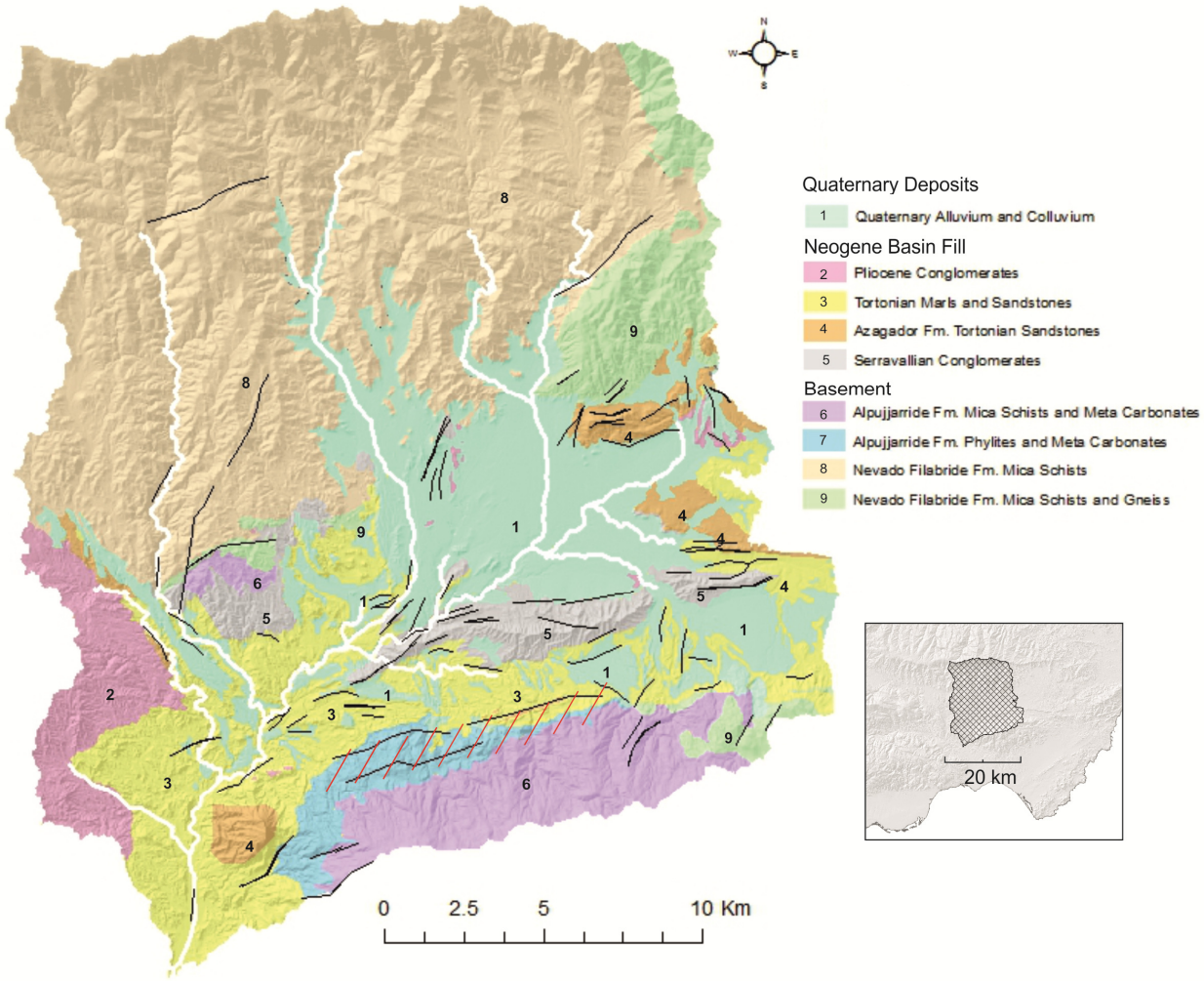

Figure 2.2 Geological map for the Tabernas Basin, revised from Instituto Geológico Minero de España Institutomap 1:50 000 map series (1030). Black lines represent faults. Diagonal red lines represent the Northern Alhamilla Fault Zone (NAF), and white lines represent major drainages.

4. *Tahal schists:* a series of light coloured feldspathic quartzites and mica schists, up to 1500 m thick, that contain relics of sedimentary structures that indicate a shallow marine origin (Gómez-Pugnaire, 2001; De Jong & Bakker, 1991).
3. *Meta-Evaporitic Formation (after Gómez- Pugnaire et al., 1994):* comprising up to 80 m of brecciated marbles, calc-schists and fine-grained scapolite-bearing metapelites with gypsum pseudomorphs, barite and halite relics (Gómez-Pugnaire et al., 1994; Gómez-Pugnaire, 2001);
2. *Marble and Calc-schist Formation (after Helmers and Voet,1967):* composed of laminated and massive calcitic and dolomitic marbles with some intercalated layers of mica schists and calc-schists, up to 1000 m thick, outcropping in the Cóbdar-Macael area only (López Sánchez-Vizcaino, 1994);
1. *Chive Formation (after Gómez- Pugnaire et al., 2012):* comprising basal heterogeneous unit of massive marbles (~50 m thick) that are capped by a series of interbedded tourmaline gneisses, dark-graphite bearing and light garnet-kyanite mica-schists, banded marbles (up to 2 m) and scarce meta-basites and serpentinite bodies;

Across the Tabernas Basin the Tahal schists are the principal sources of sediments from the northern basin margins (Gómez-Pugnaire et al., 2012). Sediment assemblages in the northern and central regions of the basin are dominated by graphite bearing mica schists and quartzites with minor gneiss inputs, with a principal sediment pathway from the Sierra de los Filabres (Fig. 2.4). The occurrence of extensive quartzite beds in both formations is thought to be a primary source of quartz rich sediments which serve the focus of Optically Stimulated Luminescence dating conducted in this study, detailed in Chapter 4.

Alpujárride complex

The Alpujárride complex occupies much of the southern margin of the Tabernas Basin, outcropping extensively in the low to middle slopes of the Sierra Alhamilla (Fig. 2.1). The Alpujárride complex consists of several tectonic units grouped into the lower, middle and

upper nappes, which increase in metamorphic grade from the lower to upper (Gómez-Pugnaire, 2001). Much like the Nevado-Filábride complex, the Alpujárride complex can also be separated in to two broad lithological zones: Pre-Permian Basement and a Mesozoic Cover (Gómez-Pugnaire, 2001).

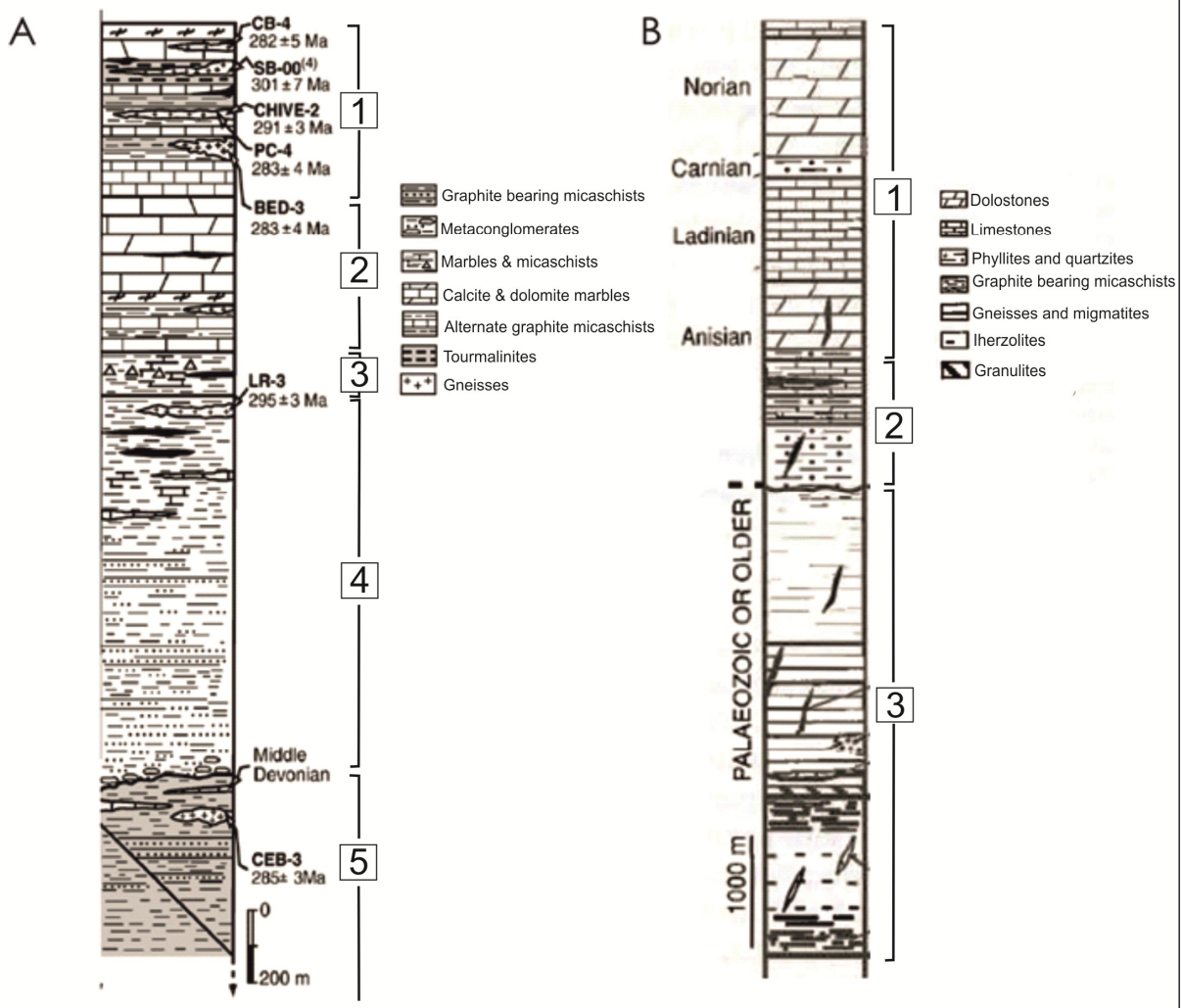

Figure 2.3 Metamorphic nappe complexes of the Tabernas region, lithostratigraphic column of the (A) Nevado-Filábride Complex and the (B) Alpujárride complex, reproduced from Gómez- Pugnaire *et al.*, (2012) & Gómez-Pugnaire (2001), respectively. Note, the numbers in boxes on the Nevado- Filábride column (A) relate to the formations of the Cover unit as described in the text.

The lithological sequence of the Alpujárride complex consists of the three main lithological units split between the two principal zones (numbers correlate to unit numbers in Fig. 2.3B units):

3. *Dark metamorphic rocks (basement):* up to 1000 m of low to intermediate grade metamorphosed graphite bearing mica schists, migmatites and quartzites.

2. *Pale phyllites and quartzites with minor carbonate (Permain-Triassic cover):* forming the basal section of the cover unit up to 1000 m thick;

1. *Thick sequence of carbonates (Triassic cover):* forming the upper section of the cover unit with up to 2000 m of shallow platform to basinal marine dolostones and limestones;

Across the Tabernas basin, sediments sourced from the Alpujárride complex occur extensively in the southern regions of the basin (south of the Serreta del Marchante anticline, Fig. 2.2 unit 3). There are multiple distinguishing lithologies which are only sourced from the Permian-Triassic age cover of the Alpujárride complex, such as brecciated limestones, carbonate conglomerates and phylittes (Fig. 2.4). When found in fluvial sections these lithologies suggest significant sediment inputs from the southerly basin margin.

2.3.2 Neogene basin fill

Neogene fills are the dominant bedrock lithology of the Tabernas Basin into which the Quaternary fluvial system has formed (Fig. 2.2). The deposition of basin fill materials across the Almería region occurred in response to variable rates of tectonic uplift coupled with climatically driven sea-level changes from the Tortonian period onward (as summarised in Table 2.1). The following section presents the chronological framework for the deposition of Neogene fill materials within the Tabernas Basin. However, the units presented often form spatially extensive lithologies, deposited in broad depositional systems that laterally span into the neighbouring Sorbas and Vera basins (Poisson *et al.*, 1999). Where significant the intrabasinal relationship of lithologies is discussed in order to formalise a regional context of Neogene sedimentation and subsequent Plio – Quaternary incision.

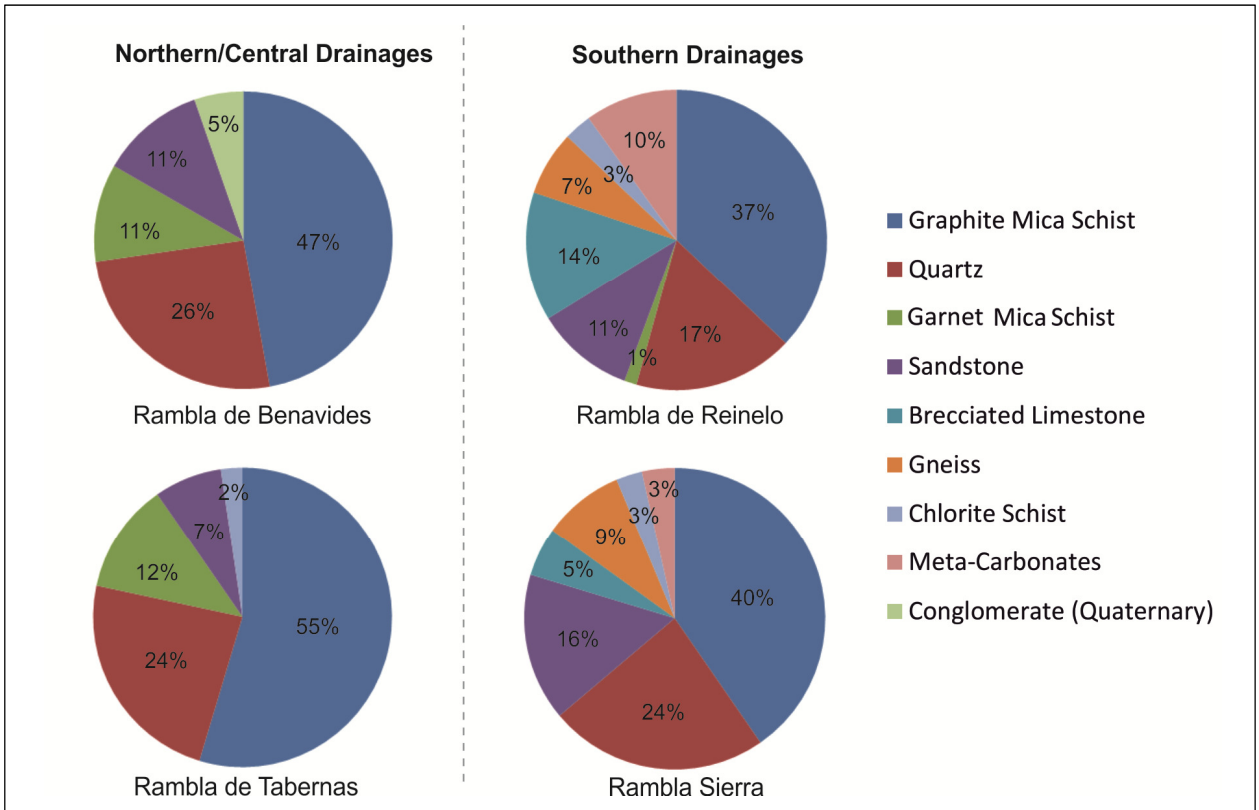

Figure 2.4 Provenance clast count data (n=300) measured from Quaternary fluvial terraces for four major basin drainages. Graphite mica schist and quartz lithologies are characteristic of drainages draining from the Sierra de los Filabres in the northern basin margin. In contrast, drainages draining from the Sierra Alhamilla in the south are rich in brecciated limestone and meta-Carbonate lithologies sourced from the Alpujárride complex which is not encountered in the northern basin margins.

Serravallian: Subaerial – Marine Successions

The oldest stage of sedimentary infill in the Tabernas Basin occurred during the transition from terrestrial to marine conditions in the Serravallian period (Fig. 2.5) (Haughton, 2001). Across the greater Almería region sea levels transgressed from south to north, with southerly areas proximal to the current Sierra Alhamilla experiencing marine conditions during the Serravallian, and northerly areas becoming marine in the Early Tortonian (Table 2.1); (Weijermars, 1991). Within the Tabernas Basin this early transgression is characterised by a cover of red continental conglomerates sourced mainly from the Alpujárride complex within the Sierra de los Filabres (see left pointed arrows at base of Tabernas Basin section in Fig. 2.5) (Weijermars et al., 1985; Haughton, 2001). These conglomerates form non-marine fan

conglomerates and coarse grained (up to boulder sized) fan-deltas which prograded in a southerly direction from the juvenile Sierra de los Filabres (Dabrio, 2009; Haughton, 2001).

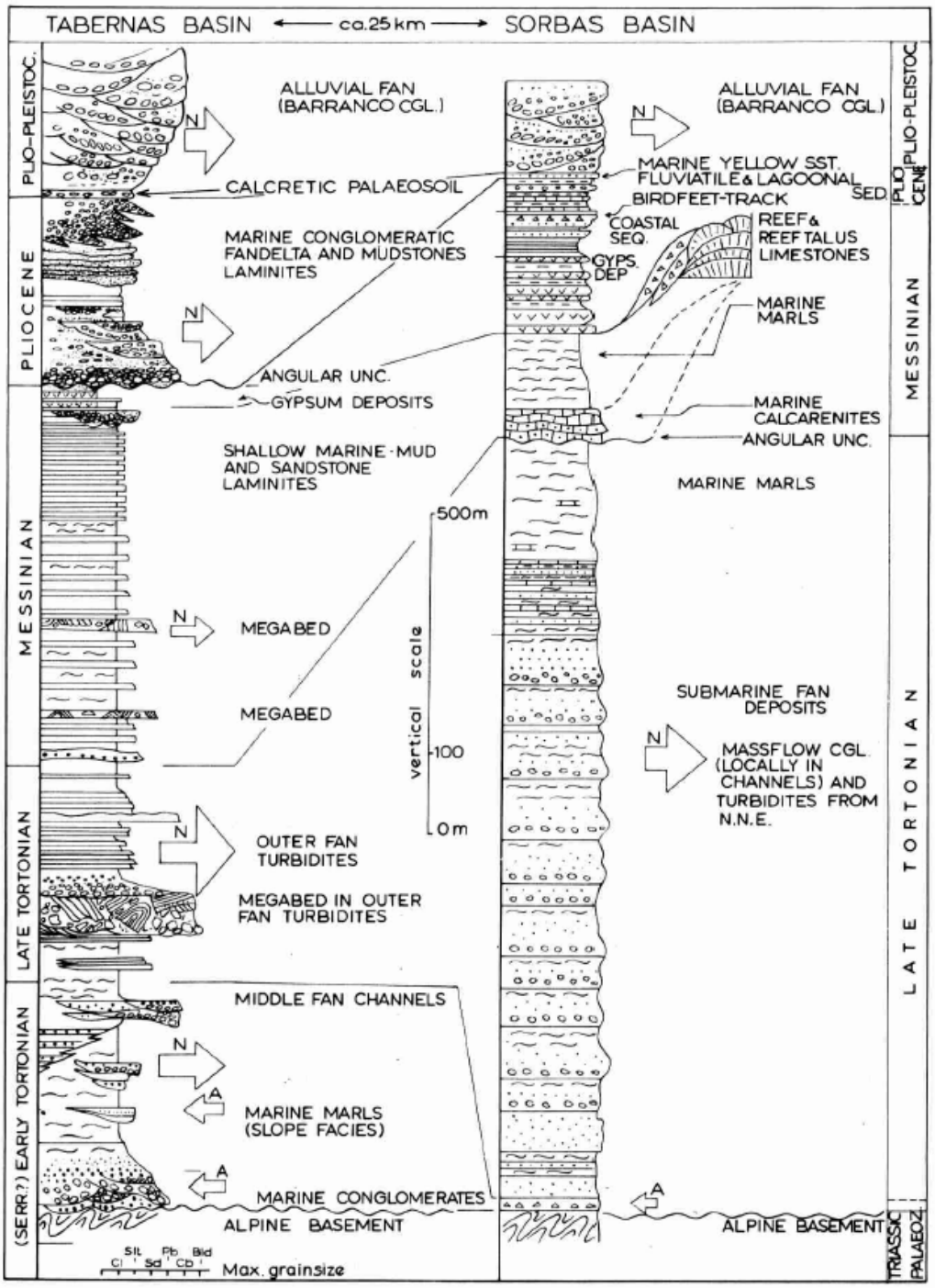

Figure 2.5 Composite stratigraphic column for the Tabernas and Sorbas basins, taken from Weijermars *et al.*, (1985). SERR is Serravallian. N and A labels relate to sediment inputs from the Nevado-Filábride and Alpujárride complex respectively.

The Serravallian conglomerates typically overlie the Alpine basement of the Sierra Alhamilla (Fig 2.5), but localised exposures can be found over older Neogene sediments in

the westerly extremes (Weijermars *et al.*, 1985). The best exposures of the unit occur within the transverse reach of Rambla Sierra, which cuts exposures through the Serreta del Marchantè anticline (Fig. 2.14). In section, the conglomerates form steeply dipping beds that exhibit well developed reverse-grading with sheared fabrics indicative of large scale sturzstrom type debris flows (Fig. 2.6) (Mather, *per comms.*). Laterally, the conglomerates extend as far as Lucainena village to the far east where they become buried under an unconformable cover of latest Tortonian, Messinian and younger fill of the Sorbas basin (Haughton, 2001). Sections are rich in graphite-bearing schists and augen gneiss sourced from the Nevado-Filábride complex in the north. When encountered by Quaternary fluvial systems, the Serravallian conglomerates present a significant lithological control upon fluvial incision. Erosional styles are typically deeply incised with a common tendency for transverse reaches, such as in the Rambla Sierra (Fig 2.7).

Figure 2.6 Sturzstrom-type debris flows in Serravallian conglomerates within Rambla Sierra with a close up of reverse grading evident within beds, Photos from A. Mather.

Figure 2.7 Serravallian conglomerates out cropping in the Serreta del Marchantè anticline being drained by the transverse Rambla Sierra drainage. The conglomerates (coloured red) dip steeply in section and are unconformably overlain by substantial Quaternary deposits (pale green). Photo facing south from UTM 30S 553302/4099656

Tortonian- Messinian: Deep- Water Successions

The most significant period of Neogene sedimentation in the Tabernas Basin occurred during the Late Tortonian - Early Messinian. During this time, a second and more significant transgression occurred with the formation of an extensive elongate deep-water trough that extended in an east-west direction from margins of the Sierra Nevada, incorporating the Tabernas and Sorbas basins (Table 2.1; Haughton, 2000; Montenat & Ott D'Estevou, 1996). The deep-water trough was bound to the north by the highlands of the Sierra de los Filabres and to the south by a subdued shallow water sill or submarine swell which had little topographic relief forming the current Sierra Alhamilla (Braga et al., 2003). Sediment inputs were in the form of turbidity currents sourced broadly from the north of the basin which delivered sediment to the E-W trending trough via well developed (10's-100's m deep) sub-marine canyons (Rogerson et al., 2006). Although the chronological links between continuous sedimentary sequences have been questioned, it is believed that turbidite deposition continued well in to the Messinian (Haughton, 2000).

Across the Tabernas and Sorbas basins, deposition within the deep water trough represents some 700 m of marine sedimentation that was subjected to distinct periods of syndepositional faulting during formation (Hodgson and Haughton, 2004). The succession can be separated into five informal stratigraphic units which represent deposition under a range of marine conditions, from bottom to top (see Fig. 2.8 for unit correlations; Haughton, 2000):

- **Unit A**: Fine grained heavily bioturbated marine marls, accumulated during flooding of the tough (Early to Late Tortonian?). The sand starved marls suggest a period of bypass in the Tabernas Basin, with axial channels transferring coarse sand deposits to easterly depocentres;

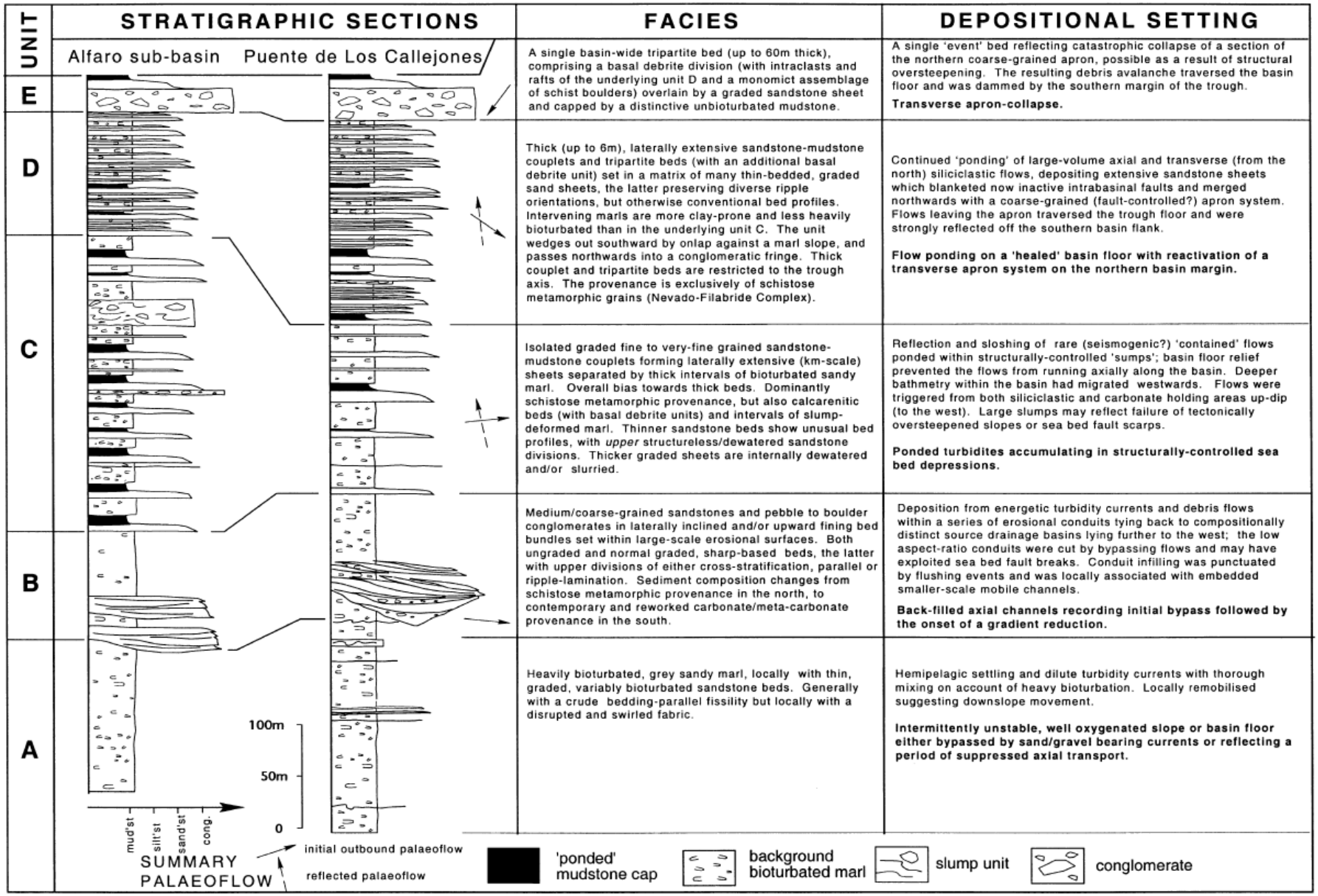

Figure 2.8- Summary stratigraphic logs of sub-Gordo sequence within the Tabernas Basin, from Haughton (2000).

- **Unit B**: Marine marls (as Unit A) with increasing numbers of embedded sand bodies that mark the boundary between the top of Unit A and base of Unit B. The sand bodies form within high-sinuosity embedded channels that back filled as a result of drainage gradient reductions;
- **Unit C**: Interbedded marls, slumps and thick sheet turbidites that show evidence of flow containment (Fig. 2.9). This unit is by far the thickest within the sequence with some 300 m of accumulation in the south of the basin. Containment is restricted to fault controlled structural depressions;

Figure 2.9 Massive slump clast in marine marls and sandstones of Unit C (terminology from Haughton, 2000). Red dashed line notes unconformable contact with Unit D comprising a series of sub-horizontally bedded sand sheets. Photo facing south from UTM 30S 550481/4098765

- **Unit D**: Sand prone sheet system comprising some 200 m of thinly bedded and thick 'contained' sandstone facies. These sand deposits form over fault-controlled topography, resultantly healing the landscape giving rise to later extensive sand sheet forms. These

units show evidence of sourcing from seismically triggered 'axial' failures and a fault controlled slope building out from northern margin of basin;

- **Unit E (Gordo Megabed)**: A basin wide debrite that forms some 60 m of massive / poorly structured conglomerates, formed as a result of a single seismically triggered mass wasting event which blanketed the basin floor.

The Tortonian-Messinian marine and turbidite sequences occur extensively across the Tabernas Basin and form much of the bedrock geology in the basin centre (Fig. 2.2). The units are typically dominated by marls of low strength and homogeneous nature which have facilitated the rapid incision, entrenchment and increased connectivity of the Quaternary drainage system (Harvey, 2002; 2007). A notable feature of the current fluvial network is the common occurrence of slot type or highly incised - laterally constrained reaches which form where drainages cut through conglomerates of the Gordo Megabed (Fig. 2.10).

Mid-Late Messinian: Evaporites

The final stages of marine basin infilling in the Tabernas Basin would have occurred in the Mid Messinian (Weijermars et al., 1985), prior to a marked period of abrupt sea-level fall and regional desiccation in the Mid – Late Messinian, termed the Messinian Salinity Crisis (MSC) (Table 2.1; Hsu et al., 1977). The MSC occurred as a result of the final closure of Tethys ocean from the Atlantic via convergence of the Betic and Rif Strait which affected much of the Mediterranean basin (Hsu et al., 1977). Across the Almería region, the MSC is notable within the geological record in the form of extensive Gypsum-rich evaporite sequences that occur in most outer basins (except the Vera Basin; Omodeo Salé et al., 2012). In the Tabernas Basin the contact between Tortonian - Messinian deep water turbidite sequences and Mid - Late Messinian shallow marine deposits is defined by an angular erosional unconformity that cross cuts bedding planes at some 60°, with no preserved sedimentary units (Weijermars *et al.*, 1985).

Figure 2.10 Slot reach in the Rambla Los Molinos as the drainage cuts through resistant massive conglomerates of the Gordo Megabad (coloured grey). Gordo megabed is unconformably overlain by gently dipping sandstones of Unit D described by Haughton, (2000) indicating a non-uniform stratigraphic relationship of the Gordo megabed across the basin. Photo facing northwest from UTM 30S 555434/4101213.

In the neighbouring Sorbas basin, extensive gypsum beds mark the transition into the Messinian Salinity Crisis, where deep water reaches of the Messinian inland sea are marked by some 130 m thick gypsum deposits (Krijgsman et al., 2001). However, in the Tabernas Basin, outcrops of gypsum are rare and only found in the far eastern (Los Yesos area) and western (Yesares area) limits associated with pre-evaporitic carbonates and fringing reef complexes (Braga *et al*., 2006). Most notably, Early-Mid Messinian pre-evaporitic deposits do not occur anywhere else in the Tabernas Basin. A hypothesis for this lack of preservation with respect to the neighbouring Sobras Basin is the high degree of Plio-Pleistocene tectonic incision which must have taken place post deposition (Harvey, 2002).

Plio-Pleistocene: Shallow Marine to Terrestrial Successions

The Plio-Pleistocene transition was the most significant period in the evolution of the current Tabernas Basin with the initial stages of drainage development under terrestrial conditions (Weijermars *et al*., 1985). Across the Almería region, the Early Pliocene was marked by a third and final transgression which led to the onset of shallow-marine conditions in basins proximal to the current Mediterranean sea (e.g. Vera, Carboneras and Almería basins; Braga et al., 2003). Water depths decreased in a landward direction, with the short lived invasion of an inland sea in the Sorbas Basin (Fig. 2.11) (Braga et al., 2003). Within the Tabernas Basin, records of the Early-Pliocene transgression are only found in the far southwest of the basin, confined within the Rioja Graben forming a minor inlet from the Almería Basin (Fig.2.11). Pliocene successions within the Rioja Graben are split in to the Gádor and Abríoja Formations which mark the transition from marine to terrestrial conditions (Postma, 1984). Of the two formations, only the Abríoja Formation is found within the current hydrological Tabernas Basin, with the Gádor Formation mainly outcropping to the south in the Tabernas-Almería Basin corridor.

The Abríoja formation unconformably overlies extensively folded Tortonian-Messinian marine and turbidite sequences, commonly outcropping in isolation in topographic highs (Fig.

2.12). In section, the Pliocene sequences often occur as localised channel cuts or dissected fan delta deposits comprised of the following units (units from bottom to top; from Postma, 1984):

1. Pro-delta sediments, with heavily bioturbated muds;
2. Lower delta slope sediments, with parallel bedded conglomerates, sandstones and pebbly mudstones;
3. Upper delta slope sediments, with tangential foresets of pebbly sandstones;
4. Sediments of a transition zone (beach, nearshore and delta front;
5. Alluvial fan and coastal plain deposits with palaeosols.

The provenance of the Pliocene conglomerates suggests reworking of materials sourced from the Sierra de los Filabres with sections dominated by graphite bearing mica schists. Post incision, the isolation of outcrops of the Abríoja Formation in topographic highs would have had limited significance upon fluvial responses other than acting as a localised source of sediments.

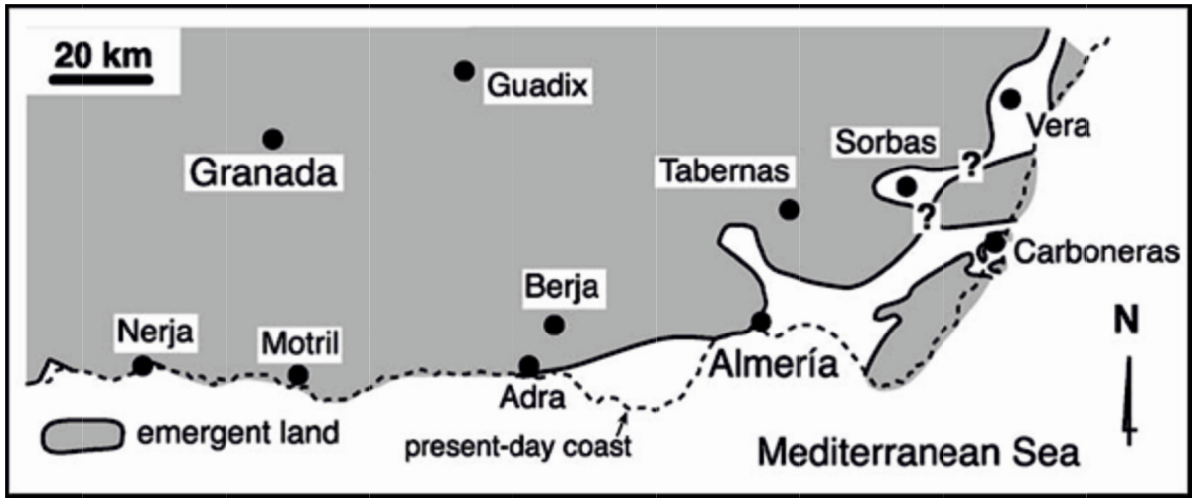

Figure 2.11 Early Pliocene Palaeography of SE Spain showing the extent of the shallow marine conditions within the Sorbas and Vera basins, from Braga *et al.,* (2003).

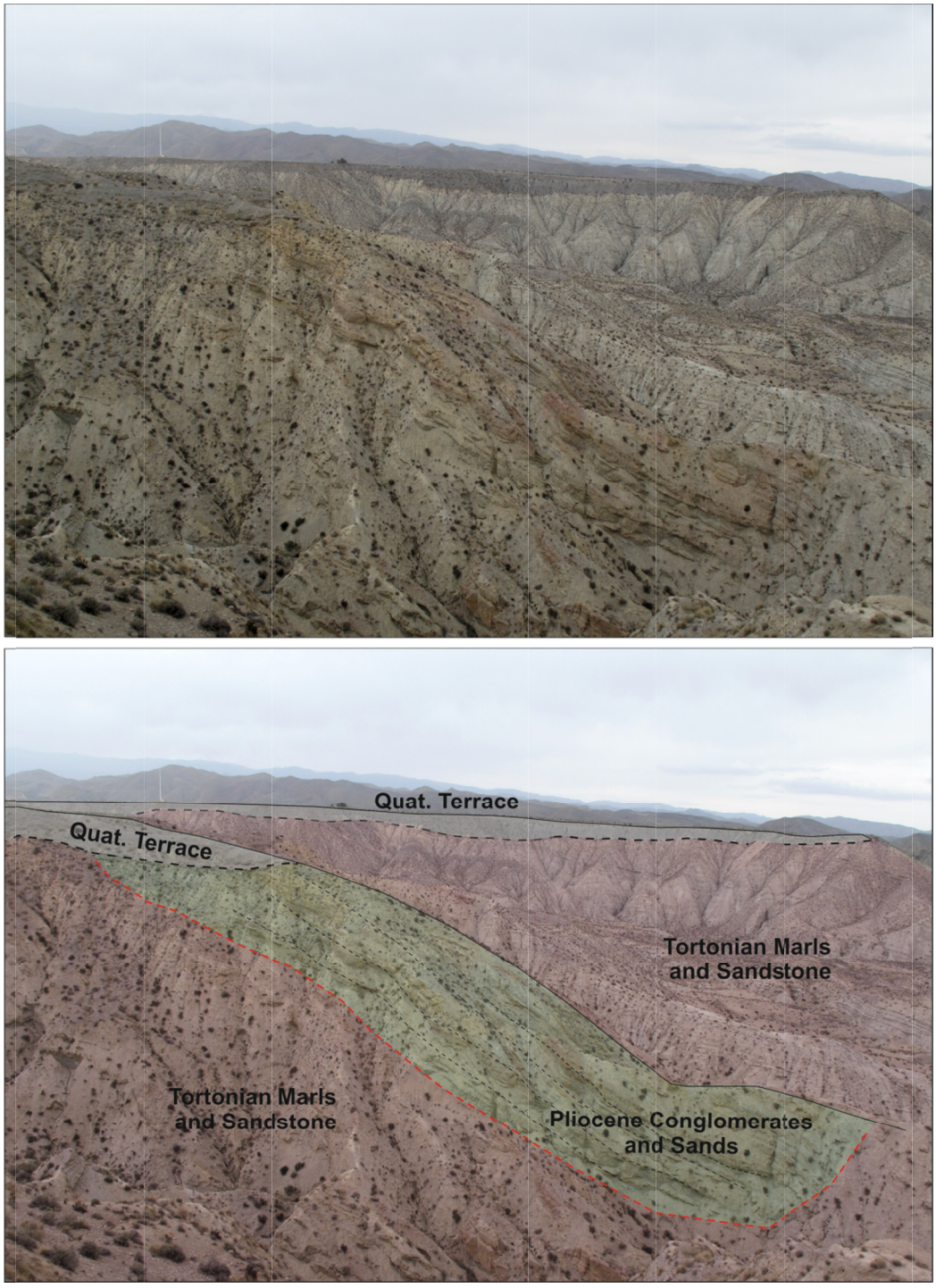

Figure 2.12 Pliocene fan-delta deposits cut into and faulted against underlying Tortonian marls and sandstone units. The Pliocene units are unconformably overlain by Quaternary terrace deposits. Picture facing east over Rambla Lanujar from UTM 30 S 547714 / 4097684.

The Early Pliocene transgression was followed by falling sea-levels and the gradual onset of terrestrial conditions across most basins in the Almería region (Terrace Sequences of Table 2.2; Braga et al., 2003). At some point in the Late Pliocene - Early Pleistocene, the terrestrial basins experienced erosional inversion documenting a switch from a pattern of regional basin infilling to sustained incision. Although currently not well understood the potential mechanisms for this switch to basin incision could include (Stokes *pers comm*.):

1. An increase in tectonic uplift via a change in neotectonic stress field in the Plio-Quaternary (e.g. Cloetingh et al., 1990);
2. Accelerated river incision as associated with the 'Mid Pleistocene Revolution' changes in duration and frequency of cold climate cycles (e.g. Gibbard & Lewin, 2009);
3. Basin scale river capture, where changes in uplift or climate-related eustacy can result in base-level lowering, headward erosion and capture (e.g. Antón et al., 2012).

Across the Tabernas Basin the onset of basin inversion and resultant incision is evidenced by a top basin fill surface of variable preservation (extensive or fragmentary; black arrows on Fig. 2.13). The basin fill surface is dissected by an inset sequence of Quaternary alluvial fan or river terrace surfaces (white arrows on Fig. 2.13), producing the current stepped landscape topography which evidences sustained base-level lowering and forms the focus of this study.

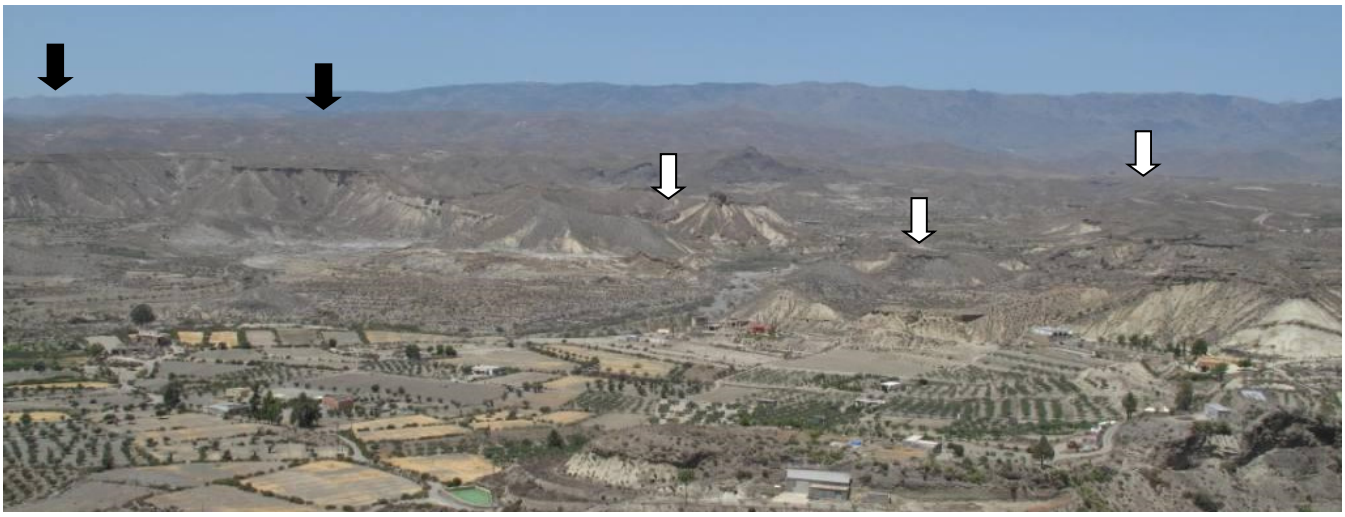

Figure 2.13 Top basin fill surface (black arrows) with inset fan / river terrace surfaces (white arrows) of the central Tabernas Basin. Photograph from M. Stokes.

2.4 Quaternary Geomorphology- Tabernas Basin

The Quaternary geomorphology of the Tabernas Basin comprises a series of incisional and depositional landform units which record the complex interactions of various forcing mechanisms over a range of spatial and temporal scales. To date, studies of the geomorphic evolution of the basin have focused on individual landscape elements, which include (Fig.2.14):

1. Alluvial fans (e.g. Harvey, 1996; 2011; Harvey et al., 2003);
2. Calcretes (e.g. Nash and Smith, 1998; 2003);

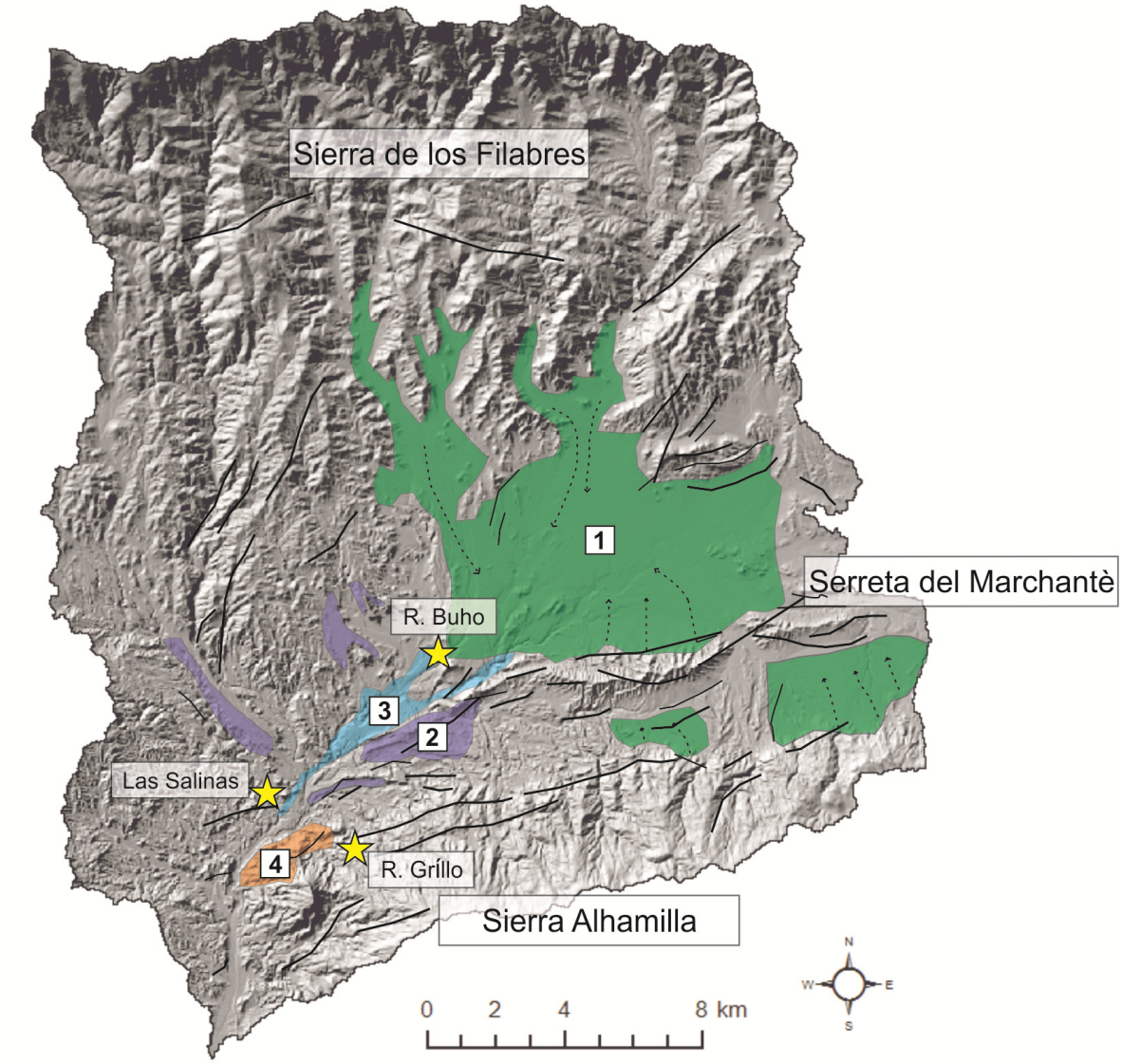

1	Alluvial fan environment; Harvey,1987; 1996; Harvey et al., 2003.
2	Calcrete development; Nash and Smith, 1998; 2003.
3	Tabernas lake systems; Harvey et al., 2003.
4	Badland formation; Alexander et al., 2008. Calvo-Cases et al., (2014)
5	Travertine development; Mather and Stokes, 1999.

Figure 2.14 Quaternary landscape elements of the Tabernas Basin. The numbers and colours relate to a specific field of study with authors detailed in the table. Note how each landscape element is spatially disconnected from each other, yet the degree of investigation covers the entire basin. Dashed arrow lines represent the directions of alluvial fan progradation

3. Quaternary lake systems (e.g. Harvey et al.,1999; 2003);
4. Badlands (e.g. Alexander et al., 2008; Calvo-Cases et al.,2014);
5. Travertines (e.g. Mather and Stokes, 1999).

Although laterally extensive across the basin, the connection between these individual landscape components is complicated by a lack of continuous spatial or temporal data. Harvey et al., (2003) focused on this lack of connectivity across the basin and attempted to apply relative dating methods (e.g. sedimentology, relative elevation, soil development and mineral magnetics) in order to link sediment sources to sinks; however, the methods applied were limited to the east of the basin alone and suffered from a lack of chronological control.

The following section aims to present the spatial and temporal connections between individual landscape elements. Initially, an overview of each landscape element is presented with focus on the mechanisms that drive their formation and preservation. A conceptual model for landscape development is presented in Section 2.4.6 which attempts to combine all individual landscape elements. The overall aim of the model is to: (i) identify the major landscape forces operating within the Tabernas Basin throughout the Quaternary, and (ii) highlight the requirement for a study of the Quaternary terrace record (presented in Chapter 3) in order to generate a full understanding of the spatial and temporal patterns of landscape evolution across the Tabernas Basin.

2.4.1 Alluvial fans

Alluvial fans form where confined streams emerge from upland catchments into zones of reduced stream power (Bull, 1979). Fans are important geomorphic features which influence fluvial system development via variations in hillslope sediment delivery from the source area in the mountain catchment to the sink in the sedimentary basin (Harvey, 1996). Across the Tabernas Basin, alluvial fans are a dominant landscape feature comprising ~ 40% of the total basin area (Fig. 2.14). Fan formation is most extensive in the east of the basin,

where sequences form large coalescent sedimentary bodies which unconformably overlie Tortonian marls and sandstones. In the east, current fan surfaces are proximally trenched but distally aggrading, recording limited incision from the current fluvial systems (i.e. decoupled from the erosional regime operating in the basin centre; Harvey et al., 1999). In comparison, fans in the west of the basin are largely dissected by the current fluvial system forming terrace remnants of variable preservation and calcrete cementation.

Across the basin, the extensive fan bodies can be separated in to three major groups (from Harvey et al., 2003) emanating from: (1) the Sierra de los Filabres along the northern basin margin, (2) the Serrate del Marchante in the centre of the basin, and (3) the Sierra Alhamilla along the southern basin margin (Fig. 2.14). A notable feature of Filabres and Marchante fans is their relatively large size in comparison to catchment area. This characteristic is related to a lack of tectonically induced dissection coupled with high rates of sediment supply which has favoured conditions of fan aggradation (Harvey, 1996). Fans emanating from the Sierra Alhamilla are poorly preserved except for the Rambla Sierra fan in the east of the basin which is fully trenched and forms fan remnants only (Harvey et al., 1999). Active tectonic deformation of all fan bodies is rare; however, passive tectonic forcing (i.e. the basin and range morphology of the region) is of primary importance in the uplift and erosion of the fan source areas (i.e. bounding sierras) and the ongoing generation of accommodation space in the basin centres (Harvey, 2011).

In the east of the basin, it is proposed that fan sedimentation has been ongoing from the Early - Mid Pleistocene as recorded by a series of distinct sedimentation events (Harvey et al., 2003). The correlation of fan aggradation sequences based on stratigraphical relationships, soil evidence and one relative date (150 ± 50 ka, Chapter 4 for detail) suggests that aggradation events are principally driven by climatic cycles (Harvey et al., 2003). Major periods of fan aggradation form in accordance with regional climate change patterns (e.g. Candy et al., 2004; Santisteban and Schulte, 2007; Schulte et al., 2008; Miekle, 2008; Ilott, 2013), with sedimentation under cold climate conditions when hillslope systems

are sparsely vegetated and relative sediment availability is high (Harvey, 1996; Harvey et al., 1999; 2003). Tentative correlations suggest two fan aggradation events occurred during the Early – Middle Pleistocene and one younger event occurred during the Holocene, as discussed further in Section 2.4.6 (Harvey et al., 2003).

2.4.2 Calcretes

Calcrete is defined as a near-surface terrestrial accumulation of calcium carbonate which occurs in a variety of forms (e.g. pedogenic and non-pedogenic; Wright and Tucker, 1991). Calcretes are of significance in studies of long-term landscape evolution as they often preserve evidence of landscape inversion (e.g. valley floor deposits isolated as elevated terrace remnants; Butt and Bristow; 2013), offer insight into the relative climatic conditions operating during their formation (e.g. Alonso-Zarza et al., 1998; Stokes et al., 2007), and offer a means of relative dating (e.g. varying stages of pedogenic carbonate accumulation and calcrete accumulation; Gile et al.,1966; Machette, 1985). Across the Tabernas Basin, multiple types of calcrete have been of significance in the extensive (basin wide) preservation of Quaternary landforms, occurring as either: (i) pedogenic, (ii) groundwater, or (iii) valley floor forms (Nash and Smith; 1998; 2003).

Pedogenic calcretes occur most extensively across the basin capping fluvial and alluvial sediments. Pedogenic forms typically occur as thin horizons of well-cemented carbonate nodules formed in the upper 50 cm of soil profiles (Nash and Smith, 1998). Unlike in the neighbouring Sorbas basin, rubification of calcreted soil profiles is highly variable and especially well developed in catchments rich in graphite schists which form the primary source of pyrites needed to generate iron rich staining (i.e. lithologies sourced from the Sierra de los Filabres; Harvey *pers. comm.*). The formation of pedogenic calcretes only occurs under conditions of severe moisture deficit when surface carbonates are not leached from the soil system (Nash and Smith, 1998). Therefore, it is likely that pedogenic calcrete formation would have taken place in Tabernas during periods of sustained decreases in

precipitation. Based on regional interpretations, this could be linked to cold climate periods when seasonal aridity was high (Macklin et al., 2002; Candy et al., 2012).

Pedogenic calcretes are found in association with laterally extensive groundwater calcretes at a range of stratigraphical positions across the Tabernas Basin (e.g. paired calcrete units; Fig. 2.15). Groundwater calcretes form thick (> 6 m) well-cemented to laminar units formed at the base of fluvial and alluvial gravel units which outcrop extensively across the central and western limits of the basin, formed as a result of the lateral transfer and cementation of carbonate-rich solutions at the boundary between unconsolidated Quaternary sediments and underlying carbon rich Tortonian marls and sandstones (Nash and Smith, 1998; 2003). The relative thickness of units represents stable or rising groundwater conditions during periods of cementation. Such conditions could infer a much wetter climate than those experienced during the formation of pedogenic calcretes (Nash and Smith, 1998).

Unlike the spatially extensive pedogenic and groundwater forms, valley floor calcretes form localised highly-cemented bases within active drainages and isolated cemented terrace remnants. Valley floor units represent the youngest phase of substantial calcium carbonate cementation in the basin (Fig. 2.15) (Nash and Smith, 2003). Valley floor cementation occurs under conditions similar to those of groundwater calcretes, with the cementation of carbonate-rich solutions at the boundary with underlying bedrock. Thicknesses vary dependent upon the conditions of formation, with thin (<0.3 m) valley floor crusts evidenced in many of the active drainages across the basin and much thicker units (2 - 4 m) exposed in major drainage knick-points (Fig. 2.15A). The similarity in formation processes between valley floor and groundwater calcretes could support a hypothesis of formation under warm climate conditions as a function of relatively high moisture availability.

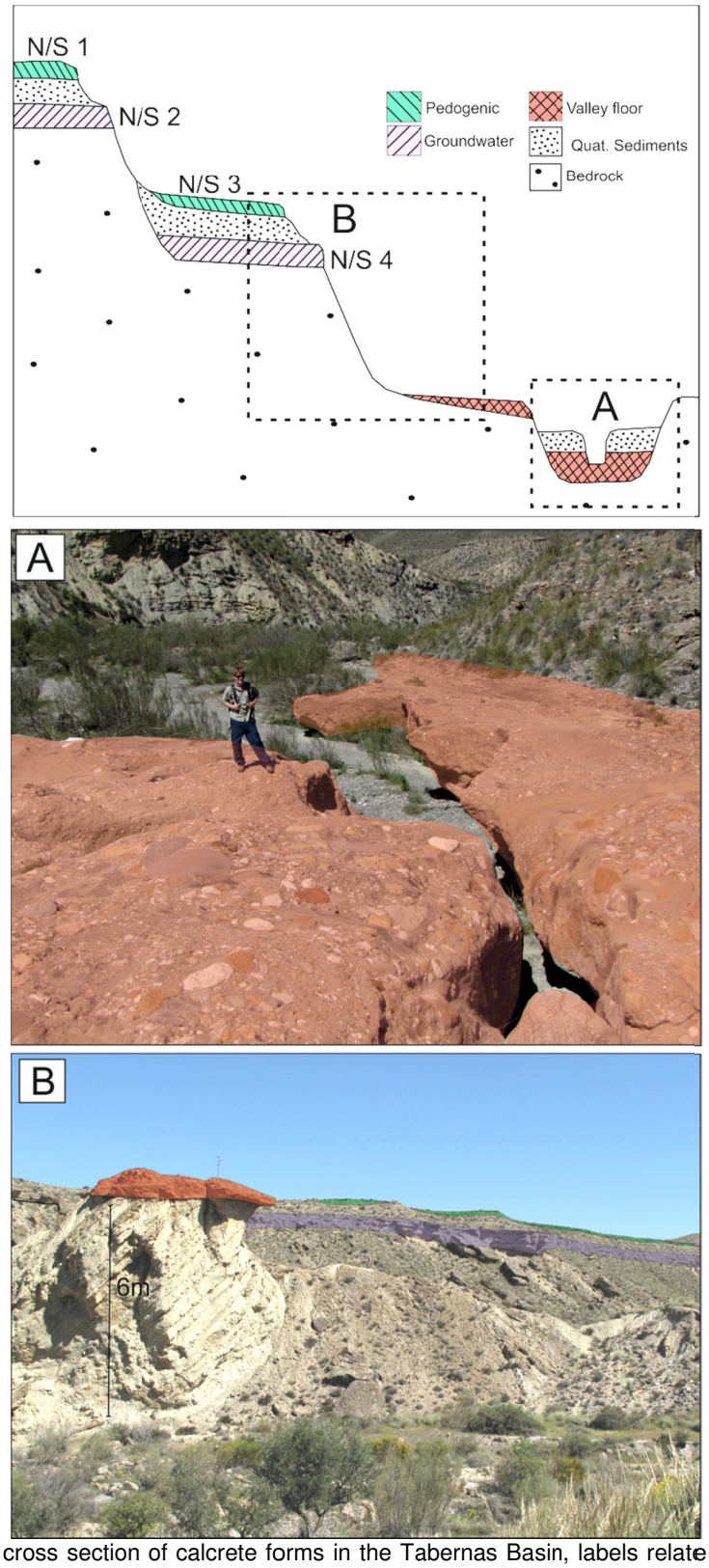

Figure 2.15 Idealised cross section of calcrete forms in the Tabernas Basin, labels relate to paired calcretes of Nash and Smith (1998). Photo A (located on cross section) shows the thickness and high degree of cementation in valley floor calcretes in current knickpoints. Photo from Rambla Sierra UTM 30S 554851/4099183. Photo B shows the pairing of pedogenic and groundwater forms and the isolated nature of typical valley floor outcrops. Photo from Rambla Reinelo UTM 30S 551535/4098058.

The suites of paired calcretes which occur at many stratigraphic levels across the Tabernas Basin highlight the complex interactions between climate and tectonics throughout the Quaternary evolution of the basin (Fig. 2.15; Nash and Smith, 2003). Variations in regional aridity promoted by Quaternary climatic fluctuations are likely linked to the differences in calcrete forms, with pedogenic calcrete development likely occurring during dry global glacial phases and groundwater/valley floor cementation during relatively wetter interglacial phases (Nash and Smith, 1998; Candy et al., 2012). Climate would further influence calcrete formation via variable rates of sediment delivery and accumulation throughout the Quaternary (i.e. the delivery of host materials). Underlying the mechanisms of climatic forcing is the ongoing pattern of base-level lowering as driven by tectonic uplift which promoted the separation of paired calcrete units at some point throughout the Quaternary (Nash and Smith, 1998; 2003; Stokes et al., 2007).

2.4.3 Quaternary lake deposits

Quaternary lake/palustrine deposits outcrop extensively along the path of the axial drainage (Rambla Tabernas) unconformably overlying low strength Tortonian marls and sandstones (Fig. 2.16). Although presented as lake units by Harvey et al., (2003) (e.g. upper and lower lake) the geomorphic units represent shallow water swamp like conditions of sediment deposition. The lake deposits form a major Quaternary depositional unit of low lithological strength often associated with areas of subsequent badland formation. Deposition of the lake deposits occurred after a stage of major base-level drop in the Early-Mid Pleistocene which promoted basin wide incision and the creation of substantial accommodation space (Chapter 5 for detail). The onset of lake sedimentation was promoted by enhanced tectonic deformation along a major anticlinal feature located in the southwest of the basin (Fig. 2.16) which impeded the main axial drainage as it runs through the constricted Tabernas-Almería basin corridor (average width ~ 250 m) (Harvey et al., 1999; 2003). At a basin scale, the lake deposits are separated into an upper and lower unit based on their relative stratigraphy and position (terminology after Harvey et al., 1999). The lower

lake formed first with the back-ponding of fine sediments ca. 10 km upstream from the deformation centre in the SW of the basin. Tectonic deformation was ongoing throughout early to middle stages of sedimentation as evidenced by the distorted nature of beds in the west of the basin (Harvey et al., 2003). Deposition took place largely under shallow water - swamp like conditions with assemblages dominated by sub-horizontal - wavy bedded mud, silt and sand facies (Harvey et al., 1999). Sediment thicknesses increase in an upstream direction (3 – 21 m) and suggest deposition onto an irregular gullied surface (Parker, 2001).

The upper lake formed as a result of the backfilling of the lower lake coupled with the progradation of tributary fan systems which blocked the upstream axial drainage above the present day Rambla Sierra (Fig. 2.16). Backfilling of the upper lake also occurred under low energy conditions with sections dominated by fine grained facies (e.g. muds, silts and sands). However, coarse grain sediment units sourced from the local hillslope system (e.g. Filabres and Marchante fans) become frequent in the later stages of infilling (Harvey et al., 1999; 2003). One relative age based on the correlation of rodent teeth to local climatic reconstructions (Chapter 4 for detail) dates the onset of upper lake formation at 150 ± 50 ka (Delgado et al., 1993). Relative correlations between the upper lake and localised fan deposits have been proposed by Harvey et al., (2003) which highlight the significance of climatically driven sediment inputs throughout the Quaternary, as detailed in Section 2.4.6.

2.4.4 Badlands

Badlands are degradational landscapes which record the complex effects of landscape forcing mechanisms upon the hillslope system over a range of temporal and spatial scales (Torri et al., 2000). Badlands form under highly erosional regimes in weak lithologies characterised by a low vegetation cover and a high drainage density, often forming short steep slopes (Calvo-Cases et al., 2014). Across the Tabernas Basin, badland styles occur extensively within the low strength Tortonian marls and unconsolidated Quaternary lake sediments, and are most pronounced in the western and central regions of

the basin where coupling between the hillslope system, tributaries and main river channels is most complete (Fig. 2.17; Alexander et al., 2008; Calvo-Cases et al., 2014).

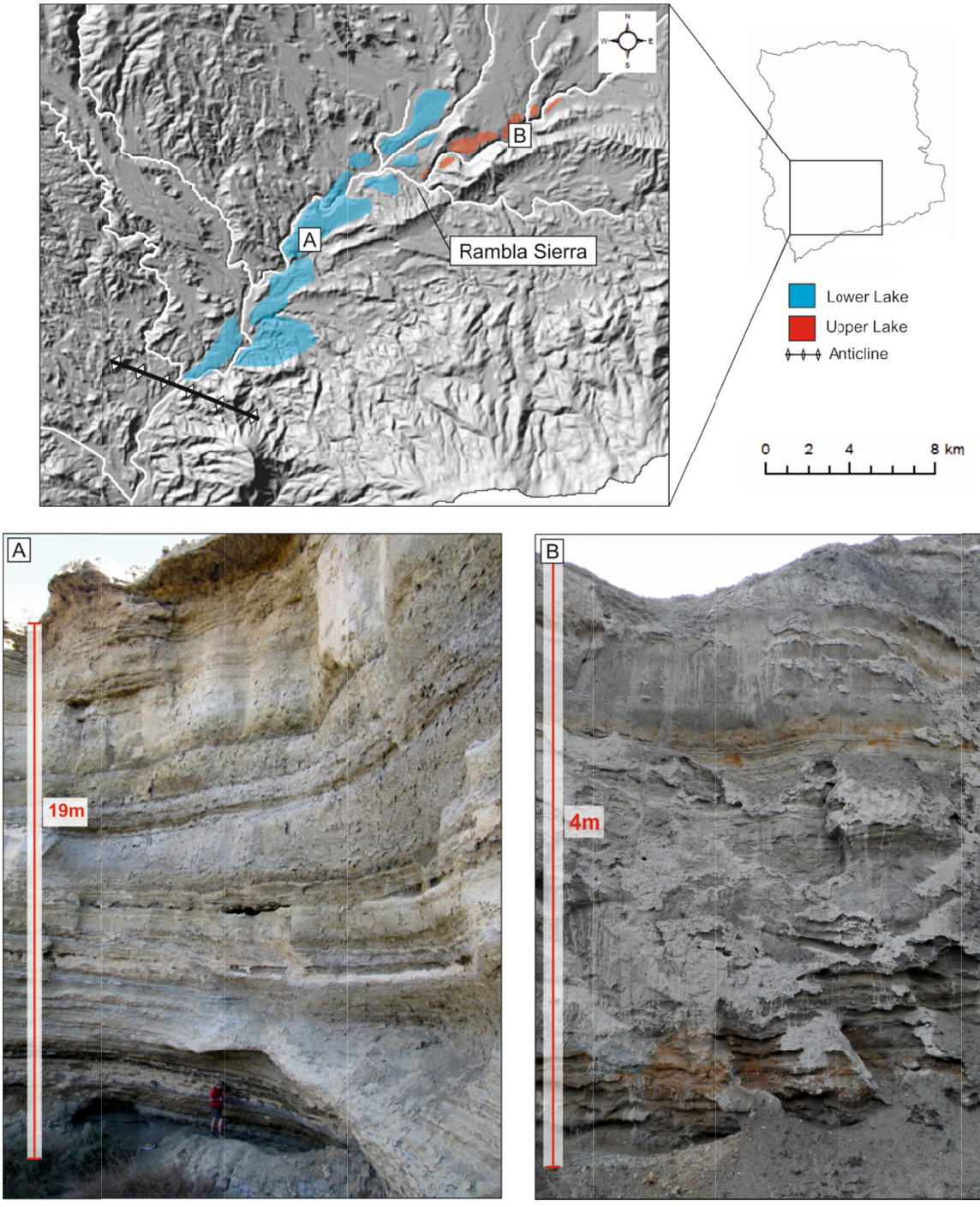

Figure 2.16 Hillshade model showing the extent of lower and upper lake deposits across the Tabernas Basin. The lower lake sections form upstream from the major anticline located in the SW corner of the basin which promoted back-ponding of sediments in the basin centre. Upper lake deposits outcrop upstream of the Rambla Sierra which would have formed an extensive aggrading fan system which blocked the upper drainage pathway. Photos A and B demonstrate the fine grained interbedded nature of lower and upper lake units, respectively. Photo locations are presented on the hillshade model.

The El Cautivo badlands, formed in the west of the basin, exhibit the most developed badland slopes in the Tabernas Basin with a mean slope range of 57º compared with a basin average of 22º (i.e. measure of difference between lowest and steepest slope gradient within a 5 m search radius based on a 5m orthocorrected DEM; Fig. 2.17).

Badland formation in Tabernas records a highly sensitive and episodic response to internal and external driving mechanisms over long timescales (Nogueras et al., 2000; Alexander et al., 1994; 2008). In El Cautivo, a series of inset remnant pediment surfaces record multiple phases of hillslope stability during the episodic erosion of the area (Alexander et al., 2008). Six stabilisation stages represent fluctuations in base-level from the Late Pleistocene onward (stability stages termed A to E from Alexander et al., 2008). Stages A to C (the early stages of evolution) formed quiescent landscapes with relatively limited incision (<3 m) and no badland formation. During this time the evolution of the hillslope system was dominated by climatic factors (i.e. sediment availability as a function of hillslope cover and low relative precipitation) with minor variations in base-level promoted by tectonic deformation centred in the SW region of the basin (Alexander et al., 2008). Post stage C and pre stage D, a substantial period of hillslope degradation occurred in El Cautivo with ~50 m of incision (Alexander et al., 2008). This dramatic base-level change, dated by unpublished optically stimulated luminescence ages at ~14 ka (Chapter 4 for detail), promoted a highly erosional regime with the onset of badland development. The increase in erosion occurred in response to the capture of internal drainages by the main axial drainage (Rambla Tabernas; Alexander et al., 2008). Capture was driven by the progressive lateral migration and headward incision of the Rambla Tabernas along a major lithological boundary (i.e. a resistant sandstone unit within the Tortonian turbidite sequence, Alexander et al., 2008).

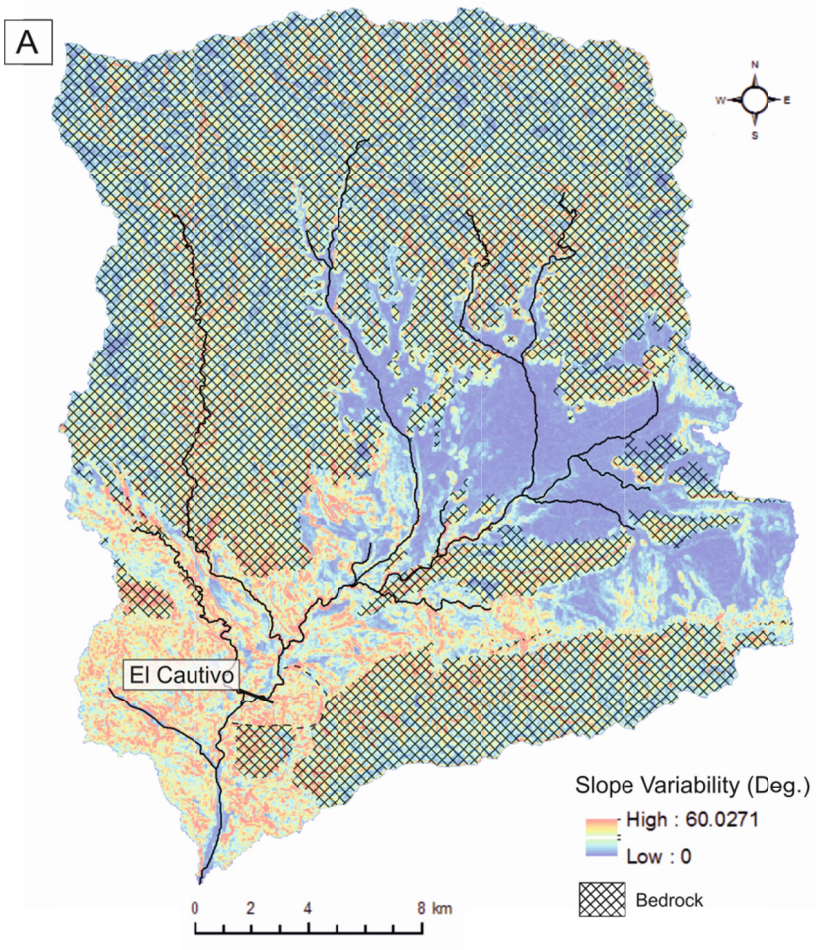

Figure 2.17 (A) Mean slope variability map for the Tabernas Basin showing the relative increase in slope difference in the western and central areas of the basin. (B) Photography of typical slope morphology in the El Cautivo badlands characterised by short, steep slopes with sparse vegetation cover and a dense drainage network. Photo from Rambla Tabernas UTM 30S 549945/4096963.

2.4.5 Travertines

Travertine is a calcium carbonate deposit precipitated from carbonate-saturated waters under subaerial conditions typically related to hot springs or caves (Pedley, 2009). In semi-arid / arid regions, travertine precipitates provide a valuable inorganic material to which absolute dating methodologies can be applied (e.g. U/Th dating; Candy et al., 2005; Díaz-Hernández et al., 2006; Schulte et al., 2008). Travertine formation in the Tabernas Basin is evidenced throughout the Quaternary forming extensive veins and caps in alluvial fan and river terraces (Fig. 2.18A). Current areas of travertine precipitation are limited to three locations: (i) Rambla del Buho; (ii) Rambla Gríllo (Mini-Hollywood) and (iii) Las Salinas (Fig 2.14). In all locations the current level of travertine formation is much lower than experienced in the past (Mather and Stokes, 1999). The most extensive travertine deposits (< 2 m thick) are preserved in an abandoned meander cut-off at Las Salinas where an active accretionary curtain forms in close proximity to fissure ridges, spring pipes and travertine barrages (Fig. 2.18B). The formation of these extensive travertine morphologies is related to carbonate-rich groundwater seepage along the local fracture system formed in accordance with a broad NE – SW trending fault system (Mather and Stokes, 1999). Travertine formation in the Rambla del Buho and Rambla Gríllo also occurs along active fault lines; however, the precipitates are much less pronounced, forming thin crusts (< 0.5 m thick) lagging the current valley floors (Fig. 2.18C).

Although dominant as a landscape feature throughout the Quaternary, the current understanding of the rates and modes of long-term travertine formation in the Tabernas Basin is limited. Preliminary work by Mather and Stokes (1999) highlights the importance of tectonic structure in the routing of carbonate rich waters to the surface and further proposed potential climatic signatures upon rates of formation. At Las Salinas, water percolation through the fracture system is noted to be highest during the winter and spring months; however, further increases in flow were noted in association with local seismic events. Unfortunately no dates are presented for the travertines in the Tabernas Basin, however

U/Th dating on travertines within the Eastern Alpujarran Corridor (to the west of the basin; Fig.1.1) suggest extensive periods of formation during marine isotope stage (MIS) 8 (García et al., 2004).

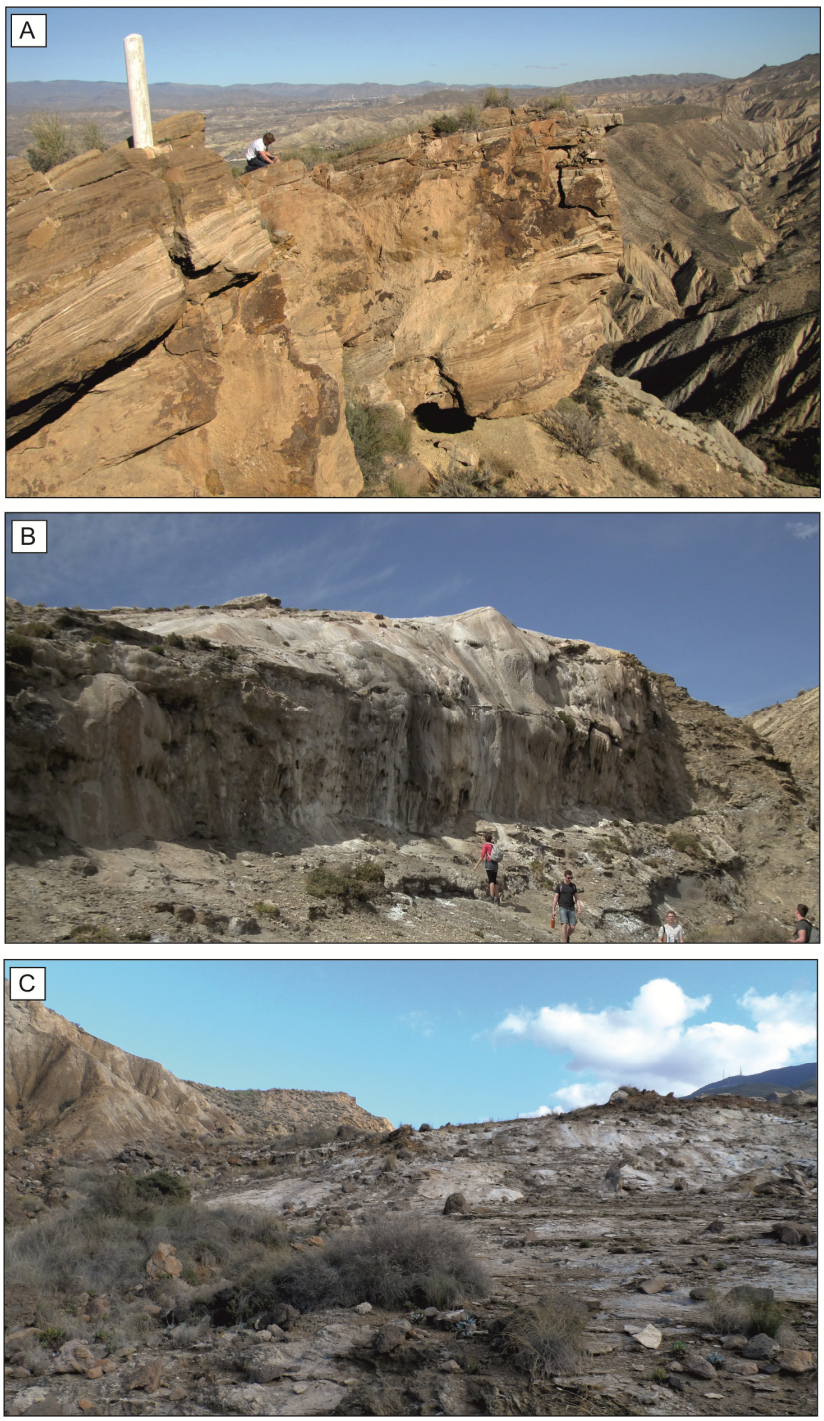

Figure 2.18 Travertine outcrops across the Tabernas Basin. (A) Travertine encrusted hilltop in isolated terrace recording 11m of travertine formation (UTM 30S 549332/4095514). (B) Travertine curtain at Las Salinas (UTM 30S 548795/4096972). (C) Travertine precipitation in the headwaters of the Rambla Grillo (UTM 30S 551160/4096319),

2.4.6 Conceptual Quaternary basin evolution model

This section integrates data collected from the literature in order to highlight (or propose) the spatial and temporal links between individual landscape elements throughout the Quaternary development of the Tabernas Basin. The conceptual model summarised in Figure 2.19 presents geomorphic connections based on broad stratigraphical and spatial relationships between often highly localised landforms. Uncertainties are highlighted where temporal and spatial constraints between elements are poorly defined. Relative timings are labelled numerically 1 - 9 (1 being the oldest and 9 the youngest); when timings are synchronous across the basin bullet points are used to relate geomorphic events.

Late Pliocene - Early Pleistocene

1. Formation of extensive paired upper calcretes in alluvial fan sediments across the basin under stable tectonic conditions (N/S 1 and N/S 2 on Fig. 2.15) (Nash and Smith,1998; 2003). Potential climatic variations during stable tectonic phase leads to the formation of paired groundwater and pedogenic calcretes?
2. Basin wide incision driven by tectonic uplift which incises and abandons upper calcretes (N/S1 and N/S2) and generates accommodation space across the basin.
3. Period of tectonic stability and climatic dominance with the onset of sedimentation and the possible formation of NS3 and NS4 calcretes (Nash and Smith, 1998)?

Middle Pleistocene- Late Pleistocene

4. Sustained periods of basin wide incision driven by tectonic uplift which lowers base-level dramatically across the basin and generates the substantial accommodation space across the basin. In the east of the basin, headwaters of Sorbas drainages are captured a diverted into the Tabernas system (Harvey et al., 1999). The basin wide incisional event could have led to the isolation of Calcretes NS3 and NS4?

- Deformation initiates along an anticline in the SW of the basin which impedes the axial drainage. This deformation stage could have occurred during sedimentation in the east

and centre of the basin with alluvial fan stage 1 (terminology from Harvey et al., 2003) and stage A pediments of Alexander et al., (2008) in the El Cautivo area;

5. Period of climatic dominance with extensive basin sedimentation. Fan stage 2 sedimentation initiates in the east of the basin, being inset in to Filabres Fan Stage 1 sediments and onlapping Marchante fans (Harvey et al., 2003). In the west and centre of the basin, back-filling of sediments in the lower lake system blocks the Rambla Sierra and the onset of sedimentation in the upper lake system. This sedimentation stage is linked with stage B pediment surfaces in El Cautivo which form minor fans aggrading into lower lake sequences (Alexander et al., 2008). Minor tectonic deformation occurs in the SW of the basin deforming lower lake sediments

Late Pleistocene – Holocene

6. Continued sedimentation of upper lake sequence with fan stage 3 sediments distally aggrading into the top of upper lake deposits dated at ~14 ka. This stage is linked with the formation of stage C pediments in El Cautivo (Harvey et al., 2003; Alexander et al., 2003);
7. Basin wide incision of the lake sequences across the basin. Extensive increase in drainage network connectivity in the El Cautivo areas leads to the onset of badland formation in the west of the basin (stage C to stage D incision in El Cautivo);
8. Sustained pattern of base-level lowering driven by tectonic uplift continues throughout the Holocene to the present day promoting the incisional variability in the current basin. Alluvial fan aggradation (fan stage 4) continued in the east of the basin which remains un-coupled with the dissected basin centres.

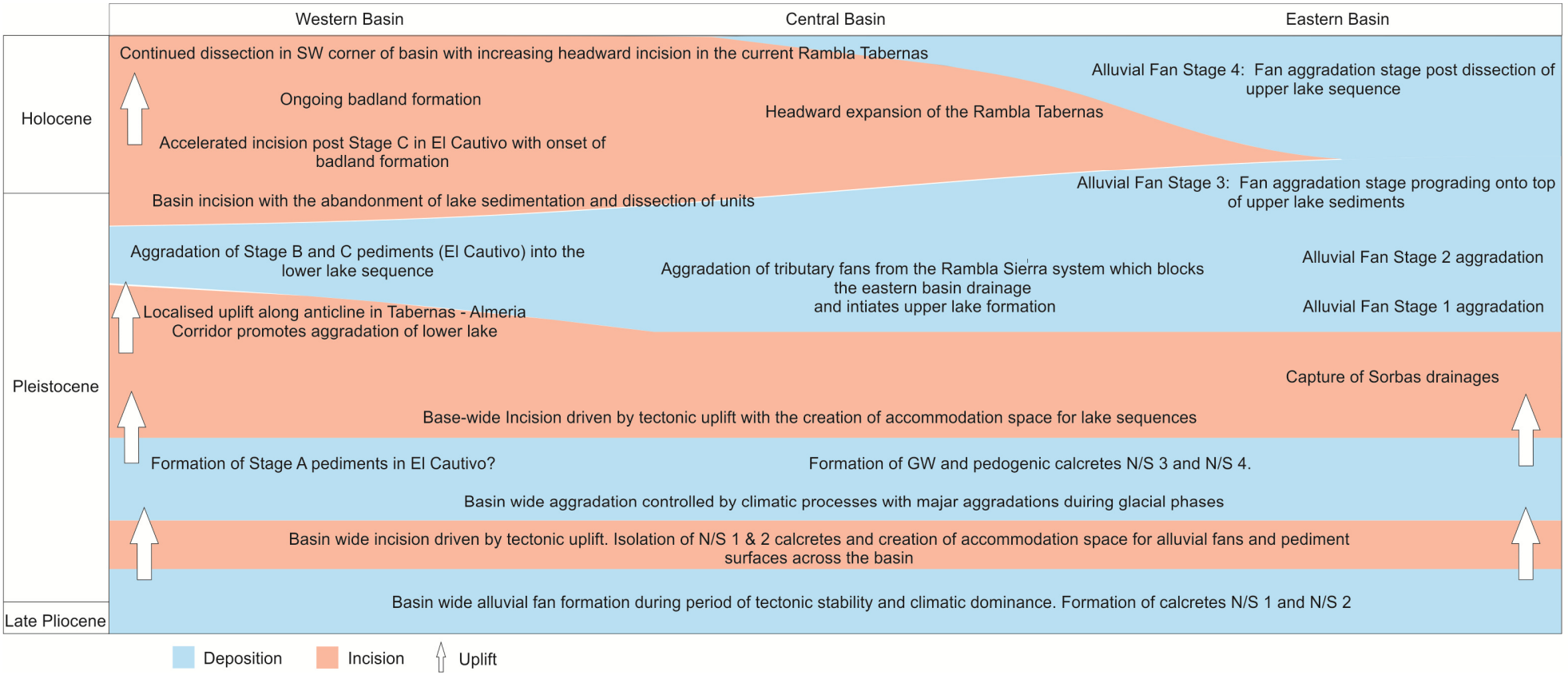

Figure 2.19 Conceptual model of Quaternary landscape evolution for the Tabernas Basin. Calcretes N/S 1- N/S4 refer to Nash and Smith (1998; 2003), Alluvial fan stages 1 – 4 refer to Harvey et al., (2003) and Stage A- Stage C pediment in El Cautivo refer to Alexander et al., (2008).

2.5 Summary

This chapter has developed the geological evolution of the Tabernas Basin, from early marine stages in the Middle to Late Miocene through to the complex terrestrial landscape of the Quaternary. Regional tectonics has been identified as a major forcing mechanism, crucial in the formation of the Tabernas Basin via the development of the characteristic basin and range morphology of the Almería region. Climatic cycles throughout the Neogene are also of regional significance promoting variations in sea-level during the early stages of basin development. Multiple sea-level transgressions deposited the extensive marine lithologies across the basin centres which have acted as a primary control upon fluvial system development throughout the Quaternary (Calvo-Cases et al., 2014).

The Quaternary landscape of the Tabernas Basin comprises a series of aggradational (e.g. alluvial fans; Harvey, 1996; Harvey et al., 2003) and degradational landforms (e.g. badlands; Alexander et al., 2008; Calvo-Cases et al., 2014) often affected by secondary processes (e.g. calcretes and travertines; Nash and Smith; 1998; 2003; Mather and Stokes, 1999). Extensive research has highlighted the significance of ongoing tectonic uplift, climatic cycles and internal feedbacks in the highly dissectional evolution of the basin. However, the relationships between individual landscape elements are typically restricted by the limited spatial occurrence of landforms and the overall lack of temporal data. This lack of spatial and temporal connectivity highlights the requirement for a study of the terrace archives which occur extensively across the basin and form an important morphological link (Fig. 2. 20).

Figure 2.20. Photograph demonstrating the extensive nature of alluvial fan and river terraces across the Tabernas Basin. Note how many of the landscape elements presented in this chapter relate to terrace morphologies across the basin. Photo taken from UTM 30S 551275/4099613 north over the Rambla Tabernas.

Chapter 3

3.1 Quaternary Landform Record- Tabernas Basin

This chapter presents a stratigraphic framework for the Quaternary landforms of the Tabernas Basin. Initially, methods of sedimentological and geomorphological analysis are presented with focus on the description and interpretation of geomorphic landforms. Sedimentary analysis of key field sections is then presented alongside morphological data in order to develop a robust relative Quaternary stratigraphy for the Tabernas Basin. This stratigraphic model forms the basis for: (i) the application of OSL dating presented in Chapter 4, (ii) conceptual modelling of the Quaternary landscape by means of geospatial interpolation (Chapter 5), and (iii) key data inputs and calibration points for numerical modelling, presented in Chapter 6.

3.2 Methodology

The techniques presented in the following section represent established research methods developed in the interpretation of the landscape system under the broad disciplines of geomorphology and sedimentology. The methods have been extensively applied in the Almería region, offering valuable data in the qualitative and quantitative assessment of Quaternary landscape evolution (e.g. Stokes, 1997; Mather, 1999; Meikle, 2008; Illot, 2013).

3.2.1 Geomorphological mapping of Quaternary landforms

Geomorphological mapping is a valuable tool which can be employed in a range of studies to assess the properties of a landscape based on units of similar surface form, materials and process characteristics (e.g. terrain assessments, resource appraisals or geohazard evaluations; Lee; 2001). At a basic level, geomorphological mapping can be split into two phases: (1) a primary data collection phase and (2) a secondary interpretation phase. During the data collection phase, the spatial extent of individual landforms is mapped with reference to their topographic position and morphological form within a given landscape

(Knight et al., 2011). This is conventionally achieved by field investigation; however, field data are often supplemented by remotely sensed data in order to add clarity and depth to sometimes geographically limited field observations (Lee, 2001). In the second phase, the mapped landscape features are interpreted based on their spatial occurrence and likely morphological origins (Knight et al., 2011). In studies of Quaternary landforms (i.e. river terraces) the focus of morphological mapping is to identify groupings of landforms based on:

- Elevation of depositional or erosional contacts of sediment bodies with relation to the current fluvial system. This can be achieved by: (i) measuring from the surface of terraces to the bed of the current channel immediately downslope of it, or (ii) by measuring the basal erosional contact of the terrace units with respect to the current fluvial system. When using measurements of the terrace surface caution should be taken as: (i) the thickness of depositional units is variable as a result of non-uniform rates of preservation of unconsolidated sediments through time (Lewin and Macklin; 2003), and (ii) the current terrace surface could represent a complex fill architecture where multiple stages of aggradation are recorded (Gibbard and Lewin, 2009). In best practice, elevation measurements are obtained from the base of sequences to the current fluvial system; however, such measurements can be limited by the extent of outcrops and the overall form of the terrace record (e.g. strath vs. fill; Stokes et al., 2012a);
- The relative thickness and structure of associated sediment bodies with focus on the likely conditions of formation and preservation (i.e. terrace sedimentology, Section 3.2.2 for detail);
- Aspects of secondary processes such as soil formation, cementation or bioturbation and any other further markers such as fossilised fauna and flora (Frye and Leonard, 1954).

Once morphological groupings are identified (e.g. landform levels or terrace groupings) it is common practice to create idealised transects (e.g. regional staircases, cross valley profiles

or longitudinal profiles) in an attempt to qualify and/or quantify rates of landscape processes at a range of spatial and temporal scales (e.g. Stokes et al., 2002; Cordier et al., 2006; Cunha et al., 2008; detailed in Chapter 5).

In this study, geomorphological mapping of Quaternary landforms was conducted in the field over a period of 24 weeks from December 2011 to March 2014. Landforms were mapped on to 1: 25,000 base maps, publically available from the Instituto Geológico y Minero de Espaňa: www.igme.es. Field mapping was conducted with the aid of a Garmin eTrex handheld GPS (vertical accuracy of ~15m) and TruPulse 360 laser range finder (vertical accuracy range of 0.5 m - 1 m). Elevation measurements were made (bases of depositional units to current channel) alongside those of sediment thickness, structure, provenance and any further secondary modification processes (detail in Section 3.2.2). The refinement and grouping of the landforms was conducted in the GIS domain, with the application of visualisation tools from the ArcGIS Spatial Analyst toolbox on 5m ortho-corrected digital elevation model (DEM) and aerial imagery with vertical accuracies of <30 cm (Fig 3.1A) (sourced from the Centro Nacional de Información Geográfica: www.centrodedescargas.cnig.es). Landform boundaries were enhanced using a high pass filter (or edge enhancement filter) applied to an output raster compiled of all major landforms. The high pass filter accentuates the differences in elevation values for a cell against that of its neighbours and is an effective tool in defining breaks in slope, such as those associated with the margins of river terraces or isolated pediment surfaces (e.g. isolated alluvial fan remnants, Fig. 3.1B).

The attributes of 188 individual landforms were collated in the GIS domain with reference to landform type, elevation, location with reference to the current fluvial system and any further details (Table 3.1). This GIS, coupled with further sedimentological data, formed the basis for the grouping of landforms into distinct terrace levels as presented in Section 3.3.

Table 3.1 Example of the GIS developed in the Arc GIS domain for the collation of landforms across the Tabernas Basin. Terrace type abbreviations present a summary of relative ages (e.g. Plio= Pliocence, Qt = Quaternary), terrace level and landform type (e.g. Af= alluvial fan, RT= river terrace,). Length and area data relate to polygons created for each mapped feature. Mean elevation is calculated from 5m orthocorrected data.

OBJECTID	Drainage	Terrace Type	Length (m)	Area (m2)	Mean Elevation (mAHD)
1	Buho	Plio-Qt/1/Af	2613.616037	142883.5453	526.62799
2	Buho	Plio-Qt/1/Af	1929.672237	69455.49448	526.62799
3	Buho	Plio-Qt/1/Af	198.997589	2516.780719	526.62799
4	Buho	Qt/2/Af	9668.514914	1141651.529	526.62799
5	Buho	Qt/3/Rt	7372.296589	904219.8668	526.62799
6	Tabernas	Qt/3/Af	8762.170133	1264782.756	356.423004
7	Tabernas	Qt/2/Af	908.200523	26572.33929	356.423004

3.2.2 Sedimentological facies analysis

When studying Quaternary sedimentary assemblages, such as river terraces or alluvial fan remnants, the application of a standardised classification system is essential for unified and consistent description and interpretation purposes (Miall, 1990; Jones, 1999). Throughout this research the well-defined method of facies analysis was adopted in the description and interpretation of key sedimentary sections (Jones, 1999). Facies analysis and further facies coding involves the detailed description of sedimentary sections in order to enable the interpretation of depositional processes and environmental settings (Miall, 1996; Tucker, 2011). The description of units based upon facies coding takes into account the physical (lithological) properties of a sedimentary unit including its texture (grain size, morphology, sorting) and structure (deformed bedding, depositional structures, bounding surfaces, sequences) (Tucker, 2011).

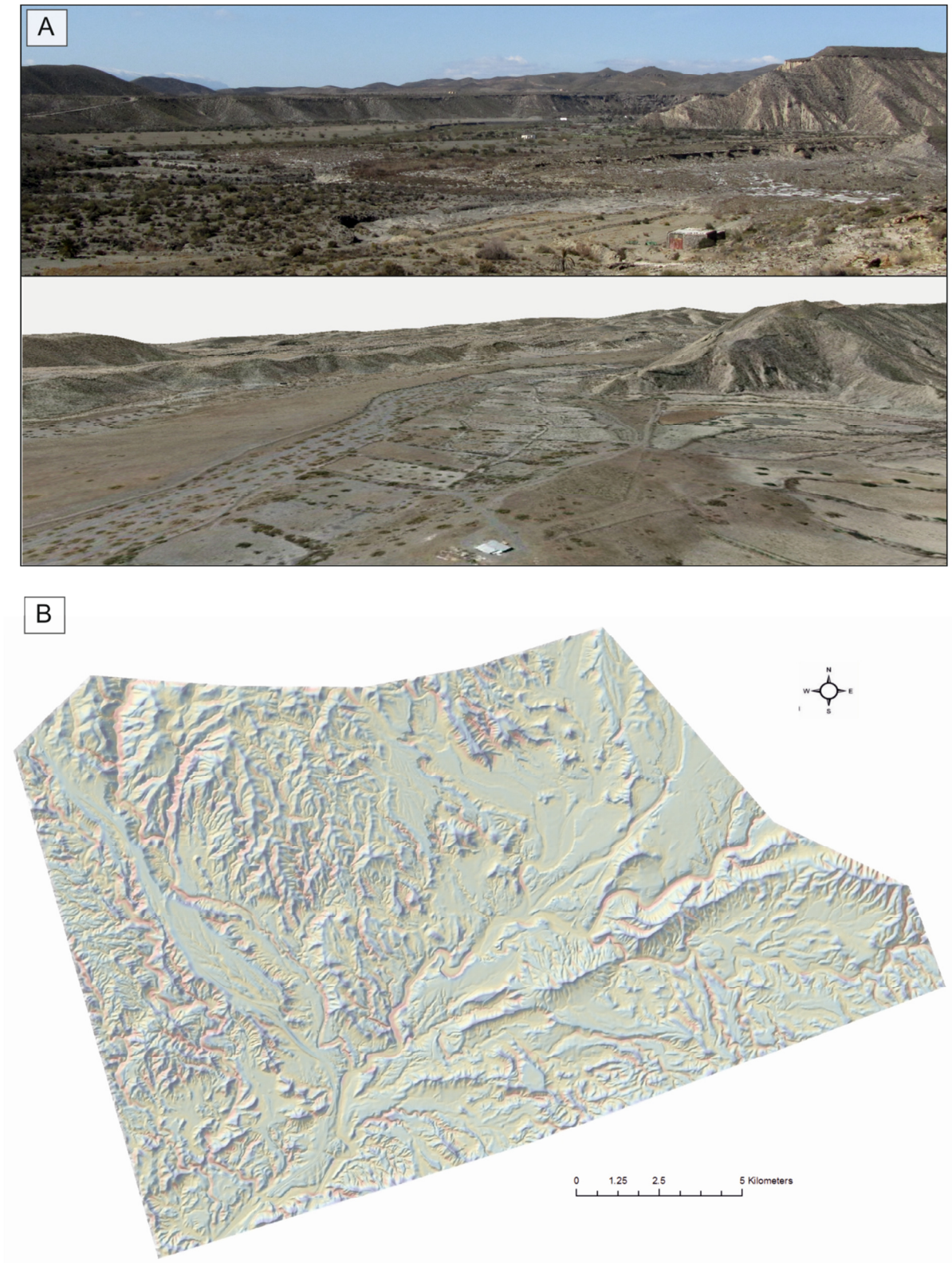

Figure 3.1 Examples of how remotely sensed data can be used alongside field investigations to help define landform features for stratigraphical and morphological interpretation. (A) Field photograph of Quaternary terrace surfaces in the Rambla Buho area (UTM 30S 553378/4101004), with the matching extract from ArcScene10 environment showing ortho-corrected aerial imagery draped over a 5m DEM. (B) Overlay of a hillshade model and high pass filter for the Tabernas Basin. The blue and red colours highlight significant breaks of slope often associated with terrace edges or highly erosional areas such as badlands.

Various schemes exist that aim to standardise the techniques and terminologies when describing sedimentary field sections (e.g. Troels-Smith, 1955; Eyles et al., 1983; Miall, 1996). Due to the negligible biological content and terrestrial nature of sedimentary deposits in the Tabernas Basin the lithofacies approach of Miall (1996) (Table 3.2) was utilised in this study. Lithofacies coding has been extensively applied to Quaternary sediment-landform records throughout the Almería region with good success (e.g. Blum, 2007; Miekle, 2008; Pla-Pueyo et al., 2009; Illott, 2013). However, caution must be taken in the interpretation stage as individual lithofacies codes often relate to multiple depositional environments (Table 3.2). In order to avoid misinterpretations in this study, individual lithofacies were grouped into facies associations representing sediment deposition in broadly similar environments (Tucker, 2003). The grouping of facies into associations is of considerable assistance in the geographical representation of depositional environments at basin scales (Tucker, 2003; Reading, 2009).

3.2.3 Logging of sedimentary profiles

Sedimentary logs were produced for type sections for all terrace levels (i.e. grouping of landforms) across the Tabernas Basin (presented in Section 3.3). Type sections were identified during extensive field investigations and were defined as the standard reference for sedimentary bodies assocaited with individual terrace levels (*sensu* North American Commission on Nomenclature, 2005). The logging exercise aimed to record all of the architectural elements of the type section (i.e.composition, texture and structure of the sedimentary deposits) in order to help develop an understanding of the conditions of deposition (*sensu* Tucker, 2011). Data were recorded in the field onto a sedimentary log with the aid of a metric tape measure and handheld GPS. A Trimble 360 TruPulse was also used for measurements which were not safely accessible on foot. Detailed photographs were taken for additional visual representation.

Table 3.2 Facies classifications applied in the description of Quaternary sedimentary sections, from Miall (1996). Attention is drawn to the limitation of applying one facies coding in the interpretation of depositional environments (possible interpretations column). In this study, groupings of facies codes are used to develop environments of deposition.

FACIES CODE	FACIES	SEDIMENTARY STRUCTURES	POSSIBLE INTERPRETATIONS
Gms	Massive, matrix supported gravel	Grading	Debris flow deposits
Gm	Crudely bedded gravel	Horizontal bedding, imbricated	Longitudinal bars, lag deposits
Gt	Gravel, stratified	Trough cross beds	Minor channel fills
Gp	Gravel, stratified	Planar cross beds	Longitudinal bars, deltaic growths from bar remnants
St	Sand, medium to coarse grain/ minor conglomerate	Solitary or grouped trough cross beds	Dune bedforms (lower flow regime)
Sp	Sand, medium to coarse grain/ minor conglomerate	Solitary or grouped planar cross beds	Transverse bars, sand waves (upper flow regime)
Sr	Sand, fine to coarse grained	Ripple cross lamination	Ripples (lower flow regime)
Sh	Sand, fine to coarse grained/ minor conglomerate	Horizontal lamination	Planar bed flow (upper flow regime)
Sl	Sand, fine to coarse grained/ minor conglomerate	Low angle cross beds (<10°)	Scour fills, antidunes
Sm	Sand, fine to coarse grained	Massive	Overbank or mudflow deposits
Fl	Sand, silt, mud interbedded	Fine laminations, interbeds <10mm sets	Overbank or waning flood
Fsc	Silt, clays	Laminated to massive	Backswamp, low energy ponded
Fm	Silt, clays	Massive, desiccation cracks	Overbank or drape deposits

The logging of type sections included the following facets (after Miekle, 2008):

1. Composition – the constituent grains which comprise a lithology. Descriptions of grain size are given using the Udden-Wentworth classification. The maximum grain size and average grain size were further utilised to give some identification of relative flow power and as a primary indicator of facies type (presented in Section 3.2.1). The composition of terrace sediments was further used to supplement provenance interpretations detailed in Section 3.2.4.
2. Colour – a distinction is made between primary and secondary colours. The primary colour is the original colour of a sediment on deposition, whilst the secondary colour is that which is produced during weathering, usually by pedogenesis or by secondary mineral enrichment processes, e.g. soil formation. Secondary colours associated with pedogenic processes were recorded using a Munsell colour chart as presented in Section 3.2.5.
3. Textural Characteristics – includes sorting of a sediment and roundness of clasts. Evaluations were made using a standard grain size comparison chart.
4. Structures – identified from differences in textural characteristics. Commonly observed sedimentary structures that include; bedding (units of sediment thicker than 1 cm), soft-sediment deformation (as associated with semi-fluid state loading/unloading), and biogenic structures that indicate the presence and activity of living organisms, with further environmental assocations (Tucker, 2011).
5. Bed thickness – offering insight into the frequency magnitude of a depositional event, with thin sporadic beds reflecting common background sedimentation, whilst thicker beds may reflect rarer, large magnitude events (Jones, 1999).
6. Channel Geometry – Architectural elements such as channel width, depth and frequency which help to define river planform types and assign bounding surfaces within a sequence.

Field logs were re-drawn in the CorelDraw X5 software package using the standard symbols presented in Figure 3.2. Lithofacies coding (Table 3.2) was added to logs based on all of the logged components of the sedimentary units.

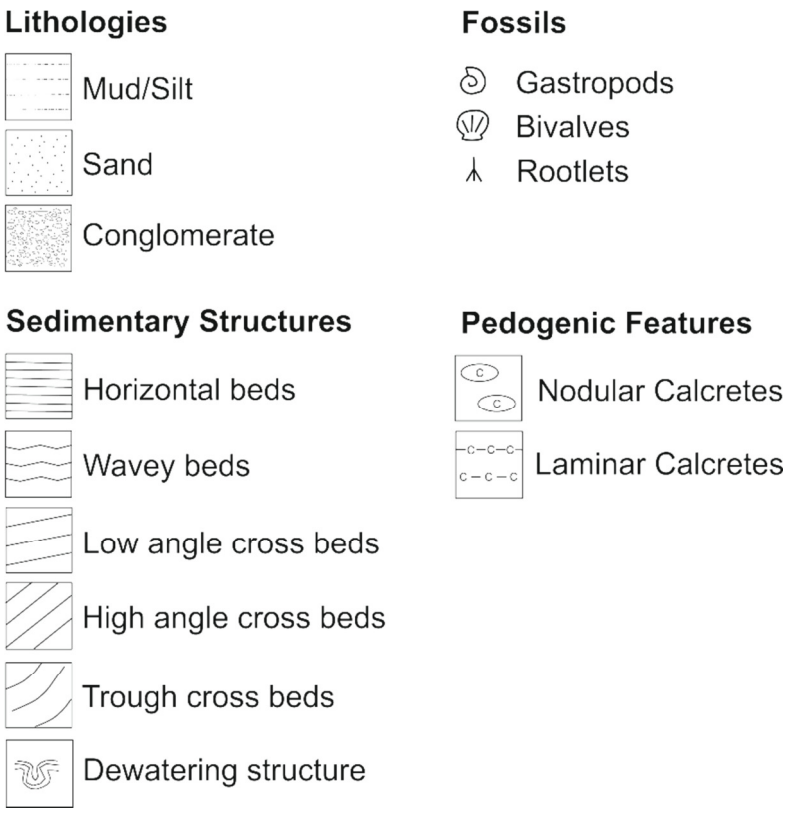

Figure 3.2 Standard logging symbols applied in the graphical representation of sedimentary sections within this thesis

3.2.4 Sediment provenance and palaeocurrent analysis

Sediment provenance and palaeocurrent analysis have proven useful tools in the identification of changes in delivery of sediments or drainage pathways throughout the evolution of Quaternary landscapes in the Almería region (e.g. Harvey and Wells, 1987; Mather, 2000; Maher, 2005; Stokes, 2008). Throughout this study, sediment provenance and paleocurrent analysis were conducted at all logged sections in order to assess spatial and temporal patterns of sediment delivery and routing in the Tabernas Basin. For sediment provenance analysis, a total of 300 random clasts within an area of $1m^2$ were analysed from

representaive sections for clast provenance purposes. The number of counts was deemed suitable based on the typical grain size of sedimentary deposits in the Tabernas Basin (e.g. conglomerates of gravel to cobble grain size). Records of lithological type and potential source areas were made in the field with the aid of a dictaphone and clasts were marked with chalk to avoid duplication. Final clast counts are graphically represented in the form of pie charts and displayed alongside sedimentary logs. It is noted that no quantatative records of clast size (i.e. laboratory analysis of grains) is presented in this thesis other than the visual description of sediment size in the logging process. This is based on the highly variable nature of grain sizes within individual terrace units and the typical indurated nature of sections.

For palaeocurrent analysis the imbrication of 100 clasts was measured from the same $1m^2$ section. Measurements were taken from clasts with an 'A' or long axis of greater than 4 cm with the aid of a compass clinometer. Clasts with a long axis of greater than 4 cm were selected because they provide a more accurare picture of channel flow directions under higher flow regimes when the whole of the channel was exploited by water and sediment flow (Tucker, 2003). Palaeocurrent data were plotted in 'Rose' diagrams in RockWorks15 software for visualisation purposes and displayed on sedimentary logs.

3.2.5 Soil and calcrete formation

The rubification of paleosol horizons and the formation of various calcrete morphologies has been utilised in the relative dating and correlation of geomorphic surfaces within the Sorbas and Vera Basins (e.g. Harvey *et al.,*1995; Candy *et al.,* 2005; Stokes *et al.*, 2007; Candy *et al.,* 2012). As presented in Chapter 2, soil and calcrete formation within Quaternary fluvial and alluvial landforms of the Tabernas Basin is well reported (Harvey et al., 2003; Nash and Smith, 2003). In this study, the B horizon soil colour was described for all logged sections using nomenclature from Munsell Soil Colour Charts, following the procedure of Harvey & Wells (1987) and Harvey et al., (1995). Soil colour codes have been added to logs and sections when encountered. However, the exposure of rubified soils across the

Tabernas Basin is limited when compared with the Quaternary records from the Sorbas Basin and does not allow for the relatvie dating of landforms at a basin scale (e.g. Harvey et al., 1995). Calcretes were described in accordance with the approaches of Nash and Smith (1998; 2003) with the assessment of calcic and petrocalcic development based on the work of Machette (1985). This classification builds on the work of Gile et al., (1966), with the application of two advanced stages of calcrete development (stages iv and v , Table 3.3). These advanced stages of development are often encountered within the Quaternary landforms of the Tabernas Basin (Nash and Smith, 1998; 2003). When encountered, stages of calcrete development are presented on sedimentary logs. However, these descriptiors are not used in the relative dating of terraces based on the limited preservation of pedogenic calcretes in the terrace record across the basin.

Table 3.3 Stages of carbonate accumulation in soils from Machette (1985) modified from Gile at al., (1966)

Stage	Soils developed in gravel	Soils developed in sand, silt or clay
i	Thin discontinuous coatings of carbonate on underside of clast	Dispersed, powdery and filamentous carbonate
ii	Continuous coating all round and, in some cases, between clasts: additional discontinuous carbonate outside main horizons	Few to common carbonate nodules and veinlets, with powdery and filamentous carbonate in places between nodules
iii	Carbonate forming a continuous layer enveloping clasts: less pervasive carbonate outside main horizon	Carbonate forming a continuous layer formed by coalescing nodules and powdery carbonate outside main horizon
iv	Upper part of solid carbonate layer with a weekly developed platy or lamellar structure capping less pervasively calcareous parts of the profile	
v	Platy or lamellar cap to the carbonate layer strongly expressed; in places brecciated and with pisolites of carbonate	
vi	Brecciation and re-cementation, as well as pisoliths, common in association with the lamellar upper layer	

3.3 Quaternary landform stratigraphy

Upon completion of detailed field mapping and sedimentary analysis in accordance with the methods presented in Section 3.2, four primary groupings of landforms were identified across the Tabernas Basin (Fig. 3.3A and Fig. 3.4). As the majority of landforms were either river terraces or alluvial fan remnants the terminology 'terrace levels' was applied to group individual landforms (e.g. terrace level 1 to terrace level 4). Terrace levels were grouped based on common mean incision depths to the current fluvial system and further supplemented by sedimentary data. This broad stratigraphical approach has been adopted in the description of Quaternary fluvial sections in the neighbouring Sorbas Basin (e.g. Harvey and Wells, 1987; Harvey et al., 1995; Maher, 2005; Illot, 2013) and was considered suitable based on climatic and process affinities between the basins. Unlike in the neighbouring Sorbas Basin, a top basin fill surface was not defined for the Tabernas Basin (i.e. Gochar fill surface; Mather, 1993). This is based on the poor preservation of the oldest terrace level (terrace level 1) and the inability to relate the terrace level with the final stages of Pliocene fill only recorded in the far west of the Tabernas Basin (Chapter 2).

The following sections (3.3.1 - 3.3.4) present an overview of the morphology, sedimentology and depositional environments for the terrace levels of the Tabernas Basin. Key sedimentary sections (type sections) are presented for each level with an overall interpretation of the geomorphic evolution of the basin presented in the summary Section 3.4. The terrace levels are presented in chronological order, with the oldest level presented first (terrace level 1). The location of sedimentary sections described throughout the sections in detail on Figure 3.3B.

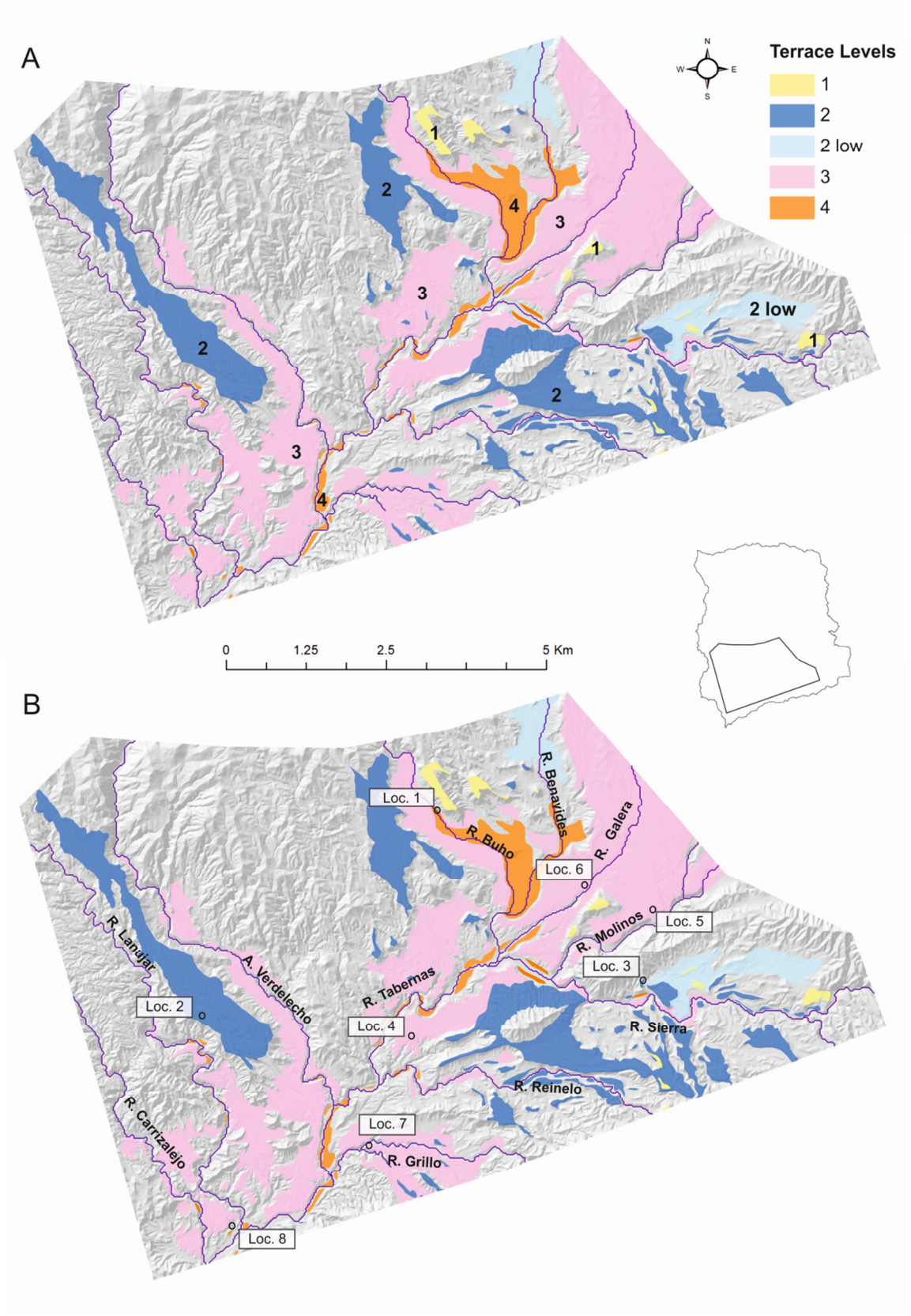

Figure 3.3 (A) Spatial extent of Quaternary terrace landforms across the Tabernas Basin.(B) Locations of type section and drainage names. The inset map shows the location of terrace units presented within the current hydrological basin.

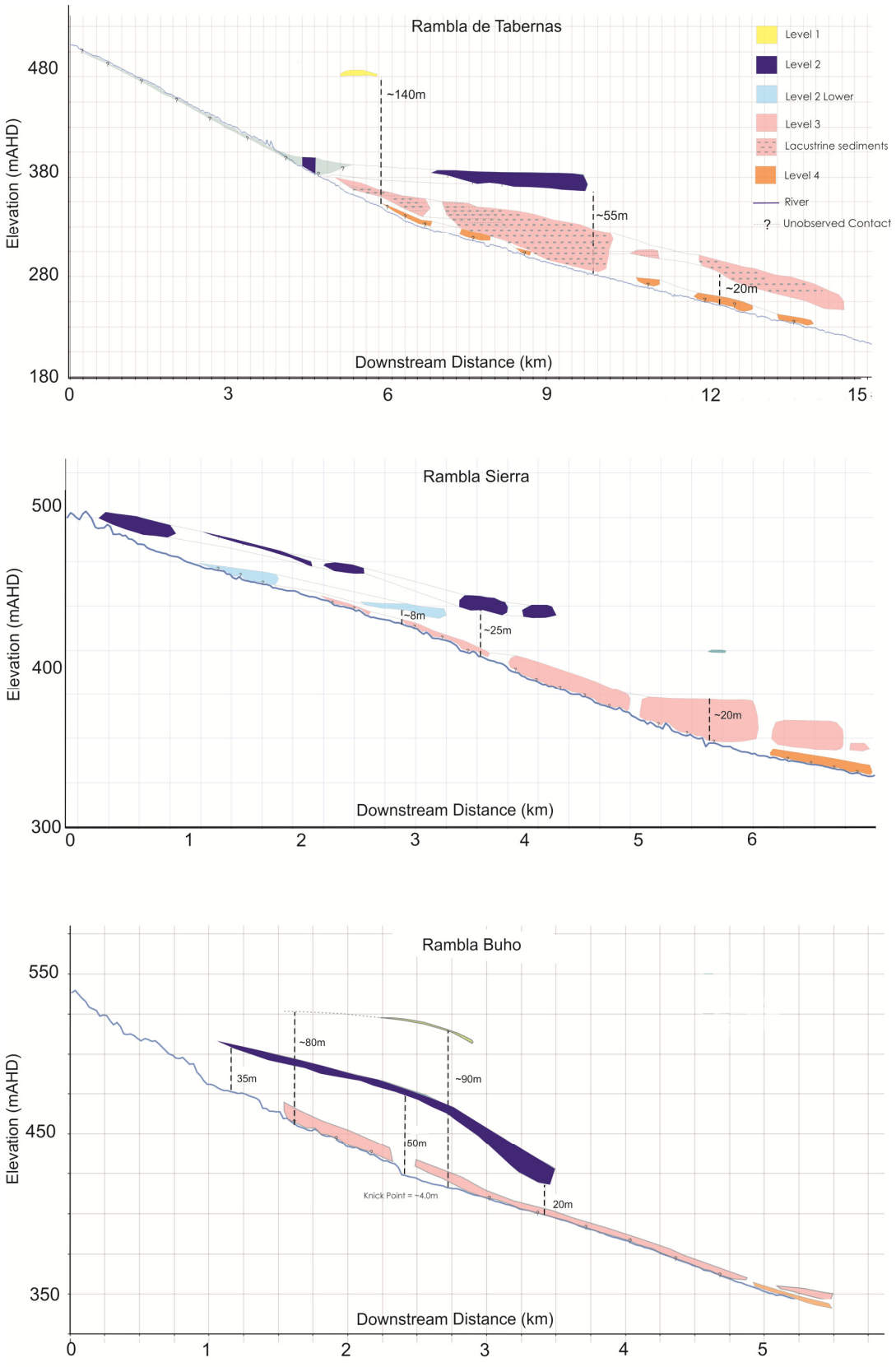

Figure 3.4 Idealised cross sections showing the elevation of terrace levels for the Rambla Tabernas and two main tributaries. Note the key presented for Rambla Tabernas applies for all sections.

3.3.1 Terrace Level 1

Terrace level 1 forms the oldest and highest Quaternary stratigraphic level in the Tabernas Basin with average incisional depths (base of sedimentary sequence to current rambla) of approximately 90 m (Fig. 3.4). The terrace level is poorly preserved across the basin with remnants only found in the east of the basin (Fig 3.3). Terrace outcrops occur as heavily calcreted isolated sedimentary units (Machette Stage V to IV) prograding off the bounding sierras in the basin centres. The terraces unconformably overlie Tortonian-Messinian submarine turbidite facies and associated deep water facies (Fig. 3.5). The thicknesses of terrace level 1 deposits varies from strath surfaces, with little or no sediment, to thin sedimentary bodies (<6m thick) which indicate either a highly erosive environment during deposition or major degradation post-deposition.

Due to the hazardous locations of outcrops, sedimentological analysis of terrace level 1 was restricted to one locality proximal to the Rambla de Buho (Loc.1 shown on Fig. 3.3B). Within this locality, fresh faces of the type section are exposed in areas of recent block failure forming obliquely to the current Rambla Buho. The preserved sediments are composed of pale brown/grey interbedded sands and conglomerates which lie unconformably over Tortonian marls and sandstones. The section can be separated into two main facies groupings, as presented in the sedimentary log and photos of Figure 3.5:

1. Basal sheet-form facies (base to 1.6 m): Characterised by interbedded sands and crudely imbricated conglomerate beds. Sand beds are of lithofacies Sm/Sh comprising fine to medium grained, weakly bedded to massive sand beds, with numerous floating gravel clasts (upto pebble sized; Fig.3.5 Photo 3). Conglomerate beds are of lithofacies Gm, forming thin (<0.35 m thick) lenses of unstructured, poorly sorted, fine to coarse grained, angular to sub-angular gravel that are laterally traceable over 3-4m. The basal contact between the sand and conglomerate beds is typically planar, however small scours do occur (<0.4 m depth);

2. Upper channel facies (1.6 m – 2.7 m): Characterised by planar cross bedded and trough cross bedded conglomerates fining upwards into sands (Photo 1 and 2 on Fig. 3.5). The conglomerate units are of lithofacies Gp comprising moderately-well sorted, clast supported, sub-angular to angular, imbricated gravel and pebbles of graphite mica schist and quartz clasts (clast count Fig.3.5). The upper 0.45 m of the units fines to lithofacies Gp/Sp comprising poorly to moderately sorted, sub-angular to angular, coarse grained sand and crudely imbricated gravel. The sand beds show signs of planar cross bedding, with individual bed thicknesses decreasing to <0.2 m, pinching out at <1 m laterally. Both the upper facies and basal sheet-form facies show a strong degree of calcretization (Stage III to IV- groundwater calcretes).

The basal sand and conlomgerate beds of lithosfacies Sm/Sh and Gm are characterised as having sheet-form geometry with a width to depth ratio in excess of 15 (Mather, 1999). The formation of sheet geometries implies sediment transportation in weakly confined to unconfined flows as associated with sheet-flood or sheet-wash conditions (Hogg, 1982; Blair & McPherson,1994). Sediment transportation would have taken place under fluid flow conditions, as supported by clast imbrication and localised basal scours (Nemec & Steel, 1984). The presence of random gravel clasts and impersistent matrix supported gravel stringers within the sands beds suggests transportation in flows that were hyperconcentrated with sediment (fluidal sediments of Nemec & Steel, 1984). The distinct sedimentary structure (cross beds), moderate degree of sorting and the imbrication of the upper channel facies of the type section suggests deposition of sediment in longitudinally migrating bar-forms or laterally active stacked channels. Both morphologies are indicactive of deposition in a radially disbursive channel network similar to those recorded in a braid-plain type environment (Miall, 1996); however, the morphology of sections indicates a lack of valley confinement.

Section Name: Terrace Level 1 Location 1
Location: E 0552076 N4102802
Surface Elev: 528-513mAHD
Base-Rambla: 80-95m

Sedimentology: Lower Section (0-1.6m) consists of fine to medium grained, massive-weakly bedded sandstones of lithofacies Sm/Sh, interbedded with clay/mudstone beds (<0.2m thick) at base (<0.4m). Basal sandstones are interbedded with mod. to poorly sorted conglomerates of lithofacies Gm. Conglomerates are massive/ structureless forming thin lensed beds typically <0.35m thick extending laterally over 3-4m.

Upper Section (1.6-2.7m) comprises mod. well sorted, clast supported planar cross bedded conglomerates of lithofacies Gp fining upward to mod.-mod. well sorted coarse grained, planar cross bedded sands /fine grained gravels.

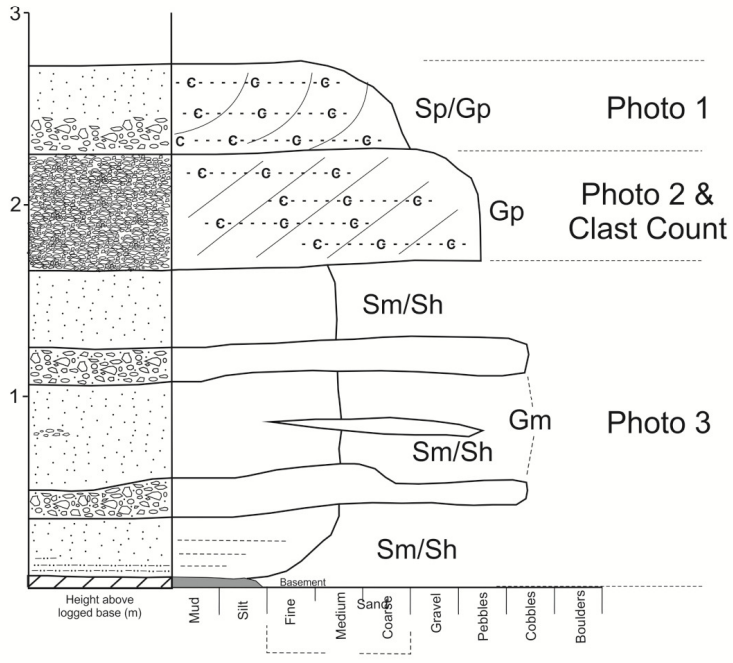

Sedimentary Log

Section
Photographs

Photo 1

Photo 2

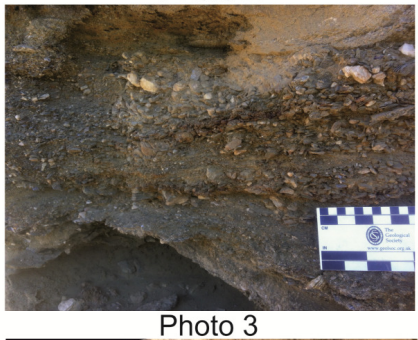

Photo 3

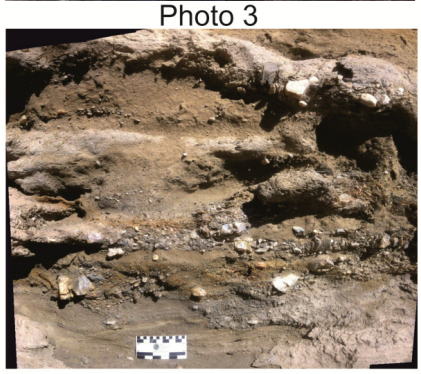

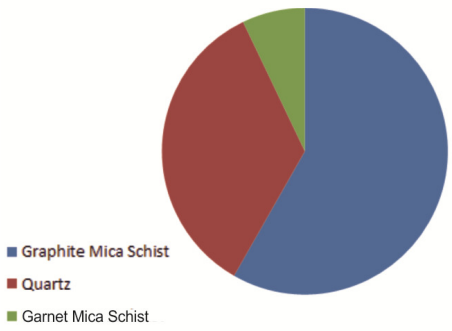

Clast Count

Figure 3.5 Sedimentary log detailing the structure and facies of terrace level 1. Location of section can be found on Figure 3.3B.

Although limited to one accessible exposure, the morphology of sections (i.e terrace remnants prograding into the basin centre from the bounding Sierras) and the sedimentary assemblages of terrace level 1 type section are indicative of deposition in an alluvial fan environment (Bull, 1977; Mather, 1999; Harvey, 2011). The progressive shift from sheet form facies (Sm/Sh) to fluvial channel facies (Gp) is typical of a distally aggrading and backfilling fan system dominated by fluvial processes (Harvey, 2002; 2011). During aggradation, the fan surfaces would have had a smooth depositional topography in comparison to characteristically steep fan surfaces associated with debris-flow processes (Harvey, 2011). Although no palaeocurrent data were collected (due to the hazardous location of the section), provenance indicators with an abundance of graphite mica schist clasts (clast count Fig. 3.5) and the morphology of the terraces would suggest sediment input from the Nevado-Filabride complex sourced from the Sierra de los Filabres to the north. The groundwater calcretes which occur throughout the section correlate with N/S1 profiles of Nash and Smith (1998; 2003) which forms the highest groundwater calcrete level within the basin (Chapter 2, Section 2.4.2).

3.3.2 Terrace level 2

The deposition of terrace level 2 deposits would have occurred after a substantial period of basin-wide incision which led to the abandonment and isolation terrace level 1 deposits (discussed in detail in Chapter 5). Across the basin, incision would have been ~40 m below the erosional contact of terrace level 1 (Table. 3.4, Fig. 3.4 and Fig. 3.6) as recorded by the extensive sedimentary archive for the terrace level (Fig. 3.3). At a basin scale, terrace level 2 landforms can be separated into two distinct units: a major unit and a lower unit (Fig. 3.3A) based on morphological and sedimentological relationships developed in this section. The lower unit forms a highly localised morphological unit preserved upstream of current drainage knickpoints which has sedimentological affinities with the majority of terrace level 2 units. A separate terrace level was not assigned to the lower unit based on its limited basin extent.

The majority of terrace level 2 outcrops (termed the major units) form extensive pediment-like surfaces linked to the bounding sierras and sloping gently into the basin centre. The pediments are best preserved along the flanks of the basin forming extensively calcreted sedimentary bodies relating to the N/S3 and N/S4 paired groundwater and pedogenic calcretes of Nash and Smith (1998; 2003). Within the basin centre, the terrace level 2 pediments are highly incised by the current fluvial system forming laterally persistent yet isolated terrace remnants (Fig. 3.3). Given the sloping nature of the pediment surfaces and the variable incisional trends in the current day fluvial system across the basin (Fig. 3.6 and Fig. 1.2B, Chapter 1), the elevation and thickness of sediment bodies varies across the basin. However, the following morphological observations can be made (summarised in Table 3.4):

- An average incisional depth (top of sediment assemblage to current river bed) of 40m is applicable for majority of terrace level 2 landforms;
- Across the basin, incisional depths increase downstream along drainages toward the axial drainage (Rambla de Tabernas);
- Incisional depths across the basin increase in a westerly direction; and
- Incisional depths with relation to the current Rambla Sierra are typically half that of other major drainages within the Tabernas Basin.

Faulting is reported in level 2 terraces in the Rambla Sierra (Harvey et al., 1999); however, at a basin scale terrace level 2 landforms show little sign of tectonic deformation in either their morphological expression or form. This observation differs from the previous text which focuses on deformation of terrace deposits around the prominent Marchante anticline (Harvey et al., 1999). Thick travertine deposits are also associated with terrace level 2 units, however, they are highly localised and only preserved at one location in the basin forming a 6m cap within terrace level 2 sediments as presented in Figure 2.18 (Chapter 2). These travertine deposits likely relate to the highly faulted northern margin of the Sierra Alhamilla, termed the Northern Alhamilla Fault Zone (NAF).

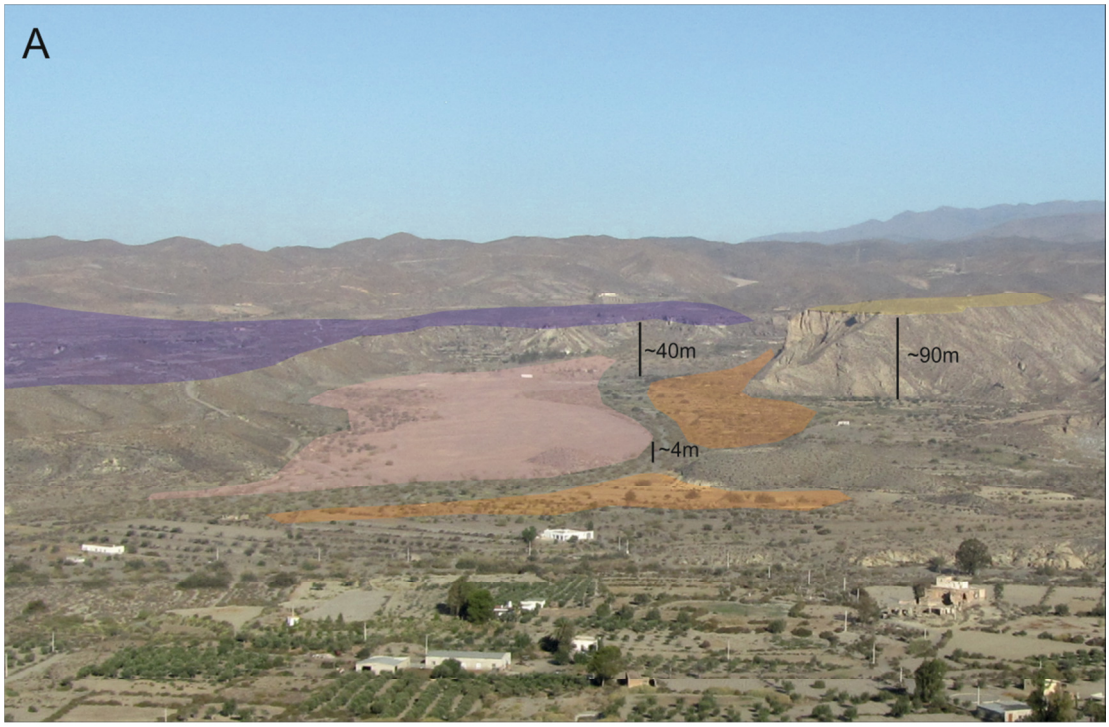

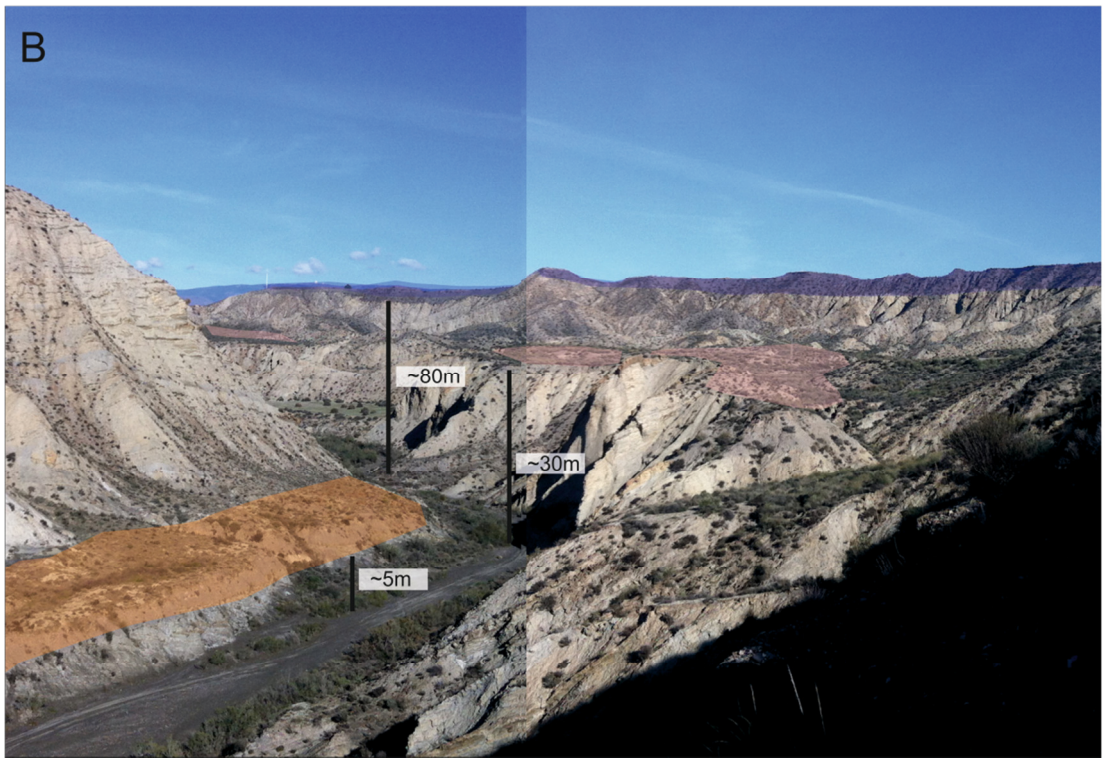

Figure 3.6 Variable incision trends across the Tabernas Basin. (A) Shows the relationships of terrace levels (coloured as Fig. 3.4) for the Rambla Buho in the east of the basin with limited separation between Levels 2 - 4 (photo facing northwest UTM 30S 553839/4100830). (B) Shows the incisional depths between terrace levels in the Rambla Lanujar in the west of the basin (photo facing northeast UTM 30S 547951/4097018).

The lower unit of terrace level 2 represents a highly localised relic landform level, inset into major terrace level 2 landforms yet above that of terrace level 3 deposits. The lower unit is isolated in occurrence and is only preserved above the current limit of incision within the Rambla Sierra and Rambla de Benavides (Fig. 3.3B) forming the active level of drainages in these locations (Fig. 3.7). The incisional base of the lower units is only exposed in knick-points, forming on average ~30 m below the incisional level of terrace level 2 major units (Table. 3.4 and Fig. 3.7).

Key sedimentary sections for both terrace level 2 units are located on Figure 3.3B. These sections represent the most complete sedimentary sequences for the major (Loc. 2 on Fig. 3.3B) and lower units (Loc. 3 on Fig. 3.3B) and characterise the typical structure for terrace level 2 landforms across the basin. The type section for terrace level 2 major units is exposed in two excavated faces that were cut during the construction of the A-92 Guadix to Almería Motorway. The section is separated into two major facies groupings which record a combined sedimentary thickness of 17 m (Fig. 3.8). The contact between the groupings is separated by a 4m gap where exposures were not safely accessed. Facies groupings include:

- Basal sheet-form facies (0 – 7 m of section): Characterised by a series of sheet-like bodies of interbedded pale grey-brown sand and conglomerate beds. Sand beds are 0.3-0.8 m thick with weak sub-horizontal and wavy bedding of lithofacies Sm/Sh. Texturally, the sand beds consist of poorly sorted, fine to coarse grained, angular, graphite rich sand. The conglomerate beds form laterally extensive (5 – 7 m) sheet-like lenses of variable thickness (0.15 - 0.6 m) with little internal structure of lithofacies Gm. In some beds coarsening upward cycles appear evident, with fine to medium gravels grading upward to cobbles (0.15 - 0.3 m ø.). Texturally the conglomerates consist of moderately well supported, clast supported, angular to sub-angular, fine to coarse gravels that are well imbricated. The conglomerates beds are rich in graphite schists (clast count; Fig. 3.8);

- Upper channelised facies (11- 17 m): Characterised by a series of minor channelised pale grey graphite schist conglomerates. Within the lower 4.5 m of the section the conglomerate beds form channel features that are up 2.5 m wide by 0.8 m deep. These channel features are infilled with moderately sorted, sub-angular, fine to coarse grained gravels that are often capped by coarse grained sand plug (lithofacies Sm). Conglomerate beds display low angle (<25°) planar cross-bedding, as represented by lithofacies Gp. The upper 1.5 m of the section is dominated by crudely bedded to massive conglomerates of lithofacies Gm. These beds display Stage III calcretization in the upper 0.6 m of section with no rubification. Conglomerates are
  imbricated toward the south/southwest.

The section for terrace level 2 lower units (Loc.3, Fig. 3.3B) records similar sedimentological styles as that of the upper 6m of the major unit. The section is exposed in a natural cut formed at the current knick-point in Rambla Sierra and is dominated by a series of weakly channelised stacked conglomerates (Fig. 3.9). The conglomerates form thin lenticular beds of varying thicknesses (<0.5 m) that pinch out laterally over 4-7m. Low angle cross bedding of lithofacies Gp is evident throughout. Texturally, the conglomerates comprise well imbricated, moderately sorted, sub-angular to angular, fine to coarse grained gravels with frequent weak fining upward trends capped by sand lags (<0.15 m thick). The conglomerates are rich in graphite schist, brecciated limestones and garnet mica schist sourced from the Sierra Alhamilla. The upper part of the section is sand rich with beds up to 1.3 m thick. The sand beds have little internal structure (lithofacies Sm) and contain frequent lenses of matrix supported, poorly sorted gravel. The top 0.35 m of the section shows Stage III calcrete formation with no subsequent rubification.

Table 3.4 Summary of morphological data for terrace level 2 landforms with reference to major basin drainages. A map of drainages is presented in Fig. 3.3B. Incisional depths calculated from base of sequence to current rambla.NO = not observed

Drainage	Min. Elevation (m AHD)	Max. Elevation (m AHD)	Mean Elevation (m AHD)	Min. Thickness (m)	Max. Thickness (m)	Mean Thickness (m)	Min. Incisional Depth (m)*	Max. Incisional Depth (m)*	Mean Incisional Depth (m)*
Rambla de Tabernas	379	409	401	1.5	14	7	69	80	75
Arroyo del Verdelecho	347	551	452	2	17	9	71	79	74
Rambla del Buho	395	521	470	5	16	8	23	51	41
Rambla de Reinelo	378	479	424	Strath	9	5	20	69	40
Rambla de Benavides	457	481	465	6	13	9	33	51	40
Rambla de Benavides (Lower Unit)*	411	451	428	NO	5	-	NO	9	-
Rambla Sierra	393	517	465	6	15	9	14	46	28
Rambla Sierra (Lower Unit)*	423	430	427	NO	8	-	NO	8	-

* Values based on limited number of exposure points

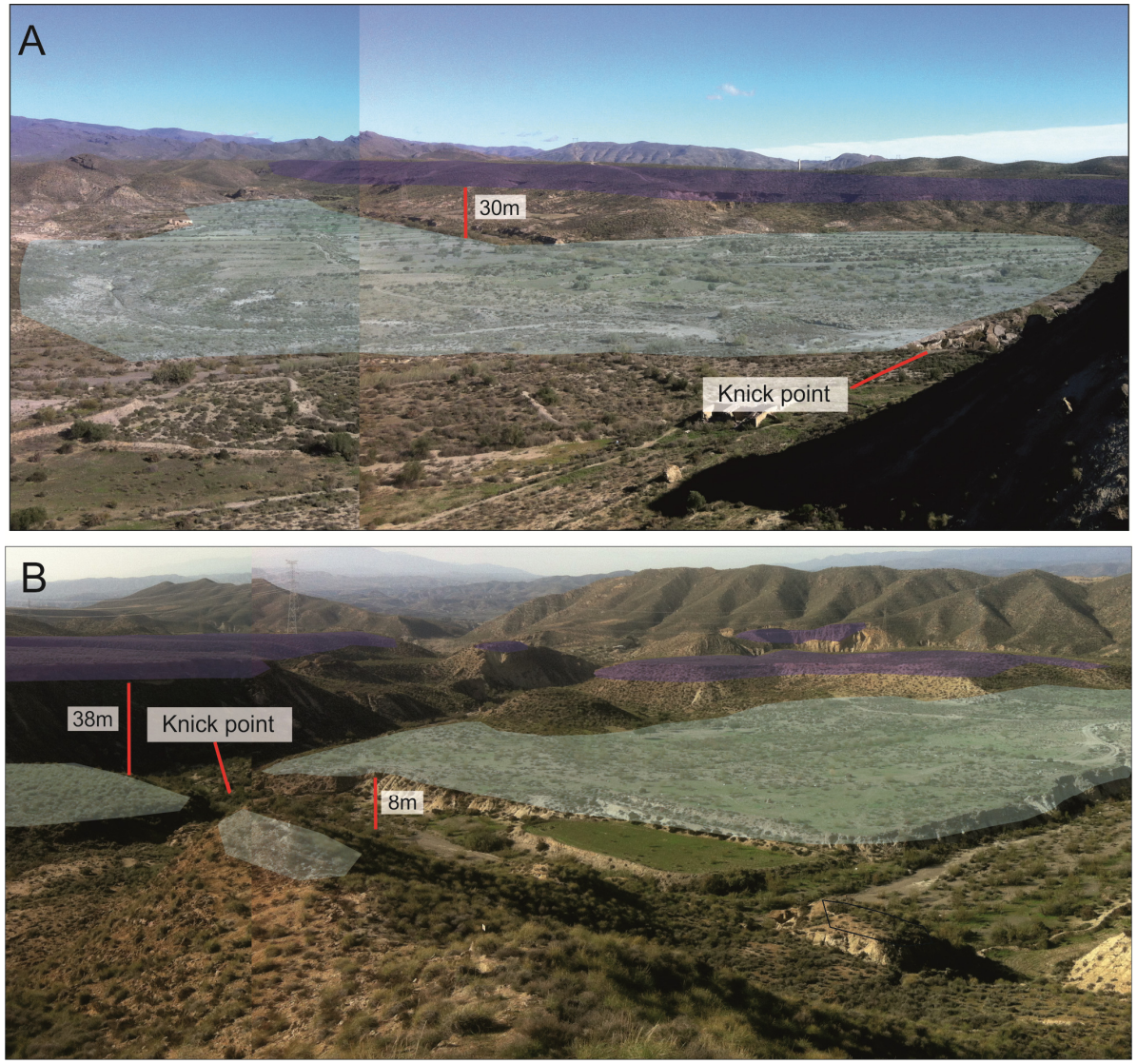

Figure 3.7 Morphological relationship of terrace level 2 and its subdivision into a main and lower unit (coloured as Fig. 3.4) for (A) the Rambla Benavides (photo facing northeast UTM 30S 552821/4102653) and (B) the Rambla Sierra (photo facing northwest UTM 30S 555633/4098931).

For the level 2 major unit type section, the basal sheet-form (width:depth ratio >15) sands and conglomerate facies (Sm/Sh and Gp/Gm) are again characteristic of weakly confined to unconfined flows, as typically assocaited with sheet-flood or sheet-flow conditions (Blair & McPherson, 1994; Mather, 1999). The textural maturity, imbrication and clast supported nature of the conglomerate beds (Gm) is indicative of transportation under water-fluid conditions (Pla-Pueyo et al., 2009). The fine grain size, poor sorting and interbedded occurrence of the sand facies (Sm/Sh) could suggest deposition during the wanning stage of flow within the sheet flow event (Mather, 1999), or during a subsequent flow event. The cross bedded conglomerates (lithofacies Gp) representative of both the upper part of the level 2 major unit and the level 2 lower unit type section are representative of deposition in longitudinal bar forms with the low angle foresets marking the direction of downstream migration (Miall, 1996; Lewis and Maddy, 1999). The stacked channels (lithofacies Gm/Sm) are representative of weakly confined and highly connected streams formed in a radial disbursive braid-plain type fluvial environment (Miall, 1996).

The facies groupings for terrace level 2 major and lower sections are indicative of deposition in a fluvially dominated alluvial fan environment, similar to those of terrace level 1 (Harvey, 2011). The morphology of the laterally extensive pediment-like surfaces would support the formation of broad coalescent fans across the basin. The dominance of fluvial processes within both terrace level 2 sections could indicate a degree of fan maturity (Harvey, 1997; 2011). For example, many Pleistocene fan sequences in the Almería region are dominated by debris flow processes in their early stages of development becoming fluvially dominated through time. This change in process dominance is related to the relative availability of sediment during climate cycles coupled with on-going patterns of tectonic uplift which generates sediments in the bounding Sierras (Harvey, 1997; 2011). The morphology and sedimentology of terrace level 2 landforms would suggest deposition in an aggrading fan system, much like those recorded in the un-trenched and active fans preserved in the east of the present day basin.

Section Name: Terrace level 2 major | **Location (base):** E 0548328 N 4098533
Surface Elev: 430-375 mAHD | **Base-Rambla**: ~70m

Sedimentology: Lower Section (0-5.7m) consists of massive-weakly sub-horizontally bedded sands of lithofacies Sm/Sh. Sands are interbedded with conglomerates of lithofacies Gm and Gp. Conglomerates are typically massive/ structureless forming thin lense type beds typically <0.5m thick extending laterally over 5-7m. In base of section conglomerates show weak low angle (<15 degrees) planar cross bedding (lithofacies Gp). Potential fining upward cycles are also noted in thick conglomerate beds, passing from fine-medium gravel to cobbles (<30cm dia.). Section dominated by Graphite Mica Schist & Quartz (Clast counts yet to be completed).

Upper Section (11-17m) consists of low angle (<25 degrees) planar cross bedded conglomerates of lithofacies (Gp). Conglomerate beds typically have channel structures (up to 2.5m wide x 0.8m deep) that contain sand plugs over channelized planar cross bedded gravels. Clast orientation to the south / southwest

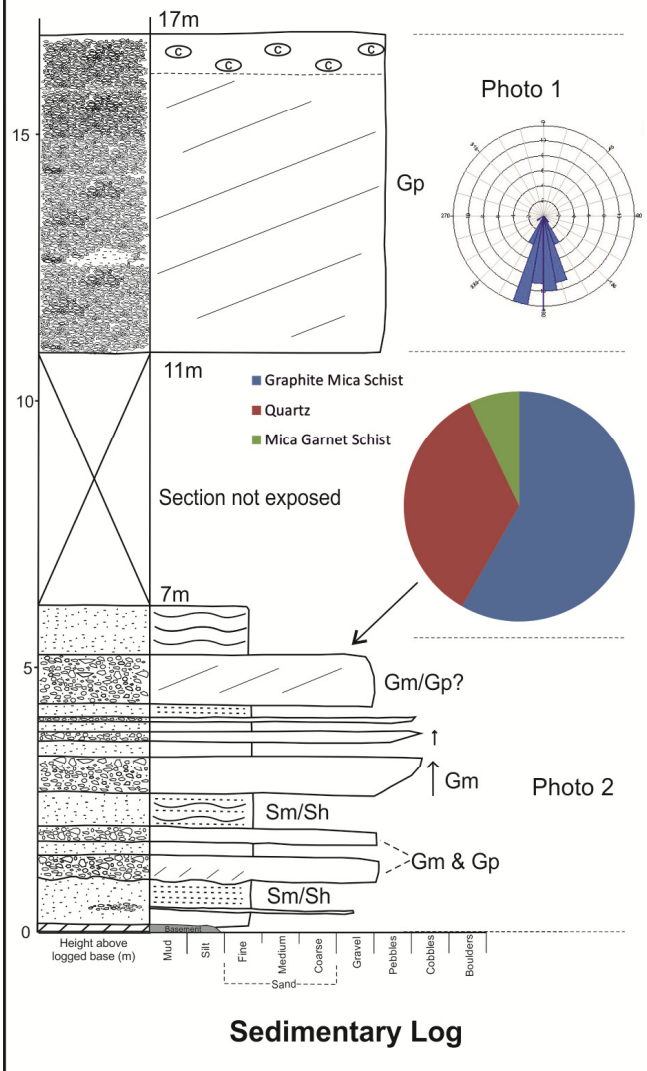

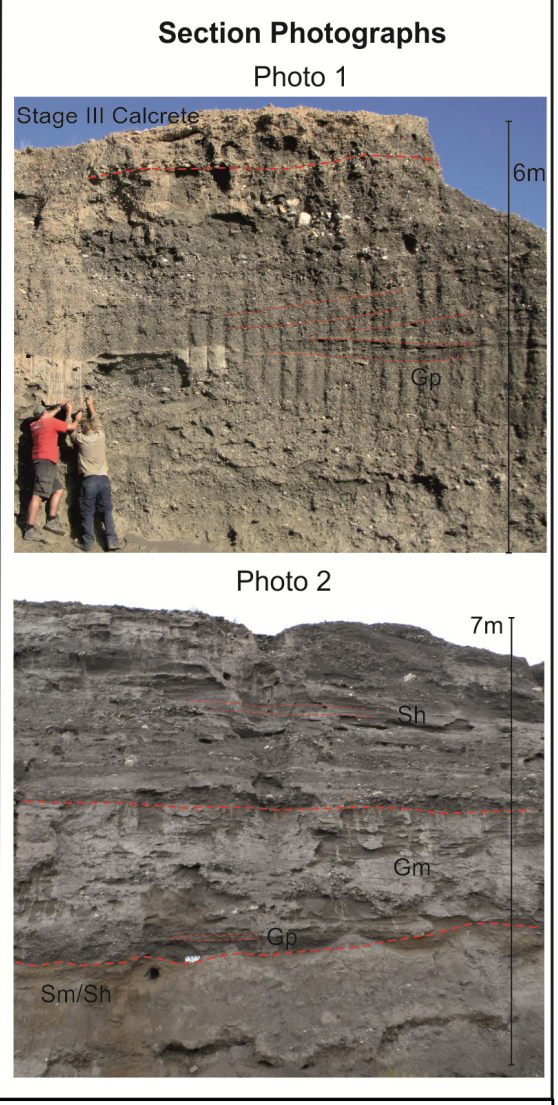

Figure 3.8 Sedimentary log detailing the structure and facies of terrace level 2 major unit type section. Location of section can be found on Figure 3.3B

Section Name: Terrace level 2 low
Location: E 0552076 N 4102802
Surface Elev: ~425mAHD
Base-Rambla: 0m

Sedimentology: Dominated by mod. well sorted, clast supported cross bedded conglomerates of lithofacies Gp. Beds are typically less than 0.5m thick and extend laterally over 4-7m. A thin sand lag (<0.15m) is often present over individual beds. Clast orientation to the west/ southwest

One crudely bedded-massive sand bed occurs from 5.9-7.35m in section, with frequent laterally inpersistent lenses of poorly sorted, matrix supported gravel.

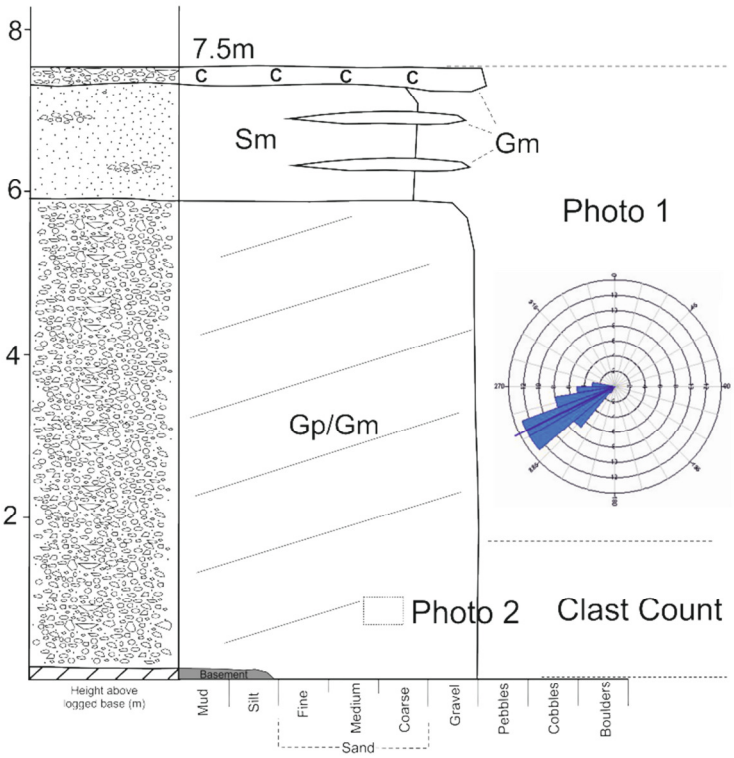

Sedimentary Log

Section Photographs

Photo 1

Photo 2

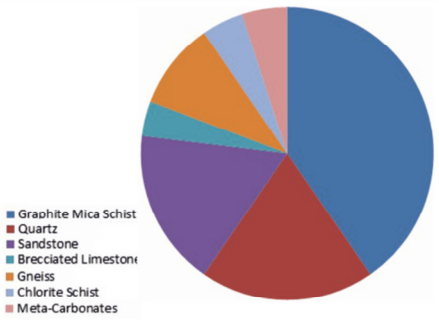

Clast Count

Figure 3.9 Sedimentary log detailing the structure and facies of terrace level 2 lower unit type section. Location of section can be found on Figure 3.3B

3.3.3 Terrace Level 3

Post deposition of terrace level 2 pediments veneers, a major period of incision took place across the Tabernas Basin. The dramatic base-level lowering event promoted basin wide incision (basin average ~60 m) as evidenced by the inset base of terrace level 3 deposits at or near the present day level of drainages (e.g. Rambla Tabernas, Sierra, Galera and Los Molinos; Fig. 3.4). Incisional depths for terrace level 3 deposits range considerably across the basin. Erosion was greatest along the axial drainage system and major tributaries (e.g. current Rambla Tabernas, Sierra and Los Molinos) with an average incisional depth of ~75 m (top of terrace level 2 to base of terrace level 3, Table 3.4). In the southern and northern margins of the basin (e.g. Ramblas Reinelo, Lanujar, Buho and Grillo) incision was almost half that of the basin centres (average of ~40 m) highlighting the variable degrees of coupling within the basin at the time. Unfortunately, the extent of incision in the east of the basin is unknown due to the current limit of incision into more recent sediment sequences (e.g. stacked alluvial fans of Harvey et al., 2003); however, substantial accommodation space must have been created during this degradational phase.

The morphology of terrace level 3 deposits is also variable across the basin (Fig. 3.10). Along the path of the axial drainage and its major tributaries (current Rambla Tabernas, Sierra and Los Molinos) terrace level 3 deposits are associated with the substantial (~20 m thick) back-ponded lacustrine sediments of the lower and upper lakes of Harvey et al., (1999; 2003) (Fig. 3.10A). In the centre and west of the basin, lower lake deposits have a highly irregular base (i.e. deposition took place into a highly incised surface; Parker, 2001) and form thick sediment bodies which outcrop extensively along the axis of the Rambla Tabernas (Fig. 3.10A). These sediments are either capped by a thin pedogenic calcrete, giving rise to a planar terrace surface, or they remain uncapped by calcrete units and form a heavily incised surface characterised by badland morphologies (Fig. 3.10C). The lower lake sediments pinch out in the southwest of the basin c.1.7 km downstream of the El Cautivo badlands. In this area, the fine grained deposits have been locally folded and faulted, with

open / undulose syndepositional deformation of sedimentary beds (Harvey et al., 1999 for detail). This deformational style forms the only evidence for syn-tectonic activity within the terrace level 3 deposits. The upper lake deposits outcrop upstream of the current confluence of the Rambla Sierra into the current Rambla Los Molinos in the east of the basin. These too have highly irregular erosional bases and variable sediment thicknesses, pinching out c. 3.6 km upstream of the Los Molinos confluence. In areas of limited dissection, the upper lake deposits are intercalated with coarse grained alluvial fan deposits (Fig 3.10B) which correlate to alluvial fan stage 3 of Harvey et al., (2003).

In contrast to the fill morphologies (terminology of Leopold and Bull, 1979) of the upper and lower lake sequences, terrace level 3 deposits preserved along the northern and southern flanks of the basin (e.g. Rambla Lanujar, Grillo and Reinelo; Fig. 3.3B for location) are typically much thinner (<6 m, Table 3.5). Sediment bodies form isolated strath terraces or surfaces commonly associated with the valley floor calcretes of Nash and Smith (1998; 2003) (Table 3.5; Fig. 3.10D). The strath terraces form well defined valley morphologies running in a broadly south-west direction (not typical of the north-south flow direction found in terrace level 1 and 2 sediments) cut into the underlying marl and sandstone beds. In the west, multiple abandoned meanders are preserved on top of strath surfaces which were resultantly isolated between deeply incised drainages upon terrace level abandonment (e.g. the Las Salina abandoned meander, Fig. 3.10A) (Harvey, 2007). Travertines also form extensively on top terrace level 3 strath surfaces, with the active precipitation of the various morphologies along localised fault systems in the Rambla de Buho, Rambla Grílllo and Las Salinas (Chapter 2, Section 2.4.5).

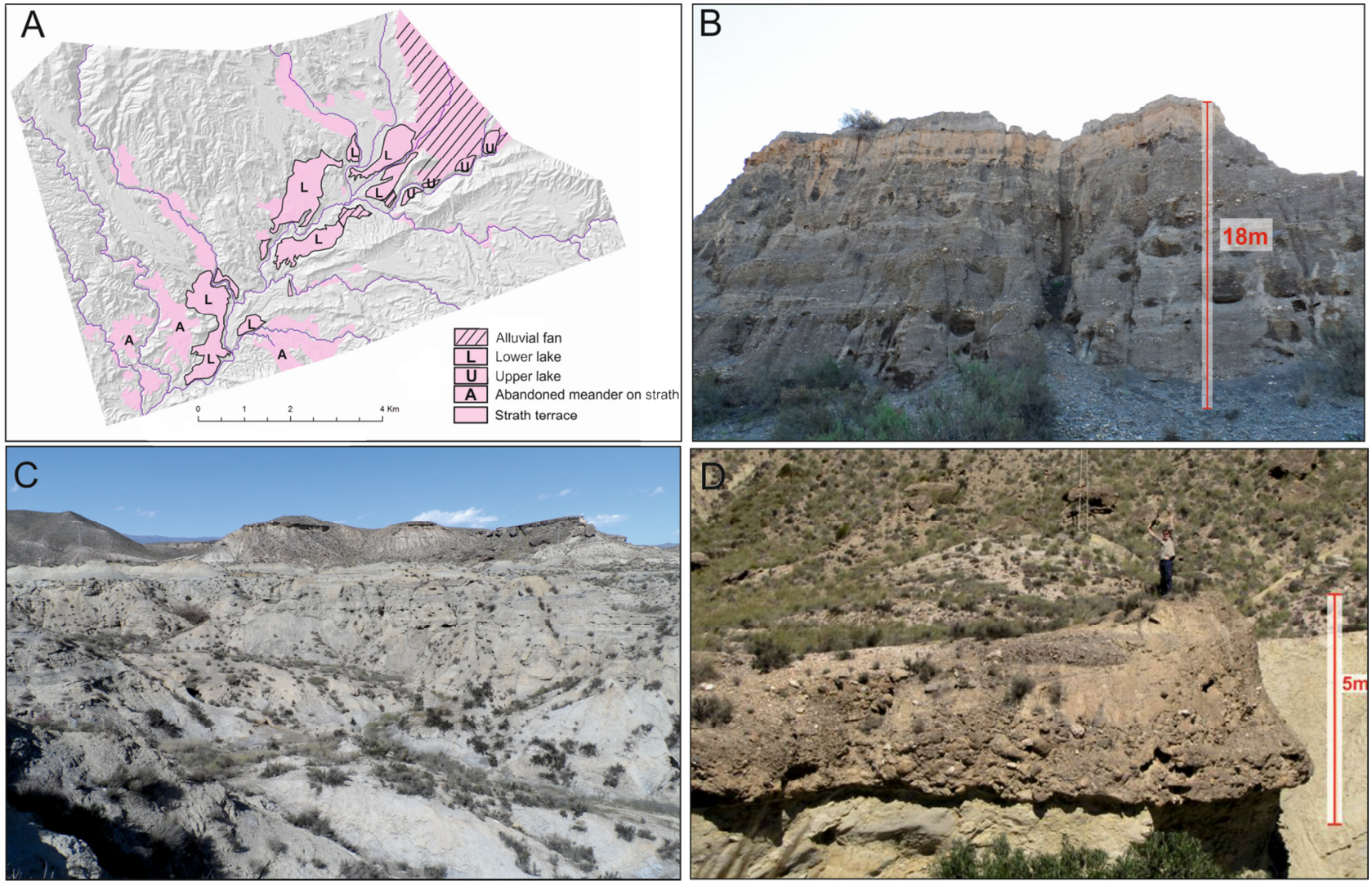

Figure 3.10 (A) Map of variable morphology of terrace level 3 deposits across the Tabernas Basin. (B) Stacked alluvial fan sediments in the Rambla Galera which are typical in the east of the basin (photo facing east from UTM 30S554445/4102269). (C) Badland morphologies developed in lower lake sediments (photo facing northeast UTM 30S 552131/4100164) and (D) calcreted strath terrace in the Rambla Reinelo typical of river terraces along the basin margins (photo facing north UTM 30S 551902/4098174).

Table 3.5 Summary of morphological data for terrace level 3 landforms with reference to major basin drainages. A map of drainages is presented in Fig. 3.3B. NO= contact not observed. Incisional depths calculated from base of sequence to current rambla.

Drainage	Min. Elevation (mAHD)	Max. Elevation (mAHD)	Mean Elevation (mAHD)	Min. Thickness (m)	Max. Thickness (m)	Mean Thickness (m)	Min. Incisional Depth (m)	Max. Incisional Depth (m)	Mean Incisional Depth (m)
Rambla de Tabernas	266	406	362	Strath	22	17	7	29	14
Arroyo del Verdelecho	271	376	331	4	10	8	9	19	16
Rambla de Lanujar	233	398	345	0	9	4	31	43	39
Barranco del Grillo	269	383	323	4	11	6	12	21	16
Rambla del Buho	356	464	403	3	12	9	2	12	9
Rambla de Reinelo	308	458	396	3	9	5	2	8	6
Rambla de Benavides	379	393	385	2	11	8	2	9	4
Rambla de los Molinos	353	423	406	3	22	16	5	20	15
Rambla Sierra	357	463	405	2	9	7	NO	12	8

The sedimentology of the third level can be separated into three principal groups which relate to the morphologies described: (1) lacustrine sediments, separated into the lower and upper lakes of Harvey et al., (2003), (2) alluvial fan sediments, associated with Filabres and Marchante Fans of Harvey, (1984) and Harvey et al., (2003) and (3) strath river terraces. Sedimentological data for the lower lake sediments presented herein develops the interpretations of type sections presented in the literature (e.g. Harvey et al.,1999; 2003); however, new type sections are presented for the upper lake, alluvial fan and river terrace deposits of terrace level 3. The addition of sections for already named depositional environments was deemed necessary in the accurate description of this complex terrace level. Where applicable the description of type sections aims to develop the environmental interpretations presented in the literature (e.g. interpretations for the lower and upper lake sections of Harvey et al., 2003).

Lower and upper lake sections

Sedimentary analysis of the lower lake type section was presented Harvey et al., (1999). The type section occurs immediately below a major knickpoint in an actively incising tributary of the Rambla Reinelo (Loc.4 on Fig. 3.3B, photo 2 on Fig. 3.11). The sedimentology of the section represents a transient shift from fluvial conditions to lacustrine/palustrine conditions which became fluvial again in the final stages of formation. The base of the section is dominated by conglomerates and sands of lithofacies Gm/Sm interbedded with silt and mud facies (Fm/Fl) deposited under fluvial conditions within a shallowing body of water (Harvey et al., 1999). The main body of the section is dominated by fine grained, massive and sub-horizontally bedded silts/muds and sands of lithofacies Fsc, Sh and Sm (Fig. 3.11), which represent sustained lacustrine/palustrine conditions with limited evidence for fluvial inputs. Frequent root casts, burrows, aquatic bivalves and gastropods are found in the sand facies (Fig. 3.11) which appear to indicate shallow water depths within a low-turbidity depositional setting (Harvey et al., 1999). Parker (2001) identified a number of gastropods (Pseudamnicola) and ostracods (Herpetocypris Brevicaudata & Heterocypris Salina) in the

lower section (<10 m) that supported the interpretation of brackish shallow water deposits (saline tolerant ostracods species representative of water depths <4 m). X-ray diffraction testing conducted on powdered sediment samples indicates a fluctuation in water depths with a relative increase in evaporite minerals (e.g. halite relative to quartz) at 5 m, 6.5 m and 17 m in the section. Channel morphologies are also noted in the lower 4m of the section with thickness of up to 2.5 m; however, no coarse grained infills are noted (Photo 3 Fig. 3.11). The upper 6 m of the lower lake section represents a transition back into coarse grained fluvial conditions with the deposition of intercalated sand and conglomeratic facies (Harvey et al., 1999; 2003). Alexander et al (2008) propose that coarse grained inputs would be sourced from the local hillslope system in the form of small scale deltaic deposits. One OSL date of 14±1 ka was obtained from a sand horizon 5m from the top of section marking the end of lacustrine sedimentation in the Late Pleistocene/ Early Holocene (discussed in detail in Chapter 4).

The upper lake type section forms in a recent cutting in the Rambla de los Molinos (Loc.5 on Fig. 3.3B) and is represented by a thickness of 22.3 m of sediment (Fig. 3.12). The lower contact of the section forms 4.2 m above the current rambla level and the upper surface of the section is dominated by agricultural terraces which indicate recent disturbance. The base of the section is characterised by <0.5 m of poorly exposed conglomerates of lithofacies Gm overlying Tortonian marls. The basal conglomerates are gravel to cobble sized (max dia. 0.4 m), sub-rounded and weakly imbricated. The basal units are overlain by the interbedded silt / mud and sand facies that dominate the upper 22 m of the section. The silt / mud and sand facies are regularly bedded in the lower section (0.5 to 7 m up section) forming laterally extensive sub-horizontal beds between 0.3 - 2.5 m thick. Many silt beds demonstrate the properties of pseudo-gley soils (sensu. Mather, 1993) with numerous ferric rich palaeosol horizons and root/rootlet traces evident. In the base of the section (<4 m) the contacts between silt/mud and sand beds are highly irregular and typical of dewatering/fluid loading structures. Sand beds decease in abundance 7 m from the base

of the section and are not present in the upper 9 m, which is dominated by silt beds of lithofacies Fl / Fsc. Calcrete nodules form abundantly in the silt beds of the upper 2.5 m where stage III calcrete formation (Machette, 1985) is evident. Palaeosol layers are also frequent throughout and are associated with orange brown colouration (possible haematite layer, Fig. 3.12). One white coloured horizon forms at 1.3 m below the upper surface of the section. The horizon is notably pale grey/white in colour, of low specific density and is laterally extensive over several tens of metres (presented as a potential diatomite/gypsum rich precipitate layer on Fig. 3.12).

Deposition of the upper lake occurred upon back-filling of the lower lake and damming of the axial drainage near the current day Rambla Sierra (Harvey et al., 1999). Deposition was likely initiated under fluvial conditions as evidenced by the grain size, clast shape and imbrication of gravel and cobbles in the base of the section (Miall, 1996). The interbedded silt and sand facies that overlie the basal conglomerates would likely have been deposited during short lived flow events, potentially of variable depth (Harvey *et al*., 2003). The lack of defined channels indicates sedimentation during unconfined flood events that were probably hyper-concentrated in sediment (Miall, 1996; Mather, 1999). The presence of palaeosol horizons and abundant root casts in the lower silts beds implies a shallowing of the water table and resultant aerial exposure of sediments prior to the onset of subsequent flood stages (Harvey *et al*.,1999; Magaldi and Tallini, 2000). The transition to massive to horizontally bedded silts in the upper 9 m of the section would indicate a shift to a low energy depositional environment, such as a body of standing water (Harvey et al., 1999). The formation of two palaeosol horizons in the upper 4 m of the section would suggest fluctuating water levels during the final stages of aggradation. However, the potential diatomite layer preserved beneath the upper paleosol horizon would indicate stable groundwater levels for a sustained period of time (5-10 yrs) (Yunker et al., 1995).

Section Name: Terrace level 3- lower lake
Surface Elev: ~340mAHD

Location (base): E 0551164 N 4098751
Base-Rambla: 0m

Sedimentology: Section is dominated by laminated and massive mud/silt and sand beds of lithofacies Fl/Fsc and Sm/Sh. Mud/Silts are pale grey/pale yellow brown in colour, sub-horizontally bedded (~20cm sets) to massive. Silt beds show characteristics of a pseudogley soil throughout with numerous rootlets. The base of the sequence is rich in gastropods, bivalves and dewatering structures.

Laterally persistent sheet form sand beds are frequent in the base of the section (lower 5m) typically less than 0.3m thick. Texturally the sandstones are weakly bedded to structureless, moderately sorted with a typical fine to medium grain size. Conglomeratic inclusions are typical in the very base and upper 2m of the section.

Mesoscale channel features are present in the lower 5m of the section as associated with abundant sandstone facies.

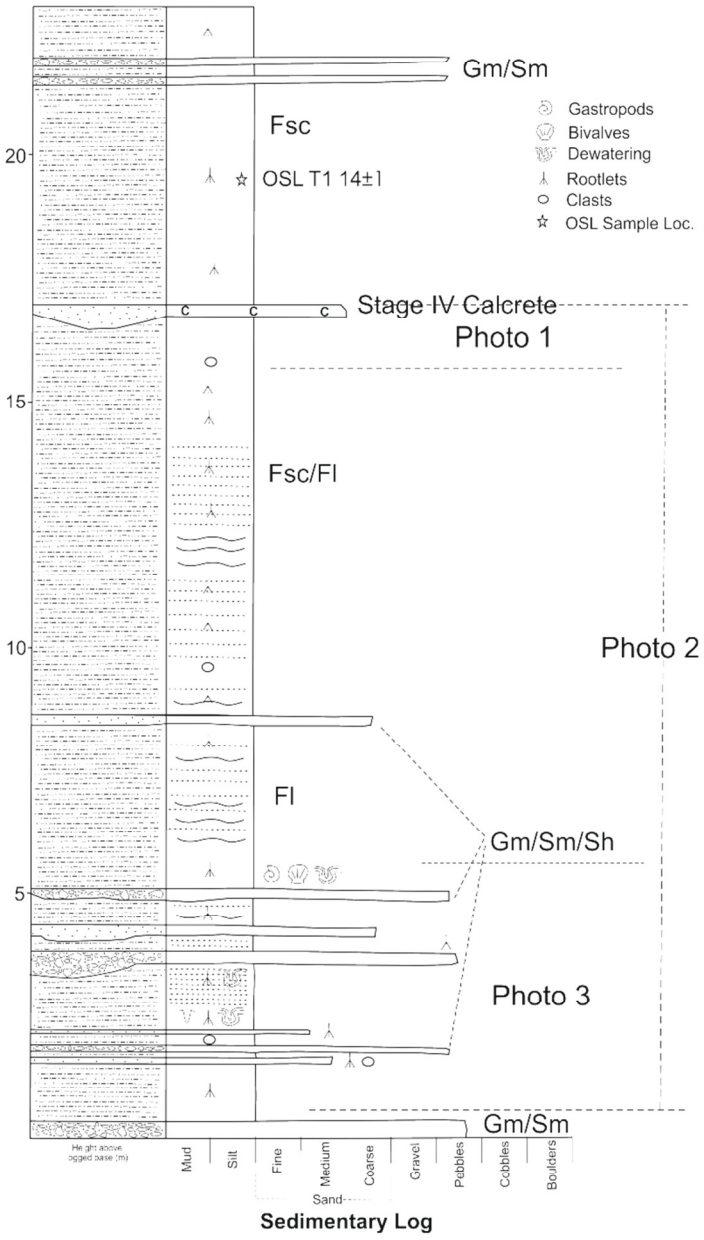

Section Photographs

Photo 1

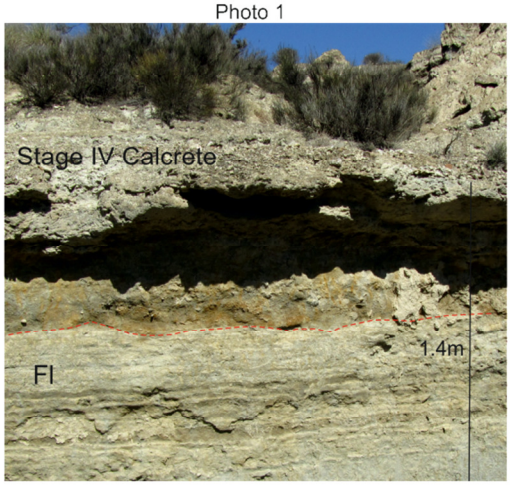

Photo 2

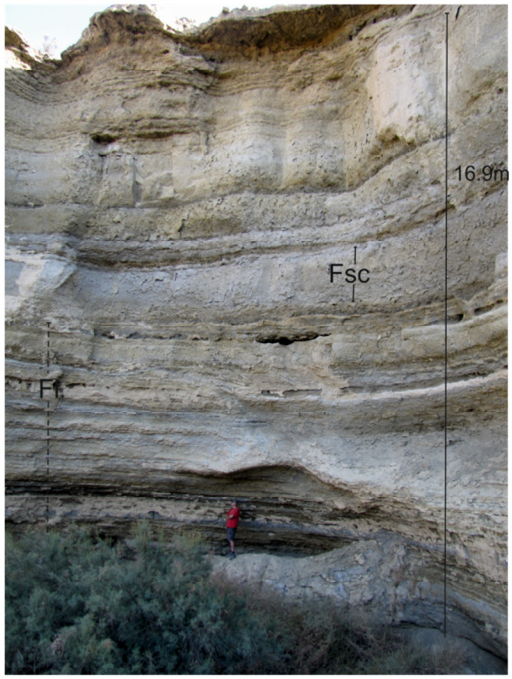

Photo 3

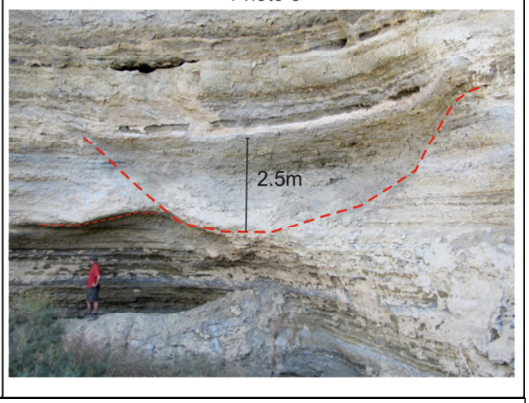

Figure 3.11 Sedimentary log detailing the structure and facies of terrace level 3 lower lake type section. Location of section can be found on Figure 3.3B marked as Location 5.

Section Name: Terrace level 3 - Upper lake
Surface Elev: ~405mAHD

Location (base): E 0555567 N 4101407
Base-Rambla: 4.2m

Sedimentology: Section is dominated by laminated silt/mud and sand beds of lithofacies Fl/Fsc and Sm/Sh. Silts/muds are blue grey in colour, sub-horizontally bedded (~40cm sets) to massive with numerous dewatering structures, root infills and palaeosol horizons that are stained orange brown. Sand beds are frequent in the base of the section (lower 6-7m) typically less than 0.4m thick- extending over some 7-9m with a sheet-form geometry. Minor evidence of fining upward sequences in sand beds with a fine gravel lag fining to a medium grained sand.

One potential diatomite layer is noted in the upper 3.8m of section. The layer is some 0.4-0.5m thick and extends laterally over several tens of metres.

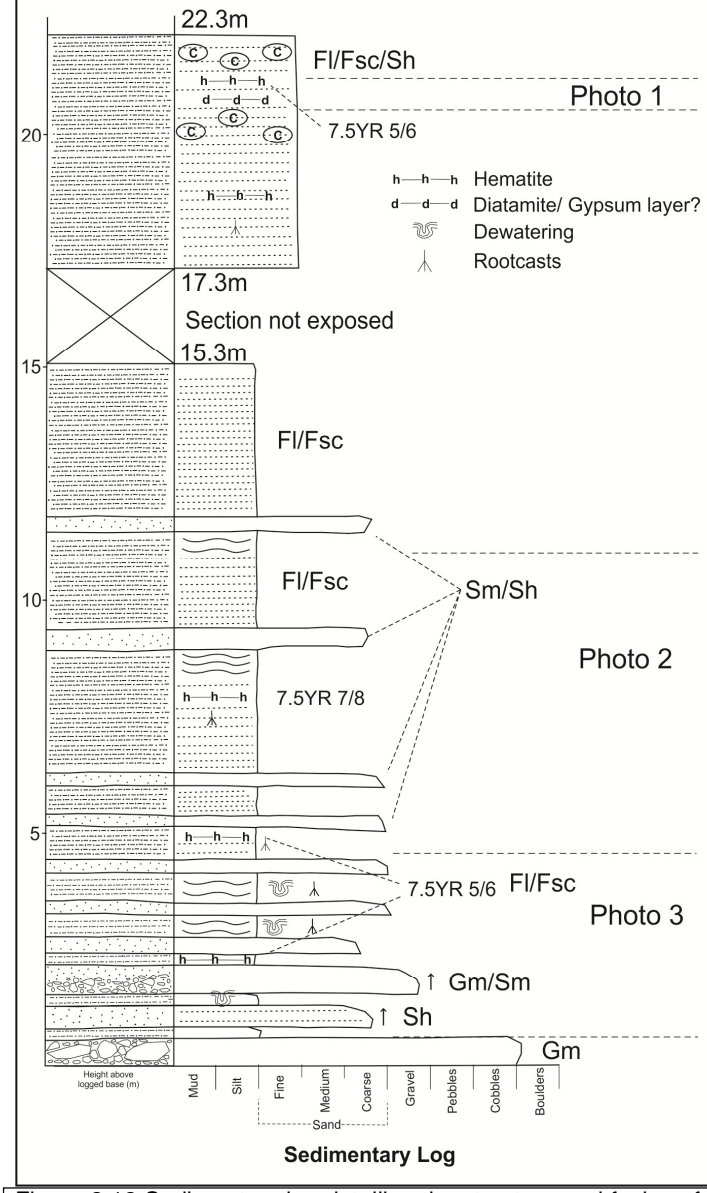

Sedimentary Log

Section Photographs

Photo 1

Photo 2

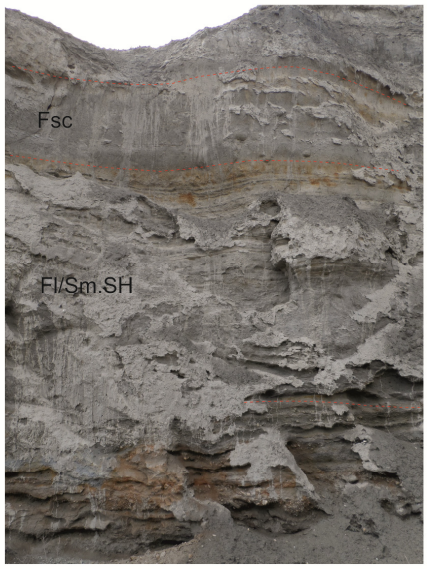

Photo 3

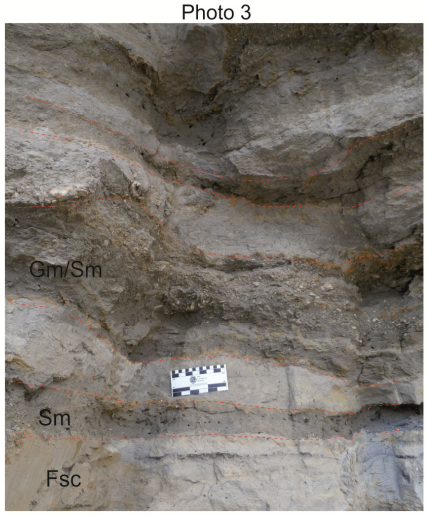

Figure 3.12 Sedimentary log detailing the structure and facies of terrace level 3 upper lake type section. Location of section can be found on Figure 3.3B.

U-Series age determination conducted by Ruiz Bustos & Martín Algarra (1991) and Delgado et al., (1993) on rodents teeth within the type section presented by Harvey et al., (1999) (~200m downstream from type section presented herein) indicates that sedimentation was occurring at 150±50 Ka in the upper lake area. However, the age determinations are based on relative associations alone and are poorly constrained (as presented in Chapter 4). The sediments of the type section presented herein are analogous with the upper lake sequences of Harvey et al.,(2003). However, the lack of coarse grain inputs encountered by Harvey et al., (2003) could relate to the recent disturbance of the section for agricultural purposes, or be a function of the increased distance from the aggrading fan fronts presented by Harvey et al., (2003).

Alluvial fan section

As presented previously, the sediments of the upper lake sequence are intercalated with aggrading alluvial fan sediments in the undissected areas in the east of the basin (e.g. Filabres and Marchante Fans; Harvey et al., 2003). The active alluvial fan systems in this region are not yet dissected by the current fluvial system and represent the most complete sedimentary archive post terrace level 2 incision and abandonment. The type section for terrace level 3 alluvial fan sediments is exposed in the Rambla Galera which marks the upper limit of incision in the current fluvial system (Loc.6 on Fig.3.3B). The section is 19m thick and dominated by planar bedded and massive conglomerates of lithofacies (Gp/Gm) and minor sand beds (Fig. 3.13). The base of the alluvial fan sequence (base - 2.9 m) comprises thin beds of conglomerate and sand (<0.7 m thick). Sand beds are typically massive or weakly horizontally bedded (lithofacies Sm/Sh) and are rich in graphite and quartz grains. The conglomerate beds typically exhibit low angle planar bedding forming extensive gravel sheets (<8 m thick) or minor channelised deposits. The contact between sand and conglomerates is often highly erosional, preserving steep channel morphologies (photo 3, Fig. 3.13). The upper fan section is dominated by thick beds of conglomerate and sands (bed thickness 1-2 m). Conglomerate beds form stacked channels up to 4.6 m wide

by 1.7 m deep. The channels are infilled with fine to coarse grained gravels which display lateral accretion surfaces (photo 2, Fig. 3.13) often capped by coarse grained sand plugs of lithofacies Sm. Two palaeosol horizons are preserved in the upper 3m of the section which relate to soil development capping Filabres fan stage 1 or 2 of Harvey et al., (2003) (photo 1, Fig. 3.13). The conglomerate beds are rich in graphite schist with imbrication to the southwest indicating sediment inputs from the bounding sierras (e.g. Sierra de los Filabres).

The alluvial fan type section represents a large aggrading fan system dominated by fluvial deposits with major channel and minor sheet geometries (lithofacies Gp/Gm and Sm/Sh). These features are typical of the Filabres fan systems presented by Harvey, (1984) and Harvey et al., (2003), lacking the proximal debris flow deposits which are characteristic of proximal fan systems emanating from the Marchante ridge anticline (Harvey, 1984). The development of terrace level 3 alluvial fan units is analogous with fan stages 2 and younger of Harvey et al., (2003) based on correlations of palaeosols horizons and phases of soil development (Chapter 2, Section 2.4.1 for detail). The presence of palaeosols within the sections suggests pronounced periods of stabilisation during fan aggradation stages and highlights the significance of climatic cycles in the generation and delivery of sediments from the hillslope system (Harvey et al., 2003).

Section Name: Terrace level 3- Alluvial fan
Surface Elev: 456 mAHD
Location (base): E 0554518 N 4102266
Base-Rambla: 0m

Sedimentology: Base- 2.9m dominated by thinly bedded conglomerate and sand units. Sand beds are typically massive or weakly horizontally bedded and range in thickness from 0.2m to 0.6m. The conglomerate beds typically form small channel features that are up 1.5m wide by 0.6m deep, with sharp contacts with sand units preserving steep channel cuts. The upper section is dominated by thicker beds of conglomerate and sands (bed thickness 2-3m). Conglomerate beds form stacked channel features upto 4.6m wide by 1.7m deep. These channel features are infilled with fine to coarse grained gravels which display lateral accretion (lithofacies Gp) and are often capped by coarse grained sand plugs (lithofacies Sm).

2 paleosol horizons (hematite orange colour) are preserved in the upper 3m

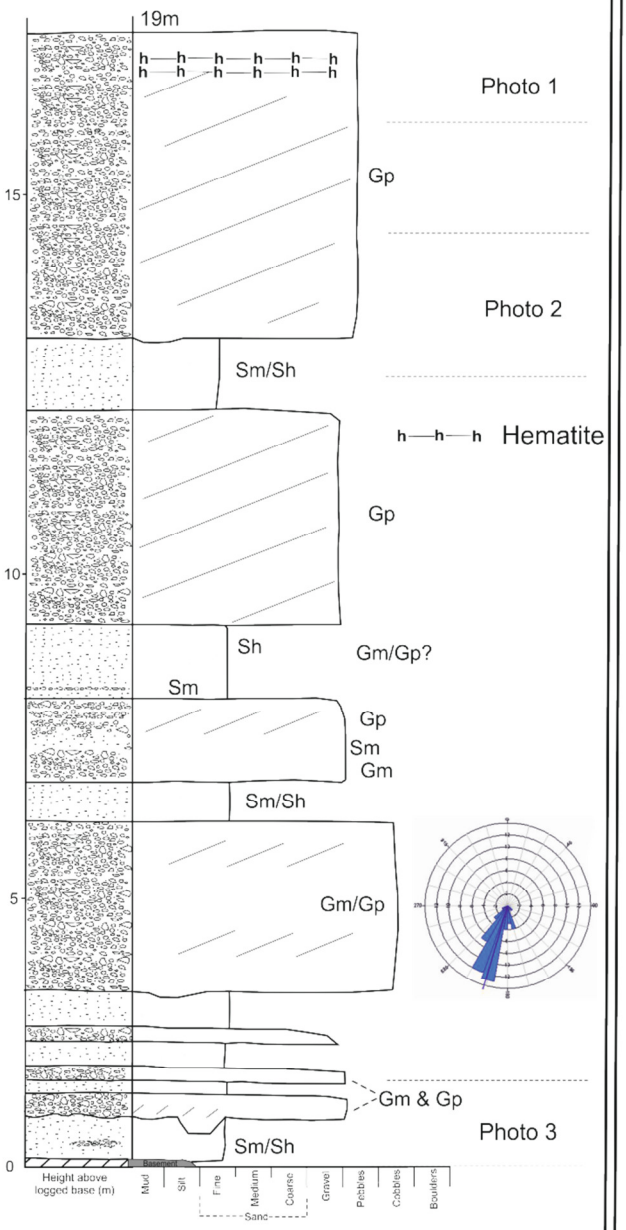

Sedimentary Log

Section Photographs

Photo 1

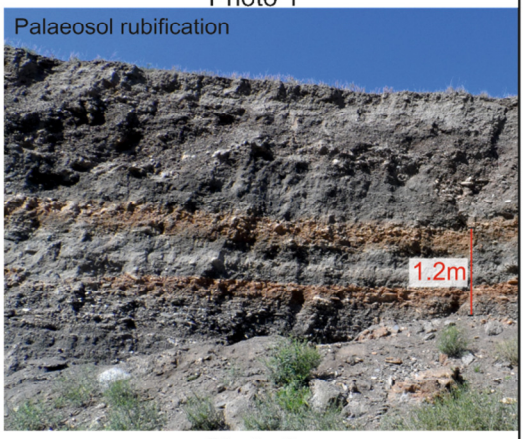

Photo 2

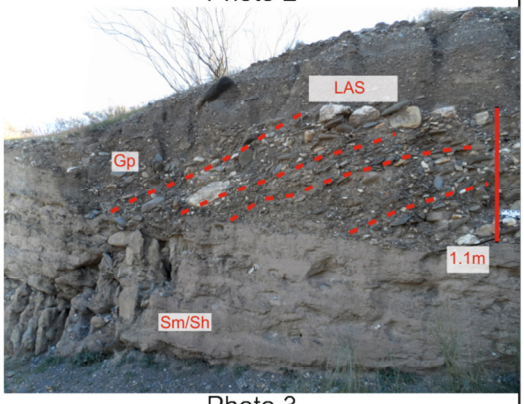

Photo 3

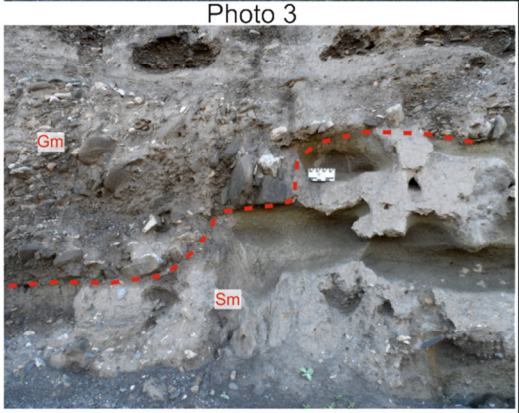

Figure 3.13 Sedimentary log detailing the structure and facies of terrace level 3 alluvial fan type section. Location of section can be found on Figure 3.3B marked as Location 6.

Section Name: Terrace level 3- River terrace **Location (base):** E 0550076 N 4097201
Surface Elev: 374 mAHD **Base-Rambla**: 21m

Sedimentology: Base of section comprises cobbles and boulders infilled with massive gravels. The main body of the section comprises fine to coarse grained gravels beds up to 1.1m thick which exhibit low angle (<15°) cross beds (Photo 1, Fig. 3.11). Small channels of <2m width by 0.5m depths are found throughout often fining upward to a sand. The upper conglomerate beds are calcreted to Stage III to IV which preserves the structure of individual gravel beds.

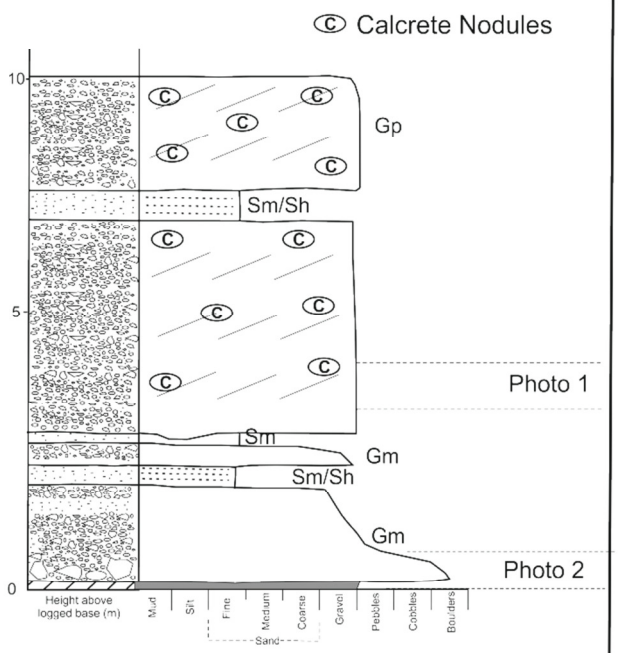

Sedimentary Log

Section Photographs

Photo 1

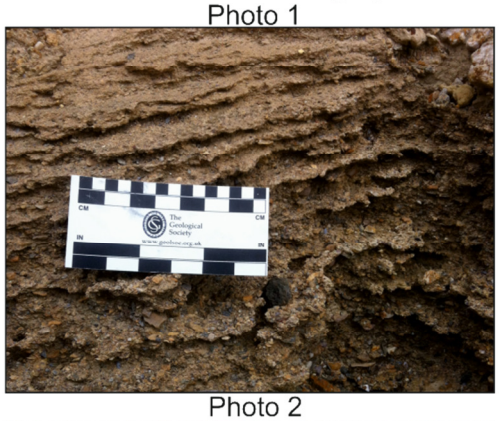

Photo 2

Photo 3- Channel cut into marls

Figure 3.14 Sedimentary log detailing the structure and facies of terrace level 3 river terrace type section. Location of section is presented on Fig. 3.3B marked as location 7. Note calcrete nodules formed insitu.

River terraces

Terrace level 3 river terraces are most common within the minor tributaries of the Tabernas Basin where fill sequences of the lower and upper lake are typically absent (e.g. Rambla Reinelo, Lanujar, Buho and Grillo). However when found together, the coarse grained terraces cap the lacustrine deposits. Although the sedimentology of individual terrace bodies is highly variable, a type section is presented here to highlight the shift to confined valley fluvial styles within the basin (Fig. 3.14). The type section for level 3 river terraces occurs in a natural cut in the Rambla Grillo (Loc.7 on Fig. 3.3B). The morphology of the section exhibits well defined valley margins cut into weak Tortonian marls with an incisional base 21 m above the current rambla (Photo 3, Fig. 3.14). The section is 10.1 m thick and extends laterally some 42 m. The sedimentology of the section is dominated by planar bedded conglomerates of lithofacies Gp with minor sand intercalations. The base of the sequence (0 - 2.3 m) is highly erosional and characterised by cobble to boulder sized clasts (D_{max} = 0.8 m) infilled with massive gravels (Photo 2, Fig. 3.14) which fine upward to massive/ weakly horizontal bedded sands. The main body of the section comprises fine to coarse grained gravels beds up to 1.1m thick which exhibit low angle (<15°) cross beds (Photo 1, Fig. 3.14). Channels of < 2m width by 0.5 m depth are found throughout often fining upward to a sand. The conglomerate beds are cemented by a Stage III to IV calcrete (Machette, 1985) which helps preserve the structure of individual gravel beds. Although variable within channels, flow imbrication is principally toward the south west.

The formation of well-defined valley morphologies cut into underlying sandstone and marl beds demonstrates the confinement of fluid flow events within the basin (Miall, 1996). The dominance of planar cross bedded conglomerates of lithofacies Gp within the river terrace type section likely represents deposition within longitudinal bar forms prograding within small fluvial channels (Miall, 1996; Pla-Pueyo et al., 2009). The stacking of small scale channels coupled with a high degree of basal scour indicates erosion at the base of beds and is typical of highly interconnected channels typical of a braided fluvial system (Miall,

1996). Deposition of cobbles and boulders at the base of section demonstrates a high transport capacity (i.e. ability of fluvial system to transport a coarse grained bedload), with major stages of deposition likely to occur during short duration - high intensity events (Lewis and Maddy, 1999). These interpretations suggest a transportation environment similar to the present day fluvial system, with bedload transportation under flash flood conditions. However, it is likely that sediment availability within channels was higher during terrace level 3 aggradations as evidenced by the characteristic choking and stacking of channels (Miall, 1996). The shift in clast imbrication towards the south-west indicates a transition from the north-south directions of flows evidenced in terrace level 1 and 2 deposits.

3.3.4 Terrace level 4

The abandonment of terrace level 3 was marked by a final period of incision within the Tabernas Basin (average incision of ~20m). At a basin scale dissection was pronounced and characterised by: (i) incision of lower and upper lake units in the Rambla Tabernas and Rambla de los Molinos (ii) the complete dissection of aggrading tributary systems in the Rambla Sierra and (iii) the abandonment of many level 3 drainage surfaces as a result of rapid headward incision (see abandonment meanders Fig. 3.10A). A brief climatic hiatus within the degradational stage could have facilitated the aggradation of terrace level 4 deposits (e.g. Younger Dryas); however, it is more likely that terrace level 4 deposits represent a minor depositional unit preserved within a broadly ongoing incisional fluvial regime. Terrace level 4 deposits are not extensive across the basin (Fig 3.3) and form localised accumulations of sediment on the inside of meander beds or along major tributary confluences. Typically, the sediment units are less than 3-4m thick and are often used for agricultural purposes when laterally extensive (Fig 3.15A). Incision into terrace level 4 units is most pronounced in the west of the basin (>7m in Rambla Tabernas, Fig. 3.15B) and decreases to the east to less than 1-2m (e.g. Rambla Buho and Rambla Benavides, Table. 3.6).

Table 3.6 Summary of morphological data for terrace level 4 landforms with reference to major basin drainages. A map of drainages is presented in Fig. 3.3B. Incisional depths are calculated to current drainage, however as base of terrace is at or below rambla level only max. Incision values are presented.

Drainage	Min. Elevation (mAHD)	Max. Elevation (mAHD)	Mean Elevation (mAHD)	Min. Thickness (m)	Max. Thickness (m)	Mean Thickness (m)	Max. Incisional Depth (m)
Rambla de Tabernas	225	375	302	<1m	7	3	7
Arroyo del Verdelecho*	267	276	271	<1m	8	3	8
Rambla de Lanujar	271	325	280	<1m	8	2	8
Rambla del Buho	350	423	374	<1m	6	2	6
Rambla de Reinelo	288	311	294	<1m	3	1	3
Rambla de Benavides	351	401	368	<1m	6	2	6
Rambla de los Molinos	346	369	355	<1m	8	4	8
Rambla Sierra	340	355	347	<1m	4	3	4

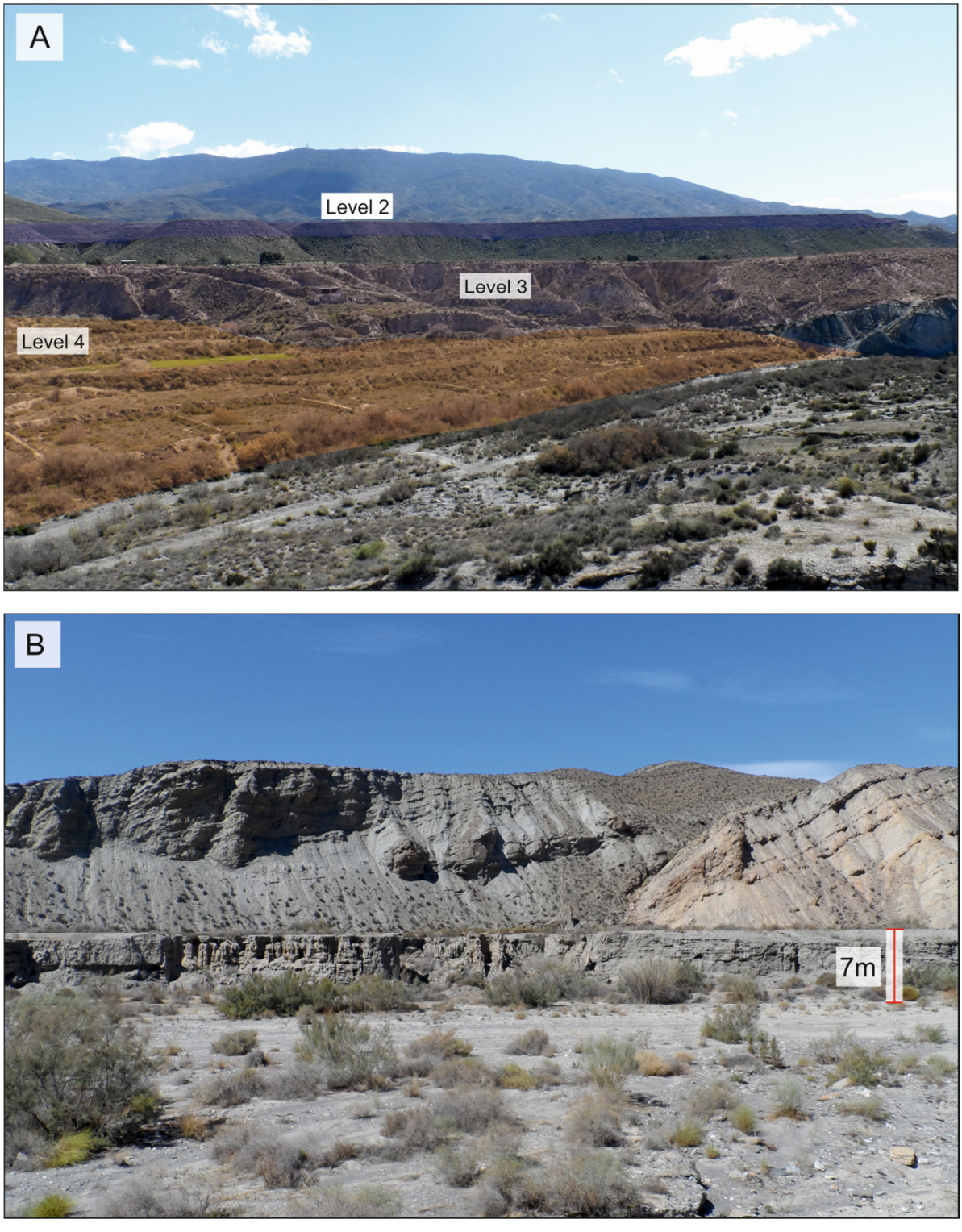

Figure 3.15 (A) Extensive deposits of terrace level 4 preserved in the confluence between Rambla Tabernas and Rambla Sierra. Surface is heavily disturbed from agricultural activity with the depositional base below the current rambla level (photo facing south UTM 30S 552538/4100756. (B) Typical incision into level 4 terrace in the west of the basin, note base of section is at or below current rambla level (photo facing north UTM 30S 547509/4094273).

The type section for terrace level 4 is located in the west of the basin where maximum incision occurs in the Rambla Tabernas (Loc. 8, Fig 3.3B). The section is 6.1 m thick with the base being at or below the current rambla level (Fig. 3.16). The sedimentology of the section can be separated in to a coarse grained basal unit and a fine grained upper unit. The base (0-3 m) is dominated by massive and low angle bedded conglomerates (lithofacies Gm and Gp) which are onlapped by horizontally bedded sands (lithofacies Sh). The conglomerates comprise cobbles and coarse gravels at the base which fine upward to a medium to coarse grained gravel. The upper gravels contain low angle cross beds and are imbricated obliquely to the section face. Bed thickness is <1 m with no visible channel forms. The sand beds that overlie the conglomerates form extensive horizontally bedded units up to 0.4 m thick. The contact between the sand and conglomerate beds is erosional and typically planar. The upper fine grained unit (3 – 6.1 m) comprises massive to weakly bedded silts and muds of lithofacies (Fm and Fl; Fig. 3.16). The beds are up to 0.5 m thick and are often interbedded with thin sand beds (<0.2m). Dewatering structures up to 0.3 m in size and laterally persistent over 3 m are found in the lower 1 m of the silt beds (photo 1 Fig. 3.16). Floating gravel clasts and carbonate nodules are common in the upper 1.5 m of the section. The contact with the underlying sand facies is erosional with minor scour infill noted at the base of the fine grained units.

The planar cross bedded conglomerates of lithofacies Gp exposed at the base of the level 4 section likely represent deposition within longitudinal bars formed within small fluvial channels under lower flow regimes (Miall, 1996; Pla-Pueyo et al., 2009). The onlapping horizontally bedded sand facies (Sh) represent a transition to planar bed flows and higher flow regimes with deposition as channel fills (Lewis and Maddy, 1999). The massive and laminated fines of lithofacies (Fl/Fm) which make up the upper 3 m of the section could represent a shift to overbank conditions of deposition, or deposition during waning floods. Minor sand sheets deposits (sh) interbedded within the fine grained units could support deposition under overbank conditions after major flow events (Pla-Pueyo et al., 2009). The

variability in facies indicates a highly mobile fluvial system such as a braided fluvial system, characterised by a coarse grained sediment supply and poorly developed laterally migrating channels (Miall, 1996). Sediment transport would have been similar to those of the current fluvial system with the transportation of coarse grained sediment during short lived high intensity flow events. The deposition of sand units could represent a shift to lower energy flow regimes within the active channel with the absence of coarse grained facies (Lewis and Maddy, 1999), or could simply record a shift in the availability of coarse grained materials within the fluvial network. The final stages of sedimentation likely occurred as overbank or flood plain deposits (Parkash et al., 2009), marking the migration of the active channel away from the type section and the resultant preservation of its deposits.

3.4 Summary: Tabernas Basin evolution

The results of morphological and sedimentological investigations presented in this chapter identify four principal terrace levels across the Tabernas Basin. Variations in the depositional environments and the intensity/duration of degradation between aggradational stages highlight the dynamic evolution of the Tabernas Basin throughout the Quaternary, as summarised in Figure 3.17. The earliest stage of deposition (terrace level 1) in the basin occurred with the aggradation of extensive alluvial fans forming off the bounding sierras into the basin centres. Although limited by exposure quality, the sediments of the terrace level 1 terraces show that the fan surfaces were dominated by radially dispersive fluvial processes with the delivery of sediment as extensive unconfined sheet flows in the early stages which became weakly channelised with time. The basin then underwent an extensive period of degradation (degradation phase 1; Fig 3.17) which lead to the abandonment and isolation of terrace level 1 deposits in the east of the basin. The timing of onset for this degradational stage is poorly constrained.

Section Name: Terrace level 4 **Location (base):** E 0550076 N 4097201
Surface Elev: 231 mAHD **Base-Rambla**: 0m

Sedimentology: Base of section comprises massive gravels exposed at current rambla level. The basal gravels are onlapped by rounded to subrounded cobbles which fine upward to fine to medium gravels (0.4 m -1.4 m). The gravel units are massive at the base of the section and form low angle cross beds in the upper 1m. Gravel units are well imbricated and rich in graphite schist, quartzite and mica schists. The lower gravel units are in turn onlapped by horizontally bedded medium to coarse grained sands (photo 2). The sand beds are < 0.4m thick with frequent thin gravel lenses.

The upper 3m of the section comprises massive silts/muds beds up to 50cm thick. The lower units contain dewatering structures upto 40cm in size and laterally persistent (photo 1). The upper 1.5m of the section becomes increasing calcreted (Stage II-III nodules). Floating gravel clasts are often found within the massive beds.

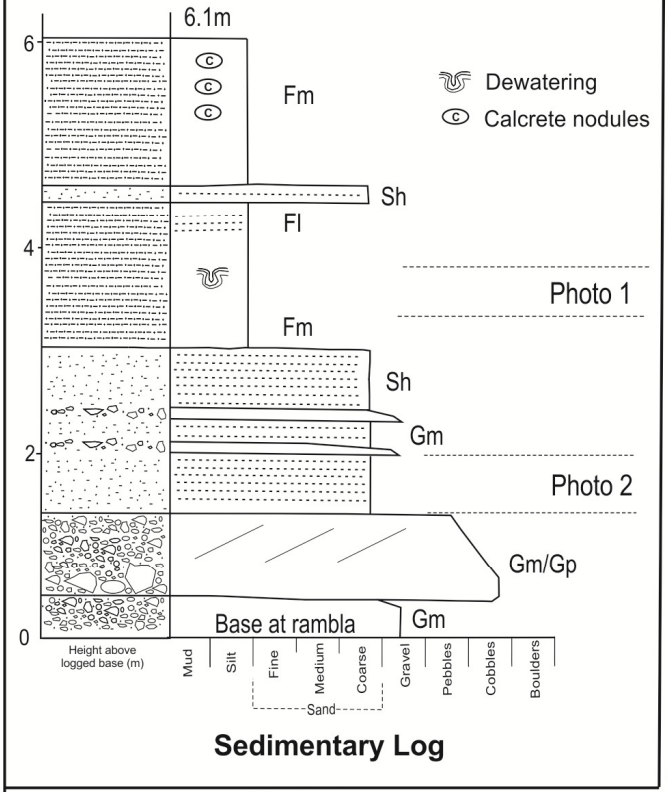

Sedimentary Log

Section Photographs

Upper Section

Photo 1

Photo 2

Figure 3.16 Sedimentary log detailing the structure and facies of the terrace level 4 type section. The location of the type section can be found on Figure 3.3B marked as location 8.

During the first incisional phase, base levels would have been lowered on average ~40m across the basin prior to the onset of the terrace level 2 aggradation. Depositional environments for terrace level 2 were dominated by large coalescent alluvial fan bodies forming off the bounding sierras, much like those preserved in the east of the current day basin. Fan surfaces would have extended into the present day basin centre and were dominated by fluvial processes with channel and sheet geometries preserved in sections across the basin. During deposition, it was likely that groundwater calcretes were forming at the base of level 2 sediment bodies, with subsequent stabilisation of the fan surfaces by pedogenic processes during periods of high aridity (Nash and Smith; 1998, 2003). Isolated travertine formation was also active in the south west margin of the basin; however, the preservation of other travertine units formed onto or within terrace level 2 deposits is limited by the amount of post-depositional incision which ensued.

Post terrace level 2 aggradation the basin experienced the most substantial Quaternary degradational stage (degradation phase 2; Fig 3.17). Again unknown in timing, this degradation period would have dramatically lowered base-levels and promoted the incision of basin drainages on average ~60m. In regions of high connectivity (i.e. along the available drainage and major tributaries), the pediment surfaces of terrace level 2 were fully dissected and large volumes of accommodation space were created (~80m of incision recorded along the Rambla Tabernas). In the east of the basin, this accommodation space was infilled by large aggrading fan systems (fan stages 1-4 of Harvey et al., 2003) which remain undissected to the present day. In the west of the basin, tectonic deformation along a major anticlinal feature blocked the axial drainage and promoted the back ponding of fine grained fluvial sediments typical of terrace level 3 in the basin centres (i.e. lower lake sediments, Harvey et al., 2003). The broad back ponding of sediments could relate to an ongoing mechanism of tectonic sag in the basin centre.

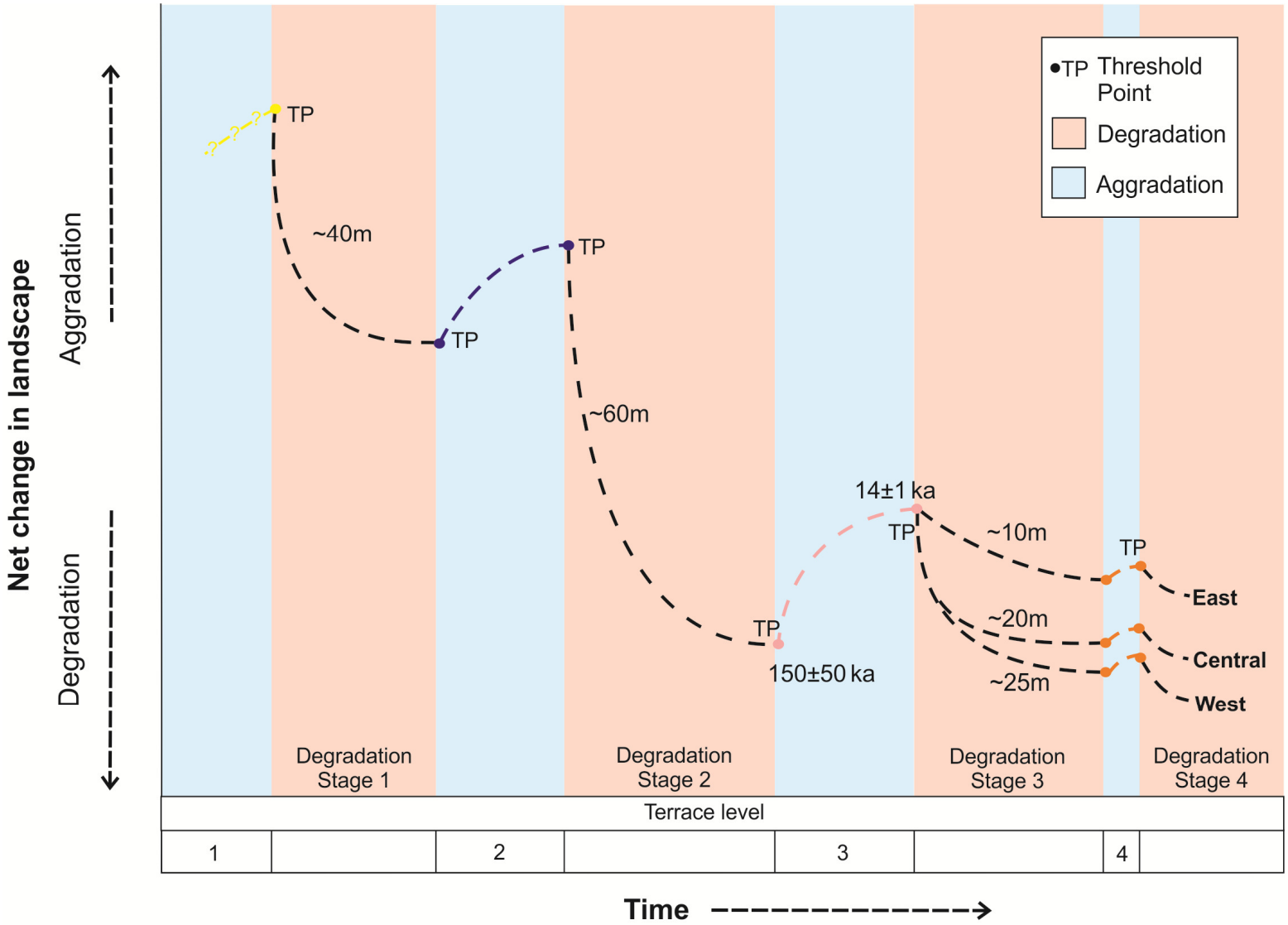

Figure 3.17 Conceptual landscape evolution model for the Tabernas Basin showing major phases of Quaternary aggradation and degradation. Measurements of aggradation/degradation are based on terrace record; however, the temporal development of the basin is largely unknown other than 2 dates presented for terrace level 3.

At the time of lower lake formation, the hillslopes were aggrading along the northern and southern basin margins with the formation of coarse grained fluvial terraces (e.g. hillslope deltas of Alexander et al., 2003). Aggradation around the present day Rambla Sierra blocked the upper reaches of the axial system (present day Rambla los Molinos) and promoted the formation of the upper lake system from at least 150 ± 50 ka (Delgado et al.,1993; Harvey et al., 2003). It was likely that aggradation was ongoing to at least 14±1 ka as dated in the lower lake section (Alexander et al., 2008), with a progressive shift to confined fluvial conditions in the final stages of development. Travertine formation at Las Salinas (Section 2.4.5, Chapter 2 for detail) was initiated at some point during this aggradation stage.

A third degradation stage occurred in the Late Pleistocene / Early Holocene as marked by the dissection of third level deposits in the west and central regions of the basin (degradation phase 3; Fig 3.17). Across the basin, incision was on average ~20m increasing in the west towards the confluence with the Río Andarax (>29m in western reaches of Rambla Tabernas). The rapid incision of drainages in the west of the basin led to the dissection of lower lake units and the abandonment of the third level terraces which preserve multiple abandonment meanders and travertine encrusted surfaces (Fig. 3.10A). Travertine formation was pronounced in the isolated meander features with precipitation ongoing to the present day (Mather and Stokes, 1999). The final stage of incision also promoted the formation of extensive badlands in the west of the basin, such as in El Cautivo (stage C to stage B transition in El Cautivo, Alexander et al., 2008). The formation of terrace level 4 deposits could have occurred during a brief climatic hiatus within this third incisional stage (e.g. Younger Dryas; degradation phase 4; Fig 3.17), or as a result of favourable preservation conditions within the incising fluvial system. The current fluvial system records ongoing incisional with trends similar to that of the terrace level 4 (e.g. focused in the west of the basin), which could support this theory of ongoing incision post terrace level 3 abandonment.

The stratigraphy presented, summarised at a basin scale in Figure 3.18, forms the underlying basis for the development of numerical and conceptual interpretations presented in Chapters 5, 6 and 7. An underlying aspect of the stratigraphy is the lack of temporal constraint presented to date. Two absolute dates are presented for terrace level 3 landforms, however, these data are limited when assessing patterns of basin evolution over a range of spatial and temporal scales. This lack of chronological control forms the basis for the application of optically stimulated luminescence dating presented in Chapter 4.

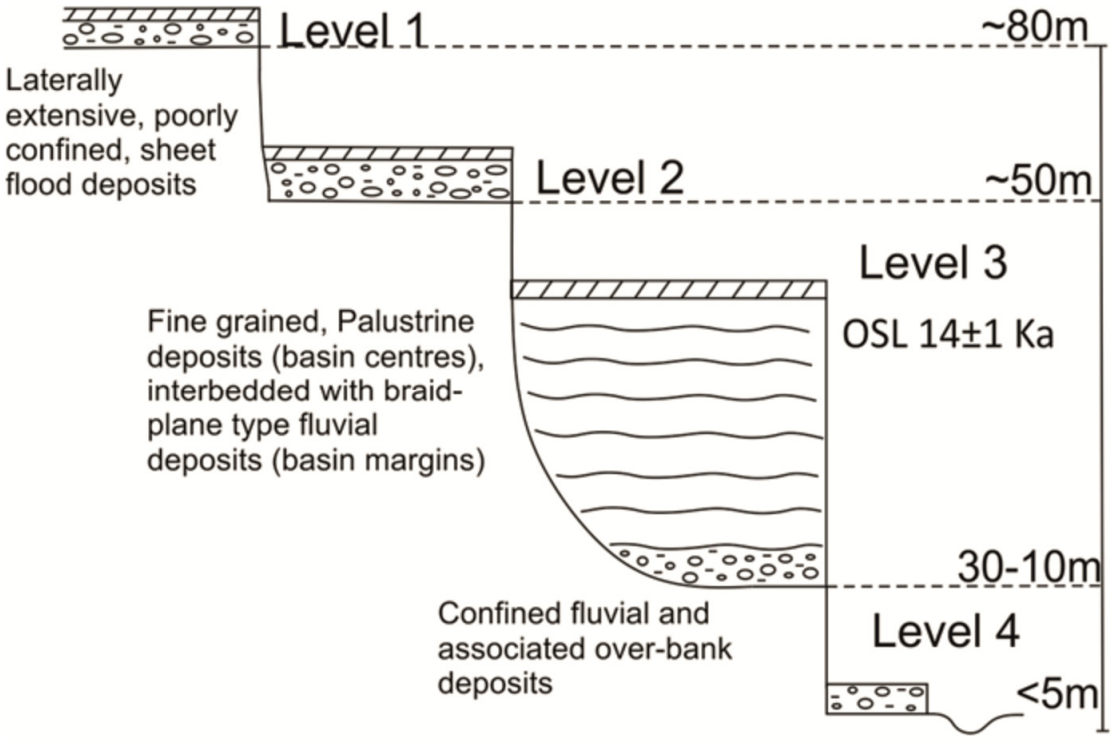

Figure 3.18 Quaternary basin stratigraphy of the Tabernas Basin, modified from Harvey et al., 2003.

Chapter 4

4.1 Optically Stimulated Luminescence (OSL) Dating

Quaternary landscapes often contain important paleoenvironmental information that archives periods of response to extrinsic (e.g. tectonics, climate and sea-level change) and intrinsic drivers (e.g. river capture, internal adjustments etc) over a range of spatial and temporal scales (Thiel, 2011). In order to gain insights into the temporal scales of landscape change and accurately reconstruct paleoenvironmental records, reliable and comprehensive absolute chronologies are required (Buylaert et al., 2012). However, in the semi-arid / arid setting the application of conventional radio carbon dating methods is limited by its upper dating capability and is often impeded by the lack of datable materials as a function of poor preservation (Macklin et al., 2002).

Across the Almería region, a lack of chronological control has occurred as a result of the poor preservation of organic materials, coupled with complications in the application of absolute dating methods (e.g. poor characteristics of materials for luminescence purposes) (e.g. Harvey, 1987; Harvey and Wells, 1987; Mather, 1993; Harvey, 2003; Maher, 2005; Stokes et al., 2007). The general absence of age estimates has promoted the interpretation of Quaternary landscapes based on the principals of relative stratigraphy via methods of lithostratigraphy, soil development and further altitudinal correlations between landform groupings (Harvey et al., 1995; 2003; Mather; 2002; Stokes et al., 2002; Miekle, 2008). However, since the late 1990's increased focus has been placed on the application of new and improved absolute dating methods across the region. At the time of writing there exists 48 U/Th dates, 23 OSL dates, 7 accelerator mass spectrometry (AMS) dates, 7 cosmogenic exposure dates and 1 electro-spin resonance date in the published literature for the Tabernas, Sorbas, Carboneras and Vera basins (Fig. 4.1; Wenzens, 1992; Kelly, 2000; Candy et al, 2005; Maher, 2005; Miekle, 2008; Schulte et al., 2008; Ilott, 2013). Although the chronologies from the Almería region are not as extensive as most northern European rivers, such as the Thames (Maddy et al., 2001) or the Rhine (Boenigk and Frechen, 2006; Frechen

et al., 2010), these dates have been vital in the interpretation of landscape responses to extrinsic and intrinsic mechanisms over Quaternary timescales (Kelly, 2000; Stokes et al., 2002; Candy et al, 2005).

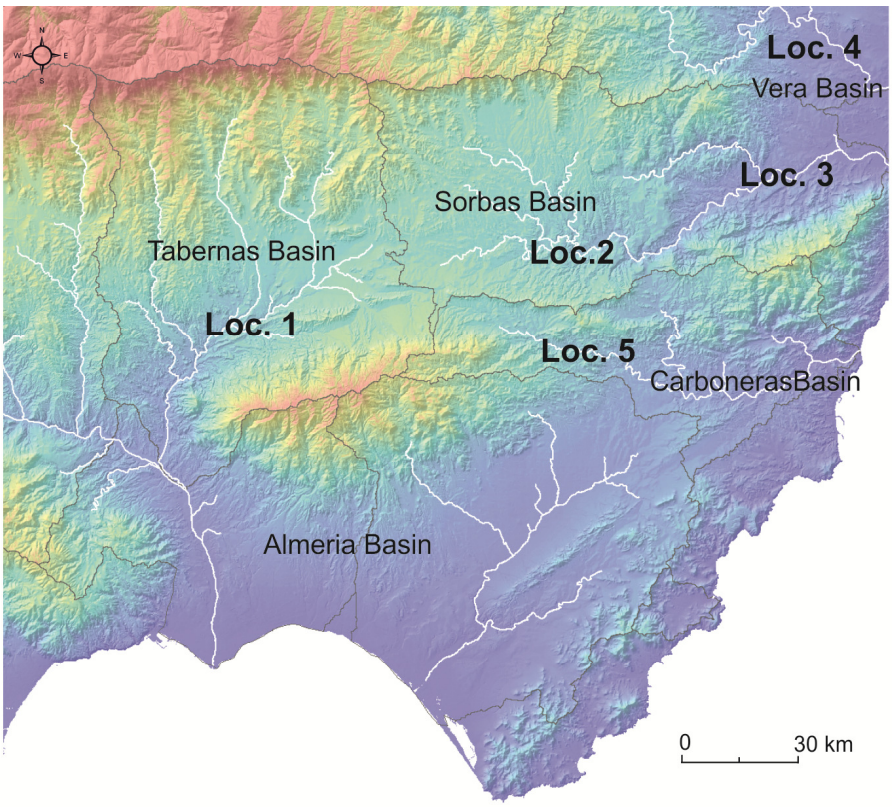

Location	Basin	Dating Method	Author
1	Tabernas	OSL & Radio Carbon	Nogueras et al., 2000; Mather, unpublished
2	Sorbas	Cosmogenic exposure & U/Th dating	Kelly et al., 2000; Candy et al., 2004; Ilott,2013
3	Sorbas / Vera	OSL, ESR & U/Th dating	Wenzens, 1991; Schulte et al., 2002; 2008
4	Vera	OSL	Miekle, 2008
5	Sorbas / Carboneras	OSL	Maher, 2005

Figure 4.1 Location of absolute age values in the published literature for the Almería region. The table details the methods applied and the associated authors.

To present, the application of dating methods in the Tabernas Basin has been limited, comprising of:

- One AMS date of between 22 - 33 ka derived from colluvial sediments in the El Cautivo Badlands (Nogueras et al., 2000);
- One optically stimulated luminescence (OSL) date of 14 ± 1 ka from the upper part of the lower lake sequence presented by Harvey et al., (2003);
- One relative age of 150 ± 50 ka from the upper lake sequence presented by Ruiz Bustos and Martín Algarra, (1991) and Delgado et al., (1993), quoted by Harvey et al., (2003) based on the correlation of rodent species (i.e. rodents teeth) to climatic chronologies generated for the Betic Cordillera.

The reliability of the age estimations is questionable. For example, sample contamination was identified in the AMS date (Alexander et al., 2008) and no analytic methods or data presented for OSL date, meaning that the reliability of the age estimation (which is presented as unpublished data by Alexander et al., 2008) cannot be scrutinised. The errors on the relative age from the upper lake sequence are large, and the correlations between the climatic chronologies are weak (Delgado et al., 1993 for detail). Furthermore the stratigraphic relationships between all age estimations are poorly defined at a basin scale.

This study aims to generate new absolute dates for the Tabernas Basin and to contribute to the greater Almería record in order to constrain temporal rates of landscape change over Quaternary timescales. Focus is placed on the use of OSL dating as a reliable absolute dating method which has been widely used in the Quaternary fluvial environment (see Rittenour, 2008 for review). Across the Almería region, OSL dating has been applied in few Quaternary landscape studies with mixed success (e.g. Maher,2005; Miekle, 2008; Schulte et al, 2008). Studies in the Vera Basin by Miekle (2008) (Loc. 4 of Fig. 4.1) adopted OSL methods using both quartz and K-feldspar grains to date fluvial and marine terraces. Age estimates derived from K-feldspar grains were taken as reliable (yet unpublished) with estimates derived from quartz grains commonly disregarded due to underestimations against

K-feldspar values. Maher (2005) attempted to date fluvial terrace deposits of the Rio Alias by methods of quartz OSL (Loc. 5 of Fig. 4.1). Two samples were analysed applying single grain techniques. Unfortunately, one sample displayed unfavourable OSL characteristics with both: (i) a low sensitivity in the number of grains that emitted a measureable OSL signal, and (ii) dose-dependent changes in sample sensitivity as a result of laboratory measurements (i.e. changes in the OSL characteristics of grains due to multiple stages of laboratory heating and irradiation; Wintle and Murray, 2006). Schulte et al., (2008) also adopted the use quartz and K-feldspar grains in the dating of travertine cemented river terraces in downstream reaches of the Rio Aguas system (Loc. 3 of Fig. 4.1). Of sixteen samples measured, only nine maximum age estimates (i.e. ages of unknown error above the true age value) were obtained from quartz grains due to incomplete resetting of the OSL signal during grain transportation and deposition.

This study aims to develop the methods of OSL application in the Almería region based on recent advances in the dating methodology (e.g. increased precision of age estimates adopting a combined quartz and K-feldspar methodology; Murray et al., 2012) combined with a full appreciation of the geomorphological evolution of the basin (e.g. basin wide terrace sedimentology and stratigraphy). Based on the findings of previous studies, both quartz and K-feldspar dosimeters are used. However, care is taken to address the issues of incomplete signal resetting and signal reproducibility in samples. Measurements are also conducted on a large sample inventory in an attempt to gain a more complete understanding of the luminescence characteristics of the region.

The following chapter details the approach used in the application of luminescence dating in the Tabernas Basin. The principals of the method applied (e.g. analytical procedure, dosimeter type, and dosimetry measurements) are discussed with regard to how they informed methods of sample acquisition (i.e. the sampling strategy) and subsequent laboratory analysis. A synthesis of the results generated is then presented for the stratigraphy developed in Chapter 3. Finally, the age estimates from the Tabernas Basin are

qualitatively compared and contrasted with chronologies derived from other sedimentary basins in the Almería region. This correlation is conducted in order assess the temporal patterns of landscape evolution at both a local (basin) and regional scale. Note that discussions of principal landscape forcing mechanisms are not explored in detail in this chapter; these interpretations are developed in detail in Chapters 6 and 7.

4.2 Fundamentals of luminescence dating

Optically stimulated luminescence is a method of determining the burial age of quartz or feldspar mineral grains based upon principles of radiation and excitation within crystal lattices, steming from the fact that imperfections in a crystal lattice have the ability to store ionizing energy (Aitken, 1998). The fundamentals of luminescence dating exploit naturally occurring ionising energy, sourced from the decay of radioactive isotopes present in the rocks and sediments that make up the Earth's surface (Huntley et al., 1985). When buried, inorganic minerals such as quartz and feldspar have the ability to trap and store energy in the form of freed electrons generated by the destabilisation of atoms within a host material (signal accrual stage Fig. 4.2). These freed electrons occupy defects or holes in the mineral crystal lattice referred to as electron traps. When exposed to sunlight or excessive heating (>~300℃), electrons stored within electron traps absorb energy and become unstable. The destabilisation of electrons from their meta-stable stores leads to recombination in luminescence centres and the resultant release of energy in the form of a single photon of light termed luminescence (Aitken, 1992).

For the purposes of luminescence dating, the natural effects of sunlight or excessive heating can be reproduced in the laboratory environment. This is achieved using either thermal or optical stimulation methods; with the release of energy termed thermoluminescence (TL) if stimulated by heating, or optically stimulated luminescence (OSL) if stimulated by light. In both instances, the measurement of luminescence signal generated from a grain (or a number of grains) is recorded using a photomultiplier housed within an OSL reader. The energy to which the photomultiplier is exposed is controlled by a series of

coloured filters, as dependent upon the mineralogy of grain being measured (see Figure 10 of Duller, 2008a). The amount of energy produced (the natural luminescence signal) is related to the total amount of radiation received during burial, referred to as the burial dose. In the laboratory, equivalent dose (D_e) estimates are made in order to best represent the burial dose. Measurements of D_e are made in the unit of absorbed radiation the gray (Gy). If measurements of the rates of radiation emission or absorption are known for the burial environment over a fixed period (per year), referred to as the dose rate (D), the depositional age for the sample can be determined by simply dividing the equivalent dose by the dose rate (Fig. 4.3; Duller, 2008a).

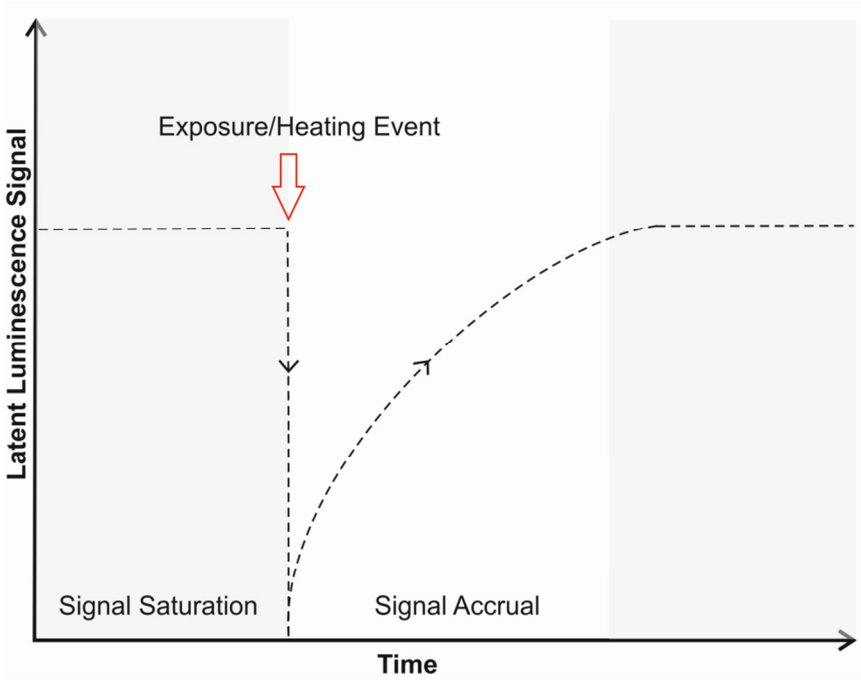

Figure 4.2 Luminescence signal growth curve showing the exponential growth of luminescence signal with time.

Key to the luminescence procedure is the assumption that all of the unstable energy (electrons) stored within a mineral grain is released upon exposure to excessive heating or sunlight (exposure / heating event Fig. 4.2). This process is termed ‘bleaching’ or ‘zeroing’, whereby the metaphorical electron clock of a mineral grain is reset to zero. In nature, the phenomenon of bleaching occurs most commonly upon exposure to sunlight during periods

of grain transportation and deposition. However, the resetting of natural signals can also be triggered by excessive heating as associated with natural (e.g. wildfires) or human activities (e.g. setting of pottery or fires for domestic purposes; Wintle, 2008). After signal resetting the electron clock of a grain has been reset to zero. Upon re-burial, zeroed grains start to absorb electrons again and the luminescence cycle is repeated (signal accrual stage in Fig.4.2).

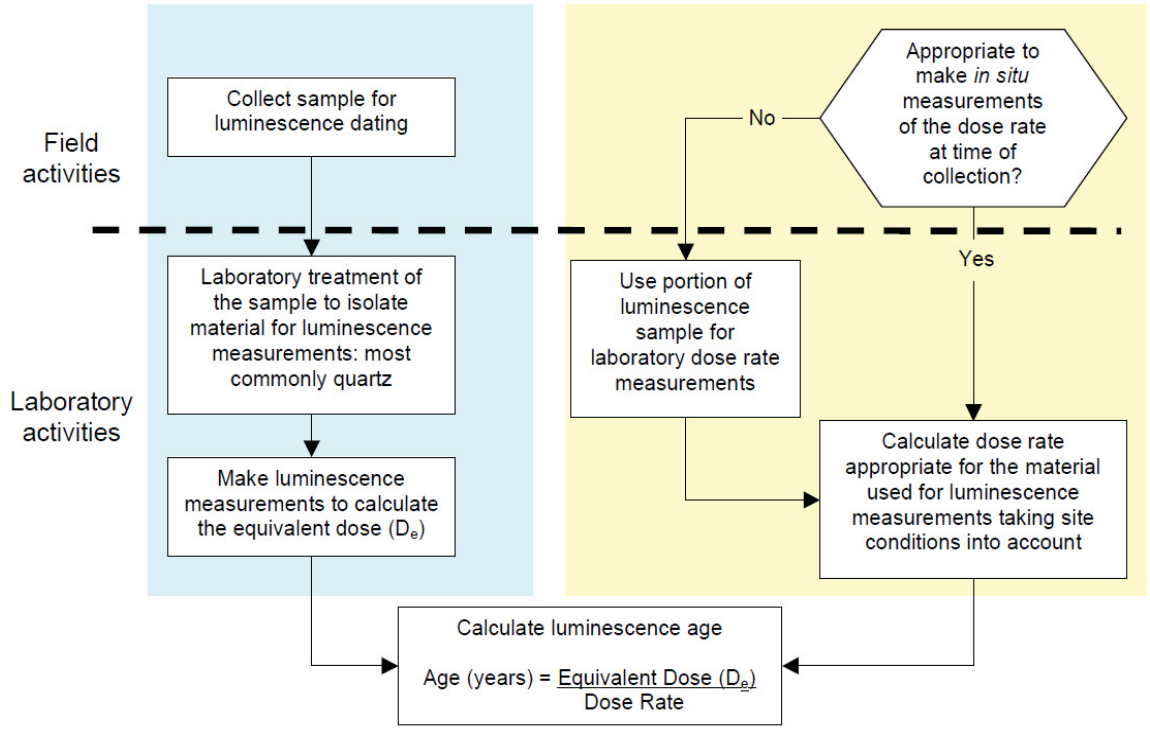

Figure 4.3 Flow chart showing procedures in the measurement equivalent dose and dose rate data for calculations of OSL ages, from Duller (2008a).

As summarised in Figure 4.4, the probability of incomplete signal resetting is high in fluvial or colluvial depositional settings due to variability in grain transportation times and variable conditions of deposition (e.g. water depth and clarity), which both affect resultant exposure times (Singarayer et al., 2005). Locally, incomplete signal resetting has been evidenced in the Vera Basin when applying OSL methods in the dating of fluvial deposits (e.g. Schulte et al.,2008). Incomplete signal resetting commonly leads to age

overestimations, therefore extensive focus is placed on assessing this fundamental aspect of the dating procedure throughout this study.

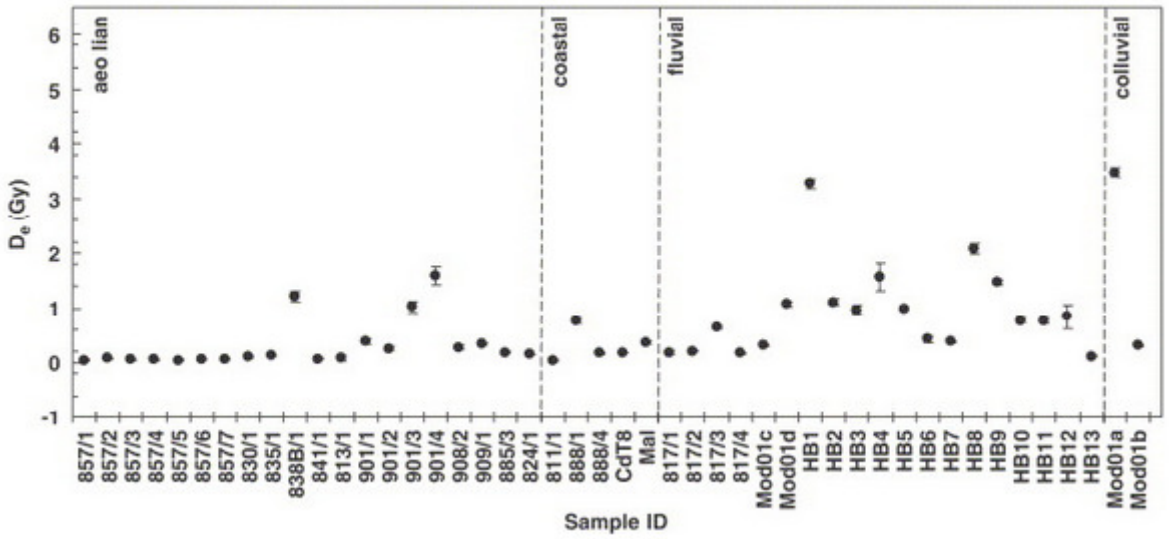

Figure 4.4 Summary of residual dose values measured from 46 modern analogue samples obtained from a range of depositional environments, Taken from Singarayer et al., (2005). Note increases in residual doses in samples obtained from a fluvial and colluvial setting.

4.3 Determination of equivalent dose values

It is established that measurements of equivalent dose (D_e) can be made using either thermal or optical stimulation methods. However, the analytical procedure applied in the generation of D_e values from either method of stimulation can vary significantly. Principally, one chooses to adopt either an additive dose or regenerative dose procedure (Murray and Wintle, 2003). In this study, regenerative methods are applied as standard. However, it is important to highlight why this decision was made. In the following sections (4.3.1 to 4.3.3) the general approaches of both procedures are presented with an overview of why the regenerative dose procedure has become favoured in standard luminescence practice.

4.3.1 Additive Dose Procedure

In the additive dose procedure a sample is initially separated into a number of subsamples (aliquots) for measurements of either: (1) the natural D_e, or (2) natural D_e with the addition of a laboratory dose, which is added as sequentially higher known amounts of

beta irradiation prior to the measurement stage. Laboratory irradiation effectively acts to reproduce the effects of natural ionising radiation that increases with exposure time during the burial period. Prior to any D_e measurements, all of the aliquots (natural and laboratory irradiated) are subjected to a phase of heating, termed the preheat. The preheat aims to remove any electrons stored in unstable electron traps which can be present prior to dose measurements. Natural and laboratory aliquots are then measured at fixed temperatures and durations in order to generate D_e estimates (Walker, 2005).

Dose estimates measured from laboratory irradiated aliquots (natural signals plus an additive dose) are plotted against the known given dose, calculated by dividing the known irradiation time by the known irradiation rate of the individual OSL reader (machine dose rate). The signals measured from the natural aliquots are also plotted against the irradiated aliquots but with no correction for additional doses. The relation between the natural and laboratory irradiated points is then fitted with a linear or exponential function in order to generate a dose response curve. The dose response curve effectively describes the growth of the luminescence signal within grains for the measured sample (Fig. 4.5A) (Walker, 2005). To determine an estimate of the natural equivalent dose (D_e) the additive growth curve is extrapolated to the dose axis (x-axis), as shown in Figure 4.5A.

4.3.2 Regenerative Dose Procedure

In the regenerative procedure all of the aliquots from a sample are measured for their natural D_e signals prior to any stages of laboratory irradiation. All of the aliquots are then subjected to sequential stages of increased laboratory irradiation in order to develop a dose response curve (Fig. 4.5B). Like in the additive dose procedure, the aliquots are subjected to a primary phase of preheating to remove unstable electrons from shallow or unstable electron traps. However, in the regenerative procedure the dose response curve is formed by the interpolation of measured luminescence values between the laboratory induced points (Murray and Wintle, 2000). D_e values are then calculated by interpolating the initial natural

signals (labelled ‘N’ on *y*-axis Fig. 4.5B) onto the dose response curve as shown on Figure 4.5B.

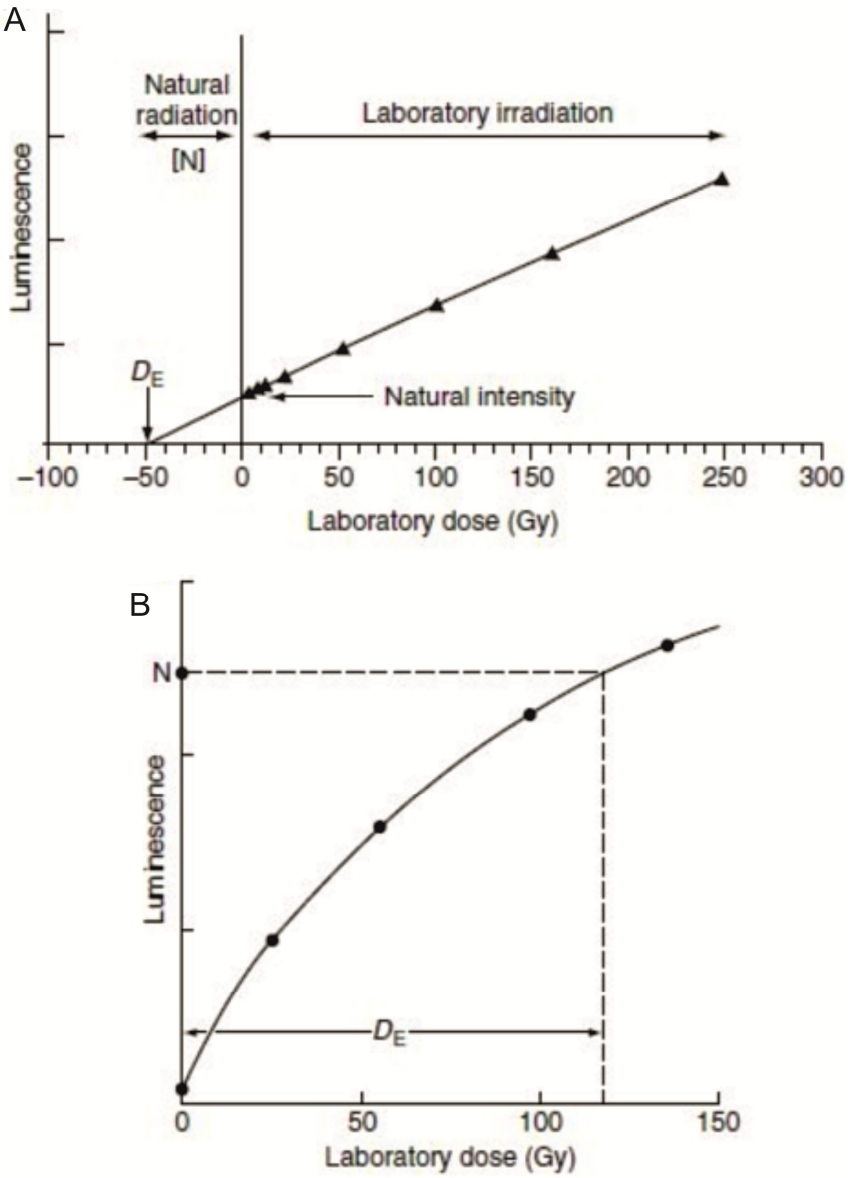

4.5 Dose response curves modelled using the additive dose (A) and regenerative dose (B) methods. In both, the DE value or the natural luminescence signal for the sample are represented in grays (Gy). Taken from Walker (2005) and references therein.

The major differences in procedures is that in regenerative methods D_e estimates are derived from each of the aliquots used, whereas in additive methods numerous aliquots are needed to produce a single D_e estimate. Furthermore in the regenerative dose procedure,

samples are not separated into aliquots for natural or laboratory purposes, but the same aliquots are used throughout. This reduces the amount of sample needed for measurements and also allows for the identification of changes in the luminescence signals within aliquots as a result of the laboratory procedure (sensitivity changes).

4.3.3 Procedure Selection

The selection of analytical procedure for this study was dependent upon a number of factors such as: inferred age, sensitivity changes, the amount of sample available, and the availability of reader/machine time. The significant increases in laboratory irradiation time (especially when dating older samples > 20 Ka) and sample amount required in the additive procedure was a major limitation and promoted the use of regenerative methods. Regenerative methods were also favoured due to the applicability of the single-aliquot regenerative (SAR) dose protocol, as proposed by Murray and Roberts (1998). The SAR protocol is a typical regenerative method (example sequence presented in Table 4.1) with the addition of a fixed radiation dose, termed the test dose, applied in the second stage of the measurement sequence (steps 5-7, Table 4.1). The test dose allows for the assessment and correction of sensitivity changes at all stages of testing (Murray and Wintle, 2000).

The SAR method was also favoured in this study as it can be applied in the appraisal of the following key factors of dating method (as summarised from Wintle and Murray, 2006):

- Dose recuperation, which tests the underlying assumption that no luminescence signal should be produced by a grain that has received no irradiation dose. This is tested by measuring the luminescence signal from a grain that has been completely reset under laboratory conditions using solar simulators over long bleaching durations. If the assumption holds true, the measured luminescence signal should be zero, however small signal increases can again occur as a result of recombination of electrons from deeper traps (typically <1-2 Gy). This stage of electron recombination is thought to be stimulated as a function of increased sensitivity of grains as a result of multiple stages of laboratory heating and irradiation;

- Thermal transfer, which is the apparent increase in luminescence signal associated with the recombination of electrons from deeper traps in a grain when subjected to higher preheat test temperatures. Thermal transfer is assessed by means of a preheat plateau test, where a range of D_e values is derived from a sample using incrementally higher preheat temperatures (160°C - 300°C). The preheat plateau test is used to define a optimum preheat temperature that does not result in markedly higher or lower D_e values;
- Signal reproducibility, which measures the ability of a grain to give reproducible D_e values. Signal reproducibility is measured using the dose recovery test. In the dose recovery test a sample is initially run using the standard SAR protocol. The sample is subsequently bleached and irradiated with a known laboratory dose close to that of the natural D_e measured in the first cycle of measurements. The sample is then run again using the SAR protocol to determine a secondary D_e value. The difference between the between the natural D_e and reproduced D_e values should be close to unity, hence evidencing the capability to make reproducible measurements under laboratory conditions;
- The significance of incomplete bleaching, where variations in the measured D_e values occur as a result of poor signal resetting in grains during transportation/deposition. Incomplete bleaching can be identified by scatter in D_e values and further is investigated using small aliquots or single grain experiments.

Table 4.1 Outline of the SAR OSL and post-IR IRSL protocols utilised in this study, following Murray and Wintle, 2003 and Buylaert et al. 2009, respectively.

Step	Quartz		K-Feldspar	
	Treatment	Observed	Treatment	Observed
1	Dose		Dose	
2	Preheat (260°c for 10 s)		Preheat (320°c for 60 s)	
3*	Blue Stimulation (125°c for 10s)	L_x	Infrared Stimulation (50°c for 100s)	$L_{x\ IR50}$
4	-		Infrared Stimulation (290°c for 100s)	$L_{x\ IR290}$
5	Test Dose		Test Dose	
6	Cut Heat (220°c)		Cut Heat (280°c)	
7*	Blue Stimulation (125°c for 40s)	T_x	Infrared Stimulation (50°c for 100s)	$T_{x\ IR50}$
8	-		Infrared Stimulation (290°c for 100s)	$T_{x\ IR290}$
9	Blue Stimulation (280°c for 40s)		Blue Stimulation (280°c for 40s)	
10	Return to Step 1		Return to Step 1	

* For quartz samples an additional step can be added to assess feldspar contamination notably infrared stimulation at 125℃ for 100s

4.4 Dosimeters in OSL Dating: Quartz vs. Feldspar

It is well established that quartz and alkali feldspars (K-feldspar) grains can provide reliable and reproducible dosimeters for luminescence purposes (e.g. Thiel et al., 2011). However, the history of both dosimeters use in the development of luminescence dating has been varied. In this study, we apply both quartz and K-feldspar dosimeters based on regional experiences (e.g Miekle, 2008; Schulte et al., 2008) in order to develop a comprehensive understanding of the luminescence characteristics of samples from the Tabernas Basin. The following sections (4.4.1 to 4.4.2) provide an overview of the benefits

and limitations of both dosimeters for dating purposes, offering insight into why the combined use of dosimeters in any study is favourable.

4.4.1 Benefits and limitations of quartz as a natural dosimeter

In early luminescence and thermoluminescence studies (e.g. Wintle and Huntley,1980; 1982; Huntley et al., 1985), quartz was commonly neglected against K-feldspar due to its relatively weak luminescence intensity and the apparent low number of grains that emitted a measureable luminescence signal. However, in the early 1970s the identification of unexpected signal loses from feldspar grains generated significant doubt about feldspar as a reliable dosimeter. The mechanism of signal loss was termed anomalous fading (Wintle, 1973) and was described as the process by which energy is transferred directly between luminescence centres within a grain by the process of radiative tunnelling (Fig. 4.6A; described further in section 4.4.2). The scientific understanding of how to account for anomalous fading was poor from detection up until the mid 2000s. This lack of knowledge typically promoted the use of quartz grains based on the relative stability of luminescence signals over Quaternary timescales (Duller, 2008a).

Quartz is further commonly favoured over K-feldspar due to the relatively short exposure period required to remove electrons in the fast - medium decay components of the luminescence signal (those commonly measured in OSL practices; Fig 4.7A). Decay components are related to three physically distinct luminescence traps (fast, medium and slow) that occur within grains with different rates of charge loss (Singarayer and Bailey, 2003). The fast-medium components are typically favoured over slow component as electrons are removed from these traps at a much faster rate and hence reduce the likelihood of incomplete signal resetting during burial and deposition (Bailey et al. 1997). This ability to reset the luminescence signal over shorter exposure periods makes quartz a useful dosimeter in many environments where incomplete signal resetting is an issue (e.g. fluvial or colluvial deposits; Singarayer et al., 2005).

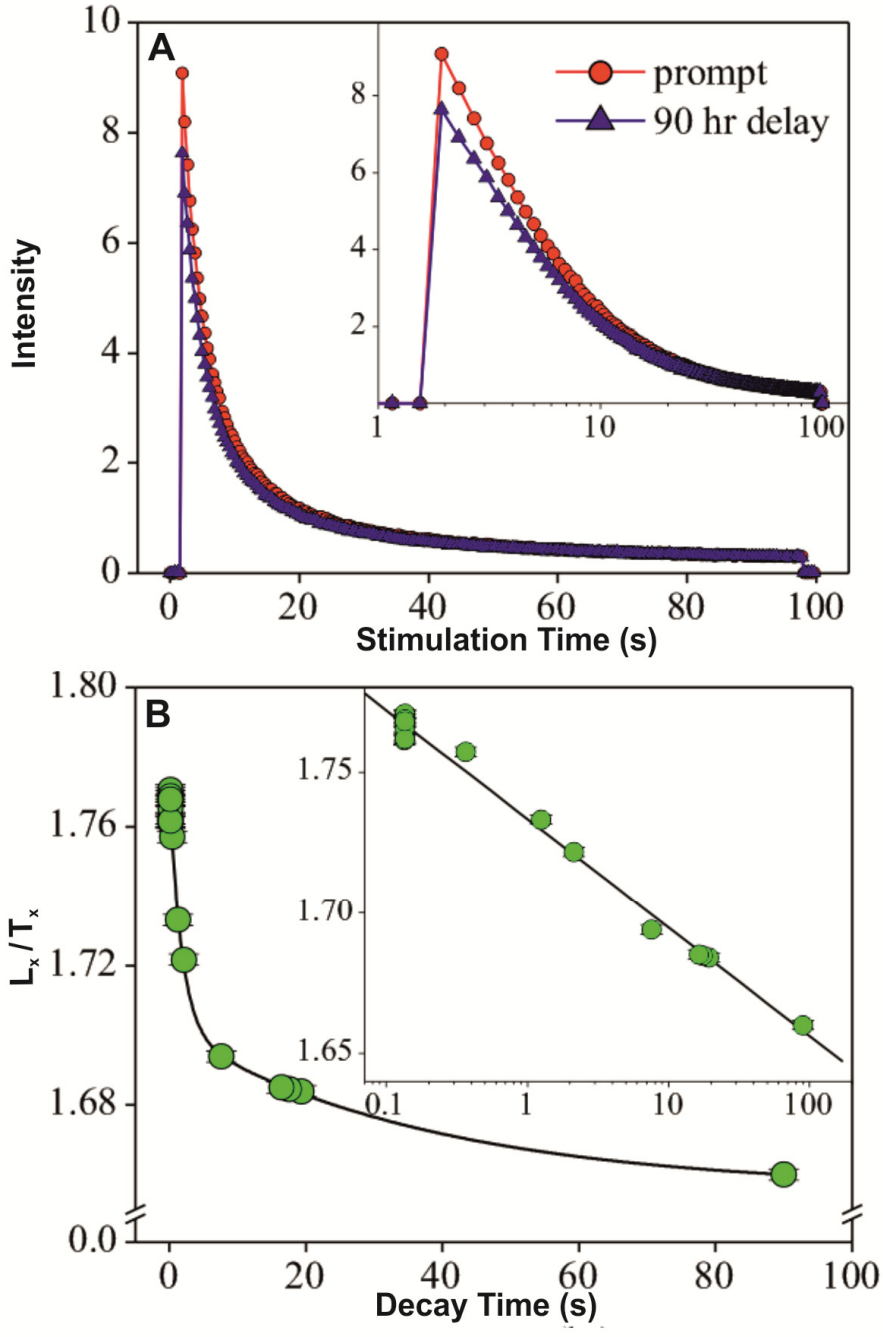

Figure 4.6 Anomalous fading in K feldspar grains taken from Thomsen et al., (2008).(A) Luminescence intensity decay curve for feldspar grains, taken initially upon sample irradiation and then after 90 hr. delay, note decrease in signal intensity as best displayed on insert. (B) Exponential fading rates in k-feldspars as evidenced by decrease in sensitivity corrected OSL signal over time.

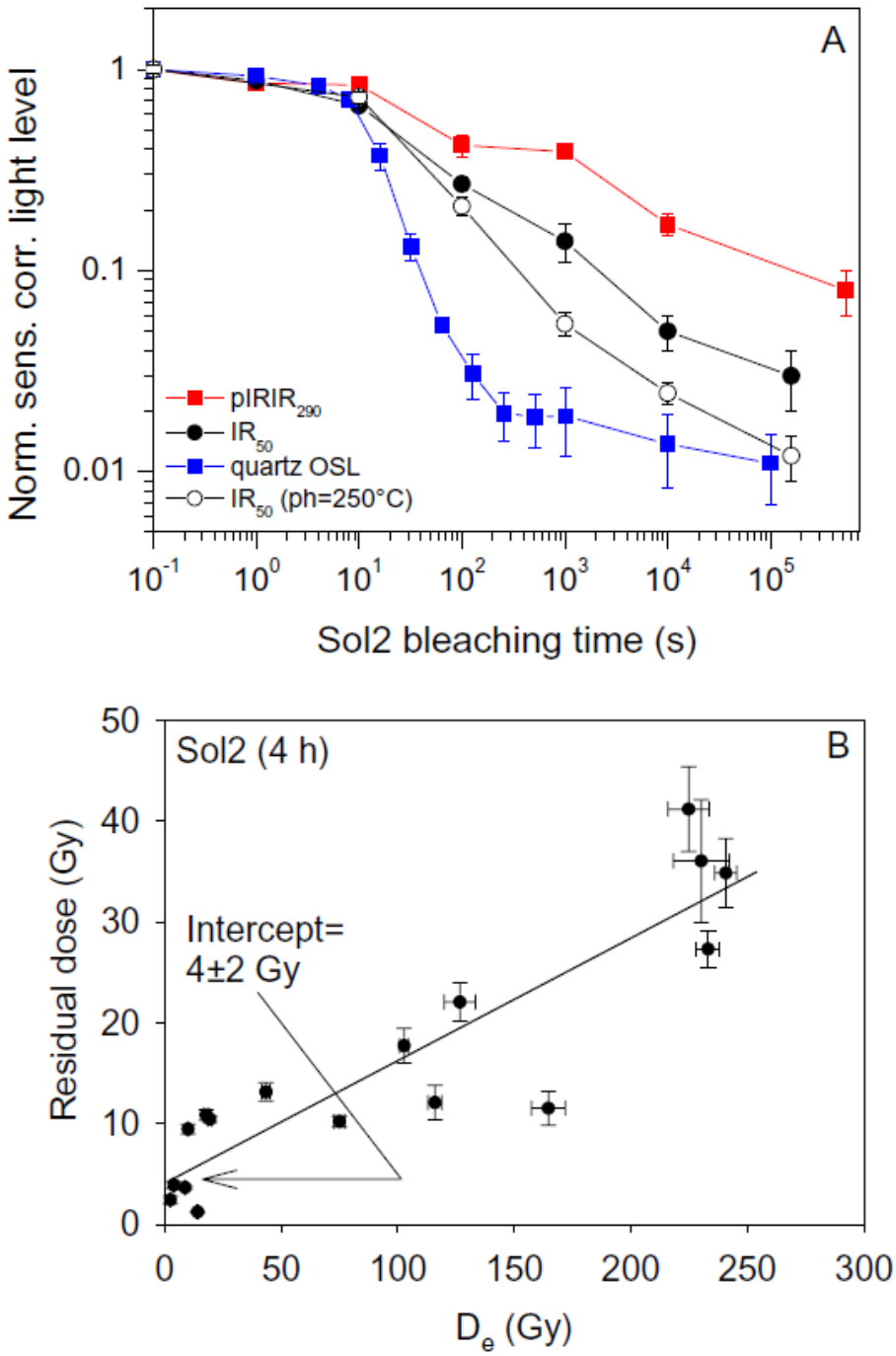

Figure 4.7 (A) Sensitivity corrected feldspar and quartz OSL plotted against exposure time in Hönle SOL2 solar simulator. Note the considerable variations in bleaching rates between Quartz and feldspar signals (labelled IR50 & PIRIR290). (B) Residual dose measurements in 15 feldspar grains after 4hrs exposure in the Hönle SOL2 solar simulator. Note how a considerable un-bleachable component remains. Both graphs from Buylaert et al. (2012).

Although quartz is commonly favoured in standard OSL practices it does have its limitations, such as:

- A low sensitivity of quartz grains (both monocrystalline and polycrystalline), where luminescence signals are either absent or non-reproducible with typically less than 5 % of grains responsible for luminescence signal (Thomsen et al.,2008);
- A low luminescence intensity from individual grains when compared with feldspar grains;
- A relatively high susceptibility of sand sized quartz to changes in environmental dose rates due to a lack of internal (beta) dose (Rittenour, 2008);
- The common presence of feldspar contaminants within quartz grains which can contribute luminescence signal during laboratory measurements (Duller, 2003);
- The limited upper age limit of the mineral grain as a function of the saturation limit of the dose response curve.

Of these limitations there is little that can be done to compensate for low luminescence sensitivity in a sample, or to accurately reconstruct changes in environmental dose-rates over long timescales. For samples with a low luminescence intensity it is current practice to perform extensive single grain experiments in order to identify the few grains giving a measureable signal within a sample (Bailey and Arnold, 2006). However, such approaches are currently at the centre of debate, with the belief that the current statistical models applied in single grain analysis are often unrepresentative (Thompson, *per comms*.). In contrast, the assessment of feldspar contaminants within quartz grains is easily measured by the calculation of an infrared (IR) depletion ratio for a sample (Duller, 2003). The IR depletion ratio calculates the ratio between the luminescence signals when stimulated with both blue and infrared light. Quartz does not emit light in the infrared spectrum and hence any signals detected during IR stimulation are associated with feldspar contaminants. Where the IR depletion ratio is greater than 10%, the contamination from feldspar is deemed too great and further treatment of the sample in hydrofluoric acid is required.

The limited upper age limit of quartz is often the greatest limitation of the mineral in studies of long-term landscape evolution for any geomorphological environment (e.g. Thomsen et al., 2008; Wintle, 2008; Buylaert et al. 2009; Thiel, 2011). The upper age limit of any dosimeter is defined by level at which the electron traps become full, termed the saturation limit. Signal saturation is mathematically expressed as twice the exponential saturation coefficient ($2D_0$) and is evidenced visually by the plateau on exponentially fitted dose response curves (Fig. 4.2; Wintle and Murray 2006). For quartz grains, the saturation limit is typically less than 200 Gy (Wintle and Murray 2006). Given an environmental dose rate of between 1.5 - 2 Gy ka^{-1}, the upper dating limit of quartz usually lies between 100 – 200 ka, restricting luminescence dating using quartz to the Late-Pleistocene (Buylaert et al., 2012). In contrast, the saturation limits for K-feldspar grains has been proven to be typically much higher, at around 1500-2000 Gy (e.g. Thomsen et al., 2008; Buylaert et al. 2009). Applying the same environmental dose rates the upper dating limit of K-feldspar increases dramatically to some 1 Ma (Buylaert et al., 2012).

4.4.2 Signal Stability in K-Feldspar and possibilities to increase the OSL age range

The significant increase in the upper dating limit of K-feldspar grains is very favourable in studies that deal with long term rates of landscape evolution. Much like quartz, K-feldspar grains are known to be widely distributed in depositional landforms (e.g. river terraces) and are typically highly abundant when found. However, the issue of anomalous fading presents a major challenge when obtaining reproducible dates (Huntley and Lamothe, 2001).Current theory on anomalous fading is based upon the hypothesis of radiative (quantum) tunnelling (Jain and Ankjærgaard, 2011) whereby electrons stored in shallow or unstable traps pass directly through internal energy barriers into nearby electron recombination centres (Wintle, 1973). It is believed that the effects of tunnelling are associated with the varying stability of luminescence signals within K-feldspar grains; as presented in the most current band-model of feldspar luminescence by Jain and Ankjærgaard (2011) (Fig. 4.8). The current band-model predicts that luminescence signals are lost over a range of states. The most unstable

signals are lost as a result of ground state tunnelling, where electron recombination occurs between shallow and unstable traps at ambient temperatures during burial (Fig. 4.8 – pathway A). The next stage of signal loss occurs when electrons pass from the ground state to an excited state as a result of laboratory infrared (IR) stimulation at low temperatures (<50 ℃), (Fig. 4.8 – pathway B). During this transition the likelihood for the recombination of distant electron pairs, which would typically occur over long timescales, is significantly increased (Buylaert et al., 2012). The final and most unlikely of signal losses occurs as a result of additional stages of IR stimulation at elevated temperatures (>200℃). Signal loss is believed to originate from the recombination of electrons as a result of band-tail migration (Fig. 4.8 – pathway C). However, at this stage electron traps are so distant from one and other that the likelihood of recombination via tunnelling is low (Jain and Ankjærgaard, 2011).

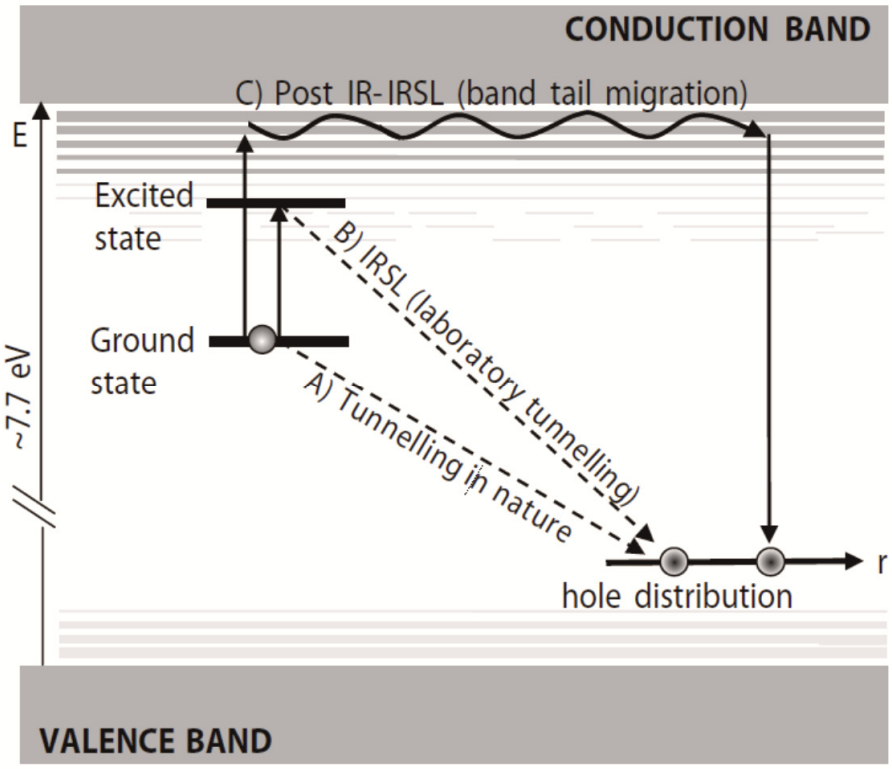

Figure 4.8 Schematic band-model that demonstrates signal stability and radiative tunnelling pathways in K-feldspar grains (Buylaert et al., 2012 and references therein).

At present, research is focused on measuring luminescence signals from K-feldspar grains based on the decreased probability of signal loss from high temperature electron traps. Significant advances have been made when applying initial stages of IR stimulation at low temperatures (<50°C) followed by additional stages of IR stimulation at high temperatures (225°C - 290°C) termed post IR-IR stimulation (Buylaert et al., 2009). Numerous studies have evidenced signal stability using the post IR-IR approach and have highlighted the application of the method when dating samples older than 20 ka (e.g. Buylaert et al., 2011; Thiel et al., 2011; Sohbati et al., 2012; Li et al., 2013). However, there are still many aspects of K-feldspar dating that are poorly understood and require further investigation (Buylaert *per comms*.). These include: (1) developing a comprehensive understanding of the generation and storage of luminescence signals (e.g. refining the current band-state model to account for numerous K-feldspar grains that do not present reproducible results under the current assumptions), and (2) to increase the reproducibility of residual or un-bleachable signals under laboratory conditions which are believed to be un-representative of natural conditions (Fig. 4.7B; Sohbati et al., 2012).

In accordance with the increased reliability of IRSL measurements it has become common to combine both quartz OSL and feldspar IRSL measurements in luminescence studies. This approach has enabled the identification of stable luminescence signals from K-feldspar grains adopting quartz OSL as a chronological control where other absolute ages are absent (Buylaert et al., 2012). Furthermore, the comparison of OSL estimates from quartz grains with the harder to reset IRSL signals from K-feldspars has become a tool in assessing the degree of sample bleaching in both dosimeters (e.g. if OSL D_e estimates agree with IRSL estimates then the quartz signal was likely well reset; Murray et al., 2012). These benefits are applicable in any study where signal resetting is likely to be of significance and hence were adopted in this study to assist in defining a highly stringent set of age estimates.

4.5 Environmental dose rate measurements

A common issue in luminescence dating is the under appreciation of environmental dose-rate measurements when compared against equivalent dose estimations. Dose rate measurements aim to best quantify the amounts of naturally occurring radiation that a sample has been exposed to during its burial (Li et al., 2008). These measurements should account for variations in dose rate contributions and are notably as important as equivalent dose estimations in the final age calculation (Fig. 4.3). The following sections (4.5.1- 4.5.3) detail the sources of radiation measured in dose rate estimations and presents the underlying assumptions in taking representative measurements. The sections aim to highlight the common problems in making accurate dose rate measurements, and identify the numerous environmental variables which must be recorded and accounted for in both the sample collection stage and in final calculations of dose rate.

4.5.1 Environmental radioactivity: Types, sources and measurements

The source of natural radiation for buried sediments comes mainly from the decay of uranium (U), thorium (Th) and potassium (K) isotopes stored within rocks and sediments of the Earth's lithosphere, with minor contributions from cosmic radiation (Duller, 2008a). Dose rate measurements quantify the gamma, beta and alpha contributions from a distinct series of radioelements which are the principal contributors of ionising radiation in the natural environment, namely: ^{40}K with a half-life of 1.25 10^9 yr^{-1}, ^{232}Th (half-life: 1.41 10^{10} yr^{-1}), ^{238}U (half-life: 4.47 10^9 yr^{-1}), ^{235}U (half-life: 7.04 10^8 yr^{-1}), and minor contributions from ^{87}Rb (half-life: 48.8 10^9 yr^{-1}) (Adamiec and Aitken, 1998). For all of these radioelements a state of equilibrium is typically assumed, whereby each member in a radioactive chain decays into the next member at the same rate at which it was produced from its proceeding parent isotope (Prescott and Hutton, 1995).

Contributions from cosmic radiation account for less than 10% of the dose-rate (Prescott and Hutton 1988) and are a function of the altitude, latitude and depth below ground level

from which a sample is taken (Prescott and Hutton,1994). Recording these factors during the sampling stage is crucial for subsequent use in the correction of the final dose rate data (Guérin et al., 2011). Of all the factors, the most significant variables are that of altitude and depth below ground. Increases in altitude lead to a notable decrease in the effects of cosmic radiation due to the relative decrease in atmospheric density (Prescott and Hutton, 1994). Increases in sample depth leads to decreased radiation contribution from cosmic sources due to cosmic ray attenuation (Guérin et al., 2011). Burial depth attenuation of cosmic rays is separated in to a soft and hard component, with the soft component of little significance upon dose rate as it becomes fully attenuated at a scale of tens of centimetres. However, the hard component has the ability to penetrate the ground at a scale of tens of metres and must be accounted for in calculations of final dose rates (Fig. 4.9) (Guérin et al., 2011).

Dose rates can be calculated by either: (i) directly counting the emission of radiation (by gamma spectrometry, beta counting or thick source alpha counting) or (ii) by measuring the concentrations of the principal radioelements and converting these concentrations to calculate radiation dose received by the sample (Duller, 2008a). Direct counting methods are often only applied when disequilibrium is thought to be an issue (i.e. the secular decay of a decay series is uniform). Measurements of dose rates can be conducted in the field with the use of portable spectrometers or artificial phosphors, or in the laboratory using various chemical methods such as high resolution gamma spectrometry, neutron activation analysis (NAA) or inductively coupled plasma mass spectrometry (ICPMS).

4.5.2 Infinite matrix theory

The infinite matrix theory is the underlying assumption applied in measurements of radioactivity for environmental dose rate purposes (Aitken, 1985). It states that for any given radioactive medium with dimensions greater than the range of ionizing radiations, all of the energy that is emitted per unit time and mass in that medium is also absorbed in the same medium (Aitken, 1985). In application, the infinite matrix theory allows for the conversion of known concentrations of selected radionuclides within a given volume of homogeneous

material into an infinite matrix dose rate (Guérin and Mercier, 2011). However, sampling in accordance with the requirements of the infinite matrix theory can be complicated by the issue of sample homogeneity. Primarily, dose-rate homogeneity is questionable as a function of the varying contributions of alpha, beta, and gamma radioactivity generated by isotopes stored in varying abundances in the ground. Of the principal isotopes, ^{40}K emits only beta and gamma radiation, yet the isotopes of uranium and thorium (^{232}Th, ^{238}U & ^{235}U) comprise alpha, beta and gamma emissions (Adamiec and Aitken, 1998).

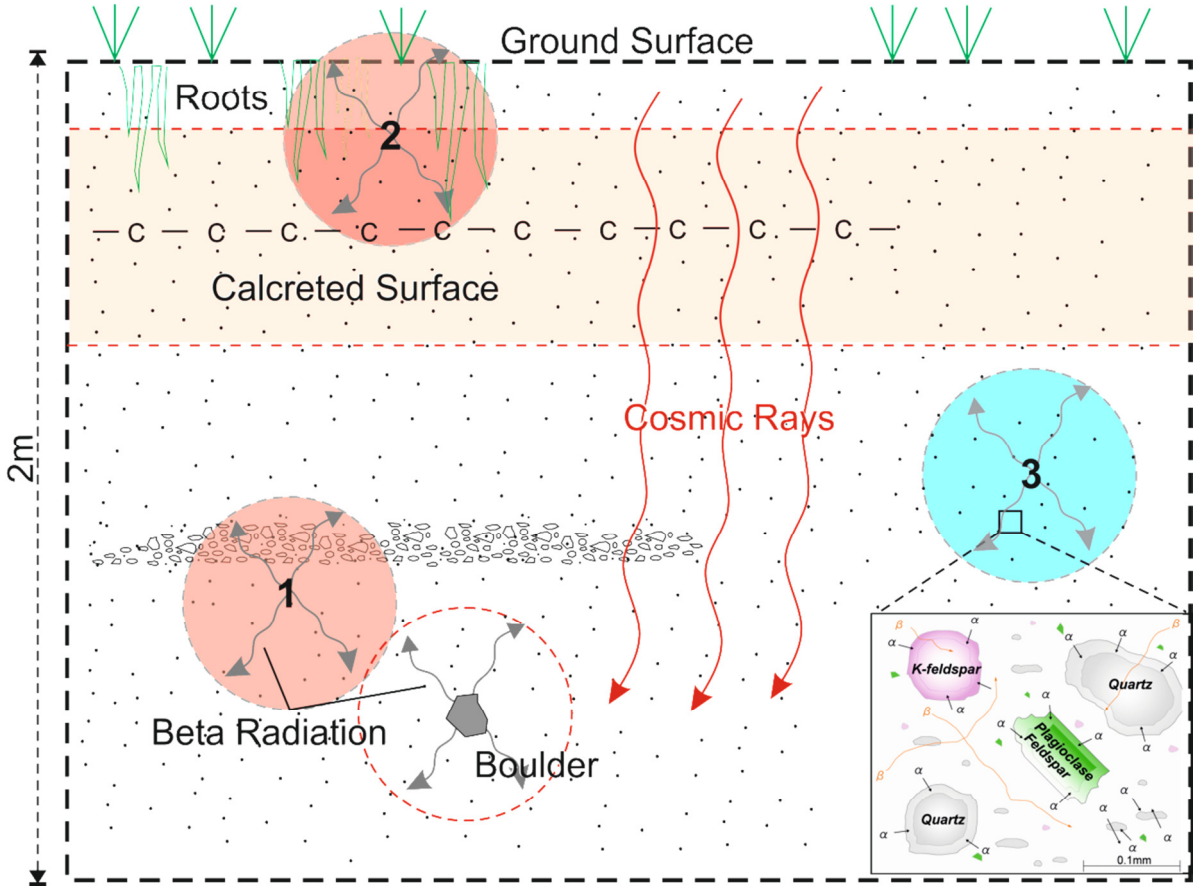

Figure 4.9 Diagram demonstrating the complications of sample homogeneity in dose rate measurements, redrawn from Aitken (1998). 3 labelled samples are first defined by gamma radiation limits of ~50cm. Sample 1 is not suitable due to close proximity to boulder and gravel horizon that both contribute heterogeneous beta and gamma dose rates. Sample 2 is not suitable due to close proximity to the ground surface and roots which alter radiation pathways and a calcrete surface that acts to attenuate beta and gamma radioactivity. Sample 3 complies with homogeneity requirements. Inset demonstrates relative scales of alpha and gamma radioactivity.

Alpha radioactivity occurs as heavy charged particles that have a high ionization power, which are significant at very short ranges (<20μm) (see inset Fig. 4.9). Beta radioactivity

forms light charge particles that have an ionising range of ~2mm, and gamma radiation forms un-massive, un-charged particles with a high ionising range of ~50cm. Therefore, to meet the assumptions made in the infinite matrix theory, all samples should be collected from a volume of sediment or rock which is: (1) homogeneous in clast size and composition, (2) has dimensions greater than $50cm^3$, and (3) is at least 50 cm from any exposed surface in order to account for variations in gamma dose rates (Fig. 4.9). The requirements for sample homogeneity are often unachievable in practice but can be overcome by either: (i) making in-situ measurements of gamma dose rates with the use of a field-spectrometer, or (ii) by modelling dose-rates from the bulk material characteristics of the surrounding volume of sediment (Duller, 2008a).

4.5.3 Sources of dose rate heterogeneity

Other than the localised differences in alpha, beta and gamma radiation, the two most common sources of dose rate heterogeneity in luminescence dating are the moisture content of the sample matrix and the internal beta dose rate contribution received by grains. Both variables further test the applicability of the infinite matrix theory as they represent highly irregular and poorly quantified variations to dose rates (Nathan and Mauz, 2008; Guèrin *et al.,* 2011). Changes in moisture content are of key significance with reference to increases in electron stopping power and the dilution of radioelement concentrations within a volume of soil or rock (Aitken and Xie, 1990; Nathan and Mauz, 2008). Increases in water content ultimately degrade the energy spectrum permeating within the soil/rock and further leads to changes in absorption efficiencies at the pore/grain interface (Nathan and Mauz, 2008). Corrections for water content have been proposed by Aitken and Xie (1990); however, they are questionable over long timescales when significant changes in moisture are likely (e.g. glacial – interglacial cycles; Duller, 2008a; Nathan and Mauz, 2008). At present, common practice applies a worse / best case scenario where the saturated moisture content (worst case) measured in the laboratory is compared against the natural moisture content from the

field (best case) (Duller, 2008a). The uncertainties associated with the variations between the values are then further accounted for in final dose-rate calculations.

Unlike the variable contributions from water content, the contributions from internal beta dose rate contributions are believed to be uniform through time (assuming no disturbance of the section occurs). Beta dose contributions are derived from the decay of radioactive elements (principally K and Rb) which occur within the lattice of a mineral (Li et al., 2008; Wintle, 2008). For sand sized K-feldspar grains, the internal contributions from the decay of ^{40}K and ^{87}Rb are a major part of the total dose rate that the grain receives and hence must be accounted for in final dose-rate calculations (Wintle, 2008). Internal dose contributions for K-feldspar grains are generated using standard concentrations of K at 13±1 % (Huntley and Baril, 1997) and a Rb concentration of 400±100 ppm (Huntley and Hancock, 2001). In comparison, the occurrence of radioactive isotopes within quartz grains is typically negligible, and hence no internal doses are generated. This lack of internal dose makes quartz grains more susceptible to changes in external dose sources through time (Guérin et al., 2012; Li et al., 2008).

4.6 Sampling methodology and locations

Sampling in accordance with the requirements of OSL dating (e.g. the infinite matrix theory) was of paramount importance in this study. However, the requirement for a full geomorphological appreciation of sample locations was of equal importance when defining a robust chronology for the Tabernas Basin. In order to meet these strict conditions the following sampling criteria was adhered to:

- Samples should only be collected from sections with a full sedimentological and stratigraphical appreciation. This includes references to Quaternary landform level, internal sedimentary stratigraphy and localised sedimentary structure (Fig. 4.10A);

- Sample locations must not be affected by processes of secondary reworking (e.g. bioturbation/calcrete formation) which might alter radiative pathways and lead to differences in environmental dose-rates within sections (Fig. 4.10B);
- Sampled sections must be of homogeneous sedimentology with unit thicknesses of at least 50 cm in order to limit the potential of radioactive heterogeneity (Fig. 4.10C);
- Where possible, sample locations should be located at the base and/or top of sedimentary units to provide insights into the timing of the onset and cessation of sedimentation of the landform;
- The complete sample inventory should aim to provide reliable age estimates for all landform levels across the basin.

Sampling was typically limited across the basin due to the highly indurated nature and highly variable sedimentology of most exposures. When suitable exposures were located, the exposure face was cleaned to remove surface weathering prior to sampling using a steel trowel. Sample faces were then logged in detail with respect to the internal stratigraphy of the landform and the component sedimentological characteristics. Sampling was conducted under blackout conditions using stainless steel tubes (8 cm x 25 cm) and light proof black bags. A lump hammer was used to assist in the sampling of weakly indurated sections. Additional bulk samples were collected for laboratory measurements of field moisture content and for material references. A total of 21 samples were collected during two field seasons from terrace levels 2 to 4 from across the Tabernas Basin. No samples were collected for terrace level 1 due to the hazardous location of outcrops. A summary of the sample locations including details of the representative terrace level, elevation, sedimentology and other contributing factors is presented in Table 4.2.

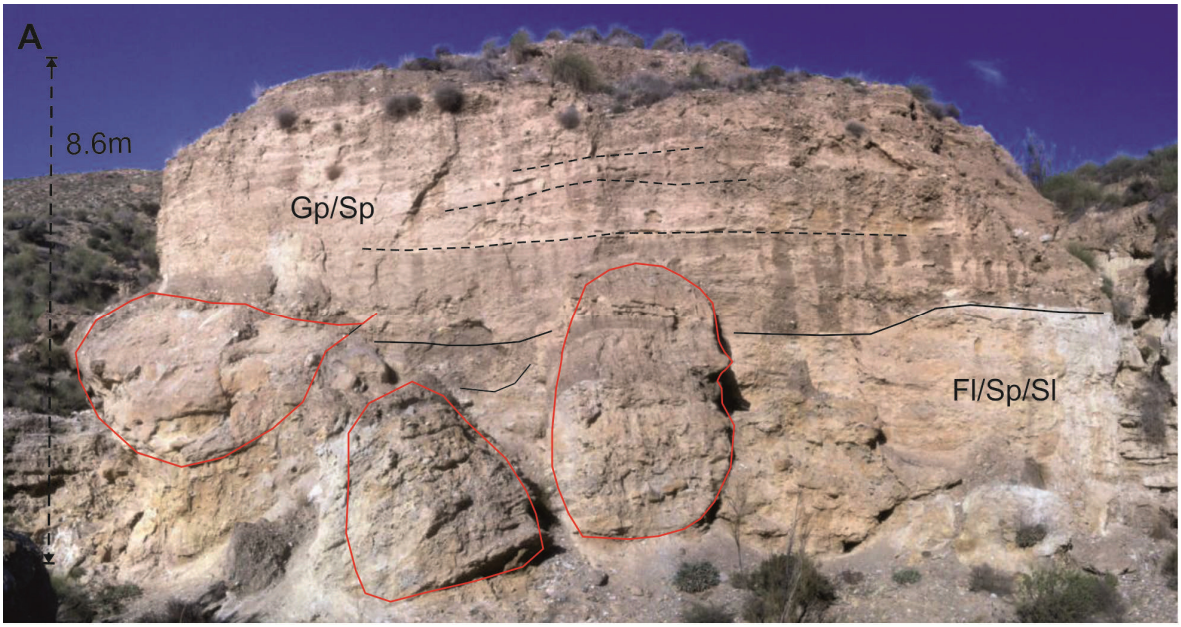

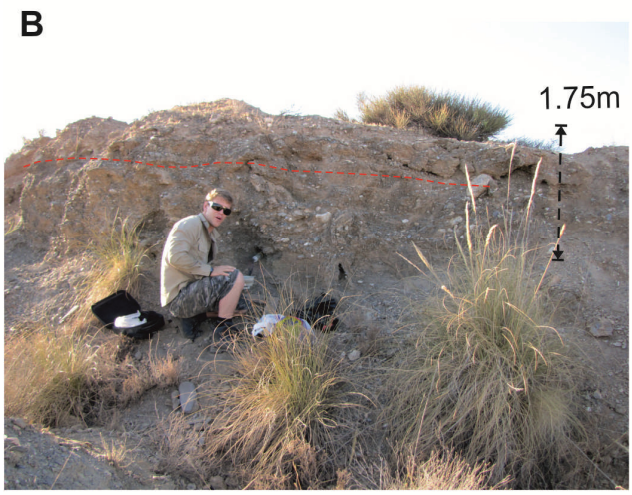

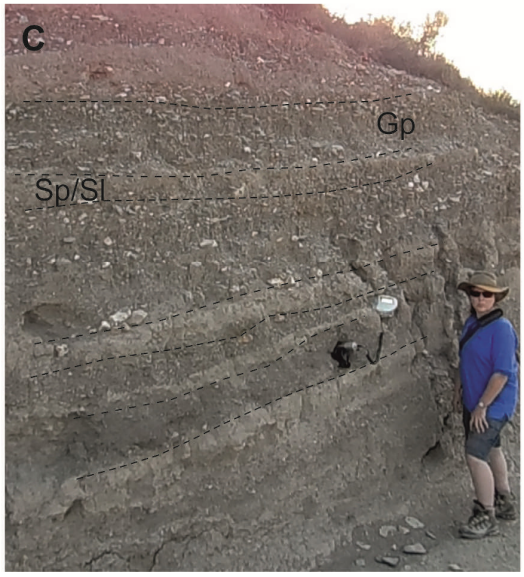

Figure 4.10 OSL sampling strategy applied in the Tabernas Basin. (A) Importance of sample strategy note red blocks represent both current and entrained hillslope topple blocks within section face, with potential for misrepresentation of section ages. Photo taken in Rambla Sierra facing south, UTM 30S 554595/4099436. (B) Sampling at least 0.5m below zone of secondary process in this case red line is pedogenic calcrete. Photo taken from motorway cut section, UTM 30S 547526/4099133 (C) Sampling from sedimentary units of greater than 0.5m thick. Photo taken in Rambla Sierra facing north west, UTM 30S 554049/4099294.

Table 4.2 Summary of OSL Sample locations. Highlighted samples were not prepared for analysis. * identifies samples prepared in the UK. Coordinates from UTM grid 30 S.

Sample	Terrace Level	Easting	Northing	Elevation (mASL)	Sedimentology & other features
Tab-1	3	554125	4099186	393	Alluvial fan: fine gravels with minor sands. Sample 4 m from top of exposed section
Tab-2*	3	554046	4099359	368	Ponded fines: clays/muds with minor sand lenses. Sample 1.8 m from current rambla base
Tab-3*	3	555833	4101629	429	Upper lake sequence: sands / silts. Sample taken 0.7 m from top of exposed section
Tab-4	2	547009	4099944	453	Fluvially dominated alluvial fan deposits: gravels/sands. Sample 0.6 m from top of exposed section
Tab-5	2	548196	4098543	405	Fluvially dominated alluvial fan deposits. Sample 13 m from base of exposed section (mid point)
Tab-6*	2	548345	4098531	389	Fluvially dominated alluvial fan deposits. Sample 1.8 m from base of exposed section
Tab-7*	3	551172	4098799	314	Lower lake sequence: ponded clays/muds/sands. Sample 8.5 m from base of exposed section
Tab-8	2	556021	4101636	402	Upper lake sequence: low energy sands/ silts. Sample 2.4 m from base of exposed section
Tab-9	3	551424	4098174	322	Fluvial terrace: gravels/sands. Sample 2.2 m from base of exposed section
Tab-10	4	549603	4097030	248	Fluvial overbanks: sands/ silts. Sample taken 1.1 m from base of exposed section
Tab-11	3	550076	4097201	256	Fluvial terrace: gravels/sands. Sample 1.4 m from base of exposed section
Tab-12	2	554811	4099886	415	Fluvial terrace: fine gravels minor sands. Sample 0.6 m from base of exposed section
Tab-13	3	552586	4100787	362	Ponded lower lake sequence: sands minor fines. Sample 1.2 m from base of exposed section
Tab-14*	2	554519	4102272	431	Alluvial fan: fine gravels with minor sands. Sample 6 m from base of exposed section
Tab-15*	3	551525	4099620	323	Ponded lower lake sequence: sands/silts/clays. Sample 0.7 m from base of exposed section
Tab-16	2	558203	4103105	456	Alluvial fan: fine to coarse gravels with minor sands. Sample 6 m from base of exposed section
Tab-17	3	547356	4092946	184	Fluvial terrace: Interbedded sands/silts/clays. Sample 1.7 m from base.
Tab-18	3	548769	4096107	247	Lower lake sections: Fluvial gravels on lapped by fines. Sample 2.4 m from top of exposed section.
Tab-19	3	552743	4101813	380	Fluvial overbanks: sands/ silts. Sample taken 0.4 m from base of exposed section
Tab-20	4	550516	4098723	295	Fluvial overbanks: sands/ silts. Sample taken 0.6 m from top of exposed section
Tab-21	4	547353	4094345	196	Fluvial terrace : gravels/ sands/ silts. Sample taken 1.4m from base of exposed section

4.7 Sample preparation and analytical facilities

4.7.1 Sample preparation and equivalent dose measurements

Sample preparation and analysis was mainly conducted during two visits to the Nordic Centre for Luminescence Research in Risø, Denmark. However, six samples were prepared at the Luminescence dating laboratory at the University of Gloucestershire prior to arrival in Denmark (Table 4.2). Two samples (Tab-5 & Tab-16) were not processed for subsequent OSL measurements as they were deemed to be of an unfavourable grain size for luminescence purposes. The remaining 19 samples were processed for luminescence purposes using standard techniques under subdued red/orange light (e.g. Thiel et al., 2011). Upon opening of sample tubes, the outer ends (~2 – 3 cm) of light exposed sediment were discarded. The samples were then wet-sieved in order to isolate the 180-250 μm grain size fraction. This fraction was treated with 10% hydrochloric acid (HCl) to remove any carbonates, followed by 10 % hydrogen peroxide to remove any organic material. Upon completion of multiple cycles of rinsing, the samples were etched with 10% hydrofluoric acid (HF) acid for a period of 40 minutes to remove the alpha irradiated surface layer and any further coatings on all grains. K-feldspar grains were then isolated from quartz grains by means of heavy liquid separation (ρ=2.58 g cm-3). The quartz extract was treated with 40% HF for 60 minutes followed by 10% HCl to remove any soluble fluorides.

All luminescence measurements were made using a Risø TL/OSL reader adopting: (1) blue light stimulation (λ = 470 nm, ~80mW cm) and photon detection through a 7.5-mm Hoya U-340 glass filter for quartz grains; or (2) infrared stimulation (λ = 875 nm,~135 mW cm) and photon detection through a Schott BG39/Corning 7-59 filter combination for K-feldspar grains. Grains were mounted as a single layer on stainless steel cups using silicone oil. Due to the relative sensitivity of the dosimeters, quartz grains were measured as large aliquots (8 mm Ø ~1000's grains), and K-feldspar grains were measured as small aliquots (2 mm Ø <100's grains). Any luminescence measurements undertaken above 200°C were conducted within a nitrogen atmosphere with pause intervals set at 10s to allow grains to attain measurement

temperature. The beta sources of all the readers used (n=5) were calibrated using standard Risø calibration quartz. Source calibrations were carried out using 180–250 mm coarse quartz grains on stainless steel cups (large aliquots~1000's grains).

4.7.2 Dosimetry

Radionuclide concentrations were either measured during the collection phase by methods of field gamma spectrometry, or in the laboratory using a high-purity germanium detector. Laboratory techniques were applied when the field detector was not available. Field gamma spectrometry was conducted using a Canberra Inspector 1000 NaI detector. The detector was calibrated using concrete calibration blocks at Oxford University following the methods of Rhodes and Schwenninger (2007). Measurements were conducted within enlarged sample holes for a counting time of 40 minutes. Final spectra were converted to concentrations of K, U and Th post fieldwork using the window-counting method of Aitken (1998). Total uncertainties are assumed at 10% for U and Th and 5% for K.

In the laboratory, radionuclide concentrations were measured on homogenised materials collected from the immediate area surrounding the three sampling locations. Approximately 200 g of material from each sample location was dried and then ashed at 450℃ for 24 h to remove any organic matter. The samples were then pulverised and homogenised for subsequent casting in a fixed wax matrix in order to prevent radon loss and to provide a reproducible counting geometry. The samples were stored for at least three weeks to enable ^{222}Rn to reach equilibrium with its parent isotope ^{226}Ra. Radionuclide concentrations (^{238}U, ^{226}Ra ^{232}Th and ^{40}K) were measured on a high-purity Germanium detector for at least 24 hours. Final dose rates were derived using the conversion factors of Adamiec and Aitken (1998) with calculations of cosmic radiation contributions based on Prescott and Hutton (1995). A nominal water content of 5 ± 4% was assumed based on the field moisture content and saturation moisture contents (derived from bulk samples). A summary of radionuclide concentrations and quartz dose rates and measurement methods for all samples is given in Table 4.3.

4.8 OSL characteristics

4.8.1 Quartz OSL characteristics

Due to the limited number of existing luminescence ages or further chronological control across the Tabernas Basin, a wide range of OSL methodologies were used in this study. Initially, focus was placed upon the application of the single aliquot regenerative (SAR) dose protocol (Murray and Wintle, 2000) in the dating of quartz grains. A summary of the SAR protocols utilised in this study is presented in Table 4.1. In accordance with the limitations of quartz dosimeters (presented in Section 4.4.1), the purity of all quartz extracts was checked for feldspar contamination prior to any dose measurements. Feldspar contributions were assessed using the IR depletion test of Duller, (2003). The contribution from IR signals was <10% of the total natural blue OSL signal for all samples and therefore all quartz extracts were suitable for further measurements.

Preheat temperatures were assessed by means of a preliminary preheat plateau test for all samples. A temperature of 260°C for a duration of 10s showed no effect on the equivalent dose values (D_e) for preheat temperature ranges from 160°C to 260°C. Fixed test doses were set at between 20-30% of the average natural dose (as determined from preliminary tests) for all samples. Cut-heats of 220°C (40°C lower than preheat temperature) were used with subsequent luminescence read-outs measured at 125°C (for 40 s) using blue light measuring 250 channels. Finally, a high-temperature blue light stimulation at 280°C was performed in order to reduce recuperation (Murray and Wintle, 2003). For D_e calculations the initial 0.8 s of the luminescence signal (fast component) less the background from the adjacent 1.6 s. Dose response curves where fitted with a single saturating exponential function.

Table 4.3 Summary of dosimetric information for all samples. se = standard error; * identifies field gamma spectrometry measurements with ^{40}K presented as %, ^{232}U & ^{232}Th presented as ppm

Sample	^{238}U (Bq kg^{-1} or ppm) ±se	^{226}Ra (Bq kg^{-1}) ±se	^{232}Th (Bq kg^{-1} or ppm) ±se	^{40}K (Bq kg^{-1} or %) ±se	Dose rate (Gy ka^{-1})
Tab-1	27.1 ± 9.0	35.3 ± 0.8	49.9 ± 1.0	566.0 ± 13.1	3.12 ± 0.14
Tab-2 *	2.9 ± 0.01	-	10.8 ± 0.01	2.2 ± 0.01	2.91 ± 0.10
Tab-3 *	1.7 ± 0.01	-	7.0 ± 0.01	0.8 ± 0.02	1.70 ± 0.11
Tab-4	39.3 ± 8.8	36.6 ± 0.8	44.1 ± 0.9	577.9 ± 14.1	3.34 ± 0.02
Tab-6 *	2.5 ± 0.01	-	10.5 ± 0.01	1.7 ± 0.01	2.74 ± 0.10
Tab-7 *	2.8 ± 0.01	-	11.9 ± 0.01	2.2 ± 0.01	3.33 ± 0.21
Tab-8	24.7 ± 9.7	27.8 ± 0.8	35.9 ± 0.9	442.1 ± 14.1	2.37 ± 0.03
Tab-9	63.3 ± 19.1	25.8 ± 1.3	35.2 ± 1.3	366.8 ± 19.6	2.49 ± 0.04
Tab-10	45.8 ± 16.1	39.1 ± 1.4	48.3 ± 1.4	486.1 ± 21.6	3.02 ± 0.03
Tab-11	27.6 ± 6.7	27.5 ± 0.6	25.7 ± 0.6	347.1 ± 9.2	2.05 ± 0.03
Tab-12	18.9 ± 4.9	30.1±1.1	40.6 ± 1.1	484.1 ± 17.5	2.98 ± 0.03
Tab-13	59.2 ± 16.4	27.5 ± 1.2	37.9 ± 1.2	426.9 ± 19.3	2.63 ± 0.03
Tab-14 *	3.0 ± 0.01	-	10.7 ± 0.01	1.8 ± 0.02	3.64 ± 0.10
Tab-15 *	2.5 ± 0.01	-	7.5 ± 0.01	1.5 ± 0.01	3.23 ± 0.10
Tab-17	38.2 ± 12.2	40.1 ± 1.0	38.1 ± 1.1	261.2 ± 10.9	2.27 ± 0.03
Tab-18	33.8 ± 9.9	27.1 ± 0.8	36.3 ± 0.9	422.5 ± 12.2	2.46 ± 0.02
Tab-19	23.0 ± 13.7	28.6 ± 1.1	28.6 ± 0.9	305.8 ± 15.9	2.05 ± 0.04
Tab-20	51.5 ± 13.8	42.7 ± 1.1	48.5 ± 1.0	472.1 ± 17.3	2.97 ± 0.02
Tab-21	40.6 ± 8.4	38.9 ± 0.8	48.6 ± 0.9	402.7 ± 10.8	2.69 ± 0.02

Due to the large amount of samples obtained from the field, an initial series of range-finder experiments were conducted on multi-grain aliquots to assess the luminescence characteristics of all samples. 5 subsamples of each sample were measured for equivalent dose values. Unfortunately, a distinct characteristic of the OSL signal from many samples was a low saturation limit. Saturation values ($2*D_0$; Wintle and Murray, 2006) were typically <50 Gy, which is notable when compared with standard saturation values of 200 Gy for quartz grains (Wintle, 2008). Taking a typical dose rate of 2.5 – 3.0 Gy/ka, the low saturation values limited the window of dating to < 16 ka. As a result, 9 samples from a range of depositional settings (Tab-1, Tab-2, Tab-6, Tab-12, Tab-13, Tab-14, Tab-15, Tab-17 & Tab-18) were discarded from further measurements due to the limited data they represent. These samples were associated with terrace levels 2 & 3 (Table 4.2). The remaining samples were measured for further natural dose measurements.

A typical dose response curve from multi-grain sample Tab-9 is presented in Figure 4.11. OSL signals were 'fast' component dominated for all remaining samples (Jain et al., 2003) with signals reaching background levels within a very short time (<2 s) (Fig. 4.11 inset). After additional dose measurements, 4 samples were identified as being in saturation (Tab-3, Tab-4, Tab-7 & Tab-8); however, the saturation doses for all samples were higher than 50 Gy, providing valuable minimum-ages for a heavily reduced sample inventory (Table 4.4). Minimum age values provide estimates of D_e based on the saturation criteria of $2*D_0$. The age estimates are minimal only, with no measure of error and must be treated with caution in terms of their chronological significance.

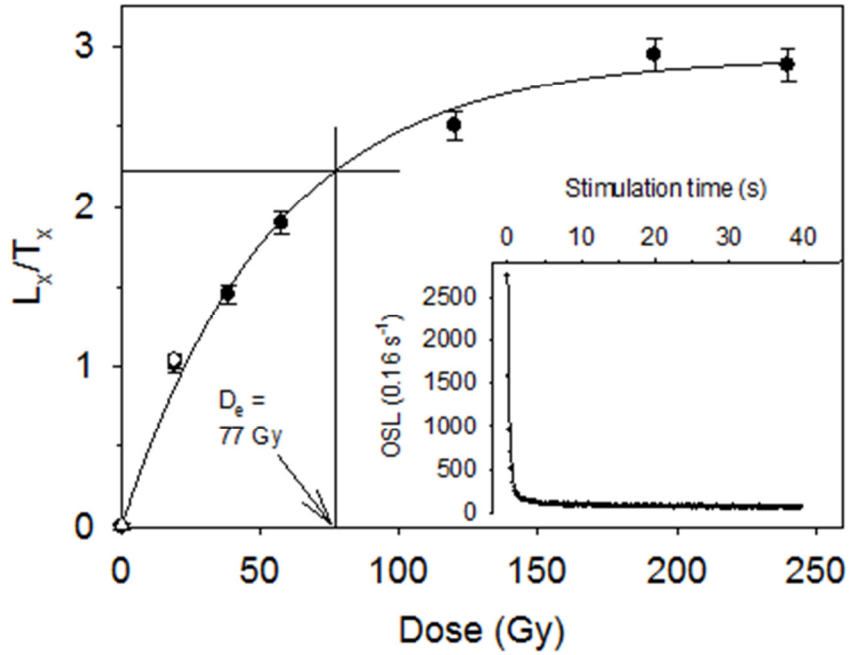

Figure 4.11 Typical dose response curve for a quartz aliquot of Tab-9. Inset presents a typical decay curve.

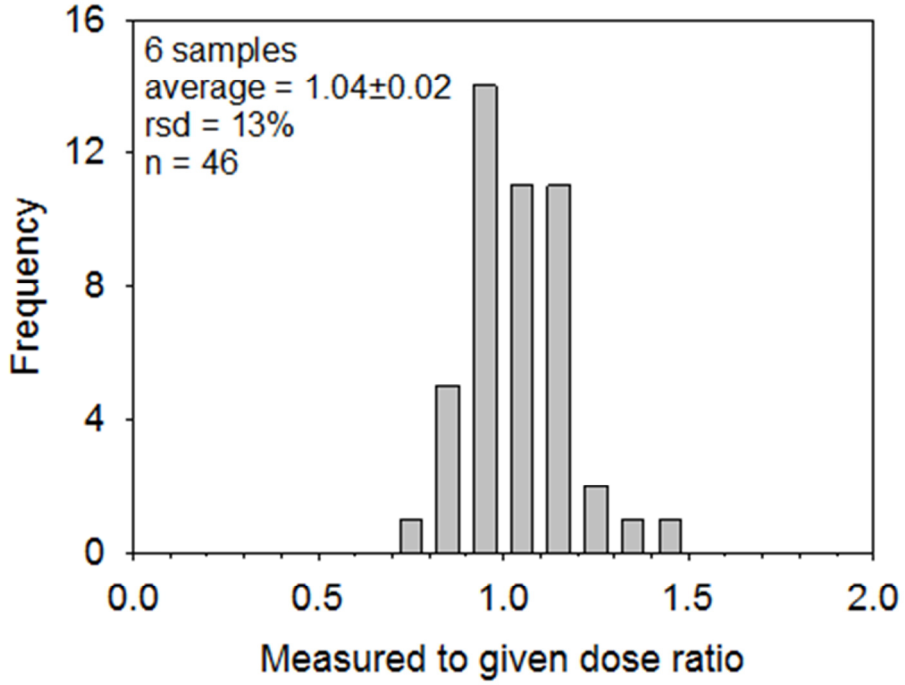

Figure 4.12 Dose recovery values for multi-grain aliquots showing results at or near unity

Recycling ratios for the remaining 6 unsaturated samples were close to unity suggesting that the test dose accurately monitored changes in luminescence sensitivity throughout the measurement sequence (Wintle and Murray, 2006). Recuperation values were less than 1% of the D_e. Dose recovery tests were undertaken on the unsaturated samples to assess the accuracy of the SAR protocol in reproducing given doses to a sample (prior to any heating). Six aliquots per sample were bleached with blue LEDs for 100 s, followed by a pause (10,000 s) and subsequent blue LED bleach (100 s). The aliquots were given a beta dose similar to their natural dose (as determined during D_e measurements) and then measured using the SAR protocol mentioned above. Dose recovery ratios were close to unity for all samples indicating that the SAR protocol is applicable in accurately determining De values for our samples (Fig. 4.12). A summary of the multi-grain aliquot D_e values for the 6 unsaturated samples and the 4 saturated samples is presented in Table 4.4.

4.8.2 K-Feldspar IRSL characteristics

Given the low saturation limits of many quartz samples further measurements were undertaken using infra-red stimulated luminescence (IRSL) from K-feldspar grains. Since identification of increased signal stability by Thomsen et al. (2008), measurements using IRSL signals from K-feldspar grains have been increasingly used to supplement quartz OSL (e.g. Wallinga et al., 2001; Thiel et al., 2011; Sohbati et al., 2012). In this study, the approach of Buylaert et al. (2012) was used, using post-IR IRSL signal measured at 290°C (referred to as $pIRIR_{290}$) after an initial low temperature IR measurement at 50°C (referred to as IR_{50}). The $pIRIR_{290}$ signal has been demonstrated to show negligible effects of anomalous fading and is becoming increasing applied in standard OSL practices (Thomsen et al., 2008; Jain and Ankjærgaard, 2011; Buylaert et al., 2012).

Following Thiel et al., (2011) and Buylaert et al. (2012) a preheat temperature of 320°C was applied for a duration of 60 s (Table 4.1). The first IR stimulation was conducted at low temperatures (50°C) with measurements of the IRSL signal for 200 s (IR_{50} signal). A second IR stimulation was then conducted at high temperatures (290°C) for 200 s ($pIRIR_{290}$

signal). Test doses were set at 40-50% of the average natural dose as determined from preliminary tests. The response to the test dose was measured in the same manner as for the natural doses. Integration intervals were set at the initial ~2 s, less a background derived from the last ~10 s. Dose response curves for both signals were fitted using a single saturating exponential function with measurements of the IR_{50} signal analysed from the same runs in which $pIRIR_{290}$ signals were made. Upon completion of all measurements a high temperature IR stimulation at 325°C was conducted to reduce the likelihood of signal carry-over.

IRSL measurements were made on seven samples (Tab-1, Tab-8, Tab-9, Tab-10, Tab-11, Tab-12 & Tab-18) from a range of terrace levels and depositional settings (e.g., fluvial terrace, palustrine, overbanks). Unfortunately, the relationships between the measured signals (IR_{50} to $pIRIR_{290}$) were non-uniform and not representative of quartz values when known (Tab-10 and Tab-11; Table 4.5). In some instances there was an apparent lack of IR_{50} signals (Tab-9 and Tab-11). The poor representation of IRSL signals suggested that the signals were either partially reset prior to measurements or the mineral grains being measured were not pure K-feldspars (e.g. Na or Ca feldspar contaminants).

To investigate the irregularities in IRSL signals, X-ray Fluorescence (XRF) analyses were conducted on three samples (Tab-9, Tab-11 & Tab-19). 6 aliquots of each sample were measured using an XRF attachment to the Risø TL/OSL reader, consisting of an X-ray tube (40 kV, 4W, Amptek Inc.) and X-ray spectrometer (X-123SDD, Amptek Inc.). Calibrated spectra for Na/K/Ca carbonates, Al2O3 and SiO2 were measured and converted to weighted percentages of K, Na and Ca. The results of the XRF analysis, as presented on Figure 4.13, identified that all three samples were not representative of pure K-feldspar. Of all the samples Tab-9 was the least contaminated, however, it still contained 20 - 30% Na content. Based on these results and the overall poor performance of the IRSL methods, feldspar dating was deemed unsuitable for this study.

Table 4.4 Summary of quartz equivalent dose values for multi-grain and single grain measurements. Note Tab-3 to Tab-8 represent minimum ages only. SE= Standard error, * Saturation values / minimum ages only, CAM = Central age model, OD= Over dispersion, CAM_{UL}=central age model un-logged.

Samp.	Equivalent Dose – Multi-grain		Equivalent Dose – Single grain								Dose rate (Gy/ka)	Multi-grain age (ka)	Single Grain Age (ka)
									$D_0 > 50$ Gy				
	N	Dose (Gy) ± SE	N	% Sat	CAM	OD CAM	CAM_{UL}	OD CAM_{UL}	CAM	CAM_{UL}			
Tab-3	23	53 ± 4*	-		-	-	-	-	-	-	1.70 ± 0.11	31.1 ± 9.8*	-
Tab-4	12	87 ± 7*	-		-	-	-	-	-	-	3.34 ± 0.02	26.4 ± 9.1*	-
Tab-7	10	52 ± 3*	-		-	-	-	-	-	-	3.33 ± 0.01	15.8 ± 6.8*	-
Tab-8	10	95 ± 4*	-		-	-	-	-	-	-	2.37 ± 0.03	41.3 ± 2.8*	-
Tab-9	18	68.4 ± 3.1	39	26	47.1 ± 8.2	77 ± 12	38.2 ± 6.8	80 ± 19	-	41.3 ± 8.2	2.49 ± 0.04	27.4 ± 1.5	25.3 ± 4.8
Tab-10	22	5.5 ± 0.2	18	5	-	-	1.6 ± 0.5	113 ± 23	-	-	3.02 ± 0.03	1.8 ± 0.1	0.5 ± 0.2
Tab-11	31	49.1 ± 1.0	66	15	33.3 ± 4.1	81 ± 10	27 ± 3	62 ± 15	41.4 ± 5.2	34 ± 4	2.05 ± 0.03	23.8 ± 1.0	20.4 ± 1.8
Tab-19	18	50.5 ± 2.1	48		-	-	-	-	-	-	2.05 ± 0.04	24.9 ± 1.2	-
Tab-20	18	5.8 ± 0.2	46	10	2.6 ± 0.7	143 ± 20	0.6 ± 0.2	70 ± 44	-	-	2.97 ± 0.02	1.9 ± 0.1	0.2 ± 0.1
Tab-21	24	17.4 ± 0.5	80	15	7.7 ± 0.8	80 ± 9	6.0 ± 0.6	64 ± 13	-	-	2.69 ± 0.02	6.5 ± 0.3	2.8 ± 0.3
MA1	12	3.6 ± 1.2	19	5	-	-	0.2 ± 0.1	-	-	-	2.22 ± 0.09	1.6 ±.0.2	0.09 ± 0.1
MA2	12	14.5 ± 2.3	22	24	-	-	0.9 ± 0.3	94 ± 48	-	-	2.22 ± 0.03	6.6 ±.1.1	0.43 ± 0.1

Table 4.5 Summary and comparison of equivalent dose values for samples measured using both quartz and K-feldspar grains. N = number of aliquots; SE = Standard Error

Sample	Equivalent Dose- Quartz*		Equivalent Dose - K-Feldspar (Gy)			
			IR_{50}		$pIRIR_{290}$	
	N	Dose (Gy) ± SE	N	Dose (Gy) ± SE	N	Dose (Gy) ± SE
Tab-1	-	-	6	79.29 ± 13.70	6	120.95 ±10.64
Tab-8	10	95 ± 3**	4	108.94 ± 1.41	6	254.88 ± 16.77
Tab-9	-	-	-	-	4	118.24 ± 23.51
Tab-10	22	5.5 ± 0.2	8	46.21 ± 0.61	4	56.40 ± 24.02
Tab-11	31	49.1 ± 1.0	-	-	2	365.88 ± 58.26
Tab-12	-	-	12	78.54 ± 8.11	15	165.00 ± 7.02
Tab-18	-	-	6	105.56 ± 17.68	8	150.90 ± 19.43

*Based on multi-grain aliquots ** Minimum age only

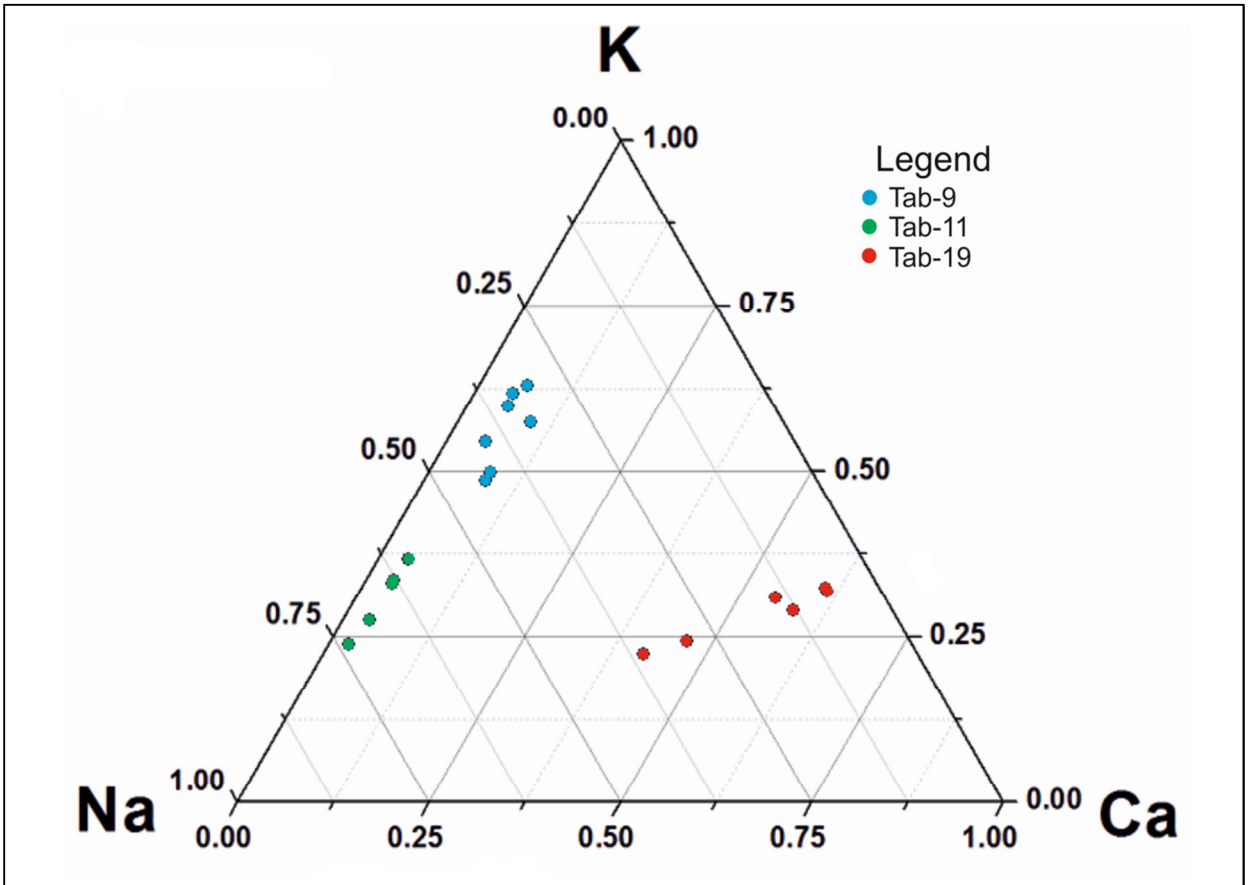

Figure 4.13 Ternary diagram showing XRF major element analysis for feldspar grains for samples Tab-9, Tab-11 and Tab-19.

4.8.3 Modern analogue samples

Due to the lack of feldspar control in assessing quartz bleaching rates, modern analogue samples were measured for quartz OSL in order to assess the likelihood of incomplete bleaching in the remaining unsaturated samples. Two samples were collected from present day depositional contexts believed to be analogous with those of the geologic samples; notably, a coarse grained sand unit (MA1) and fine grained silt/clay unit (MA2). Measurements of environmental dose rate and multi-grain quartz OSL were conducted using the same techniques detailed in Sections 4.7.1 and 4.8.1, respectively. Dose rates were 2.22 ± 0.1 Gy/ka^{-1} for both samples and the OSL characteristics were similar to that of the previous multi-grain measurements; notably, being fast component dominated with signals reaching background levels within a very short time.

4.8.4 Single grain measurements

Single grain analysis was conducted in this study to: (i) support modern analogue measurements in the assessment of sample bleaching, and (ii) to assess the accuracy of the multi-grain results derived from quartz aliquots. Single grain analysis was conducted on 5 geologic samples (Tab-9, Tab-10, Tab-11, Tab-20 and Tab-21) and both modern analogue samples (MA1 and MA2). Prior to measurements, all samples were re-sieved to the 180-250 µm grain size fraction in order to remove any fine materials that accumulated as a result of chemical treatment. Measurements were carried out on an automated Risø reader fitted with a single-grain laser attachment. The stimulation light source is a 10mW solid-state diode-pumped laser emitting at 532 nm, which is focused to a spot < 20 µm in diameter on the aluminium sample disc. Each sample disc contained 100 holes, on a 10×10 grid with 600 µm spacing between hole centres. Visual inspection under red light confirmed that a maximum of one grain was loaded into each hole.

OSL measurements were run in accordance with the SAR protocol utilised for multi-grain analysis with luminescence signals based on the initial 60 ms adopting standard single grain rejection criteria. Dose estimates were rejected if the IR depletion ratio was not within 2 s of unity or less than 0.9, and if the recuperation dose is larger than 1 Gy. Dose recovery tests were conducted on 3 samples using given doses of 15Gy, 40Gy and 60 Gy (Fig. 4.14).

Equivalent dose values were calculated from single grain measurements adopting the central age model (CAM) and CAM un-logged (CAM_{UL}), as presented in Table 4.4. Both statistical models are of value when dealing samples that show overdispersion in equivalent dose characteristics (Galbraith and Roberts, 2012). Overdispersion is a quantitative measure that refers to the relative standard deviation of the D_e distribution of true single D_e values from a central D_e value, after having allowed for estimation of the statistical error (Galbraith et al., 1999). CAM doses could only be calculated for 4 out of the 7 single grain samples (Tab-9, Tab-11, Tab-20 and Tab-21) due to the presence of multiple negative dose values. The CAM result for sample Tab-9 was calculated following the arbitrary rejection of 3 negative results. In accordance with the views of Thomsen et al., (submitted), a D_0 criteria of 50 Gy was also applied to the samples with equivalent dose values >20 Gy (Tab-9 and Tab-11). This method of analysis avoids bias to low saturation doses in the dose distribution, accepting only grains which have a D_0 greater than the average equivalent dose under discussion. This approach was deemed particularly relevant based on the characteristic low saturation limits in many of the Tabernas Basin samples.

Equivalent dose values are plotted against luminescence intensity for all samples (Fig. 4.15). A notable characteristic of all single grain measurements is the low number of grains that emitted a luminescence signal (Table 4.4). For all samples, less than 3.3% of grains emitted a measurable OSL signal. Overdispersion values were also notably high (Table 4.4) when compared with a standard ‘low dispersion’ value of 20% (Galbraith and Roberts, 2012)

Most notable is the unreported dispersion value for modern analogue sample MA1. Large overdispersion values could be a result of (i) sediment mixing during sampling stage, (ii) beta-dose rate heterogeneity, or (iii) incomplete / partial bleaching (Duller, 2008b).

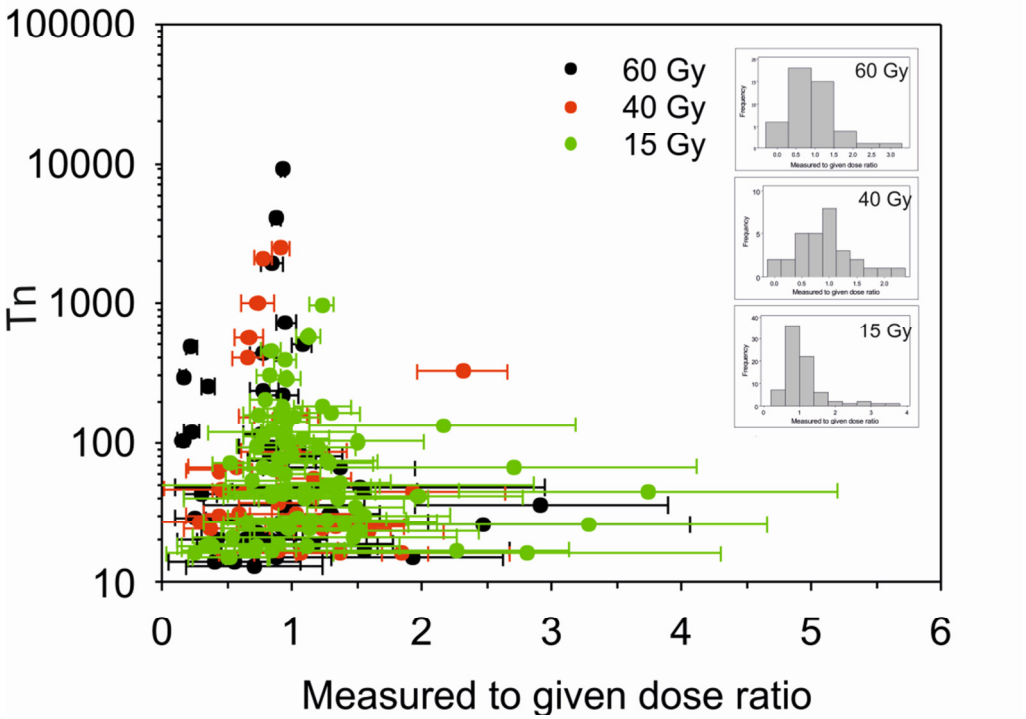

Figure 4.14 Summary of dose recovery values for single-grain measurements with 3 varying given doses at 60 Gy, 40 Gy and 15 Gy.

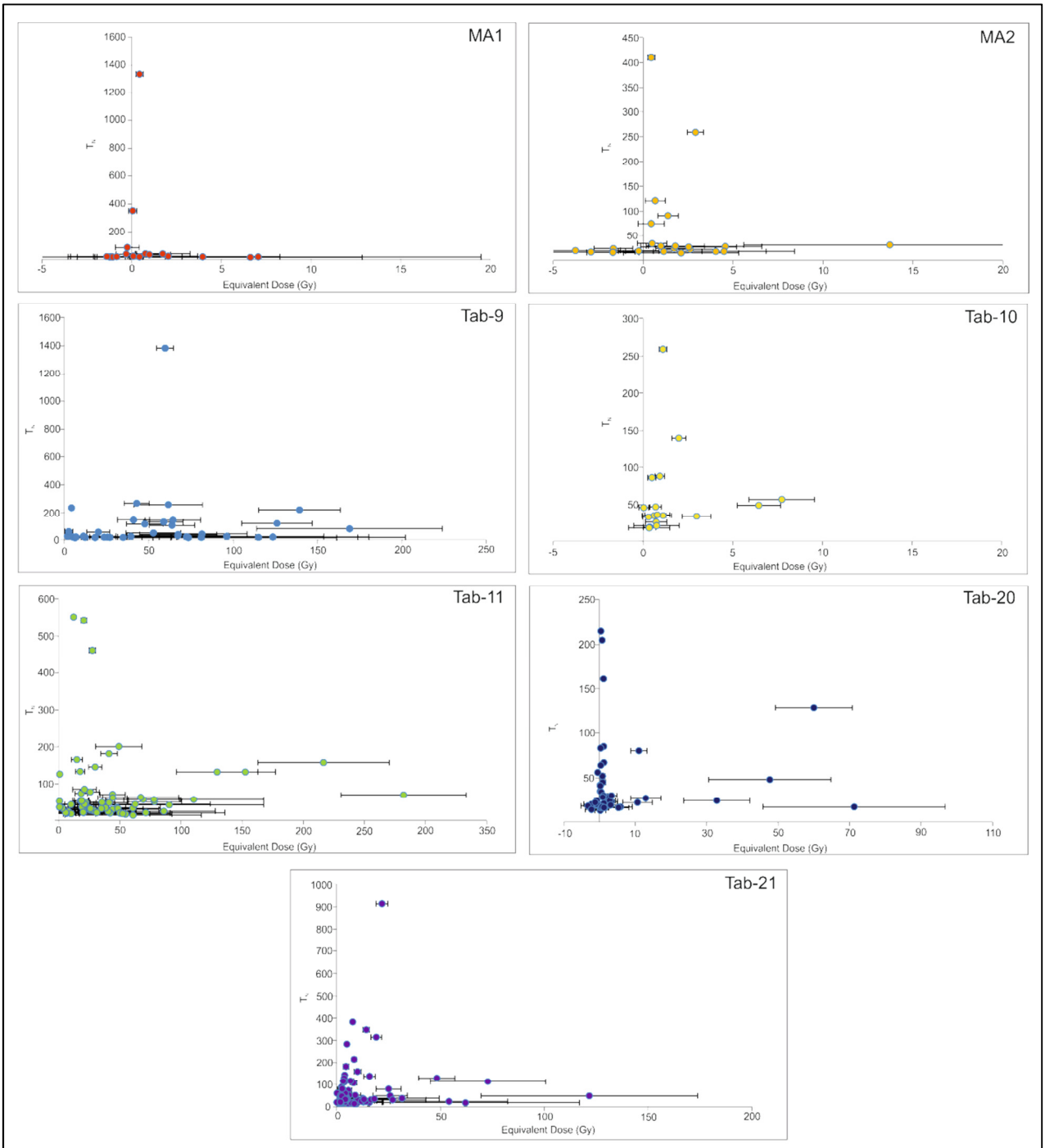

Figure 4.15 Equivalent dose vs. luminescence signal intensity plots for all single grain measurements. The large scatter in nearly all samples demonstrates the large over dispersion values.

4.9 OSL results

A summary of the quartz OSL ages calculated in this study are presented in Table 4.6. Initial analysis of modern analogue samples adopting single grain estimates shows that all samples were generally well bleached. Ages of 0.09 ± 0.1 ka and 0.43 ± 0.1 ka were calculated adopting the CAM_{UL} for samples MA1 and MA2, respectively. The results from multi-grain analysis notably overestimated the ages for the modern samples due to the presence of multiple saturated grains evidenced in single grain measurements (24% of grains in saturation for MA2; Table 4.4). This age over estimations highlight the limitations of multi-grain measurements in accurately representing modern dose distributions.

Multi-grain measurements also overestimated ages for all young samples Tab-10, Tab-20 and Tab-21 collected from terrace level 4. Calculated ages from multi-grain analysis were at least triple those from single grain measurements (Table. 4.6). Single grain CAM_{UL} estimations for terrace level 4 were between 0.2 ± 0.1 ka (Tab-20) to 2.8 ± 0.3 ka (Tab-21). The discrepancy between the multi-grain and single grain measurements is again due to the presence of a few grains in saturation, highlighting the significance of saturated grains upon dose estimations when dating young samples. The ages calculated from single grain measurements appear to relate well with the field stratigraphy (e.g. sample locations and depth) and infer a Holocene to Recent age for the lower most terrace level (level 4).

The results from multi-grain and single grain measurements (adopting the D_0 criteria) show a reasonable relationship for older samples Tab-9 and Tab-11 from terrace level 3. Calculated ages for Tab-9 fall within errors with ages at 27.4 ± 1.5 ka (multi-grain) and 25.3 ± 4.8 ka (single grain). Slight discrepancies are noted for Tab-11 with an age of 23.8 ± 1.0 ka from multi-grain measurements, compared with 20.4 ± 1.8 ka from single grain measurements. Although limited in number, the results from both older samples support the belief that multi-grain analysis sufficiently represents older samples (>10 ka) due to the decrease in importance of a few Gy's of residual (unbleached) dose when dealing with large equivalent dose values (Duller, 2008b).

Table 4.6 Summary of multi-grain and single grain OSL ages for the Tabernas Basin terrace sequence. Table includes additional date termed EX1 derived from the lower lake sequence of Harvey et al., (2003).

Samp.	Terrace Level	Depositional environment.	Multi-grain age (ka)	Single Grain Age (ka)
Tab-3	3	Upper lake sequence: sands / silts. Sample taken 0.7m from top of section	31.1 ± 9.8*	-
Tab-4	2	Rambla Verdelecho fluvially dominated alluvial fan deposits: gravels/sands. Sample 0.6m from top of section	26.4 ± 9.1*	-
Tab-7	3	Lower lake sequence: ponded clays/muds/sands. Sample 8.5m from base of section	15.8 ± 6.8*	-
Tab-8	3	Upper lake sequence: low energy sands/ silts. Sample 2.4m from base of section	41.3 ± 2.8*	-
Tab-9	3	Rambla Reinelo fluvial terrace: gravels/sands. Sample 2.2m from base of section	27.4 ± 1.5	25.3 ± 4.8
Tab-10	4	Rambla Tabernas fluvial overbanks: sands/ silts. Sample taken 1.1m from base of section	1.8 ± 0.1	0.5 ± 0.2
Tab-11	3	Rambla Grillo fluvial terrace: gravels/sands. Sample 1.4m from base of section	23.8 ± 1.0	20.4 ± 1.8
Tab-19	3	Rambla Buho fluvial overbanks: sands/ silts. Sample taken 0.4 m from base of section	24.9 ± 1.2	-
Tab-20	4	Rambla Tabernas fluvial overbanks: sands/ silts. Sample taken 0.6 m from top of section	1.9 ± 0.1	0.2 ± 0.1
Tab-21	4	Rambla Tabernas fluvial terrace : gravels/ sands/ silts. Sample taken 1.4m from base of section	6.5 ± 0.3	2.8 ± 0.3
MA1	-	Rambla Tabernas channel sands	1.6 ± 0.2	0.09 ± 0.1
MA2	-	Rambla Tabernas channel fine silts/clays	6.6 ± 1.1	0.43 ± 0.1
EX1	3	Lower lake section taken 6m from top of section	14 ± 1	-

* Minimum ages only

The minimum ages calculated from saturated doses for samples Tab-3, Tab-4, Tab-7 and Tab-8 all conform with the detailed results from multi-grain and single grain analysis. The inclusion of saturated dose values allows for the identification of a upper most depositional age for terrace level 3 upper lake sequence at 41.3 ± 2.8 ka (Tab-8; Table 4.6). The minimum ages for Tab-3 (31.1 ± 9.8 ka) and Tab-7 (15.8 ± 6.8 ka) are from the upper and lower lake sequences respectively. They support pre-existing age estimates for terrace level 3 with a depositional age ranging from 14 ± 1 ka (Sample name EX1 from Alexander et al., 2008) to 41.3 ± 2.8 ka. Unfortunately, the minimum age presented for Tab-4 (26.4 ± 9.1 ka) does not add any value for constraining the timing of deposition for terrace level 2.

4.10 Discussion

The following sections present an overview of the temporal patterns of river terrace aggradation and incision within the Tabernas Basin and further Almería region. Note that correlations principally focus on the timings of terrace formation building on the stratigraphy presented in Chapter 3. At this stage little detail is offered into the processes that promote their formation both locally and regionally (e.g. tectonics, sea-level change) which are presented in detail in Chapters 6 and 7. However, it is unavoidable to comment on the significance of climate cycles in the generation of terrace aggradation stages.

4.10.1 Tabernas Basin stratigraphy

The age estimates generated in this study add valuable information to the Tabernas Basin stratigraphy (Chapter 3 for detail) and for applying OSL more broadly within the Betic Cordillera region of SE Spain. Most notable are the age estimates for terrace levels 3 and 4 (Fig. 4.16). Adopting minimum age estimations for terrace level 3, it is inferred that deposition of the substantial lacustrine deposits characteristic along the axial drainage system was ongoing from at least 41.3 ± 2.8 ka (Tab-8 sampled 2.4m form base of upper lake sequence of Harvey et al., 2003; Table 4.5). Assuming regional patterns of terrace aggradations during cold climate phases or climatic transitions (Candy et al., 2005; Santisteban and Schulte, 2007; Bridgland and Westaway, 2008; Miekle, 2008; Schulte et al., 2008), it is likely that the aggradation of terrace level 3 occurred either during the highly variable climatic fluctuations of MIS 3, or during the transition from marine isotope stage MIS 4 to MIS 3 at ~57 ka. Assuming this date, the substantial incisional phase (degradation stage 2 on Fig 3.17, Chapter 3) which pre-dates terrace level 3 likely occurred during MIS 5.

Lacustrine/ palustrine sedimentation of terrace level 3 would have been cyclic in occurrence (as supported by the sedimentology) and ongoing throughout MIS 3 and MIS 2 as supported by dates of 31.1 ± 9.8 ka (minimum) from the upper lake sequence (Tab-3 minimum age) and 14 ± 1 ka (EX1) from the lower lake sequence of Harvey et al., (2003).

Sediment inputs from the basin margins would also have been ongoing throughout MIS2, as supported by dates of 25.3 ± 4.8ka (Tab-9) and 20.4 ± 1.8ka (Tab-11) sourced from coarse grain fluvial terraces in two major tributaries to the axial Tabernas drainage (Rambla Reinelo and Rambla Grillo; Fig 4.16). Fluvial incision and resultant terrace level 3 abandonment would likely have occurred during the transition from MIS 2 to 1 with the onset of warmer climate conditions, as supported by the youngest OSL date of 14 ± 1 ka sourced from the top of the lower lake type section of Harvey et al., (2003).

The onset of deposition for terrace level 4 is much harder to define due to the erosional base being lower than the river bed level of the current fluvial system. Dates from the lower most exposed sections for terrace level 4 (Tab-21) indicate that deposition was ongoing from 2.8 ± 0.3 ka; however, it is likely that the onset of terrace deposition occurred sometime before this. The age estimates from samples Tab-10 (0.5 ± 0.2 ka) and Tab-20 (0.2 ± 0.1 ka) support deposition for terrace level 4 throughout the late Holocene to near recent times (Fig. 4.16), but associations with the much older age estimations are hard to make given the non-continuous nature of individual terrace bodies sampled across the basin. Based on this range of dates it could be likely that terrace level 4 deposits represent isolated deposits preserved in a broadly incisional fluvial system.

4.10.2 Regional Correlations

A summary of the available chronological data obtained from the eastern Alpujarran Corridor (EAC) and the Tabernas, Sorbas and Vera basins is presented in Figure 4.17. It is important to note that the age estimates derived from other nearby basins are generated using a range of dating techniques with different inferences when dating either periods of terrace aggradations or abandonment. For example, ages derived from OSL methods are depositional in nature, yet estimates derived from U/Th dating on calcreted surface and/or cosmogenic exposure dating from terrace surfaces give a post abandonment or incisional age only (see table of content for age type in Fig. 4.17). In addition, age estimates are only

presented from studies where the chronology clearly relates to a field record. For example, numerous absolute ages are presented by Schulte et al., (2008) for Travertine sections from the middle to lower sections of the Río Aguas Quaternary system; however, the Quaternary terrace record from which these age estimates are derived (i.e. isolated travertine cemented terraces) does not correlate well with the works of Candy et al., (2005) or Ilott (2013) which date the abandonment of terrace surfaces in the upper to middle sections of the Río Aguas system.

Regardless of dating method disparities, the data derived identify regional similarities in basin evolution throughout the Quaternary period. Notable correlations can be made between the timings of terrace aggradation for the younger terrace levels for most basins. For example, terrace level 3 of the Tabernas Basin is evidenced to have been aggrading throughout MIS 3 into MIS 2 with likely abandonment and incision during the transition to warmer climate conditions (MIS 2 to MIS 1). Depositional ages (OSL age estimates) for level D of the Sorbas Basin suggest deposition was also ongoing throughout MIS 3, with subsequent abandonment sometime in the early Holocene (Candy et al., 2004), highlighting a potential link between the basins. Furthermore, based on relative positioning and the age estimations generated, it is likely that terrace level E of the Sorbas Basin is comparable with terrace level 4 of the Tabernas Basin with deposition in the Late Holocene.

Unfortunately the suggested suitable ages (quartz OSL) from the youngest terrace unit in the Vera Basin (Lorca allomember; Miekle, 2008) do not conform to age estimates from the Tabernas and Sorbas Basins (Fig.4.17). Depositional ages from quartz OSL suggest deposition during the transition from MIS 2 to MIS 1, which is typically marked as an incisional period in the Tabernas and Sorbas Basins. However, the rejected K-feldspar IRSL ages from the same samples indicate an age range of between 37.2 ± 3.4 ka to 28.5 ± 1.9 ka (Miekle, 2008). Although the reliability of the analytical procedure is poorly presented, these ages would correlate well with the findings for the Tabernas and Sorbas basins, with

deposition of the Lorca allomember during the highly variable climate of MIS 3 and/or the transition from MIS 3 to MIS 2.

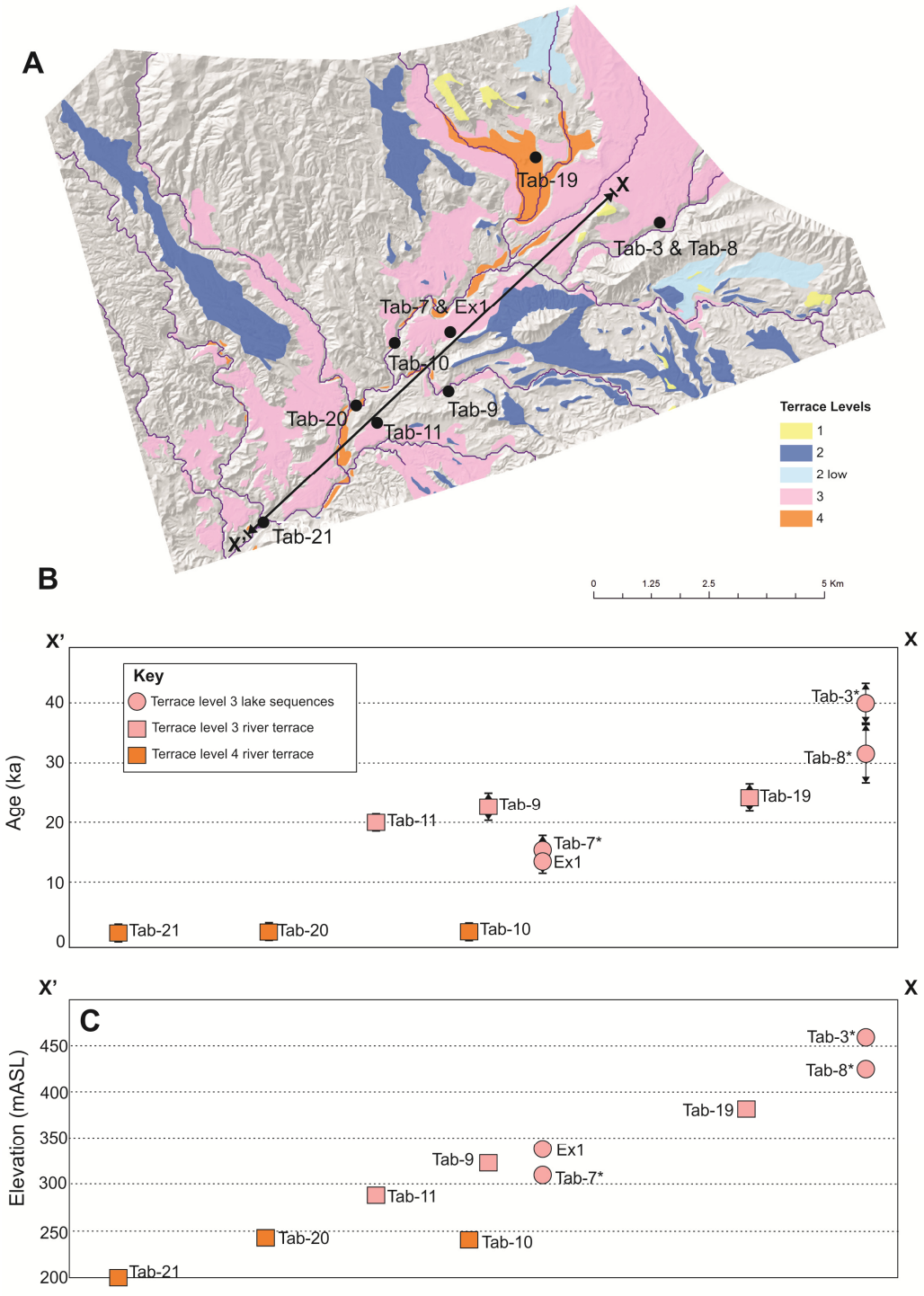

Figure 4.16 Spatial and temporal representation of OSL dates obtained in this study. (A) Location of samples from across the basin with relevant landform levels, (B) Spatial plot of OSL dates presented along transect X-X', * highlights minimum dates, and (C) Elevation plot for OSL ages. Note the clear grouping of terrace level 3 dates from both lake terraces and river terraces and the grouping of terrace level 4 dates on both B and C. It is interesting to note that fluvial terrace aggradation also occurs during periods of lake aggradations.

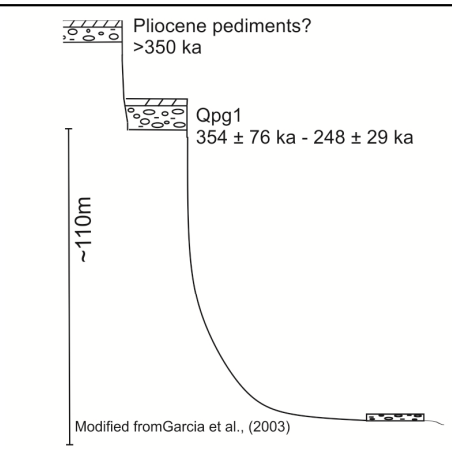

Eastern Alpujarran Corridor
(Río Andarax)

Terrace Level	Age (ka)	Method	Author
Pliocene?	> 350	U series dating / abandonment age	Garcia et al., (2003)
Qpg1	276 ± 40	U series dating / abandonment age	Garcia et al., (2003)
Qpg1	354 ± 76	U series dating / abandonment age	Garcia et al., (2003)
Qpg1	248 ± 29	U series dating / abandonment age	Garcia et al., (2003)
Qpg1	282 ± 34	U series dating / abandonment age	Garcia et al., (2003)

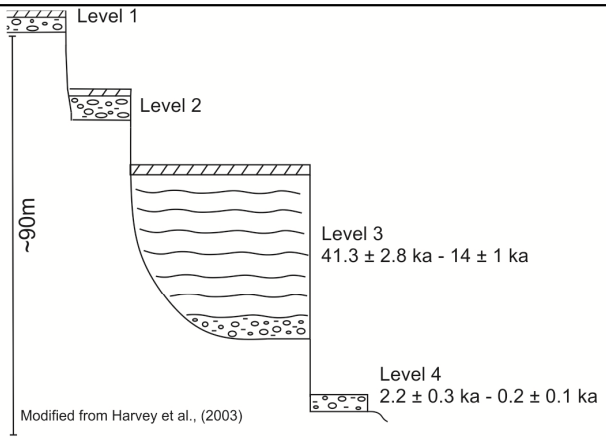

Tabernas Basin
(Río Tabernas)

Terrace Level	Age (ka)	Method	Sample
3	41.3 ± 2.8*	Quartz OSL / depositional age	Tab-8
3	31.1 ± 9.8*	Quartz OSL / depositional age	Tab-3
3	25.3 ± 4.8	Quartz OSL / depositional age	Tab-9
3	20.4 ± 3.8	Quartz OSL / depositional age	Tab-11
3	14 ± 1	Quartz OSL / depositional age	Ex1
4	2.2 ± 0.3	Quartz OSL / depositional age	Tab-21
4	0.5 ± 0.2	Quartz OSL / depositional age	Tab-10
4	0.2 ± 0.1	Quartz OSL / depositional age	Tab-20

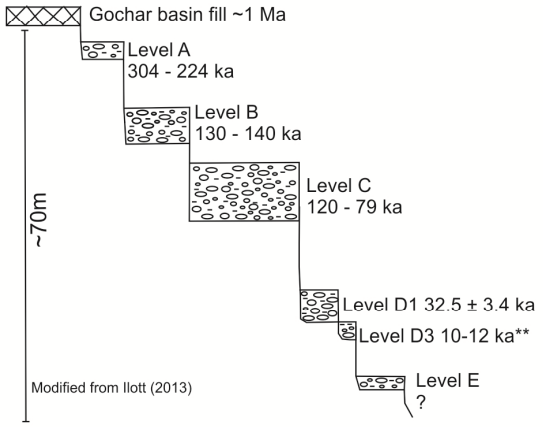

Sorbas Basin
(Upper - Middle Río Aguas)

Terrace Level	Age (ka)	Method	Author
Gochar fill	100	Cosmogenic dating / exposure age	Illott, 2013
A	304 - 224	U series dating / abandonment age	Candy et al., 2005
B	140 -130	Cosmogenic dating / exposure age	Illott, 2013
B	207 - 112	U series dating / abandonment age	Candy et al., 2005
C	120 - 79	Cosmogenic dating / exposure age	Illott, 2013
C	104 - 67	U series dating / abandonment age	Candy et al., 2005
D	30.3	U series dating / abandonment age	Candy et al., 2005

Río Alias

D	32.5 ± 3.4	Quartz OSL / depositional age	Maher,2005

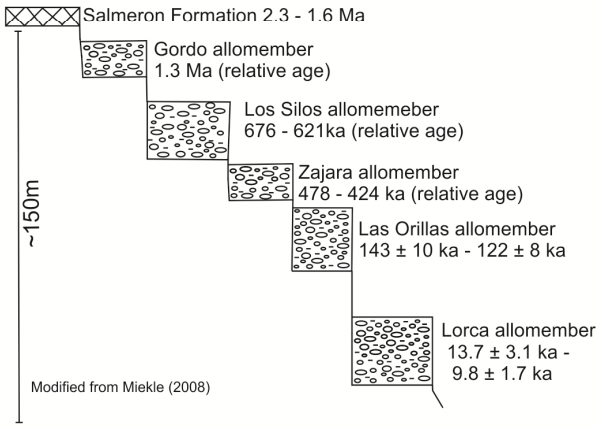

Vera Basin
(Río Almanzora)

Terrace Level	Age (ka)	Method	Author
Salmeron Form.	2300 - 1600	Electro spin resonance dating	Wenzens, 1992
Gordo	1300	Relative age based on climate aggradations	Miekle, 2008
Los Silos	676 - 621	Relative age based on climate aggradations	Miekle, 2008
Zajara	478 - 424	Relative age based on climate aggradations	Miekle, 2008
Las Orillas	143 ± 10 - 122 ± 8	K Feldspar OSL / depositional age	Miekle, 2008
Lorca	13.7 ± 3.1 - 9.8 ± 1.7	Quartz OSL / depositional age	Miekle, 2008
Lorca	37.2 ± 3.4 - 28.5 ± 1.9	K Feldspar OSL / depositional age	Miekle, 2008

Figure 4.17 Summary of basin terrace chronologies for the EAC, Tabernas, Sorbas and Vera basins. The source and method of acquisition for all dates is presented in the table below. * Minimum age value only ** Relative age derived from soil chronostratigraphy (Harvey et al., 1995).

The lack of available age estimates for terrace levels 1 and 2 in the Tabernas Basin makes correlations with the neighbouring EAC, Sorbas and Vera basins difficult. A general assumption in the region has been to accept the climatically driven modes of terrace aggradation as presented for northern European drainages by Bridgland et al., (2004), with terrace aggradation occurring during the major climatic ameliorations or during the transitions between cold and warm climate phases. This assumption fits well across the Iberian peninsula (sensu Macklin et al., 2002) and is further backed in the Almería region by the ages presented for terrace level 3 and level D of the Tabernas and Sorbas basins, respectively. These data are further supported by the age estimates generated from feldspar OSL for the Las Orillas allomember in the Vera Basin (Fig. 4.15; Miekle, 2008) recording terrace aggradation during the transition from cold to warm climate conditions (MIS 7 to MIS 6).

Accepting the abandonment age estimates presented from U series and cosmogenic methods for the Sorbas Basin and assuming similarities in basin forcing mechanisms, it is likely that older terrace aggradations occurred during major climatic forcing events such as the transition from MIS 7 to MIS 6 (~190 ka) for terrace level B, and during the major cold climate phase of MIS 4 for terrace level C. Based on this regional pattern, it is likely that terrace levels 1 and 2 aggradations in the Tabernas Basin also relate to periods of climatic amelioration or variation. However, due to the known differences in internal basin dynamics (e.g. differences in terrace level number due to river capture events between the Tabernas and neighbouring Sorbas Basin) it is difficult to prove these regional assumptions.

From the regional correlations made it is notable that the importance of constraining the onset of incisional phases is commonly neglected against the dating of aggradation events. Across the Almería region, the only incisional dates are presented for (i) the abandonment of terrace level C with focus on mechanisms of stream capture in the Sorbas Basin (Kelly et al., 2000; Candy et al., 2004) and (ii) the final stages of recorded sedimentation in the EAC (Garcia et al., 2003).

4.11 Summary

This chapter has highlighted both the use and limitations of OSL in dating Quaternary fluvial and alluvial fan deposits in the Tabernas Basin. The study has highlighted the typical restriction of the method due to unusually low saturation limits (<50 Gy) of quartz grains sourced from all terrace levels across the basin. However, some samples did have OSL characteristics favourable for age estimation purposes. Of the 21 samples taken, only eight samples were suitable for analysis using single grain, multi grain and modern analogue analysis techniques in order to develop a full understanding of the bleaching history and typical dose distributions. The results from multi-grain aliquots show that multi-grain analysis overestimates single grain results for younger samples (terrace level 4 and modern analogue) due to a number of grains in saturation. This is a common limitation of the OSL method when dealing with poorly bleached or mixed materials typically experienced in the fluvial domain. However, the results from single grain analysis applying D_0 criteria supported the dose estimations from the multi-grain analysis when dealing with older samples (terrace level 3).

Due to low saturation limits, age estimates have only been derived for the lowest two terrace levels (terrace levels 3 and 4) across the Tabernas basin. Although limited in number, these absolute ages help to identify patterns of climate driven terrace formation throughout the Quaternary and offer further insight in to the routing of sediment during terrace formations on a basin scale. In addition, this study has also allowed for the identification of the following sampling and analytical procedure which could be applied when using OSL in sedimentary basins located in the Betic Cordillera region of SE Spain:

1. Prior to the sampling stage, a full understanding of the sedimentological setting must be appreciated. This includes: (i) the relationship to other landforms across a given area (e.g. the relative position within a terrace sequence across a basin), (ii) the internal sedimentary stratigraphy of the unit which is to be sampled and (iii) any

internal structures or features which might have implications of facets of environmental dose-rate distribution (e.g. bioturbation, roots or cemented units).

2. Prior to the sampling stage, assess the likelihood of dose-rate heterogeneity. If sedimentary thicknesses are not uniform or of a notably varied grain size (e.g. numerous floating cobbles in a sand unit) collect a bulk sample of materials from the surrounding 0.5m^3 for subsequent laboratory analysis. If possible, field gamma-spectrometry should be conducted in sampled locations for further calibrations with laboratory dose-rate calculations.
3. During the sampling stage, collect modern analogue samples which are representative of the depositional environments encountered. These samples will be vital in assessing aspects of signal resetting in equivalent dose estimates.
4. If possible, collect multiple samples from a range of depositional setting, insuring a high quartz content.
5. During the sample preparation stage, retain all grain size fractions in addition to the favoured 180 – 250 μm fraction. In addition, prepare both quartz and feldspar grains for measurement purposes.
6. Prior to pulverising materials for dose-rate measurements, ensure maximum field moisture contents are measured for all samples. These values can be compared with field values, however, note that the field values typically do not represent the annual moisture contents in this region.
7. When assessing equivalent dose values, adopt a combined quartz and feldspar approach.
    i. For feldspar grains, first assess the percentage of K-feldspars in a sample. If a sample contains high percentages of Na or Ca-feldspar do not continue with IRSL measurements. If the sample has high quantities of K-feldspar, run multiple post IRSL measurements at varied cut-heats (e.g. IR_{50}, IR_{225}, IR_{250}, IR_{290}) assessing the ratios of measured signals in accordance with work of Buylaert et al., (2012).

ii. For quartz grains, run initial range-finder experiments on at least 5 multi grain aliquots of each sample to assess the equivalent dose characteristics. In addition, conduct preheats plateau tests on at least 3 samples reusing the range-finder aliquots in order to determine appropriate measurement temperatures. Give known doses close to those measured.

iii. Insure measurements are made on modern analogue samples at an early stage. This will identify any issues of incomplete bleaching and the requirement for further single grain analysis.

iv. For quartz grains, run single grain analysis if there is time and opportunity. Apply standard age model calculations as based on the distributions of the data derived (e.g. central age model or the minimum age model). If issues of low saturation occur apply the D_0 criteria proposed by Thomsen et al (in review).

v. Compare the results from both dosimeters (quartz and feldspar) in accordance with the findings of Murray et al., (2012). The results from quartz grains should be higher than the results from IR_{50} signals in a well bleached sample.

In closure, it is again highlighted that correlations presented in this chapter are based on temporal relationships in terrace aggradation and incisional stages as attributed to climate cycles alone. It is noted that regional variations in terrace records across SE Spain occur as a result of local interactions in forcing agents (e.g. tectonics and sea-level change). These aspects are further discussed in detail in Chapter 7. However, the age estimates presented herein are of vital importance in quantifying rates of long-term landscape change in both conceptual studies and further numerical modelled packages as further developed in Chapters 5 and 6.

Chapter 5

5.1 Application of geospatial interpolation techniques in Quaternary fluvial archive studies

Quaternary river terrace sequences provide valuable geomorphic records which enable the qualitative and quantitative assessment of landscape processes at a range of temporal and spatial scales (see Stokes et al., 2012). The reconstruction of global and regional terrace records has been pivotal in identifying multiple process-form relationships operating within fluvial systems over Quaternary timescales (e.g. assigning processes of climatically driven terrace formation in NW Europe largely based on two-dimensional terrace staircase transects, e.g. Bridgland and Westaway, 2008). Further studies focusing on the internal (intrinsic) characteristics of individual fluvial systems have highlighted the use of single or grouped terrace bodies when evaluating the morphological evolution of a fluvial system at timescales beyond those of the contemporary and historic record (e.g. Maizels, 1989; Vandenberghe, 1995; Daniels, 2008; Thorndycraft et al., 2008). However, in comparison to the qualification of process interactions, which mainly focus on the formation and /or dating of aggradational river deposits, the use of river terrace sequences in the quantification of the amounts and rates of landscape degradation over long timescales has been relatively limited. When adopted for quantification purposes, variations in incisional depths and thicknesses within terrace sequences has offered valuable insight into patterns of landscape degradation, sediment flux and sediment delivery within and between hydrological basins (e.g. application of mean valley width approach by Stokes et al. (2002) in the quantification of river-capture-induced base-level changes and landscape development in the Río Aguas, SE Spain; Fig. 5.1).

The following chapter focuses on the use of the Quaternary terrace records in the quantification of degradational phases in studies of long-term landscape evolution. The aim is to emphasise the importance of degradation stages within the development of fluvial systems; highlighting how an understanding of incisional rates and styles over a range of

temporal and spatial scales is a fundamental part of any fluvial archive study. The quantification of degradation stages is further used to supplement the stratigraphic framework presented in Chapter 3. The Tabernas Basin terrace record provides an opportunity to explore this statement with four major degradational phases which record a variable response to landscape forcing mechanisms throughout the Quaternary (see Fig. 3.17, Chapter 3). In this chapter, methods of geospatial interpolation are applied to the fragmentary terrace record in Tabernas to generate continuous palaeo-landsurfaces for quantification purposes. Although not routinely applied in Quaternary landscape studies, geospatial interpolation techniques have been demonstrated to offer a precise method in the reconstruction of terrace landform records when compared with conventional 2 dimensional transects and cross valley profiles (Geach et al., 2014a).

Throughout this chapter the methods of geospatial interpolation are developed in accordance with the approaches developed by Geach et al., (2014a). Initially, an overview of the multiple techniques of geospatial interpolation is presented, detailing the use and application of the method in geomorphological studies (Section 5.2). A detailed assessment of interpolation technique suitability is then presented with regard to the reconstruction of an example dataset from the Tabernas Basin terrace record (Section 5.3). Outputs from the interpolation processes are then compared with each other with focus on generating surface volume data and incisional rates for major degradation periods in the basins development (Section 5.4). The data are summarised with emphasis on developing temporal and spatial patterns of landscape development within the Tabernas Basin throughout the Quaternary period.

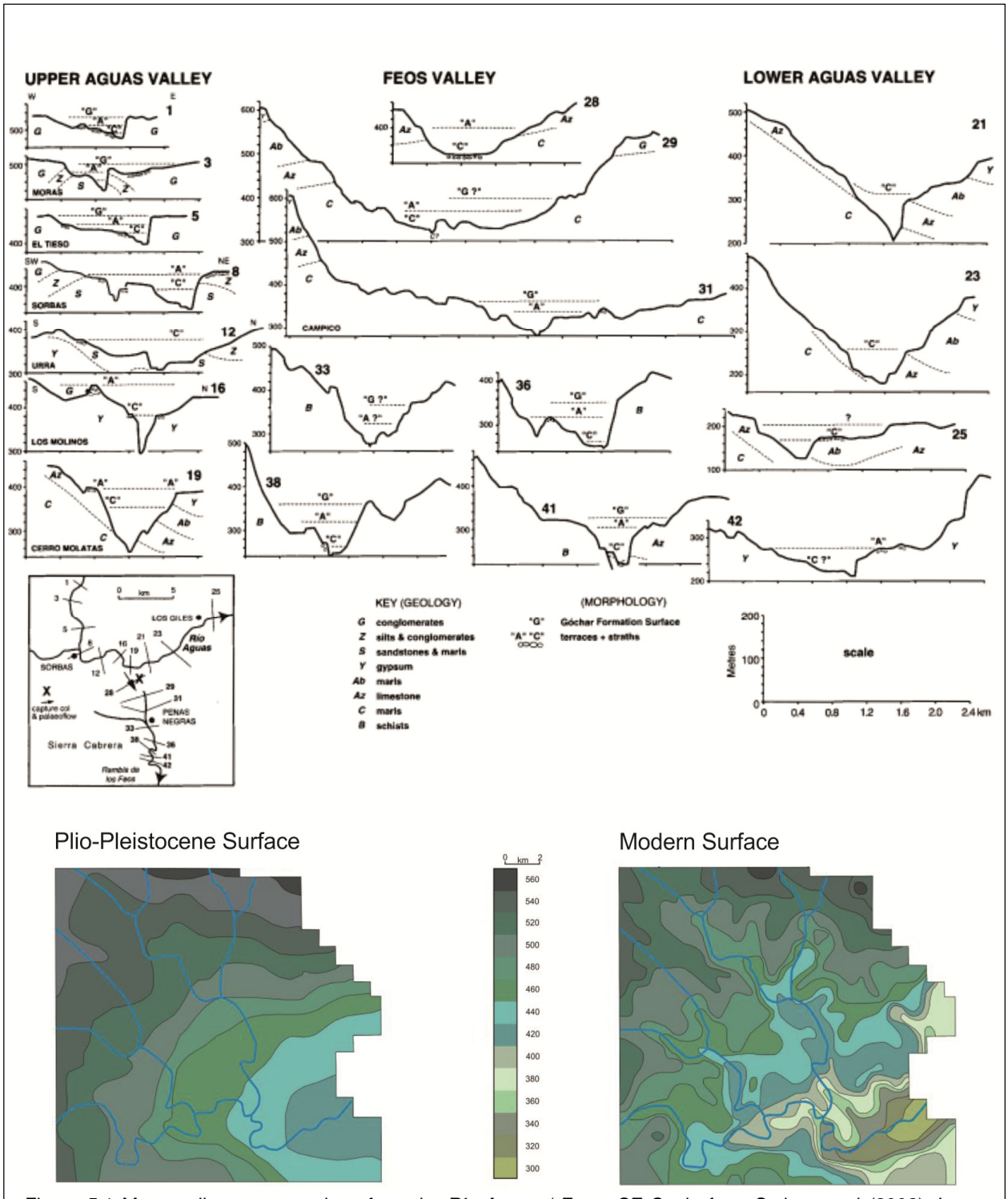

Figure 5.1 Mean valley cross sections from the Río Aguas / Feos, SE Spain from Stokes et al (2002). Insets shows a paleo-landsurface and current land surface developed from the Aguas/ Feos terrace records and current day topographic data, respectively.

5.2 Geospatial interpolation

5.2.1 Background

The purpose of the geospatial interpolation process is to enable more precise reconstructions of envirnonment phenonmena based on datasets of variable totality (Burrough and McDonnell, 1998). There are many forms of geospatial interpolation (e.g. kriging, inverse distance weighting or splines) which all effectively work by estimating the value of an environmental parameter(s) at a given point with no known direct observations using data from known point observations (Li and Heap, 2011). Interpolated values are then applied in the creation of continuous data sets or data surfaces with a known uncertaincity (Burrough and McDonnell, 1998; Chaplot et al., 2006; Haberlandt, 2007; Li and Heap, 2011). In geomorphological research, interpolation techniques have been increasingly applied in the past decade in accordance with the availability of environmental data. Typical examples include:

1. The creation of digital elevation models (DEMs) from incomplete or fragmented topographic datasets (Chaplot et al., 2006; Heritage et al., 2009; Wilson and Gallant, 2000; Bell, 2012);
2. Creation of soil moisture profiles at a range scales from limited sampling locations within river catchments (Yao et al., 2013);
3. Reconstruction of geomorphologic units within landslide complexes to assist in landscape susceptibility mapping (Gorum et al., 2008);
4. Reconstruction of historic topography data for further use in geomorphic change detection (James et al., 2012);
5. The generation of paleolandsurfaces via the reconstruction of spatially fragmented landform records for use in studies of long-term landscape evolution (Della Seta et al., 2005, 2008; Alexander et al., 2008; Calderoni et al., 2010; Troiani and Della Seta, 2011).

In this chapter, focus is placed on the use of interpolation methods in the reconstruction of river terraces for use in studies of long-term landscape evolution. The earliest application of such was conducted by Della Seta et al., (2005) and further refined by others (e.g. Della Seta et al., 2005, 2008; Calderoni et al., 2010; Troiani and Della Seta, 2011) in the reconstruction of terrace river terraces and alluvial fan remnants along the northern Marche rivers in the Umbria-Marche Apennines, Italy. Interpolation methods were used in the digital infilling (interpolation) of erosional landscape features (e.g. coastal valleys) in order to assess the significance of neotectonic processes throughout the Late Quaternary. Throughout these research examples, the value of the interpolation method was demonstrated in the identification of (i) localised variations or irregularities in erosional/depositional surfaces as a result of climatic and neotectonic factors; (ii) differences in averaged incision rates, as evidenced by variations in the height-age relationships of depositional units; and (iii) the existence of multiple depositional events within geomorphic features, as identified by more precise surface geometries and boundaries.

Adopting the broad approaches developed by Troiani and Della Seta, (2011), Geach et al., (2014a) further applied geospatial interpolation techniques in the generation of palaeo-landsurfaces from fragmentary terrace records. Using the Quaternary terrace record from the Tabernas Basin as a case study, they: (i) demonstrated the use of interpolation methods in the creation of detailed paleo-landsurfaces, (ii) highlighted the use of the method over a range of spatial (from single thread channels to basin-wide fluvial systems) and temporal scales (1 year to 100 Ka) and (iii) emphasised the applicability of the interpolation method in the creation of continuous data surfaces which form an important input of many computational modelling packages, such as FLUVER2 presented in Chapter 6. They also identified limitations in the method such as the effects of dataset parameters (e.g. surface elevation and curvature of interpolation surfaces) and known model parameters (e.g. search radius) upon the performance of individual interpolation techniques. The outcomes of the

study highlighted the requirement for a form of technique appraisal in the assessment of the interpolation techniques when applied to any geomorphological dataset.

5.2.2 Interpolation techniques overview

There are multiple techniques which exist under the heading of geospatial interpolation. In this chapter, six of the most commonly used techniques are applied in the reconstruction of Quaternary landforms from the Tabernas Basin: inverse distance weighting - fixed (IDW fix), inverse distance weighting - variable (IDW var), multiquadratic radial basis function (MRBF), ordinary kriging (OK), regularized spline with tension (RST) and universal kriging (UK). These techniques can be grouped as either deterministic or geostatistical in approach. In geostatistical techniques, data point estimations are based on quantified values of spatial autocorrelation in measured points which are derived from the entire spatial data set (e.g. OK and UK) (Eberly et al., 2004). Geostatistical methods do not require the surface used in the estimation phase to pass through all measured points of the given surface, hence making them inexact interpolators. As the relationship among known points forms the basis of estimations, a measure of the certainty or accuracy of the predictions can be generated when applying geostatistical approaches. In deterministic techniques (further known as exact interpolators), estimated point values are based on mathematical relationships developed between either (i) points of similar value (IDW fix and IDW var) or (ii) by calculating a degree of smoothing between points of a known value (MRBF and RST). Deterministic techniques are either global or local in nature. In global deterministic techniques, estimates of variables at unknown locations are generated using spatial attributes of the entire data set; whereas, in local deterministic techniques only a limited number of data points (defined by a set distance or number of points) are used (Burrough and McDonnell, 1998). An overview of the interpolation approach is presented accordingly for each technique used followed by a detailed description of the application process.

Kriging

Techniques of kriging (OK and UK) are based on the application of statistical probability theory in the prediction of unknown values at given data points (Oliver, 1990). The fundamentals of kriging assume that the distance or direction between sample points reflects a spatial correlation that can be used to explain variation in the surface (Collins and Bolstad, 1996). The relationship between points is developed in a spatial-dependence model represented by a semivariance diagram (semivariogram) (Fig. 5.2) (Oliver, 1990). The semivariogram is governed by the size (lag size) and number of distinct classes (bins) into which data points are grouped (binned) in order to reduce a large number of possible data point combinations (Fig. 5.2A) (Issacs and Srivastava, 1989). Statistical models are then applied to the semivariogram in order to develop a trend line between the data groupings (e.g., circular, spherical, exponential, and Gaussian). When fitted with the most appropriate statistical method (Fig. 5.2B), the semivariogram is used to estimate an elevation value for an unknown point (with calculated errors) as a function of its distance and degree of variation between known points (Myers, 1994). Given a degree of spatial correlation between data points, kriging can be utilised to generate uniform data surfaces from multivariate data sets (e.g. Haberlandt, 2007).

Throughout this chapter, the most appropriate statistical models and variogram parameters (i.e. lag size and bin number) were identified using the ArcGIS Geostatistical Analyst toolbox and the Average Nearest Neighbour tool in the Spatial Statistics toolbox. As a preliminary check, the data generated were assessed by methods of statistical validation. Outputs of predicted difference and standardised error were of most use in this preliminary assessment phase. In addition to the early validation stages, a fixed increase in distance search radius was conducted in order to assess the significance of this known model parameter upon technique performance. This incremental change was conducted at increased intervals of 10 points up to 100 points, with data point spacing significant at 25 m (increase in 10 points = 250 m).

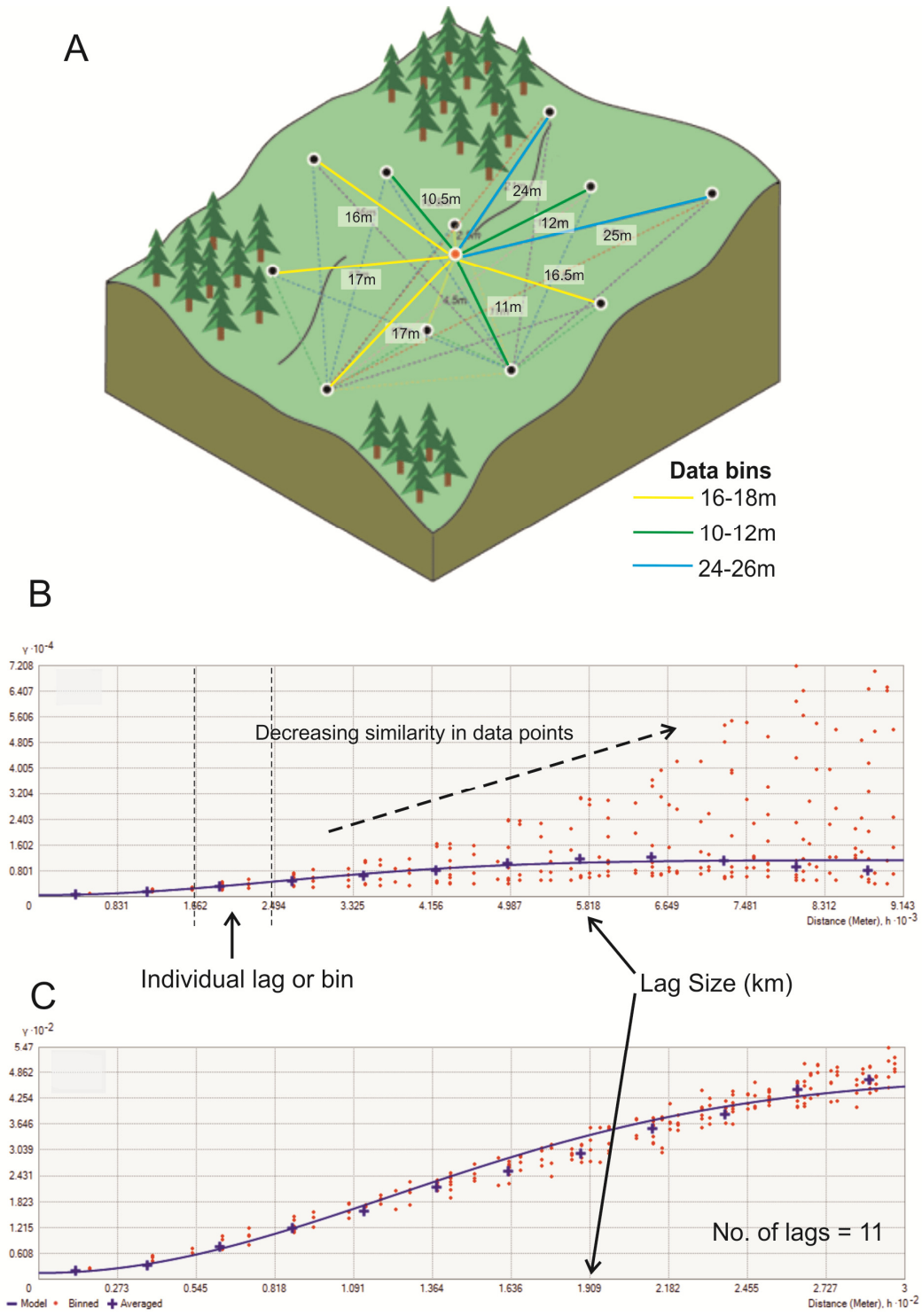

Figure 5.2 (A) Example of data point binning for a given unknown elevation point on a slope surface (red dot). The data bins in this example are 2m in size and group elevation data based on set values (e.g. 10-12m), image from ArcGIS resource centre (help.arcgic.com). The size of data bins forms the *x*-axis of the semivariograms presented in (B) and (C). (B) Shows how data are grouped in the semivariogram adopting standard groupings generated in the ArcGIS interpolation toolset for a given dataset. In B individual lags are 83m in size and fit with a spherical variogram model. Note the scatter in data at greater search distances in (B) when compared with a more representative lag size of 27m in (C) fit with the same variogram model.

The incremental increase in search radius was conducted for all of the interpolation techniques used (IDW and Spline), with data-specific parameters modelled for every stage. The nominal set distances were judged to be representative for the given spacing of the Tabernas terrace record, significant at < 200 m (i.e. typical spacing of terrace bodies was less than 200m).

Inverse distance weighting

Techniques of inverse distance weighting (IDW) determine unknown data point values using a linearly weighted combination of a set of known sample points. The weighting is a function of the inverse distance of known data points from the unknown point, which can defined by a given search radius (i.e. data points occurring outside of the search radius are not used in the interpolation function; Fig. 5.3A) (Eberly et al., 2004; Lu and Wong, 2008). The method assumes that the influence of a known data point decreases with distance from the unknown point as defined by a mathematical power parameter. A higher power parameter places more emphasis on the closest known values (e.g. red boxes over yellow boxes on Fig. 5.3B) (Watson and Philip, 1985; Lu and Wong, 2008). IDW techniques are also controlled by the number of input points used in the interpolation process. This can be defined by adopting either a fixed or variable search radius. With a variable search radius (IDW var), the number of known points used in the estimation process is set. This means that a larger search radius will be used if the density of known data points around the unknown data point is low. However, if the density of known values is large only a small search radius is required to acquire the data needed for estimation purposes. In fixed search techniques (IDW fix), a defined search radius is set along with a minimum number of known data points required to perform the interpolation calculations. If the density of data within the fixed radius is too low, the errors on the calculations are too great and the method does not work (Lu and Wong, 2008).

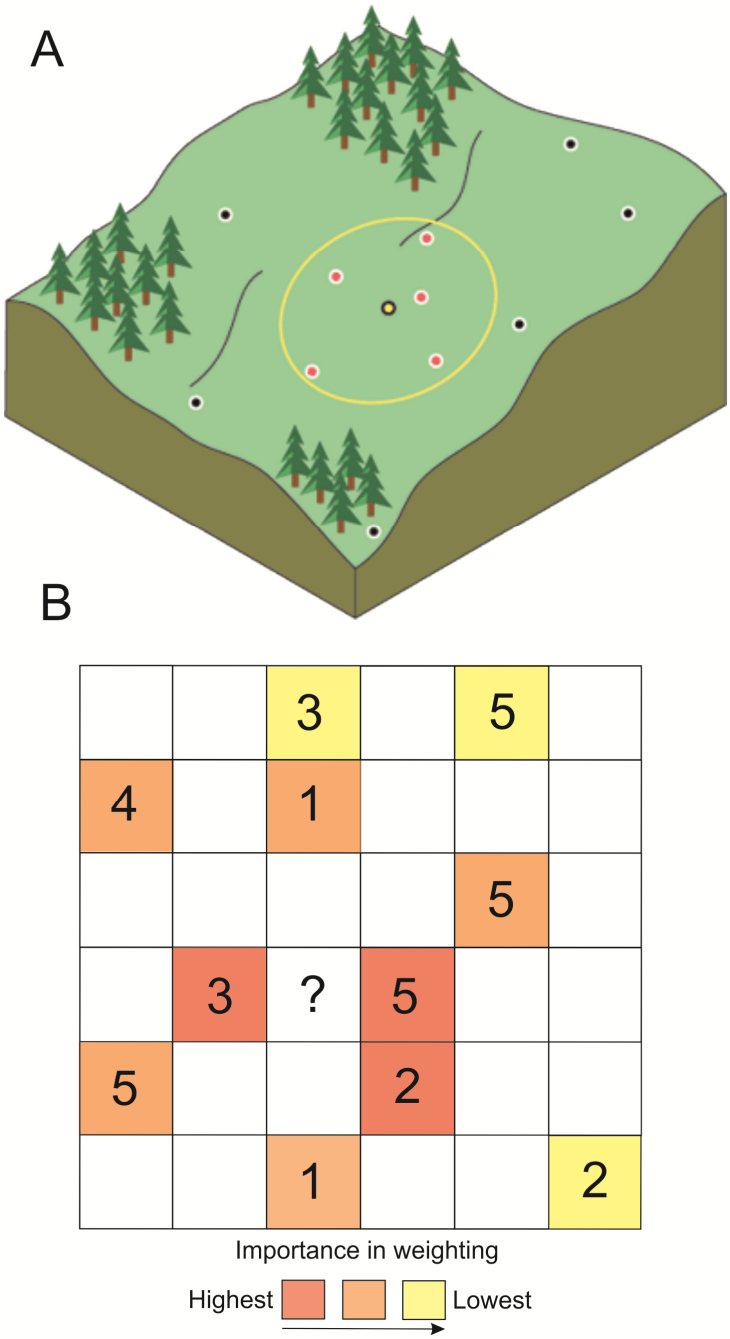

Figure 5.3 Examples of how the IDW techniques work. (A) Demonstrates how a defined search radius is applied to limit the distance of known values used in the interpolation of the unknown sample point (yellow dot). In this example any data points lying outside of the yellow circle are not used in calculations, Image from ArcGIS resource centre (help.arcgic.com). (B) Demonstrates the weighting of data with reference to the unknown cell marked by '?'. The closest cells coloured red are given a higher weighting in the interpolation calculation than those at a further distance coloured orange and yellow.

In this chapter, techniques of fixed and variable IDW were both applied. For the IDW (fix) technique, a specified fixed distance was used to define an area within which all of the input points are used for the interpolation. As with the kriging techniques, an incremental increase in search radius of 10 points up to 100 points was applied. For the IDW (var) technique, a variable search radius was used in order to find a specified minimum number of input sample points for the interpolation process. A minimum of 15 sample points for each search radius was specified. In addition, an optimal power function of 60 was used for both techniques as calculated using the optimized function in the ArcGIS Geostatistical Analyst toolbox. The power function was calculated from the root mean square prediction error value which quantifies the error of a prediction surface during cross validation, conducted within the ArcGIS Geostatistical Analyst toolbox (ArcGIS resource centre: help.arcgic.com).

Radial basis functions

Radial basis functions (RBF) are exact interpolation techniques that work by forcing a surface through a known number of input points while acting to minimise the total curvature of the surface created (Fig. 5.4A) (Bell, 2012). Radial basis functions can be grouped with IDW techniques based on their exact interpolation processes (i.e. interpolated surfaces must pass through known data points); however, they differ from IDW techniques as they allow predicted values which lie above or below the maximum values of the known data points (Fig. 5.4B). Five basis functions can be applied in the interpolation processes: thin-plate splines, splines with tension, completely regularized splines, multiquadratic functions, and inverse multiquadratic functions. Each basis function relates to a different statistical fit used when modelling the interpolated surface to the known data values. In this study we focus on the multiquadratic radial basis function (MRBF) and regularized spline with tension (RST) techniques. As presented by Geach et al., (2014a), these functions have been reported to be of use in the interpolation of geomorphic data sets of a scattered nature, such as terrace remnants (Lazzaro and Montefusco, 2002; Chaplot et al., 2006).

In the application of radial basis functions, a standard search neighbourhood was used for both MRBF and RST techniques. The standard search neighbourhood defines a circular search radius used in the weighting of input data points. As with the kriging and IDW methods, the number of neighbours was set at 10 points and increased up to 100 points (again adopting a point spacing of 25 m). Although not detailed in any of the associated literature, a kernel parameter was also deemed to be crucial during the initial stages of using the technique. The kernel parameter was applied to control the degree of localised variation in the interpolated surface. The best parameter gives the lowest root mean square error in the predicted surface in validation checks. Nominal kernel parameters were determined for each model run using the ArcGIS Geostatistical Analyst toolbox.

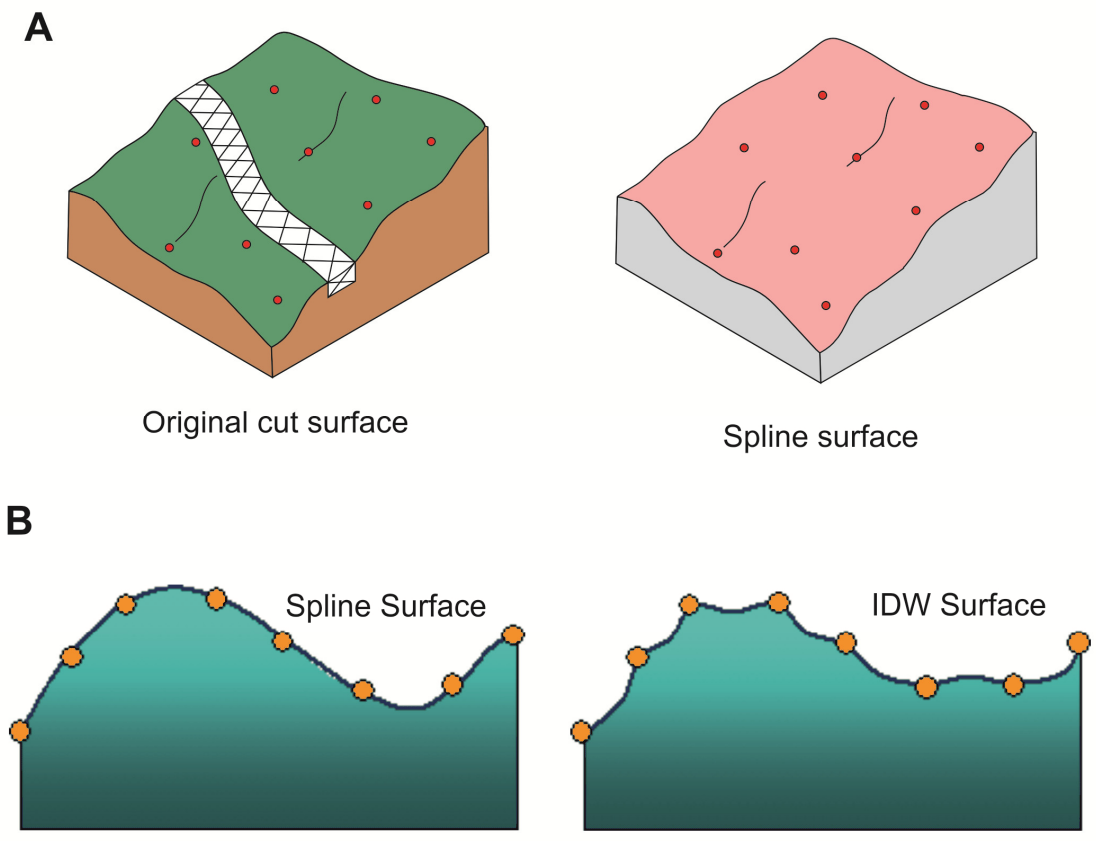

Figure 5.4 Examples of how the spline technique works. (A) Demonstrates how splines can be applied to dissected surfaces in order to generate a complete and undissected surface. Image redrawn from ArcGIS resource centre (help.arcgic.com) (B) Shows 2 idealised cross sections through an interpolated surface. Spine techniques allow for estimations of surface values above or below the data range of the known values. This is compared with IDW surfaces which does not allow for predictions outside of the original data range.

5.3 Application and validation of interpolation methods

As highlighted by Geach et al., (2014a) when assessing the use of geospatial interpolation in terrace studies; the accuracy of interpolation techniques can vary considerably as a function of both the datasets being modelled and the model parameters applied. This is well demonstrated in Figure 5.5, which represents the differences in a series of interpolated surfaces generated using methods of kriging, IDW and RBF. The implications of interpolation technique performance have significant implications in the quantification of landscape change (see surface volumes in Fig. 5.5). In this study, we apply the approaches developed by Geach et al., (2014a) in the reconstruction of terrace landforms for quantification purposes. Initially, the interpolation techniques (detailed in Section 5.2.2) are applied in the reconstruction of terrace levels with a full range of data comprising terrace levels 1 to 3 (the full dataset). In order to validate the accuracy of the data generated, the same interpolation techniques are then reapplied to the dataset with discrete islands of data removed applying a form of data 'jack-knifing' (the removed dataset). An assessment of the errors associated with the data generated from both the full and removed datasets is then analysed in the identification of the most suitable interpolation technique and model parameters (e.g. search radius).

A summary of the approach used in the interpolation process, along with an example of the validation processes is presented below. The example is based on the interpolation of terrace levels 1 to 3 from the Tabernas Basin stratigraphy (Chapter 3) conducted by Geach et al., (2014a). The aim of the technique appraisal is to highlight the requirement for an in-depth assessment of interpolation technique performance prior to the quantification and interpretation of data generated from such methods:

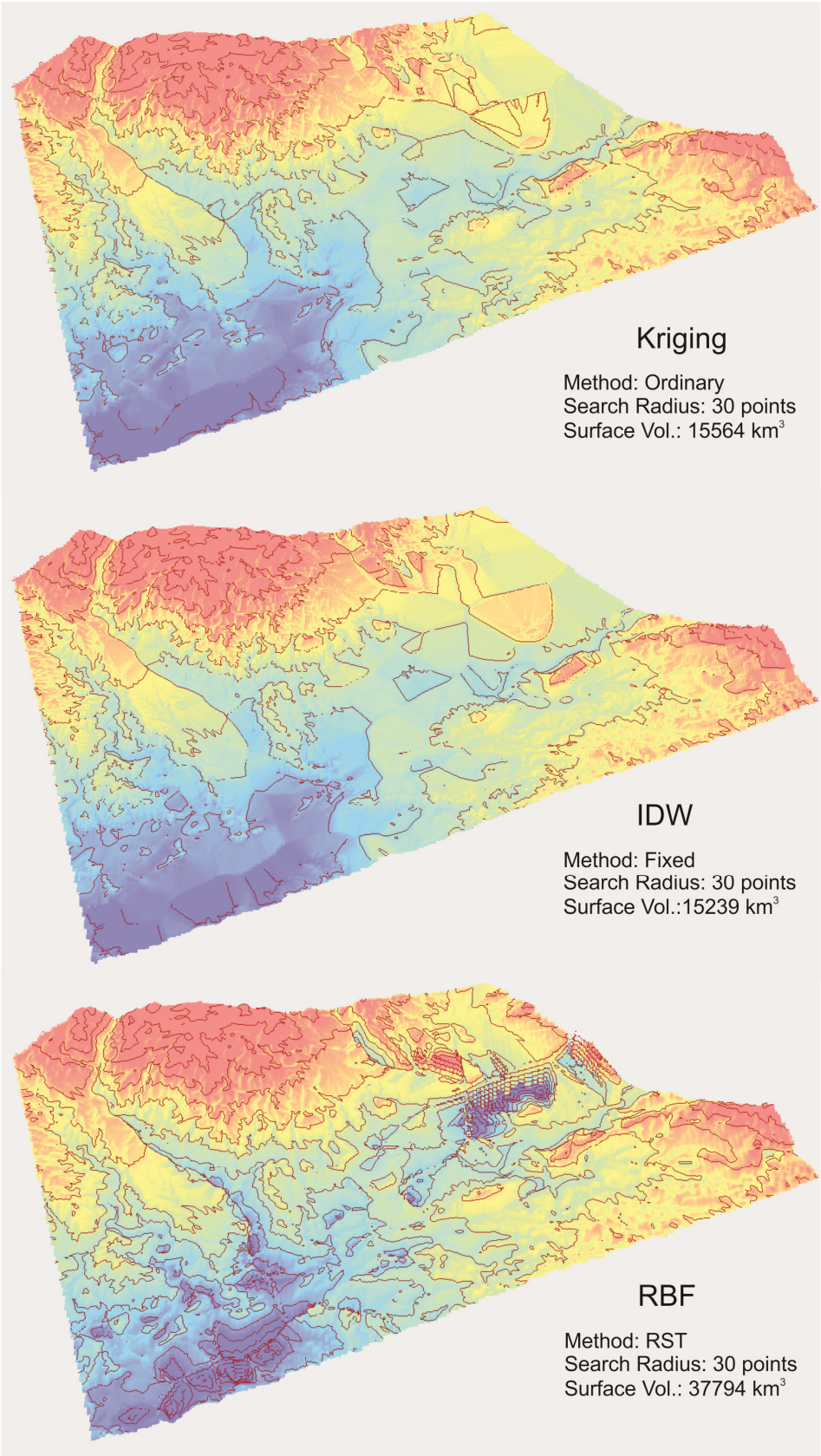

Figure 5.5 Variable results from different interpolation methods applied to the same input dataset. Note dramatic differences in surface volumes between Spline and IDW/kriging techniques when applied using standard computed values in a GIS. Volumes calculated using a top down method, where surface volume equals the volume below the highest pixel in the DEM.

5.3.1 Dataset Generation

1. Digitise the field terrace record dataset as a series of georeferenced polygons as supplement by visualisation tools in the ArcGIS domain (e.g. hillshade models).
2. Define terrace groups based on morphological and sedimentological data, presented in detail in Chapter 3.
3. Apply a high-pass filter to the topographic elevation raster in order to further refine terrace boundaries and avoid modelling of erroneous data in the interpolation process (Fig. 3.1B, Chapter 3 for example).
4. Create point datasets for all terrace levels which form the input data in the interpolation process. In order to increase the number of data points and decrease estimation errors, topographic features which occur above the height of terrace surfaces can be included in the input datasets (e.g. the bounding sierras with regard to the Tabernas Basin). In this example, a combined dataset was generated for terrace level 1, 2 and 3 deposits. This dataset is therefore representative of terrace level 3 prior to subsequent abandonment and incision.

5.3.2 Application of interpolation methods

Upon creation and refinement, the terrace level datasets are then interpolated using all techniques following the approaches detailed in Section 5.2.2. All interpolation techniques were applied in the ArcGIS10.1 software package with the use of ArcGIS Geostatistical Analyst toolbox. In order to streamline the interpolation process a circular model was generated in the ArcGIS ModelBuilder toolbox. The model automatically applied set increases in search radius for each interpolation method at the end of each model run. The function of the model is presented in Figure 5.7.

5.3.3 Validation of interpolation techniques

In order to assess the accuracy of the interpolation techniques, a stage of data jack-knifing was performed in order to assess the accuracy and precision of the interpolation processes when modelling the remaining data set (e.g. Vieira et al., 2010). For the terrace level 1 – 3 dataset, four discrete islands of data were removed from the full data set based on: (i)

surface form (i.e. flat or undulate topographic level based on surface curvature) (ii) topographic location (i.e. relative elevation of terrace top) and (iii) the difference in data setting in terms of distance to known data points (Fig. 5.7, Table 5.1). The interpolation techniques were then run again in accordance with the techniques detailed in Step 5 for the removed dataset.

Table 5.1 Summary characteristics of removed data islands (Geach et al., 2014a).

Data island	Surface area (km^2)	Topography (m)		Curvature (m)			Number of sample points
		Mean	Range	Min	Max	Range	
1	0.09	385.47	12.12	-1.38	1.18	2.57	165
2	0.05	320.21	45.16	-3.02	7.91	10.92	107
3	0.10	422.30	30.36	-5.27	2.67	7.93	202
4	0.16	252.69	33.70	-6.46	4.34	10.80	294

After application of all of the interpolation techniques to both the full and removed datasets, statistical analysis was conducted in order to assess the errors of the estimation process. The accuracy and precision of interpolation techniques was assessed by measures of mean error (ME), mean absolute error (MAE), and root mean squared error (RMSE) as detailed in Table 5.2. Mean error (ME) is commonly applied to determine the bias in estimates between data sets (Cooper and Weekes, 1983; Li and Heap, 2011). Although the measure is widely adopted, ME can be limited in applicability as negative and positive errors counteract each other, commonly leading to underestimates or overestimates of the actual error as demonstrated by Geach et al., (2014a) (Fig.5.8). MAE and RMSE are similar in approach as they give measures of average error for compared data. Both measures are useful when generating a summary of the mean difference in the units of the primary variable; however, both do not give a measure of relative size of average difference or the nature of differences comprising them (Li and Heap, 2011).

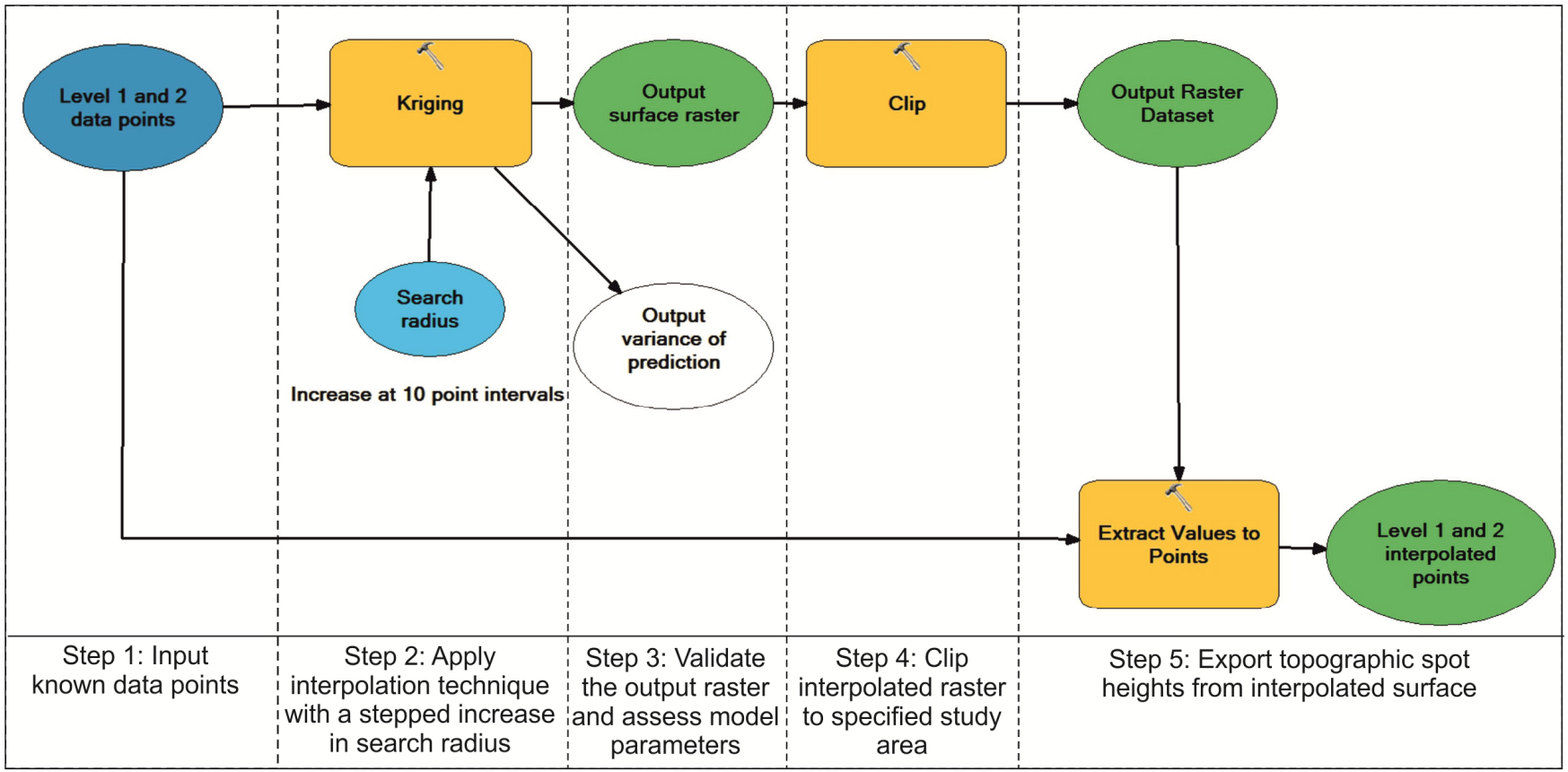

Figure 5.6 Example of the model developed in the interpolation of terrace datasets and resultant export of topographic data.

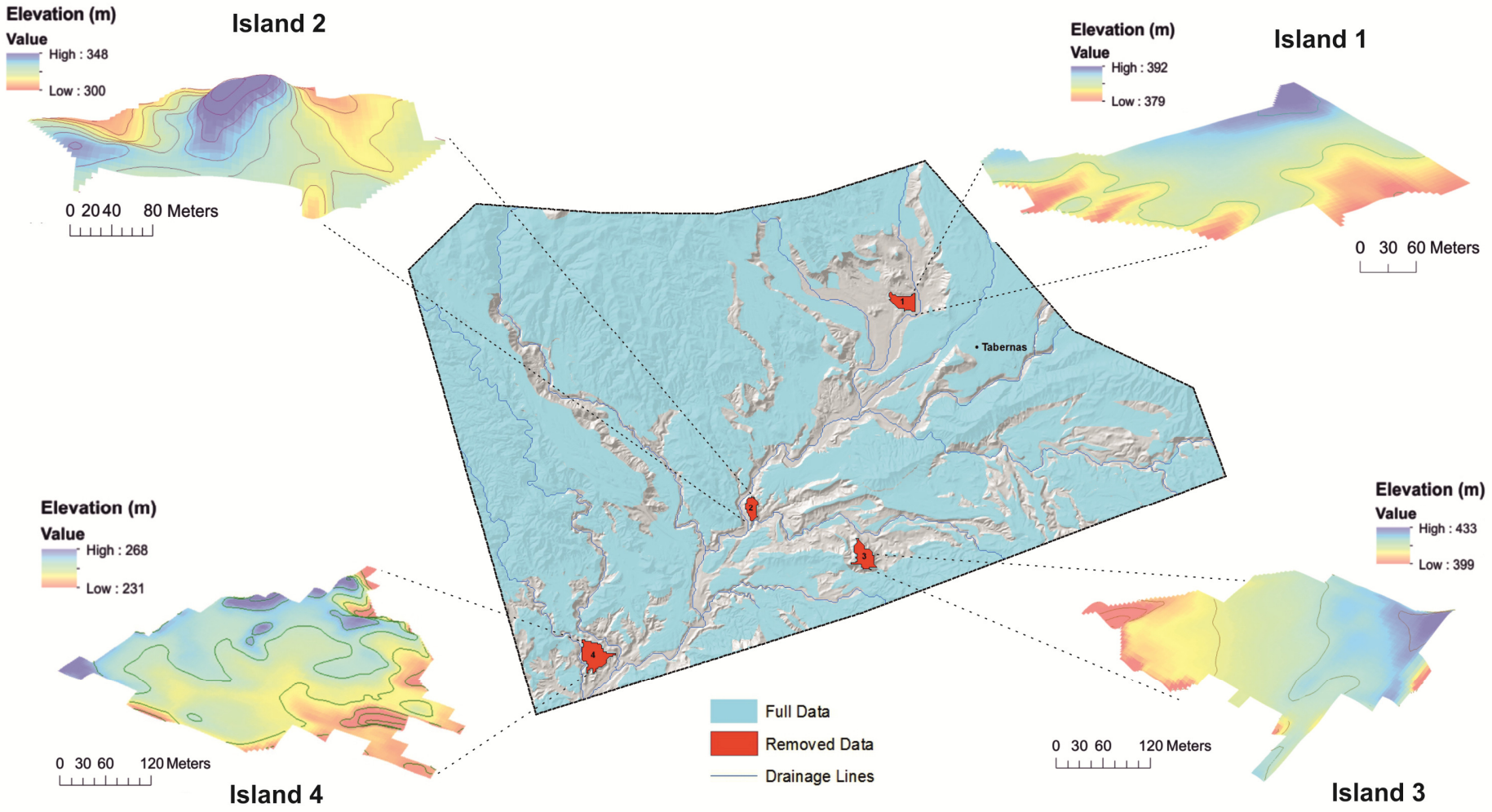

Figure 5.7 Detailed location and morphology of the islands of data removed in the jack-knifing process. Note the differences in surface elevations for each island.

Table 5.2 Error measures used to assess the performance of interpolation techniques.

Measure	Definition*
Mean error (ME)	$ME = \frac{1}{n}\sum_{i=1}^{n}(pi - oi)$
Mean absolute error (MAE)	$MAE = \frac{1}{n}\sum_{i=1}^{n}\lvert pi - oi\rvert$
Root mean square error (RMSE)	$RMSE = \left[\frac{1}{n}\sum_{i=1}^{n}(pi - oi)^2\right]^{1/2}$

*n: number of observations; o: observed values; p: predicted values

5.3.4 Results of statistical analysis

The results of statistical analysis were assessed at a number of levels in order to address the suitability of interpolation techniques. These included: (i) a primary combined assessment of technique performance for the full and removed datasets; (ii) an assessment of techniques for the individual datasets; (iii) an assessment of the importance of the removed data islands as a function of the geomorphology and position of the surface within the combined datasets; (iv) an assessment of the importance of known model parameters, and (v) an appraisal of surface volume data generated by all techniques.

With focus on the combined assessment of technique performance for both datasets, presented in Figure. 5.8, it is notable that interpolation error increased dramatically for all techniques when applied to the removed dataset. On average, MAE and RMSE values increased by 3 to 4 times. It is also noted that measures of ME dramatically underestimated MAE and RMSE values for the full dataset, highlighting the limitations of the error measure in terrace studies.

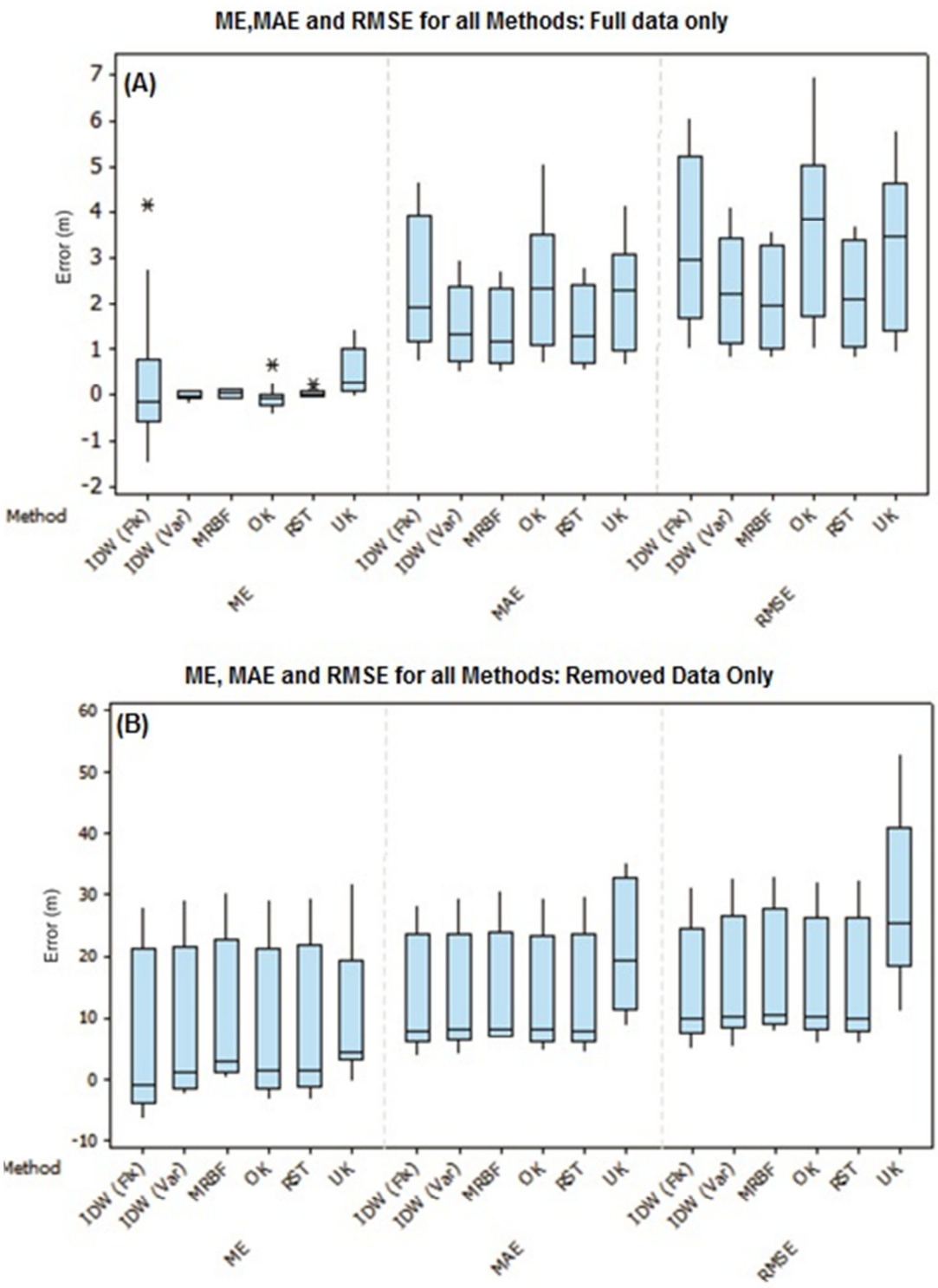

Figure 5.8 Measurements of ME, MAE, and RMSE for all interpolation methods when applied to full data (A), and to removed data (B). Note the significant underestimation of ME for the full dataset when compared with measures of MAE and RMSE. Figure from Geach et al. (2014a) as applicable for a combined terrace level 1 to 3 dataset.

When assessing the performance of techniques in the reconstruction of the full data set techniques of MRBF, RST, and IDW (var) performed well with techniques of kriging (OK and UK) and IDW (fix) being the worst (Table 5.3). The range in MAE and RMSE for all techniques was relatively small, with the largest RMSE range of 6 m for OK. Error measures in MAE and RMSE were at worst slightly positively skewed for all techniques (IDW (var), MRBF and RST - Fig. 5.8A). For the removed data set, techniques of RST and IDW (var) performed well (relative to increases in error at the data set level) (Table 5.4). The performance of OK increased significantly when compared against its performance for the full dataset; however, techniques of UK performed very poorly with an RMSE range of some 41 m (Fig. 5.8B). The range in errors between techniques was again small; however, for the removed data sets MAE and RMSE values were strongly positively skewed for most methods (Fig. 5.8B).

The accuracy of techniques in the estimation of data points for removed data islands was notably variable (Fig. 5.9). For the full dataset, measured errors were lowest for island 1 with little range in RMSE between all techniques (Table 5). In contrast, the RMSE ranges for islands 2, 3, and 4 were notably higher, increasing to 2.2 m to 3.5m (Fig. 5.9A). For the removed dataset, data Island 3 was the worst modelled with MAE and RMSE values some 3-4 times higher than the other island (Table 5). Neglecting island 3, the range in errors between all other islands was small with a MAE range < 2 m (Table 5.5). If the error contributions from the worst performing technique (UK) were neglected the difference in technique performance was relatively low for each island, with a mean RMSE range of < 6 m (see black circles Fig. 5.9).

Increases in the search radius had a highly variable effect upon technique performance (Fig. 5.10). The most notable increases in technique accuracy occurred for techniques of UK after 50 points (1250 m). The most notable decreases in technique performance occurred for methods of IDW (fix) when applied a search radius greater than 30 points (750 m). An increased search radius had little effect upon methods of IDW (var) and OK. The results

from both forms of RBF were variable. MRBF showed a slight increase in errors when search radius was increased past 40 points (1000 m); however, this trend became negligible after 70 points (1750 m). Trends from RST show no relationship to search radius at all (Fig. 5.10).

The quantification of surface volume data from the interpolated data surfaces (Table 5.5) supports the importance of dataset and model variables upon interpolation technique performance. For example, significant increases in the performance of UK techniques are noted in the volume data when the search radius applied is increased above 10 points. In addition, there is a very good degree of uniformity between the best performing interpolation methods when applied to both datasets (RST and MRBF). The results from the volumetric quantification also highlight: (i) very little difference in modelled volumes between the full and removed data sets for most methods (see difference column Table 5.5); and (ii) the volumes generated by all techniques become notably more uniform when applying a larger search radius (up to 30 points).

5.3.5 Controls upon interpolation technique performance

Although only applicable to the data modelled in this study, the results of statistical analysis conducted in this appraisal identify numerous contributing factors which influence interpolation technique performance when reconstructing fragmentary terrace records. These include: (i) the effects of dataset variables, (ii) the geomorphic attributes of the landforms being modelled and (iii) variable model parameters.

Table 5.3 MAE (m) and RMSE (m) rank for all interpolation techniques when applied to the full data set (Geach et al., 2014a).

		IDW (Fix)		IDW (Var)		MRBF		OK		RST		UK	
Search radius (points)	**Polygon**	**MAE**	**RMSE**	**MAE**	**RMSE**	**MAE**	**RMSE**	**MAE**	**RMSE**	**MAE**	**RMSE**	**MAE**	**RMSE**
10	1	6	5	1	3	2	1	5	6	3	2	4	4
10	2	5	5	1	3	2	1	6	6	3	2	4	4
10	3	6	6	2	2	1	1	5	5	3	3	4	4
10	4	4	5	3	3	1	1	6	6	2	2	5	4
20	1	5	5	3	3	1	1	6	6	2	2	4	4
20	2	5	5	3	3	1	1	6	6	2	2	4	4
20	3	6	6	2	2	1	1	4	5	3	3	5	4
20	4	4	4	3	3	1	1	6	6	2	2	5	5
30	1	6	6	3	3	1	2	5	5	2	1	4	4
30	2	5	5	3	3	1	1	6	6	2	2	4	4
30	3	6	6	3	3	1	1	4	4	2	2	5	5
30	4	4	4	3	3	1	1	6	6	2	2	5	5
Mean Rank		5.2	5.2	2.5	2.8	1.2	1.1	5.4	5.6	2.3	2.1	4.4	4.3
Combined Rank		**5**		**3**		**1**		**6**		**2**		**4**	

Table 5.4 MAE (m) and RMSE (m) rank for all interpolation techniques when applied to the removed data set (Geach et al., 2014a).

		IDW (Fix)		IDW (Var)		MRBF		OK		RST		UK	
Search radius (points)	**Polygon**	**MAE**	**RMSE**	**MAE**	**RMSE**	**MAE**	**RMSE**	**MAE**	**RMSE**	**MAE**	**RMSE**	**MAE**	**RMSE**
10	1	1	1	4	4	5	5	3	3	2	2	6	6
10	2	4	3	1	1	3	5	5	4	2	2	6	6
10	3	1	1	3	4	5	5	2	2	4	3	6	6
10	4	1	1	5	5	2	4	4	3	3	2	6	6
20	1	1	1	2	4	5	5	3	3	4	2	6	6
20	2	6	5	1	1	4	4	3	3	2	2	5	6
20	3	1	1	2	4	5	5	3	3	4	2	6	6
20	4	4	2	5	4	2	5	3	3	1	1	6	6
30	1	4	4	1	1	5	5	3	3	2	2	6	6
30	2	6	6	1	1	5	5	3	3	2	2	4	4
30	3	1	1	2	4	5	5	3	2	4	3	6	6
30	4	1	1	5	4	3	5	4	3	2	2	6	6
Mean Rank		2.58	2.25	2.67	3.08	4.08	4.83	3.25	2.92	2.67	2.08	5.75	5.83
Combined Rank		**2**		**3**		**5**		**4**		**1**		**6**	

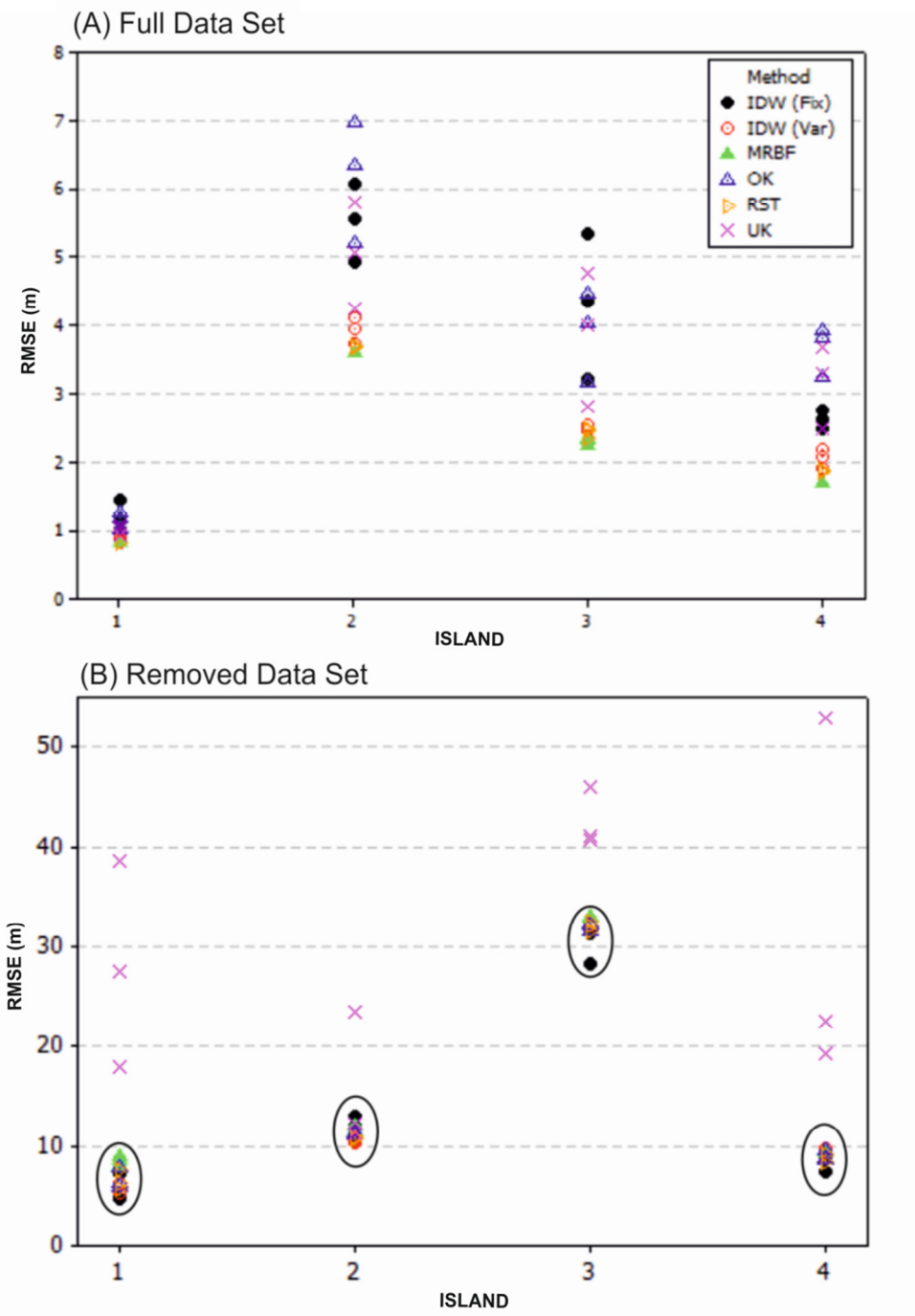

Figure. 5.9. RMSE values for removed data islands when assessed for (A) the full and (B) the removed data sets. The black circles on the removed data set (B) demonstrate the small variation in technique error when UK is neglected. Note the key in (A) is applicable to both graphs (Geach et al., 2014a).

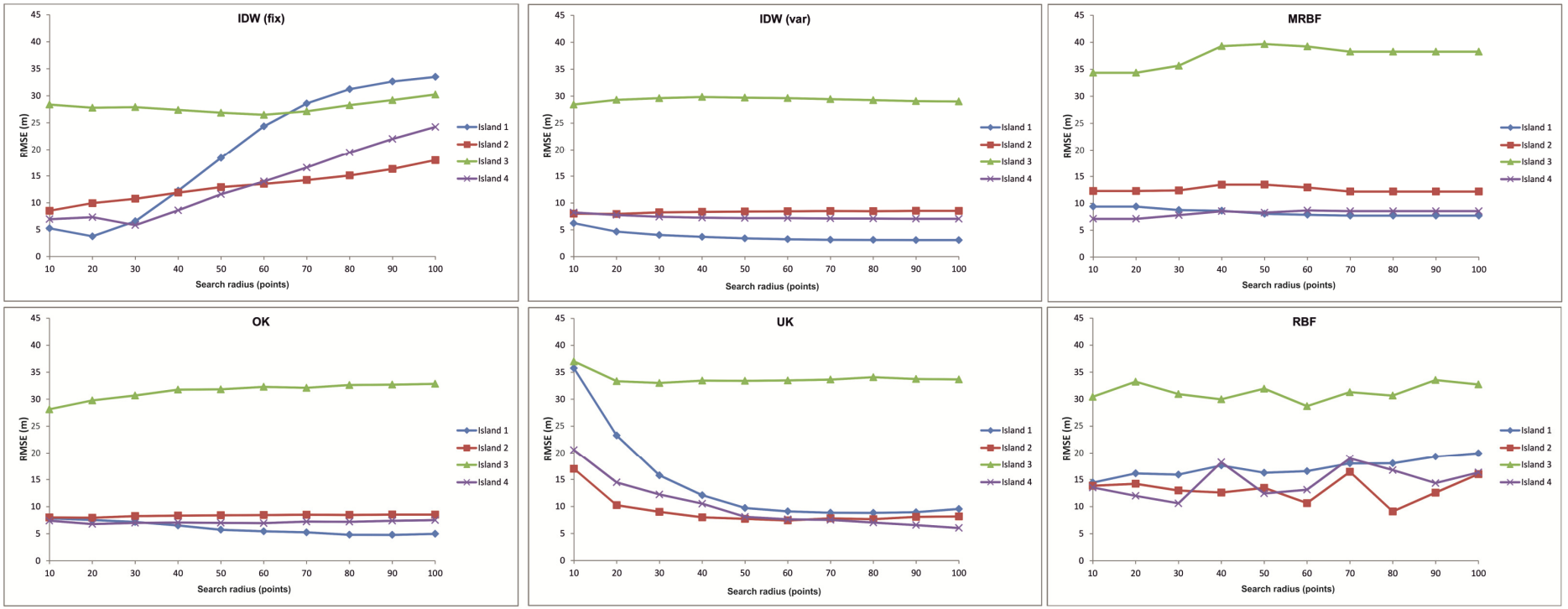

Figure 5.10 Difference in RMSE for all interpolation techniques as a result of increased search radius. Note the data presented are modelled for removed data set only as this represents the greatest modelling uncertainty (Geach et al., 2014a).

Table 5.5 Surface volumes (km^3) calculated from interpolated surfaces; values are shown as a function of search radius for the full and removed data sets (Geach et al. 2014a). Surface volumes calculated using a top down approach where the surface volume is calculated below a plane set at the level of the highest pixel in the DEM.

Method	**10 Points**			**20 Points**			**30 Points**		
	Full	Removed	Difference	Full	Removed	Difference	Full	Removed	Difference
IDW (Fix)	29673	29485	188	29797	29795	2	29871	29873	2
IDW (Var)	29359	29358	1	29410	29408	2	29469	29468	1
MRBF	29148	29145	3	29817	29812	5	27760	27755	5
OK	15843	15769	74	30588	30440	148	29968	29747	221
RST	28620	28618	2	28756	28754	2	28679	28678	1
UK	22229	30052	7823	30250	30234	16	30364	30350	14
Mean	**25812**	**27071**	**-**	**29769**	**29740**	**-**	**29351**	**29311**	**-**
St. Dev	**5634**	**5556**	**-**	**641**	**604**	**-**	**966**	**941**	**-**

Dataset parameters such as distance between known data points and density of known values appear to be a primary control upon interpolation technique performance. Although only representative of the data modelled herein, exact methods of interpolation (MRBF and RST) performed well when modelling the full data set characterised by regular data point spacing. However, when applied to the removed data set with a larger amount of estimation uncertainty both methods of IDW prevailed. This is likely a function of sample point density in the removed data set which supported the locally deterministic nature of the IDW techniques (Fisher et al., 1987; Childs, 2004; Chaplot et al., 2006). The overall poor performance of geostatistical methods (OK and UK) for both data sets could be explained by the existence of trends in the spatial attributes of the modelled data. Such trends have been noted to decrease estimation accuracy as a result of poor data representation by the sample variogram (Kravchenko, 2003).

The significance of geomorphological factors (e.g. surface elevation and surface morphology) upon technique performance are only apparent when assessing error differences at an island scale. For the full data set, variations in surface curvature promoted interpolation inaccuracy as evidenced by the poor representation of island 2 by all

techniques (Fig. 5.9A). However, surface elevation (Fig. 4) became the primary variable promoting estimation error when modelling the removed dataset as evidenced by the large modelling errors for island 3 (Fig. 5.9B). The effects of model parameters upon technique performance are governed by the inherent approach adopted in the modelling of data. For example, techniques of IDW (fix) apply a distance-decay parameter that assumes spatial uniformity in known data observations away from an unknown point. Increases in search radius, as conducted in this study, promotes estimation error due to a non-uniform distribution of observation points to the unknown point (Lu and Wong, 2008). In contrast, techniques of UK are based on an assumption of an overriding trend in the data that are modelled by the number of polynomials applied. When we increased the search radius, the number of points that fit this assumed data trend increases and reduces overall errors (Fig. 5.8) (Oliver, 1990; Collins and Bolstad, 1996).

5.3.6 Summary of approach

The outcome of the technique appraisal conducted herein highlights the significance of dataset variables, geomorphological factors and modelling parameters the accuracy of the interpolation process. The assessment conducted is of importance when applying any method in the reconstruction of data sets where the attributes of data are highly variable (*sensu* Aguilar et al., 2005). In this study, the appraisal highlights the use of RST methods when generating a continuous landsurface representative of terrace levels 1, 2 and 3. This is notable as the application of RST in an un-calibrated manner generated the worst results in initial application (Fig. 5.5). The approach presented was further applied in the generation of palaeo-landsurfaces from the other terrace levels in the Tabernas Basin for use in the quantification of incisional data, as presented in Section 5.4. The range in volumetric data generated from all interpolation techniques, presented in Table 5.5, supports the use of geospatial interpolation in the reconstruction of the Quaternary environment within the Tabernas Basin (i.e. regardless of technique used, volumetric data can be generated that fall within an order of magnitude of each other).

5.4 Quantification of basin incision

The following section details the use of interpolated palaeo-landsurfaces in the quantification of rates of landscape degradation throughout the Quaternary for the Tabernas Basin. Volumetric data were calculated by comparing the difference in paleolandsurfaces generated by the interpolation of terrace surfaces, as summarised in Figure 5.11. The most suitable interpolation techniques were assessed for all terrace level groupings in accordance with the approach detailed in Section 5.3. No reconstructions are provided for terrace level 1 deposits due to the restricted occurrence of landforms at a basin scale. This means no incisional data are presented for the first stage of basin incision (Fig. 3.17, Chapter 3). It is also highlighted that the interpolation process was conducted on data generated from the terrace surfaces for each terrace level; therefore, the volumetric data are representative of the abandonment of one terrace level to the abandonment of the next (e.g. abandonment of terrace level 2 aggradations to the abandonment of terrace level 3 aggradations). It would be possible to apply averaged incisional depths of terrace deposits along individual drainage lines in order to address the full incisional amounts between terrace levels (i.e. true degradational stages of Fig. 3.17, Chapter 3); however, the errors in the interpolation stage would be large based on a limited amount of observations at a basin scale. It is also noted that volumetric analysis is restricted by the current limit of incision in the basin. This is due to fundamental requirement for incision between terrace aggradational surfaces and represents a limitation of application to stacked terrace sequences.

Volumetric data and visual spatial representations were generated in the ArcGIS domain by comparing the comparison of interpolated datasets using the Cut and Fill tool and the Minus tool from the Spatial Analyst toolbox, respectively. The Cut and Fill function calculates the volume change between two input surfaces with results recorded as either: net gain, net loss or unchanged values based on a grouping of pixel values. As we apply inexact methods in the reconstruction of terrace records (i.e. interpolated estimations), values of extensive net

gain (i.e. elevation increases between incisional records) are taken to represent regions where the interpolation process has performed poorly (Fig. 5.12B). The Minus tool works by subtracted pixel values of one raster surface from the other. The data are reported visually and represent differences in elevation between the raster surfaces. Again, regions of net gain represent areas where the interpolation process has performed poorly as related to areas of limited terrace outcrop.

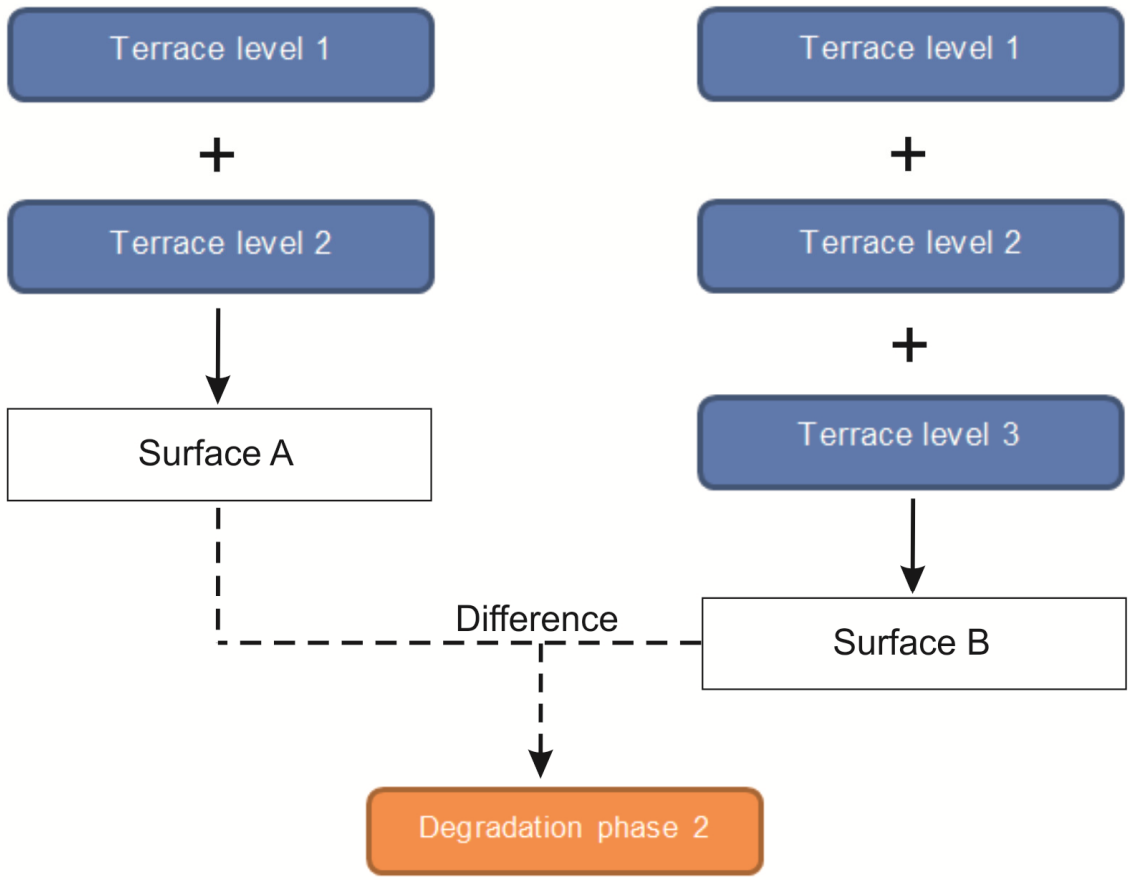

Figure 5.11 Schematic model demonstrating how terrace levels were grouped in the interpolation process to generate paleolandsurfaces and subsequent incisional data. Using degradation phase 2 as an example; terrace levels 1 and 2 were combined in the interpolation stage to generate a paleo-landsurface representative of both levels (surface A). A paleo-landsurface representative of terrace levels 1, 2 and 3 was then generated (surface B) and subsequently compared with the terrace level 1 and 2 paleo-landsurface. The difference between the two surfaces relates to degradation phase 2.

5.4.1 Degradation stage 2

As presented in Figure 5.11, spatial analysis for degradation stage 2 were conducted by removing a palaeo-DEM representative of terrace levels 1, 2 and 3 from an initial interpolated surface representative of terrace levels 1 and 2. The results of volumetric analysis are presented in Table 5.6 and visual representations are displayed in Figure 5.12. A notable feature of the net change analysis, presented in Figure 5.12A, is the variation in incisional styles across the basin. Greatest incision occurs within the centre and east of the basin focused around the Rambla Tabernas and Rambla de Buho (circles labelled 1 and 2; Fig. 5.12A). In these areas, incisional styles are laterally extensive and not constrained within current drainages. Based on the stratigraphy presented in Chapter 3, this pattern of extensive incision would have increased further into the east of the basin into the region currently infilled by undissected alluvial fans(e.g. Harvey et al., 2003); however, the stacked sequences here do not allow for analysis. In the south of the basin, incision is notably restricted near to the confluences of the Ramblas Sierra and Reinelo with the axial drainage (circles labelled 3 and 4; Fig. 5.12A). This highlights a variation in basin connectivity at this time of development, with southerly drainages relatively unaffected by the incisional event. In the west of the basin, incision is more constrained and concentrated within current drainage lines (e.g. Arroyo Verdelecho; circles labelled 5 on Fig. 5.12A).

The relative success of the interpolation process in generating representative datasets is assessed in the net change analysis presented in Fig. 5.12B and Table 5.5. Multiple regions of net gain are noted in the far east and west of the basin (circled on Fig. 5.12B); however, these values of surface increase are low when compared with the incisional data (average increase <7m). In addition, the localised regions of net gain are considerably exceeded by regions of net loss (Table 5.5). The volumetric data coupled with the visual data representations appear to support the use of the geospatial interpolation for this early stage of basin development.

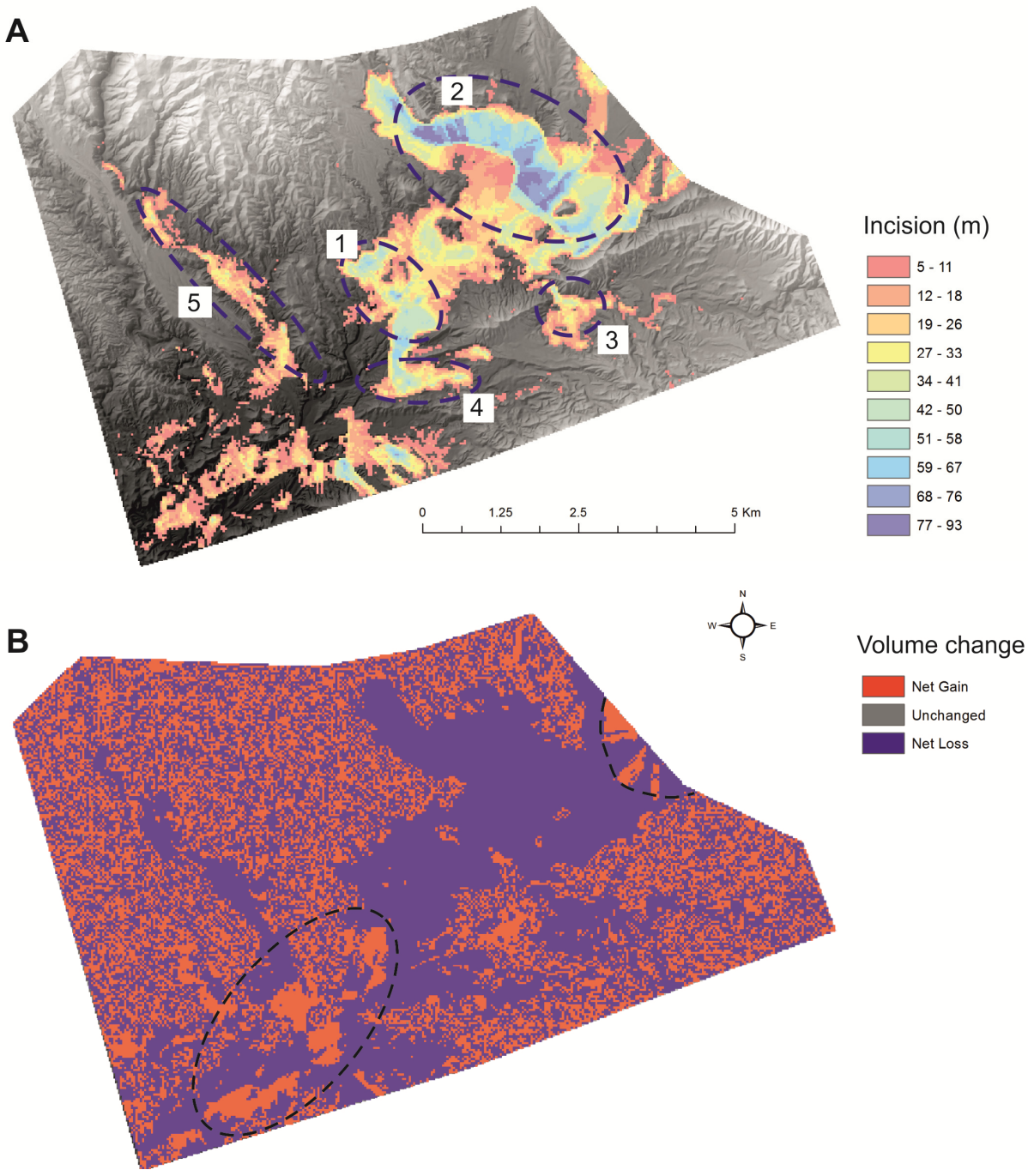

Figure 5.12 (A) Results of Minus function for degradation stage 2 showing the variations in incisional patterns across the Tabernas Basin. Labels relate to regions of incision, 1= Rambla Tabernas, 2= Rambla de Buho, 3= Rambla Sierra, 4= Rambla Reinelo, 5= Arroyo Verdelecho. (B) Output of net change analysis for degradation stage 2 demonstrating the relative success of the interpolation technique. Black circles highlight areas of concentrated net gain where the interpolation technique performed poorly. Values of net loss and gain are presented in Table 5.5.

Table 5.6 Total volumes of net change for degradation stages in the Tabernas Basin.

Degradation Stage	Net loss (km^3)	Net gain (km^3)
1 (Terrace level 1 to terrace level 2)	-	-
2 (Terrace level 1 & 2 to terrace level 3)	4722	305
3 (Terrace level 1,2&3 to terrace level 4)	807	174
4 (Terrace level 1,2,3,&4 to current rambla)	1414	187

5.4.2 Degradation stage 3

Volumetric analysis for degradation stage 3 were conducted by removing a palaeo-DEM representative of terrace levels 1, 2, 3 and 4 from an initial interpolated surface representative of terrace levels 1, 2 and 3. The results are presented in Table 5.6 and visual representations are displayed in Figure 5.13. Incision trends for degradation stage 3 are notably different to stage 2 with the majority of incision restricted along the Rambla Tabernas (Fig. 5.13A). The most intense incision is focused in two locations, notably the El Cautivo badlands (circles labelled 1; Fig. 5.13A) and the Rambla Benavides (circles labelled 2; Fig. 5.13A). The focused incisional style is unique to degradation stage 3 and shows little activity within the major basin tributaries. Volumetric data generated for degradation stage 3 are notably low when compared with the other two degradation stages (Table 5.5). Numerous regions of net gain are also noted as characterised by relatively high values of elevation increase >16m. Based on the spatial patterns and the volumetric data presented it is likely that reconstructions of degradation stage 3 were limited by the restricted nature of terrace level 4 terraces across the basin.

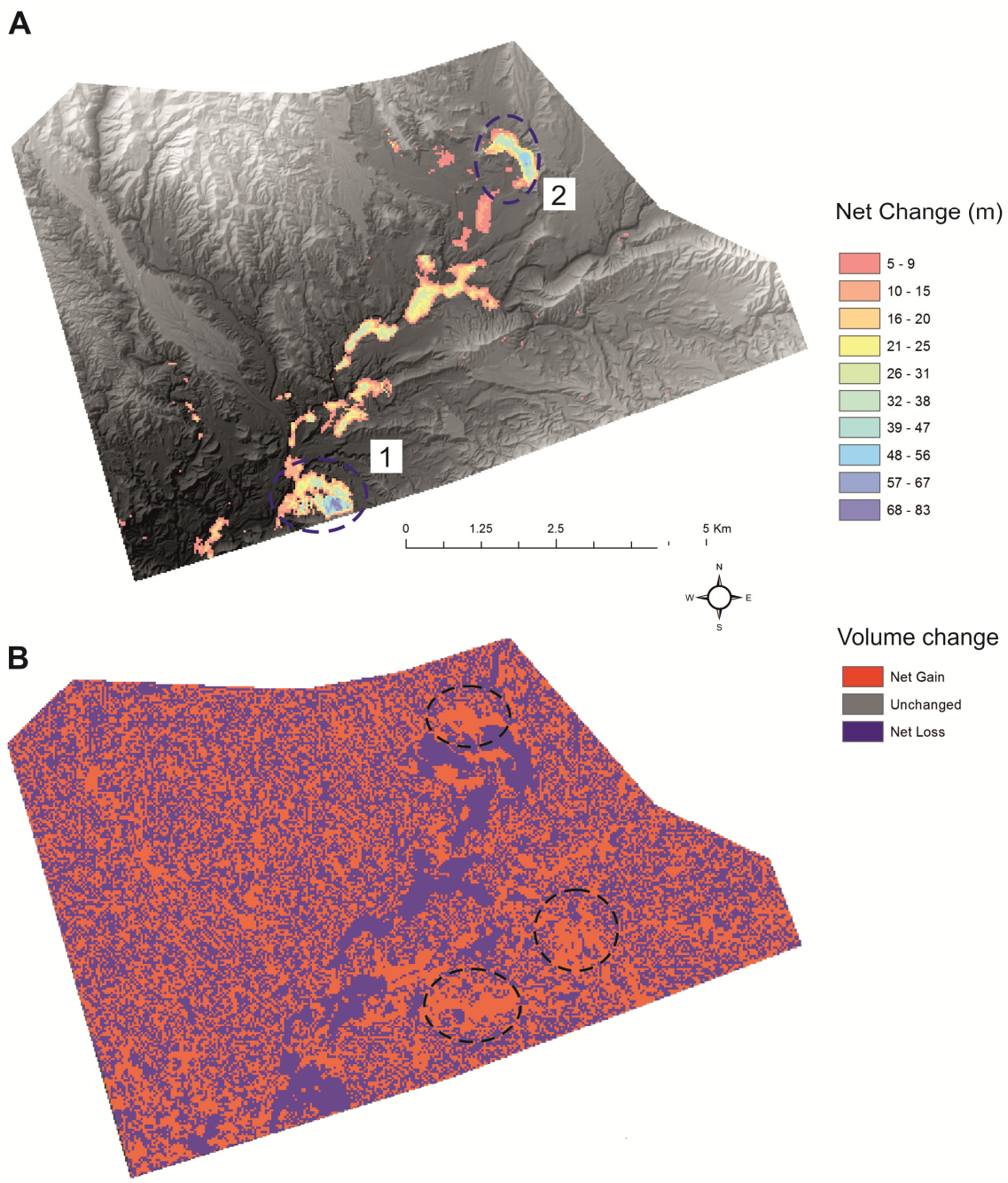

Figure 5.13 (A) Results of Minus function for degradation stage 3 showing an apparent focus of incision along the Rambla Tabernas. Labels relate to regions of incision, 1= El Cautivo badlands, 2= Rambla Benavides (B) Output of net change analysis for degradation stage 3 showing notable areas of net gain where the interpolation technique performed poorly. Values of net loss and gain are presented in Table 5.5.

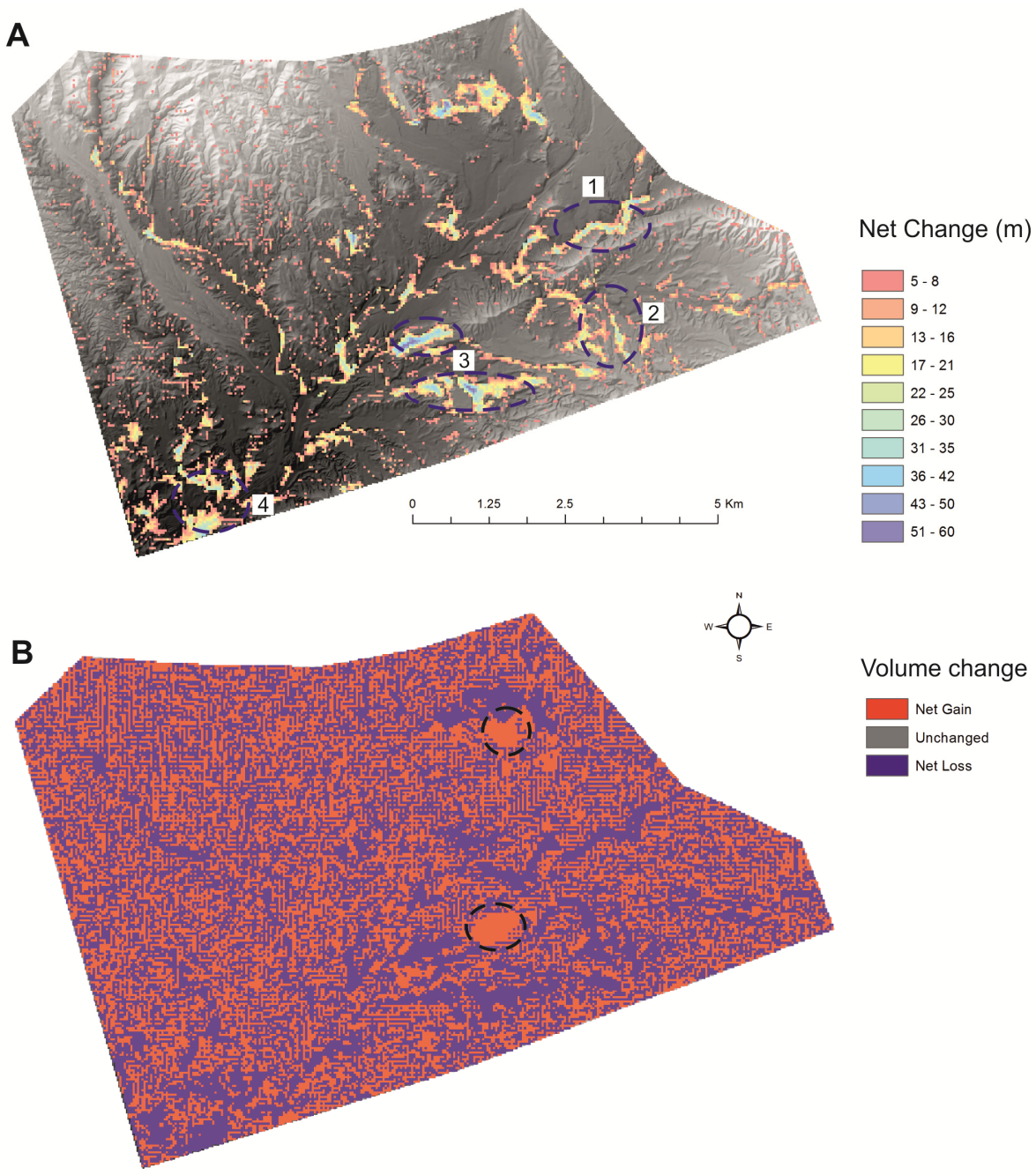

Figure 5.14 (A) Results of Minus function for degradation stage 4 showing confined incision within most of the basin tributaries. Confined incision occurs within the Rambla los Molinos, Rambla Sierra, Rambla Reinelo and south westerly corner of the basin (circles labelled 1, 2, 3 and 4 respectively (B) Output of net change analysis for degradation stage 4 showing notable areas of net gain where the interpolation technique performed poorly. Values of net loss and gain are presented in Table 5.5.

5.4.3 Degradation stage 4

Volumetric analysis for degradation stage 4 were conducted by removing the current basin DEM from an initial interpolated surface representative of terrace levels 1, 2, 3 and 4. The results of volumetric analysis are presented in Table 5.6 and visual representations are displayed in Figure 5.14. A notable feature of the spatial analysis for degradation stage 4 compared with the previous stage 3 is the dramatic increase in incision within major tributaries across the basin (Fig. 5.14A). Confined incision occurs within the Rambla los Molinos, Rambla Sierra and Rambla Reinelo (circles labelled 1, 2 and 3, respectively; Fig. 5.14A). Incision also appears concentrated in the southwest corner of the basin toward the confluence with the Río Andarax (label 4 on Fig. 5.14A. The changes in surface volumes appear representative of the incisional trends (Table 5.5). Two regions of net gain are noted; however, the values of elevation change are <5m for both.

5.4.4 Discussion of results

Although restricted by the current limits of incision across the basin, the data generated from the interpolated paleolandsurfaces highlight notable variations in incisional patterns throughout the Quaternary development of the basin. Reconstructions of degradation stage 2 highlight a major period of incision that took place across the basin post abandonment of terrace level 2. Given the extent of incision, it is likely that the degradation stage was long lived or that incisional rates were greater when compared with the following stages. Results from OSL dating suggest that degradation stage 2 likely relates to the MIS 5 (Chapter 4 for detail). The highly variable degradational styles evidenced during the incisional phase could be linked to the fluctuating climate during MIS 5 overprinted on a pattern of sustained tectonically driven base-level lowering and an inherent tectonic sag of the basin centre (e.g. Stokes et al., 2012). The relatively high frequency of climate changes during MIS 5 (e.g. sub-stages 5A to 5E) would likely have formed a highly transient fluvial system responding to short duration changes in sediment and water availability (Daniels, 2008). The effects of variable climatic conditions upon basin development (e.g. terrace level 2 sedimentation) are

further evidenced in the stages of alluvial fan development noted in the terrace stratigraphy (Chapter 3). Most notable is the transition from debris flow processes in the early stages of fan development becoming fluvially dominated through time. This change in process dominance supports the importance of sediment availability during climate cycles coupled with on-going patterns of tectonic uplift which generates sediments in the bounding Sierras (Harvey, 1997; 2011).

Notable differences in incisional styles during degradation stage 2 could also highlight the importance of various internal controls on fluvial system development. For example, incision in the east of the basin is laterally extensive creating the accommodation space into which the aggrading fan systems (e.g. Filabres fans and Marchante fans of Harvey et al., 2003) and lower and upper lake units were formed (Harvey et al., 2003). Whereas, in the west of the basin incision was confined within tributaries (e.g. Arroyo Verdelecho, Fig 5.12A) and increased toward the south west corner of the basin. These incisional styles relate well to the formation of localised strath terraces characteristic of the basin margins of terrace level 3 and support a mechanism of tectonic sag in the basin centre (Chapter 3). During degradation stage 2, basin connectivity was most pronounced in northerly drainages with limited upstream dissection in major southerly tributaries such as the Rambla Sierra and Rambla Reinelo. These patterns of variable drainage connectivity and erosion could indicate that the Tabernas Basin fluvial system was controlled by non-uniform rates of tectonically driven base-level lowering focused in the west of the basin. However, secondary controls such as lithological barriers could also have been of importance. For example, the lack of connectivity in the south of the basin could be related to the position and structure of the Marchante ridge which formed a major topographic and lithological barrier limiting erosion in the Rambla Sierra, or even be a result of enhanced calcrete cementation which limited incision in this region at the time.

During degradation stage 3, incisional patterns were largely focused around the Rambla Tabernas. Enhanced incision in the El Cautivo badlands correlates well to the

intense stage of climatically driven badland development in final stages of terrace level 3 aggradation dated at the transition from MIS 2 to MIS 1 (Chapter 3 and 4 for detail). Climatically induced incision was likely enhanced at El Cautivo by intrinsic lithological controls with the dramatic increase in erosion upon dissection of a resistant sandstone bed by the Rambla Tabernas (*sensu* Alexander et al., 2008). The focus of incision in the Rambla Benavides could link to ongoing patterns of headward incision coupled with incision within the Rambla Tabernas. However, it would be expected that incision would be ongoing in other regions of the basin. The overall lack of incision in any of the major tributaries, coupled with the relatively low volumes of material removed, could support the hypothesis that the third degradation stage represents a brief degradational period (e.g. Younger Dryas) which took place prior to the formation of terrace level 4 deposits (Section 3.4, Chapter 3). The extent of terrace 4 deposits is highly localised around the Rambla Tabernas and hence reconstructions presented are limited at a basin scale.

The results for degradation stage 4 demonstrate that incision was ongoing across the basin in the final stages of development dated at <2.2 ± 0.3 ka (Chapter 4 for detail). Incisional trends are highly confined yet occur extensively in all basin tributaries. A notable increase in the connectivity of southern drainages is also noted with the headward retreat of the Rambla Reinelo and Rambla Sierra (Fig. 5.14). Variations in spatial and volumetric data with reference to degradation stage 3 suggest that degradation stage 4 was either sustained for a longer period of time, or that incision rates were notably higher during the final stages of basin development to the current day. However, these interpretations are largely limited by the poor preservation and exposure of terrace level 4 units. For example, degradation stage 4 could simply be a continuation of degradation stage 3. The increase in drainage connectivity and incision during degradation stage 4 could also relate to an increase in tectonic activity in the Tabernas region, as evidenced by the rejuvenation of drainages along the Northern Alhamilla Fault Zone (Giaconia et al., 2012), or further external or internal changes in the internal balance of sediment delivery in the basin. Although not well

documented in the Almería region, minor fluctuations in Late Holocene climate (e.g. Little Ice Age; Wanner et al., 2008) coupled with the effects of anthropogenic forcing could have promoted the variable incisional and aggradational trends noted in the current day geomorphology of the basin. The interaction between anthropogenic and climatic forces has been evidenced in the Early to Middle Holocene fluvial records in the neighbouring Sorbas Basin with the clearing of slopes for agricultural and mining purposes (Schulte et al., 2008); however, evidence of anthropogenic activity is limited to a few locations in the Tabernas Basin (Maldonado Cabrera et al., 1991) and the understanding of the long-terms effects upon fluvial system development are limited based on a lack of chronological data. Enhanced incision in the south west corner of the basin is also noted in degradation stage 4. This pattern of variable base-level change, such as evidenced in degradation stage 2, suggests that base-level change has been non-uniform throughout multiple stages of the basin development.

5.5 Summary

This chapter has demonstrated the use of geospatial interpolation techniques in the reconstruction of incisional terrace sequences for quantification purposes. The results from the technique appraisal conducted in Section 5.3 show how an in-depth assessment of technique performance is fundamental when applying interpolation methods to any fragmentary dataset. Attributes of the dataset being modelled (e.g. distance to known data points) coupled with the geomorphic variables and further model parameters all have a significant effect upon interpolation technique performance.

Although useful in the generation of quantitative data, it is noted that the approach utilised in this study (e.g. generation of paleolandsurfaces based on current terrace surfaces) limited the full quantification of degradational stages. For exact volumetric analysis, reconstructions would have been based on the incisional base of units. However, the number of known data points needed at a basin scale to accurately represent the highly

irregular erosional contact of depositional units would not have been feasible. In addition, the requirement for elevational lowering between terrace units (i.e. a stepped strath terrace staircase) highlights another limitation of the technique when applied to the variable incisional and fill records of the Tabernas Basin. The variation in morphological styles within the Tabernas Basin is a fundamental problem when attempting to apply standard methods of landscape reconstruction.

However, the comparison of palaeo-landsurfaces representative of the major stages of basin aggradation has allowed for the subsequent assessment of incisional phases within the basins development. Unfortunately, the spatial extent of the oldest terrace record (terrace level 1) limited reconstructions to the final stages of basin development (degradation phase 2 to 4; Fig. 3.17, Chapter 3). However, notable variations in incisional amounts and styles were noted for all phases, demonstrating a variable response of landscape processes to forcing agents throughout the Quaternary. From the analysis conducted the following points can be made:

- The duration and intensity of degradation stages throughout the Quaternary evolution of the Tabernas basin were highly variable. The most substantial phases of landscape erosion occurred during degradation stage 2 when the majority of the basin was gutted. Degradation stage 3 appears to represent a limited period of basin incision mainly focused around axial drainage system; however, the reconstruction of this incisional phase was likely limited by the lateral extent of terrace level 4 units. Degradation stage 4 started at some time in the Late Holocene and is still ongoing and represents the enhanced headward incision of drainages across the basin;
- Patterns of landscape degradation evidence non-uniform rates of base-level change as potentially driven by variable rates of tectonics focused in the south west corner of the basin;

- Quaternary climate cycles were likely of significance in the evolution of the fluvial system promoting variations in sediment availability and resultant incision across the basin;
- Internal landscape controls such as lithological barriers and other factors (e.g. anthropogenic forcing) could have been of importance in the final stages of basin development.

The non-linear responses of the fluvial system to external and internal landscape forcing mechanisms form the basis of the numerical modelling presented in Chapter 6. The principal aim of numerical modelling is to offer further insight into the principal drivers of landscape change in order to develop the findings of conceptual and quantitative models of landscape evolution developed in this chapter.

Chapter 6

6.1 Numerical modelling of the Tabernas Basin Quaternary landform record

The variability of Quaternary landforms preserved in the Tabernas Basin raises numerous questions concerning the roles of external and internal controls for the evolution of the basin-wide fluvial system over late Quaternary timescales. Thus far, the mechanisms of tectonic uplift and climatically driven variations in sediment availability have been highlighted as major factors driving landscape evolution in the Tabernas Basin (Chapter 4). These external controls are overprinted on internal characteristics of the landscape which have further influenced the long-term fluvial system (e.g. variations in lithological strength). When assessing the associated literature, multiple forcing mechanisms are proposed in the evolution of the basin. For example, Harvey et al. (2003) demonstrate the importance of tectonics and climate in the formation of the lower lake units and associated alluvial fan aggradation stages. Nash and Smith (1998; 2003) identify the importance of climate cycles in the formation of terrace bodies, and further demonstrate the requirement for an ongoing pattern of tectonically driven base-level lowering in the separation of paired calcrete units. Alexander et al. (2008) support the dominance of tectonics and climate upon the hillslope system and identify further lithological controls upon vertical incision rates and system development. However, when assessing the importance of individual forcing mechanisms the qualitative assessment of landscape forces presented lacks the spatial and temporal connectivity representative of the entire basin. This lack of connectivity is a common issue in studies of fluvial terraces and forms a key driver in the development and application of landscape evolution models (LEMs) which attempt to replicate the response of Quaternary fluvial catchments (Tucker and Hancock, 2010).

Over the past decade, numerical models have been extensively applied in studies of Late Quaternary (Holocene) landscape evolution alongside qualitative field investigations in order to assess the importance of forcing mechanisms at a range of temporal and spatial scales (e.g. Veldkamp and Van Dijke, 2000; Coulthard, 2001; Coulthard et al., 2002;

Whipple and Tucker, 2002; Tucker and Hancock, 2010; Viveen et al., 2014). In accordance with the refinement of key model parameters and the ever increasing number of empirical calibrations, the outcomes of modelling exercises have: (i) supported qualitative interpretations of fluvial system development throughout the Quaternary (e.g. generation of terrace bodies during climatic transitions; Macklin et al., 2002; Bridgland and Westaway, 2008; Stange et al., 2013), (ii) enabled the quantification of landscape processes at a range of temporal and spatial scales (e.g. generation of relative uplift rates; Viveen et al., 2014), and (iii) helped to evidence poorly understood self-regulating internal controls operating within fluvial systems (e.g. sediment storage thresholds; Coulthard and Van de Wiel, 2013).

In this study, the 2-dimensional numerical model FLUVER2 is applied in accordance with the approaches of Geach et al., (submitted) in order to qualify and quantify the effects of individual forcing mechanisms (i.e. tectonic uplift and Quaternary climate cycles) in the evolution of the entire Tabernas Basin. The FLUVER2 model was favoured above its 3-dimensional counterparts (e.g. CAESAR- Coulthard 2001 and LAPSUS – Baartman et al., 2012) due to its proven applicability when modelling basin scale (10^2 – 10^5 km^2) fluvial system responses over Quaternary timescales (e.g. Tebbens and Veldkamp, 2000; Veldkamp and Van Dijke, 2000; Veldkamp and Tebbens, 2001; Stemerdink et al., 2010). Furthermore, the forward modelling approach adopted in FLUVER2 is appropriate when focusing on the intensity and interaction of landscape forming processes where model outcomes can be calibrated against field data in an attempt to limit the notions of polygenesis and equifinality (i.e. a combination of different landscape driving factors leads to the same morphological outcome; Temme et al., 2011).

The following chapter provides an overview of the FLUVER2 model, detailing the equations applied in the reconstruction of bed elevation changes through time and the overall structure of the model (Section 6.2). The input datasets used in the model exercise are then presented (e.g. discharge record and the longitudinal profile) with focus on the generation of accurate datasets representative of the Tabernas Basin system (Section 6.3).

A qualitative assessment of the model outcomes is then undertaken with correlations made to the empirical stratigraphy developed in Chapters 3 to 5 (Section 6.4).

6.2 FLUVER2: An overview

6.2.1 **Model calculations**

FLUVER2 is a river gradient model developed to quantify the effects of external and internal forcing mechanisms upon the sediment supply and transport capacity of a fluvial system over a range of spatial and temporal scales (Tebbens and Veldkamp, 2000; Veldkamp and Van Dijke, 2000). The model applies a forward-modelling approach where the dynamics of a fluvial system are simulated along a 2-dimensional longitudinal profile by calculating the incoming and outgoing sediment fluxes, resulting in either erosion or deposition along the fluvial profile. The model adopts a reductionist approach with elements of lateral channel movement and channel morphology neglected in the model structure (Stemerdink, 2007). The key calculations applied in the FLUVER2 model are (from Stemerdink, 2007):

1. **Sediment mobility:** Sediment mobility is the major variable calculated in FLUVER2 for each element of the longitudinal profile for the duration of the model period. Sediment mobility is calculated utilising the sediment continuity equation (Eq. 6.1).

$$\frac{\delta z\ (x,t)}{\delta t} = \frac{\delta qs\ (x,t)}{\delta x} + H\ (x,t) + T\ (x,t)$$

(Equation 6.1)

Changes in the height of the channel bed (z) over a set time (t) are dependent upon the change in the amount of sediment over a set distance (x), represented by the flux of sediment per unit width (qs; Fig. 6.1). H is the amount of sediment delivered from the hillslope and T is the tectonic uplift rate. Sediment flux is calculated using equation 6.2 as the difference between erosion (E) and deposition (D).

$$\frac{\delta qs\,(x,t)}{\delta x} = D - E$$

(Equation 6.2)

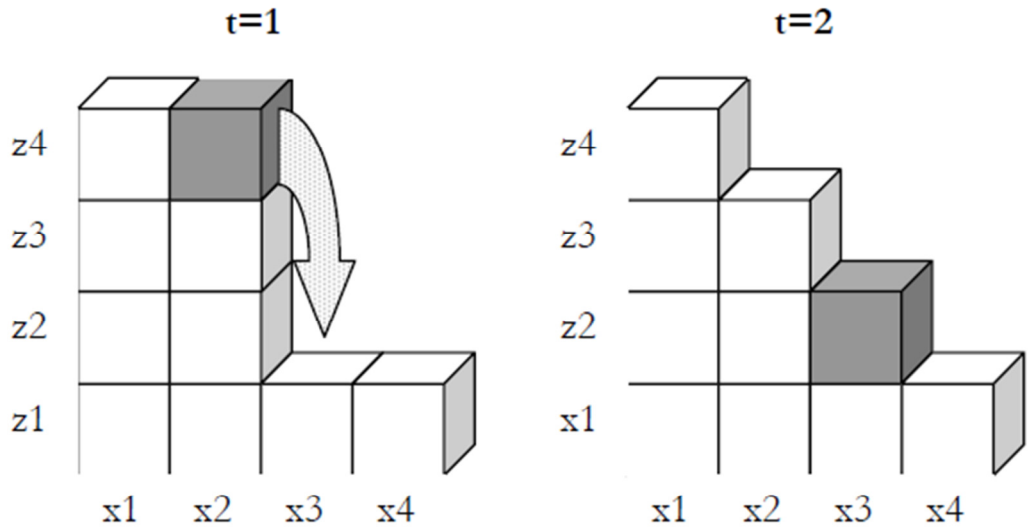

Figure 6.1 Block diagram illustrating the sediment continuity equation, from Stemerdink, 2007. The movement of sediment (grey block) over a set distance (e.g. x2 to x3) equals the change in profile height for the time step t=1 to t=2.

2. **Sediment erodibility:** The rate of erosion of the river bed is calculated for each model element as part of the sediment mobility equation. Erosion (E) is a function of the available stream power (Ω; Eq. 6.3) and the erodibility of the bed (k), shown in Equation 6.4. Stream power (Ω) is a function of the weight of water (γ), channel discharge (Q) and gradient (S). In this study, discharge and channel gradient were calculated from the input datasets presented in Section 6.3 and the weight of water is fixed.

$$\Omega = \gamma Q S$$

(Equation 6.3)

$$E = \Omega\, k$$

(Equation 6.4)

The erodibility factor (k) is an empirically derived factor representative of lithological strength calibrated in sensitivity analysis stages (Section 6.2.3; Tebbens, 1999). In this study, the erodibility factor was treated as constant in accordance with typical methods of application (e.g. Stemerdink, 2007; Viveen et al., 2013a) even though variations in lithological strength are likely across the Tabernas Basin.

3. **Sediment deposition:** The rate of sediment deposition (D) is calculated for each modelled element as a proportion of the sediment flux delivered in that segment ($sed_{(in)}$; Eq. 6.5), divided by a fixed sediment travel distance (dis). The sediment travel distance is representative of the downstream distance over which the incoming sediment flux is dispersed and is calibrated as a key constant during sensitivity analysis of the model (Section 6.2.3; Tebbens, 1999).

$$D = \frac{sed_{(in)}}{dis}$$

(Equation 6.5)

The differences in the amounts of sediment moving in and out of the individual elements for each model step determines the changes in bed height as a result of net sediment flux.

4. **Hillslope sediment supply:** In addition to sediment flux, the sediment continuity equation (Eq. 6.1) also allows for the influence of mass sediment supply from the hillslope and adjustments of elevation with regard to tectonic uplift, variables *H* and *T*, respectively. The rate of hillslope sediment supply is linked to a climatic proxy parameter (C_T) which aims to represent variations in slope vegetation cover over climate cycles. Hillslope sediment supply is further dependent upon the height of the watershed (R) relative to the elevation of the segment being modelled and an additional empirically derived constant (β) used to tune the model (Eq. 6.6). β is an

important parameter in the FLUVER2 model and was assessed in study by means of sensitivity analysis presented in Section 6.2.4.

$$H = R\,(-C_T + 1)\,\beta$$

(Equation 6.6)

The hillslope sediment supply model applies a feedback mechanism which allows for the increase in sediment supply as a function of increased slope distance; Strahler's Law (Strahler, 1950). Increases in slope distance are applied alongside changes in sediment flux when calculating net sediment gains or losses for an individual element (Stemerdink, 2007).

5. **Tectonic movement:** The final variable of the sediment continuity equation (Eq.6.1) is that of tectonic movement (*T*), typically modelled as an uplift parameter (e.g. Tebbens, 1999; Viveen et al., 2014). Individual elements are modelled with a known increase or decrease in height of the active channel at every model iteration. The tectonic movement rate can be fixed or variable for the duration of the model run. In this study, fixed uplift rates were applied in order to represent the effects of uplift upon fluvial system.

6.2.2 Model structure

The structure of the FLUVER2 model is presented in Figure 6.2. In summary, the model starts by applying a number of initial settings at time step 1 (the first model iteration) which include: (1) set data inputs, such as the shape of the longitudinal profile, the length of simulation time (model duration), the time length of each model iteration, the lateral length of model elements and the location of time series used to calibrate model outputs; and (2) model constants of sediment erodibility ('k' in Eq. 6.4), sediment travel distance ('dis' in Eq. 6.5) and the hillslope sediment supply constant ('β' in Eq. 6.6). Next, input datasets representative of climatic variables such as discharge and sea-level change are included.

These data are then subjected to fixed rates of uplift as defined by the rates of tectonic movement. The hillslope sediment supply and sediment flux rates are then calculated for each model element for the duration of the simulation run, defined in the initial settings. The outputs of the model are viewed as elevational data for the known time series locations and can also be viewed as vectorised data in GIS software packages.

In this study, model calculations were made in time steps of 20 years (length of one model iteration) for discrete 40 m steps along the longitudinal profile. The model duration was set at 250 ka based on the input terrace data presented in Section 6.3. Variations in the sediment erodibility, sediment travel distance and the hillslope sediment supply constant were assessed by means of sensitivity analysis presented in Section 6.2.4. The model inputs that serve the focus of this study are those of the discharge dataset and the rates of tectonic uplift as presented in Section 6.3. Data calibrations and further interpretations were conducted using points of known terrace data as summarised in Section 6.3.6.

6.2.3 Boundary conditions

The following boundary conditions were applied in the application of the FLUVER2 model in order to prevent numerical instability and physical impossibilities (from Tebbens, 1999; Stemerdink, 2007):

- The slope and discharge of the final model element are equal to that of that of the penultimate element. This condition avoids model collapse when calculating discharge rates for the final model element;
- The height of the active bed can never be greater than that of the watershed (catchment);
- The gradient of the active bed can never be negative, hence avoiding uphill flows;
- No negative amount of sediment can leave a segment in an attempt to avoid sediment damming in individual elements.

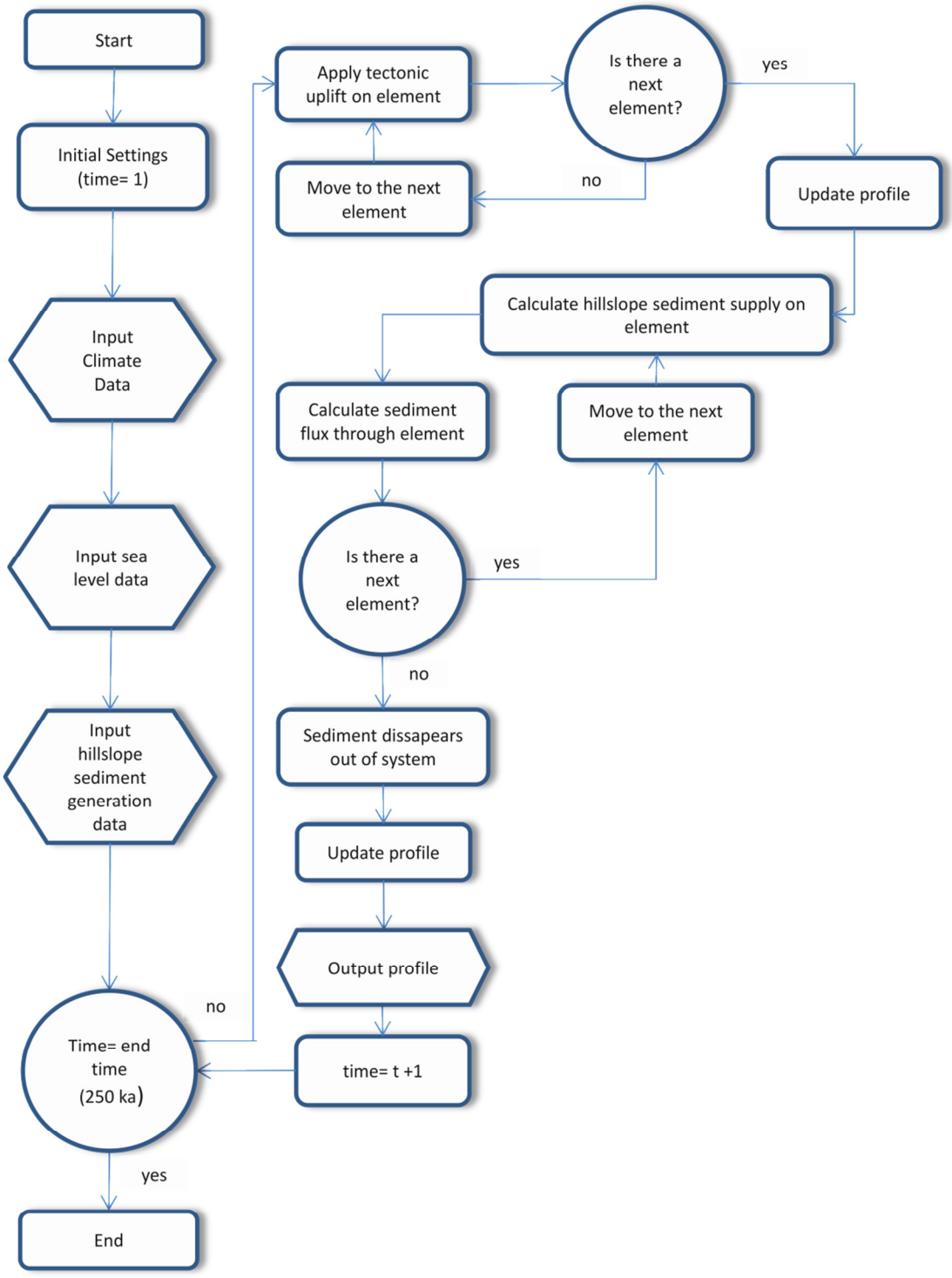

Figure 6.2 Structure and function of the FLUVER2 model modified from Stemerdink (2007). Primary model settings (rectangular boxes) such as the initial longitudinal profile, simulation time, length of one calculation step and the values of the three constants needed to calculate detachment, settlement and hillslope supply are initially determined. Next the input files with climate, sea level and hillslope sediment data are included (hexagonal boxes). The model then applies these inputs for individual tectonic uplift scenarios to calculate hillslope sediment supply and sediment flux for each element of the profile in a downstream direction as shown. Circular statements (circular boxes) must be fulfilled prior to the generation of the output profile.

6.2.4 Sensitivity Analysis

The constants of sediment erodibility, sediment travel distance and the hillslope sediment supply all need to be assessed as part of the sensitivity analysis of the FLUVER2 model. The interplay of these constants is a key part of the numerical stability of the model and determines the success of the model in reproducing natural phenomena (Tebbens, 1999). In this study, sensitivity analysis was conducted in accordance with the approaches of Tebbens (1999), Veldkamp and Van Dijke (2000), and Stemerdink (2007). Model simulations were calibrated by comparing modelled bed elevations and the duration and timings of aggradation/degradation events with field data for two known data time series locations (presented in detail in Section 6.3.6). A time series locations records the changes in bed elevation and sediment accumulation at a fixed point on the river profile.

Initially, incremental changes in the erodibility factor 'k' and the travel distance 'dis' were assessed for a fixed hillslope sediment supply rate 'β' (Fig. 6.3). The hillslope sediment supply rate was then increased and the sensitivity analysis repeated. The results of sensitivity analysis demonstrated that the FLUVER2 model was most sensitive to the hillslope sediment supply rate followed by that of the erodibility factor and sediment travel distance. If the hillslope sediment supply rate 'β' were too low, no sediment was deposited along the profile and computations often crashed (Fig. 6.4).

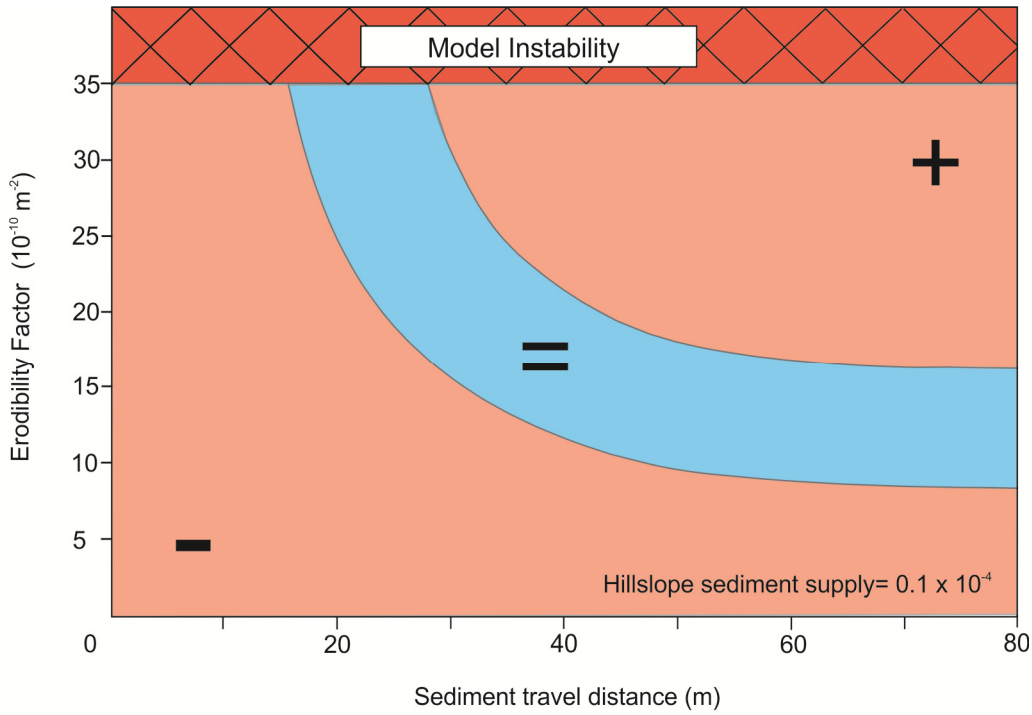

Figure 6.3 Example of the stability plots used in the analysis of model sensitivity for constants of sediment travel distance and sediment erodibility. In this example the hillslope sediment supply rate was fixed. The - field relates to constant which did not generate either the required amount of incision or sediment deposition. The + field relates to combinations which overestimated incision and sediment deposition rates. The = relates to parameter combinations which generated realistic values of incision and sediment deposition. Model instability is noted when the erodibility factor was too great.

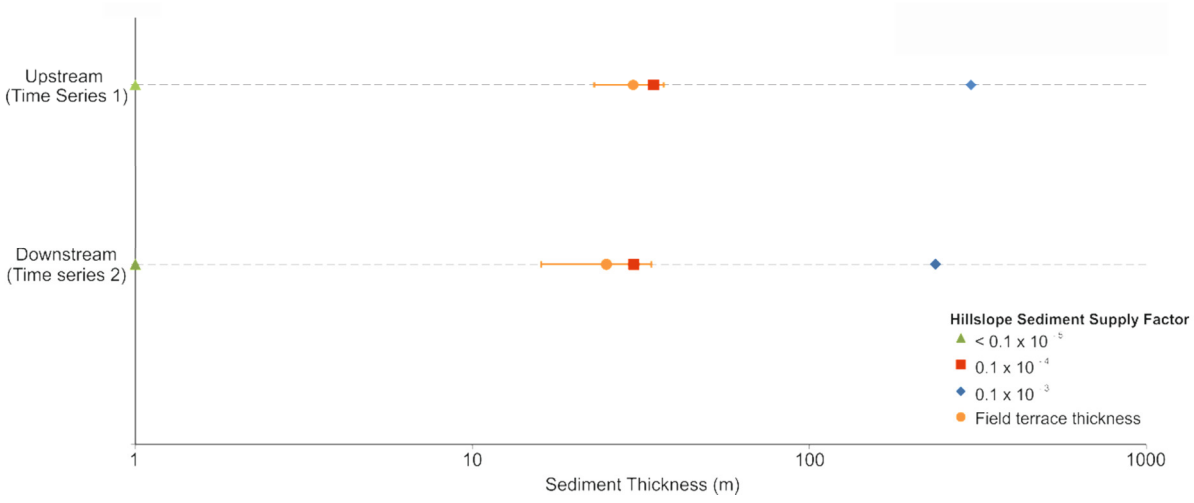

Figure 6.4 Modelled thicknesses of sediment applying a range of hillslope sediment supply factors. No sediment is recorded in the basin if sediment supply factors were less than 0.1 x 10^{-3} .Model values were most representative of field records (orange circles) when a sediment supply factor of 0.1 x 10^{-4} was applied.

6.3 Model inputs and calibration

The following section develops the techniques applied in generating the input datasets used in the FLUVER 2 model (hexagonal boxes Fig. 6.2) as presented by Geach et al., (submitted). The input records comprise the initial longitudinal profile, a palaeodischarge record, a hillslope sediment record, tectonic uplift rates and a sea level record. The accuracy and precision each of these input records is fundamental in the overall success of the modelling exercise. The section also details the use of time series in the calibration of the model parameters such as tectonic uplift rates, hillslope sediment supply and travel distances.

6.3.1 Longitudinal profile

As FLUVER2 adopts a forward modelling approach, the input longitudinal profile has to be representative of the fluvial environment at time step 1 set at 250 ka. There are obvious problems in the generation of relic longitudinal profiles that accurately represent the form of a fluvial system over long timescales (i.e. how to accurately reconstruct Quaternary landscapes). The most common approach applied in the generation of palaeo-longitudinal profiles assumes a state of semi–equilibrium in the fluvial system, meaning that any change in bed elevation was matched by periods of enhanced incision or deposition (e.g. Stemerdink et al., 2010; Viveen et al., 2013a). This approach accepts that the current configuration of the fluvial channel has not accommodated any major elevation changes via processes of lateral migration or crossed any internal thresholds which promote variable rates of incision within the system, such as river captures events (e.g. Stokes et al., 2002). Based on the results of the detailed stratigraphic and volumetric analysis presented in Chapter 3 and 5, it is unrealistic to assume a state of semi-equilibrium existed in the Tabernas Basin throughout the Quaternary period.

In this study, the approach of Bogaart and Van Balen (2000) was adopted in the use of terrace gradients to reconstruct longitudinal profiles. In this approach, the tread slope of individual strath units are used in the generation of idealised downstream profiles; however, errors often occurred as a result of high degrees of terrace separation. In this study, continuous land surfaces were generated by means of geospatial interpolation techniques, as presented in Chapter 5, for use in the generation of palaeo-longitudinal profiles. Due to the restricted occurrence of terrace level 1 deposits, geospatial reconstructions were based on a combination of terrace levels 1 and 2. Terrace elevations were based on a freely available 25m ortho-corrected DEM sourced from the Centro Nacional de Información Geográfica (CNIG, 2013). Interpolation was conducted using variable inverse distance weighting techniques applying a search radius of 30 grid cells (750m) with average basin-wide vertical errors of 6m, calculated by removing the original DEM from the interpolated surface (Geach et al., 2014a). This assessment of interpolation error was a benefit to the modelling exercise as it accounted for early stages of error propagation which can be factored in the assessment of numerical model outputs (i.e. when comparing the modelled bed elevations with the field data).

The palaeolongitudinal profile (dashed line Fig. 6.5A) was generated from the interpolated surface using standard watershed delineation tools in the ArcGIS 10.0 Hydro toolbox. Visual checks were conducted at all stages of reconstruction to ensure physical reality in all data generated. The complete palaeo-longitudinal profile had a total length of 48 km; however, the profile of focus utilised in this study starts at the current limit of incision in the east of the basin (Fig. 6.5B for location) and runs downstream to the Río Andarax confluence (total profile length 25.5 km). Minor variations in channel alignment were noted (Fig. 6.5A) however, the similarity in profiles between the current fluvial system and the relict profile was taken to represent the use of the interpolation technique.

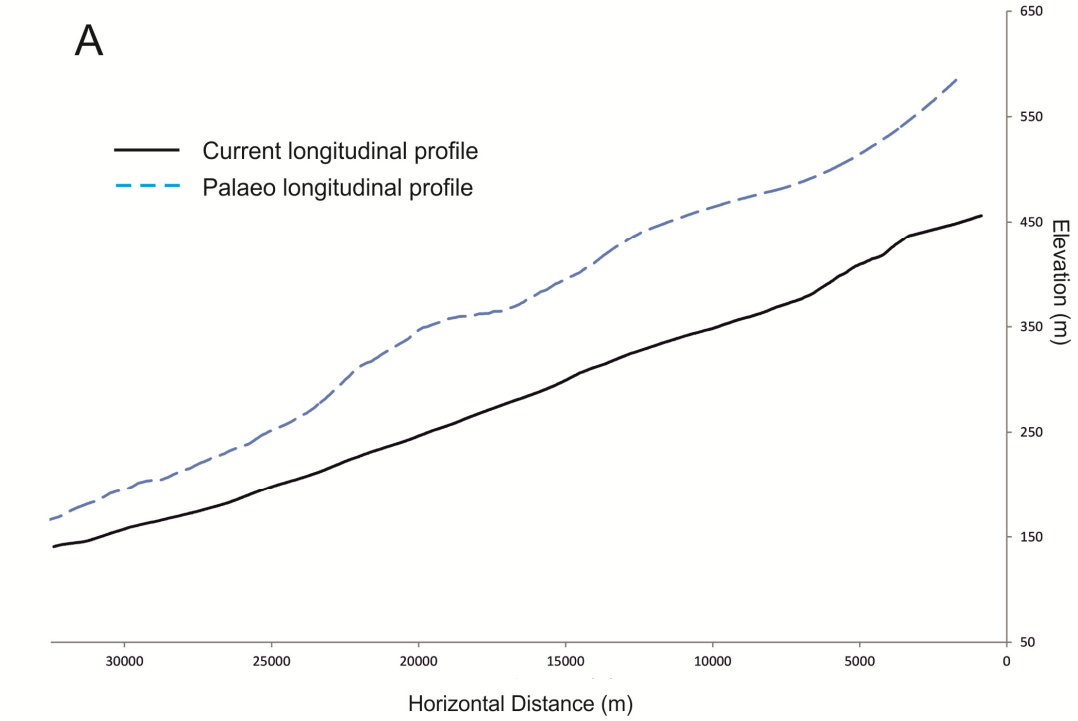

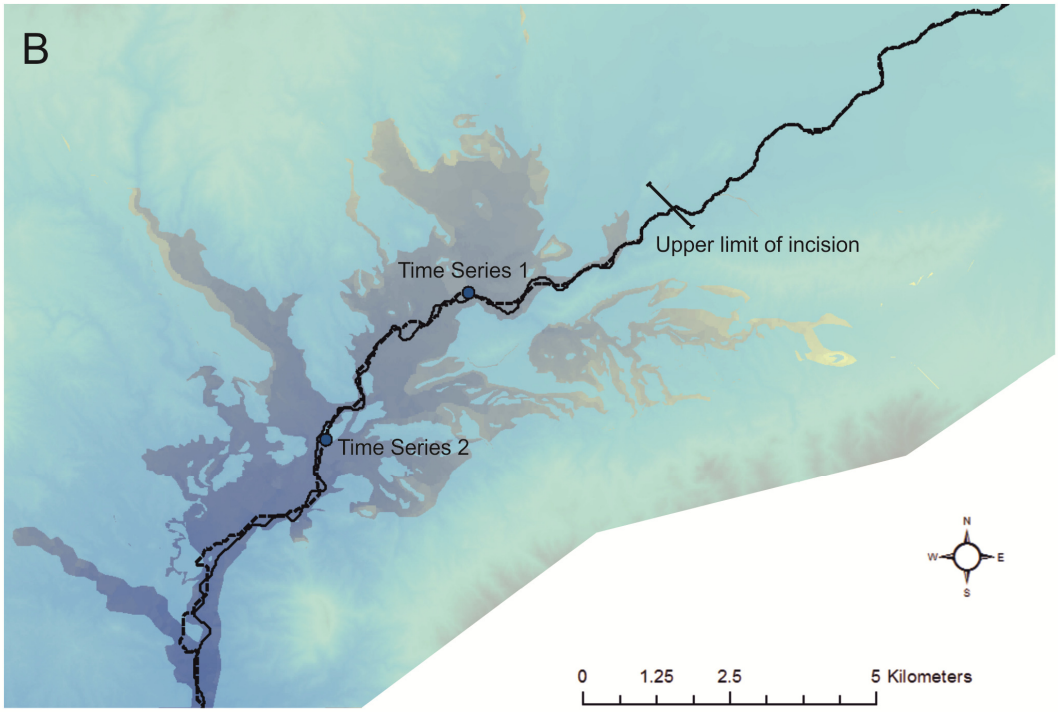

Figure 6.5 (A) Comparison of current and the relic longitudinal profile (terrace level 1 & 2) generated using interpolation techniques. (B) The spatial alignment of the current (solid black line) and palaeo (dashed black line) fluvial channels. Note the slight variation in the path of drainages. Time series used in the calibration of model data are also highlighted. Figure from Geach et al., (submitted)

Based on the correlations of terrace levels presented in Chapter 4, it is likely that terrace level 2 deposits of this study have affinities with the aggradations of terrace level B in the Sorbas Basin. Although its age cannot be confirmed with certainty, deposition of the sediments in terrace level B of the Sorbas Basin is thought to have begun before ~207 ka (Candy et al., 2005), with abandonment of the surface occurring at ~130 ka (Ilott, 2013). Based on this regional correlation, the duration of modelling applied in this study was set at 250 ka. This extended model duration was suitable in the primary generation of sediment in the early stages of the model run, and was further supported by the availability of climate proxies used in the generation of input datasets.

6.3.2 Palaeodischarge record

The discharge dataset acts to replicate the effects of variable climate cycles upon the hillslope system for the duration of the model run (e.g. relative variations in vegetation cover and hillslope runoff). There are multiple ways of generating continuous discharge datasets over Holocene timescales for modelling purposes, based on: (i) regional precipitation reconstructions from palynological data (Bohncke and Vandenberghe, 1991); (ii) the application combined atmospheric global circulation models in the generation of regional climatic data (Bogaart and van Balen, 2000) or (iii) the use of continual proxy records such as peat bogs in the generation of regional wetness indices (Coulthard et al., 2005). However, when dealing with longer Quaternary timescales relatively few methods exist (Veldkamp and Tebbens, 2001). In this study, we adopt the approach of Stemerdink et al. (2010) in the use of sea surface temperatures (SST) as a proxy for regional precipitation and discharge. Although limited by the precision of terrestrial correlations, discussed further this section, SST has been demonstrated to accurately reflect the variations in Quaternary climate required to promote variability in sediment mobility in the modelling domain. In comparison to the often fragmentary nature of Quaternary terrestrial records, offshore marine records typically contain multiple climate proxies (e.g. SST measurements, isotope records and vegetation reconstructions from pollen records) which allow for continual, high resolution

correlations (Viveen et al., 2014). This is particularly relevant in the Almería region, where terrestrial Quaternary palaeoclimate data are restricted to fragmented lacustrine records (Ortiz et al., 2004), speleothems (Hodge et al., 2008) and archaeological records found in cave settings (González-Ramón et al., 2012) of very limited quality and of an ephemeral nature. However, marine records for the Almería region cover long temporal scales which are believed to provide close correlations with the terrestrial system as a result of the sediment sources from onshore fluvial systems (e.g. correlation of marine pollen records against terrestrial records; Fletcher and Sanchez Goñi, 2008).

In this study, precipitation rates generated from palynological data were calibrated against global climatic conditions (e.g. marine oxygen isotope records) and varying rates of evapotranspiration, as associated with the dominant vegetation type of the time, to generate a hillslope discharge record (Fig. 6.6). One of the major limitations of this approach is the propagation of errors throughout the reconstruction phase. Error propagation is relevant at every level of interpretation from species biomisation of pollen data to the quantitative reconstruction of land classes and further linear correlation with SST. However, the SST approach adopted in this study has been demonstrated to be of use when reconstructing cyclic fluctuations in regional precipitation rates as recorded in both marine and terrestrial pollen records (e.g. Stemerdink et al., 2010; Viveen et al., 2013a; Geach et al., submitted).

Two deep sea cores from the Alboran Sea (ODP Hole 161-977A and MD95-2043; see Martrat et al., 2012 and Cacho et al., 1999, respectively), were used in precipitation reconstructions. The longest climate record from the ODP Hole 161-977A presents a continuous record of SST for the region (244 ka to Recent), with SST reconstructions based on alkenone assemblages and geochemistry. MD95-2043 provides a much shorter SST record (52 ka to Recent); however, a high-resolution palynological dataset is presented for the core (Fletcher and Sanchez Goñi, 2008) alongside a quantitative reconstruction of precipitation rates using the modern analogue technique (MAT; Fletcher et al., 2010). This

continual precipitation reconstruction is one of the longest palaeoclimate records for SE Spain and is pivotal in enabling more exact correlations with SST (Geach et al., submitted).

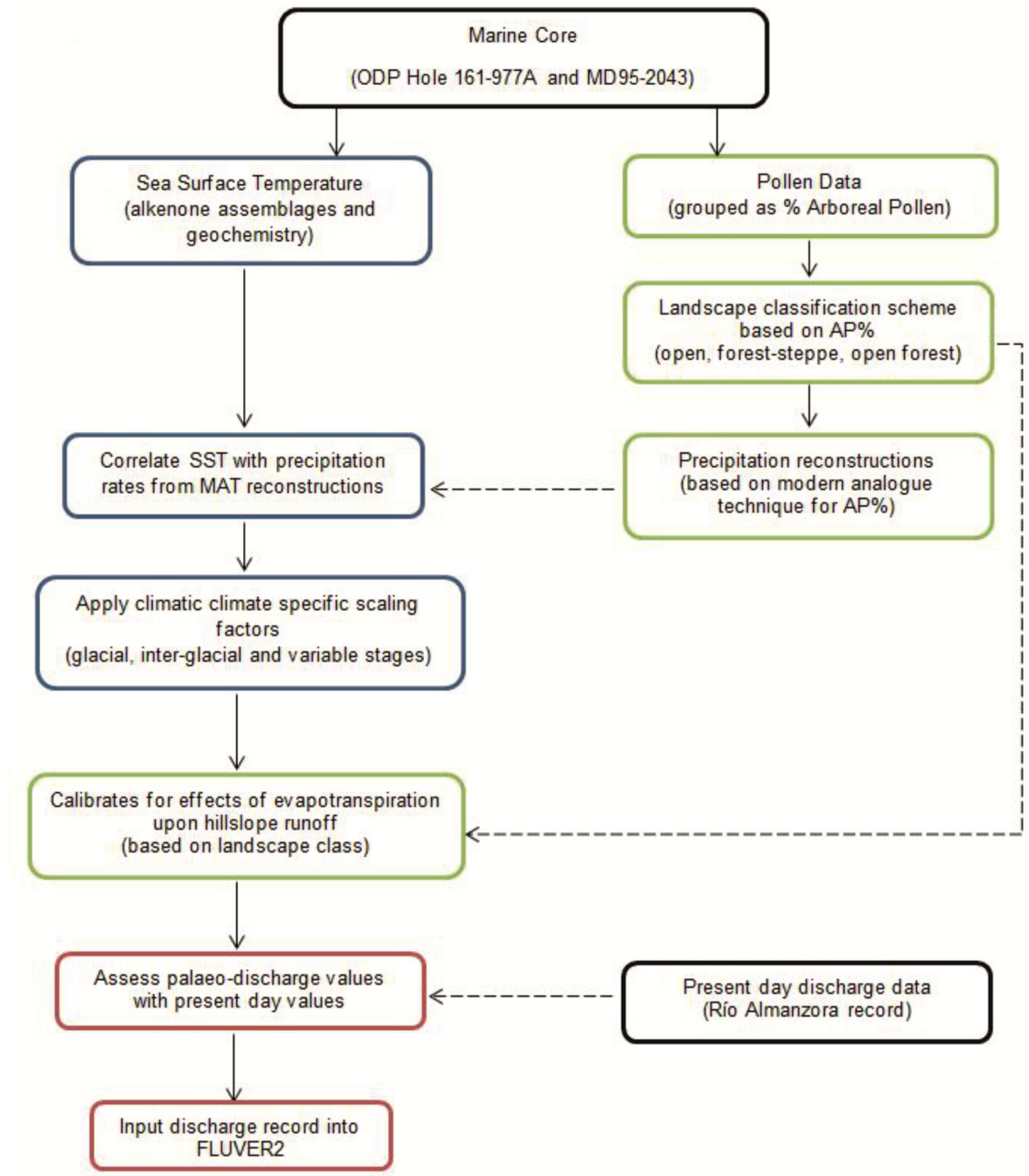

Figure 6.6 Model steps demonstrating the process applied in the generation of the discharge data input for the FLUVER2 model.

Analysis of pollen data from the MD95-2043 record shows that the Late Pleistocene to Holocene landscape was characterised by high-amplitude shifts between drought-tolerant, semi-desert vegetation over the past 50 ka, with *Artemisia* and *Chenopodiaceae* dominant during high-latitude cold episodes (stadials), and open Mediterranean forest with deciduous and evergreen *Quercus* during warm episodes (interstadials). During the last global glacial-interglacial transition and the Holocene, forest vegetation became dominant, but experienced declines during high-latitude cooling events such as the Younger Dryas, 9.3 and 8.2 ka events (Fletcher et al., 2010). Overall, the vegetation record points to a high sensitivity of southeastern Iberian vegetation cover to climatic variability, particularly to hydrological variability leading to changes in moisture availability for mesophytic forest trees (Geach et al., submitted). Marine pollen data largely conform to terrestrial records (e.g. Fletcher et al., 2010) and support the applicability of the marine records in the reconstruction of regional discharge data.

Based on the results of previous research (e.g.Stemerdink et al., 2010; Viveen et al., 2013a), correlations between the MAT precipitation record from the MD95-2043 core and the alkenone derived SSTs were made adopting a standard scaling factor (Fig. 6.7a). This simple scaling technique demonstrated that periods of forest expansion and higher steppe vegetation correlate well with reconstructed precipitation rates as associated with warmer Alboran SSTs. However, in order to further refine the correlations between SST and MAT precipitation, climate specific scaling factors were applied based on linear regression analysis for three different climate scenarios (cold climate, warm climate and variable climate). The addition of climate scenarios produced a notable increase in the accuracy of SST correlations when replicating the frequency and magnitude of change in the MAT dataset (Fig. 6.7B). However, these correlations are a limitation in the model approach, where arbitrary scaling factors are used to generate discharge data over long timescales.

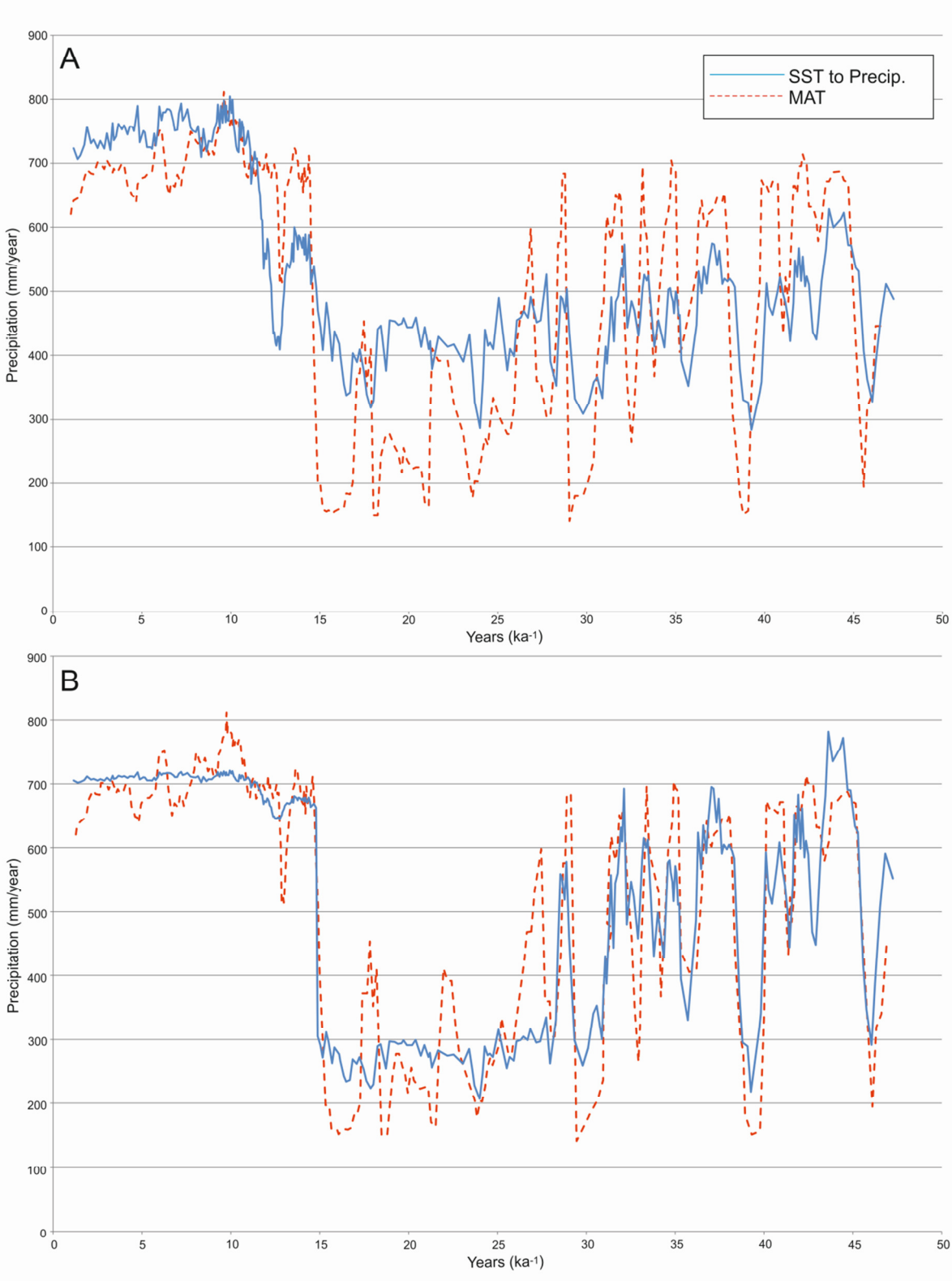

Figure 6.7 Correlations between sea surface temperature to precipitation record (SST to Precip.) and the baseline precipitation record (MAT) as calculated using: (A) a single scaling factor; and (B) climate specific scaling factors (e.g. cold, warm and variable conditions). Note the improved correlation between the records when climate specific scaling factors are applied.

The effects of vegetation slope cover and associated evapotranspiration upon rates of hillslope generated runoff must be accounted for in the generation of a discharge dataset from regional precipitation data (Fig. 6.6). In previous studies based in temperate climatic regions (e.g. Stemerdink et al., 2010; Viveen et al., 2013a), the rates of precipitation loss to evapotranspiration were generated for climatically controlled vegetation groups based on generalised temperature brackets as evidenced from the pollen record. Given that the Tabernas Basin occurs in a semi-arid to arid setting, the conversion factors representative of temperate regions were deemed unrepresentative. This is due to dominance of vegetation slope cover relative to the loss of moisture via evapotranspiration (Fletcher *per comms*.). Applying the pollen data from the MD95-2043 core, a simple land cover classification scheme was generated for the Tabernas Basin comprising of three land cover groups (open, forest-steppe, open forest) based on arboreal pollen abundances (AP%). Runoff characteristics for these land cover classes were defined with respect to the classic, negative exponential relationship between Mediterranean vegetation cover and relative runoff (Francis and Thornes, 1990, and others, as summarised in Durán and Rodríguez, 2009), with <10% runoff generated from precipitation at vegetation cover of >40% (AP% >40, open forest and forest categories); ~20% runoff at vegetation cover 20-40% (forest-steppe), and ~70% runoff at vegetation cover <20% (open) (Fig. 6.8). This classification system represents the potential for very high relative runoff and associated erosion and sediment mobilisation in settings with sparse vegetation cover, characteristic of Mediterranean landscapes under variable climatic conditions (Geach et al., submitted).

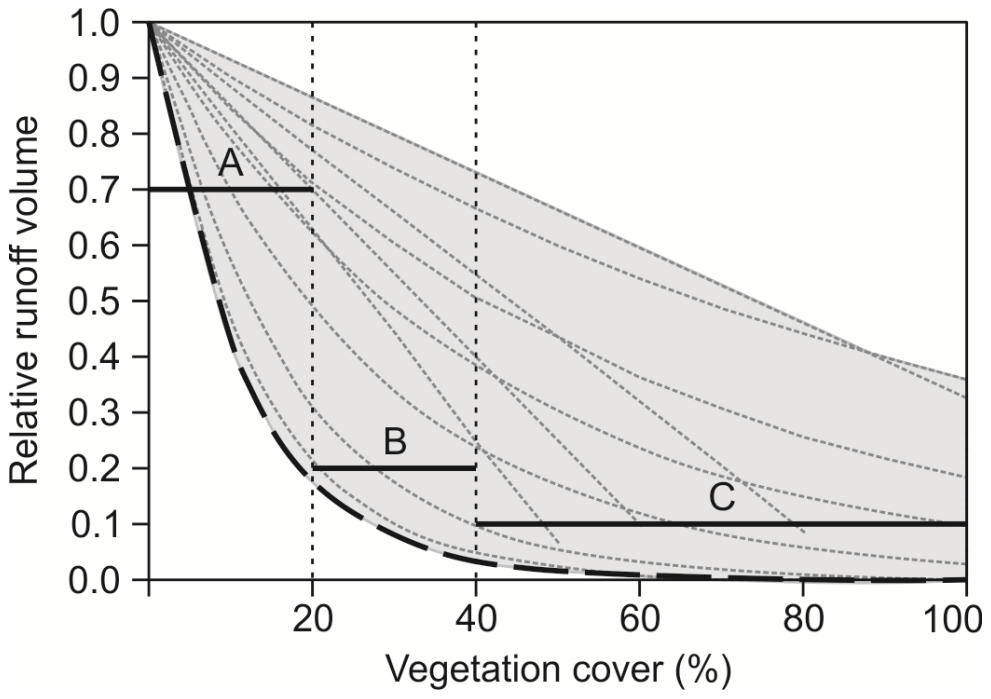

Figure 6.8 Parameterisation of runoff with respect to vegetation cover for three pollen-based vegetation classes in this study (From Geach et al., submitted): open (A), forest-steppe (B) and open forest to full forest (C). Dashed curve shows the classic negative exponential relationship reported by Francis and Thornes (1990) for Mediterranean scrubland in southeastern Spain during high intensity rainfall events. Shaded area and grey dotted lines represent the envelope of values reported in a range of other empirical studies in global semi-arid regions (adapted from Durán and Rodrguez, 2009).

As previously noted, a fundamental limitation of the SST approach is the inability to assess errors throughout the stages of data generation. An example of this would be the extensive use of AP% in the grouping of data for reconstruction purposes: however, there are several factors that support the use of vegetation data in this way. For example, a high arboreal abundance is likely to be associated with greater canopy cover, higher rainfall interception, thicker leaf litter and deeper soils, better soil infiltration, higher evapotranspiration and a more diverse mosaic of vegetation with denser patches – all of which should reduce runoff (e.g. Quinton et al., 1997; Bautista et al., 2007; Ries and Hirt, 2008; Vásquez-Mèndez et al., 2010). The use of AP% in classifications could be unreliable if dense, continuous, non-arboreal vegetation cover (e.g. grass steppe, heathlands) were persistent during the past. However, in contrast with northwestern Iberian records (e.g.

Gomez-Orellana et al., 2007; Naughton et al., 2007), grasses, heaths and associated herbaceous pollen types are never abundant in the MD95-2043 pollen record or other southern Iberian records for this time span (Lezine and Denefle, 1997). Rather, dwarf shrubs and xerophytic herbs (*Artemisia, Chenopodiaceae, Ephedra*) are characteristic during dry (cold SST) events, implying a semi-desert landscape with bare patches of ground and lower vegetation cover overall (Geach et al., submitted).

In order to generate the discharge record for the longer ODP Hole 161-977A record, the scaling factors and data generated from the MD95-2043 core were applied to the longer ODP Hole 161-977A record. Correlation of SST from both cores supports this approach (Fig. 6.9); however, the lack of pollen data for the ODP Hole 161-977A record highlights a limitation of the approach. Discharge data generated for the 250 ka period were then compared with modern day values. Unfortunately, no present day discharge data are recorded for the Tabernas Basin; instead, an annual record spanning from 1963 to 2009 from the Río Almanzora in the neighbouring Vera Basin was adopted (Fig. 6.10) (Stokes et al., 2012b). Model discharge values of 1.8 m^3/s fell well within the range of modern values, with a mean discharge value of 9.34 m^3/s and median value of 0.87 m^3/s. Although differences in catchment size are notable, the comparisons with modern day discharge data and the modelled data were acceptable based on the lack of other data for the Tabernas catchment. The use of a short discharge record of high variability is another limitation in the model application in this study.

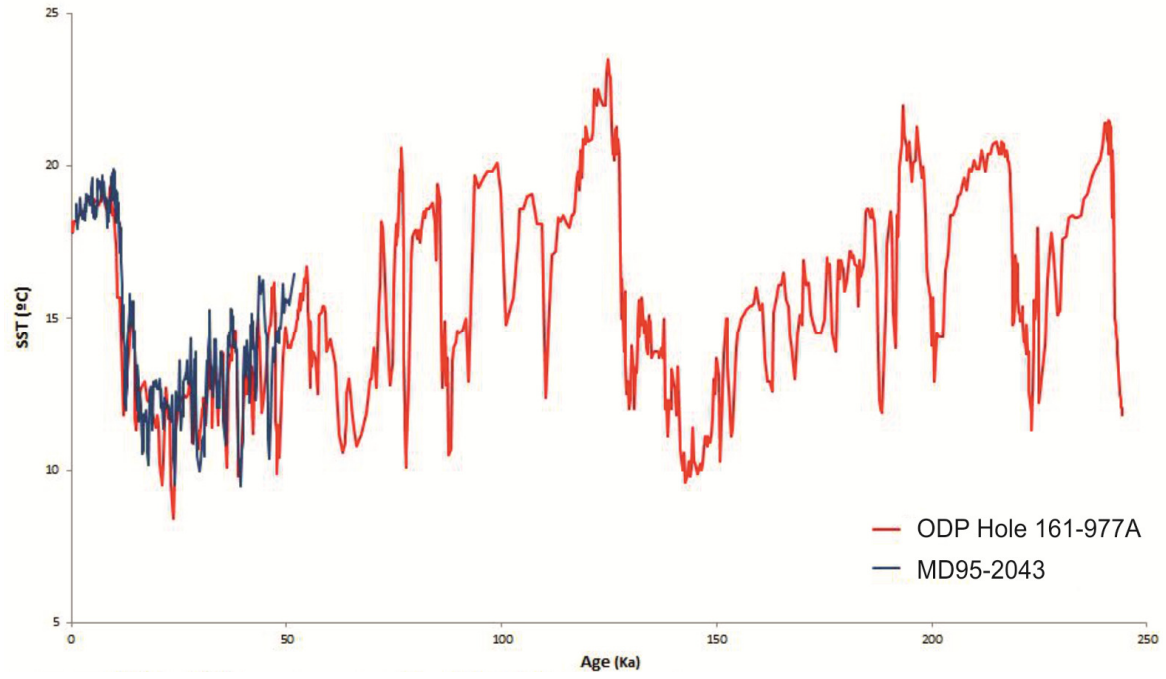

Figure 6.9 Correlation of SST records from the ODP Hole 161-997A (red line) and MD95-2043 core (blue line).

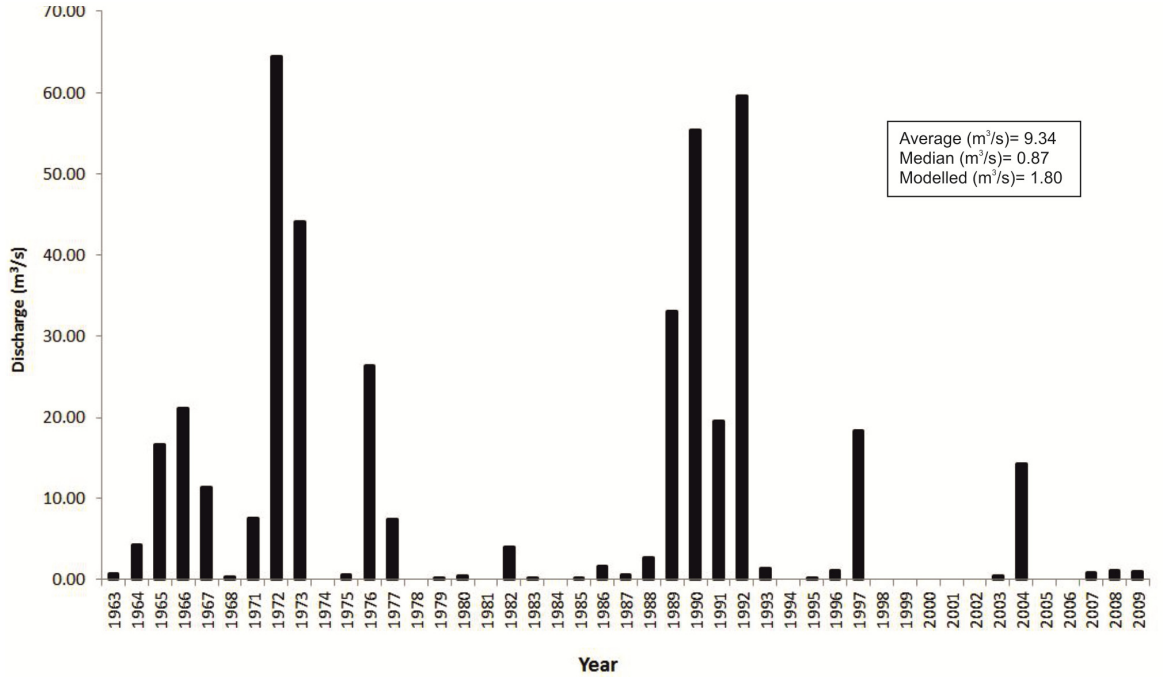

Figure 6.10 Discharge data for the Río Almanzora for period 1963-2009 is crucial in checking the relative accuracy of discharge outputs from FLUVER2 (Stokes et al., 2012b).

6.3.3 Hillslope sediment supply record.

In this study, the rate of hillslope sediment supply 'β' (Eq. 6.6) was supplemented by an additional sediment generation parameter in order to represent increases in sediment availability during Pleistocene global glacial phases in the FLUVER2 model (*sensu* Stemerdink, 2007). Given the understanding of the sediment production and storage during cold climate cycles in the Tabernas Basin, this additional parameter was deemed crucial (presented in Chapter 2, 3 and 5; Harvey et al., 1999; Harvey et al., 2003). In accordance with the assumptions made in the generation of the discharge record, sediment production was enhanced during cold periods of open vegetation. In order to reproduce cold phases in the input data, a SST temperature of <10.75 °C, assessed from SST to MAT correlations, was adopted as a threshold value from which enhanced sediment production was introduced into the system. However, when SSTs were >10.75 °C sediment was still generated applying the standard sediment mobility and hillslope sediment supply calculations adopted in the FLUVER2 model.

6.3.4 Tectonic uplift rate

As this study aims to assess the effects of tectonic uplift upon the development of the Tabernas Basin, the uplift rates applied in the FLUVER2 model are of upmost importance. It is established that the Neogene basins of the Almería region record a variable response to rates of tectonic uplift throughout the Quaternary period (Table 1.2; Chapter 1, Section 1.4.6). To date, uniform uplift rates of 0.1 to 0.2 m ka^{-1} are presented for the Tabernas Basin based on time-averaged uplift of Pliocene coastal and nearshore marine rocks (Braga et al., 2003). However, these deposits are absent across the most of the basin and cannot be easily associated with the Quaternary landscape system. In order to accurately represent uplift in the FLUVER2 model, five rates of Quaternary uplift were adopted based on regional data. The lowest uplift rate was set at 0.10 m ka^{-1} in accordance with Pliocene uplift values (Braga et al., 2003). Uplift was increased by set increments to the uppermost uplift value of 0.30 m ka^{-1} based on values presented from the Eastern Alpujarran Corridor (García et al., 2003).

6.3.5 Sea-level record

The sea level record acts as the primary base level control in the FLUVER2 model. Following the approach of Viveen et al., (2013a), the time series of Bintanja et al. (2005) was applied in the reconstruction of sea level from δ18O data. Data are presented at regular time steps of 0.1 ka making it suitable for input in the FLUVER2 model. The data were transformed to 20-year time steps by means of linear interpolation between the data points. To present, it is proposed that the effects of sea-level change have been negligible upon the evolution of the Tabernas Basin (Chapter 1, Section 1.4). In order to assess the sensitivity of the FLUVER2 model to sea-level changes and to further address the importance of sea-level change in the Tabernas Basin at a preliminary stage, the sea level record used in the model was amplified by a factor of 1.5 and 2.0. In all instances there was no effect upon the model outputs, thus ruling out the significance of this data input in the model structure. This would suggest that the Tabernas Basin drainage system has remained decoupled from the effects of sea-level as a function of its distance from coastlines during sea-level highstands.

6.3.6 Calibration of model output: time series locations

In order to assess the accuracy of the model scenarios applied (i.e. tectonic uplift rates, hillslope sediment supply rates) two time series locations were defined based on locations of known empirical data. The calibration of model parameters based on known data points builds on the approaches of sensitivity analysis (Section 6.2.4) and allows for an assessment of model reality and accuracy based on correlations with known field data (e.g. Viveen et al., 2013a). However, an element of model equifinality will always exist, whereby multiple combinations of parameters can lead to the same model output (Tucker and Hancock; 2010).

The time series locations used in this study were positioned in both an upstream (~4.6 km from point of incision shown on Fig. 6.5B; time series 1) and downstream (~ 12.6 km from point of incision; time series 2) location. At both locations a more or less a complete and well represented field terrace record was present. The field data included details of

terrace sedimentology, typical terrace thicknesses, and terrace surface elevation (Table 6.1). The time series locations were used in the calibration of model parameters with an assessment of the following modelled and field factors: (i) the number and elevation of the simulated terraces; and (ii) the timing of terrace formation and the overall thickness of the sediment deposits in the terrace record. Note that terrace level 2 lower is not recorded at either time series location and the terrace level is omitted from the modelling exercise.

Table 6.1 Field and modelled data for Tabernas basin Quaternary terrace records at time series locations 1 and 2.

Terrace Level	Surface Elevation (mAHD)	Modelled Surface Elevation (mAHD)*	Terrace Thickness (m)	Modelled Terrace Thickness (m)
	Time Series Location 1 (Upstream)			
2	395	392	10 - 21	10
3	375	378	5-10	6
4	335	358	< 2	0
	Time Series Location 2 (Downstream)			
2	338	336	6 - 15	9
3	330	334	12 - 20	18
4	290	327	< 2	0

Note terrace level 1 is not represented in this modelling exercise. * Modelled elevations represent best fit tectonic uplift scenarios of 0.13 m ka^{-1} for time series 1 and 0.25 m ka^{-1} for time series 2.

6.4 FLUVER2: Results and discussion

The following section details the results of the FLUVER2 modelling exercise adopting variable rates of tectonic uplift. The results are presented for a combination of model variables assessed in the sensitivity analysis and model calibration stage. A discussion of the model outputs are then presented based on their relation to the time-series data (Section 6.3.6). The data presented are further detailed in Geach et al., (submitted).

6.4.1 Number and elevation of the simulated terraces

The outputs from the modelling exercise show three terrace formation stages that were modelled for both time series locations over a time span of 250 ka (Fig. 6.11). Terrace aggradations were noted for all tectonic uplift scenarios; however, when applying uplift rates higher than 0.15 m ka^{-1} the model generated stacked (fill) terrace sequences whereby the younger terrace surfaces formed at elevations greater than those of older terraces (Fig. 6.11A). The generation of stacked sequences was taken to represent uplift rates much higher than those likely in the generation of the incisional record representative of this region of the Tabernas Basin. The model results highlight the further requirement for differential rates of tectonic uplift in the generation of terrace bodies at similar levels to those evidenced in the field record. For example, at time series location 1 an uplift rate of 0.13 m ka^{-1} generated terraces at elevations close to those of terrace levels 2 and 3 from the field-based survey (Fig. 6.11A). However, for the downstream time series location (time series 2), a higher uplift rate of 0.25 m ka^{-1} produced more suitable matches for terrace levels 2 and 3 (Fig. 6.11B). There were notable discrepancies between the model outputs and field records for terrace level 4 for both time series locations, with elevation differences of 23 m for time series 1 and 37 m for time series 2, assuming the best-fit uplift rates of 0.13 m ka^{-1} and 0.25 m ka^{-1}, respectively (Fig. 6.11; Table 6.1).

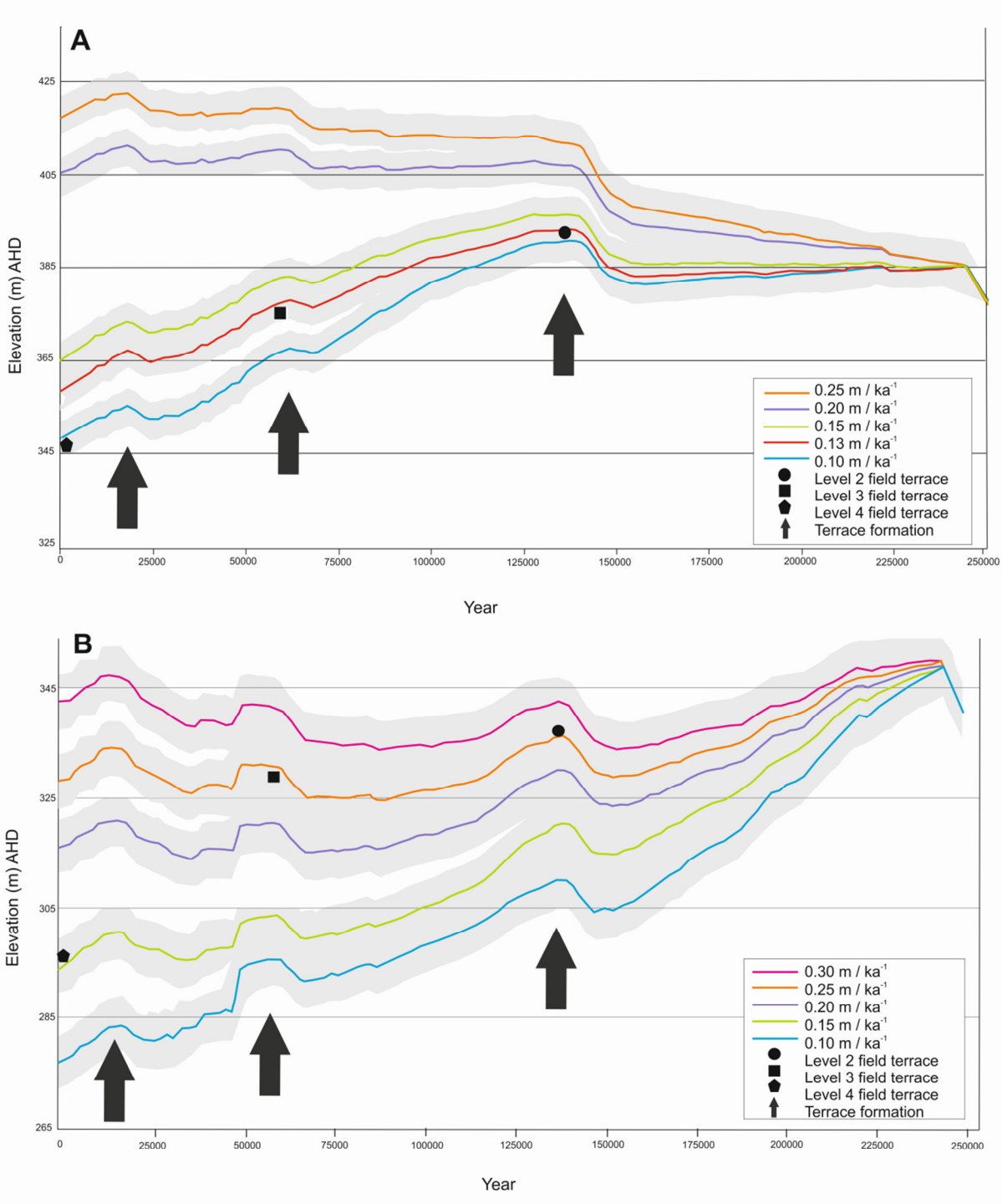

Figure 6.11 FLUVER2 output showing terrace aggradations and incisions for upstream time series location (time series 1) (A) and downstream time series location (time series 2) (B), from Geach et al (submitted). Five tectonic uplift scenarios are presented for both time series locations as referenced in the specific key. Notable correlations with the field record are presented for terrace levels 2 and 3 when applying uplift rates of 0.13 m / ka-1 for time series 1 and 0.25 m / ka- 1 for time series 2. The grey buffer around all model outcomes presents the initial errors (6m) in the generation of the palaeo-longitudinal profile. Note difference in scale on the *y- axis*. The figure supports theory of tectonic sag across the basin.

6.4.2 Timing of terrace formation and sediment stack thicknesses

The modelled rates of sediment accumulation for both time series locations are presented in Figure 6.12. A notable feature for both time series is the relative increase in sediment accumulation during the transition from MIS 6 to 5 (150 - 130 ka), and the last glacial maximum (LGM; 30 - 14 ka; Fig. 6.12). These two aggradation stages are taken to represent basin wide aggradation phases. Although dominated by the two prominent aggradation phases, variable patterns of sediment accumulation are noted in both time series locations. For example in time series 1, modelled rates of sediment deposition were greater during the first aggradation phase (MIS 6 to 5, 150 - 130 ka) when compared with the second aggradation phase (LGM, 30 - 14 ka) with modelled sediment thicknesses of 10m and 6m, respectively (Table 6.1). For time series 2, notable sedimentation was also noted during first aggradation phase (MIS 6 to 5, 150 - 130 ka); however, an additional sedimentation event occurring during the transition from MIS 5 to 4 (71 to 60 ka) which was further enhanced during the second basin wide aggradation event in the LGM (Fig. 6.12). Combined sediment thicknesses from the MIS 5-4 transition to end of the LGM aggradation stage were nearly double those of the first aggradation phase (Table 6.1). Sedimentation at both time series locations terminated at the transition to MIS 1 with no accumulation of sediment from ~12 ka onward.

.

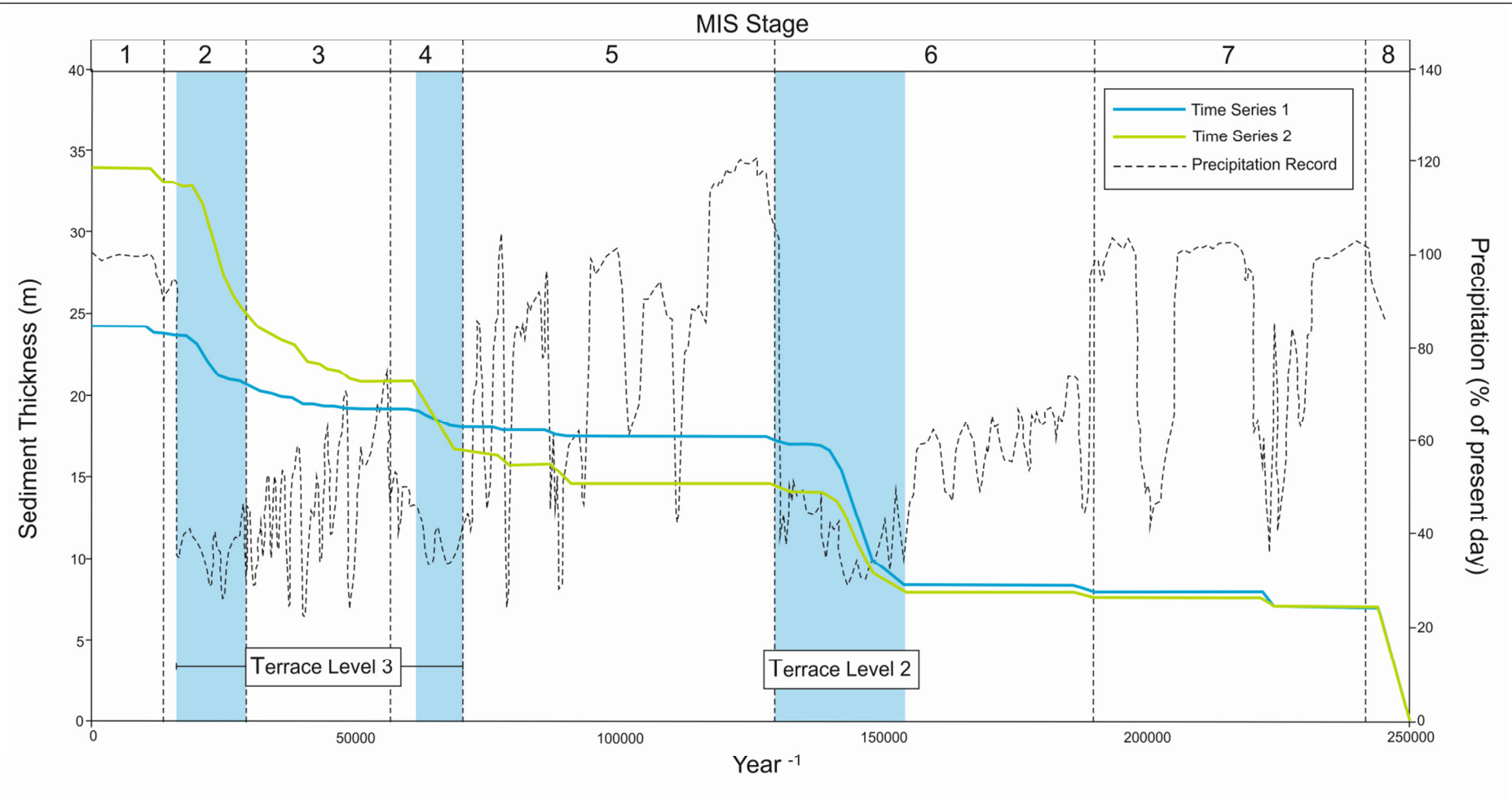

Figure 6.12 Sediment aggradation for the upstream time series (blue line) and downstream time series locations (green line) showing aggradation phases during the transition from MIS stage 6/5, MIS stage 5/4 and MIS stage 2 (LGM). Associated stages of terrace level formation are presented for levels 2 and 3. Terrace level 4 is again poorly accounted for in this output. The precipitation record presented demonstrates the success of applying SST and a long term climatic record for modelling purposes. Figure from Geach et al., (submitted).

6.4.3 Discussion

The results from the FLUVER2 model correlated well with the empirically based data (i.e. time series locations) and highlight the importance of both extrinsic and intrinsic mechanisms of landscape change with the Tabernas Basin. The sensitivity of the model to the hillslope sediment supply factor β demonstrates the importance of hillslope sediment inputs in the development of the fluvial terrace archive. The sensitivity of the model parameter offers close affinities with the actual Tabernas system, where hillslope inputs are evidenced by multiple phases of alluvial fan development. Alluvial fan progradation was characteristic in the early stages of basin evolution (terrace levels 1 and 2; Chapter 3) and is still ongoing in the undissected regions of the basin at present (Chapter 3; Harvey et al., 2003). Coupling of the hillslope system is clearly of importance throughout the evolution of the basin.

The modelled uplift rates presented in Figure 6.11 demonstrate the importance of tectonics upon the evolution of the Quaternary fluvial system. FLUVER2 results show a pronounced increase in model accuracy when applying variable uplift rates from 0.13 m ka^{-1} in the east of the basin toward 0.25 m ka^{-1} in the west for the older terrace records (terrace level 2 and 3). Increased tectonic activity in the west of the basin supports the likelihood of increased syn-tectonic deformation (*sensu* Harvey et al., 2003), and fits with the patterns of landscape degradation evidenced in the current basin geomorphology (Chapter 1, Section 1.3). This variability in Quaternary uplift rates is recorded elsewhere in the Almería region (i.e. spatial variability in uplift between the Sorbas and Vera Basins; Mather and Harvey, 1995) and fits well with regional mechanisms of enhanced tectonic uplift proposed in the EAC (0.3 - 0.7 m ka^{-1}; García et al., 2003), as summarised in Figure 6.13

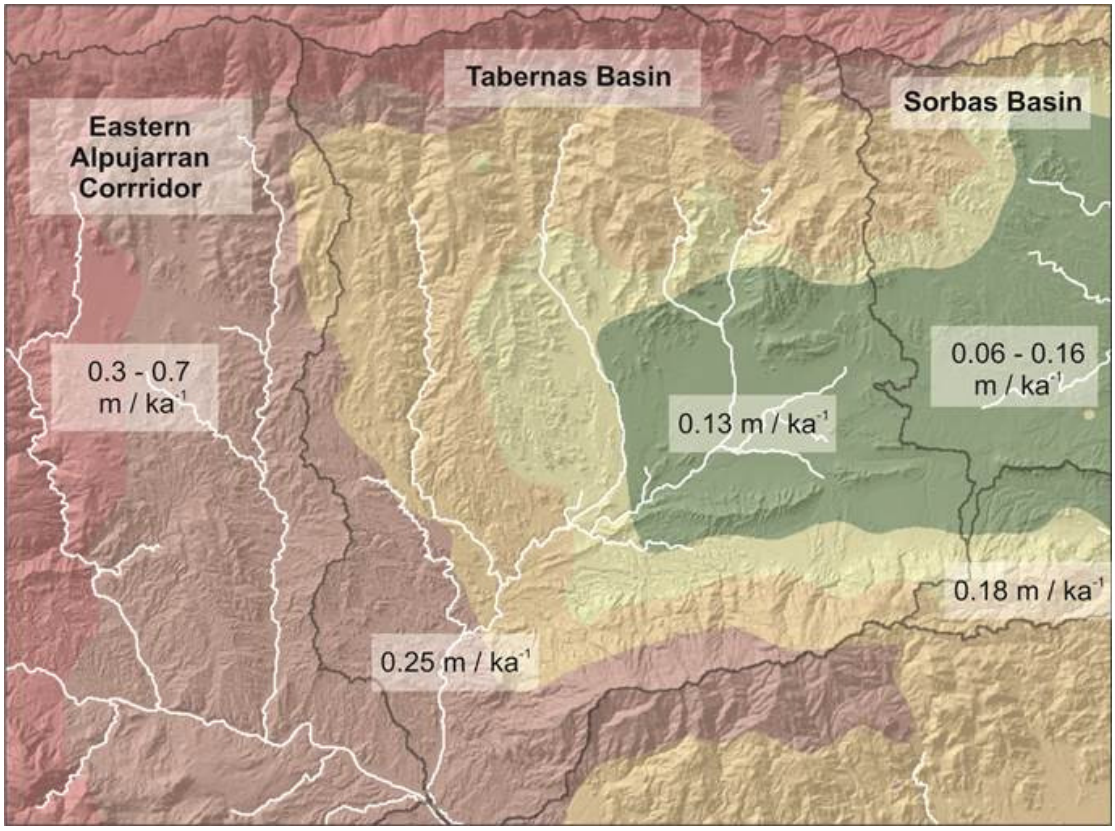

Figure 6.13 Idealised tectonic uplift map demonstrating the variability of Quaternary uplift rates for the Tabernas Basin and neighbouring Eastern Alpujarran Corridor (García et al., 2003 and Sorbas Basin (Mather,1993). Note tectonic sag in upper Tabernas basin.

The significance of climate cycles is also well simulated in the outputs of the FLUVER2 model. Periods of simulated terrace formation (Fig. 6.12) form in accordance with regional and global climatic trends, with terrace aggradations during cold climate phases (e.g. Candy et al., 2004; 2005; Maher, 2005; Miekle, 2008; Schulte et al., 2008) or climate transitions (e.g. Bridgland and Westaway, 2008) (Fig. 6.14). Major phases of aggradation were simulated during the transition from MIS 6 to MIS 5 and the LGM, with one shorter aggradation event during the transition from MIS 5 to MIS 4 (71 to 60 ka). However, lesser climatic fluctuations such as the Younger Dryas, 9.3 ka and 8.2 ka events, which have been linked to terrace formation in the neighbouring Sorbas Basin (Schulte et al., 2008) were not recorded in model outputs. The poor representation of short duration climate fluctuations could be a limitation of input discharge record, with the Holocene represented by relatively

uniform discharge data (see dashed line on Fig. 6.12). The onset of terrace incision events (Fig 6.11) also correlate well with regional models, with periods of sustained incision occur during the transition to warm interglacial conditions for both time series locations. In FLUVER2, sustained incisional events exceed aggradational events as a result of dramatic increases in discharge coupled with decreases in sediment generation between 140 to 71 ka, 60 to 30 ka and the Holocene (Fig. 6.12 dashed line). The accuracy of both depositional and incisional events in the Middle to Late Pleistocene fluvial system demonstrates the ability of FLUVER2 to represent changes in sediment flux over long timescales; however, discrepancies occur in the representation of lower magnitude Holocene climatic changes.

The amount and timings of simulated sediment deposition provides good correlations with the terrace thicknesses recorded in the field and the depositional ages derived from OSL dating, presented in Chapter 4. Most notable is the correlation between the modelled sediment thicknesses recorded during the MIS 6 to MIS 5 aggradation phase and the sediment thicknesses recorded for terrace level 2. During this aggradation event, 10 m and 9 m of sediment accumulation were modelled for time series location 1 and 2, respectively. The terrace thicknesses and modelled terrace elevations (relative to appropriate uplift rates, Fig 6.11) associate well with field deposits recorded for terrace level two (Table 4) and support a terrace formation age of ~150 and 130 ka. This age was beyond the capability of OSL dating (Chapter 4); however, it relates well to the idealised patterns of climate driven terrace formation at both global and regional scale (e.g. Santisteban and Shulte, 2007; Bridgland and Westaway, 2008) and adds valuable chronological data with regard to the early stages of basin development.

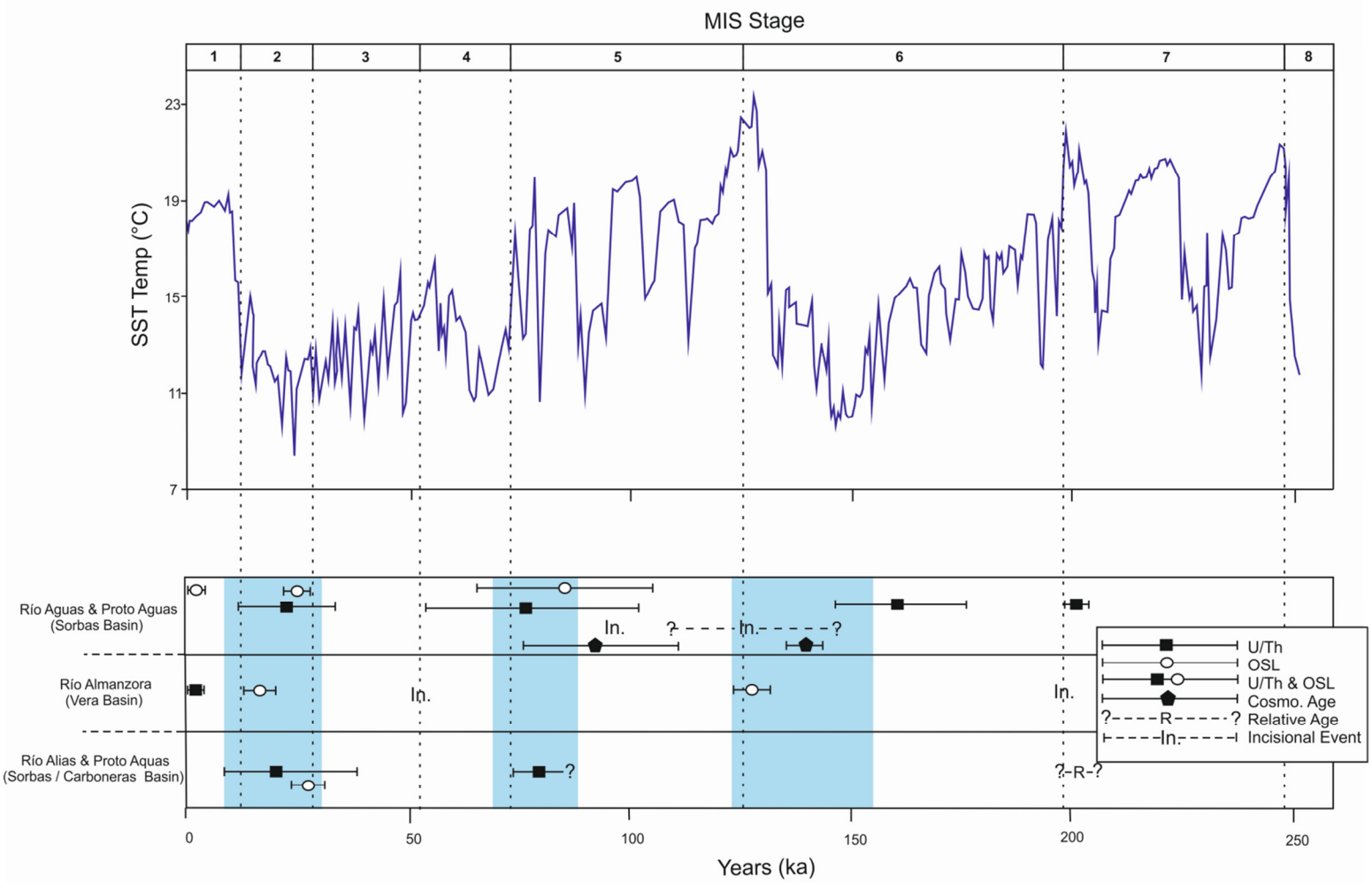

Figure 6.14 Cycles of terrace aggradation and incision for the Neogene sedimentary basins of SE Spain, from Geach et al., (submitted). The SST temperature record presented is from ODP Hole 161-977A (Martrat et al., 2012) with MIS stages from Lisiecki and Raymo (2005). Absolute and relative dates of depositional / incisional cycles sourced from Schulte (2002), Candy et al., (2004), Candy et al., (2005), Maher (2005), Schulte et al., (2008), Ilott (2013) for the Sorbas and Carboneras Basins and Schulte (2002) and Miekle (2008) for the Vera Basin.

OSL age estimates for terrace level 3 suggests that aggradation was ongoing from at least MIS 3 into MIS 2 (Chapter 4). The results from FLUVER2 support this interpretation with the onset of sedimentation modelled during the transition from MIS 5 to MIS 4 continuing into the LGM (Fig. 6.12). For the downstream time series, aggradation was modelled during the transition to MIS 4 (~70 ka) with the deposition of ~7 m of sediment (Fig. 6.12). A minor stage of incision was recorded between 54 - 50 ka followed by a substantial period of sedimentation (~14 - 16m) during the LGM. The modelled LGM aggradation phase exceeded the earlier phases of sedimentation and formed a fill terrace which entrained the older terrace of MIS 5 to MIS 4. The thickness of the fill terrace recorded in the downstream time series relates well with the fill sequences evidenced for terrace level 3 units (e.g. lower lake sequence of Harvey et al., 2003; Table 6.1). Sedimentation in the upstream time series occurred at similar timings with initial aggradations modelled during the transition in to MIS 4. However, sediment thicknesses were much lower represented by a thin veneer of deposits (2m) in the model output (Fig. 6.12). The most substantial aggradation event at the upstream time series occurred during the LGM with the aggradation of 6m of sediment. The combined model sediment thicknesses fit well within the range of the field records (5 - 10m) and are supported by the elevation data in the correlation of model outputs with terrace level 3 (Table 6.1).

No notable phases of sedimentation were modelled in either time series location after the LGM. Terrace level 4 units, dated as Late Holocene to Recent in age (Chapter 4), were not accounted for in the model. The lack of representation in sediment accumulation is further supported by inability of the model to replicate terrace level 4 units when applying a range of tectonic uplift rates (Fig. 6.11). The discrepancy between field and modelled records for terrace level 4 could be explained by complex nonlinear responses of the fluvial system through time (Coulthard and Van de Wiel, 2013). Although not directly evidenced in the Tabernas Basin, it is probable that anthropogenic activity in the catchments of the neighbouring Sorbas and Vera Basins altered the balance of sediment availability and

promoted periods of fluvial response in the Río Aguas throughout the Holocene (Schulte et al., 2008). Fire clearing of vegetation is also evidenced at Gádor to the west of the basin from *c*. 4200 cal. yr BP onward (Carrión et al., 2003). Changes in slope vegetation as a result of human activity likely altered sediment budgets throughout the Late Holocene and could be applicable in the development of the Tabernas Basin. In this study, anthropogenic signals are poorly represented in the model datasets based on the requirements of the timescales applied (e.g. averaging out Holocene fluctuations when converting SST to precipitation records over 250 ka). Intrinsic processes could also be of significance in forcing the Quaternary fluvial system through incisional thresholds. Alexander et al., (2008) propose that notable increases in incision occurred in the El Cautivo badlands in the Late Pleistocene when a major lithological threshold was crossed. Although not yet noted in the literature, the high-strength groundwater calcretes which dominate the basin would offer a further lithological control over the Quaternary fluvial system. This is well evidenced in the current styles of landscape degradation with the formation of calcreted units restricting basal incision and promoting laterally incision and localised mass wasting of the hillslope system (Fig. 6.15)

Another explanation for the poor representation of terrace level 4 units could relate to the nature of terrace formation. As presented in Chapter 3 and 5, terrace level 4 presents highly restricted terrace bodies formed along the flanks of the entrenched axial drainage. The formation of sedimentary bodies could relate to the favourable preservation of units within an actively incising and meandering fluvial system. If this is the case, terrace formation would not occur in the FLUVER2 model based on the 2 dimensional basis of the model (i.e. lateral variations in channel morphology are not accounted for). It is likely that the inability of FLUVER2 to represent nonlinear changes in fluvial system development and the restricted nature of the 2-dimsensional approaches promoted model error encountered in this study. Both aspects demonstrate major limitations when applying numerical modelling packages and highlight the requirement for: (i) improved accuracy and precision of input datasets and

(ii) increases in the ability of models to simulate variable fluvial system responses over a range of temporal scales.

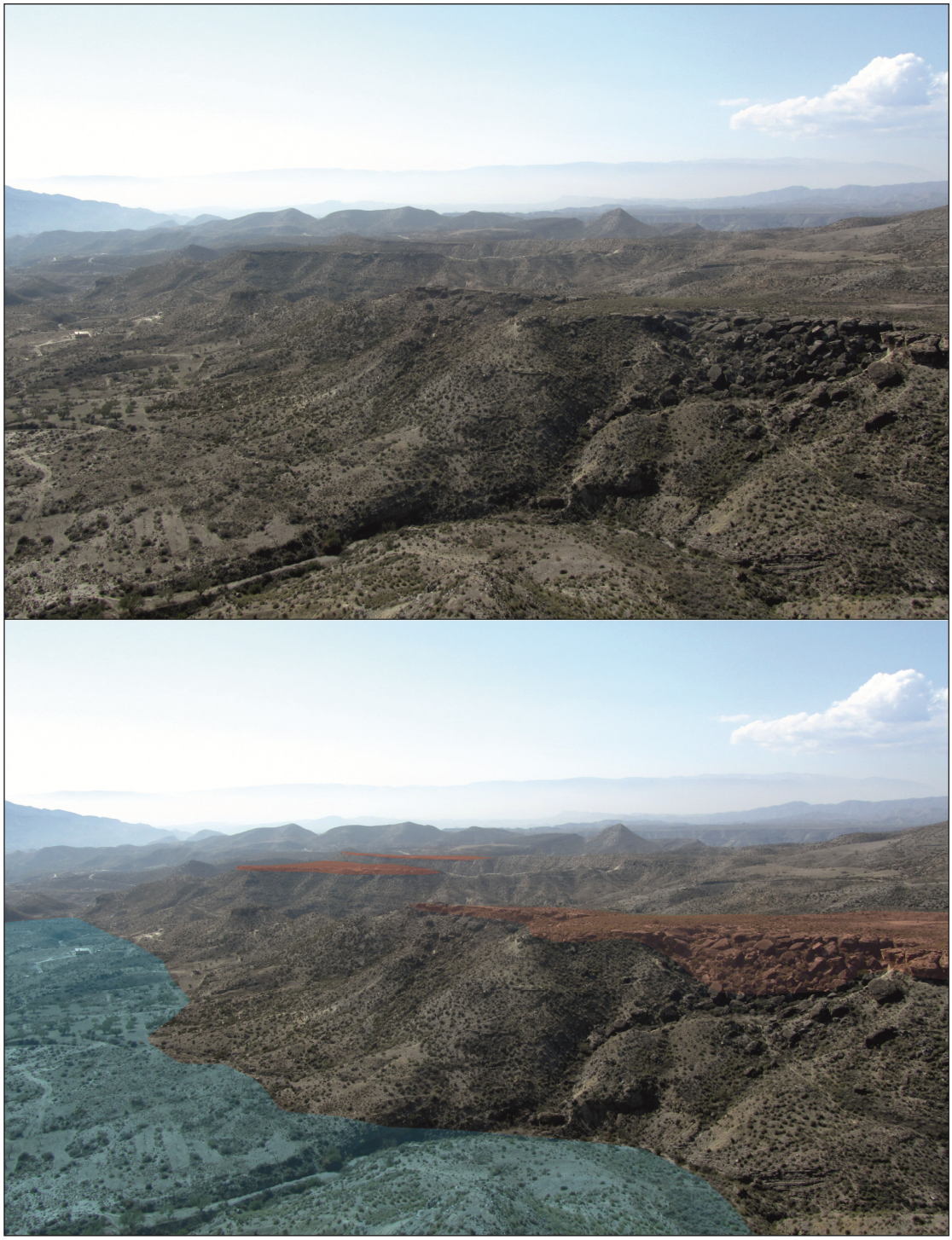

Figure 6.15 Mechanisms of hill failure typical of the central and eastern regions of the basin. Here extensive valley-floor calcretes (coloured blue) armour the current rambla bases and promote valley lateral widening. The upper groundwater calcretes (coloured red) cap upper slopes and fail as a result of gully headwall advance and undercutting.

6.5 Summary

The application of the FLUVER2 model has developed the understanding of multiple landscape forcing mechanisms upon patterns of landscape evolution in the Tabernas Basin. Calibrations between FLUVER2 outputs and empirical data points have demonstrated the importance of tectonic uplift which acts as the primary control on base-level changes throughout the Middle to Late Quaternary. The modelled data support regional uplift data and demonstrate the variable response of Quaternary landscapes to non-uniform rates of tectonic activity with the basin. FLUVER2 outputs correlate well with mapped terrace elevations, number of terraces, terrace thicknesses and available age control for the Middle to Late Pleistocene terrace records (terrace levels 2 and 3). However, the modelled outcomes correlated poorly with the Holocene record (terrace level 4).

Terrace levels 2 and 3 show affinities with modelled major aggradation events during the MIS 6 to MIS 5 transition and the LGM. The modelled correlations for terrace level 2 support regional assumptions of terrace aggradation during Pleistocene glacial phases and suggest a relative age of ~150 and 130 ka. In the model structure, climate forcing was translated to the fluvial system by increases in detached / transported sediment load and incision as a result of increases in discharge during cold climate stages. These results conform to regional trends of terrace formation during global glacial climate cycles (e.g. Candy et al., 2004; 2005; Maher, 2005; Miekle, 2008; Schulte et al., 2008; Fig. 6.14), and verify the hypothesis of terrace aggradations across the Mediterranean as a result of increasing hillslope sediment availability and increased moisture availability as principally driven by variations in precipitation throughout the Quaternary (Macklin et al., 2002; Santisteban and Schulte, 2007). Modelled sedimentation stages for terrace level 3 correlate well with minimal age values presented (MIS 3) and demonstrate that the substantial fill units characteristic of the basin centre likely represent multiple stages of sedimentation, including the lake sedimentation, starting in the transition from MIS 5 to MIS 4 and terminating in the

LGM. The sustained aggradation of terrace level 3 units throughout climatic cycles makes associations with mechanisms of formation complicated. For example, the onset of aggradation during the MIS 5 to MIS 4 climate transition fits well with conceptual global models of climate-driven terrace formation presented by Bridgland and Westaway (2008) (Fig. 6.16). In these models the majority of sediment deposition occurs during cooling transitions as a result of a relative decrease in temperature. However, sustained deposition during the LGM also associates well with regional patterns of deposition during cold climate phases, such as those evidenced in the generation of terrace level 2. The formation of the composite fill sequences of terrace level 3 under varying climate conditions also reflects the effects of localised tectonic uplift and the requirement for the formation of extensive accommodation space during the second phase of basin incision occurring post terrace level 2 (Chapter 5). This highlights the importance of internal basin dynamics in the formation of a variable terrace record.

The lack of modelled sedimentation associated with terrace level 4 units is likely a limitation in the model input data; however, the lack of sedimentation could be linked to: (i) the styles of terrace formation associated with the level (i.e. localised terrace units preserved within an incised meandering system); (ii) the importance of further intrinsic landscape properties (i.e. lithological controls); or (iii) the significance of human activity upon the landscape throughout the Late Holocene. FLUVER2 applies many simplifications in the recreation of a complex landscape system. The results of the model exercise conducted in this study develop correlations between empirical and modelled data generated from a combination of input variables (e.g. sediment travel distance and erosion factors). The combination of modelled variables worked well for the older terrace records but appear to lack the change in amplitude or frequency in sedimentation and erosion rates required to model the Holocene records. This demonstrates a fundamental limitation in many landscape evolution models (e.g. CAESAR and LAPSUS); notably that they do not accurately represent non- uniform rates of landscape processes through time (Tucker and Hancock, 2010).

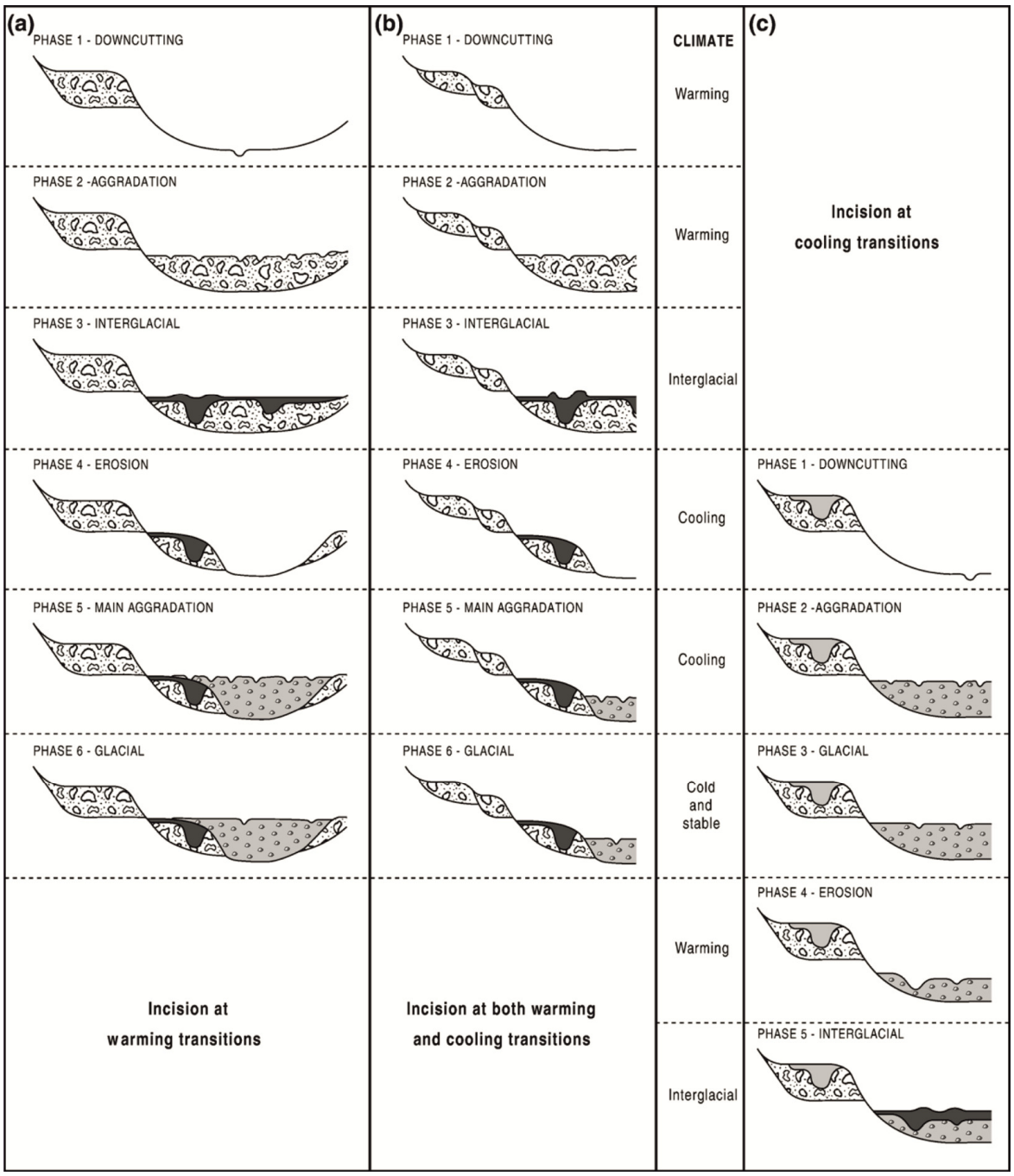

Figure 6.16 Model for terrace formation in response to climatic forcing from Bridgland and Westaway (2008). (A) Shows original model of terrace aggradation and incision with major incisional events occurring during warming climate transitions (from Bridgland, 2000). (B) Develops the original model and proposes that terrace incision can occur during both warming and cooling climate transitions (from Bridgland, 2001); However, major phases of aggradation are still related with cooling phases. (C) Demonstrates a new model of terrace incision during cooling events as evidenced in the Somme.

Chapter 7

7.1 Discussion

The following chapter presents a discussion of the principal aim of this thesis which was to ascertain the interplay and dominance of external forces (i.e. tectonic uplift and climate cycles) and/or internal landscape controls (e.g. lithological controls) upon the evolution of the Quaternary fluvial system within the Tabernas Basin. Initially, a summary of field investigations is presented alongside the results of luminescence dating, conceptual and numerical modelling with reference to Tabernas Basin alone. Where significant, unique elements of the landscape are discussed with reference their importance in the long-term evolution of the basin. The patterns of landscape development recorded in the Tabernas Basin are then compared with the understanding of long-term landscape evolution in the Almería region (e.g. the eastern Alpujarran Corridor, Sorbas and Vera Basins). The section closes by making associations with case studies from across the Iberian Peninsula and further international record where the mechanisms driving landscape evolution show inherent similarities to those recorded in the Tabernas Basin and greater Almería region.

7.2 Quaternary evolution of the Tabernas Basin

The results of the research presented in this thesis have developed the first formal Quaternary stratigraphy for the river/alluvial fan terraces and associated landforms of the entire Tabernas Basin (Chapter 3 for detail). Four terrace levels have been identified which record varying environments of deposition and highlight the transient evolution of the basin through three principal stages of landscape degradation. At a basin scale, the terrace levels typically occur at ~ 80 m (level 1: oldest), ~ 50 m (level 2), ~ 30 m - 10 m (level 3) and < 5 m (level 4: youngest) above the current drainage levels (Table 7.1).

Table 7.1 Sedimentology of the Tabernas Basin terrace record (revised from Geach et al., submitted).

Terrace Level	Sedimentary Style	Typical Sedimentary Log	Sedimentary processes and environment
1 **2**	Series of stacked, laterally persistent (10's m) interbedded conglomerates (Gm/Gp). Beds are of sheet form and thin (<1.5m), although minor channels do occur (<1m in depth). Fine to coarse grained sand lags (Sm/Sh) are common between conglomeratic units.	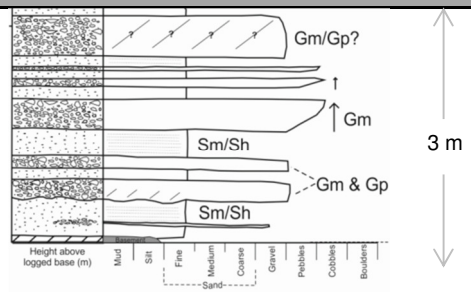	Sheet-form geometries representative of broad shallow unconfined flows formed on an aggradational alluvial fan surface. Sediments are sourced from the bounding Sierras.
3	**Basin margins:** Well defined stacked fluvial channels infilled with well imbricated conglomerates and minor sand plugs. Typical width of channels <5m and depths <2m. **Basin centres (see type log):** Series of laminated muds, silts and sands (Fl, Fsc, Sm and Sh). Typically horizontally bedded however extensive wavy bedding between facies indicates loading under semi-fluid/plastic states. Minor conglomeratic units are rare and typically occur at base of section (<0.5m thick)	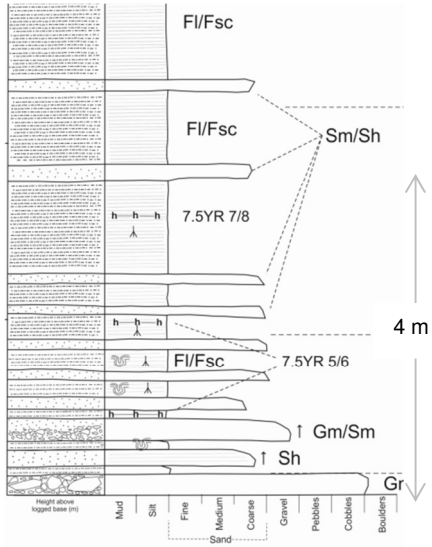	**Basin margins:** Braid plain formed on the surface of an aggradational fluvially dominated alluvial fan surface. **Basin centres: B**ack-ponding of fine grained sediments sourced from basin margins with the formation of standing bodies water in minor sinks and depressions across the basin centre. Development of palustrine / lacustrine type environments with rapid sedimentation rates.
4	Stacked channels infilled with conglomerates that are either weakly or poorly imbricated (Gm). Channel depths are shallow <0.8m and laterally in persistent (<3m wide). Overbanks (Sm/Sp) are common in laterally unconfined reaches	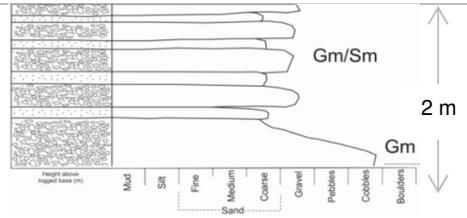	Braided fluvial conditions like that of the contemporary system. Flows are poorly confined in shallow channels that often breach during flood conditions.

The following sections present a discussion of the major phases of Quaternary basin development for the Tabernas Basin with focus on the likely mechanisms driving landscape evolution. Given the restricted observations from terrace level 1 (e.g. limited exposure and lack of any OSL or numerical modelled data) limited discussion is presented for the terrace level alone; however, the terrace level is grouped with terrace level 2 for the main discussions based on sedimentological affinities and similarities in the processes of terrace formation.

7.2.1 Basin degradation and aggradation stages: Terrace level 1 and 2

Terrace levels 1 and 2 are characterised by aggrading fill sequences (i.e. large thicknesses of sediments recording periods of terrace aggradation, using the terminology of Leopold et al., 1964) associated with deposition in a distally aggrading fluvially-dominated fan surfaces (Table 7.1, Fig. 7.1A). The morphology of fan sections suggests deposition as a continuous coalescent fan front, characterised by a radially dispersive drainage network. These alluvial fan units of terrace level 1 and 2 differ from the well-defined fluvial valley morphologies associated with terrace levels 3 and 4. The sedimentology of the level 1 and 2 fan sections lacks debris flows characteristic of later stages of Quaternary fan development (i.e. Marchante fans of Harvey et al., 2003) and indicates deposition in large fan systems with low surface gradients fed by relatively large catchments (Harvey, 2011). Fan sequences are typically tens of metres thick and were likely formed under conditions of high sediment availability and low flood discharge (Fig. 7.2A; Harvey, 2011). Clast imbrication indicates palaeoflow directions in an N – NW orientation for the southern margin; and an S–SW orientation for the northern margin, highlighting the dominance of sediment delivery from the bounding mountain ranges (Harvey et al., 2003).

A notable characteristic of level 1 and 2 alluvial fans is the pattern of sedimentation noted in both type sections. Early stages of sedimentation are dominated by unconfined sheetwash deposits which become progressively more confined through time, forming small interconnected fluvial channels characteristic of a dispersive fluvial network (Chapter 3). The

deposition of fine grained units followed by successively coarser grained materials is unusual based on the typical patterns of sedimentation, whereby coarse grained materials typically mantle the active bedrock interface prior to the deposition of fine grained materials (e.g. Jones, 2002). The inverted pattern of sedimentation recorded in level 1 and 2 sections could represent: (i) a transition between fan regions (i.e. medial to distal fan) or depositional lobes (e.g. Nichols and Hirst; 1998); (ii) backfilling of the fan (e.g. Harvey et al., 2003) or (iii) a variable response in the availability of coarse grained sediments throughout the development of the alluvial fan system (e.g. Harvey, 2011).

Given the sedimentology and relative morphology of the level 1 and 2 fan units it is unlikely that the variation in sedimentary style is related to a transition in fan regions. This is commonly recorded by the interdigitation of distinct sedimentary deposits (i.e. debris flows and stacked channel deposits; see dashed box on Fig. 7.2B) which record a change in geomorphic slope, such as the transition from the relatively steep fan surface into a horizontal alluvial plain (Fig. 7.2B) (Nichols and Hirst; 1998). However, the sedimentology of the level 1 and 2 alluvial fans appears to record a progressive shift in sedimentological styles from unconfined flow events, dominated by fine grained deposits, to confined flow events dominated by coarse grained facies. Furthermore, the morphology of sections (i.e. nature and dip of beds) does not record a notable change in fan gradient. The use of type sections for terrace level 1 and 2 units limits interpretations based on the switching of fan lobes in the development of fan sequences. A switch in the depositional front of the fan could result in the sedimentary architecture recorded, with coarse grained units deposited along the main areas of sedimentation (i.e. fan apex) and fine grained units deposited in marginal regions of the active lobe. If lobe switching is recorded in level 1 and 2 sections, the lateral extent of sedimentary units (>300m) would suggest large fan areas.

Backfilling of alluvial fans is well recorded in the development of the modern Tabernas Basin and could be associated with the sedimentary sequences noted in level 1 and 2 sections. Fans in the east of the modern basin record ongoing aggradation from the Mid-

Late Pleistocene onwards, with aggradation events driven by increases in sediment availability relative to low flood discharges during cold climate phases (Harvey et al., 1995; Harvey et al.,2003). Backfilling of the terrace level 1 and 2 alluvial fans would account for the transition in sedimentological styles and would be further supported by the lateral extent and morphology of the associated terrace remnants (Chapter 3). Terrace level 2 units show that fan surfaces would have formed coalescent fronts which aggraded well into the basin centre (Fig. 7.1A). The morphology of the level 1 and 2 fans would be similar to those preserved in the current eastern limits of the basin and would have recorded limited dissection and the dominance of aggradation in the distal zones of the fan (e.g. Harvey, 2002). The coalescent fans would have acted as a dominant buffer zone between the mountain catchments and the major basin drainages and would suggest poor coupling of the slope-channel fluvial system during the early stages of basin formation (Harvey, 2002; Fryirs et al., 2007). The level 1 and 2 fan sequences of the Tabernas Basin are characteristic of the early Quaternary depositional units found in the neighbouring Sorbas and Vera Basins (Mather et al., 2000; Stokes, 2008). Early Quaternary basin infills in both basins are dominated by extensive fluvially dominated alluvial fan environments which relate to a period of tectonic quiescence or an important threshold whereby limited incision is recorded (Mather et al., 2000).

Variability in the size and amount of sediment available in the evolution of alluvial fan systems is also well demonstrated in the Tabernas Basin. For example, in the younger Marchante fan sequences Harvey (1990) highlights the dominance of debris flow processes in the early stages of fan development, which become dominated by sheet-form and channel flow processes through time. The shift in flow processes is related to the availability of sediment during climate cycles coupled with on-going patterns of tectonic uplift which generates sediments in the bounding Sierras (Harvey, 2007; 2011). However, for terrace level 1 and 2 it would appear that coarse grained materials were either: (i) not abundant in the fan catchments in the early stages of fan development; (ii) that the flow conditions experienced were not sufficient enough to mobilise coarse materials from the catchments;

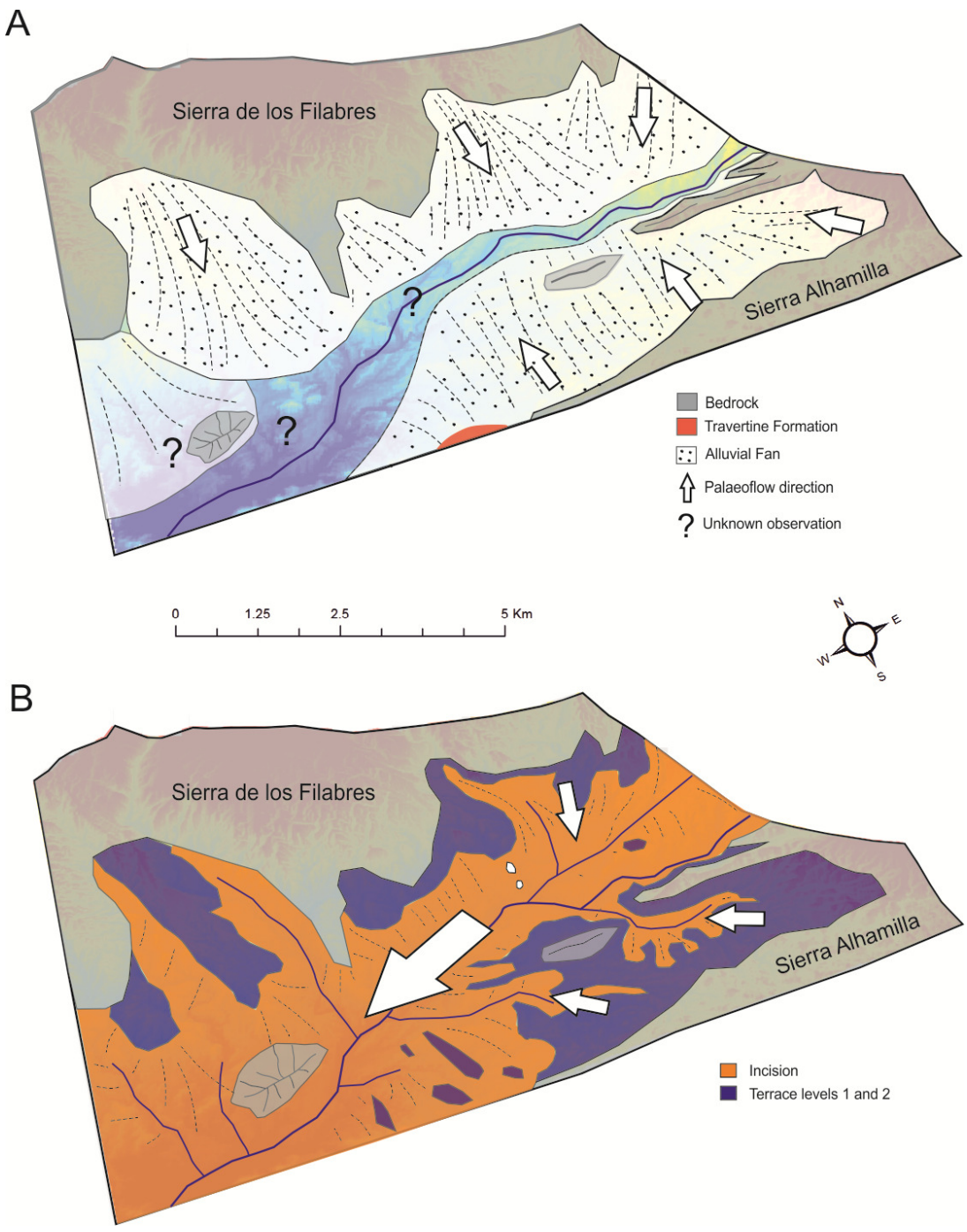

Figure 7.1 Conceptual landscape model for early stages of basin evoltuion. (A) Shows formation of coalscent alluvial fans typically of terrace levels 1 and 2. (B) Major stage of landscape degradation which occurred post terrace level 2 aggradation.

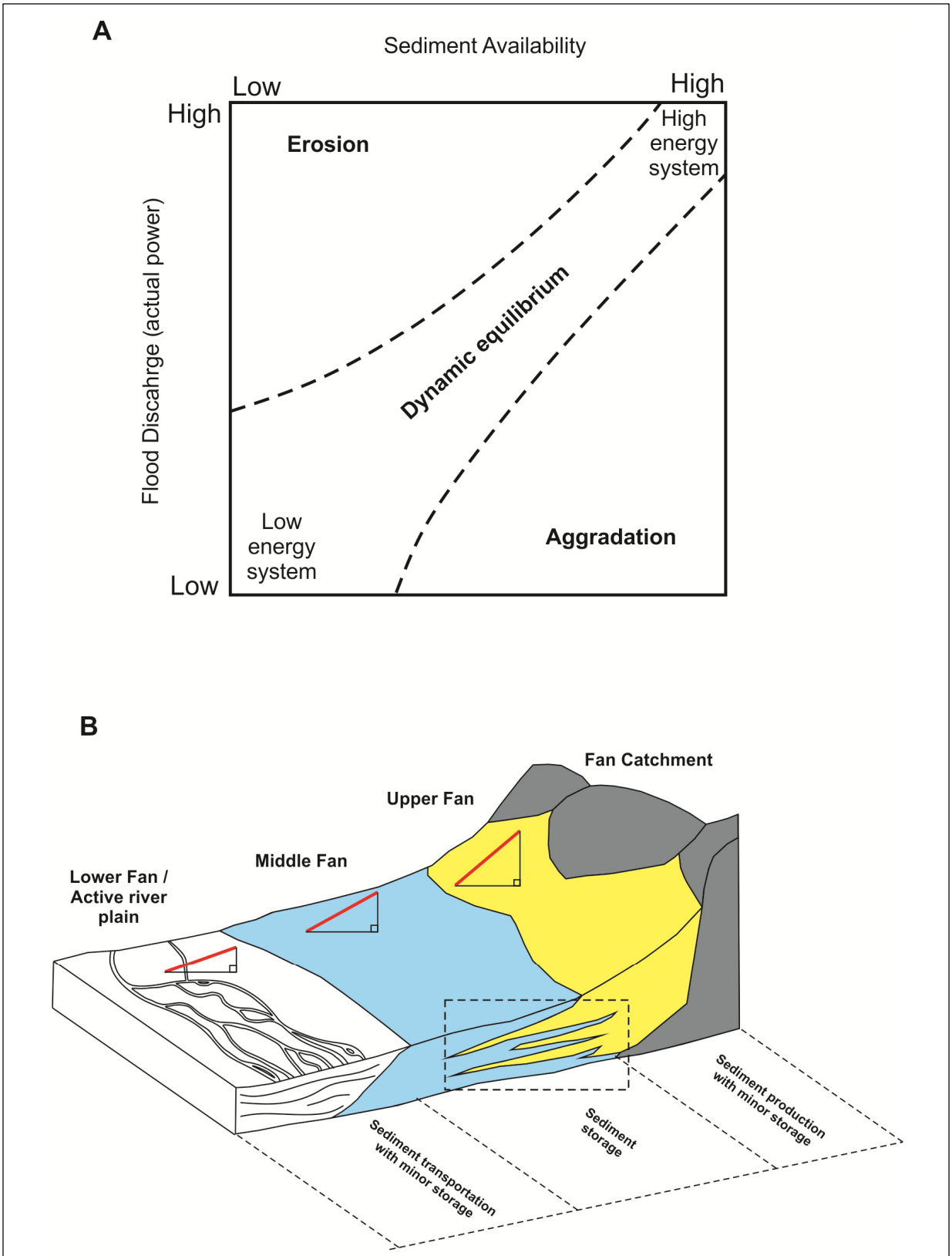

Figure 7.2 (A) Theoretical relationships between critical power and sediment availability in the promotion of erosion or deposition in the alluvial fan environment, from Harvey (2011). (B) Conceptual model of the alluvial fan zones (different coloured regions) showing the interdigited styles of sedimentary units and the decrease in fan surface gradients.

or (iii) that wet/drying cycles of the cohesive basin infills (i.e. Tortonian Marls) formed a pseudo-armour layer in the active zone and coarse grained materials were not required to initiate sedimentation (e.g. mineral soil crust formation of Cantón et al., 2001). These factors would highlight a variable response of the Early Quaternary landscape in response to: (i) non-uniform uplift in the mountain catchments, (ii) relative decreases in the intensity of flow events as associated with regional climatic patterns, and/or (iii) internal slope processes/characteristics which are an important part of the geomorphic configuration of the basin.

A notable feature of terrace level 1 and 2 is the high degree of calcrete formation which acts as a principal factor in the preservation of Quaternary terraces bodies. Although likely limited by exposure extent in terrace level 1, calcretes form extensively across the basin within terrace level 2 deposits. The development of both groundwater and pedogenic calcretes highlights the variability of groundwater levels throughout the early development of the basin in relation to variable climatic signals (e.g. formation of pedogenic calcretes in periods of sustained aridity; Nash and Smith, 2003). However, periods of climate dominance are overprinted on a pattern of sustained base-level lowering driven by tectonic uplift which led to the separation of calcrete bodies (Nash and Smith, 1998; 2003). The preservation of thick travertine units along fault lines in the Northern Alhamilla Fault Zone (Mather and Stokes, 1999) attests to the importance of tectonic activity in the early development of the basin, and could further relate to: (i) relative increases in groundwater availability driven by the climatic cycles (i.e. increase in available moisture during warmer climate periods; Santisteban and Schulte, 2007) or (ii) the enhanced routing of groundwater flows along tectonic features during periods of enhanced tectonic activity (e.g. Stokes et al., 2007). The travertine caps which on-lap isolated terrace level 2 outcrops would indicate that travertine formation occurred post terrace level 2 deposition, likely highlighting a strong climatic control with formation during the transition to basin incision in warm climate phases (based on cold climate sedimentation events).

Unfortunately, no absolute dates are provided for either terrace levels 1 or 2 alluvial fan units and little is known about the period of degradation that led to the formation of separate terrace levels (degradation stage 1, Chapter 5). However, it is proposed that a sustained period of base-level lowering was required to obtain the ~30m separation preserved between the alluvial fan terraces in the east of the basin. The results of numerical modelling suggest that terrace level 2 aggradations likely occurred during the transition from MIS 6 to MIS 5 (Chapter 6). This pattern of climatically driven aggradation under cold climate conditions fits well with the conceptual models of Bridgland and Westaway (2008) and further regional models of terrace formation (e.g. Miekle, 2008; Santisteban and Schulte, 2007; Stokes, 2008) presented in detail in Section 7.3. Accepting these models of climatic forcing, it is likely that terrace level 1 aggradations occurred during MIS 8 to MIS 7, with subsequent incision during MIS 7/ MIS 6. These relative dates associated well with the older terrace levels in the Sorbas Basin (Level A deposits = MIS 8, Level B deposits = MIS 6; Ilott, 2013), yet correlations with the Vera Basins are poor (Zajara allomember = MIS 12, Miekle, 2008) (Fig. 7.3). The reconstruction of terrace level 2 lower in Tabernas is omitted from regional correlations based on its limited exposure. Adopting simple stratigraphic correlations, the unit could relate to terrace level C in the Sorbas Basin, yet these correlations are weak based on a lack of temporal data. Plio/Pleistocene final stage basin fills (e.g. Gochar and Salmerón formation) dated at 1 Ma by cosmogenic exposure dating in the Sorbas Basin (Ilott, 2013) and 1.6 Ma by Electron Spin Resonance techniques in the Vera Basin (Wenzens,1992) are not preserved within the main part of the Tabernas Basin (Fig. 7.3). The accuracy of dates generated for the final stage basin fills are questionable based on recent developments in the dating methodologies applied.

7.2.2 Basin degradation and aggradation stage: Terrace level 3

Upon deposition and abandonment of terrace level 2 units a substantial incision phase dominated the Tabernas Basin. This incisional stage promoted the large scale decoupling of the fluvial systems from the adjacent hillslopes (degradation stage 2, Chapter 5) and could be analogous with earlier stages of prolonged incision which stripped the majority of Miocene deposits from the basin in the Early to Middle Pliocene (Harvey, 2002). Across the basin, the alluvial fan units of terrace levels 1 and 2 were dissected by headward migrating fluvial systems (Fig.7.1B) which completely gutted the Tabernas Basin and promoted the capture of small fluvial systems from the far western catchment of the Sorbas Basin (*sensu* Harvey, 2002).

Although hard to confirm based on limited absolute dates, the results of numerical modelling suggest that the degradation phase was sustained for the duration of MIS 5 (~70 ka). This prolonged period of incision by far exceeds the prior phase of modelled aggradation for terrace level 2 which lasted ~20 ka (MIS 6 to MIS 5 transition). A pattern of sustained degradation relative to aggradation is noted in all stages of basin development in numerical outputs and differs from conceptual models of terrace formation as a result of climate forcing, where incisional events are believed to be short lived relative to aggradation events (Fig. 7.4) (Bridland and Westaway, 2008). The only other basin to record a highly degradational record in the Almería region is the neighbouring Eastern Alpujarran Corridor (EAC), where enhanced tectonic activity coupled with the localised capture of inter fan drainages has promoted sustained incision from MIS 8 onward (García et al., 2003).

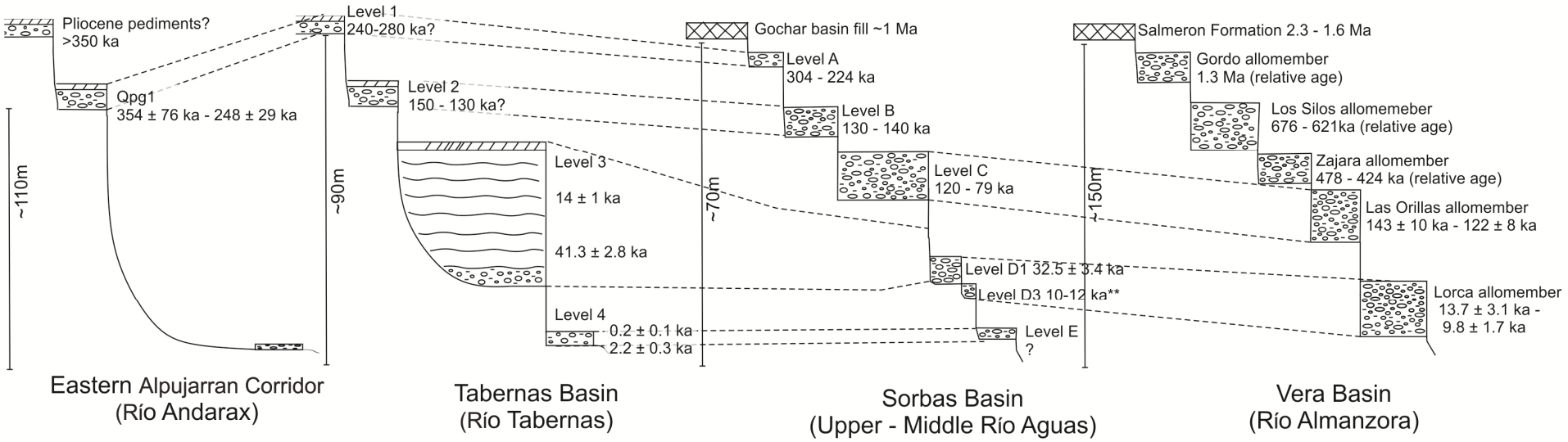

Figure 7.3 Correlation of dated terrace sequences across the Almería region. Note correlations are based on the limited a chronology obtained from a number of dating techniques as detailed in Chapter 4.

Terrace level 3 deposits record a notable shift in sedimentological style across the Tabernas Basin with the onset of confined fluvial conditions along the basin margins as recorded by strath terraces with well-defined valley margins (Fig. 7.5). Channel structures indicate shallow flow depths in a braided fluvial system (<1 - 2m; Table 7.1) with clast imbrication toward the confluence with the present day Río Andarax. The extent of fluvial deposits highlights an increase in headward expansion of fluvial systems across the western and central regions of the basin (Fig. 7.5). In the east of the basin, terrace level 3 is characterised by extensive alluvial fan deposits which relate to the Filabres Fans and Marchante Fans of Harvey et al., (2003). In these sequences multiple stages of fan sedimentation are recorded which date from the Mid-Late Pleistocene onward (Harvey et al., 2003). Sedimentation stages were promoted by variations in hillslope sediment supply as controlled by Quaternary climate cycles with little effect from tectonically (local) induced base-level change (Harvey, et al., 1999; 2003). Much like the fan sequences of terrace levels 1 and 2; the alluvial fans of terrace level 3 were dominated by fluvial processes and were distally aggrading recording little to no incision. The fan bodies formed extensive coalescent alluvial bodies (still present in the east of the basin) which acted as a major store of sediments from the upstream catchments (Fig. 7.1B). The presence of both aggrading alluvial fans and headward incising fluvial systems highlights a progressive increase in basin-wide slope-channel connectivity, promoted by an interplay of climatic forces in the east of the basin and sustained patterns of tectonically driven base-level lowering in the west.

In the centre of the basin, fine-grained fill deposits of the upper and lower lake sequences are key components of the terrace level 3 units (Harvey et al., 2003) (Table 7.1). These fill deposits are considered to have formed as a result of tectonic deformation along a major SW-NE trending anticline in the far SW corner of the basin (Fig. 7.5). Deformation and surface uplift near the main drainage outlet resulted in the wide spread ponding / sediment backfilling and preservation of fine grained sediments in the major basin depo-centres (Harvey et al., 1999; Harvey et al., 2003). A mechanism of enhanced tectonic activity in the

west of the basin is supported by the outcomes of numerical modelling, which indicate that uplift rates needed to obtain the separation recorded between terrace bodies in the west of the basin were near double than those in the east of the basin (0.25 m ka^{-1} in the west and 0.13 m ka^{-1} in the east) and would fit a pattern of regional increases in uplift focused in the EAC, discussed in detail in Section 7.3.

Sedimentological analysis of the lower and upper lake sequences of Harvey et al., (2003) indicates a lower energy depositional setting than those of the basin margin fluvial systems with the preservation of distal muds, silts and sands sediments derived from the hillslope system. The results of OSL dating suggest that the fine-grained fill deposits were aggrading from at least MIS 3 into MIS 2 (minimum age of 41.3 ± 2.8 ka (Tab 8), Chapter 4). FLUVER2 outputs support an interpretation of climatically forced aggradation with the onset of sedimentation modelled during the transition from MIS 5 to MIS 4 continuing into the LGM (Fig. 7. 4). The phase of aggradation modelled during the LGM exceeded the earlier phases of sedimentation and formed the 20 m fill terrace evidenced in the field record which entrained the older terrace of MIS 5 to MIS 4 (Geach et al., submitted).

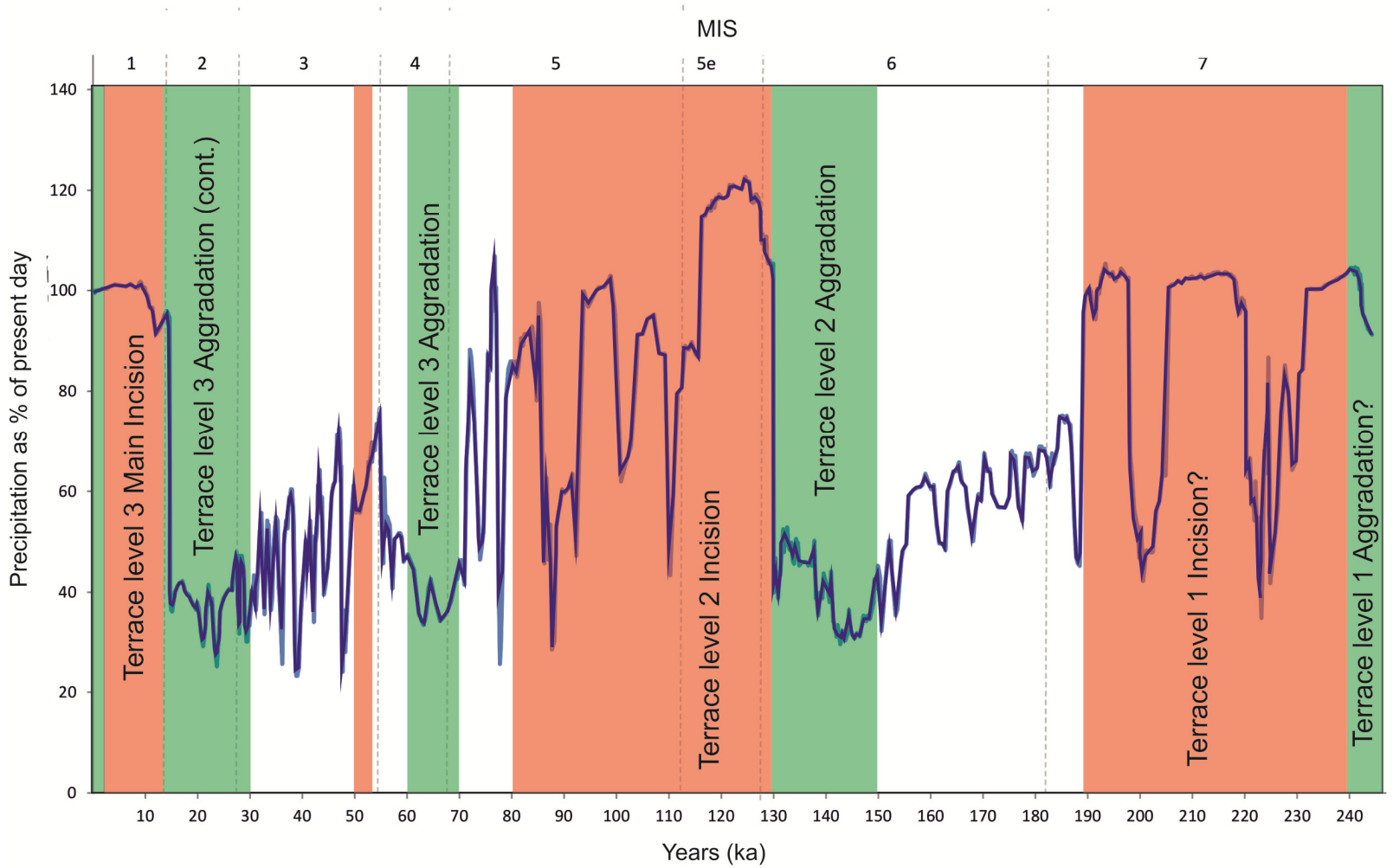

Figure 7.4 Terrace aggradation and incisional phases for the Tabernas Basin from FLUVER2 model outputs presented in Chapter 6. The blue line represents relative precipitation for the model duration of 250 ka as developed by Geach et al., (Submitted). Green regions represent preiods of aggradation, red regions indiciate periods of incision and white regions demonstrate periods of modelled stability and no net change in channel elevation.

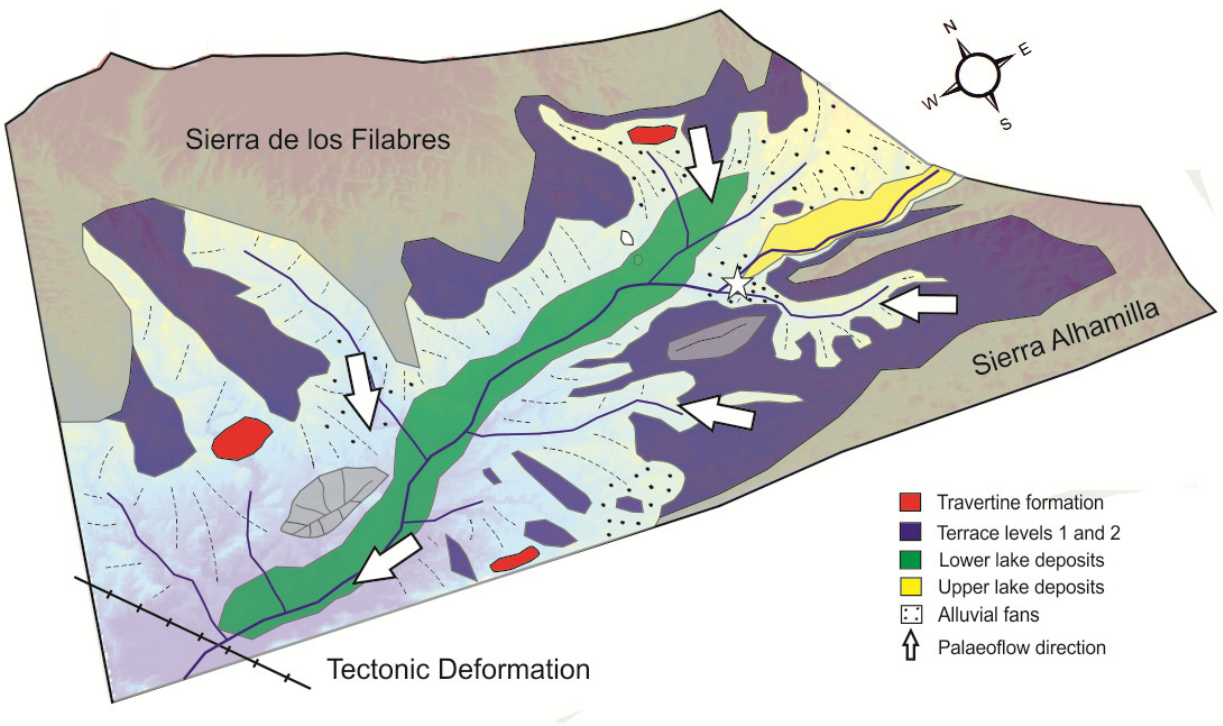

Figure 7.5 Conceptual model of landscape development for terrace level 3 deposits. Star indicates the location of upstream blockage of basin drainage and locus of upper lake formation.

OSL results for the basin margin fluvial systems supports deposition during the LGM with age estimates of 25.3 ± 4.8 ka (Tab-9) and 20.4 ± 1.8 ka (Tab-11) (Chapter 4), highlighting the coupling of the basin hillslope and fluvial systems in the later stages of terrace level development (*sensu* Alexander et al., 2008). However, the lack of coarse grained sediments recorded in the fine grained fill deposits (i.e. lower and upper lake) poses questions with regard to the connectivity of landscape elements which could relate to: (i) the significant sediment buffering effects of the extensive alluvial fan units formed in the east of the basin, and/or (ii) the internal configuration of the landscape and aspects of favourable preservation of fine grained materials in major depositional centres of the basin. Age estimates for the composite terrace level 3 recorded in the Tabernas Basin correlate well for the Level D units of the Sorbas Basin (MIS 3) and the Lorca Allomember of the Vera Basins (LGM) (Fig. 7.3) and likely support regional interpretations of climatically driven terrace formation, discussed further in Section 7.3.2.

Compared with terrace levels 1 and 2, calcrete formation is less extensive in terrace level 3 and is restricted to valley floor or thin (<1 m) groundwater morphologies which record groundwater tables higher than present. The lack of extensive pedogenic morphologies limits the application of soil calcrete development stages for the basin (e.g. Harvey et al., 1995). However, the differences in calcrete thickness and maturity could relate to: (i) variations in deposition environments (e.g. shift from laterally extensive alluvial fans to a more incised landscape); (ii) changes in moisture availability in accordance with fluctuations in the frequency or duration of periods of climatic change (Nash and Smith; 2003); and/or (iii) a relative decrease in the availability of free carbonates in the later stages of basin evolution. Variability in climate cycle duration and relative discharge during MIS 3 and MIS 4 is well represented in precipitation record developed for the FLUVER 2 model and could highlight the importance of non-uniform rates of moisture availability during short term climatic oscillations across the basin (e.g. D/O or Heinrich Events, Section 7.3 for detail). However, calcrete formation is recorded in the Sorbas and Vera Basins for the respective terrace levels. This would support a hypothesis of local variations in the carbonate availability in the Late Pleistocene development of Tabernas Basin with respect to the preceding phases of calcrete formation evidenced in the Terrace levels 1 and 2.

The effects of variable climate cycles upon secondary processes of calcrete formation could be further evidenced in the numerous travertines associated with the terrace level (*sensu*. Mather and Stokes, 1999) (Fig. 7.5). However, travertines associated with terrace level 3 form within the sedimentary units and would suggest formation during or shortly after terrace aggradations. This pattern of travertine formation differs from terrace level 2 units and supports deposition during cold climate phases or warming transitions. The routing of groundwater flows along tectonic pathways coupled with aspects of moisture availability as a result of short term climate cycles forms the basis of ongoing investigations in the Tabernas Basin by means of isotope analysis of travertine samples (Mather, *per comms*.).

7.2.3 Basin degradation and aggradation stage: Terrace level 4

The abandonment of terrace level 3 was marked by a period of degradation which led to focused incision within the major drainages of the western and central regions of the basin (degradation stage 3, Chapter 5). This degradational period was less extensive than the preceding incisional phase (degradation stage 2) and did not affect the alluvial fans of terrace level 3 in the east of basin, except by fanhead trenching ad renewed distal aggradation. The focus of incision was in the west of the basin, which supports patterns of tectonically driven uplift modelled for terrace level 3 aggradations, (Chapter 6) and highlights the contrast in landscape processes within the final stages of basin evolution (e.g. climatically controlled aggradational sequences in the east vs. patterns of tectonically induced base-level lowering and incision in the west). Enhanced base-level lowering in the west of the basin promoted the abandonment of multiple drainage pathways, which became preserved as km-scale abandoned meanders in the terrace record (e.g. Las Salinas) (Harvey, 2007), and initiated substantial badland formation (e.g. post stage C development in El Cautivo; Alexander et al., 2008) (Fig.7.6). The degradation phase was likely initiated in the Late Pleistocene as constrained by OSL age estimates (lake abandonment ages of ~14 ka) and further supported by the results of numerical modelling (Fig. 7.4). Onset of incision during the transition to the current interglacial period fits well with conceptual and regional models of climatically driven terrace formation (e.g. Bridgland and Westaway, 2008; Santisteban and Schulte, 2007).

Terrace level 4 deposits occur as localised terrace aggradations preserved in the outside of valley meander loops or at the confluence of major basin drainages (Fig. 7.6). The terrace level forms at or near the current river level (<5 m) and is associated with braided conditions much like that of the current fluvial system (Table 7.1). At a basin scale, terrace thicknesses notably increase in a westerly direction (4 - 7 m) in association with increased levels of tectonically driven base-level lowering. As in many terrace studies, it is hard to discern if terrace level 4 forms a true stratigraphic unit, or if the sedimentary assemblages

simply form as part of the current fluvial system (i.e. favourably preserved overbank and channel margin deposits). For example, Level E of the Río Aguas system is not presented as a true terrace level by Ilott, (2013) as it is taken to represent the current level of the active drainage.

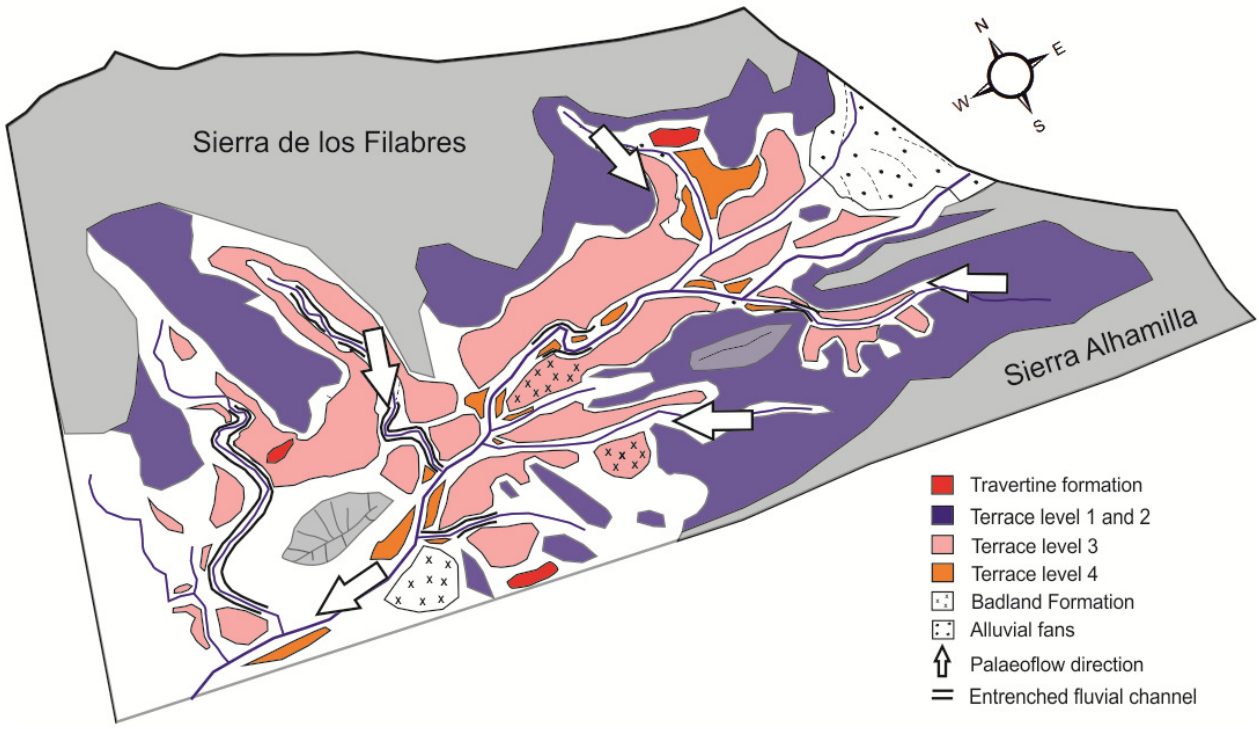

Figure 7.6 Landscape units associated with terrace level 4 and current basin development.

Given the restricted extent of deposits along the current axial drainage (Rambla Tabernas) it is proposed that terrace level 4 likely represents a grouping of terraces which form well within the active limits of the current basin drainage. However, the terrace remnants do provide evidence for an increase in focused vertical down-cutting in the majority of basin drainages in the west of the basin (entrenched drainages: Fig.7.6). OSL age estimates suggest that the formation of terrace level 4 occurred as a transient unit throughout the Late Holocene to recent (2.8 ± 0.3 ka to 0.2 ± 0.1 ka). This pattern of terrace formation does not form in accordance with previous stages of basin development (e.g.

aggradations during climate transitions) and is poorly represented in the results of numerical modelling (Section 6.4.3, Chapter 6). The discrepancy in formation processes could be related to: (i) the non-linear response of the fluvial system as it crossed an important internal threshold (e.g. lithological barrier or occurrence of a local capture event), and/or (ii) the effects of anthropogenic forcing which are well recorded in the region throughout the Mid-Late Holocene (Chapter 6 for detail). Calcrete formation in terrace level 4 units is non-existent suggesting that sustained periods of groundwater flow were likely short lived prior to terrace abandonment.

7.2.4 Basin degradation stage: Current basin development

The final stage of basin development relates to the period of ongoing basin degradation operating in the current fluvial system. Results from conceptual modelling presented in Chapter 5 highlight the continued focus of tectonically driven base-level lowering in the west of basin which is promoting the ongoing headward migration of basin drainages. The current limit of incision of the active fluvial system is focused near the town of Tabernas, marked by the presence of undissected alluvial fans in the east of basin on Figure 7.6. In these regions, the formation of knickpoints within larger knickzones demonstrates the ongoing retreat of the drainages into the major aggradational fan sequences dating from the Mid-Late Pleistocene (Fig. 7.7A). Aggradation events in active alluvial fans in the east of the basin are largely limited to the proximal regions of the fans systems and are notably limited in size and lateral extent when compared with their older Quaternary counterparts. This is likely a factor of limited sediment availability as promoted by the rehabilitation of vegetation in the upper catchments and use of fan surfaces for agricultural purposes (Bellin et al., 2011).

In the western and central regions of the basin, badland formation is sustained and most notable in areas where coupling between the hillslopes and main channels is complete (Calvo-Cases et al., 2014). This is particularly evident in areas of recent agricultural practice, where sub-surface pipes evolve into large gullies and badland slopes (Fig. 7.7B). The weathering of slopes is promoted by the geophysical/chemical properties of the underlying

Tortonian mudstones which are easily weathered by wetting and drying sequences (Cantón et al. 2001). However, due to the relative lack of intense rainfall events sediment runoff is notably low (Calvo-Cases et al., 2014). Calcrete formation is present with the formation of valley floor calcretes in the major basin drainages (Fig. 7.7C). The active formation of calcretes could relate to relatively stable or rising groundwater tables in the current fluvial system (Nash and Smith, 1998). However, the cementation of fluvial channels poses a considerable internal barrier to vertical incision and promotes lateral channel migration. The undercutting of calcrete capped hillslopes as a result of increased vertical increase promotes mass wasting of the hillslope system in the form of rock topples which create minor sediment contributions to the current fluvial system.

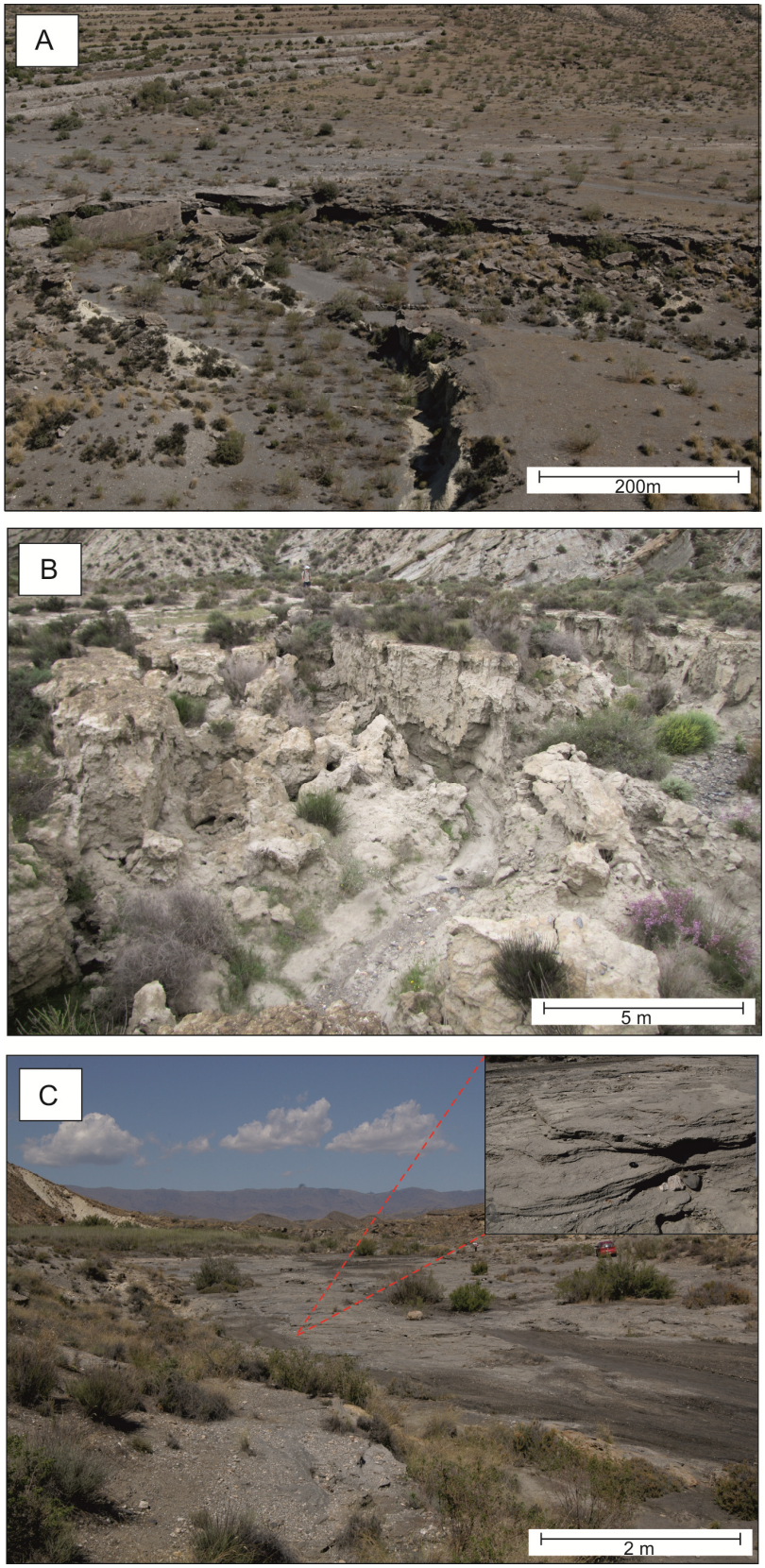

Figure 7.7 Variable landforms of the current Tabernas Basin. (A) Zone of knick-point retreat in the Rambla Benavides (UTM 30S 552788/4103042); (B) Extensive piping and onset of badland formation in an agricultural terrace in Rambla Seca (UTM 30S 546789/4094486); (C) Valley floor calcrete formation in the bed of the Rambla Benavides (UTM 30S 552790/4103002).

7.3 Regional correlations

The importance of external forcing mechanisms (e.g. tectonics and climate) and internal landscape controls (e.g. lithological thresholds) upon patterns of long-term landscape evolution is well demonstrated in the Tabernas Basin. The following sections aim to further address the importance of such forcing mechanisms across the Almería region. Comparisons are presented for basins where an understanding of the mechanisms of long-term landscape evolution has been investigated from Quaternary terraces and associated landforms (e.g. Sorbas Basin, Vera Basin and the EAC). The section is separated into discussions which focus on the importance of individual forcing mechanisms; however, where appropriate reference is made to the interaction of processes at a regional scale.

7.3.1 Tectonics

The four tiered terrace staircase of the Tabernas Basin correlates well with the four principal terrace levels recorded in the neighbouring Sorbas and Vera Basins (Mather and Harvey, 1995; Stokes and Mather, 2003; Maher, 2005; Miekle, 2008; Ilott, 2013). However, correlations with the EAC to the west are poor (García et al 2003; 2004). Based on the chronological data available for both the Tabernas Basin and the EAC, it is likely that the final three stages of aggradation recorded in the Tabernas Basin (terrace levels 2-4) are not represented in the highly erosional setting of the EAC (Fig. 7.3). The Plio-Quaternary deposits of the EAC (e.g. Qt / Qpg units of García et al, 2003) form one stratigraphic level deposited under cold climate conditions during MIS 8 (~245 ka) based on U/Th dates from travertines deposited within terrace units (García et al, 2003). The aggradation of hillslope sequences during MIS 8 relates to a regional increase in sediment supply during a period termed the Middle Pleistocene fluvial-aggradation maximum (Harvey, 1990; García, 2001; García et al., 2004). Upon cessation of terrace aggradation, ongoing base-level lowering has been sustained in the EAC in response to high tectonic uplift rates (0.3-0.7 m/ka^{-1}) focused along two principal fault lines that bound the northern and southern margins of the EAC

between the Sierra de Gadór and Sierra Nevada. Post Miocene uplift has accommodated between 40 and 75 km of right-lateral strike-slip separation and up to 2 km of vertical separation (Sanz de Galdeano, 1996). Rapid uplift has sustained a wave of tectonically driven incision throughout the Middle Pleistocene to Holocene, evidenced by the headward advance of fluvial systems and the decoupling of hillslope systems which are buffered by large scale alluvial fans forming off the bounding sierras (Garcia et al., 2004).

In comparison to the dominance of tectonics in the EAC, the fluvial archives of the Sorbas and Vera Basins record a more 'typical' response to cyclic changes in Quaternary climate overprinted on patterns of tectonically driven base-level lowering (e.g. Starkel, 2003). Notable periods of terrace formation occurred during cold climate phases when the availability of hillslope sediment outweighs the erosive capacity of fluvial systems as a function of decreased precipitation and relative increases in hillslope vegetation cover (Mather and Harvey, 1995; Stokes and Mather, 2003; Maher, 2005; Miekle, 2008; Ilott, 2013). Tectonic uplift has led to formation of incisional terrace sequences; however, variability in uplift rates both between and within the basins has promoted differences in the degree of separation between terrace units and the capture of major drainage pathways (Harvey, 1987; Mather and Harvey, 1995; Maher, 2007; Stokes, 2008; Ilott, 2013).

At a regional scale, Quaternary incision is believed to have initiated in the Sorbas Basin as a result of increased rates of uplift in relation to the neighbouring Vera Basin (Ilott, 2013 and references therein). This pattern of variable uplift promoted a major capture event (c. 69 ka; Candy et al., 2004) which had major repercussions upon the landscape system, with the formation of extensive landscape instabilities (i.e. landslides and badland formation) and variations sediment budgets/fluxes both between and within basins from the Mid-Pleistocene onward (Griffiths et al., 2002; Mather, 2002; Stokes et al., 2002). In the Sorbas Basin, four terrace levels of varying degrees of separation (Stages A-D of Mather and Harvey, 1995) represent the variable response of the Río Aguas fluvial system to non-uniform rates of tectonic uplift operating across the basin (Fig. 7.3) (Mather and Harvey, 1995; Mather, 2000;

Ilott, 2013). Uplift is thought to be focused in the southern and central regions of the basin as recorded by relative increases in fluvial incision and the rejuvenation fluvial systems along the northern flank of the Sierra Alhamilla (Mather, 1991; Mather and Westhead, 1993; Giaconia et al., 2012; Ilott, 2013). The effects of non-uniform temporal rates of uplift have also been noted upon fluvial system development throughout the Quaternary. Ilott (2013) proposes that variations in the spacing between terraces in the upper and middle Río Aguas are principally linked to varying rates of uplift. Adopting the approaches of Maddy and Bridgland (2000), the separation of terrace units of known absolute age was modelled for different uplift scenarios (Fig. 7.8). Results indicate that: (i) uplift was low during the early stages of basin development (i.e. the dissection of Pliocene Góchar basin fill surface prior to aggradation of Terrace A units), and (ii) that uplift increased during the later stages of basin development in accordance with the increase in spacing in the younger terraces (e.g. post Terrace B and C; Fig. 7.8) (Ilott, 2013). Signs of active tectonics are also well recorded in the Sorbas Basin with the offset of the main channel of the Río Aguas along a NNE-SSW lineament (the Infierno Marchalico Lineament; Mather & Westhead, 1993; Mather, 2000) and the faulting of Terrace C deposits in the north of the basin (Ilott,2013).

It is hard to discern if rates of tectonic uplift in the Tabernas Basin were as temporally variable as noted in the Sorbas Basin. For example, were the effects of tectonics present throughout the Quaternary or did the basin undergo periods of episodic tectonic pulses? This is a function of a number of factors, such as: (i) the limited terrace exposure and age control for Terrace Level 1, which restricts interpretations of the early stages of basin evolution; and (ii) the apparent dominance of spatial variations in uplift from the Mid-Pleistocene onward (e.g. focus of tectonically driven base-level change in the west of the basin).

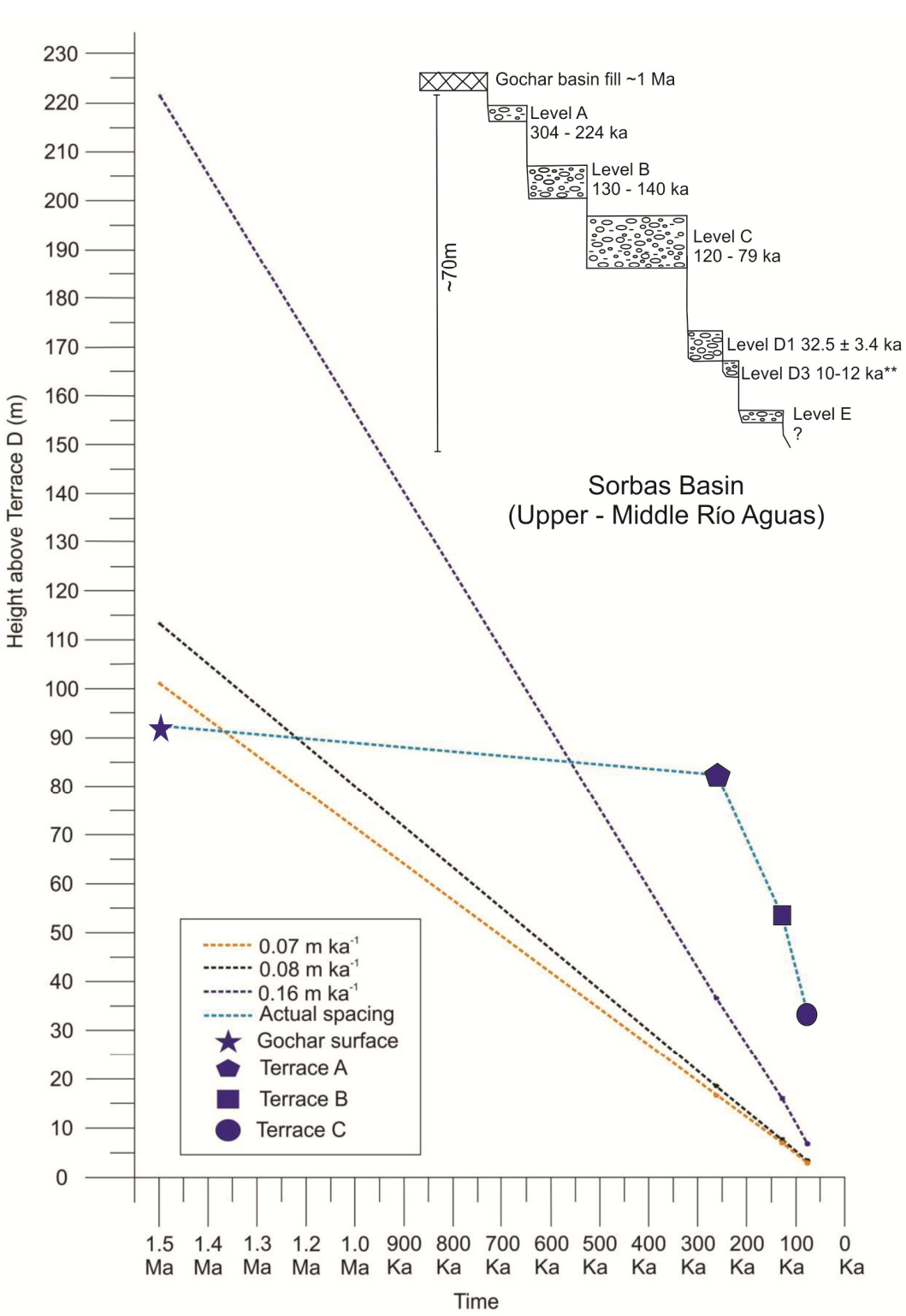

Figure 7.8 Comparison of modelled uplift rates against actual field record for the Upper-Middle Rio Aguas system in the Sorbas Basin, from Ilott (2013). Results demonstrate how relative uplift between the dissection of the Góchar top basin fill and Terrace A units was lower than subsequent stages of basin development. A notable increase in incision occurs between Terrace B and C units.

The development of the fluvial network in the Vera Basin is attributed to differential uplift in the early stages of formation coupled with the effects of Quaternary climate cycles and relative changes in sea level (Wenzens and Wenzens, 1997; Miekle, 2008; Stokes, 2008). The Vera Basin Quaternary record is similar in part to that of the Sorbas Basin, with the dissection of a Plio-Pleistocene final basin fill surface (the Salmerón Formation) and the development of a four tiered fluvial terrace staircase (Stokes, 1997). In the early stages of terrestrial development, the Vera Basin was internally draining; however, low rates of uplift across the basin (0.01 - 0.02 m ka^{-1}) relative to those of the neighbouring basins (Sorbas: 0.06 - 0.16 m ka^{-1}; Huercal–Overa: > 0.5 m ka^{-1}) increased regional gradients and promoted the capture of multiple drainages under conditions of sustained headward incision initiating a switch to an externally draining system (Stokes, 2008).

The switch to basin incision and subsequent aggradation of incisional terrace units forms in accordance with conceptual models of Bridgland and Westaway (2008), with climatic signals overprinted on a record of tectonically driven base-level lowering. Basin wide incision occurred during warming transitions and sediment deposition during cold stages and cooling transitions (Miekle, 2008). A uniform uplift rate of 0.072 m ka^{-1} has been calculated from dated terrace sequences across the basin; however, little mention of non-uniformity in uplift rates is presented based on the separation of terrace units alone (Miekle, 2008). Active tectonics is well evidenced in the form of extensional faulting concentrated within the final basin fill sediments (Salmerón Formation) and Pleistocene Level 1 landforms (Stokes and Mather, 2000; Stokes, 2008). The early stages of active tectonism have been highlighted to coincide with the onset of fluvial incision in the basin (Stokes, 2008). The style and orientation of faulting suggests increases in north–south compression, as probably linked to increases in activity along the Palomares Fault (Booth-Rea et al., 2004; Stokes, 2008).

The proposed onset of regional incision in the Sorbas basin relative to its surrounding basins (cf. Ilott, 2013) is well supported with reference to the Vera Basin but is unrealistic in accordance with the findings from the Tabernas Basin and EAC. The rates of uplift calculated from Quaternary terraces across the region develop a pattern of sustained incision in the EAC which occurs in response to its proximity to a major deformation centre expressed by the Sierra Nevada (García, 2001; García et al., 2003). As in the EAC, the Tabernas Basin records notable periods of tectonically driven base-level change which promoted major waves of incision that stripped the basin throughout its evolution (degradation stages, Chapter 5). Modelled uplift rates for the Tabernas Basin and EAC are in excess of values generated for the Sorbas Basin (Tabernas= 0.13- 0.25 m ka^{-1}; Sorbas= 0.06 - 0.16 m ka^{-1}) and show substantial increases towards the west of the region. Uplift rates decrease towards the east across the Sorbas Basin into the Vera Basin (Fig 7.9) in accordance with the lack of major Quaternary dissectional events (i.e. the stripping of the entire basin). This focus of regional uplift shows a pattern of tectonic sag in the upper part of the Tabernas Basin and conforms well to Neogene uplift patterns as analysed from well dated Coral reefs and coastal conglomerates (Braga et al., 2003). From the Late Messinian onward, records of uplift were highest at the western margins of the Almería region focused around the Sierra Nevada, decreasing to the east of this major relief. The results from this study support the underlying importance of tectonic uplift upon patterns of landscape development in the Almería region.

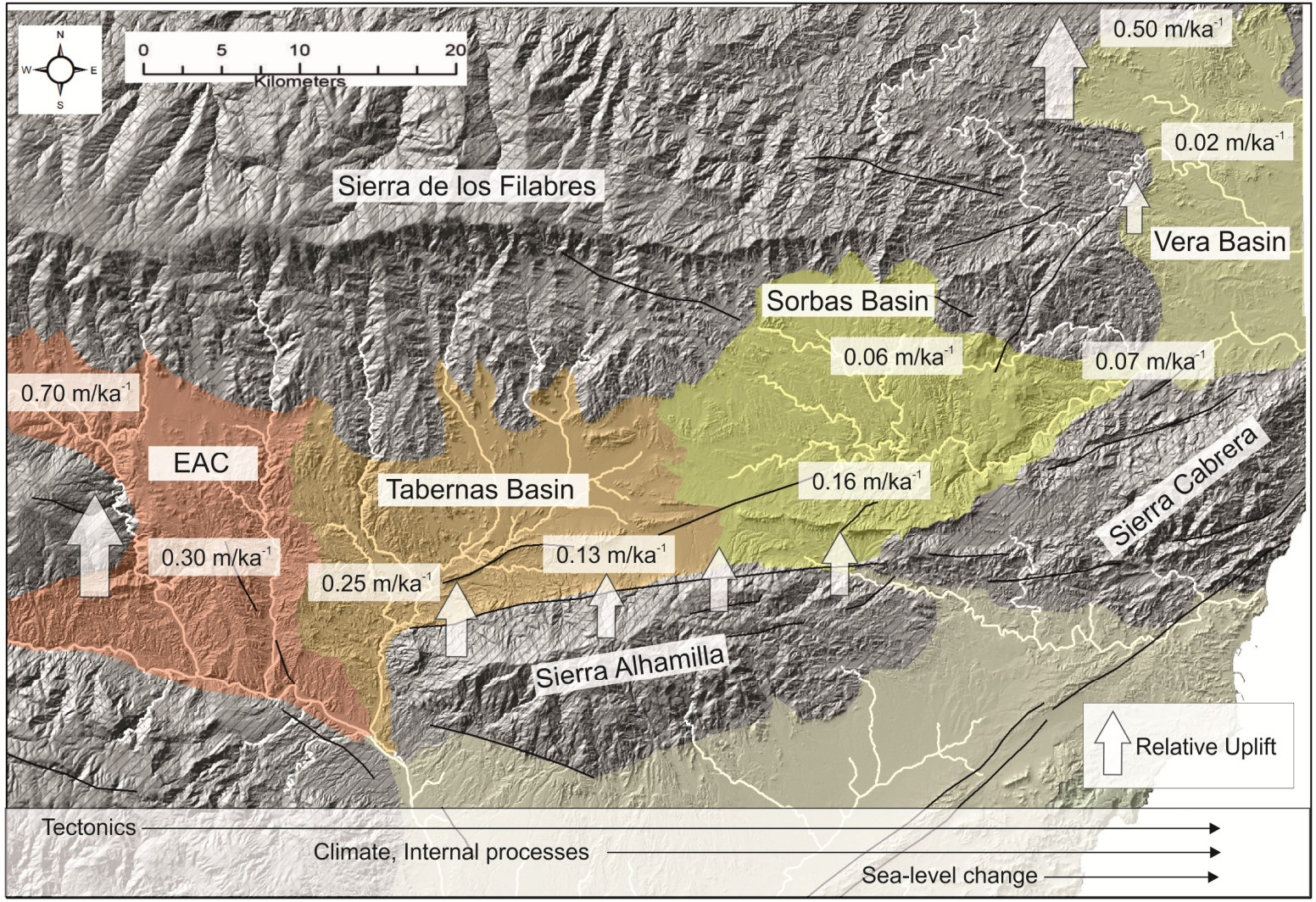

Figure 7.9 Patterns of uplift and major controls of landscape evolution within the Almería region. Uplift rates from García et al., (2003) for the EAC, Mather, (1991); Mather and Harvey, (1995); Mather et al., (2002) for the Sorbas Basin; Stokes, (1997), Miekle, (2008) for the Vera Basin. Arrows represent relative uplft rates at given locations across the region. The variation in uplift shows tectonic sag in the upper part of the Tabernas Basin.

7.3.2 Climate

The importance of Quaternary climate cycles upon fluvial system development has been developed throughout this thesis with reference to the conceptual models of Bridgland and Westaway (2008). Examples of river terrace development from across the globe suggest terrace formation occurs in accordance with fluctuations in precipitation and vegetation cover as driven by 100 ka climatic cycles (Bridgland and Westaway, 2008 and references therein). At a regional scale, the response of fluvial systems in all of the Almería basins (Tabernas, Sorbas and Vera Basins) appear to show good correlation in terms of aggradations during cold climate periods (e.g. Maher, 2005; Schulte et al., 2008; Miekle, 2008; Ilott, 2013), which are often sustained well into the transitional warming phases (e.g. LGM aggradations in the Sorbas Basin [e.g. Schulte et al., 2008] and the Tabernas Basin, as presented in this research). Sediment availability increased during cold climate phases in response to relative decreases in vegetation cover characterised by high-amplitude shifts between drought-tolerant, semi-desert vegetation during cold episodes (stadials), and open Mediterranean forest with deciduous and evergreen *Quercus* during warm episodes (interstadials) (Geach et al., *submitted*).

Decreases in slope vegetation cover were promoted by relative decreases in regional precipitation which are further recorded by variations in $\delta^{13}C$ precipitates preserved in speleothems records in the north of the Almería region (e.g. Gitana Cave, Fig. 7.10; Hodge et al., 2008). Relative increases in $\delta^{13}C$ are taken to represent changes in soil microbial activity and vegetation respiration as controlled by decreasing moisture availability during the growing season (Hodge *et al*., 2008). The most notable stages of decreased effective precipitation are recorded during MIS 6 with steady decreases further recorded in MIS 4 (Hodge *et al*., 2008). These phases of decreased precipitation correspond well with the precipitation record generated for the FLUVER2 model and associated with terrace level 2 and 3 aggradations in the Tabernas Basin during MIS 6-5 transition and MIS 4, respectively (Fig. 7.10).

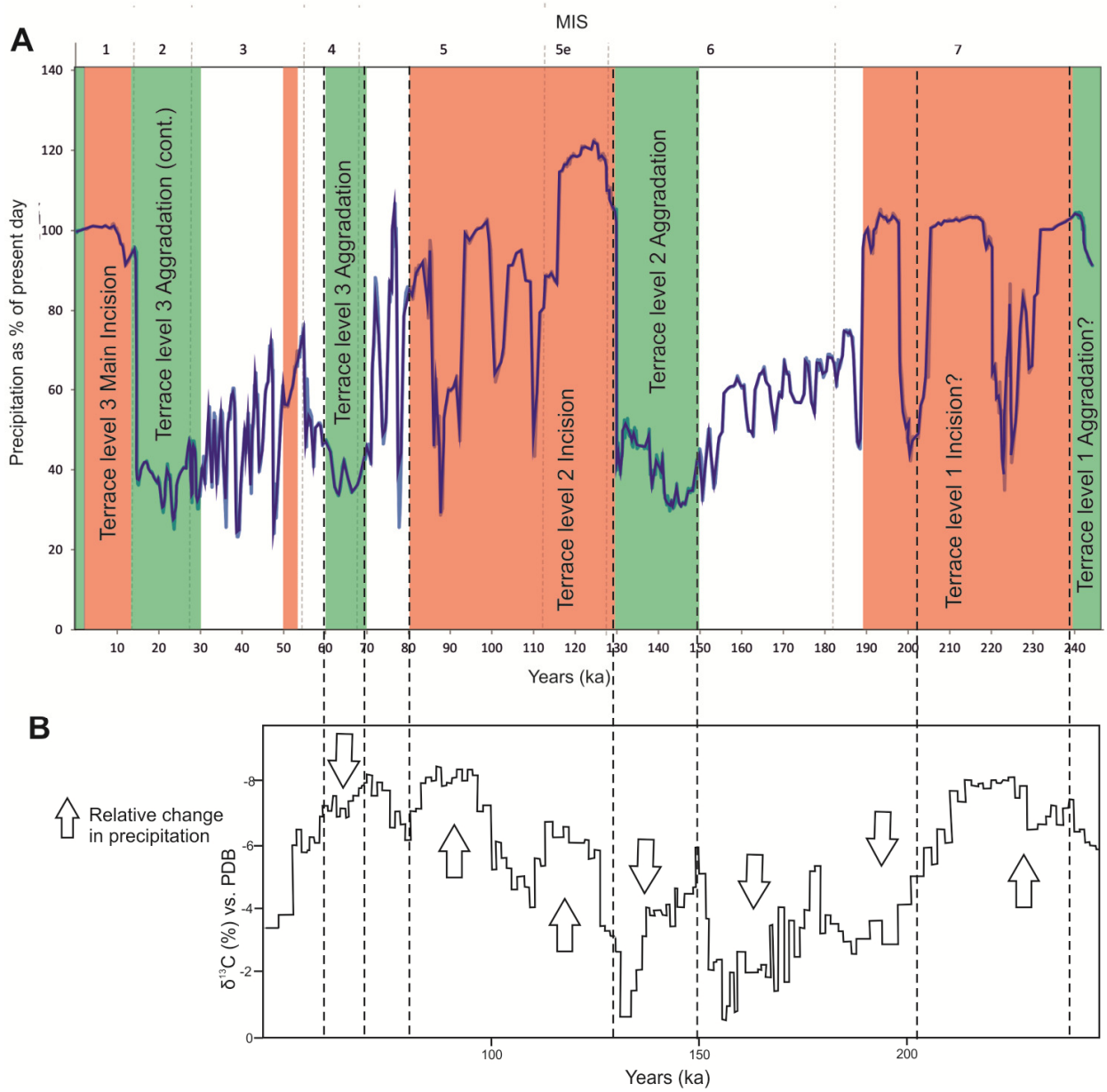

Figure 7.10 Correlation of precipitation record generated for FLUVER2 model in the Tabernas Basin (A) against relative precipitation records from speleothems (B), Gitana Cave (from Hodge et al., 2008). Periods of terrace aggradation and incision match relative changes in precipitation as recorded in the speleothem record.

In accordance with regional models of terrace formation (e.g. Santisteban and Schulte, 2007), phases of incision in all basins are likely to have occurred during warm climate periods as a result of relative decreases in sediment availability from the hillslope systems coupled with relative increases in precipitation (Macklin et al.,1995; 2002; Santisteban and Schulte, 2007; Bridgland and Westaway, 2008). Patterns of increased effective precipitation

are recorded in speleothem records during the transition from MIS 8 to MIS 7 and MIS 6 to MIS 5 (Hodge et al., 2008). These changes relate well to the precipitation record for the Tabernas Basin (Fig. 7.10) and further correspond to relative increases in flood discharges recorded in terrace record sedimentology of the Vera and Sorbas Basins (Stokes et al., 2012; Ilott, 2013).

Palaeoflood reconstructions conducted in the Vera and Sorbas Basins (e.g. Stokes et al., 2012; Ilott, 2013) are based on the application of a series of flood estimation techniques (e.g. Manning's and Darcy–Weisbach flow competency equations) in the quantification of flood discharge values from terrace records (e.g. Stokes et al, 2012 and references therein). The correlation of palaeoflood discharge values with the speleothem records show that rapid increases in effective precipitation, observed in $\delta^{13}C$ levels during the MOIS 6/5 transition, could relate to the larger palaeoflood estimates calculated for terrace Level 4 and Level C deposits of the Vera and Sorbas basins, respectively (Stokes et al., 2012; Ilott, 2013). However, correlations between the palaeoenvironmental datasets are limited by the accuracy of reconstructions based on the highly fragmentary nature of terrace development. (i.e. the inability to assess if the formation of terraces was as a result of one or multiple flow events, and the requirement for multiple regional datasets in order to generate meaningful time averaged peak flow or discharge data).

The impact of short duration climatic oscillations, such as Dansgaard-Oeschger (D/O) cycles and Heinrich events (HE), has been proposed upon fluvial system development across the Mediterranean region (Macklin and Lewin, 2008). D/O cycles are a series of abrupt temperature changes recorded as variations in the $\delta^{18}O$ signal in the Greenland ice-core (Dansgaard et al., 1993). The warming period associated with a D/O cycle is thought to be triggered by re-establishment of the North Atlantic thermohaline circulation (Maslin et al., 2001). Heinrich events represent ice-rafting episodes that are thought to have originated through the internally forced collapse of the Laurentide ice sheet in eastern Canada (Bond et al., 1999). In the Mediterranean region, cold D/O events (stadials) and Heinrich events are

evidenced in marine core records by periods of lower SST and higher aridity (Fig. 7.11). Increases in aridity were a function of more vigorous north-westerly winds over the northwestern Mediterranean coupled with an intensification of warm and dry Saharan winds (Moreno et al., 2004). In contrast, the D/O interstadials are characterised by warmer temperatures, higher continental humidity and increased primary productivity in the Alboran Sea as a consequence of a southward shift in the north-westerly winds (Fig. 7.11) (Moreno et al., 2004). Further to these Northern Atlantic forcing mechanisms, short duration climatic changes in the Iberian Peninsula could also be driven by salinity drops along the Mediterranean Iberian margin as driven by large discharges from Mediterranean rivers, enhanced by seasonal melting from glaciated mountains (Lewis et al., 2009; Benito et al., 2010).

Across the Almería region, little focus has been placed upon the significance of short duration climatic cycles upon patterns of fluvial development. Miekle (2008) proposed a lack of terrace aggradation in the Vera Basin during MIS 4 to MIS 2 due to reduced climatic fluctuations during these stages; however, interpretations of terrace formation are based on a weak chronology. Schulte (2002) also propose a stage of terrace aggradation in the downstream Río Aguas during MIS 2 that could be linked to Heinrich Event H1, yet the correlations are tentative and based on a single absolute age. The poor resolution of Quaternary landform chronologies across the region limits correlations with short duration climate changes at the current time. However, the results of numerical modelling conducted for the Tabernas Basin present the first continual relative record of fluvial system evolution for the Almería region (Chapter 6). The FLUVER2 results support the conceptual patterns of climatically driven aggradation and incision during climatic transitions (Santisteban and Schulte, 2007); however, they do not associate well with shorter duration climatic fluctuations (Fig. 7.12). Model phases of sediment aggradation and incision both exceed short duration climatic oscillations even though they are well represented in the precipitation record utilised in the FLUVER2 model (Fig. 7.12).

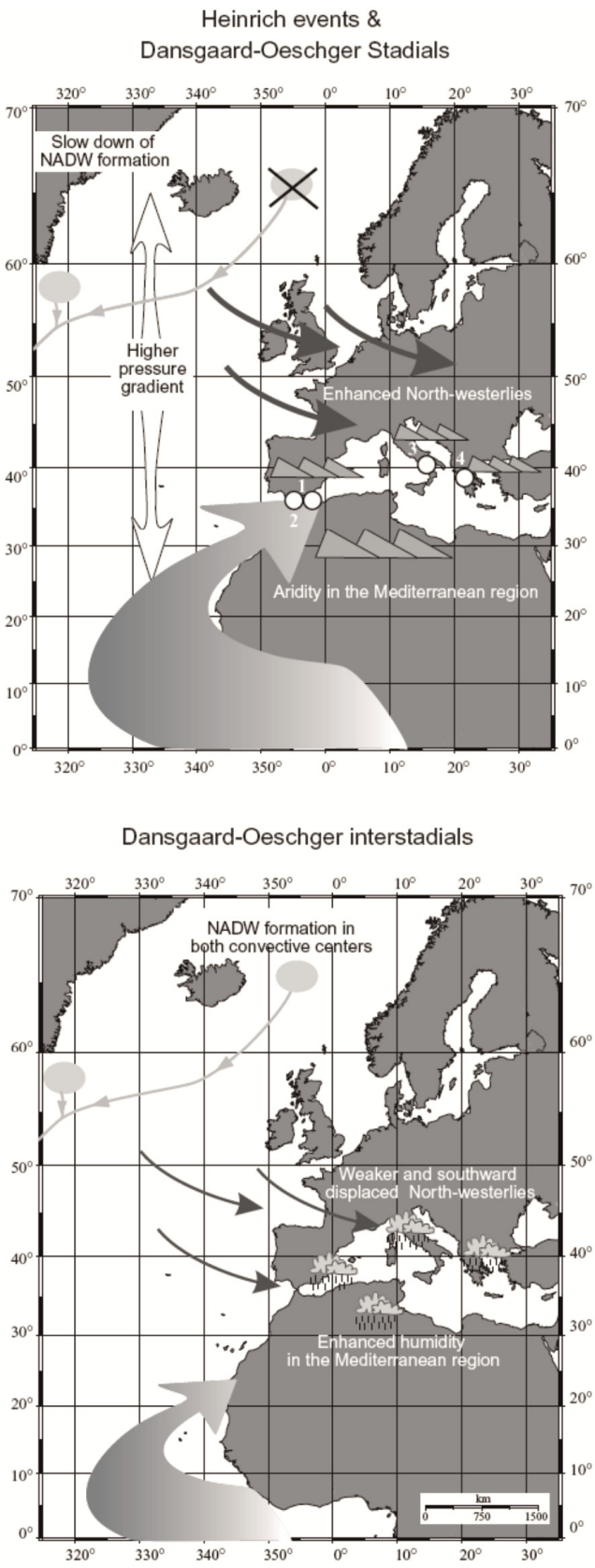

Figure 7.11 D/O scenarios that summarize the main processes and features that controlled the Alboran climate record during Heinrich events and D/O stadials and D/O interstadial periods after Moreno *et al.*, (2005).

This poor correlation would suggest that short duration climatic cycles did not have a major effect upon terrace formation in the Almería region. This is likely due to the relative response time and sensitivity of fluvial systems to external driven change. However, the poor correlation could be a result of the coarseness of fluvial archives which often only record large magnitude climatic signatures (Vandenberghe, 2003).

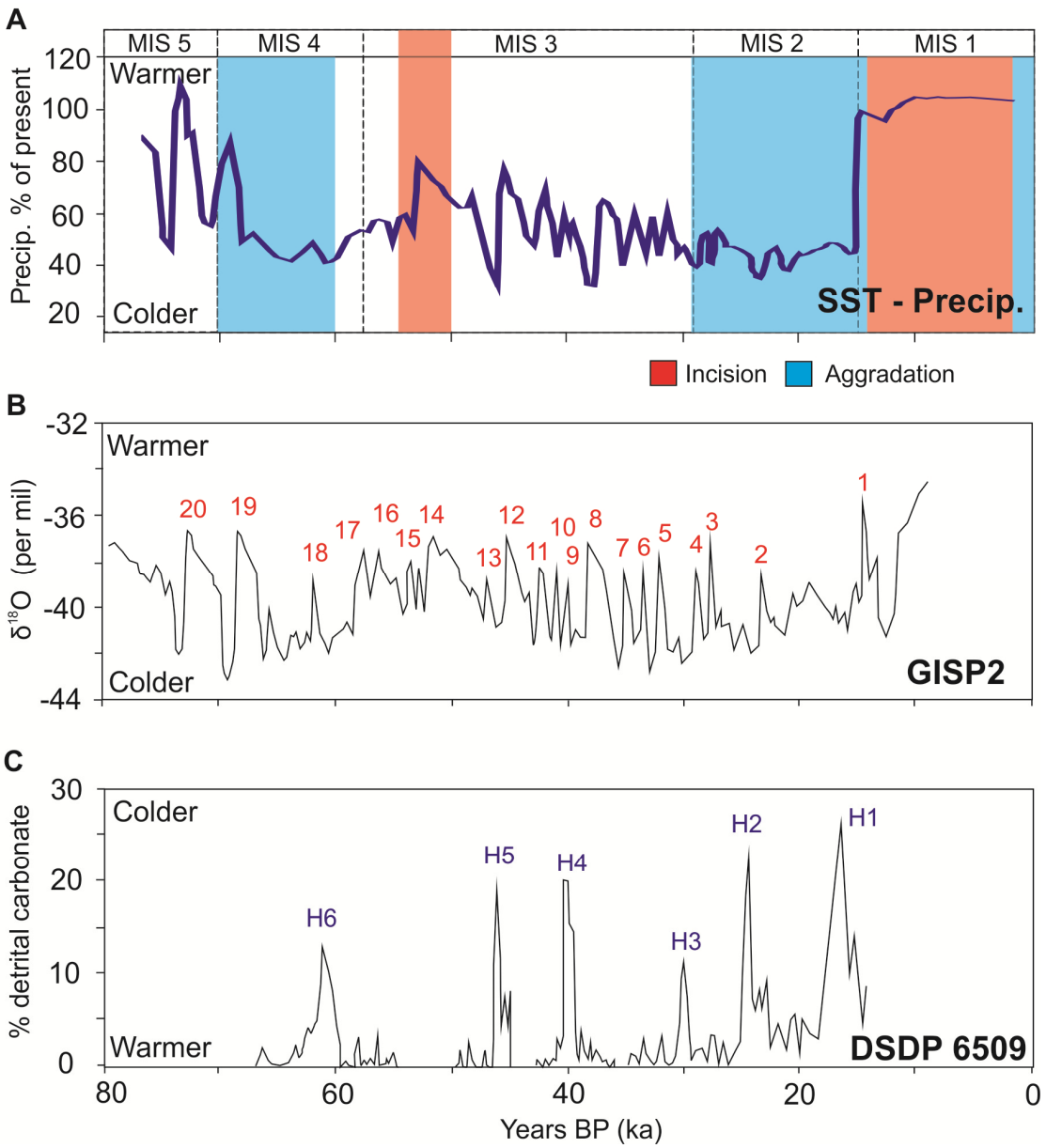

Figure 7.12 Comparison of short term climatic oscillations against the precipitation record generated as part of FLUVER2 inputs for the Tabernas Basin (A). (B) The δ18O record from the GISP2 ice core in Greenland, showing 20 of the 25 observed Dansgaard-Oeschger events during the last glacial period (Grootes et al., 1993). (C) A record of ice-rafted material during Heinrich events from a deep-sea core in the North Atlantic (Bond and Lotti, 1995). Note the correlation between climate forcing events and the relative changes in precipitation in the FLUVER2 dataset (A).

7.3.3 Internal controls - Lithology, drainage rearrangements and anthropogenic forcing

Lithological controls have been well evidenced upon patterns of drainage development throughout the Holocene in the Tabernas Basin (e.g. Alexander et al., 2008) and are significant in the current day fluvial system. Across the basin, resistant lithologies associated with the Gordo Megabed, Serravallian conglomerates and Tortonian sandstone beds have promoted the vertical incision and confinement of fluvial systems in highly entrenched, slot-like canyons (Chapter 2). In these relatively more resistant lithologies, fluvial systems are unable to erode laterally and patterns of landscape degradation become confined to the vertical down-cutting of channels with limited opportunity for river terrace formation. In contrast, the effects of resistant Tortonian sandstone beds and the extensive groundwater or valley floor calcretes evidenced across the Tabernas Basin act to limit basal incision, promoting the lateral erosion of fluvial systems and patterns of landscape degradation associated with the undercutting of calcrete capped slopes (Fig. 6.15, Chapter 6).

In both the Sorbas and Tabernas Basins, the development of the major drainage systems (Río Aguas and Rambla Tabernas, respectively) has been controlled by variability in the erodibility of basin lithologies overprinted upon the inherited tectonic structure of the basins. The Plio-Pleistocene fluvial systems of both basins exploited a weak band of marls characteristic of the basin centres, allowing them to erode headwards and expand the drainage network (Mather and Harvey, 1995). Both drainages follow the strike of the bedding which is controlled by the weakly synclinal folding of the basin created due to the uplift of the mountain ranges (Harvey, 1987). Much like in the Tabernas Basin, terrace formation is limited in the Sorbas Basin to areas of weaker lithology, with the development of highly incised slot type canyons in stronger metamorphic basement (Ilott, 2013). The metamorphic basement in the Sorbas Basin also acts to buffer the effects of the ~90m base-level drop, triggered by the major Late Pleistocene capture event which promoted a wave of incision that was easily transmitted in fluvial systems cutting through weak marl beds (Mather et

al.,2002; Stokes et al., 2002). Unlike in the Tabernas and Sorbas Basins, the effects of lithology upon drainage development in the Vera Basin and the EAC is less discussed in the literature (e.g. García et al., 2003; Stokes and Mather, 2003; Miekle, 2008).

Mechanisms of river capture / piracy have had a significant impact upon the development of the Quaternary landscape in both the Sorbas and Vera Basins (e.g. Mather, 1991; Stokes, 1997; Mather et al., 2000). As detailed in previous sections, the creation of steep regional gradients as a result of variable rates of tectonic uplift has promoted the headward incision of fluvial systems through largely weak marine marl/sandstone lithologies (Mather, 2000; Stokes et al., 2002; Stokes, 2008). In the Sorbas Basin, the effects of the c.69 ka capture event (Candy et al., 2004) promoted the removal of ~0.86 km^3 of material along the trunk drainages of the basin (Mather et al., 2002; Stokes et al., 2002). In the Vera Basin, multiple capture events promoted the shift to externally draining conditions and marked the onset of fluvial incision recorded in the Quaternary terrace record (Stokes, 2008). Across the Tabernas Basin, the effects of capture events have been limited throughout the basin's development. It is likely that during degradation stage 2 (Chapter 5) the headwaters of minor tributaries in the far west of the Sorbas Basin were captured and redirected through the Tabernas Basin (Mather and Harvey, 1995). However, the increases in discharge would have been limited due to the minor re-arrangement of the upper basin headwaters when compared with larger regional counterparts where catchment areas increase notably in size (e.g. <2% increase in Tabernas Basin catchment size compared to a 50% (c. 225 km^2) increase in the Río Aguas catchment after the c. 69 ka capture event, Stokes et al., 2002). A minor capture could be evidenced in the final stages of basin development represented by the non-uniform rates of landscape development for terrace level 4 (Chapter 6). However, it is likely that such shifts represent a transition of the fluvial system as a result of human or lithological forcing.

The effects of human activity upon fluvial systems in the Almería region have principally been studied in the downstream Río Aguas and Río Antas systems (Sorbas and Vera

Basins). Schulte (2002) highlights that Holocene deposits represent aggradational episodes during the Atlantic period (7.5 - 5 ka), early Middle Ages, Little Ice Age (LIA) (430± 50 yr B.P.) and the 20th century. Terrace formation was principally attributed to fluctuations in regional precipitation as evidenced by palynological data supported by limited 14C, IRSL and U/Th radiometric age estimations. However, during the last 500 years it is likely that human interference had a influence upon fluvial system dynamics (Schulte, 2002). This is characterised by the abandonment of agricultural land and infrastructure during the Christian conquest in the 16th century, and increases in charcoal production during the mining boom of the 19th century. During both periods, slope instability would have notably increased and surface runoff during torrential rainstorm events would have reinforced erosion processes and enhanced sediment supply in the river systems (Chapman et al., 1998; Schulte, 2002). Early human activity (e.g. Neolithic period) is believed to have had little effect upon fluvial systems across the Sorbas and Vera Basins as suggested by a lack of archaeological data (Schulte, 2002).

Results from the Tabernas Basin highlight relative changes in sediment delivery in the final stages of basin development (Holocene) through to the current day landscape (Chapter 6). Although, not substantiated by palaeoenvironmental data (i.e. pollen data) there is evidence of early human occupation of the Tabernas Basin. Most notable is the extensive occurrence of Neolithic to Bronze Age settlements and burial sites situated within a densely populated corridor termed the '*Pasillo de Tabernas'* (Fig. 7.13). The density of settlements within the east of Tabernas Basin was attributed to the rich alluvial soils and presence of natural springs which enabled early forms of agriculture along major drainages, such as the Rambla de los Molinos (Maldonado Cabrera et al., 1991). Minor communities were also thought to reside in the upper catchments of the Sierra de los Filabres; however, it is likely that these populations were mobile adapting to seasonal changes in growing periods (Maldonado Cabrera et al., 1991). Although limited by a lack of quantified data (e.g. pollen records or detailed archaeological data), the early stages of land clearing for agricultural

purposes could have promoted net changes in sediment availability from the Bronze Age onwards.

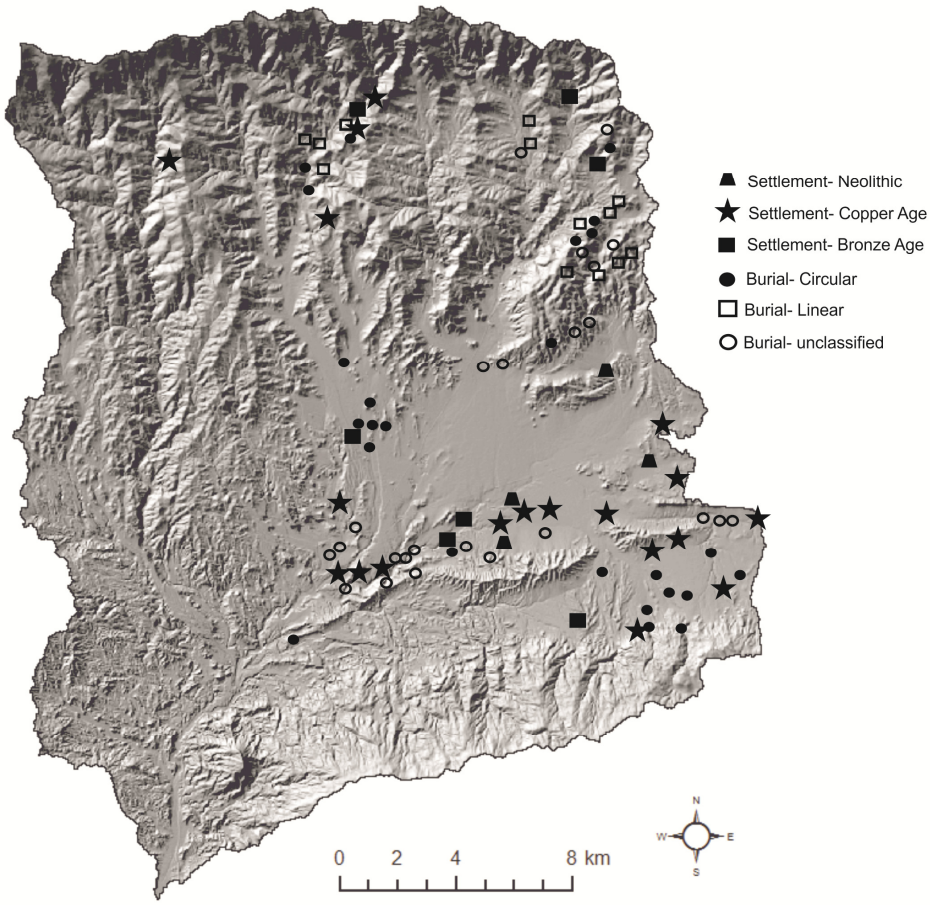

Figure 7.13 Distribution of Neolithic to Bronze Age sites within the Pasillo de Tabernas, redrawn from Maldonado Cabrera et al., (1991)

.

7.4 International significance

Although the Neogene basins of the Almería region are relatively small when compared with their Iberian (e.g. Tejo, Ebro, Duero rivers) or international counterparts (e.g. Rhine, Thames, Moselle), the detailed understanding of fluvial responses to both external and internal forcing mechanisms developed in the region offers a valuable case study of semi-arid/ arid region Quaternary landscape evolution, as well as an example of intramontane Quaternary basin development in a collisional mountain belt setting. Most notable are the interactions between external forcing mechanisms overprinted upon a suit of complex internal processes that have promoted non-uniformity in rates of landscape development. The following sections present an overview of the significance of these process interactions as compared with case-studies from the Iberian Peninsula and further international fluvial systems where relevant.

7.4.1 External forcing mechanisms: Tectonics and climate

The dominance of tectonically driven changes in base-level upon patterns of long-term landscape evolution is well recorded across the Iberian Peninsula. Although limited in geographical size, the effects of variable rates of uplift noted in the Almería region are often reproduced as 'scaled-up' versions, both spatially and temporally, across the greater peninsula. For example, the main rivers that drain the central and northern regions of the Iberian Peninsula (e.g. Tejo, Duerdo and Guadalquivir) have developed as a result of non-uniform rates of tectonic uplift driven by Alpine convergence at the northern and southern Iberian borders (Pyrenees and Betics). In west Iberia, convergence has been accommodated in left-lateral strike-slip corridors subjected to moderate levels of deformation (De Vicente and Vegas, 2009). The creation of regional drainage gradients between the inland Cenozoic Basins and the coastal plains has facilitated the capture and opening of formerly closed (endorheic) fluvial systems in a broadly E-W direction into the Atlantic Ocean (e.g. Duero and Tejo Basins; Martín-Serrano, 1991, Cuhna et al., 2005; Antón et al. 2012;

2014) (Fig. 7.14). The capture of large inland basins has had major repercussions upon the development of landscape system as a result of dramatic increases in catchment size and sediment budgets in the subsequent pirating drainage systems (e.g. capture of the Duero Basin increased the catchment size by > 50,000 km^2; Antón et al. 2012). Variations in uplift have further promoted changes in the styles and rates of fluvial system development across the peninsula. For example, in regions of limited uplift, such as the Ródão depression located along the Tejo river on the Portuguese / Spanish border, river terrace formation is noted to have occurred under braided fluvial conditions with the formation of thick sediment sequences and laterally extensive terrace bodies (Cuhna et al., 2005). This is comparable with regions of high uplift, where the Tejo takes on a narrow valley form, incised in the Hercynian basement with little to no terrace formation coupled with straight reaches that correspond to NE–SW and NNW–SSE faults (Cuhna et al., 2005). Variations in temporal uplift rates are further recorded as associated with varying degrees of terrace separation between older Tejo terraces (Cuhna et al., 2005). Although issues occur in the upscaling of forcing mechanisms from low to high order drainages (e.g. transition from continental drainage configurations which record effects of African-European plate collision to regional drainages which record the local effects of Neogene uplift) (Merritts et al., 1994), these mechanisms of tectonic variability appear similar to those recorded in the Tabernas, Sorbas and Vera Basins, and demonstrate the importance of tectonic forcing upon patterns of long-term landscape development.

Regional scale capture events driven by tectonic forcing are further recorded in the south of the Iberian Peninsula. In the Guadix Basin, a major drainage reversal occurred which rerouted the internally drained Plio-Pleistocene fluvial system of the Guadix Basin northwards into the headward eroding tributaries of the Guadalquivir River (Calvache and Viseras, 1997). Capture was further enhanced by the progressive shift of the axial fluvial system in response to the northward tilting of the basin, driven by localised uplift of a central sector of the Betic Cordillera during the Upper Pleistocene (Calvache and Viseras, 1997).

Although not well represented in the Quaternary record for the Almería region, the effects of tectonic tilting along active basin margins (e.g. active northern margin of the Sierra Alhamilla relative to inactive southern margin of the Sierra de los Filabres; Giaconia et al., 2012) could be of significance in the future development of the axial fluvial systems and warrants further investigation.

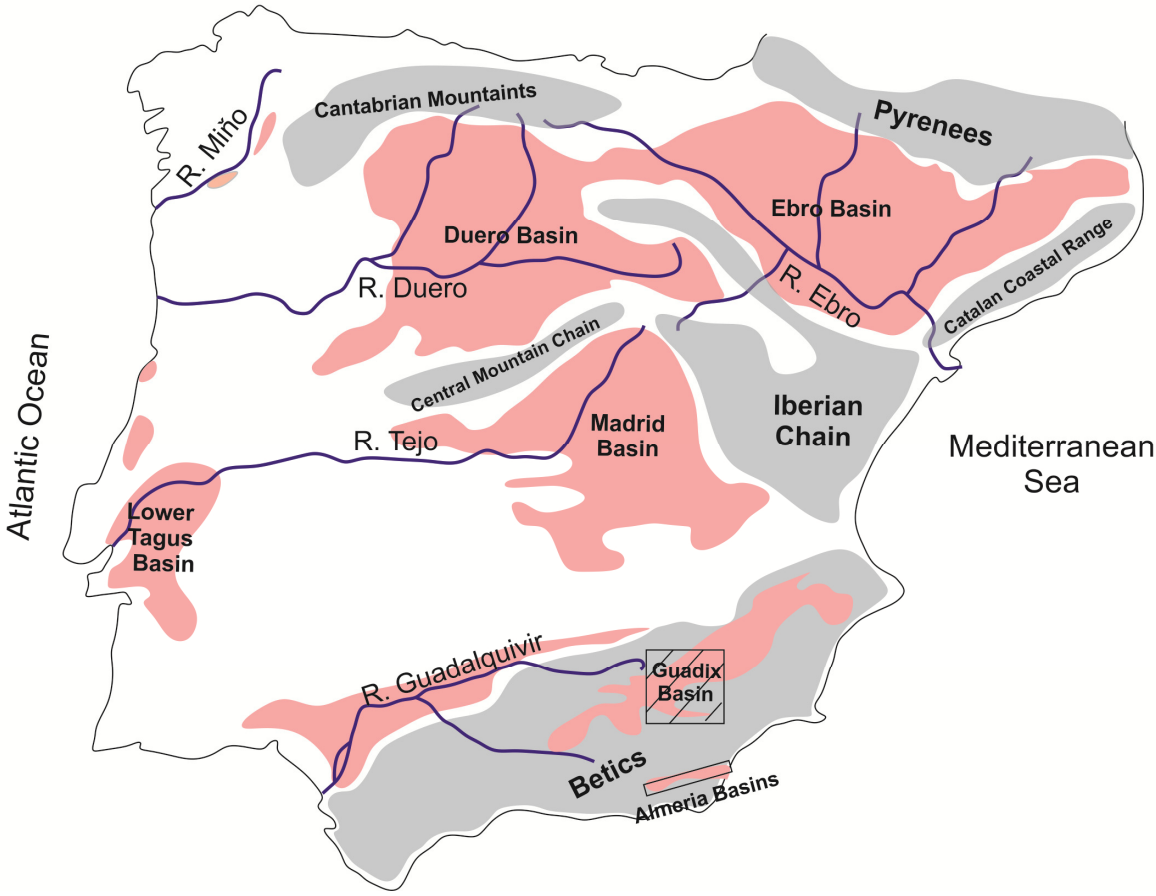

Figure 7.14 Map of the major basins (coloured pink), drainages (blue lines) and mountain ranges of the Iberian Peninsula (coloured blue).

In the northeast of the Iberian Peninsula (Fig. 7.14), the Ebro Basin records the effects of capture as promoted by the localised interplay of tectonic forces. The Ebro Basin formed as a result of regional subsidence related to the growth of the surrounding Alpine ranges (Pyrenees to the north, Catalan Coastal Range to the southeast and the Iberian Range to the southwest) which closed the western connection of the basin to the Atlantic Ocean in the earliest Late Eocene. The basin was syntectonically and post tectonically backfilled under

endorheic conditions during the Early to Middle Oligocene (Fig. 7.15A). Ongoing regional subsidence was reinforced by extensional tectonics during the Late Oligocene, which promoted rifting in the Catalan range (Coney et al., 1996). The formation of topographical barriers in the south-western margins of the basin confined fluvial system development for a further ~15 Ma, with the subsequent capture of the Ebro system and onset of externally draining conditions in the Late Miocene (Garcia-Castellanos et al., 2003). The opening of the drainage was likely promoted by a combination of tectonic and climatic forces. Increases in precipitation during a long term climate transition in the Late Miocene coupled with a period of relative tectonic quiescence promoted the over topping of the Ebro Basin lake sequence and the development of an external drainage network (Garcia-Castellanos et al., 2003). The capture of the Ebro basin promoted large variations in sediment budgets with ~40,000 km^3 of sediment modelled as an input into the Ebro Delta from the Late Miocene onward (Fig. 7.15).

The coupled relationship between climatic and tectonic forcing is well evidenced in fluvial systems across the Iberian Peninsula and further Mediterranean region. The in-depth review of Macklin et al., (2002) of Spanish, Greek and Libyan river basins demonstrates fluvial system response to glacial and interglacial cycles with at least 13 major alluviation episodes over the past 200 ka. Although the onset of alluviation episodes is variable as a function of the size, position and altitude of catchments, it is apparent that climate-related changes in catchment hydrology and vegetation cover over the last 200 ka were the primary control of large-scale (catchment wide) sedimentation over time periods of between 10^3 and 10^4 years (Macklin et al., 2002).

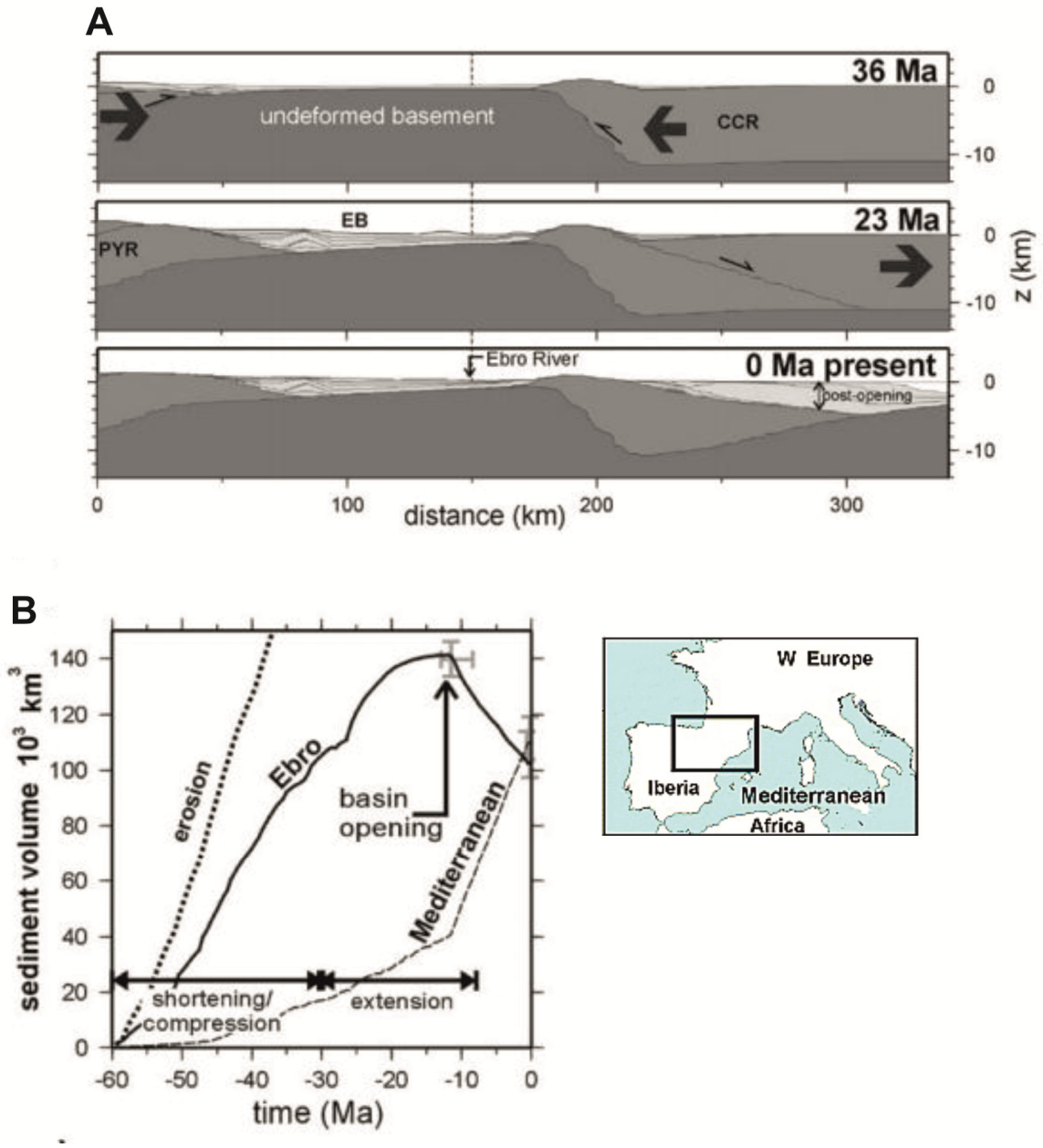

Figure 7.15 (A) Cross sections showing the development of the Ebro Basin as a result of early stages compressional tectonics which become extensional from 23 Ma onward. Note the significant delivery of sediment into the Ebro delta post capture (23 Ma to present). (B) Modelled sediment volumes representative of lake fill units of the Ebro Basin. Post capture internal sediment fluxes decrease by 40 x 10^3 km^3. Both figures from Garcia-Castellanos et al., (2003).

Patterns of sedimentation in the Almería region fit well with conceptual models of climatically driven terrace formation across the Mediterranean basins with sustained periods of terrace aggradation during cold climate or warming transitions (Mather and Harvey, 1995; Candy et al., 2004; Miekle, 2008, Ilott, 2013). Terrace formation in the Río Aguas, Antas and Almanzora systems records a notable shift in fluvial styles from extensive pediment and terrace surfaces in the Late Pliocene - Early Pleistocene to confined and narrow terrace remnants in the Middle Pleistocene to Holocene terraces (Harvey, 2002; Santisteban and Schulte, 2007; Ilott, 2013). The broad change in valley morphology and increases in terrace formation from the Middle-Late Pleistocene onwards is believed to be a function of the shift from low-amplitude to high-amplitude climatic cycles during the Mid-Pleistocene revolution (MPR). The MPR is well recorded in the south of the Iberian Peninsula; however, patterns of terrace formation in accordance with 100ka eccentricity cycles are not uniform in the central and northern regions of the peninsula (Santisteban and Schulte, 2007). The disparity between terrace records is likely a result of the local configuration of drainage networks as associated with relative tectonic activity and further internal factors such as the ongoing adjustment of fluvial systems to external capture events (e.g. Antón et al., 2012).

Although patterns of river aggradation are well demonstrated across the Mediterranean region, the relative importance of degradation stages in the development of fluvial systems is often neglected (e.g. the focus of Macklin et al., 2002 upon alluviation episodes alone). This is likely a function of the poor temporal constraint of incisional stages, which are typically derived from the 'gaps' in aggradation records (Fig. 7.16), coupled with the spatial variations in incisional records, such as those evidenced in this research from the Tabernas Basin, which are hard to discern from a non-existent record. Working with depositional records allows for collection of factual data from which tangible qualitative and quantitative interpretations can be made, rather than modelling events that lack any accurate measurable index. Yet the results of numerical modelling conducted in this study demonstrate that the duration of incisional phases in the Tabernas Basin exceeds that of

aggradational stages, and that degradational stages represent important geomorphic periods in the evolution of the basin (Section 6.4.3, Chapter 6).

With focus on the application of numerical models, the results from the Tabernas Basin are supported by the results of FLUVER2 modelling conducted in the Miño fluvial system in the northwest of the Iberian Peninsula (Fig. 7.14 for location) and the upstream Maas fluvial system in the southern Netherlands. In the Miño River, classified as a bedrock fluvial system (i.e. river developed into thin sediment accumulations, Baker, 1984), modelled incision accounts for 80% of fluvial activity in the last 600ka of basin development (Fig. 7.17) (Viveen et al., 2013). In the Maas River, an alluvial system (i.e. river cuts into and reworks substantial thicknesses of alluvium), the duration of modelled incisional events are typically longer than aggradation periods yet they are shown to decrease in a downstream direction, from 75% of modelled duration (400 ka) in the upper system (550km from river source) to 20% in the lower reaches of the system (720km from source) (Fig. 7.17) (Veldkamp and Van Dijke, 2000). Decreases in the duration of incisional events are likely a function of internal characteristics of the Maas fluvial system with reference to elements of sediment storage, transportation and reworking coupled with the decrease effects of climate cycles in the downstream fluvial system (Veldkamp and Van Dijke, 2000). Based on the combined results of these numerical modelling studies, it would appear that the conceptual models of river incision during climatic transitions alone (e.g. Bridgland and Westaway, 2008) require modification for low order and intramontane fluvial systems. Numerical modelling results do support the initiation of incisional events during climatic transitions, yet incision appears to be sustained between climatic cycles with relative rates of incision being largely controlled by internal system dynamics (e.g. Veldkamp and Van Dijke, 2000; Coulthard et al., 2013).

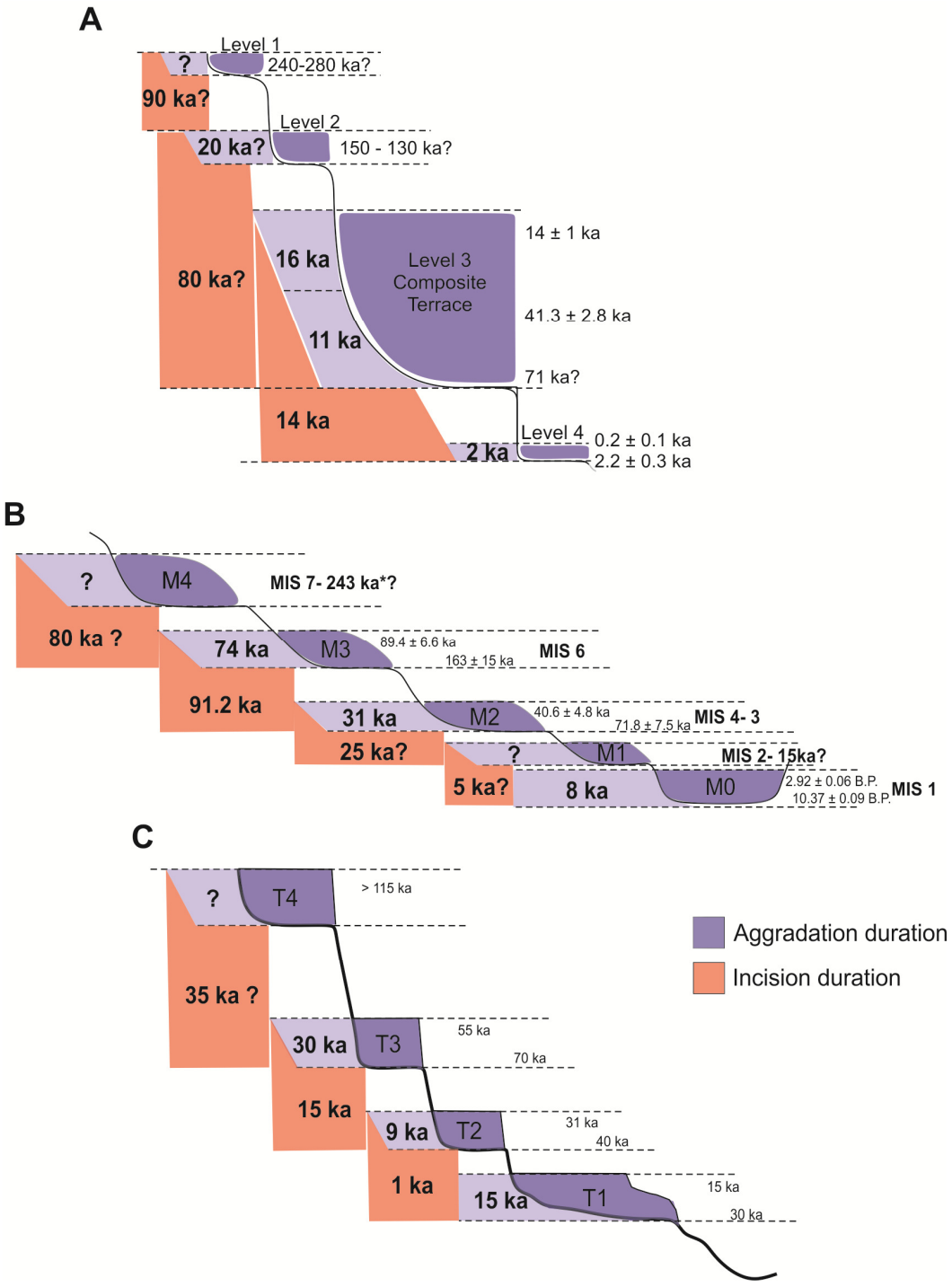

Figure 7.16 Comparison of Tabernas terrace record (A) against two well dated fluvial archives demonstrating variations in aggradational and incisional period durations. (B) Chronostratigraphy of the middle-lower terraces of the Meurthe- Moselle valleys, from Cordier et al., (2006). Age estimates based on IRSL dating of fluvial sediments. The relative chronology is limited by lack of known ages for terraces M4 and M1, with estimations of incisional stages during glacial stages. (C) Composite correlation of fluvial terraces is presented for eight non-glacial catchments of the eastern North Island, New Zealand (from Litchfield and Berryman, 2005). Ages from radiocarbon and OSL dating of fluvial deposits and loess. Note how incisional events in the final stages of fluvial development are separated by unrealistic time gaps (e.g. 1ka between T2 and T1),

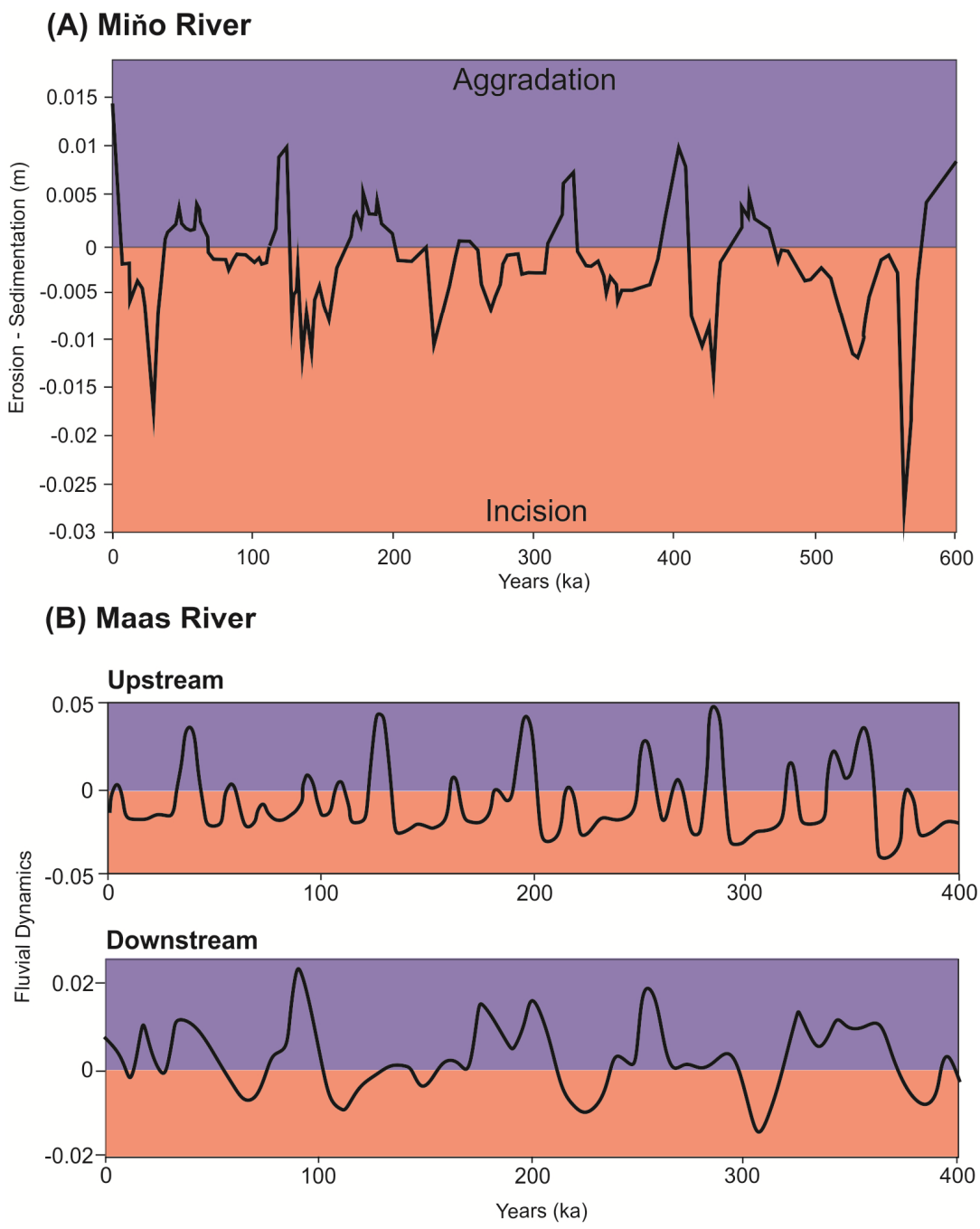

Figure 7.17 FLUVER2 outputs sedimentation outputs for the Miño River (A) and the Maas River (B). (A) Demonstrates the relative amounts of incision account for 80% of the model window for the Miño system, from Viveen et al., (2013). (B) Demonstrates the decrease in duration of incision in the downstream section of the Maas River, this is attributed to variations in internal sediment dynamics, from Veldkamp and Van Dijke, (2000).

7.4.2 Internal forcing mechanisms

The internal characteristics of landscapes are a fundamental element of any fluvial system (Schumm, 1979). In this research, the importance of lithological controls and internal thresholds has been clearly demonstrated for the Almería region (Chapter 6). The underlying significance of basin lithology is evident in most studies of fluvial system development across the Iberian Peninsula. For example, the formation of highly incised, laterally confined fluvial channels in the Duero and Tejo Rivers has been limited to regions of high lithological strength that are exposed to conditions of sustained tectonically driven base-level lowering (Cunha et al., 2005; Antón et al., 2012). However, other than the qualitative observations made from variations in fluvial incisional styles little work has attempted to quantify the variations in the rates of incision as a function of lithological strength (Stokes *per comms.*). This is likely a function of the limitations in making representative and reproducible rock strength measurements throughout an entire catchment.

In comparison to the well evidenced effects of lithology upon fluvial system development, the understanding of how internal thresholds affect long-term patterns of fluvial system development remain poorly addressed. This is ultimately due to the limitations of terrace datasets, which provide a biased and fragmentary insight into how fluvial systems evolve (Coulthard and Van de Wiel, 2013). In a global context of terrace studies, the significance of internal thresholds are commonly cited when patterns of fluvial system development do not fit with conceptual models of landscape forcing as a result of external forcing mechanisms such as tectonics, climate or sea-level change (Vandenberghe et al., 2010). Therefore, when patterns of fluvial development occur within the understanding of current theory, the importance of internal thresholds in the development of fluvial systems are commonly overlooked, based on the overly simplistic observations made from a fragmentary dataset (Vandenberghe et al., 2010). However, the importance of intrinsic thresholds can be demonstrated on a range of scales. These include: (1) the short-term activity of lateral channel migration which acts to alter sediment budgets and further inhibit or promote terrace

preservation (Lewin and Macklin, 2003) through to (2) variations in sediment availability as related to the identity of any given catchment, which is subject to geomorphic–hydrological laws, such as sediment load, downstream gradient and pre-existing topography (e.g. Rose et al., 1999).

In this research, the importance of intrinsic thresholds was developed by the conceptual and numerical modelling of the Tabernas Basin fluvial system (Chapter 6). The datasets generated from numerical modelling packages offers valuable continual quantitative data which can be correlated against real world data. Although still at the forefront of development, applications of landscape evolution models have offered much insight into the importance of external forcing mechanisms upon the landscape system, as developed throughout this discussion, and also highlighted the relative importance of intrinsic thresholds (e.g. the development of the Maas River presented in Section 7.4.1; Velkdkamp and Van Dijke, 2000). Increases in the accuracy and precision of numerical models are likely to offer further insight into the complex interplay of external and internal drivers of landscape change. However, the need for model development highlights the importance of comprehensive field data for use in the calibration stage.

7.5 Summary

The discussions presented in this chapter have developed the local, regional and international significance of the Quaternary landscape development in the Tabernas Basin. The results generated from a combination of field investigations, including conceptual and numerical modelling have highlighted the importance of tectonically driven base-level controls upon landscape evolution in the Tabernas Basin and within the broader Almería region. At a regional scale, the data presented have shown that non-uniform rates of uplift, focused in the west of the region, have been of significance in driving variations in base-level throughout the Quaternary evolution of the Almería basins. Variations in tectonically driven base-level change are recorded by a series of river capture events in the eastern basins,

which appears to be a prevalent process driving the evolution of drainage networks across the Iberian Peninsula. The effects of climatically driven variations in sediment availability associated with Quaternary global glacial and interglacial cycles are also well evidenced in the Tabernas Basin and greater Almería region. Patterns of terrace aggradation fit well with conceptual models of climatically driven terrace formation (e.g. .Bridgland and Westaway, 2008); however, incisional trends based on numerical outputs appear to show discrepancies. Results of numerical modelling conducted in this research support numerous previous studies, and suggest that the duration of incisional phases initiated at climatic transitions are long lived and typically exceed that of aggradation cycles. However, the validity of this observation is restricted by the resolution of current chronological stratigraphies for global fluvial systems. The results of numerical modelling also highlight the importance of non-linearity in the development of the Tabernas Basin. Variations in incisional styles are likely associated with either the crossing of internal landscape thresholds or the effects of human activity upon the landscape. Both factors have been demonstrated to be of importance in the development of fluvial systems throughout the Quaternary in both the Almería region and greater Iberian sub-continent.

Chapter 8

8.1 Conclusion

This study aims to ascertain the interplay and dominance of external forces (i.e. tectonic uplift and climate cycles) and/or internal controls (e.g. lithological controls) upon the evolution of the Quaternary fluvial system within the Tabernas Basin. Throughout the study, a combined research approach was applied in order to develop an understanding of long-term landscape evolution. Initial focus was placed on the detailed field based geomorphological mapping and sedimentological analysis of landform units (Chapter 3). The results of field investigations were supplemented by chronological data derived from optically stimulated dating methods in order to develop the temporal patterns of basin development (Chapter 4). The Quaternary landforms of the Tabernas Basin were then investigated by methods of quantitative landscape modelling (Chapters 5 and 6). Patterns of landscape evolution as attributed to one or more forcing mechanism were qualitatively compared and contrasted with: (i) the regional records of Quaternary landscape change from other sedimentary basins located in the Betic Cordillera region of SE Spain (e.g. Sorbas and Vera Basins) and (ii) further studies of long-term landscape evolution within the Iberian Peninsula.

8.1.1 Quaternary evolution of the Tabernas Basin.

Four Quaternary fluvial terrace levels were identified for the Tabernas Basin. These terraces levels occur at ~ 80 m (level 1: oldest), ~ 50 m (level 2), ~ 30 m - 10 m (level 3) and < 5 m (level 4: youngest) above the current channel. The broad sedimentology of the terrace levels indicates deposition in laterally extensive, fluvially dominated alluvial fans for terrace levels 1 and 2 with a shift to more confined, braided conditions for levels 3 and 4. Age estimates from OSL dating demonstrate that terrace deposition occurred as a result of climatic forcing during transitional phases, which was likely sustained under cold climate conditions throughout global glacial stages (Fig. 8.1). Age estimates of 41.3 ± 2.8 ka to 14 ± 1 ka (MIS 3 to MIS 2) were derived for terrace level 3 and 2.8 ± 0.3 ka to 0.2 ± 0.1 ka (Holocene – Recent) for terrace level 4. Unfortunately, the application of OSL dating for

terrace levels 1, 2 and 3 was limited by the low saturation levels of quartz grains, coupled with a lack of potassium feldspars across the basin (Chapter 4). Detailed analysis applying both single grain and multi grain measurements further demonstrated the increased effects of partial signal resetting upon the age estimations from young samples (< 5 ka). However, the age estimates generated offer valuable data for further studies of landscape evolution both within the basin and across the Almería region.

The results of numerical modelling were used to supplement field and chronological data. Modelled outputs suggest that: (i) terrace level 2 formation likely occurred during the transition from MIS 6 to MIS 5; (ii) terrace level 3 formation was initiated during the transition from MIS 5 to MIS 4 and was sustained well into the LGM (MIS 2), as supported by the OSL data; and (iii) the aggradation of terrace level 4 units did not occur as a result of climatic forcing; however, sediment deposition was promoted by the crossing of an internal system threshold as forced by lithological and / or anthropogenic factors. Unfortunately, no relative age estimates are presented for terrace level 1 due to the limited extent of terrace outcrops across the basin which limited model reconstruction. Based on patterns of climatically driven terrace formation, terrace level 1 sedimentation likely took place during the transition from MIS 8 to MIS 7.

The application of geospatial interpolation successfully allowed for the generation of continual palaeolandsurfaces from terrace landforms. The reconstructed terrace levels were then compared in the GIS domain in order to assess patterns of landscape degradation. The separation of terrace levels across the Tabernas Basin occurred during four major degradation stages. Basin incision was promoted by non-uniform rates of tectonically driven base-level change focused in the west of the basin, as evidenced in the current basin geomorphology (Chapter 5) and supported by numerical model data (uplift rates of 0.13 m ka^{-1} in the east against 0.25 m ka^{-1} in the west, Chapter 6). The most pronounced degradational stage occurred post terrace level 2 formation, with the complete dissection of the basin from its confluence with the Río Andarax in the west, and lateral incision well into

the Sorbas Basin in the east (Chapter 5). Relative increases in the intensity of incision likely occurred as a result of enhanced base-level lowering within the Río Andarax as it passed through the rapidly uplifting eastern Alpujarran Corridor (EAC). The timing of degradation stages is hard to define based on limited chronological data; however, results from numerical modelling would suggest the following:

- Degradation stage 1 (terrace level 1 to terrace level 2) likely took place during MIS 7
- Degradation stage 2 (terrace level 2 to terrace level 3) was long-lived and sustained throughout MIS 5 (~140 to 71 ka);
- Degradation stage 3 (terrace level 3 to terrace level 4) was short lived and occurred during the transition from MIS 2 to MIS 1;
- Degradation stage 4 (terrace level 4 to present) initiated at some point in the Late Holocene and is still ongoing in the current fluvial system.

Due to the lack of exposure across the basin, the understanding of terrace level 2 lower remains poor. In conclusion, it is proposed that long-term landscape evolution in the Tabernas Basin was primarily governed by non-uniform rates of tectonically driven base-level change coupled with the effects of Quaternary climate cycles. Rates of tectonic uplift have been spatially and temporally non-uniform as evidenced by variations in the intensity of degradational stages and the highly variable landscape response to base-level changes focused in the west of the basin. Quaternary climatic cycles forced fluvial system development via alterations in precipitation and vegetation cover. Notable periods of fluvial system aggradation occurred during cold climate phases. Degradational periods typically occurred during warming transitions; however, sustained incision throughout climate cycles (e.g. MIS 5) could relate to the dominance of tectonically driven base-level changes. Although limited to the most recent terrace records, internal threshold conditions are also of significance in the development of the Tabernas Basin. These thresholds could be related to the geomorphic attributes of the landscape or further aspects of anthropogenic forcing.

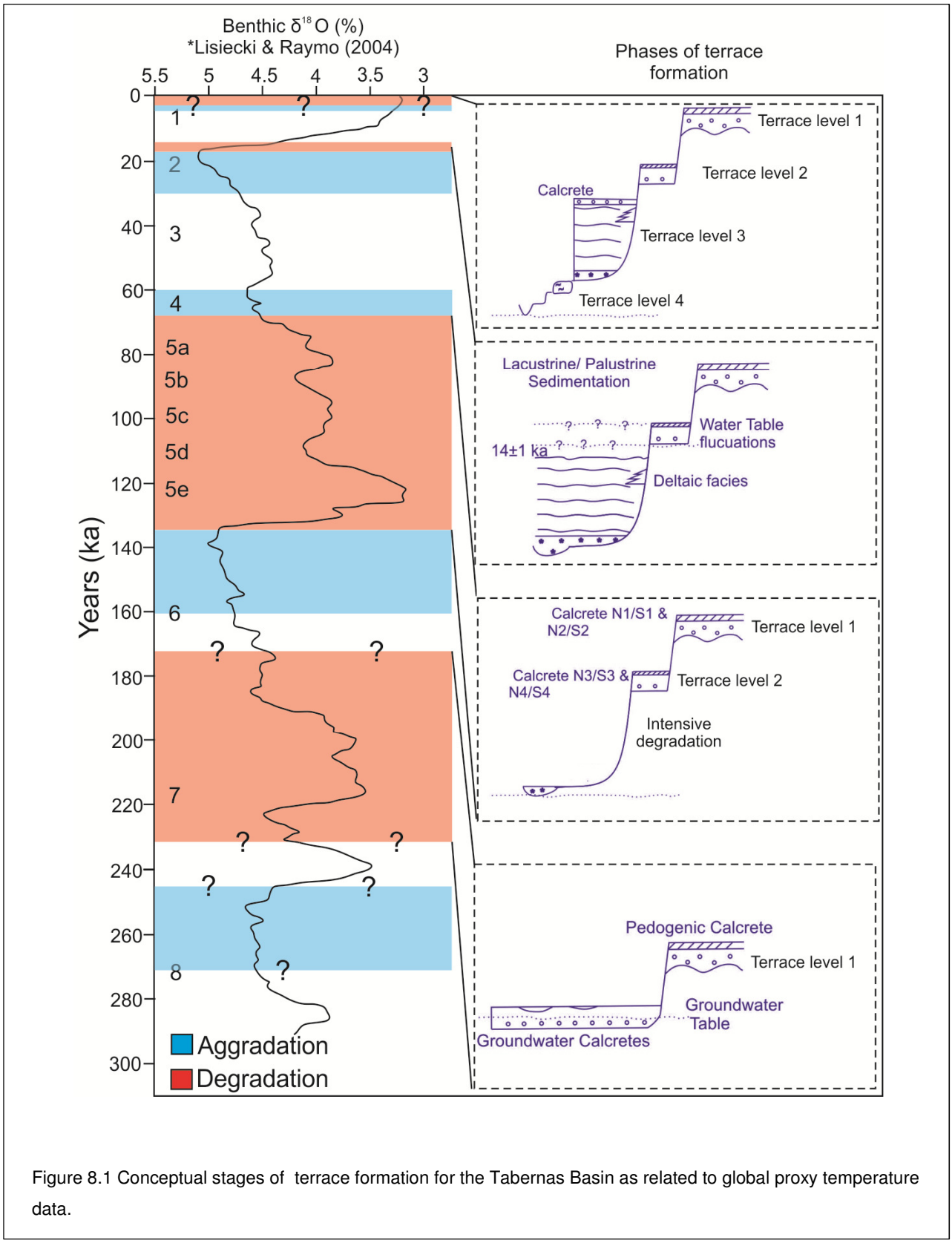

Figure 8.1 Conceptual stages of terrace formation for the Tabernas Basin as related to global proxy temperature data.

8.1.2 Developing the regional understanding of Quaternary landscape evolution

The findings of this study offer valuable data in regional interpretations of long-term landscape evolution. Most notable is the underlying significance of variable rates of tectonic uplift in the generation of localised patterns of landscape evolution (Chapter 7). The modelled uplift rates generated for the Tabernas Basin link the neighbouring Sorbas Basin and the EAC, and develop a focus of uplift around the Sierra Nevada in the west of the Almería region. The results from OSL dating offer further valuable age estimates to an ever increasing regional record. Interpretations from multiple chronological datasets highlight the patterns of climatically forced terrace formation across the Almería region and further away in the Iberian Peninsula. However, the significance of long lived incisional periods evidenced in the EAC, Tabernas Basin and Sorbas Basin demonstrates the underlying importance of tectonically controlled base-level changes upon patterns of landscape evolution. Internal landscape thresholds are also important at a regional scale. This is well demonstrated by the importance of river capture events and aspects of anthropogenic land clearance which has forced fluvial system development at accelerated rates when compared with those of external forcing mechanisms.

The detailed analysis of qualitative field, chronological and conceptual modelling data by means of numerical modelling offered the first continual record of landscape development for the Almería region. Although limited by the accuracy and reliability of modelling software, the outcomes of the modelling exercise associate well with regional trends (i.e. uplift rates) and offer valuable information with regard to the continual development of fluvial systems in southeast Spain. Results from Tabernas would suggest that: (i) aggradation and incisional trends correlate well with Quaternary climatic cycles which were enhanced post Mid Pleistocene Revolution (~MIS 8) and (ii) short duration climatic cycles (D/O and Heinrich Events) are not well evidenced in the Quaternary fluvial archive of the Almería; however, this observation requires additional investigation based on other well dated and modelled catchments.

8.1.3 Key conclusions

The key conclusions of this research are:

- The Quaternary landforms of the Tabernas Basin form four terrace levels;
- Optically stimulated luminescence dating has been applied with variable success in the dating of Quaternary fluvial deposits;
- A combined research approach (i.e. field investigations, conceptual and numerical modelling) has enabled detailed interpretations of long-term landscape evolution for the Tabernas Basin;
- Patterns of Mid to Late Pleistocene landscape evolution in the Tabernas Basin are principally controlled by the effects of climatic forcing overprinted on a pattern of non-uniform tectonic uplift;
- Early stages of terrace formation took place during climate transitions and were likely sustained throughout global glacial phases;
- The Holocene development of the Tabernas Basin is likely linked to the internal characteristics of the landscape coupled with the effects of anthropogenic forcing;
- At a regional scale, patterns of landform development in the Tabernas Basin concur with neighbouring basins and develop a regional context for the effects of non-uniform rates of tectonic uplift throughout the Quaternary which are focused in the west of the region.
- The ongoing development of numerical software packages will enable detailed quantification of landscape processes over Quaternary timescales.

8.2 Ongoing investigations

The results of this study have highlighted multiple factors which warrant further research, these include:

- An investigation into the importance of calcrete and travertine development across the Almería region. Both secondary precipitates form important geomorphic features in terms of their physical attributes and act as valuable stores of palaeoclimatic data within the Quaternary landscape. Given the focus of this study, limited detail has been placed on the understanding of these landform features in terms of their detailed morphology or geochemical composition (e.g. isotopic analysis). However, an understanding of the detailed climatic conditions of formation would provide a vital proxy record for the Tabernas Basin and greater Almería region.
- A detailed investigation into the precision and accuracy of numerical modelling results presented from the FLUVER2 model. It is currently well understood that 2-D models do not accurately represent highly complex natural landscapes (Tucker and Hancock, 2010). Given this understanding, are the results of this investigation simply a representation of a number of parameter interactions which generated a dataset representative of reality? There are now a number of 3-D model packages that have to capability to model landscape evolution at Pleistocene timescales (e.g. LAPSUS, CHILD). A comparison of model outcomes would offer insight into the limitations of the FLUVER2 model and highlight the requirement for further development.
- Focus on the development of a robust absolute chronology for the Almería region. It is evident from the outcomes of this research that the sedimentary basins of SE Spain offer valuable insight to the long-term development of the Mediterranean region. At present, the major interpretations of landscape evolution are based on a weak chronological framework. Many of the dates obtained for the region have been generated by continually advancing dating techniques which warrant further application in a region of extensive geomorphological knowledge.

- Quantification of the effects of rock mass strength upon the development of long-term fluvial systems. This principal landscape control is highlighted in most terrace studies; however, little focus is ever placed on developing a quantified dataset which investigates the empirical relationships between lithological strength and incisional rates. These data form crucial inputs into landscape evolution models and are at present based on limited laboratory data and theoretical relationships between rock strength and sediment production. These data often do not account for variable rates of weathering and or the coupled effects of rock mass strength (Sklar and Dietrich, 2001).

References

Adamiec, G., Aitken, M.J., 1998. Dose-rate conversion factors: update. Ancient TL, 16, 37-50

Aguilar, F.J., Aguera. F., Aguilar, M.A., Carvajal. F, 2005. Effects of terrain morphology, sampling density and interpolation methods on grid DEM accuracy. Photogrammetric Engineering and Remote Sensing, 71, 805-816.

Aitken M.J. 1985. Thermoluminescence dating. Academic press: London

Aitken, M.J., 1992. Optical dating. Quaternary Science Reviews, 11, 127-131.

Aitken, M.J., 1998. Introduction to Optical Dating. Oxford University Press, Oxford.

Aitken M.J., Xie, J. 1990. Moisture correction for annual gamma dose. Ancient TL, 8, 6-9.

Alexander, R.W., Harvey, A.M., Calvo, A., James, P.A., Cerda, A., 1994. Natural stabilisation mechanisms on badlands slopes: Tabernas, Almería, Spain. In: Millington, A.C., Pye, K. (Eds.), Environmental Change in Drylands: Biogeographical and Geomorphological Perspectives. Wiley, Chichester, pp. 85-111.

Alexander, R.W., Calvo-Cases, A., Arnau-Roalen, E., Mather, A.E., Lazaro- Suau, R., 2008. Erosion and stabilisation sequences in relation to base level changes in the El Cautivo badlands, SE Spain. Geomorphology, 100, 83-90.

Alonso-Zarza, A.M., Silva, P.G., Goy, J.L., Zazo, C., 1998. Fan-surface dynamics and biogenic calcrete development: interactions during ultimate phases of fan evolution in the semiarid SE Spain (Murcia). Geomorphology, 24, 147-167.

Amor, J.M., Florschutz, F., 1964. Results of the preliminary palynological investigation of samples fro a 50m boring in Southern Spain. Boletin de la Real Sociedad Espanola de Historia Natural, 62, 251-255.

Antoine, P., Lautridou, J.P., Laurent, M., 2000. Long-term fluvial archives in NW France: response of the Seine and Somme rivers to tectonic movements, climatic variations and sea-level changes. Geomorphology, 33, 183-207.

Antón, L., Rodés, A., De Vicente, G., Pallàs, R., Garcia-Castellanos, D., Stuart, F.M., Braucher, R., Bourlès, D., 2012. Quantification of fluvial incision in the Duero Basin (NW Iberia) from longitudinal profile analysis and terrestrial cosmogenic nuclide concentrations. Geomorphology, 165–166, 50-61.

Antón, L., De Vicente, G., Muñoz-Martín, A., Stokes, M., 2014. Using river long profiles and geomorphic indices to evaluate the geomorphological signature of continental scale drainage capture, Duero basin (NW Iberia). Geomorphology, 206, 250-261.

Azañón, J.M., Azor, A., Perez-Pena, J.V., Carrillo, J.M., 2005. Late Quaternary large-scale rotational slides induced by river incision: The Arroyo de Gor area (Guadix basin, SE Spain). Geomorphology, 69, 152-168.

Baartman, J.E.M., Veldkamp, A., Schoorl, J.M., Wallinga, J., Cammeraat, L.H., 2011. Unravelling Late Pleistocene and Holocene landscape dynamics: The Upper Guadalentín Basin, SE Spain. Geomorphology, 125, 172-185.

Baartman, J.E.M., van Gorp, W., Temme, A.J.A.M., Schoorl, J.M., 2012. Modelling sediment dynamics due to hillslope–river interactions: incorporating fluvial behaviour in landscape evolution model LAPSUS. Earth Surface Processes and Landforms, 37, 923-935.

Baker, R.V., 1984. Flood Sedimentation in Bedrock Fluvial Systems. Sedimentology of Gravels and Conglomerates. In: Koster, E.H., Steel, R.J. (Eds.), Sedimentology of

Gravels and Conglomerates, Canadian Society of Petroleum Geologists, Calgary, pp. 87 – 98
Bailey, R., Smith, B., Rhodes, E., 1997. Partial bleaching and the decay form characteristics of quartz OSL. Radiation Measurements, 27, 123-136.
Bailey, R.M., Arnold, L.J., 2006. Statistical modelling of single grain quartz De distributions and an assessment of procedures for estimating burial dose. Quaternary Science Reviews, 25, 2475-2502.
Bautista, S., Mayor, A.G., Bourakhouadar, J., Bellot, J., 2007. Plant spatial pattern predicts hillslope runoff and erosion in a semiarid Mediterranean landscape. Ecosystems, 10, 987-998
Bell, A.D.F., 2012. Creating DEMs from survey data: interpolation methods and determination of accuracy. In: Clarke, L.E. (Ed.), Geomorphological Techniques (Online Edition). British Society for Geomorphology, London, Chap. 2, Sec. 3.1.
Bellin, N., Vanacker, V., van Wesemael, B., Solé-Benet, A., Bakker, M.M., 2011. Natural and anthropogenic controls on soil erosion in the Internal Betic Cordillera (southeast Spain). Catena, 87, 190-200.
Benito, G., Rico, M., Sánchez-Moya, Y., Sopeña, A., Thorndycraft, V.R., Barriendos, M., 2010. The impact of late Holocene climatic variability and land use change on the flood hydrology of the Guadalentín River, southeast Spain. Global and Planetary Change, 70, 53-63.
Bintanja R, Van de Wal RSW, Oerlemans J. 2005. Modelled atmospheric temperatures and global sea levels over the past million years. Nature, 437, 125-128
Bishop, P., 1995. Drainage rearrangement by river capture, beheading and diversion. Progress in Physical Geography, 19, 449-473.
Blair, T.C., McPherson, J.G., 1994. Alluvial Fan Processes and Forms. In: Parsons, A.J., Abrahams, A.D. (Ed.), Geomorphology of Desert Environments. Chapman & Hall, London, pp 354-402.
Blum, A.J., 2007. Controls on Long-Term Drainage Development of the Carboneras Basin, SE Spain. University of Plymouth, Plymouth, PhD Thesis
Blum, M.D., 1993. Genesis and architecture of incised valley fill sequences; a late Quaternary example from the Colorado River, Gulf Coastal Plain of Texas. In: Weimer, P., Posamentier, H.W. (Eds.), Siliciclastic sequence stratigraphy; recent developments and applications: AAPG Memoir, 58, pp. 259-283.
Blum, M.D., Tornqvist, T.E., 2000. Fluvial responses to climate and sea-level change: a review and look forward. Sedimentology, 47, 2-48.
Boenigk, W., Frechen, M., 2006. The Pliocene and Quaternary fluvial archives of the Rhine system. Quaternary Science Reviews, 25, 550-574.
Bohncke, S., Vandenberghe, J., 1991. Palaeohydrological development in the Southern Netherlands during the last 15000 years. In: Starkel, K.J.G. L, Thornes, J.B. (Eds.), Temperate Palaeohydrology. Wiley, New York, pp. 253-281.
Bogaart, P.W., van Balen, R.T., 2000. Numerical modeling of the response of alluvial rivers to Quaternary climate change. Global and Planetary Change, 27, 147-163.
Bond, G.C., Lotti, R., 1995. Iceberg discharges into the North Atlantic on millennial time scales during the last glaciation. Science, 267, 1005-1010.
Bond, G.C., Showers, W., Elliot, M., Evans, M., Lotti, R., Hajdas, I., Bonani, G., Johnson, S., 1999. The North Atlantic's 1–2 kyr climate rhythm: relation to Heinrich events, Dansgaard/Oeschger cycles and the little ice age. In: Clark. P.U., Webb. R.S.,

Keigwin, L.D. (Eds.), Mechanisms of Global Change at Millennial Time Scales, Geophysical Monograph 112. American Geophysical Union, Washington DC, pp. 59-76.
Bonham-Carter, G.F., 1994. Geographic Information Systems for Geoscientists: Modelling with GIS. Computer Methods in the Geosciences, 13. Elsevier Butterworth-Heinemann, Oxford, UK, 398 pp.
Booth-Rea, G., Azañón, J.-M., Azor, A., García-Dueñas, V., 2004. Influence of strike-slip segmentation on drainage evolution and topography. A case study: the Palomares Fault Zone (Southeastern Betics, Spain). Journal of Structural Geology, 26, 1615–1632.
Bowman, D., Svoray, T., Shapira, I., Laronne, J.B., 2010. Extreme rates of channel incision and shape evolution in response to a continuous,rapid base-level fall, the Dead Sea, Israel. Geomorphology, 114, 227-237.
Braga, J.C., Martin, J.M., Quesada, C., 2003. Patterns and average rates of late Neogene–Recent uplift of the Betic Cordillera, SE Spain. Geomorphology, 50, 3-26.
Bridgland, D.R., 2000. River terrace systems in north-west Europe: an archive of environmental change, uplift and early human occupation. Quaternary Science Reviews, 19, 1293-1303.
Bridgland, D.R., 2001. The Pleistocene evolution and Palaeolithic occupation of the Solent River. In: Wenban-Smith, F.F., Hosfield, R.T. (Eds.), Palaeolithic Archaeology of the Solent River. Lithic Studies Society Occasional Paper. Lithic Studies Society, London, pp. 15-25.
Bridgland, D., Maddy, D., Bates, M., 2004. River terrace sequences: templates for Quaternary geochronology and marine- terrestrial correlation. Journal of Quaternary Science, 19, 203-218.
Bridgland, D., Westaway, R., 2008. Climatically controlled river terrace staircases: A worldwide Quaternary phenomenon. Geomorphology, 98, 285-315.
Bridgland, D.R., Westaway, R., Romieh, M.A., Candy, I., Daoud, M., Demir, T., Galiatsatos, N., Schreve, D.C., Seyrek, A., Shaw, A.D., White, T.S., Whittaker, J., 2012. The River Orontes in Syria and Turkey: Downstream variation of fluvial archives in different crustal blocks. Geomorphology, 165–166, 25-49.
Brunsden, D., 2001. A critical assessment of the sensitivity concept in geomorphology. Catena, 42, 99-123.
Bull, W.B., 1977. The alluvial-fan environment. Progress in Physical Geography, 1, 222-270.
Bull, W.B., 1979. Threshold of critical power in streams. Geological Society of America Bulletin, 90, 453-464.
Bull, W.B., 1991. Geomorphic Responses to Climate Change. Oxford University Press, Oxford.
Bull, W.B., 2007. Tectonic Geomorphology of Mountains: A New Approach to Paleoseismology. Blackwell Sciences, Oxford.
Burrough, P.A., McDonnell, R., 1998. Principles of GIS. Oxford University Press, London.
Butt, C.R.M., Bristow, A.P.J., 2013. Relief inversion in the geomorphological evolution of sub-Saharan West Africa. Geomorphology, 185(0), 16-26.
Buylaert, J.-P., Murray, A.S., Thomsen, K.J., Jain, M., 2009. Testing the potential of an elevated temperature IRSL signal from K-feldspar. Radiation Measurements, 44, 560-565.

Buylaert, J.-P., Thiel, C., Murray, A.S., Vandenberghe, D.A.G., Yi, S., Lu, H., 2011. IRSL and post-IR IRSL residual doses recorded in modern dust samples from the Chinese Loess Plateau. Geochronology, 38, 432-440.

Buylaert, J.-P., Jain, M., Murray, A.S., Thomsen, K.J., Thiel, C., Sohbati, R., 2012. A robust feldspar luminescence dating method for Middle and Late Pleistocene sediments. Boreas, 41, 435-451.

Cacho, I., Grimalt, J.O., Pelejero, C., Canals, M., Sierro, F.J., Flores, J.A., Shackleton, N. 1999. Dansgaard-Oeschger and Heinrich event imprints in Alboran Sea paleotemperatures. Palaeoceanography, 14, 698-705.

Calderoni, G., Della Seta, M., Fredi, P., Palmieri, E.L., Nesci, O., Savelli, D., Troiani, F., 2010. Late Quaternary geomorphological evolution of the Adriatic coast reach encompassing the Metauro, Cesano and Misa river mouths (northern Marche, Italy). In: Valemsise, G., Pantosi, D. (Eds.), Geology of the Adriatic Area, GeoActa Special Publication, 3, pp. 109-124.

Calvache, M.E., Viseras, C., 1997. Long-term control mechanisms of stream piracy processes in Southeast Spain. Earth Surface Processes and Landforms, 22, 93-105.

Calvo Cases, A., Harvey, A.M., Alexander, R.W., Cantón, Y., Lázaro- Suau, R., Solè-Benet, A., Puigdefábregas, J., 2014. Badlands in the Tabernas Basin, Betic Chain. In: Gutièrrez, F., Gutièrrez, M. (Eds.), Landscape and landforms of Spain. Springer, Netherlands, pp. 197-211

Candy, I., Black, S., Sellwood, B.W., 2004. Interpreting the response of a dryland river system to Late Quaternary climate change. Quaternary Science Reviews, 23, 2513-2523.

Candy, I., Black, S., Sellwood, B.W., 2005. U-series isochron dating of immature and mature calcretes as a basis for constructing Quaternary landform chronologies for the Sorbas basin, southeast Spain. Quaternary Research, 64, 100-111.

Candy, I., Adamson, K., Gallant, C.E., Whitfield, E., Pope, R., 2012. Oxygen and carbon isotopic composition of Quaternary meteoric carbonates from western and southern Europe: Their role in palaoenvironmental reconstruction. Palaeogeography, Palaeoclimatology, Palaeoecology, 326–328, 1-11.

Cantón, Y., Domingo, F., Solé-Benet, A., Puigdefábregas, J., 2001. Hydrological and erosion response of a badlands system in semiarid SE Spain. Journal of Hydrology, 252, 65-84.

Carrión, J.S., Sánchez-Gómez, P., Mota, J.F., Yll, R., Chaín, C., 2003. Holocene vegetation dynamics, fire and grazing in the Sierra de Gádor, southern Spain. The Holocene, 13, 839-849.

Challis, K., 2006. Airborne laser altimetry in alluviated landscapes. Archaeological Prospection, 13, 103-127.

Charlton, R., 2008. Fundamentals of Fluvial Geomorphology. Routledge, Oxon.

Chaplot, V., Darboux, F., Bourennane, H., Leguédois, S., Silvera, N., Phachomphon, K., 2006. Accuracy of interpolation techniques for the derivation of digital elevation models in relation to landform types and data density. Geomorphology 77, 126-141.

Chapman, R.W., Delibes, G., Escoriza, T., Fernandez-Posse, J.L., Lopez Castro, C., Martın Morales, C., Menasanch, M., 1998. Demography and settlement. In: P.V. Castro (Ed.), Aguas Project. Palaeoclimatic Reconstruction and the Dynamics of Human Settlement and Land-use in the Area of the Middle Aguas (Almerıa), in the South-east of the Iberian Peninsula. European Commission Contract Number EV5V-Cf94-0487, Luxembourg, pp. 68–72.

Chen, C., Yue, T., 2010. A method of DEM construction and related error analysis. Computers and Geosciences, 36, 717-725.
Childs, C., 2004. Interpolating surfaces in ArcGIS spatial analyst. ArcUser Magazine, July-September, 32-35.
Cloetingh, S., 1986. Intraplate stresses: a new tectonic mechanism for fluctuations of relative sea level. Geology, 14, 617-620.
Cloetingh, S., Gradstein, F.M., Koo, H., Grant, A.C., Kaminski, M., 1990. Plate reorganization: a cause of rapid late Neogene subsidence and sedimentation around the North Atlantic. J. Geol. Soc. London, 147, 495-506.
Cloetingh, S., Willett, S.D., 2013. TOPO-EUROPE: Understanding of the coupling between the deep Earth and continental topography. Tectonophysics, 602, 1-14
Coleman, J.M., Gagliano, S.M., Webb, J.E., 1964. Minor sedimentary structures in a prograding distributary. Marine Geology, 1, 240-258.
Collins, F.C., Bolstad, P.V., 1996. A comparison of spatial interpolation techniques in temperature estimation. Poster Presentation: Proceedings of the Third International Conference / Workshop on Integrating GIS and Environmental Modeling. National Center for Geographic Information Analysis, Santa Fe, NM, January 21-25,
Coney, P.J., Munoz, J.A., McKlay, K.R., Evenchick, C.A., 1996. Syntectonic burial and post-tectonic exhumation of the Southern Pyrenees foreland fold-thrust bel. J. Geol. Soc. London, 153, 9-16.
Cooper, R.A., Weekes, A.J., 1983. Data, Models and Statistical Aanalysis. Philip Allan, Oxford, UK.
Cordier, S., Harmand, D., Frechen, M., Beiner, M., 2006. Fluvial system response to Middle and Upper Pleistocene climate change in the Meurthe and Moselle valleys (Eastern Paris Basin and Rhenish Massif). Quaternary Science Reviews, 25, 1460-1474
Coulthard, T.J. 2001. Landscape evolution models: a software review. Hydrological Processes, 15, 165-173.
Coulthard, T.J., Macklin, M.G., Kirkby, M.J. 2002. A cellular model of Holocene upland river basin and alluvial fan evolution. Earth Surface Processes and Landforms, 27, 269-288.
Coulthard TJ, Lewin J, MG, M., 2005. Modelling differential catchment response to environmental change. Geomorphology, 69, 222-241.
Coulthard, T.J., Van de Wiel, M.J., 2013. Climate, tectonics or morphology: what signals can we see in drainage basin sediment yields? Earth Surf. Dynam. Discuss., 1, 67-91.
Cunha, P.P., Antunes Martins, A., Daveau, S., Friend, P.F., 2005. Tectonic control of the Tejo river fluvial incision during the late Cenozoic, in Ródão—central Portugal (Atlantic Iberian border). Geomorphology, 64, 271-298.
Cunha, P.P., Martins, A.A., Huot, S., Murray, A., Raposo, L., 2008. Dating the Tejo river lower terraces in the Ródão area (Portugal) to assess the role of tectonics and uplift. Geomorphology, 102, 43-54.
Dabrio, C.J., 2009. Fan-Delta Facies Associations in Late Neogene and Quaternary Basins of Southeastern Spain. In: Colella, A., Prior, D. (Eds.), Coarse-Grained Deltas. Special Publication, IAS, 10, pp. 91-111.
Daniels, M.J., 2008. Distinguishing allogenic from autogenic causes of bed elevation change in late Quaternary alluvial stratigraphic records. Geomorphology, 101, 159-171.
Dansgaard, W., Johnsen, S.J., Clausen, H.B., Dahl-Jensen, D., Gundestrup, N.S., Hammer,C.U., Hvidberg, C.S., Steffensen, J.P., Sveinbjörnsdottir, A.E., Jouzel, J.,

Bond,G.C., 1993. Evidence for general instability of past climate from a 250-kyr ice-core record. Nature, 364, 218-220.
De Jong, K., Bakker, H.E., 1991. The Mulhacen and Alpujarride Complex in the Sierra de los Filabres, SE Spain: lithostratigraphy. Geol. Mijnbouw, 70, 93-103.
De Larouzière, F., Bolze, J., Bordet, P., Hernandez, J., Montenat, C., Ott d'Estevou, P., 1988. The Betic segment of the lithospheric Trans-Alboran shear zone during the Late Miocene. Tectonophysics, 152(1), 41-52.
De Vicente, G., Vegas, R., 2009. Large-scale distributed deformation controlled topography along the western Africa–Eurasia limit: Tectonic constraints. Tectonophysics, 474(1–2), 124-143
Delgado, C. L., Pascual Molina, A., Ruiz Bustos, A., 1993. Geology and Micromammals of the Serra 1 Site (Tabernas Basin, Betic Cordillera). Estudios Geol, 49, 361-366.
Della Seta, M., Fredi, P., Lupia Palmieri, E., Nesci, O., Savelli, D., Troiani, F., 2005. River terraces in the Fiume Tronto drainage basin: a contribution to morphotectonic investigations. Geografia Fisica e Dinamica Quaternaria, Suppl. VII, pp. 123-135.
Della Seta, M., Del Monte, M., Fredi, P., Miccadei, E., Nesci, O., Pambianchi, G., Piacentini, T., Troiani, F., 2008. Morphotectonic evolution of the Adriatic piedmont of the Apennines: an advancement in the knowledge of the Marche-Abruzzo border area. Geomorphology 102, 119-129.
Díaz-Hernández, J.L., Juliá, R., 2006. Geochronological position of badlands and geomorphological patterns in the Guadix–Baza basin (SE Spain). Quaternary Research, 65, 467-477.
Duller, G.A.T., 2003. Distinguishing quartz and feldspar in single grain luminescence measurements. Radiation Measurements, 37, 161-165.
Duller, G.A.T., 2008a. Luminescence Dating:guidelines on using luminescence dating in archaeology. English Heritage, Swindon.
Duller, G.A.T., 2008b. Single-grain optical dating of Quaternary sediments: why aliquot size matters in luminescence dating. Boreas, 37, 589-612.
Duller, G.A.T., Wintle, A.G., 2012. A review of the thermally transferred optically stimulated luminescence signal from quartz for dating sediments. Quaternary Geochronology, 7, 6-20.
Durán Zuazo, V.H., Rodríguez Pleguezuelo, C.R. 2009. Soil-erosion and runoff prevention by plant covers: a review. In: Lichtfouse E, Navarrete M, Debaeke P (Eds).Soil-Erosion and Runoff Prevention by Plant Covers: A Review. Springer, Netherlands, pp. 785-811.
Eberly, S., Swall, J., Holland, D., Cox, B., Baldridge, E., 2004. Developing Spatially Interpolated Surfaces and Estimating Uncertainty. U.S Environmental Protection Agency Report EPA-454/R-04-004, New York, 159 pp.
Egeler, C.G., Simon, O.J., 1969. Orogenic evolution of the Betic Zone (Betic Cordilleras, Spain), with emphasis on nappe structures. Geol. Mijnbouw, 48, 296-305.
Eyles, N., Eyles, C.H., Miall, A.D., 1983. Lithofacies types and vertical profile models; an alternative approach to the description and environmental interpretation of glacial diamict and diamictite sequences. Sedimentology, 30, 393-410.
Eriksson, M.G., Olley, J.M., Kilham, D.R., Pietsch, T., Wasson, R.J., 2006. Aggradation and incision since the very late Pleistocene in the Naas River, south-eastern Australia. Geomorphology, 81, 66-88.

Fabres, J., Calafat, A., Sanchez-Vidal, A., Canals, M., Heussner, S. 2002. Composition and spatio-temporal variability of particle fluxes in the Western Alboran Gyre, Mediterranean Sea. Journal of Marine Systems, 33, 431-456

Fisher, N.I., Lewis, T., Embleton, B.J.J., 1987. Statistical Analysis of Spherical Data. Cambridge University Press, Cambridge.

Fletcher, W.J, Sánchez Goñi, M.F. 2008. Orbital-and sub-orbital-scale climate impacts on vegetation of the western Mediterranean basin over the last 48,000 yr. Quaternary Research, 70, 451-464

Fletcher, W.J., Sánchez Goñi, M.F., Allen, J.R., Cheddadi, R., Combourieu-Nebout, N., Huntley, B., Lawson, I., Londeix, L., Magri, D., Margari, V. 2010. Millennial-scale variability during the last glacial in vegetation records from Europe. Quaternary Science Reviews, 29, 2839-2864

Francis, C.F., Thornes, J. 1990. Runoff hydrographs from three Mediterranean vegetation cover types. In: Francis, C.F. (Ed). Vegetation and Erosion: Processes and Environments. British Geomorphological Research Group Symposia Series, London, pp 365-384.

Frechen, M., Ellwanger, D., Hinderer, M., Lämmermann-Barthel, J., Neeb, I., Techmer, A., 2010. Late Pleistocene fluvial dynamics in the Hochrhein Valley and in the Upper Rhine Graben: chronological frame. International Journal of Earth Sciences, 99, 1955-1974.

Frye, J.C., Leonard, A.R., 1954. Some problems of alluvial terrace mapping. American Journal of Science, 252, 242-251.

Fryirs, K.A., Brierley, G.J., Preston, N.J., Kasai, M., 2007. Buffers, barriers and blankets: The (dis)connectivity of catchment-scale sediment cascades. Catena, 70, 49-67.

Galbraith, R.F., Roberts, R.G., 2012. Statistical aspects of equivalent dose and error calculation and display in OSL dating: An overview and some recommendations. Quaternary Geochronology, 11, 1-27.

García, A.F., 2001. Quaternary stream incision and topographic development in the eastern Alpujarran Corridor, Betic Cordillera, southern Spain (Almería). The University of California, Santa Barbara, USA, PhD thesis.

García, A.F., Zhu, Z., Ku, T.L., Sanz de Galdeano, C., Chadwick, O.A., Chacón Montero, J., 2003. Tectonically driven landscape development within the eastern Alpujarran Corridor, Betic Cordillera, SE Spain (Almería). Geomorphology, 50, 83-110.

García, A.F., Zhu, Z., Ku, T.L., Chadwick, O.A., Chacón Montero, J., 2004. An incision wave in the geologic record, Alpujarran Corridor, southern Spain (Almería). Geomorphology, 60, 37-72.

Garcia-Castellanos, D., Vergés, J., Gaspar-Escribano, J., Cloetingh, S., 2003. Interplay between tectonics, climate, and fluvial transport during the Cenozoic evolution of the Ebro Basin (NE Iberia). Journal of Geophysical Research: Solid Earth, 108, 2347-2353.

Geach, M.R., Stokes, M., Telfer, M.W., Mather, A.E., Fyfe, R.M., Lewin, S., 2014a. The application of geospatial interpolation methods in the reconstruction of Quaternary landform records. Geomorphology, 216, 234-246.

Geach, M.R., Thomsen, K.J., Buylaert, J-P., Murray, A.S. 2014b. A chronological framework for the Quaternary landform records of the Tabernas Basin, SE Spain. Poster presented at the 14th Luminescence and Electron Spin Resonance Dating conference, Montreal, Canada.

Geach, M.R., Viveen, W., Mather, A.E. , Telfer, M.W., Fletcher, W.J., Stokes, M. (In review). An integrated field and numerical modelling study of controls on Late Quaternary fluvial landscape development (Tabernas, SE Spain). Earth Surface Processes and Landforms.

Giaconia, F., Booth-Rea, G., Martinez-Martinez, J.M., Azanon, J.M., Perez-Pena, J.V., Perez-Romero, J., Villegas, I., 2012. Geomorphic evidence of active tectonics in the Sierra Alhamilla (eastern Betics, SE Spain). Geomorphology, 145, 90-106.

Gibbard, P.L., Lewin, J., 2003. The history of the major rivers of southern Britain during the Tertiary. Journal of the Geological Society, 160, 829–845.

Gibbard, P.L., Lewin, J., 2009. River incision and terrace formation in the Late Cenozoic of Europe. Tectonophysics, 474, 41-55.

Gile, L.H., Petersen, F.F., Grossman, R.B., 1966. Morphological and genetic sequences of carbonate accumulation in desert soils. Soil Science, 101, 347-360.

Gómez-Pugnaire, M.T., 2001. The basement geology of the Almeria Province. In: Mather, A.E., Martin, J.M., Harvey, A.M., Braga, J.C. (Eds.), A Field Guide to the Neogene Sedimentary Basins of the Almeria Province, SE Spain. Blackwell Science, Oxford, pp. 33 ‑ 58

Gómez-Pugnaire, M.T., Franz, G., Sánchez-Vizcaino, V.L., 1994. Retrograde formation of NaCl-scapolite in high pressure metaevaporites from the Cordilleras Béticas (Spain). Contr. Mineral. and Petrol., 116(4), 448-461.

Gómez-Pugnaire, M.T., Rubatto, D., Fernández-Soler, J.M., Jabaloy, A., López-Sánchez-Vizcaíno, V., González-Lodeiro, F., Galindo-Zaldívar, J., Padrón-Navarta, J.A., 2012. Late Variscan magmatism in the Nevado-Filábride Complex: U-Pb geochronologic evidence for the pre-Mesozoic nature of the deepest Betic complex (SE Spain). Lithos, 146–147, 93-111.

Gómez-Orellana L, Ramil-Rego P, Muñoz Sobrino C. 2007. The Würm in NW Iberia, a pollen record from area Longa (Galicia). Quaternary Research, 67, 438-452

González-Ramón A, Andreo B, Ruiz-Bustos A, Richards DA, López-Sáez JA, Alba-Sánchez F. 2012. Late Quaternary paleoenvironmental record from a sedimentary fill in Cucú cave, Almería, SE Spain. Quaternary Research, 77, 264-272

Gorum, T., Gonencgil, B., Gokceoglu, C., Nefeslioglu, H.A., 2008. Implementation of reconstructed geomorphologic units in landslide susceptibility mapping: the Melen Gorge (NW Turkey). Natural Hazards, 46, 323-351.

Graziano, A., Raulin, M., 1989. Research Methods: A Process of Inquiry. HarperCollins, New York.

Griffiths, J.S., Mather, A.E., Hart, A.B., 2002. Landslide susceptibility in the Río Aguas catchment, SE Spain. Quarterly Journal of Engineering Geology and Hydrogeology, 35, 9-17.

Grootes, P.M., Stuiver, M., White, J.W.C., Johnsen, S.J., 1993. Comparison of oxygen isotope records from the GISP2 and GRIP Greenland ice cores. Nature, 366, 552-554.

Guérin, G., Mercier, N., Adamiec, G., 2011. Dose-rate conversion factors: update. Ancient TL, 29, 5-8.

Guérin, G., Mercier, N., Nathan, R., Adamiec, G., Lefrais, Y., 2012. On the use of the infinite matrix assumption and associated concepts: A critical review. Radiation Measurements, 47, 778-785.

Hack, J.T., S, 1957. Studies of longitudinal stream profiles in Virginia and Maryland, U.S. U.S. Geol. Surv. Professional Paper .294-B, 97.
Haberlandt, U., 2007. Geostatistical interpolation of hourly precipitation from rain gauges and radar for a large-scale extreme rainfall event. Journal of Hydrology, 332, 144-157.
Haines-Young, R.H., Petch, J.R., 1986. Physical geography: its nature and methods. Harper & Row, London.
Hartkamp, A.D., De Beurs, K., Stein. A, White, J.W., 1999. Interpolation Techniques for Climate Variables. NRG-GIS Series Report 99-01, CIMMYT, Mexico, 26 pp.
Harvey, A.M., 1984. Debris flows and fluvial deposits in Spanish Quaternary alluvial fans: implications for fan morphology. In: Koster, E.H., Steel, R.J., (Eds.), Sedimentology of Gravels and Conglomerates, Canadian Society of Petroleum Geologists, Calgary, pp. 123-132.
Harvey, A.M., 1987. Patterns of Quaternary Aggradation and Dissectional Landform Development in the Almería Region, southeast Spain: a dry-region, tectonically active landscape. Die Erde, 188, 193-215.
Harvey, A.M., 1990. Factors influencing Quaternary alluvial fan development in southeast Spain. In: Rachocki, A.H., Church, M. (Eds.), Alluvial Fans: A Field Approach. Wiley, Chichester, pp. 247–269.
Harvey, A.M., 1996. The role of alluvial fans in mountain fluvial systems of southeast Spain: implications of climatic change. Earth Surface Processes and Landforms, 21, 543-553.
Harvey, A.M., 2002. The relationships between alluvial fans and fan channels within Mediterranean mountain fluvial systems. In: Bull, L.J., Kirkby, M.J. (Eds.), Dryland Rivers: Hydrology and Geomorphology of Semi-arid Channels. John Wiley & Sons Ltd., Chichester, UK, pp. 205-226.
Harvey, A.M., 2007. High sinuosity bedrock channels: response to rapid incision - examples in SE Spain. Revista C&G, 21, 21-47.
Harvey, A.M., 2011. Dryland Alluvial Fans. In: D.S.G. Thomas (Ed.), Arid Zone Geomorphology. John Wiley & Sons, Oxford, UK, pp. 333-371.
Harvey, A.M., Wells, S.G., 1987. Response of Quaternary fluvial systems to differential epeirogenic uplift: Aguas and Feos river systems, southeast Spain. Geology, 15, 689-693.
Harvey, A.M., Miller, S.Y., Wells, S.G.,1995. Quaternary soil and river terrace sequences in the Aguas/Feos river system. In: Lewin, J., Macklin, M.G., Woodward, J.C. (Eds.) Mediterranean Quaternary River Environments.Balkema, Rotterdam, pp. 263–281.
Harvey, A.M., Foster, G., Hannam, J., Mather, A.E., 1999. Mineral magnetic characteristics of the soils and sediments of the Tabernas alluvial and ‘‘lake’’ system. In: Mather, A.E., Stokes, M., (Eds.), BSRG/BGRG SE Spain Field Meeting Guide Book, University of Plymouth, pp. 43– 61.
Harvey, A.M., Foster, G., Hannam, J., Mather, A.E., 2003. The Tabernas alluvial fan and lake system, southeast Spain: applications of mineral magnetic and pedogenic iron oxide analyses towards clarifying the Quaternary sediment sequences. Geomorphology, 50, 151-171.
Haughton, P.D.W., 2000. Evolving turbidite systems on a deforming basin floor, Tabernas, SE Spain. Sedimentology, 47, 497-518.
Haughton, P.D.W., 2001. Tectonics and sedimentation: the evolving turbidite systems of the Tabernas basin. In: Mather, A.E., Martin, J.M., Harvey, A.M., Braga, J.C. (Eds.), A

Field Guide to the Neogene Sedimentary Basins of the Almeria Province, SE Spain. Blackwell Sciences, Oxford, pp. 89-115.
Helmers, H., Voet, H.W., 1967. Regional extension of Nevado-Filabride Nappes in eastern and central Sierra de los Filabres (Betic Cordilerras, SE Spain). Proceedings of the Koninklije Nederlandse Akademie Van Wetenschappen Series B- Physical Sciences, 70, 239-245.
Heritage, G.L., Milan, D.J., Large, A.R.G., Fuller, I.C., 2009. Influence of survey strategy and interpolation model on DEM quality. Geomorphology 112, 334-344.
Hitchcock, E., 1824. Remarks on the geology of the district adjoining the Erie Canal. In: E. Amos (Ed.), A geological and agricultural survey of the district adjoining the Erie Canal in the State of New York; taken under the direction of the Hon. Stephen Van Rensselaer; Part I, Containing a description of the rock formations together with a geological profile extending from the Atlantic to Lake Erie. Packard and van Benthuysen, Albany, NY, pp. 158 -163.
Hodge, E.J., Richards, D.A., Smart, P.L., Ginés, A., Mattey, D.P., 2008. Sub-millennial climate shifts in the western Mediterranean during the last glacial period recorded in a speleothem from Mallorca, Spain. Journal of Quaternary Science, 23, 713-718.
Hodgson, D.M., Haughton, P.D.W., 2004. Impact of syndepositional faulting on gravity current behaviour and deep-water stratigraphy: Tabernas-Sorbas Basin, SE Spain. In: Lomas, S., Joseph, P. (Eds.), Confined Turbidites Systems, Geological Society, London, Special Publications, 222, pp. 135 – 152
Hogg, S.E., 1982. Sheetfloods, sheetwash, sheetflow, or ... ? Earth-Science Reviews, 18, 59-76.
Hsu, K.J., Montadert, L., Bernoulli, D., Cita, M.B., Erickson, A., Garrusib, R.E., Melieres, F., Muller, C., Wright, R., 1977. History of the Mediterranean salinity Crisis. Nature, 267, 399–403.
Huntley, D.J., Godfrey-Smith, D.I., Thewalt, M.L.W., 1985. Optical dating of sediments. Nature, 313, 105-107.
Huntley, D.J., Baril, M.R., 1997. The K content of the K-feldspars being measured in optical dating or in thermoluminescence dating. Ancient TL, 15, 11–13.
Huntley, D.J., Hancock, R.G.V., 2001. The Rb contents of the K-feldspar grains being measured in optical dating. Ancient TL, 19, 43-46.
Huntley, D.J., Lamothe, M., 2001. Ubiquity of anomalous fading in K-feldspars and the measurement and correction for it in optical dating. Canadian Journal of Earth Sciences, 38, 1093-1106.
Ilott, S.H., 2013. Cosmogenic dating of fluvial terraces in the Sorbas basin, SE Spain. University of Plymouth, PhD Thesis.
Isaacs, E.H., Srivastava, M., 1989. An Introduction to Applied Geostatistics. Oxford University Press, Oxford.
Jain, M., Murray, A.S., Bøtter-Jensen, L., 2003. Characterisation of blue-light stimulated luminescence components in different quartz samples: implications for dose measurement. Radiation Measurements, 37, 441-449.
Jain, M., Ankjærgaard, C., 2011. Towards a non-fading signal in feldspar: Insight into charge transport and tunnelling from time-resolved optically stimulated luminescence. Radiation Measurements, 46, 292-309.

Jones, A.P., 1999. Background the sedimentary facies. In: Jones, A.P., Tucker, M.E., Hart, J.K. (Eds.), Technical Guide Number 7: The description and analysis of Quaternary stratigraphic field sections. Quaternary Research Association, London, pp 1- 18

Jones, S.J., 2002. Transverse rivers draining the Spanish Pyrenees: large scale patterns of sediment erosion and deposition. In Jones, S.J., Frostick, L.E. (Eds.), Sediment Flux to Basins: Causes, Controls and Consequences. Geological Society, London, Special Publications, 191,pp. 171-185.

Jones, S.J., Frostick, L.E., Astin, T.R., 1999. Climatic and tectonic controls on fluvial incision and aggradation in the Spanish Pyrenees. J. Geol. Soc., 156, 761-769.

Kelly, M., Black, S., Rowan, J.S., 2000. A calcrete-based U/Th chronology for landform evolution in the Sorbas basin, southeast Spain. Quaternary Science Review, 19, 995-1010.

Knight, J., Wishart, W.A., Rose, J., 2011. Geomorphological field mapping. In: Smith, M., Paron, P., Griffiths, J.S. (Eds.), Geomorphological mapping methods and applications, Elsevier, Oxford, pp. 151-180.

Kravchenko, A.N., 2003. Influence of spatial structure on accuracy of interpolation methods. Soil Sci. Soc. Am. J., 67, 1564-1571.

Krijgsman, W., Fortuin, A.R., Hilgen, F.J., Sierro, F.J., 2001. Astrochronology for the Messinian Sorbas basin (SE Spain) and orbital (precessional) forcing for evaporite cyclicity. Sedimentary Geology, 140, 43-60.

Lane, E.W., 1955. The importance of fluvial morphology in hydraulic engineering. American Society of Civil Engineers Proceedings, 81, 1-17.

Larouzière, F.D., Bolze, J., Bordet, P., Hernandez, J., Montenat, C., Ott d'Estevou, P. 1988. The Betic segment of the lithospheric Trans-Alboran shear zone during the Late Miocene. Tectonophysics, 152, 41-52.

Lázaro, R., Rey, J.M., 1990. Sobre el clima de la provincia de Almería (SE Ibérico): primer ensayo de cartografía automática de medias annuals de temperatura y precipitación. Suelo y Planta, 1, 61-68.

Lazzaro, D., Montefusco, L.B., 2002. Radial basis functions for the multivariate interpolation of large scattered data sets. Journal of Computational and Applied Mathematics, 140, 521-536.

Lee, E.M., 2001. Geomorphological mapping. In: J.S. Griffiths (Ed.), Land Surface Evaluation for Engineering Practice, Geological Society, London, Engineering Geology Special Publications, 18, pp. 53 – 56

Leopold, L.B., Wolman, M.G., Miller, J.P., 1964. Fluvial Processes in Geomorphology. Freeman, San Francisco

Leopold, L.B., Bull, W.B., 1979. Base level, aggradation, and grade. Proceedings of the American Philosophical Society, Vol. 123, No. 3, pp.168-202.

Lesley, J.P., 1878. On terrace levels in Pennsylvania. American Journal of Science, 16, 68-69.

Lewin, J., Macklin, M.G., 2003. Preservation potential for Late Quaternary river alluvium. Journal of Quaternary Science, 18, 107-120.

Lewin, J., Gibbard, P.L., 2010. Quaternary river terraces in England: Forms, sediments and processes. Geomorphology, 120, 293-311.

Lewis, C.J., McDonald, E.V., Sancho, C., Peña, J.L., Rhodes, E.J., 2009. Climatic implications of correlated Upper Pleistocene glacial and fluvial deposits on the Cinca

and Gállego Rivers (NE Spain) based on OSL dating and soil stratigraphy. Global and Planetary Change, 67, 141-152.
Lewis, S.G., Maddy, D., 1999. Description and analysis of Quaternary fluvial sediments: A case study from the upper River Thames, UK. In: Jones, A.P., Tucker, M.E., Hart, J.K. (Eds.), Technical Guide Number 7: The description and analysis of Quaternary stratigraphic field sections. Quaternary Research Association, London, pp. 111-135.
Lézine, A-M., Denèfle, M. 1997. Enhanced anticyclonic circulation in the eastern North Atlantic during cold intervals of the last deglaciation inferred from deep-sea pollen records. Geology, 25, 119-122.
Li, B., Li, S.-H., Wintle, A., 2008. Overcoming Environmental Dose Rate Changes in Luminescence Dating of Waterlain Deposits. Geochronometia, 30, 33–40.
Li, B., Li, S.-H., 2011. Thermal stability of infrared stimulated luminescence of sedimentary K-feldspar. Radiation Measurements, 46, 29-36.
Li, J., Heap, A.D., 2011. A review of comparative studies of spatial interpolation methods in environmental sciences: performance and impact factors. Ecological Informatics, 6, 228-241.
Li, B., Jacobs, Z., Roberts, R.G., Li, S.-H., 2013. Extending the age limit of luminescence dating using the dose-dependent sensitivity of MET-pIRIR signals from K-feldspar. Quaternary Geochronology, 17, 55-67.
Lisiecki, L. E., & Raymo, M. E., 2004. A Pliocene Pleistocene stack of 57 globally distributed benthic δ18O records. Palaeoceanography, 20,1-17
Liritzis, I., Singhvi, A.K., Feathers, J.K., Wagner, G.A., Kadereit, A., Zacharias, N., Li, S.-H., 2013. Luminescence Dating in Archaeology, Anthropology, and Geoarchaeology: An Overview. Springer Briefs In Earth System Sciences. Springer, London.
Litchfield, N.J., Berryman, K.R., 2005. Correlation of fluvial terraces within the Hikurangi Margin, New Zealand: implications for climate and baselevel controls. Geomorphology, 68, 291-313.
López Sánchez-Vizcaino, V., 1994. Evolución petrológica y geoquímica de las rocas carbonáticas en el área de Macaèl-Cóbdar, Complejo Nevado-Filábride, SE España., University of Granada, Spain, PhD Thesis.
Lu, G.Y., Wong, D.W., 2008. An adaptive inverse-distance weighting spatial interpolation technique. Computers and Geosciences, 34, 1044-1055.
Machette, M.N., 1985. Calcic soils of the southwestern United States. In: Weide, D.L. (Ed.), Soils and Quaternary Geology of the Southwestern United States Geological Society of America. Special Paper, 203, pp. 1– 21.
Mackey, S.D., Bridge, J.S., 1995. Thrre-dimensional model of alluvial stratigraphy: theory and application. Journal of Sedimentary Research, 65, 7 - 31.
Macklin, M.G., Lewin. J., Woodward, J.C., 1995. Quaternary fluvial systems in the Mediterranean. In: Lewin, J., Macklin, M.G., Woodward, J.C. (Eds.), Mediterranean River Environments. Balkema, Rotterdam, pp. 1 ‑ 25
Macklin, M.G., Fuller, I.C., Lewin. J., Maas, G.S., Passmore, D.G., Rose, J., Woodward, J.C., Black, S., Hamlin, R.H.B., Rowan, J.S., 2002. Correlation of fluvial sequences in the Mediterranean basin over the last 200 ka and their relationship to climate change. Quaternary Science Review, 21, 1633-1641.
Macklin, M.G., Lewin, J., 2008. Alluvial responses to the changing Earth system. Earth Surface Processes and Landforms, 33, 1374-1395.

Maddy, D., 1997. Uplift-driven valley incision and river terrace formation in southern England. Journal of Quaternary Science, 12, 539-545.
Maddy, D., Bridgeland, D.R., 2000. Accelerated uplift resulting from Anglian glacioisostatic rebound in the Middle Thames Valley, UK?: evidence from the river terrace record. Quaternary Science Reviews, 19, 1581-1588.
Maddy, D., Bridgland, D., Westaway, R., 2001. Uplift-driven valley incision and climate-controlled river terrace development in the Thames Valley, UK. Quaternary International, 79, 23-36.
Magaldi, D., Tallini, M., 2000. A micromorphological index of soil development for the Quaternary geology research. Catena, 41, 261-276.
Maher, E., 2005. The Quaternary evolution of the Rio Alias southeast Spain, with emphasis on sediment provenance. University of Liverpool, PhD Thesis.
Maher, E., 2007. The impact of a major Quaternary river capture on the alluvial sediments of a beheaded river system, the Río Alias SE Spain. Geomorphology, 84, 344-356.
Maher, E., Harvey, A.M., 2008. Fluvial system response to tectonically induced base-level change during the late-Quaternary: The Río Alias southeast Spain. Geomorphology, 100, 180-192.
Maizels, J.K., 1989. Sedimentology and palaeohydrology of Holocene flood deposits in front of a jökulhlaup glacier, South Iceland. In: Bevan, K., Carling, P. (Eds.), Floods. Hydrological, Sedimentological and Geomorphological Implications: an Overview. John Wiley & Sons, New York, pp. 239–253
Maldonado Cabrera, G., Molina Gonzalec, F., Hernandez, F.A., Camara Serrano, J.A., Gonzalez, V.M., Ruiz Sanchez, V., 1991. The social role of the Megaliths in the Southeast of the Iberian Península. The megalithic communities from "Tabernas" corridor. CuAo. PREH. GR., 16-17, 167-190.
Maldonado, A., Somoza, L.s., Pallarés, L., 1999. The Betic orogen and the Iberian–African boundary in the Gulf of Cadiz: geological evolution (central North Atlantic). Marine Geology, 155, 9-43.
Mardikis, M.G., Kalivas, D.P., Kollias, V.J., 2005. Comparison of interpolation methods for the prediction of reference evapotranspiration-an application in Greece. Water Resources Management 19, 251-278.
Martrat, B., Jimenez, P., Zahn, R., Grimalt, J.O. 2012. Sea surface temperatures, alkenones and sedimentation rates at the Alboran basin. In Supplement to: Martrat, B; Jimenez, A.P., Zahn, R., Grimalt, J. O. (2014): Similarities and dissimilarities between the last two deglaciations and interglaciations in the North Atlantic region. Quaternary Science Reviews, 99, 122-134
Martín-Serrano, A., 1991. La definición y el encajamiento de la red fluvial actual sobre el Macizo Hesérico en el marco de su geodinámica alpina. Revista de la Sociedad Geológica de Espana, 4, 337–351.
Martínez-Martínez, J., Azañón, J., 1997. Mode of extensional tectonics in the southeastern Betics (SE Spain): Implications for the tectonic evolution of the peri-Alborán orogenic system. Tectonics, 16, 205-225.
Maslin, M., Seidov, D., Lowe, J. , 2001. Synthesis of the nature and causes of rapid climate transitions during the Quaternary. In: Seidov, D , Haupt, B.J., Maslin, M. (Eds.), Oceans and Rapid Climate Change: Past, Present and Future. Geophysical Monograph- EGU, pp. 9-51.
Mather, A.E., 1991. Late Cenozoic drainage evolution of the Sorbas Basin, southeast Spain, University of Liverpool, Unpublished PhD Thesis.

Mather, A.E., 1993. Basin inversion: some consequences for drainage evolution and alluvial architecture. Sedimentology, 40, 1069-1089.
Mather, A.E., 1999. Alluvial Fans: a case study from the Sorbas Basin, Southeast Spain. In: Jones, A.P., Tucker, M.E., Hart, J.K. (Eds.), Technical Guide Number 7: The description and analysis of Quaternary stratigraphic field sections. Quaternary Research Association, London, pp. 77-110.
Mather, A.E., 2000. Adjustment of a drainage network to capture induced base-level change: an example from the Sorbas Basin, SE Spain. Geomorphology, 34, 271-289.
Mather, A.E., 2009. Tectonic setting and landscape development. In: J.C. Woodward (Ed.), The Physical Geography of the Mediterranean. Oxford University Press, Oxford, pp. 5- 32.
Mather, A.E., Westhead, K., 1993. Plio/Quaternary strain of the Sorbas Basin, SE Spain: evidence from soft sediment deformation structures. Quaternary Proceedings, 3, 57-65.
Mather, A.E., Harvey, A.M., 1995. Controls on drainage evolution in the Sorbas Basin, southeast Spain. In: Lewin, J., Macklin, M.G., Woodward, J.C. (Eds.), Mediterranean Quaternary River Environments. A.A.Balkema, Rotterdam, pp. 65-76.
Mather, A.E., Stokes, M., 1999. Pleistocene travertines and lakes of Tabernas: evidence for a wetter climate? In: Mather, A.E., Stokes, M. (Eds.), BSRG/BGRG SE Spain field meeting. University of Plymouth Field Guide, pp. 63-71.
Mather, A.E., Harvey, A.M., Stokes, M., 2000. Quantifying long-term catchment changes of alluvial fan systems. Geological Society of America Bulletin, 112, 1825-1833.
Mather, A.E., Stokes, M., Griffiths, J.S., 2002. Quaternary Landscape Evolution: A Framework for Understanding Contemporary Erosion, SE Spain. Land Degradation & Development, 13, 89-109.
Matoshko, A., Gozhik, P., Danukalova, G., 2004. Key Late Cenozoic fluvial archives of eastern Europe: the Dniester, Dnieper, Don and Volga. Proceedings of the Geologists' Association, 115, 141-173.
Merritts, D.J., Vincent, K.R., Wohl, E.E., 1994. Long river profiles, tectonism, and eustasy: A guide to interpreting fluvial terraces. Journal of Geophysical Research: Solid Earth, 99,14031-14050.
Miall, A.D., 1990. Principles of sedimentary basin analysis. Springer-Verlag, New York.
Miall, A.D., 1996. The Geology of fluvial deposits. Springer Verlag, Berlin.
Miekle, C.D., 2008. The Pleistocene Drainage Evolution of the Río Almanzora, Vera Basin, SE Spain. Newcastle University, PhD Thesis.
Montenat, C.H., D'estevou, P.O., 1996. Late Neogene basins evolving in the Eastern Betic transcurrent fault zone: an illustrated review. In: Friend, P.F., Dabrio, C.J. (Eds.), Tertiary Basins of Spain: The Stratigraphic Record of Crustal Kinematic. Cambridge University Press, Cambridge, pp. 372-386
Moreno, A., Cacho, I., Canals, M., Grimalt, J.O., Sánchez-Goñi, M.F., Shackleton, N., Sierro, F.J., 2005. Links between marine and atmospheric processes oscillating on a millennial time-scale. A multi-proxy study of the last 50,000 yr from the Alboran Sea (Western Mediterranean Sea). Quaternary Science Reviews, 24, 1623-1636.
Murray, A.S., Roberts, R.G., 1998. Measurement of the equivalent dose in quartz using a regenerative-dose single-aliquot protocol. Radiation Measurements, 29, 503-515.
Murray, A.S., Wintle, A.G., 2000. Luminescence dating of quartz using an improved single aliquot regenerative-dose protocol. Radiation Measurements, 32, 57-73.

Murray, A., Wintle, A., 2003. The single aliquot regenerative dose protocol: potential for improvements in reliability. Radiation Measurements, 37, 377-381.
Murray, A.S., Thomsen, K.J., Masuda, N., Buylaert, J.P., Jain, M., 2012. Identifying well-bleached quartz using the different bleaching rates of quartz and feldspar luminescence signals. Radiation Measurements, 47, 688-695.
Myers, D.E., 1994. Spatial interpolation: an overview. Geoderma, 62, 17-28.
Nalder, I.A., Wein, R.W., 1998. Spatial interpolation of climatic normals: test of a new method in the Canadian boreal forest. Agricultural and Forest Meteorology, 92, 211-225.
Nash, D.J., Smith, R.F., 1998. Multiple calcrete profiles in the Tabernas Basin, SE Spain: Their origins and geomorphic implications. Earth Surface Processes and Landforms, 23, 1009-1029.
Nash, D.J., Smith, R.F., 2003. Properties and development of channel calcretes in a mountain catchment, Tabernas Basin, southeast Spain. Geomorphology, 50, 227-250.
Nathan, R.P., Mauz, B., 2008. On the dose-rate estimate of carbonate-rich sediments for trapped charge dating. Radiation Measurements, 43, 14-25.
Naughton, F., Sanchez Goni, M., Desprat, S., Turon, J-L., Duprat, J., Malaizé, B., Joli, C., Cortijo, E., Drago, T., Freitas, M. 2007. Present-day and past (last 25000 years) marine pollen signal off western Iberia. Marine Micropaleontology, 62, 91-114
Nebout, N.C., Turon, J.L., Zahn, R., Capotondi, L., Londeix, L., Pahnke, K. 2002. Enhanced aridity and atmospheric high-pressure stability over the western Mediterranean during the North Atlantic cold events of the past 50 k.y. Geology, 30, 863-866.
Nemec, W., Steel, R.J., 1984. Alluvial and coastal conglomerates: their significant features and some comments on gravely mass-flow deposits. In: Koster, E.H., Steel, R.J., (Eds.), Sedimentology of Gravels and Conglomerates, Canadian Society of Petroleum Geologists, Calgary, pp. 1-31.
Nichols, G.J., Hirst, P.J., 1998. Alluvial Fans and Fluvial Distributary Systems, Oligo-Miocene, Northern Spain: Contrasting Processes and Products. Journal of Sedimentary Research, 68, 879-889.
Nogueras, P., Burjachs, F., Gallart, F., Puigdefábregas, J., 2000. Recent gully erosion in the El Cautivo badlands (Tabernas, SE Spain). Catena, 40, 203-215.
North American Commission on Nomenclature. 2005. North American Stratigraphic Code. The American Association of Petroleum Geologists Bulletin, 89, 1547-1591.
Oliver, M.A., 1990. Kriging: a method of interpolation for geographical information systems. International Journal of Geographic Information Systems, 4, 313-332.
Olley, J.M., Murray, A., Roberts, R.G., 1996. The effects of disequilibria in the Uranium and Thorium decay chains on burial dose rates in fluvial sediments. Quaternary Science Review, 15, 751-760.
Omodeo Salé, S., Gennari, R., Lugli, S., Manzi, V., Roveri, M., 2012. Tectonic and climatic control on the Late Messinian sedimentary evolution of the Nijar Basin (Betic Cordillera, Southern Spain). Basin Research, 24, 314-337.
Ortiz, J.E., Torres, T., Delgado, A., Julià, R., Lucini, M., Llamas, F.J., Reyes, E., Soler, V., Valle, M., 2004. The palaeoenvironmental and palaeohydrological evolution of Padul Peat Bog (Granada, Spain) over one million years, from elemental, isotopic and molecular organic geochemical proxies. Organic Geochemistry, 35, 1243-1260.
Parkash, B., Awasthi, A., Gohain, K., 2009. Lithofacies of the Markanda terminal fan, Kurukshetra district, Haryana, India. In: Collinson, J.D., Lewin, J. (Eds.), Modern and

Ancient Fluvial Systems, Spec. Publ. Cambridge University Press, Cambridge, pp. 337-344
Parker, A., 2001. A palaeoenvironmental investigation of Quaternary lake sediments in the Tabernas Basin, SE Spain. University of Plymouth. MRes Thesis.
Pazzaglia, F.J., Gardner, T.W., Merritts, D.J., 1998. Bedrock fluvial incision and longitudinal profile development over geologic time scales determined by fluvial terraces. In: Tinkler, K.J., Wohl, E.E. (Eds.), Rivers over rock: Fluvial processes in bedrock channels. American Geophysical Union, Florida, pp. 207-235.
Pedley, M., 2009. Tufas and travertines of the Mediterranean region: a testing ground for freshwater carbonate concepts and developments. Sedimentology, 56, 221-246
Pla-Pueyo, S., Gierlowski-Kordesch, E.H., Viseras, C., Soria, J.M., 2009. Major controls on sedimentation during the evolution of a continental basin: Pliocene–Pleistocene of the Guadix Basin (Betic Cordillera, southern Spain). Sedimentary Geology, 219, 97-114.
Poisson, A.M., Morel, J.L., Andrieux, J., Coulon, M., Wernli, R., Guernet, C., 1999. The origin and development of Neogene basins in the SE Betic Cordileera (SE Spain): A case study of the Tabernas-Sorbas and Huercal-Overa Basins. Journal of Petroleum Geology, 22, 97-114.
Pons, A., Reille, M. 1988. The Holocene-and Upper Pleistocene pollen record from Padul (Granada, Spain): a new study. Palaeogeography, Palaeoclimatology, Palaeoecology, 66, 243-263
Poolton, N.R.J., Kars, R.H., Wallinga, J., Bos, A.J.J., 2009. Direct evidence for the participation of band-tails and excited-state tunnelling in the luminescence of irradiated feldspars. Journal of Physics: Condensed Matter, 21, 485505.
Posamentier, H.W., Vail, P.R., 1988. Eustatic controls on clastic deposition II- sequence and sytems tract models. In: Wilgus, C.K., Hastings, B.S., Kendall, C.G.S.C., Posamentier, H.W., Ross, C.A., Van Wagoner, J.C. (Eds.), Sea-Level Changes-An Integrated Approach, The Society of Economic Palaeontologists and Mineralogists, SEPM Special Publication No. 42, pp. 109 - 124.
Posamentier, H.W., Allen, G.P., 1993. Variability of the sequence stratigraphic model: effects of local basin factors. Sedimentary Geology, 86, 91-109.
Postma, G., 1984. Mass-flow conglomerates in a submarine canyon; Abrioja fan-delta, Pliocene, southeast Spain. Canadian Society of Petroleum Geosciences, Memoir 10, 237-258.
Prescott, J.R., Hutton, J.T., 1994. Cosmic ray contributions to dose rates for luminescence and ESR dating: Large depths and long-term time variations. Radiation Measurements, 23, 497-500.
Prescott, J.R., Hutton, J.T., 1995. Environmental dose rates and radioactive disequilibrium from some Australian luminescence dating sites. Quaternary Science Reviews, 14, 439-448.
Prince, P.S., Spotila, J.A., Henika, W.A., 2011. Stream capture as driver of transient landscape evolution in a tectonically quiescent setting. Geology, 39, 823-826.
Quinton JN, Edwards G, Morgan R. 1997. The influence of vegetation species and plant properties on runoff and soil erosion: results from a rainfall simulation study in south east Spain. Soil Use and Management, 13, 143-148
Reading, H.G., 2009. Sedimentary environments: processes, facies and stratigraphy, Fourth Edition. John Wiley & Sons, Chichester, UK.

Reusser, L.J., Bierman, P.R., Pavich, M.J., Zen, E.-a., Larsen, J., Finkel, R., 2004. Rapid Late Pleistocene Incision of Atlantic Passive-Margin River Gorges. Science, 305, 499-502.

Ries, J.B., Hirt, U. 2008. Permanence of soil surface crusts on abandoned farmland in the Central Ebro Basin/Spain. Catena, 72, 282-296

Rittenour, T.M., 2008. Luminescence dating of fluvial deposits: applications to geomorphic, palaeoseismic and archaeological research. Boreas, 37, 613-635.

Rhodes, E., Schwenninger, J., 2007. Dose rates and radioisotope concentrations in the concrete calibration blocks at Oxford. Ancient TL, 25, 5-8.

Robeson, S.M., 1997. Spherical methods for spatial interpolation: review and evaluation. Cartography and Geographic Information Systems, 24, 3-20.

Roep, T.B., Beets, D.J., Dronkert, H., Pagnier, H. 1979. A prograding coastal sequence of wave-built structures of Messinian age, Sorbas, Almeria, Spain. Sedimentary Geology, 22 , 135-163.

Rogerson, M., Kouwenhoven, T.J., van der Zwaan, G.J., O'Neill, B.J., van der Zwan, C.J., Postma, G., Kleverlaan, K., Tijbosch, H., 2006. Benthic foraminifera of a Miocene canyon and fan. Marine Micropaleontology, 60, 295-318.

Rose, J., Meng, X., Watson, C., 1999. Palaeoclimate and palaeoenvironmental responses in the western Mediterranean over the last 140 ka: evidence from Mallorca, Spain. J. Geol. Soc., 156, 435-448.

Rosenberg, T.M., Preusser, F., Wintle, A.G., 2011. A comparison of single and multiple aliquot TT-OSL data sets for sand-sized quartz from the Arabian Peninsula. Radiation Measurements, 46, 573-579.

Ruiz Bustos, A., Martín Algarra, A., 1991. Propuesta de esquema cronologico y biostratigrafico del Cuaternario en las Cordillera Beticas, VII Reunion Nacional sobre Cuaternario, Valencia, pp. 34-35.

Santisteban, J.I., Schulte, L., 2007. Fluvial networks of the Iberian Peninsula: a chronological framework. Quaternary Science Reviews, 26, 2738-2757.

Sanz de Galdeano, C., 1990. La prolongación hacia el sur de las fosas y desgarres del norte y centro de Europa: una propuesta de interpretación. Revista de la Sociedad Geológica de España, 3, 231-241.

Sanz de Galdeano, C., 1996. The E-W segments of the contact between the External and Internal Zones of the Betic and Rif Cordilleras and the E–W Corridors of the Internal Zone (a combined explanation). Estudios Geologicos, 52, 123-136.

Sanz de Galdeano, C., Vera, J.A., 1992. Stratigraphic record and palaeogeographic context of the Neogene basins in the Betic Cordillera, Spain. Basin Research, 4, 21-36.

Sanz de Galdeano, C., Alfaro, P., 2004. Tectonic significance of the present relief of the Betic Cordillera. Geomorphology, 63, 175-190.

Sanz de Galdeano, C., Shanov, S., Galindo-Zaldívar, J., Radulov, A., Nikolov, G., 2010. A new tectonic discontinuity in the Betic Cordillera deduced from active tectonics and seismicity in the Tabernas Basin. Journal of Geodynamics, 50, 57-66.

Schoorl, J.M., Temme, A.J.A.M., Veldkamp, A. 2014. Modelling centennial sediment waves in an eroding landscape – catchment complexity. Earth Surface Processes and Landforms, 39, 1526-1537

Schulte, L., 2002. Climatic and human influence on river systems and glacier fluctuations in southeast Spain since the Last Glacial Maximum. Quaternary International, 93-94, 85-100.

Schulte, L., Julià, R., Burjachs, F., Hilgers, A., 2008. Middle Pleistocene to Holocene geochronology of the River Aguas terrace sequence (Iberian Peninsula): Fluvial response to Mediterranean environmental change. Geomorphology, 98, 13-33.
Schumm, S.A., 1977. The fluvial system. John Wiley and Sons, New York.
Schumm, S.A., 1979. Geomorphic thresholds: the concept and its applications. Transactions of the Institute of British Geographers, 4, 485-515.
Schumm, S.A., 1993. River Response to Baselevel Change: Implications for Sequence Stratigraphy. The Journal of Geology, 101, 279-294.
Schumm, S.A., Parker, R.S., 1973. Implications of complex response of drainage systems for Quaternary alluvial stratigraphy. Nature (Physical Science) 243, 99-103.
Schumm, S.A., Dumont, J.F., Holbrook, J.M., 2000. Active Tectonics and Alluvial Rivers. Cambridge University Press, Cambridge, UK.
Seale, P., 1999. Quality in qualitative research. Qualitative Inquiry, 5, 465-478.
Siddall, M., Rohling, E.J., Almogi-Labin, A., Hemleben, C., Meischner, D., Schmelzer, I., Smeed, D.A., 2003. Sea-level fluctuations during the last glacial cycle. Nature, 423, 853-858.
Singarayer, J.S., Bailey, R.M., 2003. Further investigations of the quartz optically stimulated luminescence components using linear modulation. Radiation Measurements, 37, 451-458.
Singarayer, J.S., Bailey, R.M., Ward, S., Stokes, S., 2005. Assessing the completeness of optical resetting of quartz OSL in the natural environment. Radiation Measurements, 40, 13-25.
Sklar, L.S., Dietrich, W.E., 2001. Sediment and rock strength controls on river incision into bedrock. Geology, 29, 1087-1090.
Sohbati, R., Murray, A.S., Buylaert, J.-P., Ortuño, M., Cunha, P.P., Masana, E., 2012. Luminescence dating of Pleistocene alluvial sediments affected by the Alhama de Murcia fault (eastern Betics, Spain) – a comparison between OSL, IRSL and post-IRIRSL ages. Boreas, 41, 250-262.
Stange, K.M., van Balen, R., Vandenberghe, J., Peña, J.L., Sancho, C. 2013. External controls on Quaternary fluvial incision and terrace formation at the Segre River, Southern Pyrenees. Tectonophysics, 602 (0), 316-331.
Starkel, L., 2003. Climatically controlled terraces in uplifting mountain areas. Quaternary Science Reviews, 22, 2189-2198.
Stemerdink, C. 2007. A Numerical Model of Post-Anglian Longitudinal Profile Development of the River Thames in the Upper Thames Basin. Newcastle University, PhD Thesis.
Stemerdink, C., Maddy, D., Bridgland, D.R., Veldkamp, A., 2010. The construction of a palaeodischarge time series for use in a study of fluvial system development of the Middle to Late Pleistocene Upper Thames. Journal of Quaternary Science, 25, 447-460.
Stokes, M., 1997. Plio-Pleistocene Drainage Evolution of the Vera Basin, SE Spain. University of Plymouth, Plymouth, PhD Thesis.
Stokes, M., 2008. Plio-Pleistocene drainage development in an inverted sedimentary basin: Vera basin, Betic Cordillera, SE Spain. Geomorphology, 100, 193-211.
Stokes, M., Mather, A.E., 2000. Response of Plio-Pleistocene alluvial systems to tectonically induced base-level changes, Vera Basin, SE Spain. J. Geol. Soc., 157, 303-316.
Stokes, M., Mather, A.E., Harvey, A.M., 2002. Quantification of river capture induced base-level changes and landscape development, Sorbas Basin, SE Spain. In: Jones, S.J.,

Frostick, L.E. (Eds.), Sediment Flux to Basins: Causes, Controls, Consequences. Geological Society, London, Special Publication, 191, pp. 23– 35.
Stokes, M., Mather, A.E., 2003. Tectonic origin and evolution of a transverse drainage: the Rıo Almanzora, Betic Cordillera , Southeast Spain. Geomorphology, 50, 59-81.
Stokes, M., Nash, D.J., Harvey, A.M., 2007. Calcrete 'fossilisation' of alluvial fans in SE Spain: The roles of groundwater, pedogenic processes and fan dynamics in calcrete development. Geomorphology, 85, 63-84.
Stokes, M., Cunha, P.P., Martins, A.A., 2012a. Techniques for analysing Late Cenozoic river terrace sequences. Geomorphology, 165–166, 1-6.
Stokes, M., Griffiths, J.S., Mather, A., 2012b. Palaeoflood estimates of Pleistocene coarse grained river terrace landforms (Río Almanzora, SE Spain). Geomorphology, 149–150, 11-26.
Strahler, A.N., 1950. Equilibrium theory of erosional slopes approached by frequency distribution analysis. Part I. American Journal of Science, 248, 673-696
Tarasov, P., Williams, J.W., Andreev, A., Nakagawa, T., Bezrukova, E., Herzschuh, U., Igarashi, Y., Müller, S., Werner, K., Zheng, Z. 2007. Satellite-and pollen-based quantitative woody cover reconstructions for northern Asia: verification and application to late-Quaternary pollen data. Earth and Planetary Science Letters, 264, 284-298
Tebbens, L.A., 1999. Late Quaternary evolution of the Meuse fluvial system and its sediment composition. A reconstruction based on bulk sample geochemistry and forward modelling. Wageningen University, The Netherlands, PhD Thesis.
Tebbens, L.A., Veldkamp, A., 2000. Late Quaternary evolution of fluvial sediment composition: a modeling case study of the River Meuse. Global and Planetary Change, 27, 187-206.
Thiel, C., 2011. On the applicability of post-IR IRSL dating to different environments, Freien Universität Berlin, PhD Thesis.
Thiel, C., Buylaert, J.-P., Murray, A., Terhorst, B., Hofer, I., Tsukamoto, S., Frechen, M., 2011. Luminescence dating of the Stratzing loess profile (Austria) – Testing the potential of an elevated temperature post-IR IRSL protocol. Quaternary International, 234, 23-31.
Thomsen, K.J., Murray, A.S., Jain, M., Bøtter-Jensen, L., 2008. Laboratory fading rates of various luminescence signals from feldspar-rich sediment extracts. Radiation Measurements, 43, 1474-1486.
Thomsen, K.J., Murray, A.S., Buylaert, J.P., Jain, M., Hansen, J.H. , Aubry,T., In review. Testing single-grain quartz OSL methods using known age samples from the Bordes-Fitte rockshelter (Roches d'Abilly site, Central France). Quaternary Geochronology
Thorndycraft, V.R., Benito, G., Gregory, K.J., 2008. Fluvial geomorphology: A perspective on current status and methods. Geomorphology, 98, 2-12.
Torri, D., Calzolari, C., Rodolfi, G., 2000. Badlands in changing environments: an introduction. Catena, 40, 119-125.
Trochim, W. 2006. The Research Methods Knowledge Base, 2nd Edition. Internet www page at URL : > http://www.socialresearchmethods.net/kb/dedind.php (Last accessed 4th June 2013).
Troels-Smith, J., 1955. Characterization of unconsolidated sediments. Geological survey of Denmark: iv. Series. Vol. 3, C. A. Reitzels forlag, Copenhagen, 77 pp.

Troiani, F., Della Seta, M., 2011. Geomorphological response of fluvial and coastal terraces to Quaternary tectonics and climate as revealed by geostatistical topographic analysis. Earth Surface Processes and Landforms, 36, 1193-1208.
Trudgill, B.D., 2002. Structural controls on drainage development in the Canyonlands grabens of southeast Utah. AAPG Bulletin, 86, 1095-1112.
Tucker, G.E., 2003. Sedimentary Rocks in the field, Third Edition. John Wiley and Sons Ltd., Chichester, UK.
Tucker, G.E., 2011. Sedimentary Rocks in the field, Fourth Edition. John Wiley and Sons Ltd., Chichester, UK.
Tucker, G.E., Hancock, G.R. 2010. Modelling landscape evolution. Earth Surface Processes and Landforms, 35, 28-50.
Twidale, C.R., 2004. River patterns and their meaning. Earth-Science Reviews, 67,159-218.
Van den Berg, M.W., van Hoof, T., 2001. The Maas Terrace sequence at Maastricht, SE Netherlands; evidence for 200 m of late Neogene and Quaternary surface uplift. In: Maddy, D., Macklin, M.G., Woodward, J.C. (Eds.), River basin sediment systems; archives of environmental change. A.A. Balkema, Netherlands, pp. 45-86.
Van Gorp, W., Temme, A.J.A.M., Baartman, J.E.M., Schoorl, J.M., 2014. Landscape Evolution Modelling of naturally dammed rivers. Earth Surface Processes and Landforms, 39, 1587-1600.
Vandenberghe, J., 1995. Timescales, climate and river development. Quaternary Science Reviews, 14, 631-638.
Vandenberghe, J., 2003. Climate forcing of fluvial system development: an evolution of ideas. Quaternary Science Reviews, 22, 2053-2060.
Vandenberghe, J., Cordier, S., Bridgland, D.R., 2010. Extrinsic and intrinsic forcing of fluvial development: understanding natural and anthropogenic influences. Proceedings of the Geologists' Association, 121, 107-112
Vásquez-Méndez, R., Ventura-Ramos, E., Oleschko, K., Hernández-Sandoval, L., Parrot, J.-F., Nearing, M.A., 2010. Soil erosion and runoff in different vegetation patches from semiarid Central Mexico. Catena, 80, 162-169.
Veldkamp, A., Van Dijke, J.J., 2000. Simulating internal and external controls on fluvial terrace stratigraphy: a qualitative comparison with the Maas record. Geomorphology, 33, 225-236.
Veldkamp, A., Tebbens, L.A., 2001. Registration of abrupt climate changes within fluvial systems: insights from numerical modelling experiments. Global and Planetary Change, 28, 129-144.
Vera, J.A., 2001. Evolution of the South Iberian continental margin. In: Ziegler, P.A., Cavazza, W., Robertson, A.H.F., Crasquin-Soleau, S. (Eds.), Peri-Tethys Memoir 6: Peri-Tethyan Rift/Wrench Basins and Passive Margins. Mémoires du Muséum national d'Histoire naturelle (Paris), 186, pp. 109–143.
Vieira, S R.,Carvalho, J.R P., González, A P., 2010. Jack knifing for semivariogram validation. Bragantia, 69, 97-105.
Visocekas, R., 1985. Tunnelling radiative recombination in labradorite: Its association with anomalous fading of thermoluminescence. Nuclear Tracks Radiation Measurements, 10, 521-529.
Viveen, W., Braucher, R., Bourlès, D., Schoorl, J.M., Veldkamp, A., van Balen, R.T., Wallinga, J., Fernandez-Mosquera, D., Vidal-Romani, J.R., Sanjurjo-Sanchez, J., 2012. A 0.65Ma chronology and incision rate assessment of the NW Iberian Miño

River terraces based on 10Be and luminescence dating. Global and Planetary Change, 94–95, 82-100.
Viveen, W., Schoorl, J.M., Veldkamp, A., van Balen, R.T., Desprat, S., Vidal-Romani, J.R., 2013a. Reconstructing the interacting effects of base level, climate, and tectonic uplift in the lower Miño River terrace record: A gradient modelling evaluation. Geomorphology, 186, 96-118.
Viveen, W., Schoorl, J.M., Veldkamp, A., van Balen, R.T., Vidal-Romani, J.R., 2013b. Fluvial terraces of the northwest Iberian lower Miño River. Journal of Maps, 9, 513-522.
Viveen, W., Schoorl, J.M., Veldkamp, A., van Balen, R.T., 2014. Modelling the impact of regional uplift and local tectonics on fluvial terrace preservation. Geomorphology, 210, 119-135.
Wanner, H., Beer, J., Bütikofer, J., Crowley, T.J., Cubasch, U., Flückiger, J., Goosse, H., Grosjean, M., Joos, F., Kaplan, J.O., Küttel, M., Müller, S.A., Prentice, I.C., Solomina, O., Stocker, T.F., Tarasov, P., Wagner, M., Widmann, M., 2008. Mid- to Late Holocene climate change: an overview. Quaternary Science Reviews, 27, 1791-1828.
Waters, J.M., Allibone, R.M., Wallis, G.P., 2006. Geological subsidence, river capture, and cladogenesis of galaxiid fish lineages in central New Zealand. Biological Journal of the Linnaean Society, 88, 367-376.
Walker, M., 2005. Radiometric Dating: Radiation Exposure Dating. In: M. Walker (Ed.), Quaternary Dating Methods. John Wiley & Sons, Ltd, Chichester, UK, pp. 93-120.
Wallinga, J., Murray, A.S., Duller, G.A.T., Törnqvist, T.E., 2001. Testing optically stimulated luminescence dating of sand-sized quartz and feldspar from fluvial deposits. Earth Planet. Sci. Lett., 193, 617-630.
Wallinga, J., 2002. Optically stimulated luminescence dating of fluvial deposits: a review. Boreas, 31, 303-322.
Watson, D.F., Philip, G.M., 1985. A refinement of inverse distance weighted interpolation. Geoprocessing, 2, 315-327.
Weijermars, R., 1991. Geology and tectonics of the Betic Zone, SE Spain. Earth-Science Reviews, 31, 153-236.
Weijermars, R., Roep, T.B., Van den Eeckhout, B., Postma, G., Kleverlaan, K., 1985. Uplift history of a Betic fold nappe inferred from Neogene–Quaternary sedimentation and tectonics (in the Sierra Alhamilla and Almeria, Sorbas and Tabernas Basins of the Betic Cordilleras, SE Spain). Geologie en Mijnbouw, 64, 397-411.
Wenzens, E., 1992. Mid-Quaternary climatic conditions and relief development in the Vera Basin, southeast Spain. Eiszeitalter und Gegenwart, 42, 121-133.
Wenzens, E., Wenzens, G., 1997. The influence of tectonics, sea-level fluctuations and river capture on the Quaternary morphogenesis of the semi-arid Pulpi Basin (southeast Spain). Catena, 30, 283-293.
Westaway, R., 2002. Long-term river terrace sequences: Evidence for global increases in surface uplift rates in the Late Pliocene and early Middle Pleistocene caused by flow in the lower continental crust induced by surface processes. Netherlands Journal of Geosciences, 81, 305-328.
Westaway, R., 2006. Investigation of coupling between surface processes and induced flow in the lower continental crust as a cause of intraplate seismicity. Earth Surface Processes and Landforms, 31, 1480–1509.

Westaway, R., Bridgland, D.R., Sinha, R., Demir, T., 2009. Fluvial sequences as evidence for landscape and climatic evolution in the Late Cenozoic: A synthesis of data from IGCP 518. Global and Planetary Change, 68, 237-253.

Whipple, K.X., Tucker, G.E. 2002. Implications of sediment-flux-dependent river incision models for landscape evolution. Journal of Geophysical Research: Solid Earth, 107, 310-320.

Williams, J.W, Jackson ST. 2003. Palynological and AVHRR observations of modern vegetation gradients in eastern North America. The Holocene, 13, 485-497

Wilson, J.P., Gallant, J.C., 2000. Terrain Analysis: Principles and Applications. John Wiley and Sons, New York.

Wintle, A.G., 1973. Anomalous fading of thermoluminescence in mineral samples. Nature, 245, 143-144.

Wintle, A.G., 2008. Luminescence dating: where it has been and where it is going. Boreas, 37, 471-482.

Wintle, A.G., Huntley, D.J., 1980. Thermoluminescence dating of ocean sediments. Canadian Journal of Earth Sciences, 17, 348-360

Wintle, A.G., Murray, A.S., 2006. A review of quartz optically stimulated luminescence characteristics and their relevance in single-aliquot regeneration dating protocols. Radiation Measurements, 41, 369–391.

Wright, V.P., Tucker, M.E., 1991. Calcretes. Blackwell Scientific Publications., London.

Yao, X., Fu, B., Lu, Y., Sun, F., Wang, S., 2013. Comparison of four spatial interpolation methods for estimating soil moisture in a complex terrain catchment. PLoS ONE, 8, e54660.

Yunker, M.B., Macdonald, R.W., Veltkamp, D.J., Cretney, W.J., 1995. Terrestrial and marine biomarkers in a seasonally ice-covered Arctic estuary — integration of multivariate and biomarker approaches. Marine Chemistry, 49, 1-50

Zaprowski, B.J., Evenson, E.B., Epstein, J.B., 2002. Stream piracy in the Black Hills: a geomorphology lab exercise. Journal of Geoscience Education, 50, 380-388.

Zazo, C., Goy, J.L., Dabrio, C.J., Bardají, .T, Hillaire-Marcel, C., Ghaleb, B., González-Delgado, J.A., Soler, V., 2003. Pleistocene raised marine terraces of the Spanish Mediterranean and Atlantic coasts: records of coastal uplift, sea-level highstands and climate changes. Marine Geology, 194, 103-133.

Zielhofer, C., Faust, D., Linstädter, J., 2008. Late Pleistocene and Holocene alluvial archives in the Southwestern Mediterranean: Changes in fluvial dynamics and past human response. Quaternary International, 181, 39-54.

Zimmerman, D., Pavlik, C., Ruggles, A., Armstrong, M.P., 1999. An experimental comparison of ordinary and universal kriging and inverse distance weighting. Mathematical Geology, 31, 375-390.